DEEP PELAGIC ECOSYSTEM DYNAMICS IN A HIGHLY IMPACTED WATER COLUMN: THE GULF OF MEXICO AFTER DEEPWATER HORIZON

EDITED BY: Tracey T. Sutton, Heather Bracken-Grissom, Jose V. Lopez, Michael Vecchione and Marsh J. Youngbluth

PUBLISHED IN: Frontiers in Marine Science

frontiers Research Topics

frontiers

ISSN 1664-8714
ISBN 978-2-88966-716-1
DOI 10.3389/978-2-88966-716-1

About Frontiers

Frontiers is more than just an open-access publisher of scholarly articles: it is a pioneering approach to the world of academia, radically improving the way scholarly research is managed. The grand vision of Frontiers is a world where all people have an equal opportunity to seek, share and generate knowledge. Frontiers provides immediate and permanent online open access to all its publications, but this alone is not enough to realize our grand goals.

Frontiers Journal Series

The Frontiers Journal Series is a multi-tier and interdisciplinary set of open-access, online journals, promising a paradigm shift from the current review, selection and dissemination processes in academic publishing. All Frontiers journals are driven by researchers for researchers; therefore, they constitute a service to the scholarly community. At the same time, the Frontiers Journal Series operates on a revolutionary invention, the tiered publishing system, initially addressing specific communities of scholars, and gradually climbing up to broader public understanding, thus serving the interests of the lay society, too.

Dedication to Quality

Each Frontiers article is a landmark of the highest quality, thanks to genuinely collaborative interactions between authors and review editors, who include some of the world's best academicians. Research must be certified by peers before entering a stream of knowledge that may eventually reach the public - and shape society; therefore, Frontiers only applies the most rigorous and unbiased reviews.
Frontiers revolutionizes research publishing by freely delivering the most outstanding research, evaluated with no bias from both the academic and social point of view. By applying the most advanced information technologies, Frontiers is catapulting scholarly publishing into a new generation.

What are Frontiers Research Topics?

Frontiers Research Topics are very popular trademarks of the Frontiers Journals Series: they are collections of at least ten articles, all centered on a particular subject. With their unique mix of varied contributions from Original Research to Review Articles, Frontiers Research Topics unify the most influential researchers, the latest key findings and historical advances in a hot research area! Find out more on how to host your own Frontiers Research Topic or contribute to one as an author by contacting the Frontiers Editorial Office: frontiersin.org/about/contact

DEEP PELAGIC ECOSYSTEM DYNAMICS IN A HIGHLY IMPACTED WATER COLUMN: THE GULF OF MEXICO AFTER DEEPWATER HORIZON

Topic Editors:
Tracey T. Sutton, Nova Southeastern University, United States
Heather Bracken-Grissom, Florida International University, United States
Jose V. Lopez, Nova Southeastern University, United States
Michael Vecchione, National Oceanic and Atmospheric Administration (NOAA), United States
Marsh J. Youngbluth, Florida Atlantic University, United States

The Topic Editors Tracey Sutton, Heather Bracken-Grissom, Jose Lopez, Michael Vecchione and Marsh Youngbluth declare that they are affiliated with the DEEPEND consortium on the biotic composition, distribution, and abundance of deep-pelagic (0-1500 m depth) assemblages.

Citation: Sutton, T. T., Bracken-Grissom, H., Lopez, J. V., Vecchione, M., Youngbluth, M. J., eds. (2021). Deep Pelagic Ecosystem Dynamics in a Highly Impacted Water Column: The Gulf of Mexico After Deepwater Horizon. Lausanne: Frontiers Media SA. doi: 10.3389/978-2-88966-716-1

Table of Contents

frontiers in Marine Science

EDITORIAL
published: 09 March 2021
doi: 10.3389/fmars.2021.653074

Editorial: Deep Pelagic Ecosystem Dynamics in a Highly Impacted Water Column: The Gulf of Mexico After *Deepwater Horizon*

Tracey T. Sutton[1], Kevin M. Boswell[2], Heather D. Bracken-Grissom[2], Jose V. Lopez[1], Michael Vecchione[3] and Marsh Youngbluth[4]*

[1] Guy Harvey Oceanographic Center, Halmos College of Arts and Sciences, Nova Southeastern University, Dania Beach, FL, United States, [2] Department of Biological Sciences, Institute of Environment, Florida International University, North Miami, FL, United States, [3] NMFS National Systematics Laboratory, National Museum of Natural History, Washington, DC, United States, [4] Harbor Branch Oceanographic Institution at Florida Atlantic University, Fort Pierce, FL, United States

Keywords: epipelagic, mesopelagic, bathypelagic, ecology, biodiversity, connectivity, biophysical coupling

Editorial on the Research Topic

Deep Pelagic Ecosystem Dynamics in a Highly Impacted Water Column: The Gulf of Mexico After Deepwater Horizon

OPEN ACCESS

Edited and reviewed by:
Eva Ramirez-Llodra, REV Ocean, Norway

****Correspondence:***
Tracey T. Sutton
tsutton1@nova.edu

Specialty section:
This article was submitted to Deep-Sea Environments and Ecology, a section of the journal Frontiers in Marine Science

Received: *13 January 2021*
Accepted: *12 February 2021*
Published: *09 March 2021*

Citation:
Sutton TT, Boswell KM, Bracken-Grissom HD, Lopez JV, Vecchione M and Youngbluth M (2021) Editorial: Deep Pelagic Ecosystem Dynamics in a Highly Impacted Water Column: The Gulf of Mexico After Deepwater Horizon. Front. Mar. Sci. 8:653074. doi: 10.3389/fmars.2021.653074

AIMS AND OBJECTIVES OF RESEARCH TOPIC

The intermediate-sized midwater fauna (fishes, shrimps, and cephalopods; "micronekton" collectively) are dominant components of the pelagic ocean, which is by far the largest ecosystem type on Earth by several metrics (volume, organismal numbers, biomass, and productivity). Deep-pelagic micronekton, those animals residing in the water column below 200 m depth during the day, are the direct link between plankton and oceanic top predators, and through the linked processes of feeding and daily vertical migration facilitate one of Earth's most important ecosystem services to humans, carbon sequestration. Despite increasing recognition of this importance, a disconnect exists between stewardship and human impact; only a miniscule fraction of the deep-pelagic ocean has been studied in detail, while anthropogenic threats to that system are increasing rapidly. Perhaps nowhere on Earth is that dichotomy more demonstrable than the Gulf of Mexico (Gulf hereafter), a complex, high-diversity ecosystem under intense human usage and subjected to arguably the worst marine pollution event in human history.

Assessment of the impacts of the *Deepwater Horizon* disaster to the deep-pelagic biota was impeded from the start by the lack of pre-event information, both in terms of baselines (faunal composition, abundance, and distribution) and in terms of understanding natural variability, against which impacts of anthropogenic disturbance could be detected and quantified. In this Research Topic, we present a description of three interlinked research programs (ONSAP, DEEPEND, and DEEPEND|RESTORE, described below) that began in 2010 and continue as of this writing. These programs were designed to investigate key aspects of the Gulf pelagic ecosystem, including its faunal structure, biophysical drivers of that structure, organismal and community ecology, natural variability, and potential resilience to disturbance. The contributed papers are grouped below by major themes, indicated in the conceptual model (**Figure 1**) of DEEPEND (Deep Pelagic Nekton Dynamics; www.deependconsortium.org), the largest of the three aforementioned research programs.

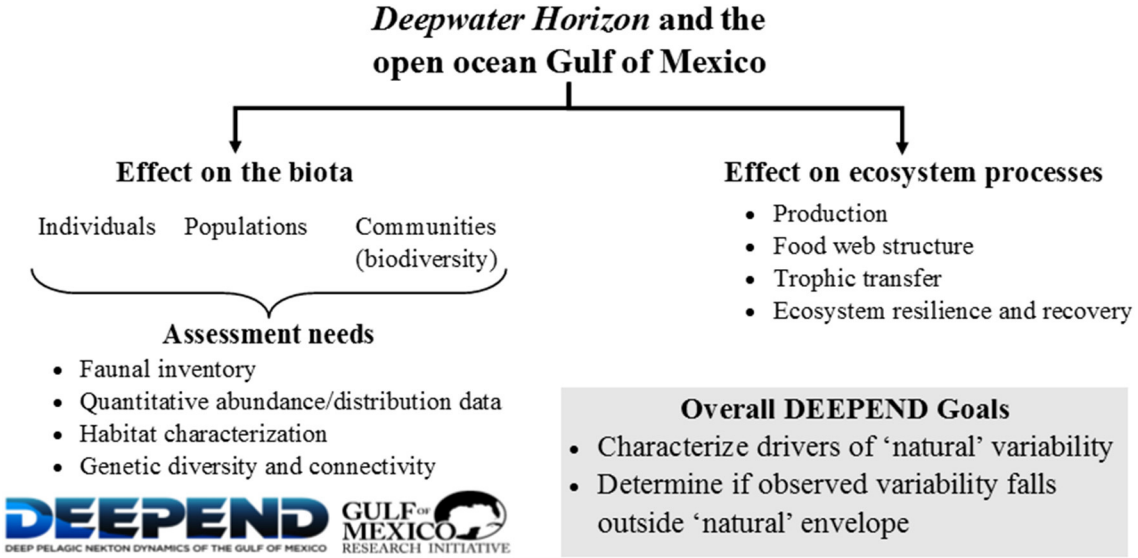

FIGURE 1 | The conceptual framework of the DEEPEND research consortium.

INTEGRATED, MULTIDISCIPLINARY RESEARCH TO TACKLE A COMPLEX TOPIC

The pelagic Gulf is characterized by dynamic physical oceanography, high species richness (as determined by the research programs described herein), and complex faunal distributions resulting from the interplay between daily vertical animal movement and current-mediated horizontal transport. Thus, assessment of the system and the potential effects of the *Deepwater Horizon* disaster (DWH hereafter) on that system required a multidisciplinary approach, as described in Cook et al., Boswell et al., Easson et al., and Timm et al. The full suite of integrated approaches included *in situ* sampling, water column profiling, acoustic sensing, satellite remote sensing, microbial and metazoan genetic analysis, trophic analysis using traditional and biochemical methodologies, petrogenic contamination analysis, imaging, AUV sensing, and numerical modeling.

The primary focus of research devoted to this Research Topic issue was research conducted by DEEPEND, a 5-year (2015–2020), 102-member, 19-organization research consortium supported by The Gulf of Mexico Research Initiative (GoMRI; https://gulfresearchinitiative.org). DEEPEND was an expanded successor of the NOAA-supported Offshore Nekton Sampling and Analysis Program (ONSAP; 2010–2015), whose explicit mission was to provide faunal composition and abundance information for NOAA's DWH natural resource damage assessment (Sutton et al., 2020). DEEPEND's approaches included: (1) a direct assessment of Gulf deep-pelagic community structure, from the surface to 1,500 m, with simultaneous investigation of the physical and biological (including microbial; Easson and Lopez, 2019) drivers of this structure; (2) quantification of 'natural' variability against which longer-term disturbance and recovery trends could be detected; (3) a time-series biophysical modeling approach comparing data collected shortly after DWH (2010–2011; ONSAP sampling) to 2015–2018 (DEEPEND sampling); and (4) an assessment of the extant and potential future consequences of DWH on the pelagic biota of the Gulf. At the culmination of the 10-year tenure of GoMRI in 2020, DEEPEND was funded to continue time-series analysis and to translate information gained into resource management products via the NOAA RESTORE Science Program.

COMMUNITY ECOLOGY: DIVERSITY, POPULATION DYNAMICS, AND REPRODUCTION

Several papers provided corroboration for the classification of the Gulf as one of the global ocean's most speciose mesopelagic ecosystems (Sutton et al., 2017). A highly resolved inventory of biological diversity is critical in systems exposed to intense natural and anthropogenic perturbations (such as the Gulf), as diversity is a fundamental emergent property of ecosystems, reflecting complexity and resilience, as well as indicating regime shifts and alternate stable states. Moore et al. highlighted the dominant contribution of a chronically overlooked pelagic faunal group, eels (specifically, leptocephalus larvae), including numerous new records for the Gulf, while Frank et al., Judkins and Vecchione, Meinert et al., and Milligan and Sutton provided detailed quantitative faunal inventories of euphausiids ("krill"), cephalopods, ichthyoplankton, and lanternfishes, respectively.

Other papers examined aspects of the abundance, distribution, and reproduction of foundational oceanic taxa of the Gulf. These papers relate to the spatial and temporal attributes of the pelagic fauna as a function of DWH exposure. Were some

fauna more prevalent in the DWH footprint, and did key ecological processes, such as reproduction, coincide with the DWH? Frank et al. examined the euphausiid assemblage of the Gulf and its relationship to the "oceanic rim," reporting higher abundances but lower diversity over the continental slope (200–1,000 m bottom depth) compared to open water (>1,000 m bottom depth). These authors also noted evidence for seasonal spawning in the Gulf, a critical element of vulnerability to, and recovery from, point-source disturbances. Marks et al. highlighted the dearth of information about the organismal biology of deep-pelagic species in general and provided the first reproductive information about the dominant mesopelagic fish predators of the Gulf (dragonfishes, Family Stomiidae). They found that dragonfishes are gonochoristic (separate sexes and not hermaphroditic), iteroparous, batch spawners with protracted reproductive capacity throughout the year. Such data are crucial for understanding what may be the largest data gap in deep-pelagic ecology, the reproductive timing and rates of its constituents.

VERTICAL MIGRATION DYNAMICS

The largest coordinated animal movement on Earth happens every day in the pelagic ocean in the form of diel (daily) vertical migration (DVM), with meso- and sometimes bathypelagic animals ascending from deep daytime residence depths to shallower nighttime depths to feed, then descending again at daybreak. DVM is one of the primary elements of the "biological pump," whose value to humans in sequestering carbon has been estimated in the 100's of billions to trillions of dollars (USD; Hoagland et al., 2019). Boswell et al. used integrated acoustical, remote sensing and net-sampling data to illustrate relationships of depth and intensity of "deep scattering layers" (i.e., layers of maximal faunal abundance, inferred from acoustic backscatter) with oceanographic conditions and light intensity. This was particularly evident within the Gulf's major oceanographic feature, the Loop Current, where they acoustically estimated that biomass was two to four times lower than residual Gulf waters. Easson et al. found shifting environmental DNA (eDNA) profiles tied to DVM, providing another tool with which to study DVM dynamics. Judkins and Vecchione found that a very large percentage (95%) of the Gulf's cephalopod assemblage is distributed at the deep-meso/bathypelagic interface (1,000–1,400 m depth), coincident with a large subsurface hydrocarbon/dispersant plume that developed after DWH (Camilli et al., 2010). Milligan and Sutton reported that the strong DVM habits of lanternfishes (Family Myctophidae) paired with depth-specific, multidirectional current shear resulted in the broad distribution of the assemblage as a whole. In essence, the entire lanternfish assemblage of the northern Gulf can be treated and managed as one contiguous stock.

MESOSCALE BIOPHYSICAL COUPLING

Assessment of pelagic community structure, and its variation, in a given area is complicated by the effect of constant water movement and water mass replacement, akin to the adage "you never put your foot in the same river twice." In both the Gulf and pelagic regions worldwide, depth is the primary determinant of community structure, with the proviso that depth is a multivariate factor; light, heat, pressure, water density, sound transmission, and food availability all vary directly with depth. In the horizontal/geographical context of the Gulf, mesoscale oceanographic features are the primary components of habitat variability (see Johnston et al., 2019), and thus putative drivers of community structure. In addition to findings of Boswell et al. mentioned previously, Meinert et al. reported in this Research Topic that cyclonic eddies, frontal features, and areas of upwelling are areas of higher biodiversity of fish larvae, and that the mixed layer is an essential habitat for deep-pelagic fishes during early-life stages. In a study of larval and juvenile tunas of the Gulf, Pruzinsky et al. reported that over large spatial scales, early-life-history stages of commercially important species partition habitat on the mesoscale in addition to the temporal scale tied to adult spawning. These factors are important for spatially and temporally explicit modeling developed to predict stock sizes of higher trophic levels in oceanic ecosystems. Timm et al. investigated comparative population genomics and biophysical oceanography, which suggested that vertical migration habits (or lack thereof) have important implications for horizontal transport between the Gulf and adjacent waters via the fast moving waters of the Loop Current. Studies such as these are essential to establish an envelope of natural variability against which variability caused by a pollution event can be compared.

PELAGIC ECOSYSTEM CONNECTIVITY

The pelagic ocean has been historically delineated into depth strata based on light penetration (epipelagic, mesopelagic, and bathypelagic domains, representing the photic, disphotic, and aphotic layers of the water column, respectively). Research has often been stratified in this manner as well, with little or no integration across depths and oceanographic subdisciplines. Thus, the connectivity between these depth zones is poorly documented (Sutton, 2013). Likewise, connectivity between ocean basins and sub-basins, and connectivity between the neritic and pelagic domains, are understudied. Several DEEPEND publications have examined vertical distribution patterns within and between pelagic populations, including Boswell et al., Easson et al., Judkins and Vecchione, Milligan and Sutton, and Timm et al. from this Research Topic (please see D'Elia et al., 2016; Sutton et al., 2020 for references of previous works). Milligan and Sutton and Timm et al. also added a horizontal connectivity component, both within the Gulf basin proper and the adjacent seas, respectively. Frank et al. reported increased euphausiid abundances over the continental slope compared to open water, emphasizing the important connectivity of oceanic and coastal ecosystems through "boundary communities" of putatively enhanced trophic interaction. In terms of ecological connectivity, the study of Richards et al. determined that isotopic values of particulate organic matter can vary significantly over relatively small horizontal and vertical scales, and that baseline

variation can be conserved in the signatures of higher-order consumers. In terms of DWH, one of the primary attributes of this disaster compared to those that preceded it was the wide range of habitats effected, in other words the high connectivity of the disaster. Research on connectivity of the biota affected must be conducted on a similar scale for this and future large-scale pollution events.

IMPLICATIONS FOR RESOURCE MANAGEMENT

One of the grand challenges of deep-sea research is convincing the public, stake holders, resource managers and even other scientists that the deep sea really matters (Jamieson et al., 2020). The need for such awareness is manifest in the summary findings of DEEPEND and its associated programs, namely that the Gulf is a highly integrated unit that should be managed holistically rather than in parts. The current efforts of the DEEPEND consortium, and future work funded by the NOAA RESTORE Science Program (www.restoreactscienceprogram.noaa.gov), are focused on that theme. For example, Romero et al. in this and previous works (e.g., Romero et al., 2018) emphasized the need for long-term monitoring of petrogenic contamination in the deep-pelagic fauna to ascertain the persistence of oil spill effects and reverberate after the source has been contained. With the steadily increasing depths of oil production in the Gulf (Gulf "ultra-deep" wells now provide the majority of US oil production; Murawski et al., 2019) and the likelihood of accidents increasing with platform depth (Muehlenbachs et al., 2013), deep oils spills are not just possible, they are likely. Resource management efforts such as NOAA's Natural Resource Damage Assessments require such information now and in response to future spills. Multiple authors in this Research Topic have also shown that the northern Gulf is a critical habitat for the juveniles of commercially important fish and invertebrate species, as well as other coastal, demersal, and benthic species (Pruzinsky et al.; Meinert et al.; Moore et al.). The deep-pelagic micronekton are vital components of oceanic food webs (Frank et al.; Judkins and Vecchione; Milligan and Sutton,; Richards et al.), the trophodynamics of which represent one of the major data gaps with respect to the stewardship of apex predatory fishes, cetaceans, and seabirds (including endangered species).

The DWH disaster emphasized the lack of faunal inventories and baselines for deep-sea pelagic ecosystems being exposed to industrial disturbance. In creating quantitative and genetic inventories for the pelagic Gulf (e.g., Frank et al.; Moore et al.), the DEEPEND group had to sequentially decipher information written in English, French, Russian, Spanish, and Italian. These data are now accessible in a collated form for use in resource management. We anticipate that this Research Topic will serve to advance deep-sea research beyond the strictly "*Challenger*-era" domain of descriptive science. Although description is an absolutely essential first step and one from which we are still very far away for much of the global ocean, the next-level analyses presented here of emergent properties, ecosystem functioning, and ecosystem resilience are necessary for understanding the ecosystem as well as results of human impacts on it.

AUTHOR CONTRIBUTIONS

TS, KB, HB-G, JL, MV, and MY conceived the Research Topic and wrote the manuscript. All authors approved the submitted version.

ACKNOWLEDGMENTS

We would like to thank the collaboration of 36 reviewers for making this collection of papers possible. We thank the 42 authors for their tireless pursuits during the DEEPEND program, and for sharing the products of their research for this issue. Last but not least, we thank The Gulf of Mexico Research Initiative, the NOAA Office of Response and Restoration, and the NOAA RESTORE Science Program for funding the research encompassed herein.

REFERENCES

Camilli, R., Reddy, C. M., Yoerger, D. R., Van Mooy, B. A. S., Jakuba, M. V., Kinsey, J. C., et al. (2010). Tracking hydrocarbon plume transport and biodegradation at Deepwater Horizon. *Science* 330, 201–204. doi: 10.1126/science.1195223

D'Elia, M., Warren, J. D., Rodriguez-Pinto, I., Sutton, T. T., and Cook, A. B. (2016). Diel variation in the vertical distribution of deep-water scattering layers in the Gulf of Mexico. *Deep-Sea Res. I* 115, 91–102. doi: 10.1016/j.dsr.2016.05.014

Easson, C. G., and Lopez, J. V. (2019). Environmental drivers of bacterioplankton community structure in the northern Gulf of Mexico. *Front. Microbiol.* 9:3175. doi: 10.3389/fmicb.2018.03175

Hoagland, P., Jin, D., Holland, M., Kostel, K., Taylor, E., Renier, N., et al. (2019). Ecosystem services of the mesopelagic. *Woods Hole Oceanographic Inst.* 2019:35. doi: 10.1575/1912/25013

Jamieson, A. J., Singleman, G., Linley, T. D., and Casey, S. (2020). Fear and loathing of the deep ocean: why don't people care about the deep sea? *ICES J. Mar. Sci.* fsaa234. doi: 10.1093/icesjms/fsaa234

Johnston, M., Milligan, R., Easson, C., DeRada, S., Penta, B., and Sutton, T. (2019). An empirically-validated method for characterizing pelagic habitats in the Gulf of Mexico using ocean model data. *Limnol. Oceanogr. Meth.* 17, 362–375. doi: 10.1002/lom3.10319

Muehlenbachs, L., Cohen, M. A., and Gerarden, T. (2013). The impact of water depth on safety and environmental performance in offshore oil and gas production. *Energy Policy* 55, 699–705. doi: 10.1016/j.enpol.2012.12.074

Murawski, S., Ainsworth, C., Gilbert, S., Hollander, D., Paris, C., Schlüter, M., et al. (2019). *Scenarios and Responses to Future Deep Oil Spills: Fighting the Next War*. Springer. doi: 10.1007/978-3-030-12963-7

Romero, I. C., Sutton, T. T., Carr, B., Quintana-Rizzo, E., Ross, S. W., Hollander, D. J., et al. (2018). Decadal assessment of polycyclic aromatic hydrocarbons in mesopelagic fishes from the Gulf of Mexico reveals exposure to oil-derived sources. *Envir. Sci. Tech.* 52, 10985–10996. doi: 10.1021/acs.est.8b02243

Sutton, T. T. (2013). Vertical ecology of the pelagic ocean: classical patterns and new perspectives. *J. Fish Biol.* 83, 1508–1527. doi: 10.1111/jfb.12263

Sutton, T. T., Clark, M. R., Dunn, D. C., Halpin, P. N., Rogers, A. D., et al. (2017). A global biogeographic classification of the mesopelagic zone. *Deep Sea Res. I* 126, 85–102. doi: 10.1016/j.dsr.2017.05.006

Sutton, T. T., Frank, T. M., Romero, I. C., and Judkins, H. (2020). "As Gulf oil extraction goes deeper, who is at risk? Community structure, distribution, and connectivity of the deep-pelagic fauna," in *Scenarios and Responses to Future Deep Oil Spills – Fighting the Next War*, eds S. A. Murawski, C. Ainsworth, S. Gilbert, D. Hollander, C.B. Paris, M. Schlüter, and D. Wetzel (Cham: Springer), 403–418. doi: 10.1007/978-3-030-12963-7_24

Conflict of Interest: The authors declare that the research was conducted in the absence of any commercial or financial relationships that could be construed as a potential conflict of interest.

frontiers in Marine Science

ORIGINAL RESEARCH
published: 07 February 2020
doi: 10.3389/fmars.2020.00019

Comparative Population Genomics and Biophysical Modeling of Shrimp Migration in the Gulf of Mexico Reveals Current-Mediated Connectivity

Laura E. Timm [1,2], Lys M. Isma [1], Matthew W. Johnston [3] and Heather D. Bracken-Grissom [1]*

[1] CRUSTOMICS Laboratory, Department of Biological Sciences, Institute of Water and Environment, Florida International University, North Miami, FL, United States, [2] Evolutionary Genomics Laboratory, Department of Biochemistry and Molecular Genetics, University of Colorado-Anschutz Medical Campus, Aurora, CO, United States, [3] Oceanic Ecology Laboratory, Halmos College of Natural Sciences and Oceanography, Nova Southeastern University, Dania Beach, FL, United States

OPEN ACCESS

Edited by:
Tracey T. Sutton, Nova Southeastern University, United States

Reviewed by:
Alastair Brown, University of Southampton, United Kingdom
Ann I. Larsson, University of Gothenburg, Sweden

****Correspondence:***
Laura E. Timm
laura.timm@cuanschutz.edu

Specialty section:
This article was submitted to Deep-Sea Environments and Ecology, a section of the journal Frontiers in Marine Science

Received: *31 July 2019*
Accepted: *13 January 2020*
Published: *07 February 2020*

Citation:
Timm LE, Isma LM, Johnston MW and Bracken-Grissom HD (2020) Comparative Population Genomics and Biophysical Modeling of Shrimp Migration in the Gulf of Mexico Reveals Current-Mediated Connectivity. Front. Mar. Sci. 7:19. doi: 10.3389/fmars.2020.00019

The Gulf of Mexico experiences frequent perturbations, both natural and anthropogenic. To better understand the impacts of these events, we must inventory natural variability within the ecosystem, communities, species, and populations, and contextualize these findings in relation to physical features. Here, we present an integrated study of comparative population genomics and biophysical oceanography. Targeting three species of mesopelagic shrimp common to the Gulf of Mexico midwater (*Acanthephyra purpurea*, *Systellaspis debilis*, and *Robustosergia robusta*), we analyzed genetic diversity and population connectivity as proxies for species health and resilience, respectively. We also simulated a range of vertical migratory behaviors for the shrimp to infer the relationship between diel vertical migration and horizontal transmission between the Gulf of Mexico and the greater Atlantic Ocean. This study aims to establish biological baselines and characterize these values in terms of the prevailing oceanographic feature of the midwater: the Gulf Loop Current. Generally, the oplophorid species (*A. purpurea* and *S. debilis*) exhibit lower genetic diversity and higher interpopulation homogeneity compared to the sergestid (*R. robusta*). Biophysical simulations suggest the differences in vertical migratory regimes between these two groups have important implications for horizontal transport out of the Gulf of Mexico. Because of the difference in vertical migration patterns, access to the Gulf Loop Current varies across taxa and impacts inter-basin migration. Our findings suggest a negative correlation between surface abundance and genetic diversity in these three shrimp species. We hypothesize that this correlation may be due to the relationships between surface abundance and access to the fastest moving waters of the Gulf Loop Current.

Keywords: genetic diversity, connectivity, biophysical oceanographic modeling, diel vertical migration, midwater shrimp, Gulf Loop Current, Gulf of Mexico, Bear Seamount

INTRODUCTION

The Gulf of Mexico experiences frequent environmental perturbations. In the past decade alone, the region has been struck by two major hurricanes: Hurricane Ike in 2008 (Kraus and Lin, 2009) and Hurricane Harvey in 2017 (van Olderborgh et al., 2017). Additionally, three major oil spills have impacted the region: the Deepwater Horizon Oil Spill in 2010 (Beyer et al., 2016), the Shell Brutus Platform Spill in 2016, and an additional pipeline rupture 40 miles south of the Louisiana coastal city of Venice in 2017 (Nelson and Grubesic, 2018). The Gulf of Mexico also hosts a hyper-diverse mesopelagic zone (Sutton et al., 2017) and is described as a unique biogeographic ecoregion, distinct from the Caribbean Sea, Sargasso Sea, and greater Atlantic Ocean (Backus et al., 1977; Gartner, 1988). The frequent perturbations, both natural and anthropogenic, may have a drastic impact on the Gulf mesopelagic given its unique biological community and connections (St. John et al., 2016). Research efforts must focus on diagnosing Gulf health, contextualizing health in relation to the Gulf's relationship to the greater Atlantic, and understanding the role(s) of major oceanographic features on inter-basin population connectivity.

Genetic diversity and genetic connectivity, common metrics targeted in population genomics, provide especially valuable information about enigmatic species, serving as established proxies for species health and resilience, respectively (Hellberg et al., 2002; Hughes and Stachowicz, 2004; Danovaro et al., 2008; Cowen and Sponaugle, 2009). Genetic diversity is measured as the number of alleles present within a population or species. A population's or species' ability to adapt to new or changing environments is closely tied to higher genetic diversity (Hughes and Stachowicz, 2004; Danovaro et al., 2008; Cowen and Sponaugle, 2009). Thus, local adaptation can be crucial to a population's maintained health in the face of environmental disturbances. The movement and distribution of genes within or between systems is described by population connectivity. Population connectivity can be characterized as inter-population gene flow or migration, or the historical demography of populations, such as recent separation or re-mixing of distinct populations and/or changes to population size (Cowen et al., 2007). The ecological implications of these population dynamics are crucial to species resilience: following a localized perturbation event, gene flow between geographically separated populations can provide a functional genetic reservoir outside the disturbed area (Hellberg et al., 2002; Cowen and Sponaugle, 2009).

This study focuses on population genomics and biophysical connectivity of three mesopelagic crustacean species in relation to the Gulf Loop Current (GLC) and associated eddies, the principal mixing features in the Gulf of Mexico. Generally, the GLC enters the Gulf of Mexico through the Yucatan Channel and exits through the Florida Straits, occupying the upper (surface to ∼800 m) water column (Oey et al., 2005; Hamilton et al., 2014). The GLC is characterized by relatively warm, fast-moving water with speeds as swift as 1.7 m s^{-1} (Forristall et al., 1992) in surface waters (e.g., the top 100 m of the water column; Hamilton et al., 2014), decreasing to a maximum speed of 0.4 m s^{-1} between 100 and 200 m depth, and continuing to slow with depth. Below 1,000 m depth, water movement is generally considered to be independent of the Gulf Loop Current (Oey et al., 2005; Hamilton et al., 2014). Recent work focused on characterizing water masses in the Gulf presents evidence of distinctly structured microbial communities associated with mesoscale features (Johnston et al., 2019). Given that the Loop Current has been associated with lower biomass and abundances of pelagic organisms (Biggs, 1992; Biggs and Muller-Karger, 1994; Zimmerman and Biggs, 1999; Wells et al., 2017), it is not unrealistic to conclude the current has real, biologically significant impacts on the diversity and distribution of pelagic fauna within the Gulf.

Many midwater organisms exhibit diel vertical migratory behavior, occupying deeper water during the day and moving into epipelagic/surface water at night (Loose and Dawidowicz, 1994; Brierley, 2014). This behavior results in substantial, diel increases in surface abundances for a number of "midwater" species. However, differences in migratory behavior (ranging from "non-migratory," wherein depth-discrete abundances remain unchanged over a solar cycle, to different degrees of migratory) can be described in terms of migratory regimes (Brierley, 2014). Recently, a population genetics/genomics study of three mesopelagic cephalopod species, representing a range of migratory regimes, found evidence for a correlation between surface abundance and inter-basin population dynamics in the Gulf of Mexico and the greater Atlantic Ocean (Timm et al., 2020). The authors posit that this putative relationship between surface abundance and inter-basin population dynamics is due to the division of these regimes into concomitant "tiers" of access to the Gulf Loop Current. Here, we seek to further investigate this trend through the addition of biophysical modeling of migration regimes and the population genomics analysis of three crustacean species.

All three species targeted in this study (**Figure 1**) vertically migrate to some degree, but exhibit contrasting life histories, specifically in reproductive behavior and generation time. The oplophorids *Acanthephyra purpurea* (Milne-Edwards, 1881a) and *Systellaspis debilis* (Milne-Edwards, 1881b) brood their eggs (Herring, 1967, 1974a,b) and can live multiple years (Ramirez Llodra, 2002). The sergestid species, *Robustosergia robusta* (Smith, 1882) reproduces by releasing fertilized eggs into the water column (Vereshchaka, 2009) and lives ∼15 mo (based on studies of co-occurring sergestid species, see Genthe, 1969; Uchida and Baba, 2008). Additionally, surveys have indicated that *R. robusta* diel vertical migratory behavior differs geographically (Foxton, 1970; Donaldson, 1975; Froglia and Giannini, 1982; Froglia and Gramitto, 2000; Vereshchaka, 2009) and ontologically: larvae migrate into shallower waters than juveniles, which in turn migrate into shallower waters than adults (Flock and Hopkins, 1992). Such ontological shifts in diel vertical migratory behavior have also been found in *A. purpurea* and *S. debilis* (Roe, 1984; De Robertis, 2002). These insights into diel vertical migration make Gulf-specific observations of vertical migratory behavior necessary for both oplophorid species (Burdett et al., 2017) and *R. robusta* (Frank, pers. comm.). Combined with our increased understanding of the complexities of the Gulf Loop Current (Johnston et al., 2019) and the short lifespan of *R. robusta*, this behavior

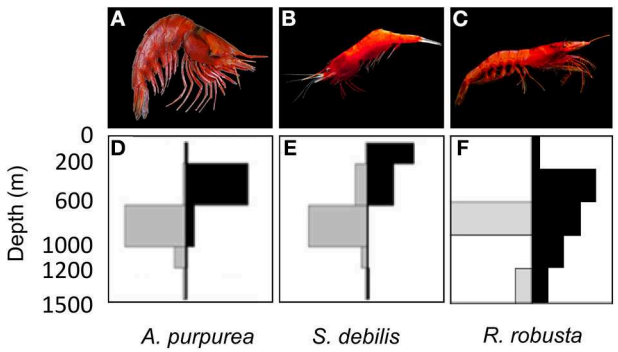

FIGURE 1 | Three species of mesopelagic shrimp targeted in this study, including the oplophorids **(A)** *Acanthephyra purpurea* (Milne-Edwards, 1881a) (photo credit: Dr. T.-Y. Chan) and **(B)** *Systellaspis debilis* (Milne-Edwards, 1881b) (photo credit: Dr. Danté Fenolio), and the sergestid **(C)** *Robustosergia robusta* (Smith, 1882) (photo credit: Dr. Danté Fenolio). Discrete depth abundances are reported for *A. purpurea* and *S. debilis* **(D,E)**, respectively (Burdett et al., 2017) and *R. robusta* **(F)** (Frank, pers. comm.). Relative abundances, indicated by bar length, are plotted by depth (in meters) and solar cycle ("Day" is represented by gray bars to the left; "Night" is represented by black bars to the right).

may have an amplified impact on population dynamics. In short, we expect this study to yield great insight into the interplay between behavior and population dynamics in the Gulf midwater.

The research presented here seeks fine-scale resolution to identify differences in diversity and connectivity (the latter, both genetic and biophysical) in non-model organisms across relatively small geographic distances. To quantify genetic diversity and inter-basin gene flow with the greatest power realistically available, we utilized a powerful next-generation sequencing (NGS) method, double digest Restriction site Associated DNA sequencing (ddRADseq, as described by Peterson et al., 2012). This approach allowed us to query a representative, reproducible fraction of the genome and generate orders of magnitude more data with greater statistical power than traditional population genetics studies have done (Davey and Blaxter, 2010; Peterson et al., 2012; Reitzel et al., 2013; Catchen et al., 2017). Next, we employed a biophysical dispersal model to simulate the migration behaviors and subsequent residency within the Gulf of Mexico of both diel migrators and non-migrators. The model integrated ocean circulation in the upper 1,500 m of the water column from the Hybrid Coordinate Ocean Model (HYCOM) and passive dispersal (exclusive of diel migrations) of particles representing our study species. The goal was to emulate the overall displacement effect of swift surface waters on migrators vs. non-migrators. Integrating the results from these two approaches, genetic and biophysical, allowed us to objectively define migration regimes and test for regime effect on population genomics across species.

Our study represents a comparative, integrative NGS and biophysical modeling investigation into the role of behavior and oceanography on population dynamics in three species of crustacean ubiquitous in the mesopelagic Gulf. This study utilizes a dual approach to infer biological resilience in the Gulf and model the role of the Gulf Loop Current in maintaining this resilience. To accomplish this goal we (1) quantify genetic diversity in each species and compare between the Gulf and Bear Seamount in the northern Atlantic; (2) characterize population connectivity between the Gulf and greater Atlantic from a hybrid population genomics-biophysical modeling perspective; (3) correlate surface abundance with diversity and connectivity; and (4) improve our understanding of crustacean health and resilience in the region, specifically in the context of species- and/or population-specific diel vertical migratory behavior and the major oceanographic feature of the region, the Gulf Loop Current.

MATERIALS AND METHODS

Adult specimens of *A. purpurea*, *S. debilis*, and *R. robusta* were collected from the northern Gulf of Mexico during the wet (August) and dry (May) seasons of 2015 and 2016 as part of the Gulf of Mexico Research Initiative (GOMRI)-funded Deep Pelagic Nekton Dynamics of the Gulf of Mexico (DEEPEND) project on the R/V Point Sur (**Figure 2**). During the DEEPEND cruises, every collection site was sampled twice: a day sample (entire water column from 0 to 1,500 m depth, sampled at noon) and a night sample (0–1,500 m depth, sampled at midnight). Gulf samples were collected with a Multiple Opening/Closing Net and Environmental Sensing System (MOC-10) rigged with six 3-mm mesh nets, allowing for collected specimens to be assigned to a depth bin (0–200 m, 200–600 m, 600–1,000 m, 1,000–1,200 m, and 1,200–1,500 m; the sixth net sampled from 0 to 1,500 m). In 2016, samples of *A. purpurea* and *S. debilis* were also collected from the Florida Straits aboard the R/V Walton Smith. Maximum sampling depth in the Florida Straits was determined by water depth and trawls ran every few hours. For this cruise, specimens were collected with a 9 m^2 Tucker trawl fitted with a cod-end capable of closure at-depth, allowing for discrete depth sampling. All three species were collected from Bear Seamount in the Northern Atlantic in 2014 as part of the Deepwater Systematics project, funded by the NMFS Northeast Fisheries Science Center and conducted on the R/V Pisces. Samples were collected from Bear Seamount with a modified Irish herring trawl.

All samples were identified to species and collected as whole-specimens, either in 70% EtOH or a RNA-stabilizing buffer, and stored at −20°C onboard the vessel before being transferred to a −80°C freezer in the Florida International University Crustacean Collection (FICC). Collected samples were then given a unique voucher ID in the FICC database, including all relevant collection data. Muscle tissue was plucked for each specimen and stored in 70% EtOH or a RNA-stabilizing buffer, in accordance with how the whole-specimen was originally collected, and stored in a −80°C freezer. Voucher specimens were preserved in 70% EtOH and deposited in the FICC. In total, 247 samples of *A. purpurea* were collected, 218 samples of *S. debilis*, and 95 samples of *R. robusta*. For each species, a subset of individuals was selected to provide adequate representation for each sampling locality (Bear Seamount, Florida Straits, and the Gulf of Mexico). These subsets

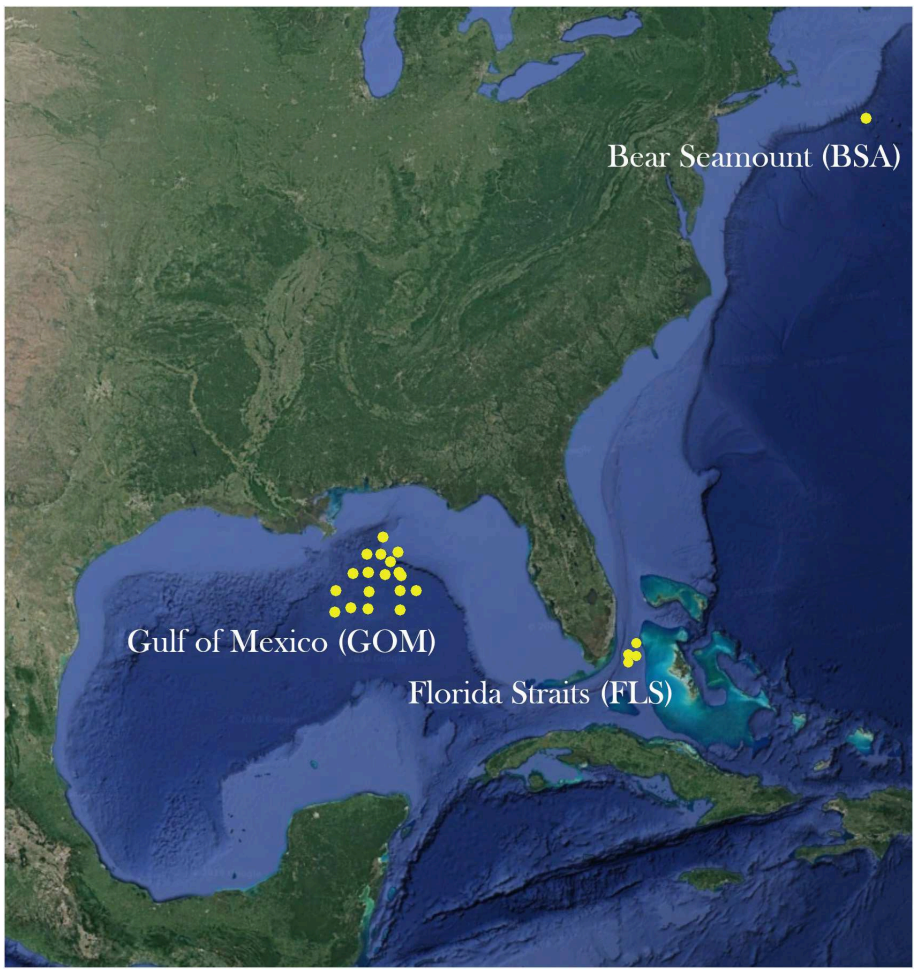

FIGURE 2 | A map of sites sampled from the Gulf of Mexico, the Florida Straits, and Bear Seamount in the Atlantic Ocean.

and metadata associated with each specimen are included in this study are detailed in **Supplemental Information 1.**

DNA Extraction and Sample Barcoding

DNA was extracted with the DNeasy Blood and Tissue Kit (Qiagen), following the protocol provided by the manufacturer. Due to the high quality of DNA necessary for robust ddRADseq data, several quality control measures were taken, many of which are detailed in O'Leary et al. (2018). First, the amount of DNA was ascertained with the Qubit dsDNA High Sensitivity Assay (Thermo Fisher). Next, DNA extractions were visualized on a 2% agarose gel with GelRed (Biotium) run for 90 min at 100 V to ensure the presence of exclusively high molecular weight DNA. Samples with <500 ng DNA and/or a preponderance of degraded DNA were excluded from library preparation.

Finally, every individual eligible for ddRADseq library preparation was barcoded with the 16S ribosomal subunit, 16S (*A. purpurea* and *S. debilis*) or cytochrome oxidase subunit I, COI (*R. robusta*). Because these barcodes were used solely to confirm taxonomic species identification (and not for downstream analyses), genes were selected based on ease of amplification for each species (that is, universal primers were effective). Polymerase Chain Reaction (PCR) occurred in 25-µl volumes: 12.5 µl GoTaq DNA Polymerase (Promega), 1 µl of each primer, 8.5 µl of sterile distilled water, and 2 µl of template DNA. The primer combinations, sequences, and references, as well as annealing temperatures and amplicon length (in base pairs) are presented in **Supplemental Information 2**. All PCR products were visualized on a 1% agarose gel in the same manner as the DNA extractions.

Amplicons were cleaned and sequenced at the Genewiz sequencing facility in Newark, NJ, USA. Quality filtering of raw reads, contig assembly, ambiguity determination, primer removal, and alignment with MAFFT (Katoh and Standley, 2013) occurred in Geneious v.9.3 (Kearse et al., 2012). The alignment was visually inspected for errors in MEGA7 (Kumar et al., 2016) before determining the reading frame and codon position of COI.

Cleaned, aligned sequences were queried against the NCBI GenBank database using the Basic Local Alignment Search Tool (BLAST) for standard nucleotide. Before querying, we confirmed

that all three species were present in the database for the locus we sequenced (16S or COI). A barcode was considered a match when the percent identity of the match was ≥99%. Only individuals whose taxonomic identification was supported by BLAST results were included in ddRADseq library preparation.

Next-Generation Sequencing With ddRADseq

Library Preparation

Double digest RADseq libraries were successfully prepared for 96 individuals of *A. purpurea*, 96 individuals of *S. debilis*, and 95 individuals of *R. robusta*. Reduced representation libraries were prepared according to the double digest RADseq (ddRADseq) method (Peterson et al., 2012). Generally, enzyme trials were completed to determine the appropriate enzyme combinations and size selection windows. DNA was digested with a combination of two enzymes (New England Biolabs) and custom barcoded adapters were synthesized and ligated to the fragments resulting from double digest. Once barcoded, samples could be pooled into sublibraries, which were size selected on a PippinPrep (Sage Science). Specific enzyme combinations, custom barcoded adapter sequences, and size selection schemes are reported in **Supplemental Information 3.** Size selected fragments were then amplified via PCR with Phusion Hi-Fidelity Polymerase (Thermo Scientific), which also incorporated indices (i7) and Illumina adapters into the fragments and allowed for pooling of sublibraries into the final libraries; 12 sublibraries per library and one library per species. The final libraries were quality checked on an Agilent BioAnalyzer 2100 (Agilent Technologies) before the library was sent for sequencing on an Illumina NextSeq, SE75 high output, at the Georgia Genomics Facility at the University of Georgia.

Quality Filtering and Data Assembly

Raw sequence files were processed with the STACKS v1.45 (Catchen et al., 2013) pipeline on the FIU High Performance Computing Cluster (HPCC). In process_radtags, reads were demultiplexed, cleaned (-c), and quality-filtered (-q). The ustacks program aligned identical reads within each individual, then these consensus reads were cataloged in cstacks. All putative loci were queried against this catalog with sstacks before rxstacks corrected individual genotype calls according to the accumulated population data. Here, "population" is determined by the collection location of each specimen; for example, all specimens collected from the Gulf of Mexico were labeled as members of the "Gulf" population. Finally, the populations program output a file of aligned, putatively unlinked single-nucleotide polymorphisms (SNPs). Two requirements had to be met for a given SNP to be called: first, the minimum read depth (-m = 5) had to be met; second, the SNP needed to be found in 25% of the individuals of a population (-r = 0.25) for the SNP to be called for that population. After SNPs were called according to these parameters, two additional requirements needed to be met for a given SNP to be retained: the SNP had to be present in all populations (Bear Seamount, Florida Straits, and Gulf) and, to increase the likelihood of excluding linked loci, only one random SNP was called per locus (–write_random_snp). These parameter settings were chosen to exclude reads originating from mitochondrial and ribosomal sequences (relative to nuclear sequence, these are generally considered to differ substantially in frequency, thus these are functionally removed with the stack depth parameter) and to prevent the inclusion of paralogs (also controlled with stack depth).

Each file of aligned SNPs then underwent an iterative missing data filter. Loci with >95% missing data were removed, followed by individuals with >95% missing data. This was repeated with 90% missing data, then 85%, and so on. This was repeated until only 10% missing data was allowed by locus and individual or until ∼500 loci remained. This "500 SNP" rule was necessary in the case of the oplophorids *A. purpurea* and *S. debilis*, as strict filtering resulted in data sets reduced to unusably small sizes. This is likely the result of very large genome sizes: the amount of data returned from the Illumina NextSeq is relatively fixed, therefore larger genomes will yield smaller amounts of consistently reproducible reads across individuals. Finally, we used BayeScan v2.1 (Foll and Gaggiotti, 2008) to identify F_{ST} outliers within each filtered data set. Any loci identified as outliers were removed. Sample sizes for each species following quality filtering are reported in **Table 1**.

Molecular Data Analysis

Several genetic diversity indices were calculated in GENODIVE v2.0b23 (Meirmans and Van Tienderen, 2004), including observed heterozygosity (H_o), the inbreeding coefficient (G_{IS}), and expected heterozygosity (H_e, which was calculated from the H_o and G_{IS} values). Jackknifing over loci was used to calculate standard deviation.

GENODIVE was also used to measure population differentiation (F_{ST}) and calculate hierarchical Analyses of Molecular Variance (AMOVAs, including F_{IT} and F_{IS}) with the Infinite Allele Model. Both analyses were run under 999 permutations to assess significance. For the AMOVAs, missing data were replaced with randomly drawn alleles determined by overall allele frequencies.

We employed the Bayesian program STRUCTURE v2.3.4 (Pritchard et al., 2000) to test for population structure within the data. Seven *K*-values were tested ($K = 1$–7) 10 times each under the admixture model. Following a burn-in of 20,000 generations, 200,000 Markov Chain Monte Carlo generations ran. In STRUCTURE HARVESTER v0.6.94 (Earl and VonHoldt, 2012), STRUCTURE results were collated and *ad hoc* posterior probability models (Pritchard et al., 2000) and the Evanno method (Evanno et al., 2005) were used to infer the optimal *K* value. STRUCTURE HARVESTER also generated CLUster Matching and Permutation Program (CLUMPP) files for individuals and populations. These files were input into CLUMPP v1.1.2 (Jakobsson and Rosenberg, 2007), resulting in input files compatible with distruct v1.1 (Rosenberg, 2004) and facilitating the visualization of estimated membership coefficients.

Two additional, non-model based methods were also employed for inferring and visualizing population structure: multi-dimensional scaling (MDS) plots and Principle Component Analyses (PCAs) were rendered for each data set using the R packages MASS (Venables and Ripley, 2002)

TABLE 1 | Sample sizes and diversity indices, including observed heterozygosity (Ho) and expected heterozygosity (He), for the three targeted species: *Acanthephyra purpurea, Systellaspis debilis*, and *Robustosergia robusta*.

	N				H_o				H_e				AMOVA Results		
	Overall	Atlantic	FL straits	Gulf	Overall	Atlantic	FL straits	Gulf	Overall	Atlantic	FL straits	Gulf	F_{IT}	F_{IS}	F_{ST}
A. purpurea	86	17	15	54	0.057	0.058	0.063	0.044	0.122	0.116	0.127	0.114	83.9%	16.1%*	0.0%
S. debilis	91	8	14	69	0.054	0.070	0.039	0.048	0.094	0.080	0.093	0.098	80.6%	19.4%*	0.0%
R. robusta	37	10	–	27	0.089	0.090	–	0.089	0.104	0.105	–	0.104	71.9%	11.9%*	16.2%*

*Results of the hierarchical AMOVAs conducted to characterize genetic variation among individuals (F_{IT} = 71.9%–83.9%), among individuals within populations (F_{IS} = 11.9%–19.4%), and among populations (F_{ST} = 0%–16.2%). The Infinite Allele Model was used with 999 permutations to assess statistical significance, which is reported in parentheses. Any missing data was replaced with randomly drawn alleles determined by the overall allele frequencies of the data set. AMOVA results indicate the vast majority of variance is due to differences between individuals (F_{IT}), regardless of the region from which they were sampled. *$p < 0.05$.*

and adegenet (Jombart and Ahmed, 2011), respectively. These methods are very similar, however MDS preserves distance/dissimilarity between data points while PCA preserves covariance within the data.

Biophysical Oceanographic Simulations

To further assess the potential population connectivity between the Gulf of Mexico (GOM) and greater Atlantic for the three target species, *R. robusta*, *A. purpurea*, and *S. debilis*, we ran a suite of simulations representing both migrating and non-migrating deep-sea fauna (hereafter "particles") using a derivation of a particle-tracking, Lagrangian biophysical model previously used to study the dispersal of marine organisms (Johnston and Bernard, 2017; Riegl et al., 2018). The purpose was to assess if strong surface circulation had an overall effect on the diffusion of diel migrators vs. non-migrators outside of the GOM (i.e., a proxy for connectivity to the greater Atlantic). Please see **Supplemental Information 4** for a complete description of the model logic following the Overview, Design concepts, and Design (ODD) protocol as per (Grimm et al., 2006, 2010; Grimm and Railsback, 2005). The following is an abbreviated description of the simulations that were run, including their parameterization.

The primary "model domain" spanned 98–76.5°W longitude and 18–35°N latitude, encompassing the entire GOM and the Eastern Florida Shelf northward to 35°N. Ocean condition data for the simulations were derived from the GOM 1/25° resolution Hybrid Current Ocean Model (HYCOM). HYCOM simulation data are high resolution approximations of water flow that have been used in many previous studies that rely on particle-tracking biophysical models (e.g., Kool et al., 2010; Johnston and Purkis, 2015; Johnston and Bernard, 2017). We used three-dimensional daily snapshot (i.e., at 00:00 UTM) HYCOM data for the upper 1,500 m of the water column for the year 2015 and ran 60-day simulations, commencing on January 1, 2015. The year 2015 was chosen as it was a typical, representative year in the GOM when the Gulf Loop Current (GLC) was in an extended state and 2015 also corresponds to the start of the sampling period by the DEEPEND Consortium which provided the samples for our genetic analysis. It should be noted that during the GLC's extended state is when connectivity outside of the GOM should be at its maximum and connectivity would expectedly be lower when the GLC is in a retracted state.

At the start of each simulation, we released five particles at each of the 46 stations (total $n = 230$ per simulation) in the DEEPEND sample grid in the northern GOM (**Figure 3**), a quantity we deemed sufficient to demonstrate the potential for individual retention and/or export out of the GOM. We ran 15 simulations (see **Supplemental Information 5** for a summary of all simulations) to represent non-migrating particles (hereafter the "non-migratory simulations"), with releases at 100 m water depth increments, spanning 1,500 to 100 m. These simulations emulated the dispersal of particles that do not migrate vertically and inhabit discrete depths. We next ran a suite of 105 simulations over all possible combinations of diel vertical migration patterns (hereafter the "migratory simulations") from 1, 500 to 100 m in 100 m increments (i.e., from 1,500 to 1,400 m, from 1,500 to 1,300 m, from 1,400 to 1,300 m, from 1,400 to 1,200 m, and so on) to represent the range of diel migratory behaviors (see **Supplemental Information 6** for the animation showing migrators vs. non-migrators).

During each simulation, particles were reliant upon water flow for dispersal, with the exception of the inclusion of a small percentage of stochasticity to represent eddy diffusivity and small-scale animal movement (see SI for the specifics). Migratory particles underwent a diel migration from the depths to the surface waters to the depths over a 4-hr span in each direction. Morning migrations downwards began at 5:00 a.m. at the starting depth and ended at 9:00 a.m. at the bottom depth, as specified in **Supplemental Information 5.** Evening migrations started from the bottom depth at 5:00 p.m. and ended in shallow waters at 9:00 p.m. Particles were tracked for 60 days, during which we corrected their position hourly and recorded their cumulative horizontal displacement distance. For the purposes of determining connectivity outside of the GOM, we considered those particles that were transported east of −80° to be exported from the GOM and into the western Atlantic. Finally, we summed both the total particle movements for each simulation and those movements which occurred outside of the GOM to calculate retention and export percentages. We also averaged the overall cumulative distance traveled of each particle for each simulation to demonstrate the horizontal dispersal distance per scenario. Though we were primarily interested here in the outputs that represented the specific behaviors of *R. robusta*, *A. purpurea*, and *S. debilis*, the suite of simulations we completed may be useful in

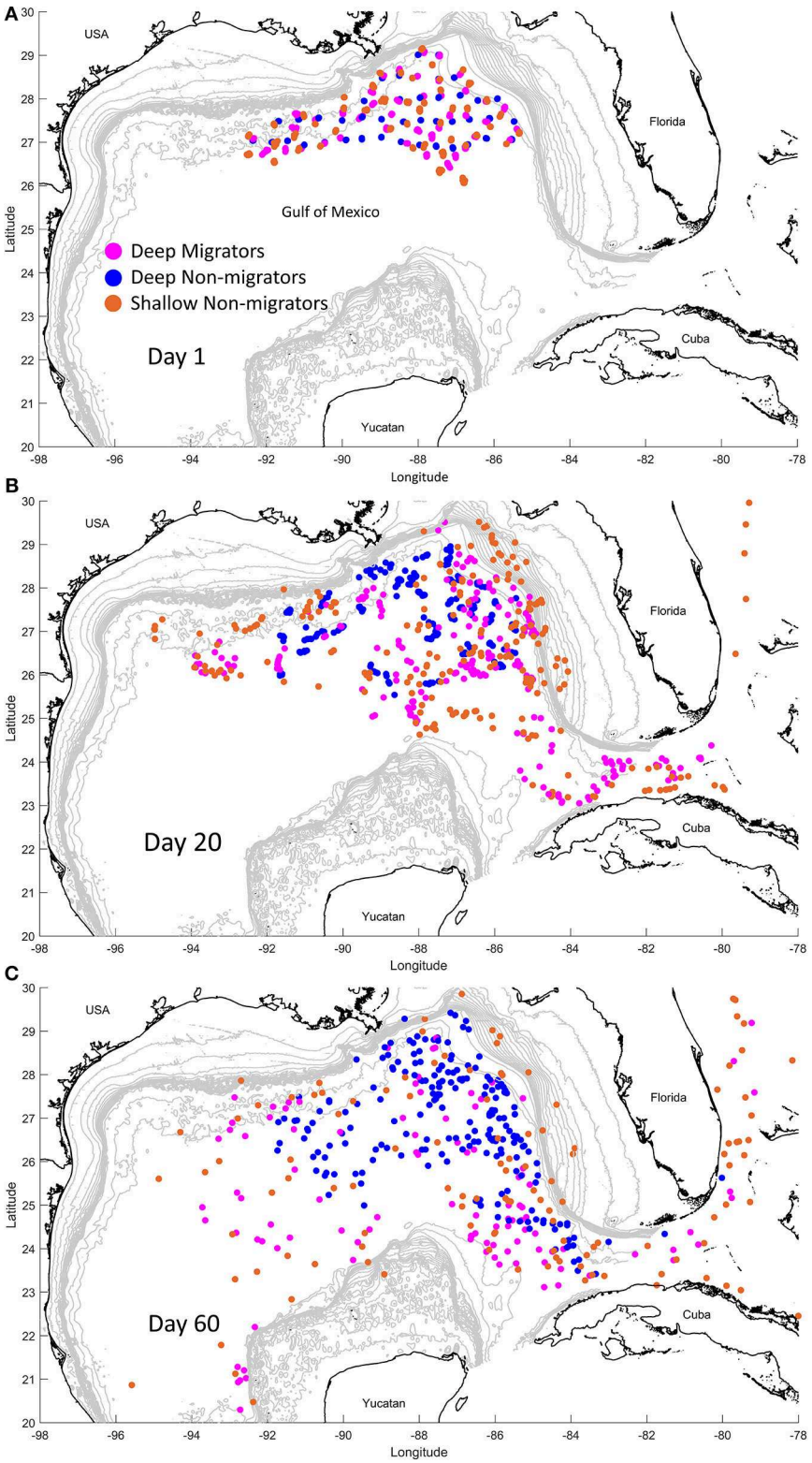

FIGURE 3 | Snapshots of the biophysical modeling simulation at day 1 **(A)**, day 20 **(B)**, and day 60 **(C)**. Particles that exhibit diel vertical migration ("Migrators") from 900 m to 200 m are in pink. Particles that do not exhibit this behavior, instead residing at 900 m (blue, "Deep Non-migrators") or 100 m (orange, "Shallow Non-migrators"), are also depicted.

the future to study the connectivity of other diel migrating and non-migrating deep-sea fauna in the GOM.

Integrating Analyses and Comparing Migration Regimes

Biophysical oceanographic modeling (BPOM) results were used alongside discrete depth abundance data (Burdett et al., 2017; Frank, pers. comm.) to distinguish between migration regimes, based on the depths at which modeled particles were exported from the Gulf, and classify each species as shallow non-migrator, deep non-migrator, strong migrator, or weak migrator. Based on the depths at which modeled particles were exported from the Gulf, each species was classified as a shallow non-migrator, deep non-migrator, strong vertical migrator, or weak vertical migrator. Once these evidence-based regimes were identified, data from species targeted in this study, as well as those targeted in Timm et al. (2020), were classified and binned by migration regime. To test for general correlation between surface abundance and genetic diversity indices, we began by defining "surface abundance" as the percent of total day abundance found above 600 m at night, as determined by MOC-10 net abundances (**Figure 1**). This cutoff was informed by the BPOM results: in migrators, particle export from the GOM ceased below 500 m; in non-migrators, export ceased at 500 m (**Table 2**). Because we did not have a net that discretely sampled above and below 500 m, we instead used 600 m as the cutoff. We plotted each diversity index (observed and expected heterozygosity and the inbreeding coefficient) against surface abundance for each species. Data from Timm et al. (2020) was also included to increase sample size. A trendline was fit to each index and R^2 was used to determine goodness-of-fit. To statistically test for correlation, we calculated Kendall's τ and Spearman's rank. We did not calculate Pearson's index because the data was not normally distributed.

RESULTS

Of the 288 prepared libraries (96 individuals within each species), 279 could be aligned and assembled within STACKS (95 of *A. purpurea*, 95 of *S. debilis*, and 89 of *R. robusta*). The initial data sets included: 596 SNPs (*A. purpurea*), 652 SNPs (*S. debilis*), and 4,196 SNPs (*R. robusta*). After applying the missing data filter, the *A. purpurea* data set included 522 SNPs across 87 individuals, the *S. debilis* data set included 525 SNPs across 91 individuals, and the *R. robusta* data set included 1,066 SNPs across 37 individuals. Across all data sets, only the *R. robusta* set was found to contain F_{ST} outliers: three SNPs were identified by BAYESCAN and removed from the final data set. This information is summarized in **Supplemental Information 1** and demultiplexed fastq reads have been uploaded and are publicly available through the Gulf of Mexico Research Initiative's Information & Data Cooperative (Timm et al., 2019), as well as on NCBI's SRA database under BioProject PRJNA553831. The SNP counts for each species in this data set are relatively low for a ddRADseq study, where tens of thousands of SNPs might be genotyped. We attribute the low counts to two primary causes: first, no genomes have been annotated, assembled, or even sequenced for any of the targeted species, lowering confidence in SNP calls; second, the oplophorid species, for which SNP counts were very low, are hypothesized to have large genome sizes (the only oplophorid with a genome size estimate, *Hymenodora sp.*, has a C-val of 38.00; Dixon et al., 2001). DNA barcoding efforts confirmed taxonomic identification of 90 specimens of *A. purpurea* (90 *de novo* sequences of 16S: GenBank Accessions MN507733-MN507822) and 80 specimens of *S. debilis* (80 *de novo* sequences of 16S: GenBank Accessions MN507553-MN507632). Sanger sequencing of the COI gene in *R. robusta* generated 57 *de novo* sequences (GenBank Accessions MN510870-MN510926). However, due to a lack of archived COI sequences for *R. robusta* in GenBank, BLAST results identified five individuals as *Robustosergia regalis*, none of which were included in downstream analyses.

Population Genomics

Genetic Diversity

Values across species were very similar (H_o: 0.057–0.089; H_e: 0.094–0.122) with exception of the inbreeding coefficient which was highest in *A. purpurea* (0.534), slightly lower in *S. debilis* (0.425), and lowest in *R. robusta* (0.146). As the inbreeding coefficient reflects the relationship between H_o and H_e ($[H_e$-$H_o]/H_e$), it ranges from −1 to 1, with positive values indicating inbreeding or a recent decrease in population size. These results are reported in **Table 1.**

Observed heterozygosity is the actual, measured amount of heterozygosity found in a population and can be impacted by an excess of homozygosity. Expected heterozygosity, however, describes the theoretical amount of heterozygosity present assuming the population of interest is in Hardy-Weinberg Equilibrium. It considers the number of alleles as well as their abundance, regardless of homozygosity. These two metrics, observed and expected heterozygosity, are compared using the inbreeding coefficient, as described in the Materials and Methods section. In all species and basins studied here, expected heterozygosity was found to be higher than observed heterozygosity, with the largest difference in *A. purpurea*, followed by *S. debilis*, then *R. robusta*. Generally, inbreeding coefficients approaching 1 indicate decreases in population size or local purifying selection, suggesting that the oplophorids have experienced population decreases or uneven selection pressures that *R. robusta* has not faced.

When genetic diversity was compared by basin (Gulf of Mexico [GOM] vs. Bear Seamount in the greater Atlantic [BSA]), both *A. purpurea* and *R. robusta* exhibited slightly higher diversity in the greater Atlantic (*A. purpurea* BSA $H_E = 0.116$ > GOM $H_E = 0.114$; *R. robusta* BSA $H_E = 0.105$ > GOM $H_E = 0.104$), while *S. debilis* had higher diversity in the Gulf (H_E BSA $= 0.080 < H_E$ GOM $= 0.098$). In *R. robusta*, the inbreeding coefficient was found to be slightly lower in the Gulf than the greater Atlantic (BSA $G_{IS} = 0.148$ > GOM $G_{IS} = 0.143$). The oplophorids had significantly higher G_{IS} in the Gulf compared to the greater Atlantic (*A. purpurea* BSA $G_{IS} = 0.500 <$ GOM $G_{IS} = 0.614$; *S. debilis* BSA $G_{IS} = 0.126$; GOM $G_{IS} = 0.510$). This is illustrated in **Figure 4**.

TABLE 2 | Characterization of each species by migratory regime based on biophysical oceanographic modeling (BOM) (export ceases for migrators below 600 m and non-migrators below 500 m) and recorded diel vertical migratory behavior (difference in depth-discrete abundance by solar cycle and proportion of individuals above or below the BOM export depths).

Species	Taxonomic Group	Migratory Regime	Justification
Acanthephyra purpurea	Crustacea	Migrator: strong	difference in solar cycle, majority of ind above 600 m at night & below during day
Systellaspis debilis	Crustacea	Migrator: strong	difference in solar cycle, majority of ind above 600 m at night & below during day
Robustosergia robusta	Crustacea	Migrator: weak	difference in solar cycle, plurality of ind above 600 m at night & majority below during day
Cranchia scabra	Cephalopoda	Non-migrator: shallow	no difference in solar cycle, majority of ind above 600 m
Pyroteuthis margaritifera	Cephalopoda	Migrator: weak	difference in solar cycle, plurality of ind above 200 m at night & majority below during day
Vampyroteuthis infernalis	Cephalopoda	Non-migrator: deep	no difference in solar cycle, majority of ind below 600 m

Justification for each characterization is included.

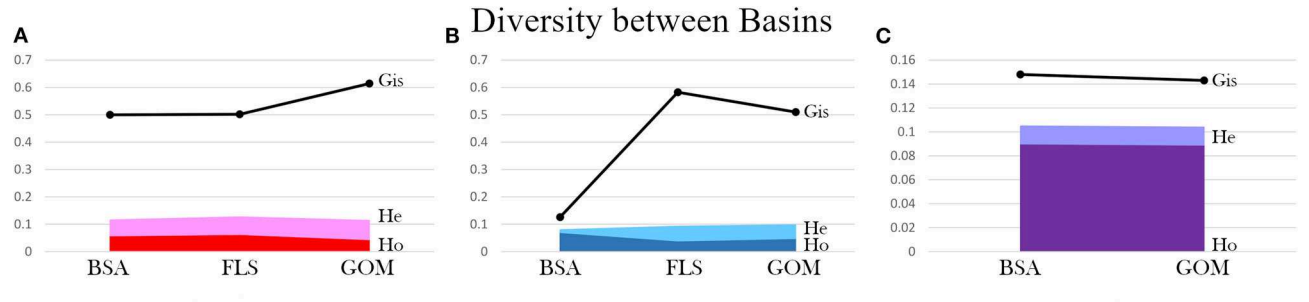

FIGURE 4 | Diversity metrics (observed heterozygosity Ho, expected heterozygosity He, and inbreeding coefficient Gis) are compared between collection localities: Bear Seamount in the Atlantic (BSA), Florida Straits (FLS), and the Gulf of Mexico (GOM) for **(A)** *Acanthephyra purpurea*, **(B)** *Systellaspis debilis*, and **(C)** *Robustosergia robusta* (note the change in y-axis scale).

Population Differentiation and Structure

AMOVA results, reported in **Table 1**, indicate a lack of population differentiation between basins in the oplophorids: F_{IT} ranged from 80.6% in *S. debilis* to 83.9% in *A. purpurea* and the rest of molecular variance was accounted for by F_{IS} (19.4% in *S. debilis* and 16.1% in *A. purpurea*). The majority of variance in *R. robusta* was from F_{IT} (71.9%), however the remainder was comprised of F_{IS} (11.9%) and F_{ST} (16.2%), indicating statistically significant genetic differentiation between the Gulf and the Atlantic.

STRUCTURE results strongly support and aptly illustrate the AMOVA results for each species (**Figure 5**). For the oplophorids, optimal K was determined to be 2; for *R. robusta*, $K = 3$ was deemed optimal. In the oplophorids, the admixture of ancestral populations within each individual is nearly identical across BSA, the Florida Straits, and the GOM, while there is some variation within each sampling locality. *R. robusta*, however, exhibits a dramatic difference in admixture proportion between the GOM and BSA. While admixture from all three ancestral populations is present in every individual, the individuals from the Atlantic consist of nearly equal admixture from populations 1 and 2, with the majority from population 3, while individuals from the Gulf have a very small proportion of admixture from population 3, nearly identical proportions of admixture from population 1 as seen in BSA, and the vast majority of admixture from population 2.

The PCAs and MDSs present these results another way: both oplophorid species have all individuals fall into a single cluster, regardless of collection locality. Conversely, the population differentiation seen in the AMOVA results for *R. robusta*, as well as the STRUCTURE analysis, is made further evident in the PCA and MDS: both plots show two distinct clusters, one containing individuals from Bear Seamount in the northern Atlantic and the other containing Gulf specimens. Results from PCA and MDS are depicted in **Figure 5**.

Biophysical Oceanographic Simulations

In the non-migratory simulations, dispersal out of the GOM (and inferred external connectivity to the greater Atlantic) primarily occurred in particles that were resident in water depths of 600 m or shallower (**Table 2** and **Figure 3**). The percentage range of particle movements outside of the GOM was a minimum of 0.14% for those residing at 600 m to a maximum of 15.72% for those found at 100 m water depth. Average horizontal dispersal distance for the non-migrating particles ranged from 422.03 km (1,500 m residents) to 2,558.25 km

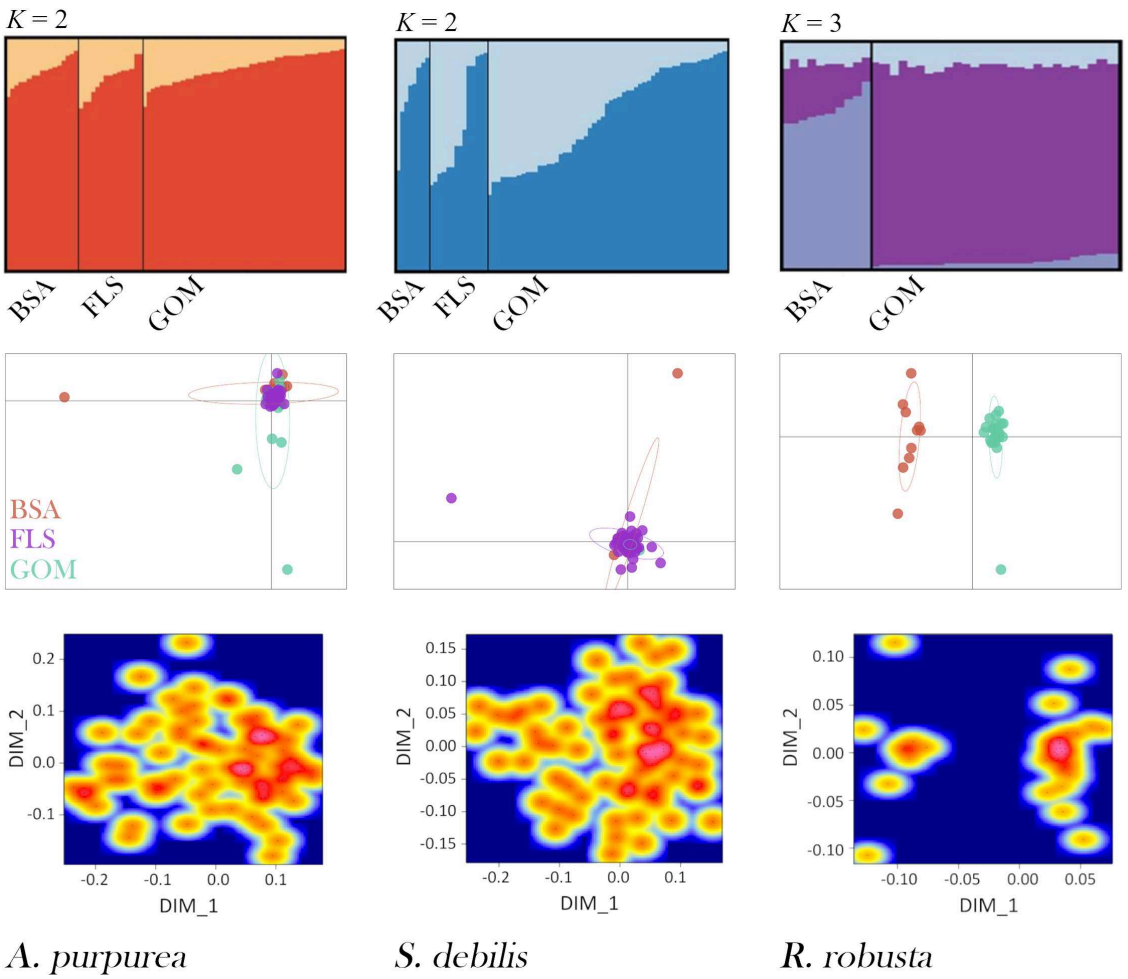

FIGURE 5 | DISTRUCT plots **(top)**, Principal Component Analyses (PCAs; **middle**), and multidimensional scaling (MDS) heat maps **(bottom)** for *Acanthephyra purpurea*, *Systellaspis debilis*, and *Robustosergia robusta*. Collection localities are denoted "BSA" for Bear Seamount in the north Atlantic, "FLS" for the Florida Straits, and "GOM" for the Gulf of Mexico., The first two principal components shown for each species are as follows: *A. purpurea* PC1 = 3.5%, PC2 = 3.1%, *S. debilis* PC1 = 2.7%, PC2 = 2.5%, and *R. robusta* PC1 = 5.9%, PC2 = 3.6%.

(100 m residents), demonstrating that those residing at shallower depths were dispersed much greater distances than those inhabiting the deep.

For the migratory simulations, dispersal out of the GOM was associated with those migrations that occurred from the deepest depths (e.g., 1,500–1,000 m) to a minimum of 500 m water depth, with increases in both the percentage of export and horizontal dispersal distance in depths shallower than 500 m. When migrating from midwater depths (e.g., 900–200 m), increases in the percentage of export and horizontal distance were again seen with shallower migrations, however almost all midwater simulations showed some level of export from the GOM. The maximum export percentage measured was 14.94% and the maximum horizontal displacement was 3,824.88 km, both in particles that migrated from 200 to 100 m water depth on a diel cycle.

Integrating Analyses and Comparing Migration Regimes

BPOM identified minimum depths for export out of the Gulf of Mexico for both migrators (500 m) and non-migrators (600 m). These values, along with discrete depth abundances calculated from MOC-10 capture, were used to characterize each of the six species (**Table 2**): the three species of mesopelagic shrimp and three species of mesopelagic cephalopod included from Timm et al. (2020). Generally, a negative correlation between surface abundance and genetic diversity was statistically supported (**Figure 6**). Across analyses, correlation was strongest between surface abundance and observed heterozygosity ($R^2 = 0.868$, rs $= -0.942$, τ statistically significant; **Table 3**). Correlation between surface abundance and expected heterozygosity was weaker ($R^2 = 0.494$, rs $= -0.543$, τ not statistically significant; **Table 3**). Inbreeding coefficient was not found to be correlated to

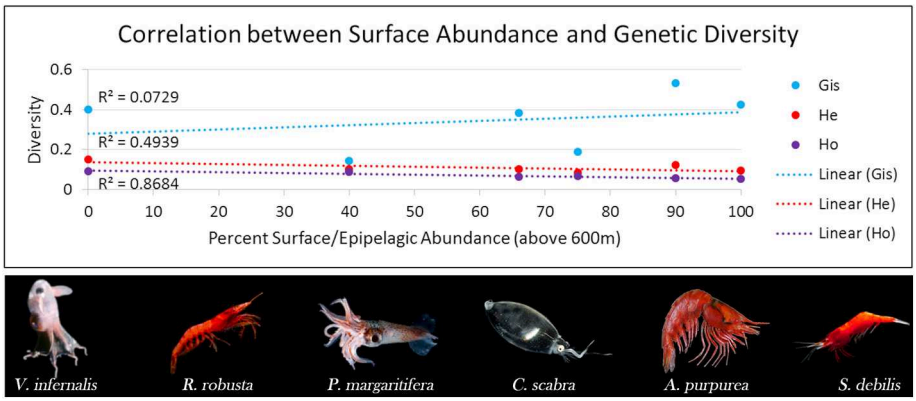

FIGURE 6 | Graph relating genetic diversity (inbreeding coefficient [G_{IS}] in blue, expected heterozygosity [H_e] in red, and observed heterozygosity [H_o] to abundance in the surface/epipelagic (here, we define this as above 600 m) across midwater invertebrate species with differing diel vertical migratory behaviors. We find an indirect relationship, with diversity decreasing as the percent of individuals found in the surface/epipelagic increases. This correlation is strongest in H_o (R^2 = 0.87) compared to H_e (R^2 = 0.49) and G_{IS} (R^2 = 0.073). *Robustosergia robusta, Pyroteuthis margaritifera, Cranchia scabra*, and *Systellaspis debilis* photo credit: Dr. Danté Fenolio. *Vampyroteuthis infernalis* photo credit: David Wrobel. *Acanthephyra purpurea* photo credit: Dr. T.-Y. Chan.

TABLE 3 | Results of testing for correlation between surface/epipelagic abundance ("SA," here defined as above 600 m) and three diversity metrics: inbreeding coefficient (G_{IS}), expected heterozygosity (H_e), and observed heterozygosity (H_o).

	R^2	Spearman	Kendall
SA x G_{is}	0.073	−0.543*	Not sig
SA x H_e	0.494	−0.543*	Not sig
SA x H_o	0.868	−0.942*	Sig

*R^2 is taken from the trendline and has been discussed in a previous figure. As our data are not normally distributed, correlation was tested with Spearman's rs and Kendall's τ (non-parametric tests). Spearman's rs ranges from −1 (strong negative/indirect correlation) to 1 (strong positive/direct correlation) with values closer to 0 indicating weak correlation. When |rs| > 0.5, the correlation is considered strong. Here, this is indicated with *. Kendall's τ is compared to a critical value. When |τ| > critical value, correlation is not significant ("Not sig„" in table). When |τ| </= critical value, correlation is significant ("Sig").*

surface abundance ($R^2 = 0.073$, rs $= -0.543$, τ not statistically significant; **Table 3**).

DISCUSSION

Through the integrated analysis of genomic proxies, namely diversity and connectivity, and biophysical models, we are beginning to address a persistent data gap in the mesopelagic Gulf by establishing biological baselines. We investigated how genetic diversity is organized between the Gulf of Mexico and the greater Atlantic, including the Florida Straits. Between basins, expected and observed heterozygosity paralleled each other well in each species, with the exception of *S. debilis* in the north Atlantic, wherein the two were nearly equal, greatly decreasing the inbreeding coefficient. In the oplophorids, inbreeding was lower in samples collected from Bear Seamount in the greater Atlantic compared to the Gulf, with the Florida Straits being nearly equal to Bear Seamount (in the case of *A. purpurea*) or significantly higher than the Gulf (in the case of *S. debilis*). This may be indicative of Gulf-localized perturbation or purifying selection affecting the oplophorids. However, the low inbreeding coefficient, high diversity, and small inter-basin diversity differences seen in *R. robusta* suggest quite different population dynamics.

To better understand the processes maintaining these contrasting dynamics, we investigated how this inter-basin organization is maintained through population structure and genetic connectivity and also modeled physical connectivity. Here again, we found a notable difference between the oplophorids and *R. robusta*. The oplophorids exhibited high population connectivity, indicating historical and current gene flow. Results of population structure analyses indicate each oplophorid species consists of a single population spanning the Gulf, Florida Straits, and the north Atlantic. Individuals from these populations are comprised of admixture from two ancestral populations of each species. *R. robusta*, however, exhibits significant population differentiation between basins. Analyses of population structure indicate this is coupled with different patterns of admixture from three ancestral populations, forming two distinct genetic signatures. Both of these results were echoed in our biophysical model results: the strong migrators (i.e., the oplophorids) were flushed from the Gulf while the weak migrators (i.e., *R. robusta*) were retained in the Gulf over the simulation timeframe (**Table 2** and **Figure 3**).

High connectivity and little population structure in oplophorids, evidenced by high F_{IT}, low F_{ST}, and results of structure analyses, may constrain genetic diversity through purifying selection: in both species, a single population must contend with two very different basins and environments (Backus et al., 1977; Gartner, 1988; Sutton et al., 2017). Any potential local or basin-specific adaptations must also be fit for the other basin. Additionally, in the case of *S. debilis*, it seems the entire inter-basin population is impacted by local perturbations: a localized die-off in the Gulf of Mexico can be seen in the overall population (Gulf and northwestern

Atlantic, see **Table 1** F_{IS} results). *R. robusta*, however, exhibits the highest diversity and lowest inbreeding of species included in this study. This may be attributable to a larger number of ancestral populations (three, instead of two in the oplophorids) or potentially local adaptation to the Gulf of Mexico and the Atlantic Ocean, relatively independently. Random genetic drift within each basin may also explain the results we see. Relatively high, statistically significant F_{ST}, indicating population differentiation between basins, could suggest local adaptation following the recent separation and isolation of two distinct subspecies. However, more work is needed to fully address this, specifically a comprehensive phylogeny of sergestids.

Previous work investigating genetic connectivity between the Gulf of Mexico and the greater Atlantic has largely focused on shark species with high potential dispersal distances. Research into population connectivity in Atlantic sharpnose sharks and sandbar sharks (conducted with mitochondrial RFLP and allozymes) found a single continuous population in both cases (Heist et al., 1995, 1996; Heist and Gold, 1999). A study of blacktip sharks (incorporating microsatellite data as well as the mitochondrial control region) identified population structure between the basins and largely attributed this to female shark preference for their own natal nursery grounds for parturition (Keeney et al., 2005). A study of genetic connectivity of the coral *Montastraea cavernosa* collected from across the Atlantic identified three populations; one of which (the Caribbean-North Atlantic) spans Bear Seamount and the Gulf of Mexico (Nunes et al., 2009). The authors attribute this connectivity to larval dispersal across long distances, while acknowledging the difficulties of modeling dispersal purely in terms of current-mediated transport. They cite larval lifespan, predation, micro-environmental fluctuations, and active swimming behavior as complicating variables in modeling larval dispersal via currents; all of which may also apply to the shrimp species targeted in this study.

Across the analyses presented here, results exhibited fairly clear distinctions between two taxonomic groups that represent distant evolutionary histories: the oplophorids *A. purpurea* and *S. debilis*, and the sergestid *R. robusta*. These two groups differ in many ways, including reproductive behavior and strength of diel vertical migration. Brooding behavior, exhibited by the oplophorids, may contribute greatly to connectivity between basins by facilitating inter-basin migration: while fecundity may differ by reproductive strategy (Ramirez Llodra, 2002), brooded young tend to have a better chance of survivorship (MacIntosh et al., 2014). Moreover, a survey of *R. robusta*, which releases fertilized eggs without brooding, from 1992 describes an ontological shift in diel vertical migration strength, with juvenile shrimp exhibiting stronger migration behavior than adults (Flock and Hopkins, 1992). As such, though larvae of *R. robusta* may have better access to the fastest moving waters of the Gulf Loop Current, they may also be less likely to survive and contribute to the effective population. The authors have noted this anecdotally: on research cruises to the Florida Straits, adults of *A. purpurea*, *S. debilis*, and sergestids known to exhibit strong diel vertical migration (Flock and Hopkins, 1992) were quite abundant, but adults of *R. robusta* were functionally absent and non-migrating sergestid larvae were neither collected nor noted. However, as mentioned, this requires confirmation. Statistical analysis of size distributions along the depth gradient is needed to clarify the role of larvae as migrants connecting the Gulf and Atlantic. While larvae can be critical for population connectivity in marine species (Palumbi, 2003; Gaines et al., 2007; Cowen and Sponaugle, 2009), there is also strong evidence that potential dispersal is rarely correlated with realized dispersal (Shanks, 2009).

Despite the potentially confounding variables identified in determining dispersal through current-mediated transport (e.g., disparity between potential and realized dispersal, oversimplifying active swimming behaviors, and ignoring the importance of rare individuals dispersing long distances; see Shanks, 2009 for a more thorough discussion), biophysical modeling can be used in concert with genetic evidence to improve our understanding of the dynamic relationships between marine organisms and their environment (Liggins et al., 2013). This integrative approach has been used to differentiate between broad-ranged natural populations and exotic introduced populations in the globally-distributed moon jellyfish genus, *Aurelia* (Dawson et al., 2005). Combining thorough empirical genetic sampling with biophysical modeling of dispersal has also proved valuable in explaining population structure in the highly dispersive spiny lobster, *Panulirus argus* (Truelove et al., 2017).

Our study particularly focused on diel vertical migration of adults, resultant surface/epipelagic abundance and transport on swift surface currents, and population dynamics. Including data from Timm et al. (2020), we find a trend of high surface abundance associated with low (if not absent) population differentiation between basins. However, this relationship appears to be binary. More stringent, statistical testing, across as many species as possible is needed to properly investigate this putative relationship. Genetic diversity shows much higher variability, allowing for statistical testing of correlation. Generally, an indirect/negative correlation was found, with higher surface abundance associated with lower genetic diversity. This relationship was clearest in observed heterozygosity, though still present in expected heterozygosity. It was nearly absent in the inbreeding coefficient. In the context of our simulation results, we suspect species with higher surface abundance have better access to the Gulf Loop Current, promoting inter-basin migration and homogenizing the population.

Testing for an effect of migration regime, informed by discrete depth abundance observations combined with oceanographic modeling, provides compelling evidence that vertical migration behavior alone is not sufficient to explain differences in genetic diversity across these species. Generally, modeling indicated an increase in export from the Gulf of Mexico into the greater Atlantic and an increase in dispersal distance as simulated particles reached shallower depths. Indeed, we find that minimum depth reached by each species during a diel cycle may be particularly indicative of access to the Gulf Loop Current and ability to migrate between basins.

In many ways, this study only begins to uncover the mechanisms driving and maintaining natural variability in the mesopelagic species inhabiting the Gulf of Mexico and between the Gulf and the greater Atlantic. The establishment of baselines for genetic diversity and connectivity is crucial to understanding the Gulf and for future appraisal of damages following disturbance events. We hypothesize that specific differences in population dynamics may be explained by access to the Gulf Loop Current: populations with higher abundance in the surface or epipelagic potentially have greater access to the fastest moving waters of the Gulf Loop Current. It can be logically reasoned that this access could maintain a single population spanning the Gulf and Atlantic in the strong vertical migrators, homogenizing if not functionally preventing local adaptation and population differentiation.

The results presented here, contextualized in terms of environment (the Gulf Loop Current) and life history (reproductive strategy and diel vertical migratory behavior), serve as the first glimpse of the natural variability present in the Gulf midwater and begin to describe potential drivers of this variability. First, we find that genetically, the oplophorids included in this study, *A. purpurea* and *S. debilis*, each form a single population spanning the eastern Gulf of Mexico and the northwest Atlantic. While this is associated with lower diversity, suggesting a lack of natural variability within each population and raising some concern over these species' health, it also indicates unimpeded gene flow between basins, a result also indicated in our model simulations. This is a good prognosis for genetic rescue potential and resilience in the Gulf. *Robustosergia robusta*, however, shows an opposite trend: high diversity, indicative of natural variability and species health, and genetic population differentiation between basins with low physical connectivity suggests lower potential for genetic rescue—a strategy for replenishing lost genetic diversity following a localized environmental perturbation (Mussmann et al., 2017). The unique genetic signatures of each basin may mean that, despite gene flow between basins, diversity lost within one basin may not be easily replaced through inter-basin migration.

FUTURE DIRECTIONS

In light of the immense difficulties associated with deep-sea specimen collection (especially of deep, non-migrating species), we recognize that continued collection efforts are needed to increase sample sizes. Additionally, before attempts to model surface abundance-genetic diversity correlation are undertaken, the correlation should be tested in more species. As fishes represent a major proportion of the mesopelagic biomass and are generally better studied, a similar study to the one presented here, focused on fish species, could substantially improve our understanding of the state and flux of genetic diversity in the mesopelagic Gulf of Mexico. When model testing begins, pervasive depth-dependent environmental variables (i.e., salinity, temperature, hydrostatic pressure, dissolved oxygen concentration, and chlorophyll concentration) should be considered as well as physical oceanographic parameters, such as water velocity and direction in relation to the Florida Straits, and biological traits such as active retention within the GOM via directional swimming during diel vertical migration.

DATA AVAILABILITY STATEMENT

All data are publicly available through the Gulf of Mexico Research Initiative Information & Data Cooperative (GRIIDC) at https://data.gulfresearchinitiative.org (doi: 10.7266/n7-3p3y-g470) and from NCBI (BioProject PRJNA553831).

AUTHOR CONTRIBUTIONS

LT and HB-G contributed conception and design of the study. Population genomics data generation and analysis was conducted by LT and LI. MJ carried out the biophysical modeling component of the study. MJ and LT worked together to integrate the results from population genomics and biophysical modeling. LT wrote the manuscript, with the exception of the biophysical modeling sections, which were written by MJ. All authors contributed to the revision process, have read, and approve this manuscript.

FUNDING

This research was made possible in part by a grant from The Gulf of Mexico Research Initiative to the Deep Pelagic Nekton Dynamics of the Gulf of Mexico (DEEPEND) Consortium, as well as a Division of Environmental Biology National Science Foundation (NSF) grant awarded to HB-G (DEB#1556059). Samples from Bear Seamount were collected through the Deepwater Systematics project, funded by the NMFS Northeast Fisheries Science Center. Funding was also provided by the Florida International University (FIU) Presidential Fellowship, the FIU Doctoral Evidence Acquisition Fellowship, and the FIU Dissertation Year Fellowship.

ACKNOWLEDGMENTS

We would like to specially thank Dr. Tammy Frank and Dr. Rosanna Milligan for their support in sample collection and statistical analysis, as well as Mr. Jorge Perez-Moreno and Mr. Charles Golightly for support in initial sample processing. We also thank LT's Ph.D. committee: Dr. José Eirin-Lopez, Dr. Mauricio Rodriguez-Lanetty, Dr. Eric von Wettberg, and Dr. Wensong Wu. We especially thank Dr. Emily Warschefsky, Dr. Joseph Ahrens, and Mr. Jordon Rahaman for advice and feedback on ddRADseq library prep and data assembly. Finally, we thank the reviewers for feedback on earlier versions of this manuscript. The work presented here is part of LT's doctoral dissertation (Timm, 2018) and is publicly available online. This is contribution #174 from the Coastlines and Oceans Division of the Institute of Environment at Florida International University.

SUPPLEMENTARY MATERIAL

The Supplementary Material for this article can be found online at: https://www.frontiersin.org/articles/10.3389/fmars.2020.00019/full#supplementary-material

Supplemental Information 1 | Metadata for all samples included in this study, including: the Illumina i7 index and custom barcode combination, listed under "Idx-BC," sample ID (HBG number), species, date and basin of collection, as well as the Station ID and coordinates for the collection site, and the depth range from which the sample was collected. The gene targeted for Sanger sequencing, to be used for DNA barcoding to confirm taxonomic identification, was either the 16S small ribosomal subunit (16S) or cytochrome c oxidase subunit I (COI). This is reported under "Gene" and the associated GenBank Accession number is also listed.

Supplemental Information 2 | The primer pairs and annealing temperatures associated with PCR amplification of two mitochondrial genes targeted for DNA barcoding of samples included in the ddRADseq library preparations.

Supplemental Information 3 | Details of ddRADseq protocol for each species, including enzymes, custom-made barcoded-adapter sequences, and size selection schemes. Both strands of each adapter are given (1.1 and 1.2) in the 5′ to 3′ direction. These strands are annealed prior to ligation to the ddRADseq fragments. The barcode section of the adapter is underlined. Note that the overhang in the 1.1 strands differs between the "oplo" and the "flex" adapters. Illumina i7 adapters were also used, specifically index 1, 3, 7, 12, 13, 16, 21, 24, 29, 37, 42, and 43.

Supplemental Information 4 | This model description follows the Overview, Design concepts, and Details (ODD) protocol for describing individual- and agent-based models (Grimm and Railsback, 2005; Grimm et al., 2006) and consists of seven elements. The first three elements provide an overview of the model, the fourth element explains general concepts underlying the model's design, and the remaining three elements provide details of the model processes.

Supplemental Information 5 | Summary of the dispersal of migrators and non-migrators within and outside of the GOM.

Supplemental Information 6 | Three-dimensional animation of the dispersal of migrating species vs. non-migrating species spanning 80 days. Blue dots represent non-migrating animals at 900 m depth and pink represent animals with a diel vertical migration range of 200 m to 900 m depth.

REFERENCES

Backus, R. H., Craddock, J. E., Haedrich, R. L., and Robison, B. H. (1977). Atlantic mesopelagic zoogeography. *Fish. Western N. Atlantic* 7, 266–287 doi: 10.1575/1912/4359

Beyer, J., Trannum, H. C., Bakke, T., Hodson, P. V., and Collier, T. K. (2016). Environmental effects of the Deepwater Horizon oil spill: a review. *Mar. Pollut. Bull.* 110, 28–51. doi: 10.1016/j.marpolbul.2016.06.027

Biggs, D. C. (1992). Nutrients, plankton, and productivity in a warm-core ring in the western Gulf of Mexico. *J. Geophys. Res.* 2, 2143–2154. doi: 10.1029/90JC02020

Biggs, D. C., and Muller-Karger, F. E. (1994). Ship and satellite observations of chlorophyll stocks in interacting cyclone-anticyclone eddy pairs in the western Gulf of Mexico. *J. Geophys. Res.*4, 7371–7384. doi: 10.1029/93JC02153

Brierley, A. S. (2014). Diel vertical migration. *Curr. Biol.* 24, R1074–R1076. doi: 10.1016/j.cub.2014.08.054

Burdett, E. A., Fine, C. D., Sutton, T. T., Cook, A. B., and Frank, T. M. (2017). Geographic and depth distributions, ontogeny, and reproductive seasonality of decapod shrimps (Caridea: Oplophoridae) from the northeastern Gulf of Mexico. *Bull. Mar. Sci.* 93, 743–767. doi: 10.5343/bms.2016.1083

Catchen, J., Hohenlohe, P. A., Bassham, S., Amores, A., and Cresko, W. A. (2013). Stacks: an analysis tool set for population genomics. *Mol. Ecol.* 22, 3124–3140. doi: 10.1111/mec.12354

Catchen, J. M., Hohenlohe, P. A., Bernatchez, L., Funk, W. C., Andrews, K. R., and Allendorf, F. W. (2017). Unbroken: RADseq remains a powerful tool for understanding the genetics of adaptation in natural populations. *Mol. Ecol. Res.* 17, 362–365. doi: 10.1111/1755-0998.12669

Cowen, R. K., Gawarkiewicz, G., Pineda, J., Thorrold, S. R., and Werner, F. (2007). Population connectivity in marine systems. *Oceanography* 20, 14–21. doi: 10.5670/oceanog.2007.26

Cowen, R. K., and Sponaugle, S. (2009). Larval dispersal and marine population connectivity. *Ann. Rev. Mar. Sci.* 1, 443–466. doi: 10.1146/annurev.marine.010908.163757

Danovaro, R., Gambi, C., Dell'Anno, A., Corinaldesi, C., Fraschetti, S., Vanreusel, A., et al. (2008). Exponential decline of deep-sea ecosystem functioning linked to benthic biodiversity loss. *Curr. Biol.* 18, 1–8. doi: 10.1016/j.cub.2007.11.056

Davey, J. L., and Blaxter, M. W. (2010). RADseq: next-generation population genetics. *Brief. Funct. Genom.* 9, 416–423. doi: 10.1093/bfgp/elq031

Dawson, M. N., Gupta, A. S., and England, M. H. (2005). Coupled biophysical global ocean model and molecular genetic analyses identify multiple introductions of cryptogenic species. *Proc. Natl. Acad. Sci. U.S.A.* 102, 11968–11973. doi: 10.1073/pnas.0503811102

De Robertis, A. (2002). Size-dependent visual predation risk and the timing of vertical migration: an optimization model. *Limnol. Oceanogr.* 47, 925–933. doi: 10.4319/lo.2002.47.4.0925

Dixon, D. R., Dixon, L. R. J., Wilson, J. T., and Pascoe, P. L. (2001). Chromosomal and nuclear characteristics of deep-sea hydrothermal-vent organisms: correlates of increased growth rate. *Mar. Biol.* 139, 251–255. doi: 10.1007/s002270100564

Donaldson, H. A. (1975). Vertical distribution and feeding of sergestid shrimps (Decapoda: Natantia) collected near Bermuda. *Mar. Biol.* 31, 37–50. doi: 10.1007/BF00390646

Earl, D. A., and VonHoldt, B. M. (2012). STRUCTURE HARVESTER: a website and program for visualizing STRUCTURE output and implementing the Evanno method. *Conserv. Gene. Res.* 4, 359–361. doi: 10.1007/s12686-011-9548-7

Evanno, G., Regnaut, S., and Goudet, J. (2005). Detecting the number of clusters of individuals using the software STRUCTURE: a simulation study. *Mol. Ecol.* 14, 2611–2620. doi: 10.1111/j.1365-294X.2005.02553.x

Flock, M. E., and Hopkins, T. L. (1992). Species composition, vertical distribution, and food habits of the sergestid shrimp. *J. Crustacean Biol.* 12, 210–223. doi: 10.2307/1549076

Foll, M., and Gaggiotti, O. (2008). A genome-scan method to identify selected loci appropriate for both dominant and codominant markers: a Bayesian perspective. *Genetics* 180, 977–993. doi: 10.1534/genetics.108.092221

Forristall, G. Z., Schaudt, K. J., and Cooper, C. K. (1992). Evolution and kinematics of a loop current eddy in the Gulf of Mexico during 1985. *J. Geophys. Res.* 97, 2173–2184. doi: 10.1029/91JC02905

Foxton, P. (1970). The vertical distribution of pelagic decapods (Crustacea: Natantia) collected on the Sond cruise 1965 II. the Penaeidea and general discussion. *J. Mar. Biol. Assoc. U.K.* 50, 961–1000. doi: 10.1017/S0025315400005907

Froglia, C., and Giannini, S. (1982). Osservazioni sugli spostamenti verticali nictemerali di *Sergestes arcticus* kroyer e *Sergia robusta* (Smith) (Crustacea, Decapoda, Sergestidae) nel Mediterraneo occidentale. *Atti Del Convegno Delle Unità Operative Afferenti Ai Sottoprogetti Risorse Biologiche e Inquinamento Marino*. 1, 311–319.

Froglia, C., and Gramitto, M. E. (2000). A new pelagic shrimp of the genus *Sergia* (Decapoda, Sergestidae) from the Atlantic Ocean. *J. Crustacean Biol.* 20, 71–77. doi: 10.1163/1937240X-90000009

Gaines, S., Gaylord, B., Gerber, L., Hastings, A., and Kinlan, B. (2007). Connecting places: the ecological consequences of dispersal in the sea. *Oceanography* 20, 90–99. doi: 10.5670/oceanog.2007.32

Gartner, J. V. (1988). The lanternfishes (Pisces: Myctophidae) of the eastern Gulf of Mexico. *Fish. Bull.* 85, 81–98.

Genthe, H. C. (1969). The reproductive biology of *Sergestes similis* (Decapoda, Natantia). *Mar. Biol.* 2, 203–217. doi: 10.1007/BF00351142

Grimm, V., Berger, U., Bastiansen, F., Eliassen, S., Ginot, V., Giske, J., et al. (2006). A standard protocol for describing individual-based and agent-based models. *Ecol. Model.* 198, 115–126. doi: 10.1016/j.ecolmodel.2006.04.023

Grimm, V., Berger, U., DeAngelis, D. L., Polhill, J. G., Giske, J., and Railsback, S. F. (2010). The ODD protocol: a review and first update. *Ecol. Model.* 221, 2760–2768. doi: 10.1016/j.ecolmodel.2010.08.019

Grimm, V., and Railsback, S. F. (2005*). Individual-Based Modeling and Ecology*. Princeton, NJ: Princeton Unviersity Press.

Hamilton, P., Donohue, K., Hall, C., Leben, R., Quian, H., Sheinbaum, J., et al. (2014). *Observations and Dynamics of the Loop Current*. OCS Study BOEM 5015-006. New Orleans, LA.

Heist, E. J., and Gold, J. R. (1999). Microsatellite DNA variation in sandbar sharks (*Carcharhinus plumbeus*) from the Gulf of Mexico and Mid-Atlantic Bight. *Copeia* 1999, 182–186. doi: 10.2307/1447399

Heist, E. J., Graves, J. E., and Musick, J. A. (1995). Population genetics of the sandbar shark (*Carcharhinus plumbeus*) in the Gulf of Mexico and Mid-Atlantic Bight. *Copeia* 1995, 555–562. doi: 10.2307/1446752

Heist, E. J., Musick, J., and Graves, J. E. (1996). Mitochondrial DNA diversity and divergence among sharpnose sharks, *Rhizoprionodon terraenovae*, from the Gulf of Mexico and Mid-Atlantic Bight. *Fish. Bull.* 94, 664–668.

Hellberg, M. E., Burton, R. S., Neigel, J. E., and Palumbi, S. R. (2002). Genetic assessment of connectivity among marine populations. *Bull. Mar. Sci.* 70, 273–290.

Herring, P. J. (1967). Observations on the early larvae of three species of *Acanthephyra* (Crustacea, Decapoda, Caridea). *Deep Sea Res. Oceanogr.* 14, 325–329. doi: 10.1016/0011-7471(67)90075-7

Herring, P. J. (1974a). Observations on the embryonic development of some deep-living decapod crustaceans, with particular reference to species of *Acanthephyra*. *Mar. Biol.* 25, 25–33. doi: 10.1007/BF00395105

Herring, P. J. (1974b). Size, density and lipid content of some decapod eggs. *Deep-Sea Res. Oceanograp. Abst.* 21, 91–94. doi: 10.1016/0011-7471(74)90023-0

Hughes, A. R., and Stachowicz, J. J. (2004). Genetic diversity enhances the resistance of a seagrass ecosystem to disturbance. *Proc. Natl. Acad. Sci. U.S.A.* 101, 8998–9002. doi: 10.1073/pnas.0402642101

Jakobsson, M., and Rosenberg, N. A. (2007). CLUMPP: a cluster matching and permutation program for dealing with label switching and multimodality in analysis of population structure. *Bioinformatics* 23, 1801–1806. doi: 10.1093/bioinformatics/btm233

Johnston, M. W., and Bernard, A. M. (2017). A bank divided: quantifying a spatial and temporal connectivity break between the Campeche Bank and the northeastern Gulf of Mexico. *Mar. Biol.* 164:12. doi: 10.1007/s00227-016-3038-0

Johnston, M. W., Milligan, R. J., Easson, C. G., DeRada, S., English, D. C., Penta, B., et al. (2019). An empirically validated method for characterizing pelagic habitats in the Gulf of Mexico using ocean model data. *Limnol. Oceanograp.* 17, 363–375. doi: 10.1002/lom3.10319

Johnston, M. W., and Purkis, S. J. (2015). A coordinated and sustained international strategy is required to turn the tide on the Atlantic lionfish invasion. *Mar. Ecol. Prog. Ser.* 533, 219–235. doi: 10.3354/meps11399

Jombart, T., and Ahmed, I. (2011). Adegenet 1.3-1: New tools for the analysis of genome-wide SNP data. *Bioinformatics* 27, 3070–3071. doi: 10.1093/bioinformatics/btr521

Katoh, K., and Standley, D. M. (2013). MAFFT multiple sequence alignment software version 7: improvements in performance and usability. *Mol. Biol. Evol.* 30, 772–780. doi: 10.1093/molbev/mst010

Kearse, M., Moir, R., Wilson, A., Stones-Havas, S., Cheung, M., Sturrock, S., et al. (2012). Geneious basic: an integrated and extendable desktop software platform for the organization and analysis of sequence data. *Bioinformatics* 28, 1647–1649. doi: 10.1093/bioinformatics/bts199

Keeney, D. B., Heupel, M. R., Hueter, R. E., and Heist, E. J. (2005). Microsatellite and mitochondrial DNA analyses of the genetic structure of blacktip shark (*Carcharhinus limbatus*) nurseries in the northwestern Atlantic, Gulf of Mexico, and Caribbean Sea. *Mol. Ecol.* 14, 1911–1923. doi: 10.1111/j.1365-294X.2005.02549.x

Kool, J. T., Paris, C. B., Andréfouët, S., and Cowen, R. K. (2010). Complex migration and the development of genetic structure in subdivided populations: an example from Caribbean coral reef ecosystems. *Ecography* 33, 597–606. doi: 10.1111/j.1600-0587.2009.06012.x

Kraus, N. C., and Lin, L. (2009). Hurricane Ike along the upper Texas coast: an introduction. *Shore Beach.* 77, 3–8.

Kumar, S., Stecher, G., and Tamura, K. (2016). MEGA7: Molecular evolutionary genetics analysis version 7.0 for bigger datasets. *Mol. Biol. Evol.* 33, 1870–1874. doi: 10.1093/molbev/msw054

Liggins, L., Treml, E. A., and Riginos, C. (2013). Taking the plunge: an introduction to undertaking seascape genetic studies and using biophysical models. *Geo. Comp.* 7, 173–196. doi: 10.1111/gec3.12031

Loose, C. J., and Dawidowicz, P. (1994). Trade-offs in diel vertical migration by zooplankton: the costs of predator avoidance. *Ecology* 75, 2255–2263. doi: 10.2307/1940881

MacIntosh, H., de Nys, R., and Whalan, S. (2014). Contrasting life histories in shipworms: growth, reproductive development and fecundity. *J. Exp. Mar. Biol. Ecol.* 459, 80–86. doi: 10.1016/j.jembe.2014.05.015

Meirmans, P. G., and Van Tienderen, P. H. (2004). GENOTYPE and GENODIVE: two programs for the analysis of genetic diversity of asexual organisms. *Mol. Ecol. Notes* 4, 792–794. doi: 10.1111/j.1471-8286.2004.00770.x

Milne-Edwards, A. (1881a). "Compte rendu sommaire d'une exploration zoologique faite dans l'Atlantique, a bord du navire le Travailleu," in *Comptes Rendus Hebdomadaires de Séances de l'Académie des Sciences, Vol. 93* (Paris), 931–936.

Milne-Edwards, A. (1881b). Description de quelques crustacés macroures provenant des grandes profondeurs de la Mer des Antilles. *Ann. Sci. Nat.* 6, 1–15.

Mussmann, S. M., Douglas, M. R., Anthonysamy, W. J. B., Davis, M. A., Simpson, S. A., Louis, W., et al. (2017). Genetic rescue, the greater prairie chicken and the problem of conservation reliance in the anthropocene. *R. Soc. Open Sci.* 4:160736. doi: 10.1098/rsos.160736

Nelson, J. R., and Grubesic, T. H. (2018). The implications of oil exploration off the Gulf Coast of Florida. *J. Mar. Sci. Eng.* 6, 1–21. doi: 10.3390/jmse6020030

Nunes, F., Norris, R. D., and Knowlton, N. (2009). Implications of isolation and low genetic diversity in peripheral populations of an amphi-Atlantic coral. *Mol. Ecol.* 18, 4283–4297. doi: 10.1111/j.1365-294X.2009.04347.x

Oey, L.-Y., Ezer, T., and Lee, H.-C. (2005). "Loop current, rings, and related circulation in the Gulf of Mexico: a review of numerical models and future challenges," in *Circulation in the Gulf of Mexico: Observations and Models,* eds W. Sturges and A. Lugo-Fernandez (Washington, DC: American Geophysical Union), 31–56.

O'Leary, S. J., Puritz, J. B., Willis, S. C., Hollenbeck, C. M., and Portnoy, D. S. (2018). These aren't the loci you're looking for: principles of effective SNP filtering for molecular ecologists. *Mol. Ecol.* 27, 3193–3206. doi: 10.1111/mec.14792

Palumbi, S. R. (2003). Population genetics, demographic connectivity, and the design of marine reserves. *Ecol. Appl.* 13, S146–S158. doi: 10.1890/1051-0761(2003)013<0146:PGDCAT>2.0.CO;2

Peterson, B. K., Weber, J. N., Kay, E. H., Fisher, H. S., and Hoekstra, H. E. (2012). Double digest RADseq: an inexpensive method for *de novo* SNP discovery and genotyping in model and non-model species. *PLoS ONE* 7:e37135. doi: 10.1371/journal.pone.0037135

Pritchard, J. K., Stephens, M., and Donnelly, P. (2000). Inference of population structure using multilocus genotype data. *Genetics* 155, 945–959.

Ramirez Llodra, E. (2002). Fecundity and life-history strategies in marine invertebrates. *Adv. Mar. Biol.* 43, 87–170. doi: 10.1016/S0065-2881(02)43004-0

Reitzel, A. M., Herrera, S., Layden, M. J., Martindale, M. Q., and Shank, T. M. (2013). Going where traditional markers have not gone before: utility of and promise for RAD sequencing in marine invertebrate phylogeography and population genomics. *Mol. Ecol.* 22, 2953–2970. doi: 10.1111/mec.12228

Riegl, B., Johnston, M., Purkis, S., Howells, E., Burt, J., Steiner, S. C. C., et al. (2018). Population collapse dynamics in *Aropora downingi*, an Arabian/Persian Gulf ecosystem-engineering coral, linked to rising temperature. *Glob. Change Biol.* 24, 2447–2462. doi: 10.1111/gcb.14114

Roe, H. S. J. (1984). The diel migrations and distributions within a mesopelagic community in the north east Atlantic (2): vertical migration

and feeding of mysids and decapod Crustacea. *Prog. Oceanogr*. 13, 269–318. doi: 10.1016/0079-6611(84)90011-9

Rosenberg, N. A. (2004). DISTRUCT: A program for the graphical display of population structure. *Mol. Ecol. Notes* 4, 137–138. doi: 10.1046/j.1471-8286.2003.00566.x

Shanks, A. L. (2009). Pelagic larval duration and dispersal distance revisited. *Biol. Bull*. 216, 373–385. doi: 10.1086/BBLv216n3p373

Smith, S.I. (1882). *Reports on the Results of Dredging Under the Supervisión of Alexander Agassiz, on the East Coast of the United States During the Summer of 1880, by the U.S. Coast Survey Steamer "Blake", Commander J.R. Bartlett, U.S.N., Commanding*. Bulletin of the Museum of comparative Zoology at Harvard College, Vol. 10, 1–108.

St. John, M. A., Borja, A., Chust, G., Heath, M., Grigorov, I., Mariani, P., et al. (2016). A dark hole in our understanding of marine ecosystems and their services: perspectives from the mesopelagic community. *Front. Mar. Sci*. 3:31. doi: 10.3389/fmars.2016.00031

Sutton, T. T., Clark, M. R., Dunn, D. C., Halpin, P. N., Rogers, A. D., Guinotte, J., et al. (2017). A global biogeographic classification of the mesopelagic zone. *Deep-Sea Res. Part I Oceanogr. Res. Pap*. 126, 85–102. doi: 10.1016/j.dsr.2017.05.006

Timm, L. E. (2018). *Evolutionary and population dynamics of crustaceans in the Gulf of Mexico* (doctoral dissertation). Miami, FL: Florida International University.

Timm, L. E., Bracken-Grissom, H. D., Sosnowski, A., Breitbart, M., Vecchione, M., and Judkins, H. (2020). Population connectivity of three deep-sea cephalopod species between the Gulf of Mexico and northwestern Atlantic Ocean. *Deep Sea Res. I*. 103222. doi: 10.1016/j.dsr.2020.103222

Timm, L. E., Isma, L. M., and Bracken-Grissom, H. D. (2019). Single-locus barcodes and demultiplexed ddRADseq data for comparative population genomic analysis of the mesopelagic shrimp species *Acanthephyra purpurea*, *Systellaspis debilis*, and *Robustosergia robusta*. Gulf of Mexico Research Initiative Information and Data Cooperative (GRIIDC), Harte Research Institute, Texas A&M University – Corpus Christi. doi: 10.7266/n7-3p3y-g470

Truelove, N. K., Kough, A. S., Behringer, D. C., Paris, C. B., Box, S. J., Preziosi, R. F., et al. (2017). Biophysical connectivity explains population genetic structure in a highly dispersive marine species. *Coral Reefs* 36, 233–244. doi: 10.1007/s00338-016-1516-y

Uchida, H., and Baba, O. (2008). Fishery management and the pooling arrangement in the Sakuraebi Fishery in Japan. *Case Studies Fish. Self Governance* 504, 175–190.

van Olderborgh, G. J., van der Wiel, K., Sebastian, A., Singh, R., Arrighi, J., Otto, F., et al. (2017). Attribution of extreme rainfall from Hurricane Harvey, August 2017. *Environ. Res. Lett*. 12:124009. doi: 10.1088/1748-9326/aa9ef2

Venables, W. N., and Ripley, B. D. (2002). *Modern Applied Statistics With S, 4th Edn*. New York, NY: Springer.

Vereshchaka, A. L. (2009). Revision of the genus *Sergestes* (Decapoda: Dendrobranchiata: Sergestidae): taxonomy and distribution. *Galathea Rep*. 22, 7–104.

Wells, R. J. D., Rooker, J. R., Quigg, A., and Wissel, B. (2017). Influence of mesoscale oceanographic features on pelagic food webs in the Gulf of Mexico. *Mar. Biol*. 164, 1–11. doi: 10.1007/s00227-017-3122-0

Zimmerman, R. A., and Biggs, D. C. (1999). Patterns of distribution of sound-scattering zooplankton in warm- and cold-core eddies in the Gulf of Mexico, from a narrowband acoustic doppler current profiler survey. *J. Geophys. Res. Oceans* 104, 5251–5262. doi: 10.1029/1998JC900072

Conflict of Interest: The authors declare that the research was conducted in the absence of any commercial or financial relationships that could be construed as a potential conflict of interest.

The reviewer AL declared a past co-authorship with one of the authors MJ to the handling editor.

frontiers in Marine Science

ORIGINAL RESEARCH
published: 12 February 2020
doi: 10.3389/fmars.2020.00015

Dispersion Overrides Environmental Variability as a Primary Driver of the Horizontal Assemblage Structure of the Mesopelagic Fish Family Myctophidae in the Northern Gulf of Mexico

Rosanna J. Milligan and Tracey T. Sutton*

Halmos College of Natural Sciences and Oceanography, Nova Southeastern University, Dania Beach, FL, United States

OPEN ACCESS

Edited by:
Ana Colaço, Marine Research Institute (IMAR), Portugal

Reviewed by:
Xabier Irigoien, King Abdullah University of Science and Technology, Saudi Arabia
Verena Wang, The University of Southern Mississippi, United States

***Correspondence:**
Rosanna J. Milligan
R.Milligan@nova.edu

Specialty section:
This article was submitted to Deep-Sea Environments and Ecology, a section of the journal Frontiers in Marine Science

Received: *31 July 2019*
Accepted: *09 January 2020*
Published: *12 February 2020*

Citation:
Milligan RJ and Sutton TT (2020) Dispersion Overrides Environmental Variability as a Primary Driver of the Horizontal Assemblage Structure of the Mesopelagic Fish Family Myctophidae in the Northern Gulf of Mexico. Front. Mar. Sci. 7:15. doi: 10.3389/fmars.2020.00015

The lanternfishes (Myctophidae) are a highly speciose, globally-distributed family of fishes that constitute a dominant component of the global pelagic fauna. As a vertically-migrating taxon of oceanic micronekton, myctophids play vital ecological roles in the biological carbon pump and as an important prey group for several commercially-important species. However, our knowledge of the ecology of this taxon remains incomplete, and as anthropogenic impacts continue to develop and extend into deeper waters, there is a clear need for a better understanding of its ecological role and assemblage dynamics. The aim of the present study was to examine the distribution patterns of the myctophid assemblage within a 200 km × 700 km grid of the northern Gulf of Mexico (GoM) in relation to major mesoscale hydrographic features. The 22 dominant myctophid species (>0.05% by relative abundance) were analyzed from a total of 302 trawl samples collected between January and September 2011, from 0 to 1000 m depth. Redundancy analysis (RDA) indicated that measured environmental variables and spatial patterning explained an average of 12% (range: 0–27%) of the observed variance in the myctophid assemblage. Distance-based Moran's Eigenvector Mapping (dbMEM) and trend analysis (RDA) indicated limited significant spatial coherence within the assemblage at the scales considered. Local contribution to beta diversity scores corroborated these findings, indicating that the majority of samples were not significantly different from the mean assemblage structure. Taken together, these results suggest that the myctophid assemblage in the northern GoM is well-mixed and highly dispersed at the sub-basin scale (at least), likely the result of the interaction between vertical migration and depth-specific lateral advection. Findings such as these inform our approach to assessing impacts in a large, dynamic, pelagic ecosystems. It is essential to know over what spatial scales assessments of pelagic

faunal impacts, and potential recoveries, must be based. In cases of large, spatially integrated pelagic assemblages, high dispersal rates may serve to either ameliorate the effects of a disturbance through immigration or spread the effects across a wider spatial area than the disturbance phenomenon footprint itself.

Keywords: beta diversity, deep sea, micronekton, Myctophidae, spatial analysis

INTRODUCTION

Understanding how biodiversity is structured within ecosystems can provide insight into both the natural variability and functioning of those ecosystems and their stability in the face of natural or anthropogenic disturbance (e.g., Tilman et al., 2014). Nonetheless, there are significant gaps in our knowledge of many ecosystems, which can hinder our ability to predict future changes. This is especially true of the deep-pelagic realm, which has historically received relatively little scientific attention (Webb et al., 2010) and yet is likely to provide a wide range of essential ecosystem functions and services that are of global importance (e.g., Gjosaeter and Kawaguchi, 1980; Robinson et al., 2010; St. John et al., 2016).

One pelagic taxon of particular ecological interest is the Myctophidae, which is a highly speciose and globally-distributed family of fishes containing 251 recognized species from 32 genera (Fricke et al., 2019). Like much of the mesopelagic fauna, almost all myctophid species undertake diel vertical migrations (DVMs). While DVM behaviors are influenced by species identity, life-history stage, and environmental variables, the most common migratory pattern for myctophids involves individuals remaining at mesopelagic depths (c. 200–1000 m) during the day to avoid predation, and then migrating to epipelagic depths (c. 0–200 m) at night to feed (e.g., Gjosaeter and Kawaguchi, 1980; Sutton, 2013). DVM behaviors directly facilitate the active transport of carbon from the surface ocean to depth (e.g., Robinson et al., 2010), suggesting that myctophids and other migratory animals may play important roles in pelagic biogeochemical cycling and climate regulation. Similarly, myctophids are an important food source for numerous predators, including commercially-valuable and deep-living fish species, marine mammals and seabirds (e.g., Sutton and Hopkins, 1996; Beamish et al., 1999; Pusineri et al., 2008), and create important trophic connections between open oceans and terrestrial, coastal, and seafloor ecosystems. When one considers that the mesopelagic realm contains by far the highest biomass of fish on the planet (Kaartvedt et al., 2012; Irigoien et al., 2014) and that myctophids are once again being considered as a potential fishery resource (St. John et al., 2016), the importance of better understanding the spatial and temporal dynamics of these fishes is clear.

In recent years, there has been growing interest in identifying ecologically-meaningful predictors of deep-pelagic community structure, particularly in relation to mesoscale oceanographic features (i.e., those that occur over 10s to 100s of kilometers). The Gulf of Mexico (GoM) is a particularly interesting location to study mesoscale processes of deep-pelagic fishes, as it harbors an especially diverse myctophid assemblage (Gartner et al., 1987; Biggs and Ressler, 2001), as well as a number of relatively well-defined mesoscale oceanographic features of potential biological importance. The offshore GoM also has the potential to be heavily impacted by human activities, as was highlighted by the *Deepwater Horizon* oil spill in 2010, and there is therefore an urgent need to better understand the natural drivers of offshore, pelagic fauna to predict their effects on pelagic ecosystems in the future and how they may interact with anthropogenic impacts.

One of the major mesoscale oceanographic features influencing the upper circulation (<1000 m) of the GoM is the loop current (LC) and its associated eddies. The LC enters the GoM through the Yucatan Channel in the south, bringing warm, saline subtropical underwater (STUW; Rivas et al., 2005) into the GoM before exiting to the NW Atlantic through the Florida Straits (c. 750 m maximum depth). Anti-cyclonic Loop Current Eddies (LCEs) are formed from northward intrusions of the LC into the GoM, and are typically large (100s of kilometers in diameter), downwelling features associated with low surface productivity that generally persist for several months or years, and may extend to depths of several 100 m (e.g., Elliott, 1982; Biggs, 1992; Oey et al., 2003). LCEs can be identified within the GoM as regions of high sea surface height anomalies (SSHA; e.g., Zimmerman and Biggs, 1999; Jochens and DiMarco, 2008), and from temperature-salinity and temperature-depth profiles, where STUW is warmer than the surrounding water mass types below c. 200 m (Herring, 2010; Johnston et al., 2019). Over time, LCEs propagate westwards through the GoM, gradually mixing with Gulf Common Water (GCW) as they age and decay (Vukovich, 2007). Upwelling cyclonic eddies (CEs) are relatively small (10s km), transient (days–weeks) features that can form along the boundaries of LCEs (Vukovich, 2007). In the northeast GoM, cyclone-anticyclone confluences can draw productive coastal and riverine waters offshore (Biggs and Muller-Karger, 1994; Biggs and Ressler, 2001), usually following the summer rainy season when river outflows are highest (Morey et al., 2003).

In this manner, LCEs have the potential to facilitate the physical transport of fauna both between ocean basins, as well as between coastal and offshore ecosystems (e.g., Olson, 1991). However, they are also hypothesized to affect faunal distributions through local influences on primary productivity, with LCEs creating low-productivity regions, and CEs and riverine inputs creating high productivity regions respectively. In an acoustic study of the GoM, Zimmerman and Biggs (1999) reported greater abundances of mesopelagic fauna within more productive cyclonic eddies compared to less productive LCEs, and similar observations have been made for anticyclonic eddies in the Pacific Ocean (Barnett, 1984; Drazen et al., 2011). Similarly, Godo et al. (2012) reported that higher faunal biomasses were associated

with an anticyclonic eddy in the Norwegian Sea that contained high-productivity coastal waters. To date, the effects of riverine waters as transient regions of enhanced productivity have not been studied for any offshore fauna in the GoM.

It is notable that most previous studies have focused on patterns of abundance and biomass, and less is known about how mesoscale features may influence biodiversity patterns within regional basins (but see Potier et al., 2014; Olivar et al., 2016). In the present study, we aim to determine the relative importance of major mesoscale environmental features and spatial processes on the beta diversity of myctophids, using data collected from the upper 1000 m of the northern GoM between a continuous January-to-September 2011 survey. For the present study, we define beta diversity as the variation in assemblage composition between samples following Legendre et al. (2005).

MATERIALS AND METHODS

Data Collection and Filtering

A 10-m^2 Multiple Opening-Closing Net and Environmental Sensing System (MOCNESS) was used to sample 46 locations across the northern GoM during three consecutive sampling campaigns conducted between January 2011 and September 2011 (**Figures 1**, **2**) as part of the Offshore Nekton Sampling and Analysis Program (ONSAP; Cook et al., unpublished). Each campaign was designed to survey all stations over a period of 3 months (January–March; April–June; July–September). For the purposes of defining the spatiotemporal scales of the analyses, each campaign was considered to be a replicate survey of the northern GoM. The spatial extent was therefore c. 200 km × 700 km with a spatial grain of c. 50 km and temporal resolution of c. 3 months.

Each location was visited once per campaign, during which two MOCNESS deployments were conducted, centered around solar noon and midnight. Each deployment produced five depth-stratified samples from 0 to 1500 m, with the depth ranges chosen to reflect classical ecological divisions of the pelagic ocean (Sutton, 2013) and the approximate depth (1000–1200 m) of the deep-water oil plume observed after the *Deepwater Horizon* oil spill (Camilli et al., 2010).

A number of quality filters were applied to the data to reduce the effects of sampling errors and random noise. Firstly,

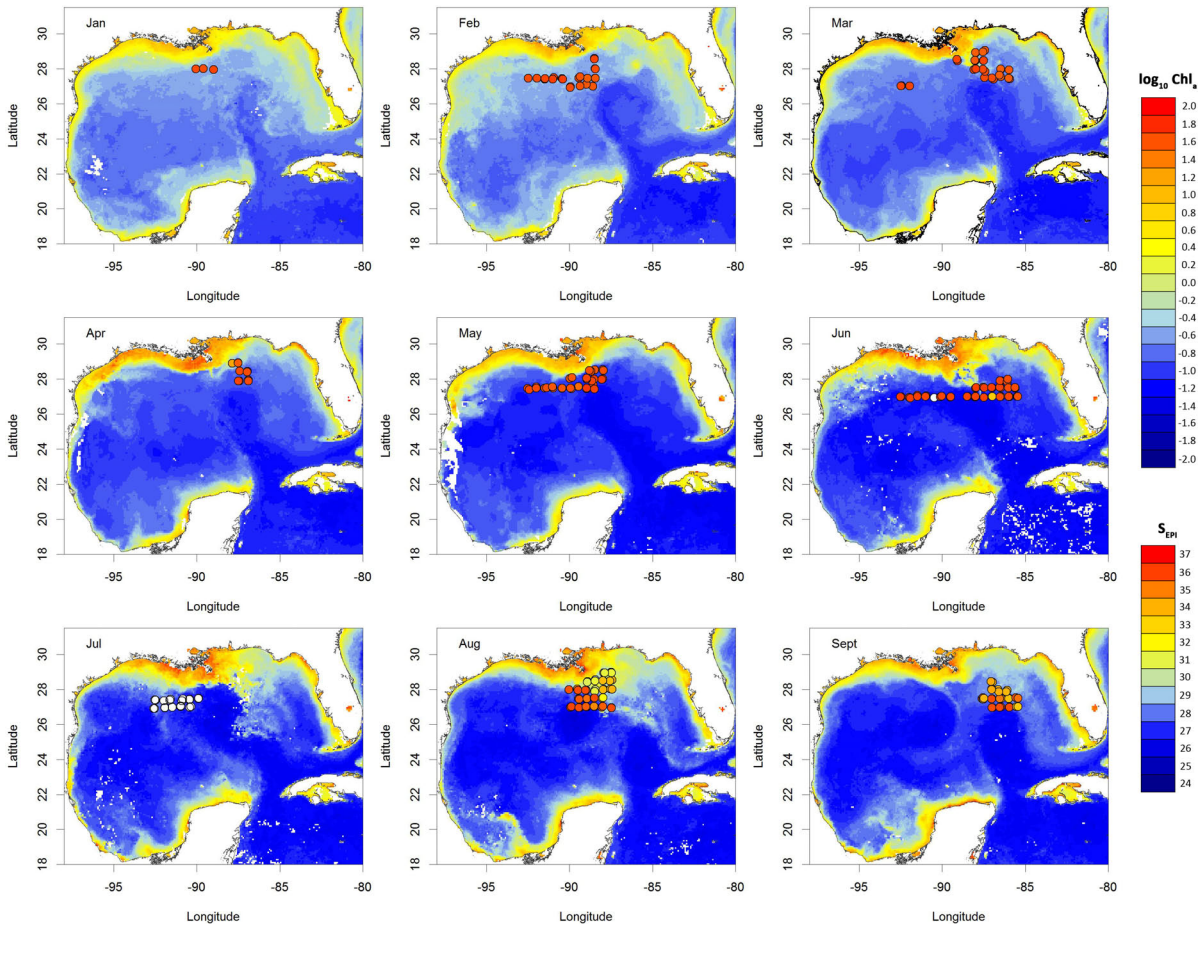

FIGURE 1 | Maps showing the satellite-derived $\log_{10}$ Chl_a concentrations across the GoM per month. Each point is a MOCNESS sample, colored according to the S_{EPI} values recorded by the MOCNESS sensors at the time of collection. White points indicate no MOCNESS sensor data were available. Chart datum: WGS84.

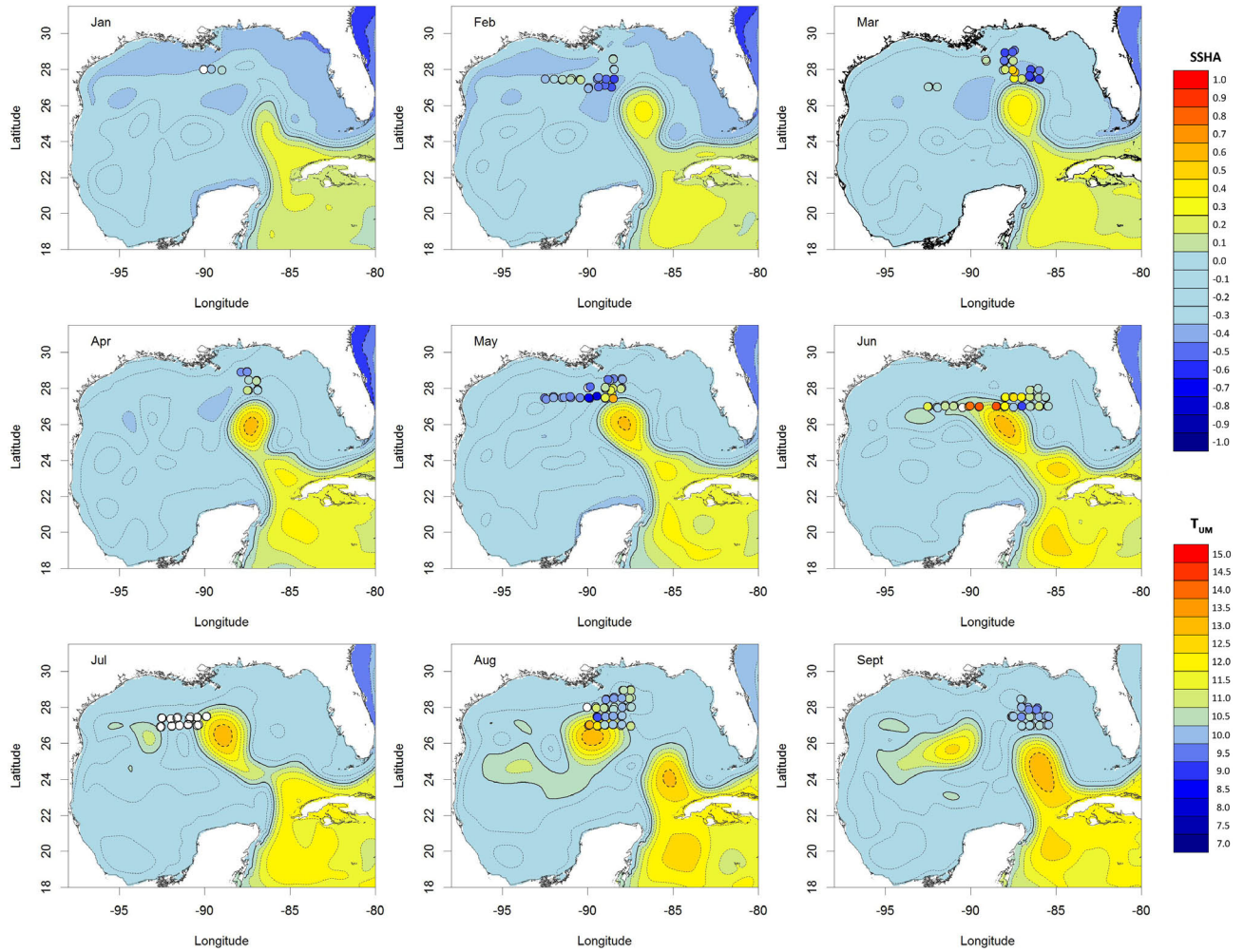

FIGURE 2 | Maps showing satellite-derived, integrated SSHA data per month (from CMEMS). Contour lines mark 0.1 m intervals; 0 m is indicated by the solid line. Each point is a MOCNESS sample, colored according to the T_{UM} at the time of collection. White points indicate no MOCNESS sensor data were available. Chart datum: WGS84.

only daytime samples collected from the upper (200–600 m) and lower mesopelagic (600–1000 m), and night-time samples from the epipelagic (0–200 m) were included in the analyses. These depth strata contain the majority of the captured myctophids, and reflects their DVM behaviors (**Supplementary Figure 1**). Secondly, only myctophids identified to species level were retained in the dataset. Finally, myctophid counts were standardized by trawl volume (as recorded by the MOCNESS sensors) and only those species comprising > 0.5% of the total myctophid fauna were retained for further analysis.

To test the effects of mesoscale features on the myctophid assemblage composition, six physical and chemical variables were selected as indicators of either coastal and riverine inputs to the GOM, or of anti-cyclonic LCEs (**Table 1**). Conceptually, these spatial variables were considered to represent either "static" spatial processes with no biologically-relevant temporal component (e.g., distance from the 200 m isobath), or "dynamic" spatial processes. The values of the dynamic processes at a location represent effectively instantaneous measurements [e.g., mean temperature in the upper mesopelagic (200–600 m; T_{UM}); minimum surface salinity (S_{EPI})], up to integrated monthly measures [e.g., SSHA; chlorophyll *a* concentration (Chl_a)]. Any samples for which MOCNESS sensor data were unavailable were excluded from further analysis, which included all samples collected in July 2011.

Community Analysis

The myctophid assemblage data were analyzed using three separate analyses: redundancy analysis (RDA; following Legendre and Legendre, 2012) to identify linear trends in assemblage composition using the Cartesian co-ordinate data; RDA to examine the effects of the mesoscale variables of interest on assemblage composition (**Table 1**); and distance-based Moran's Eigenvector Maps to quantify spatial patterning within the assemblage (dbMEM; Dray et al., 2006). These three analyses were then followed by variance partitioning

TABLE 1 | Environmental variables selected for inclusion in the multivariate analyses and their suggested interpretation.

Variable	Units	Indicative of:	Temporal resolution	Spatial resolution	Data product	Source
Distance to 200 m isobaths	km	Coastal influences and/or topographic association	Effectively invariant	1/120°	The GEBCO_2014 Grid, version 20141103	General Bathymetric Chart of the Oceans (GEBCO), http://www.gebco.net
Sea surface height anomaly (SSHA)	m	Loop current and associated eddies	Monthly	1/12°	GLOBAL_ANALYSIS_FORECAST_PHY_001_024	E.U Copernicus Marine Service (CMEMS)
Mean temperature between 200 and 600 m (T_{UM})	°C	Loop current and associated eddies	Instantaneous	<1 m		*In situ* MOCNESS sensors
Min. surface salinity (S_{EPI})	n/a	Coastal runoff; riverine input	Instantaneous	<1 m		*In situ* MOCNESS sensors
Mean Chl. a concentration (Chl_a)	mg m^{-3}	Surface productivity; coastal runoff; riverine input	Monthly	9 km^2	Moderate-resolution Imaging Spectroradiometer (MODIS) Aqua Chlorophyll Data; 2018 Reprocessing	Nasa Goddard Space Flight Center, Ocean Ecology Laboratory, Ocean Biology Processing Group, 2018

(Peres-Neto et al., 2006) to quantify the relative effects of the three sets of variables in shaping the myctophid beta diversity across the northern GoM. These multivariate analyses are particularly useful in that they allow spatial autocorrelation in the environmental variables and assemblage data to be explicitly accounted for Dormann et al. (2007) and partitioned within the statistical framework, reducing the risk of type 1 errors when determining the importance of the environmental conditions. Data from each depth stratum and survey campaign were analyzed separately. All analyses were conducted using R software (R Core Team, 2018) and results were considered significant at $p < 0.05$. Where significance was determined by permutation testing, 10000 permutations were used.

Prior to analysis, the myctophid count data were Hellinger transformed and converted to a Hellinger distance matrix (Legendre and Gallagher, 2001). Geographic position data (latitude and longitude) corresponding to each sample were transformed to Cartesian coordinates using the "geoXY" function in the SoDA package (Chambers, 2013), and the mesoscale variables were scaled and centered using the "scale" function. The overall relationship between the geographic distance and the Hellinger distance between samples was examined using Pearson's correlation coefficient, and conducted separately for each of the survey periods and depth strata examined.

The analyses were then conducted in the following sequence. First, linear spatial trends in the myctophid data were identified by testing the Cartesian coordinate data against the myctophid data with the "rda" and "anova.cca" functions in the vegan package (Oksanen et al., 2017). If a significant overall effect of latitude or longitude was detected, the significant variable(s) were identified by forward selection using the double-stopping criterion described by Blanchet et al. (2008) and implemented in the "forward.sel" function in the packfor package (Dray, 2013). Any significant coordinate variable(s) were used to detrend the myctophid data prior to any further analyses. Next, RDA and forward selection were used to identify any significant effects of mesoscale variables on the (detrended) myctophid data. Variance inflation factor (VIF) scores were checked following RDA using the "VIF" function, and any variables with a score > 5 (indicating collinearity) were excluded and the model refitted.

To assess the spatial scales of variation within the data, a geographic distance matrix was generated for all sample locations by applying the Euclidean distance function "dist" to their Cartesian coordinates. The dbMEM eigenfunctions were generated from this distance matrix using the "PCNM" function in the PCNM package (Dray et al., 2015), where the truncation distance was set to the minimum distance required to connect all locations within a minimum spanning tree (here, c. 75–100 km). Moran's I was used as the measure of spatial autocorrelation, where positive values indicate positive spatial autocorrelation and negative values indicate negative spatial autocorrelation. Since identifying positive spatial correlation was of most ecological interest, only those eigenfunctions with positive Moran's I values were retained, and tested for overall significance using the "anova.cca" function. If the overall test indicated significant effects, forward selection was conducted as before. To identify whether the groups covaried with the observed mesoscale variables, the significant RDA axes from each group were regressed against the mesoscale variables using linear models ("lm" function).

Finally, variance partitioning was conducted with respect to any significant linear trends, significant dbMEM eigenfunctions, and significant mesoscale variables identified during the previous analyses using the "varpart" function in the vegan package.

As a complement to the spatial eigenfunction analyses, local contribution to beta diversity (LCBD; Legendre and de Caceres, 2013) scores were generated for each sample and used to identify those samples where the assemblage composition differed significantly from that of the mean assemblage. LCBD scores were generated from the Hellinger distance matrix for the myctophid data using the "LCBD.comp" function in the adespatial package (Dray et al., 2016). The resulting p-values were adjusted using the Holm correction for multiple comparisons. Linear models (LMs) were fitted to identify whether LCBD scores correlated with different environmental conditions or with Hellinger-transformed abundances of particular species. In both cases, term selection was conducted by backward selection using AIC scores as the selection criterion. Variables were retained

in the model if their exclusion resulted in the AIC score increasing by ≥ 4.

RESULTS

Environmental Setting

The physical and chemical conditions varied over the course of the sampling period, with temporal and spatial patterns evident in the data (**Figures 1**, **2**). S_{EPI} were typically high between January and June (January–June) with much lower values recorded later in the year (August–September). The Chl_a concentrations showed a similar pattern, suggesting that offshore transport of coastal and riverine water occurred during late summer 2011. The mean monthly SSHA maps indicate that a LCE began to form in February–March 2011, but that the core of the eddy remained south of the surveyed area during 2011. During April–June 2011, SSHA strongly covaried with T_{UM} and S_{EPI} and so was excluded from the analyses.

Community Analyses

A total of 20,953 myctophids from were collected from 302 non-empty net samples from the epipelagic (night) and mesopelagic (day), representing 18.2% of the total number of fishes captured in these depths (the numerically-dominant gonostomatid, *Cyclothone* spp. comprised 50.1%). The dominant taxa included in the analyses comprised 20,325 individuals from 22 species (**Table 2**), which represented c. 80% of all myctophids captured during 2011 by number. Some temporal variation in the rank order of the dominant species was observed through the survey period (**Table 2**), though species composition otherwise remained relatively consistent. All myctophids were adults, with standard lengths ranging from 7–77 mm (epipelagic; night), and 7–99 mm (mesopelagic; day).

Epipelagic Depths (0–200 m; Night)

Between January and March 2011, the composition of myctophids between 0 and 200 m was significantly correlated with S_{EPI} [R^2 (adj.) = 0.11; $p < 0.001$]. A longitudinal trend in the data was identified, but did not remain significant after variance partitioning (**Figure 3**). No environmental variables were significantly correlated with assemblage composition between April and June ($p = 0.07$), though a latitudinal trend was evident [R^2 (adj.) = 0.05; $p = 0.01$]. In August and September, myctophid assemblage composition was significantly correlated with SSHA [R^2 (adj.) = 0.04; $p = 0.014$] and Chl_a concentration [R^2 (adj.) = 0.03; $p = 0.023$]. Significant spatial patterning (dbMEM: $p = 0.0001$) were also evident in the data (**Figure 4A**). The first pattern (Axis 1) correlated significantly with SSHA [$p = 0.001$; R^2 (adj.) = 0.29]. Both dbMEM and environmental variables remained significant following variance partitioning (**Figure 3**). Pearson's correlation between Hellinger and geographic distances showed a significant positive relationship between samples collected in August and September (**Table 3**), indicating that samples at greater distances from each other were less similar in terms of myctophid assemblage composition. No other results were significant.

TABLE 2 | Percentage contribution to the total myctophid assemblage captured during 2011 from each cruise series.

Species	Percentage of myctophids captured			
	Overall *(Rank)*	**January–March 2011** *(Rank)*	**April–June 2011** *(Rank)*	**July–September 2011** *(Rank)*
Lampanyctus alatus	17.19 *(1)*	20.67 *(1)*	20.80 *(1)*	14.23 *(2)*
Ceratoscopelus warmingii	15.31 *(2)*	7.12 *(5)*	18.50 *(2)*	13.28 *(3)*
Diaphus dumerilii	10.60 *(3)*	5.07 *(6)*	11.64 *(4)*	18.22 *(1)*
Benthosema suborbitale	9.99 *(4)*	14.52 *(3)*	11.90 *(3)*	6.97 *(7)*
Notolychnus valdiviae	9.53 *(5)*	15.72 (2)	7.15 *(5)*	9.41 *(5)*
Hygophum benoiti	9.05 *(6)*	–	5.52 *(7)*	7.24 *(6)*
Lepidophanes guentheri	6.87 *(7)*	7.75 *(4)*	6.46 *(6)*	9.94 *(4)*
Myctophum affine	2.42 *(8)*	0.75 *(18)*	2.09 *(9)*	2.50 *(9)*
Diogenichthys atlanticus	2.35 *(9)*	4.07 *(8)*	1.95 *(10)*	2.47 *(10)*
Diaphus mollis	2.11 *(10)*	2.33 *(10)*	2.56 *(8)*	2.68 *(8)*
Notoscopelus resplendens	2.07 *(11)*	4.80 *(7)*	1.79 *(11)*	–
Hygophum taaningi	1.93 *(12)*	1.85 *(11)*	1.55 *(12)*	1.68 *(11)*
Bolinichthys photothorax	0.90 *(13)*	0.81 *(16)*	1.05 *(13)*	1.14 *(14)*
Bolinichthys supralateralis	0.88 *(14)*	1.10 *(14)*	–	1.21 *(13)*
Diaphus lucidus	0.88 *(14)*	1.06 *(15)*	0.71 *(15)*	0.86 *(17)*
Hygophum hygomii	0.83 *(16)*	3.61 *(9)*	–	–
Diaphus splendidus	0.86 *(17)*	0.60 *(20)*	0.82 *(14)*	1.32 *(12)*
Lobianchia gemellarii	0.73 *(18)*	1.16 *(12)*	0.55 *(18)*	1.08 *(16)*
Lampanyctus lineatus	0.70 *(19)*	1.14 *(13)*	–	0.70 *(18)*
Lampadena luminosa	0.69 *(20)*	–	0.59 *(17)*	1.09 *(15)*
Hygophum macrochir	0.68 *(21)*	0.77 *(17)*	0.62 *(16)*	–
Hygophum reinhardtii	–	0.69 *(19)*	–	–

'–' indicates those species that did not contribute more than 0.5% of the combined myctophid fauna captured within the mesopelagic (day only) and epipelagic (night only).

Upper Mesopelagic Depths (200–600 m; Day)

Between January and March 2011, the composition of myctophids between 200 and 600 m was significantly correlated with both T_{UM} [R^2 (adj.) = 0.07; $p = 0.01$] and SSHA [R^2 (adj.) = 0.06;

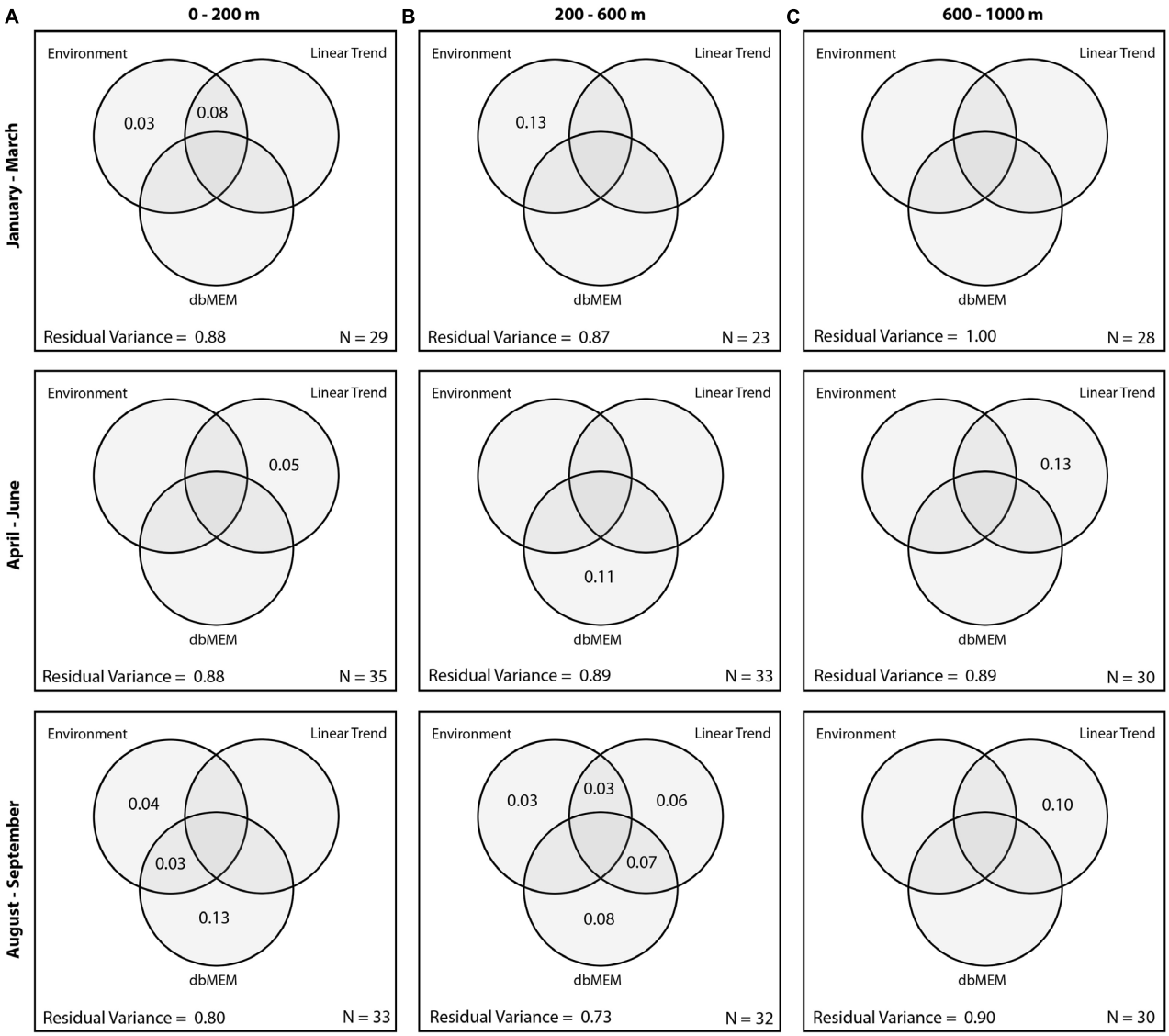

FIGURE 3 | Venn diagrams showing the relative variance explained by significant environmental and spatial variables at **(A)** 0–200 m (Night); **(B)** 200–600 m (Day); **(C)** 600–1000 m (Day).

p = 0.001]. Significant spatial patterning was evident in April–June [dbMEM: R^2 (adj.) = 0.11; p = 0.04; **Figure 4B**]. The finer-scale pattern was significantly correlated with S_{EPI} (p = 0.005) and T_{UM} (p = 0.002; overall adj. R^2 = 0.33). In August and September, myctophid assemblage composition was significantly correlated with a latitudinal trend [R^2 (adj.) = 0.05; p = 0.013], and with SSHA [R^2 (adj.) = 0.08; p = 0.012] and distance to the 200 m isobath [R^2 (adj.) = 0.06; p = 0.019]. A marginally significant spatial pattern (dbMEM: p = 0.045) was also evident in the data (**Figure 4C**), which correlated significantly with SSHA [p = 0.004, R^2 (adj.) = 0.28], Chl_a concentration (p = 0.040) and T_{UM} [p = 0.047; overall adj. R^2 (adj.) = 0.27]. All dbMEM, latitudinal trend and environmental variables remained significant following variance partitioning (**Figure 3**). Pearson's correlation between Hellinger and geographic distances showed a significant positive relationship between samples collected in August and September (**Table 3**), indicating that samples at greater distances from each other were less similar in terms of myctophid assemblage composition. No other results were significant.

Lower Mesopelagic Depths (600–1000 m; Day)

Myctophid assemblage composition in lower mesopelagic depths were significantly correlated with latitude [R^2 (adj.) = 0.13; $p < 0.001$] between April and June, and with both latitude [R^2 (adj.) = 0.055; p = 0.01] and longitude [R^2 (adj.) = 0.095; p = 0.001] in August and September (**Figure 3**). Pearson's correlation between Hellinger and geographic distances showed significant relationships between samples collected in all survey periods,

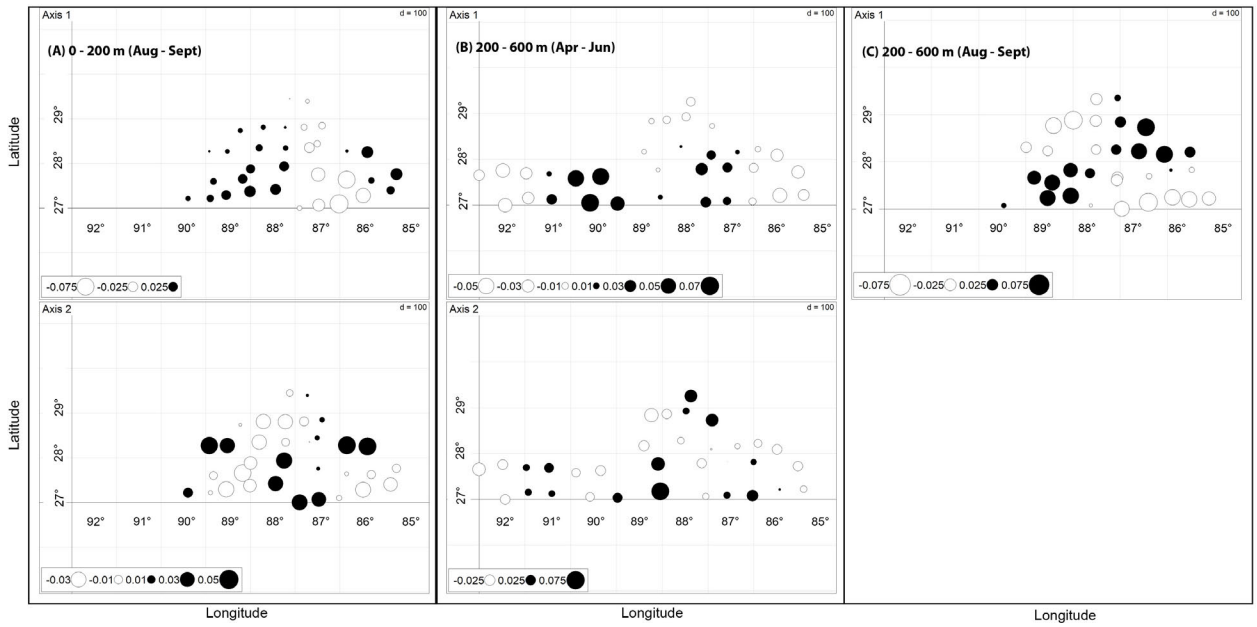

FIGURE 4 | dbMEMs showing significant correlation to myctophid assemblage composition following RDA in **(A)** 0–200 m (August–September); **(B)** 200–600 m (April–June); **(C)** 200–600 m (August–September). In **(A,B)** two significant axes were identified; in **(C)** only a single significant axis was identified. Circle color and size represents the values of the eigenvalues that model positive spatial correlation and indicate the scales of spatial patterning in the assemblage data.

TABLE 3 | Summary of the correlation between Hellinger distance (dissimilarity) and geographic (Euclidian) distance for samples collected from each survey period and depth stratum.

Survey period	Depth stratum	Pearson's correlation coefficient	*p*-Value
January–March 2010	0–200 m	0.08	0.144
	200–600 m	−0.03	0.620
	600–1000 m	−0.29	<0.001
April–June 2010	0–200 m	−0.03	0.489
	200–600 m	0.06	0.198
	600–1000 m	0.22	<0.001
August–September 2010	0–200 m	0.09	0.030
	200–600 m	0.27	<0.001
	600–1000 m	0.28	<0.001

with a negative correlation observed between January and March, and positive correlations between April and September (**Table 3**). No other results were significant.

Local Contribution to Beta Diversity (LCBD)

Local contribution to beta diversity scores indicated that five samples from epipelagic depths, and four samples from upper mesopelagic depths were significantly different to the other samples within each survey period (**Figure 5**). One additional sample from the upper mesopelagic was marginally significant (p = 0.056). No samples from lower mesopelagic depths were significantly different to the others (**Figure 5**). LMs indicated that LCBD scores correlated negatively with SSHA only (**Supplementary Table 1**). Samples with significantly different LCBD scores occurred with SSHA was in the range −0.37 and −0.13 m, compared with a range of −0.37 to 0.45 m for the remaining samples. LMs also indicated that high LCBD scores were correlated with lower relative abundances of the seven most abundant myctophid species, plus *Notoscopelus resplendens, Hygophum taaningi,* and *Lampanyctus lineatus* (**Supplementary Table 2**).

DISCUSSION

This study examined the spatial distributions of the myctophid assemblage in the northern Gulf of Mexico over a 9-month period in 2011 in relation to Loop Current origin water and a summer plume of low-salinity coastal and riverine runoff. Overall, the myctophid assemblage composition showed limited horizontal structuring at the spatial and temporal scales considered, suggesting that discrete, geographically maintained assemblages are not maintained in the northern Gulf, and that the greater assemblage can be treated as a single unit. The dbMEM and RDA analyses indicated that environmental and spatial variables together explained an average of 12% (range: 0–27%) of the variance in the myctophid beta diversity (i.e., the variation in assemblage composition between samples) over the 9-month survey period, but that the significant environmental variables and spatial patterns varied with both water depth and time of year. We found no evidence to suggest that Loop Current eddies contained a unique myctophid fauna compared to the rest of the GoM. While relatively little is known about the biodiversity patterns of mesopelagic fauna in general, these findings are

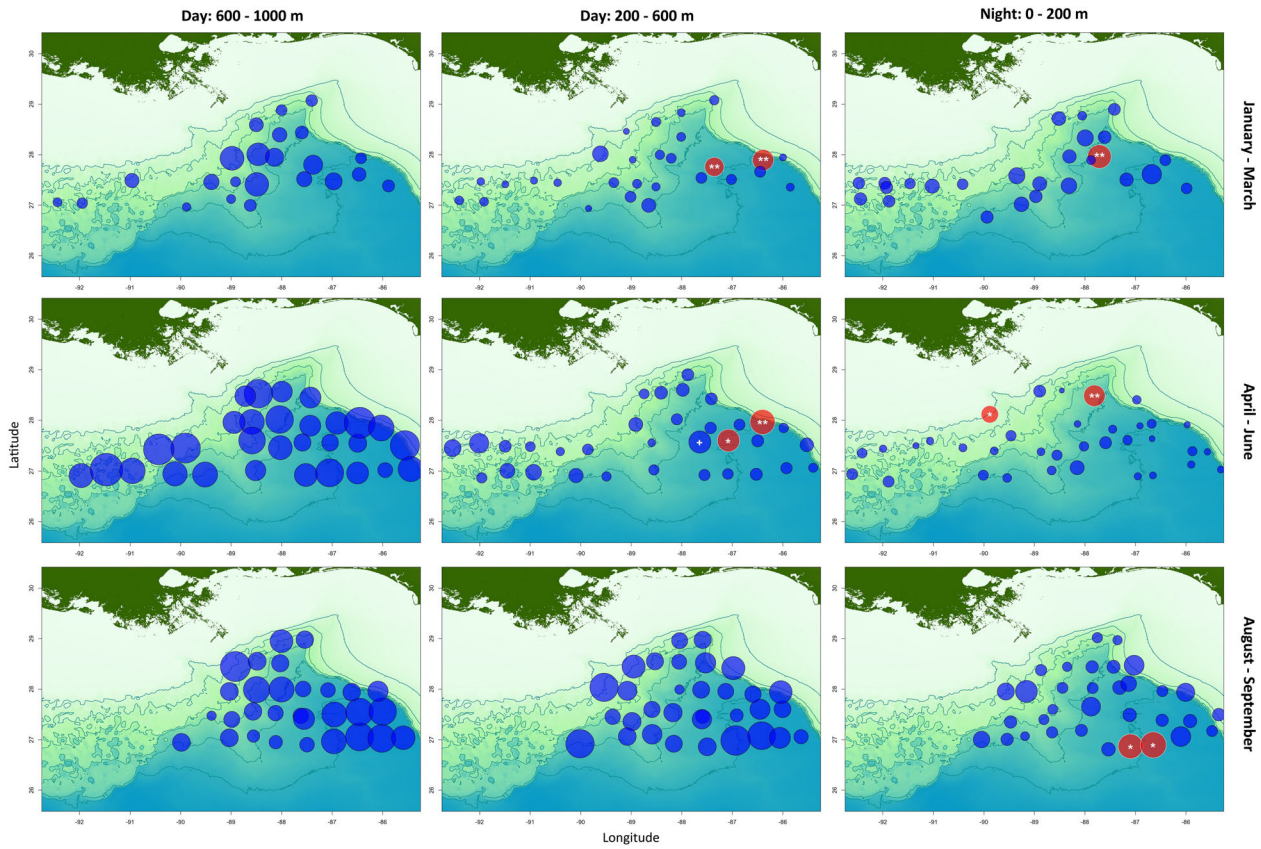

FIGURE 5 | Local contribution to beta diversity (LCBD) scores of each sample, subdivided by depth band and cruise program. Red circles indicate samples that are significantly different to the mean community; blue circles are samples that are not significantly different. The radii of the circles correspond to the LCBD scores. The significance (with Holm correction) is indicated as: $^{+}p < 0.1$; $^{*}p < 0.05$; $^{**}p < 0.01$.

similar to those reported in other oceans when examined at the sub-ecoregion (*sensu* Spalding et al., 2007; Sutton et al., 2017) level. For example, Olivar et al. (2016) determined that physical and chemical variables explained only 10% of the variance in myctophid composition across the Atlantic, Indian and Pacific Oceans, with 17% of the variance explained by spatial variables.

Within the upper 600 m, the results suggested significant, albeit weak, effects of variables associated with Loop Current eddies and low-salinity coastal water between January and March, and August and September. It is notable that the Loop Current eddy-associated variables were not significant between April and June, when the strongest Loop Current eddy conditions occurred within the survey region (**Figure 2**). Higher LCBD scores were associated with lower SSHA values, which can be indicative of cyclonic eddies (Vukovich, 2007). As upwelling features, cyclonic eddies would contain cooler water than the surrounding Gulf Common Water however, which was not evident from the T_{UW} data. It may be that the discrepancy reflects the temporal scales measured by each metric, where the monthly-averaged SSHA could have provided an indication of previous oceanographic conditions (or the formation of new conditions) at each sample site that were not detected *in situ,* but which nonetheless influenced faunal distributions enough for a residual (or pre-emptive) effect to be detected. However, given the relatively small number of samples ($N = 9$) identified as having a significantly different faunal composition, it is possible that these findings could simply reflect the patchy distributions of micronekton in the water column (e.g., Benoit-Bird and Au, 2003) and further, targeted study of these features is needed.

In the lower mesopelagic zone (600–1000 m), patterns of beta diversity were simpler and only significantly structured by linear spatial gradients, which explained 10–13% of the variation in species composition, though significant positive and negative correlations between Hellinger distance and geographic distance were identified in all samples collected from 600 to 1000 m. The LCBD analyses however suggested that the myctophid assemblage below 600 m was homogeneous across the northern GoM at the time of the study. Circulation patterns within the GoM are believed to comprise of an upper layer and a lower layer that become effectively decoupled from each other at c. 800–1200 m depth (Hamilton and Lugo-Fernandez, 2001). While further work is needed, it is nonetheless possible that the transition from an upper- to lower-level circulation pattern may explain the different spatial patterns observed in the lower mesopelagic samples compared to those collected above 600 m, where the influence of Loop Current origin

waters is strongest. Taken together, our findings indicate that the myctophid assemblage within the upper 1000 m of the GoM showed only weak horizontal structuring over the study period at the spatial (75–700 km) and temporal (<3 months) scales considered.

Significant broad-scale spatial structuring was identified between April and September (0–600 m) that was not fully explained by the measured environmental variables. While it is important not to over-interpret the patterns observed from a small number of dbMEMs (Legendre and Legendre, 2012), there are several possible explanations that may account for some of the observed spatial structuring, including unmeasured or "historic" environmental conditions, or biotic and stochastic processes that are not under environmental control (Legendre and Legendre, 2012). Current speed and direction were not included in the present study for example, but convergence or divergence fronts could feasibly explain some additional portion of the variance observed in the assemblage structure by physically aggregating or dispersing the fauna, respectively (Olson et al., 1994; Potier et al., 2014). Similarly, better understanding of circulatory patterns in the deep GoM may also provide insight into the spatial structuring of the micronekton in lower mesopelagic and bathypelagic (>1000 m) depths. It is also possible that the myctophid fauna were less affected by their immediate conditions than by a set of conditions that they encountered at some earlier point in time, leading to detection of a residual effect. Biotic responses may include inter-specific interactions such as competition for resources (e.g., with other zooplanktivorous organisms (e.g., engraulid fishes) that may be seasonally abundant), or predator-prey relationships, which are likely to be important in structuring mesopelagic assemblages at fine spatial (meters) and temporal (minutes–hours) scales (Benoit-Bird and McManus, 2014; Koslow et al., 2014). Alternatively, the observed differences in rank dominance of myctophid species between sampling campaigns may be indicative of underlying seasonal changes in the myctophid assemblage related to their underlying population dynamics for example.

One explanation for the weak horizontal structuring within the myctophid assemblage is the high dispersal potential of pelagic organisms. With few hard barriers to dispersal, mobile pelagic organisms have relatively unrestricted access to all parts of their environment (given sufficient time; Heino et al., 2015). In a recent review, Gaither et al. (2016) highlighted that most circumtropical fishes are pelagic and deep-living (i.e., occurring below 200 m), with myctophids comprising 17% of all known circumtropical species. Gaither et al. (2016) suggested that highly dispersed taxa tended to be those with highly mobile adult stages and which are habitat generalists (or prefer widely-distributed habitats), and that passive transport of planktonic pelagic species and larvae by oceanic currents is also likely to promote dispersal (Gaither et al., 2016; Allen et al., 2018). Both larval and adult myctophids are pelagic, and while their small size may preclude long-distance swimming, their ability to undertake DVMs and onshore-offshore migrations (Benoit-Bird and Au, 2006) indicates that they are capable of actively choosing favorable environmental conditions at scales of at least 100–1000s m, and of tolerating a wide range of environmental conditions associated with changing depth (e.g., temperature, salinity, pressure, light levels).

Changing vertical distributions may also play an important role in promoting horizontal dispersal. Ontogenetic changes in vertical distributions are common amongst myctophids, with many species having non-migratory, epipelagic larval and juvenile stages, with adults moving into progressively deeper waters as they age (e.g., Badcock and Merrett, 1976; Gartner et al., 2008). Adult myctophids also typically perform DVMs to feed and reproduce in the surface waters, but the proportions of individuals migrating on a given day can be highly variable (Watanabe et al., 1999) and may be influenced by environmental (Badcock and Merrett, 1976; Linkowski, 1996; Ekau et al., 2010; Drazen et al., 2011) or biotic (e.g., Angel and Pugh, 2000) conditions. Additionally, since the speed and direction of water currents in the upper 1000 m of the GoM vary with depth (Jochens and DiMarco, 2008), vertically-migrating species have the potential to be passively moved relatively large horizontal distances, at different speeds and in different directions depending on their preferred vertical distribution at any given life-history stage. All these traits could promote dispersal, and lead to a more homogeneous assemblage than would be observed if species were structured only by environmental variables (Heino et al., 2015), or if species maintained geographic integrity via active station-keeping. In a recent circumglobal study, Villarino et al. (2018) came to a similar conclusion regarding the relative dispersal potential of myctophid fishes, where passive drift was hypothesized to dominate their distribution patterns at small sizes, with vertical migration rather than horizontal movements dominating their dispersal behaviors as adults.

While the results presented here indicate that myctophid distributions are not directly driven by environmental parameters at the scales studied, it is possible that some drivers may not be detected by the methods used in this study. By using Hellinger distances in the analyses, we implicitly define "assemblage composition" as the relative abundance of species within a given sample. Changes in the relative abundance species within samples are accounted for, but differences in absolute abundance between samples are not. In the GoM, Loop Current eddies have been previously associated with a lower abundance and biomass of pelagic fauna (if not explicitly myctophids; Zimmerman and Biggs, 1999; Wells et al., 2017), but these differences would not be detected by the methods used here, and will require further study to quantify.

Assuming that high dispersal and mixing rates drive myctophid assemblage distributions within the northern GoM, it is possible to make some inferences about how offshore assemblages may be impacted by stressors and disturbance events. Within the GoM, such information is particularly useful for understanding any potential impacts from the *Deepwater Horizon* oil spill on the deep-pelagic fauna, given the lack of pre-spill data for the region, and in predicting how offshore ecosystems may be impacted by future spills. For example, metacommunity theory suggests that assemblages with high

dispersal rates are likely to be more resilient because individuals can recolonize local areas rapidly after a disturbance event (Heino, 2013). However, the extent to which "local areas" or refugia might exist within the pelagic realm is unclear. Physical and chemical boundaries (e.g., pycnoclines) may preclude the mixing of spilled oil to some extent, but these are not hard barriers to micronekton movements. If a disturbance is detectable by the fauna, but not immediately lethal, mobile individuals may be able to move away from the impacted area before it has a major impact on their health. Such avoidance behavior has been observed in mobile demersal fishes exposed to oil spills in other regions (Elmgren et al., 1983; Law and Kelly, 2004), but it is unclear how well micronekton would be able to actively avoid impacted areas, particularly on the scale of DWHOS. In open ecosystems like those in the pelagic realm, local or point-source disturbances could have a greater footprint than they might in more enclosed ecosystems. It is also possible that high dispersal rates in a pelagic system could lead to increased rates of lethal or sub-lethal exposure than would be expected in more static or enclosed ecosystems, since a greater number of individuals could move into (and out of) the disturbed area over the duration of the event (Heino, 2013; Heino et al., 2015).

The present study makes use of an exceptionally large dataset of deep-pelagic fishes, and provides the first spatially-explicit analysis of myctophid beta diversity patterns in the GoM. While these findings represent a snapshot view of the conditions and fauna during a single year, they nonetheless provide novel insights into how deep-pelagic biodiversity is structured and provide support for the idea that myctophid assemblages are well-mixed and highly dispersed. We anticipate that these findings will provide a useful basis upon which to build further analyses examining seasonal and inter-annual changes in the abundance and biodiversity patterns of deep-pelagic fishes, as well as further exploration of the importance of biotic interactions and behavioral choices amongst the fauna. Given the importance of myctophids in delivering vital ecosystem services such as carbon sequestration from the surface ocean to depth, and as prey for numerous commercially and ecologically important species (e.g., St. John et al., 2016), we anticipate that these findings will also provide valuable, necessary scientific data upon which to build reliable offshore management strategies to protect the functioning and resilience of deep-pelagic ecosystems.

DATA AVAILABILITY STATEMENT

The faunal data used in this study are publicly available through the Gulf of Mexico Research Initiative Information & Data Cooperative (GRIIDC) at https://data.gulfresearchinitiative.org (doi: 10.7266/N7VX0DK2). Additional data were sourced from the E.U. Copernicus Marine Service (GLOBAL_ANALYSIS_FORECAST_PHY_001_024), the GEBCO_2014 Grid (version 20141103), and NASA's Ocean Biology Processing Group (doi: 10.5067/AQUA/MODIS/L3M/CHL/2018).

AUTHOR CONTRIBUTIONS

TS designed and conducted the surveys presented here, and identified the myctophid specimens. RM conducted the data analyses, prepared the figures, and wrote the first manuscript draft. Both authors reviewed and edited the final draft.

FUNDING

This research was funded in part by the NOAA Office of Response and Restoration and in part by a grant from the Gulf of Mexico Research Initiative (GoMRI).

ACKNOWLEDGMENTS

We would like to thank A. Cook for her assistance and data management during both the ONSAP program. We also thank K. Bowen, K. Lord, L. Malarkey, M. Novotny, A. Pickard, and N. Pruzinsky for assistance with quantitative sample processing. We would also like to thank the crew and scientific staff of the M/V *Meg Skansi* and R/V *Point Sur*.

SUPPLEMENTARY MATERIAL

The Supplementary Material for this article can be found online at: https://www.frontiersin.org/articles/10.3389/fmars.2020.00015/full#supplementary-material

REFERENCES

Allen, R. M., Metaxas, A., and Snelgrove, P. V. R. (2018). Applying movement ecology to marine animals with complex life cycles. *Ann. Rev. Mar. Sci*. 10, 19–42. doi: 10.1146/annurev-marine-121916-063134

Angel, M. V., and Pugh, P. R. (2000). Quantification of diel vertical migration by micronektonic taxa in the northeast Atlantic. *Hydrobiologia* 40, 161–179. doi: 10.1007/978-94-017-1982-7_16

Badcock, J., and Merrett, N. R. (1976). Midwater fishes in the eastern north Atlantic–1. *Prog. Oceanogr*. 7, 3–58. doi: 10.1016/0079-6611(76)90003-3

Barnett, M. A. (1984). Mesopelagic fish zoogeography in the central tropical and sub-tropical Pacific-ocean – species composition and structure at representative locations in 3 ecosystems. *Mar. Biol.* 82, 199–208. doi: 10.1007/bf00394103

Beamish, R. J., Leask, K. D., Ivanov, O. A., Balanov, A. A., Orlov, A. M., and Sinclair, B. (1999). The ecology, distribution, and abundance of midwater fishes of the Subarctic Pacific gyres. *Prog. Oceanogr*. 43, 399–442. doi: 10.1016/s0079-6611(99)00017-8

Benoit-Bird, K. J., and Au, W. W. L. (2003). Spatial dynamics of a nearshore, micronekton sound-scattering layer. *ICES J. Mar. Sci*. 60, 899–913. doi: 10.1016/S1054-3139(03)00092-4

Benoit-Bird, K. J., and Au, W. W. L. (2006). Extreme diel horizontal migrations by a tropical nearshore resident micronekton community. *Mar. Ecol. Prog. Ser*. 319, 1–14. doi: 10.3354/meps319001

Benoit-Bird, K. J., and McManus, M. A. (2014). A critical time window for organismal interactions in a pelagic ecosystem. *PLoS One* 9:e97763. doi: 10.1371/journal.pone.0097763

Biggs, D. C. (1992). Nutrients, plankton, and productivity in a warm-core ring in the western Gulf of Mexico. *J. Geophys. Res. Oceans* 97, 2143–2154.

Biggs, D. C., and Muller-Karger, F. E. (1994). Ship and satellite-observations of chlorophyll stocks in interacting cyclone-anticyclone eddy pairs in the western Gulf of Mexico. *J. Geophys. Res. Oceans* 99, 7371–7384.

Biggs, D. C., and Ressler, P. H. (2001). Distribution and abundance of phytoplankton, zooplankton, ichthyoplankton, and micronekton in the deepwater Gulf of Mexico. *Gulf Mex. Sci.* 19, 7–29.

Blanchet, F. G., Legendre, P., and Borcard, D. (2008). Forward selection of explanatory variables. *Ecology* 89, 2623–2632. doi: 10.1890/07-0986.1

Camilli, R., Reddy, C. M., Yoerger, D. R., Van Mooy, B. A. S., Jakuba, M. V., Kinsey, J. C., et al. (2010). Tracking hydrocarbon plume transport and biodegradation at Deepwater Horizon. *Science* 330, 201–204. doi: 10.1126/science.1195223

Chambers, J. M. (2013). *Functions and Examples for Software for Data Analysis*. *R Package Version 1.0-6*.

Dormann, C. F., Mcpherson, J. M., Araujo, M. B., Bivand, R., Bollinger, J., Carl, G., et al. (2007). Methods to account for spatial autocorrelation in the analysis of species distributional data: a review. *Ecography* 30, 609–628. doi: 10.1111/j.2007.0906-7590.05171.x

Dray, S. (2013). Packfor: Forward Selection with Permutation (Canoco p.46). R Package Version 0.0-8/r109. Available at: https://R-Forge.R-project.org/projects/sedar/ (accessed December 17, 2019).

Dray, S., Blanchet, G., Borcard, D., Guenard, G., Jombart, T., and Larocque, G. (2016). *Adespatial: Multivariate Multiscale Spatial Analysis*, *R Package Version 0.0-7*. Available at: https://CRAN.R-project.org/package=adespatial (accessed December 17, 2019).

Dray, S., Legendre, P., Borcard, D., and Blanchet, G. (2015). *PCNM Spatial Eigenfunctions*. Available at: http://r-forge.r-project.org/R/?group_id=195 (accessed June 9, 2016).

Dray, S., Legendre, P., and Peres-Neto, P. R. (2006). Spatial modelling: a comprehensive framework for principal coordinate analysis of neighbour matrices (PCNM). *Ecol. Modell.* 196, 483–493. doi: 10.1016/j.ecolmodel.2006.02.015

Drazen, J. C., De Forest, L. G., and Domokos, R. (2011). Micronekton abundance and biomass in Hawaiian waters as influenced by seamounts, eddies, and the moon. *Deep Sea Res. Part I Oceanogr. Res. Pap.* 58, 557–566. doi: 10.1016/j.dsr.2011.03.002

Ekau, W., Auel, H., Poertner, H. O., and Gilbert, D. (2010). Impacts of hypoxia on the structure and processes in pelagic communities (zooplankton, macro-invertebrates and fish). *Biogeosciences* 7, 1669–1699. doi: 10.5194/bg-7-1669-2010

Elliott, B. A. (1982). Anticyclonic rings in the Gulf of Mexico. *J. Phys. Oceanogr.* 12, 1292–1309. doi: 10.1175/1520-0485(1982)012<1292:aritgo>2.0.co;2

Elmgren, R., Hansson, S., Larsson, U., Sundelin, B., and Boehm, P. D. (1983). The Tsesis oil-spill – acute and long-term impact on the benthos. *Mar. Biol.* 73, 51–65. doi: 10.1007/bf00396285

Fricke, R., Eschmeyer, W. N., and Van der Laan, R. (eds) (2019). *Eschmeyer's Catalog of Fishes: Genera, Species, References. Electronic Version*. Available at: http://researcharchive.calacademy.org/research/ichthyology/catalog/fishcatmain.asp (accessed July 20, 2019).

Gaither, M. R., Bowen, B. W., Rocha, L. A., and Briggs, J. C. (2016). Fishes that rule the world: circumtropical distributions revisited. *Fish Fish.* 17, 664–679. doi: 10.1111/faf.12136

Gartner, J. V. Jr., Sulak, K. J., Ross, S. W., and Necaise, A. M. (2008). Persistent near-bottom aggregations of mesopelagic animals along the North Carolina and Virginia continental slopes. *Mar. Biol.* 153, 825–841. doi: 10.1007/s00227-007-0855-1

Gartner, J. V., Hopkins, T. L., Baird, R. C., and Milliken, D. M. (1987). The lanternfishes (pisces, myctophidae) of the eastern Gulf of Mexico. *Fis. Bull.* 85, 81–98.

Gjosaeter, J., and Kawaguchi, K. (1980). *A Review of the World Resources of Mesopelagic Fish Fao Fisheries Technical Paper No. 193*. Rome: Food and Agriculture Organization of the United Nations, 1–151.

Godo, O. R., Samuelsen, A., MacAulay, G. J., Patel, R., Hjollo, S. S., and Horne, J. (2012). Mesoscale eddies are oases for higher trophic marine life. *PLoS One* 7:e30161. doi: 10.1371/journal.pone.0030161

Hamilton, P., and Lugo-Fernandez, A. (2001). Observations of high speed deep currents in the northern Gulf of Mexico. *Geophys. Res. Lett.* 28, 2867–2870. doi: 10.1029/2001gl013039

Heino, J. (2013). The importance of metacommunity ecology for environmental assessment research in the freshwater realm. *Biol. Rev.* 88, 166–178. doi: 10.1111/j.1469-185X.2012.00244.x

Heino, J., Melo, A. S., Siqueira, T., Soininen, J., Valanko, S., and Mauricio Bino, L. (2015). Metacommunity organisation, spatial extent and dispersal in aquatic systems: patterns, processes and prospects. *Freshw. Biol.* 60, 845–869. doi: 10.1111/fwb.12533

Herring, H. J. (2010). *Gulf of Mexico Hydrographic Climatology and Method of Synthesizing Subsurface Profiles From the Satellite Sea Surface Height Anomaly*. Report No. 122. Silver Spring, MD: United States Department of Commerce National Oceanographic and Atmospheric Administration.

Irigoien, X., Klevjer, T. A., Rostad, A., Martinez, U., Boyra, G., and Acuna, J. L. (2014). Large mesopelagic fishes biomass and trophic efficiency in the open ocean. *Nat. Commun.* 5:3271. doi: 10.1038/ncomms4271

Jochens, A. E., and DiMarco, S. F. (2008). Physical oceanographic conditions in the deepwater Gulf of Mexico in summer 2000–2002. *Deep Sea Res. II* 55, 2541–2554. doi: 10.1016/j.dsr2.2008.07.003

Johnston, M. W., Milligan, R. J., Easson, C. G., Derada, S., English, D. C., and Penta, B. (2019). An Empirically-validated method for characterizing pelagic habitats in the Gulf of Mexico using ocean model data. *Limnol. Oceanogr. Methods* 17, 362–375.

Kaartvedt, S., Staby, A., and Aksnes, D. L. (2012). Efficient trawl avoidance by mesopelagic fishes causes large underestimation of their biomass. *Mar. Ecol. Prog. Ser.* 456, 1–6. doi: 10.3354/meps09785

Koslow, J. A., Davison, P., Lara-Lopez, A., and Ohman, M. D. (2014). Epipelagic and mesopelagic fishes in the southern California current system: ecological interactions and oceanographic influences on their abundance. *J. Mar. Syst.* 138, 20–28. doi: 10.1016/j.jmarsys.2013.09.007

Law, R. J., and Kelly, C. (2004). The impact of the "Sea Empress" oil spill. *Aquat. Living Resour.* 17, 389–394. doi: 10.1051/alr:2004029

Legendre, P., Borcard, D., and Peres-Neto, P. R. (2005). Analyzing beta diversity: partitioning the spatial variation of community composition data. *Ecol. Monogr.* 75, 435–450. doi: 10.1890/05-0549

Legendre, P., and de Caceres, M. (2013). Beta diversity as the variance of community data: dissimilarity coefficients and partitioning. *Ecol. Lett.* 16, 951–963. doi: 10.1111/ele.12141

Legendre, P., and Gallagher, E. D. (2001). Ecologically meaningful transformations for ordination of species data. *Oecologia* 129, 271–280. doi: 10.1007/s004420100716

Legendre, P., and Legendre, L. (2012). *Numerical Ecology*. Oxford: Elsevier.

Linkowski, T. B. (1996). Lunar rhythms of vertical migrations coded in otolith microstructure of North Atlantic lanternfishes, genus *Hygophum* (Myctophidae). *Mar. Biol.* 124, 495–508. doi: 10.1007/bf00351031

Morey, S. L., Schroeder, W. W., O'Brien, J. J., and Zavala-Hidalgo, J. (2003). The annual cycle of riverine influence in the eastern Gulf of Mexico basin. *Geophys. Res. Lett.* 30:1867.

Nasa Goddard Space Flight Center, Ocean Ecology Laboratory, Ocean Biology Processing Group (2018). *Moderate-Resolution Imaging Spectroradiometer (MODIS) Aqua Chlorophyll Data 2018 Reprocessing*. Greenbelt, MD: NASA (OB.DAAC). doi: 10.5067/AQUA/MODIS/L3M/CHL/2018

Oey, L. Y., Lee, H. C., and Schmitz, W. J. (2003). Effects of winds and Caribbean eddies on the frequency of loop current eddy shedding: a numerical model study. *J. Geophys. Res. Oceans* 108:3324.

Oksanen, J., Blanchet, G., Friendly, M., Kindt, R., Legendre, P., McGlinn, D., et al. (2017). *vegan: Community Ecology Package. R Package Version 2.4-2*. Available at: https://CRAN.R-project.org/package=vegan

Olivar, M. P., Gonzalez-Gordillo, J. I., Salat, J., Chust, G., Cozar, A., Hernandez-Leon, S., et al. (2016). The contribution of migratory mesopelagic fishes to neuston fish assemblages across the Atlantic. *Indian Pac. Oceans Mar. Freshw. Res.* 67, 1114–1127.

Olson, D. B. (1991). Rings in the ocean. *Ann. Rev. Earth Planet. Sci.* 19, 283–311.

Olson, D. B., Hitchcock, G. L., Mariano, A. J., Ashjian, C. J., Peng, G., Nero, R. W., et al. (1994). Life on the edge: marine life and fronts. *Oceanography* 7, 52–60. doi: 10.1016/j.marenvres.2018.09.010

Peres-Neto, P. R., Legendre, P., Dray, S., and Borcard, D. (2006). Variation partitioning of species data matrices: estimation and comparison of fractions. *Ecology* 87, 2614–2625. doi: 10.1890/0012-9658(2006)87%5B2614:vposdm%5D2.0.co;2

Potier, M., Bach, P., Menard, F., and Marsac, F. (2014). Influence of mesoscale features on micronekton and large pelagic fish communities in the Mozambique channel. *Deep Sea Res. Part II Top. Stud. Oceanogr.* 100, 184–199. doi: 10.1016/j.dsr2.2013.10.026

Pusineri, C., Chancollon, O., Ringelstein, J., and Ridoux, V. (2008). Feeding niche segregation among the Northeast Atlantic community of oceanic top predators. *Mar. Ecol. Prog. Ser.* 361, 21–34. doi: 10.3354/meps07318

R Core Team (2018). *R: A Language and Environment for Statistical Computing*. Vienna: R Foundation for Statistical Computing.

Rivas, D., Badan, A., and Ochoa, J. (2005). The ventilation of the deep Gulf of Mexico. *J. Phys. Oceanogr.* 35, 1763–1781. doi: 10.1175/jpo2786.1

Robinson, C., Steinberg, D. K., Anderson, T. R., Aristegui, J., Carlson, C. A., Frost, J. R., et al. (2010). Mesopelagic zone ecology and biogeochemistry – a synthesis. *Deep Sea Res. Part II Top. Stud. Oceanogr.* 57, 1504–1518. doi: 10.1016/j.dsr2.2010.02.018

Spalding, M. D., Fox, H. E., Allen, G. R., Davidson, N., Ferdaña, Z. A., Finlayson, M., et al. (2007). Marine ecoregions of the world: a bioregionalization of coastal and shelf areas. *Bioscience* 57, 573–583. doi: 10.1641/b570707

St. John, M. A., Borja, A., Chust, G., Heath, M., Grigorov, I., and Mariani, P. (2016). A dark hole in our understanding of marine ecosystems and their services: perspectives from the mesopelagic community. *Front. Mar. Sci.* 3:31. doi: 10.3389/fmars.2016.00031

Sutton, T. T. (2013). Vertical ecology of the pelagic ocean: classical patterns and new perspectives. *J. Fish Biol.* 83, 1508–1527. doi: 10.1111/jfb.12263

Sutton, T. T., Clark, M. R., Dunn, D. C., Halpin, P. N., Rogers, A. D., Guinotte, J., (2017). A global biogeographic classification of the mesopelagic zone. *Deep Sea Res. Part 1 Oceanogr. Res. Pap*. 126, 85–102. doi: 10.1016/j.dsr.2017.05.006

Sutton, T. T., and Hopkins, T. L. (1996). Trophic ecology of the stomiid (Pisces: Stomiidae) fish assemblage of the eastern Gulf of Mexico: strategies, selectivity and impact of a top mesopelagic predator group. *Mar. Biol.* 127, 179–192. doi: 10.1007/bf00942102

Tilman, D., Isbell, F., and Cowles, J. M. (2014). "Biodiversity and ecosystem functioning," in *Annual Review of Ecology, Evolution, and Systematics*, Vol 45, ed. D. J. Futuyma (Palo Alto, CA: Annual Review).

Villarino, E., Watson, J. R., Jonsson, B., Gasol, J. M., Salazar, G., and Acinas, S. G. (2018). Large-scale ocean connectivity and planktonic body size. *Nat. Commun.* 9:142. doi: 10.1038/s41467-017-02535-8

Vukovich, F. M. (2007). Climatology of ocean features in the Gulf of Mexico using satellite remote sensing data. *J. Phys. Oceanogr.* 37, 689–707. doi: 10.1175/jpo2989.1

Watanabe, H., Moku, M., Kawaguchi, K., Ishimaru, K., and Ohno, A. (1999). Diel vertical migration of myctophid fishes (Family Myctophidae) in the transitional waters of the western North Pacific. *Fish. Oceanogr.* 8, 115–127. doi: 10.1046/j.1365-2419.1999.00103.x

Webb, T. J., Vanden Berghe, E., and O'Dor, R. (2010). Biodiversity's big wet secret: the global distribution of marine biological records reveals chronic under-exploration of the deep pelagic ocean. *PLoS One* 5:e1022. doi: 10.1371/journal.pone.0010223

Wells, R. J. D., Rooker, J. R., Quigg, A., and Wissel, B. (2017). Influence of mesoscale oceanographic features on pelagic food webs in the Gulf of Mexico. *Mar. Biol.* 164:92.

Zimmerman, R. A., and Biggs, D. C. (1999). Patterns of distribution of sound-scattering zooplankton in warm- and cold-core eddies in the Gulf of Mexico, from a narrowband acoustic Doppler current profiler survey. *J. Geophys. Res. Oceans* 104, 5251–5262. doi: 10.1029/1998jc900072

Conflict of Interest: The authors declare that the research was conducted in the absence of any commercial or financial relationships that could be construed as a potential conflict of interest.

frontiers in Marine Science

ORIGINAL RESEARCH
published: 19 February 2020
doi: 10.3389/fmars.2020.00051

Oceanographic Structure and Light Levels Drive Patterns of Sound Scattering Layers in a Low-Latitude Oceanic System

Kevin M. Boswell[1], Marta D'Elia[1], Matthew W. Johnston[2], John A. Mohan[3], Joseph D. Warren[4], R. J. David Wells[3,5] and Tracey T. Sutton[2]*

[1] Department of Biological Sciences, Marine Science Program, Florida International University, North Miami, FL, United States, [2] Halmos College of Natural Sciences and Oceanography, Nova Southeastern University, Dania Beach, FL, United States, [3] Department of Marine Biology, Texas A&M University at Galveston, Galveston, TX, United States, [4] School of Marine and Atmospheric Sciences, Stony Brook University, Southampton, NY, United States, [5] Department of Wildlife and Fisheries Sciences, Texas A&M University, College Station, TX, United States

OPEN ACCESS

Edited by:
Cristina Gambi, Marche Polytechnic University, Italy

Reviewed by:
M. Pilar Olivar, Superior Council of Scientific Investigations (CSIC), Spain
Thor Aleksander Klevjer, Norwegian Institute of Marine Research (IMR), Norway

***Correspondence:**
Kevin M. Boswell
kevin.boswell@fiu.edu

Specialty section:
This article was submitted to Deep-Sea Environments and Ecology, a section of the journal Frontiers in Marine Science

Received: *28 August 2019*
Accepted: *27 January 2020*
Published: *19 February 2020*

Citation:
Boswell KM, D'Elia M, Johnston MW, Mohan JA, Warren JD, Wells RJD and Sutton TT (2020) Oceanographic Structure and Light Levels Drive Patterns of Sound Scattering Layers in a Low-Latitude Oceanic System. Front. Mar. Sci. 7:51. doi: 10.3389/fmars.2020.00051

Several factors have been reported to structure the spatial and temporal patterns of sound scattering layers, including temperature, oxygen, salinity, light, and physical oceanographic conditions. In this study, we examined the spatiotemporal variability of acoustically detected sound scattering layers in the northern Gulf of Mexico to investigate the drivers of this variability, including mesoscale oceanographic features [e.g., Loop Current-origin water (LCOW), frontal boundaries, and Gulf Common Water]. Results indicate correlations in the vertical position and acoustic backscatter intensity of sound scattering layers with oceanographic conditions and light intensity. LCOW regions displayed consistent decreases, by a factor of two and four, in acoustic backscatter intensity in the upper 200 m relative to frontal boundaries and Gulf Common Water, respectively. Sound scattering layers had greater backscatter intensity at night in comparison to daytime (25x for frontal boundaries, 17x for LCOW, and 12x for Gulf Common Water). The importance of biotic (primary productivity) and abiotic (sea surface temperature, salinity) factors varied across oceanographic conditions and depth intervals, suggesting that the patterns in distribution and behavior of mesopelagic assemblages in low-latitude, oligotrophic ecosystems can be highly dynamic.

Keywords: sound scattering layers, diel vertical migration, oceanographic features, eddy, Gulf of Mexico

INTRODUCTION

The oceanic biome is approximately 71% of the planet's area and much more of the planet's living space by volume, yet it remains vastly understudied (Childress, 1983; Webb et al., 2010). Perhaps the most conspicuous features of this biome are the persistent and ubiquitous sound scattering layers (Marshall, 1954; Barham, 1966; Gjosaeter and Kawaguchi, 1980; Irigoien et al., 2014; Cade and Benoit-Bird, 2015; Davison et al., 2015) formed by zooplankton and micronekton (Kloser et al., 2002; Irigoien et al., 2014; Béhagle et al., 2017). These organisms are responsible for the Earth's largest animal migration, a process known as diel vertical migration (DVM)

(Marshall, 1954; Pearre, 2003; Brierley, 2014; Aksnes et al., 2017; Behrenfeld et al., 2019). Recently, the fish component of the global mesopelagic micronekton community (crustaceans, cephalopods, and fishes, ∼2–10 cm in length) was estimated to exceed 5 billion tons (Irigoien et al., 2014; Klevjer et al., 2016; Aksnes et al., 2017).

The migrating layers serve as important trophic pathways linking meso- and bathypelagic habitats with the epipelagic through active vertical movement of animals. In general, micronekton actively swim toward the surface at dusk, seeking foraging opportunities (Merrett and Roe, 1974; Brodeur et al., 2005; Bianchi et al., 2013; Sutton, 2013; Sutton et al., 2020), and descend at dawn into the deep ocean. An important consequence of DVM is that it facilitates trophic interactions and biogeochemical exchange, vertically integrating the world's oceans (Sutton and Hopkins, 1996a; Hidaka et al., 2001; Davison et al., 2013, Davison et al., 2015; Schukat et al., 2013; Hudson et al., 2014; Trueman et al., 2014; Ariza et al., 2016; Sutton et al., 2020) through extensive, coordinated animal movement. In addition to significant contributions to the biological pump, mesopelagic communities also serve an important role in oceanic food webs by facilitating linkages among secondary producers (zooplankton) and higher-level consumers, including oceanic apex predators (Robertson and Chivers, 1997; Potier et al., 2007; Spear et al., 2007; Benoit-Bird et al., 2017). In spite of the fundamental ecological importance for open-ocean functioning, and increasing interest in commercial exploitation, the mesopelagic community remains one of the least-studied components of oceanic systems (Handegard et al., 2013; Irigoien et al., 2014; Davison et al., 2015).

The spatial and temporal variability observed in the sound scattering layers are known to fluctuate horizontally and vertically across abiotic and biotic gradients, primarily temperature (Kumar et al., 2005; Brierley, 2014; Béhagle et al., 2017; Proud et al., 2017), oxygen content (Devol, 1981; Bertrand et al., 2010; Brierley, 2014; Béhagle et al., 2017), salinity (Forward, 1976; Wang et al., 2014), and light intensity (Frank and Widder, 1997; Aksnes et al., 2009; Lebourges-Dhaussy et al., 2014; Last et al., 2016; Aksnes et al., 2017; Kaartvedt et al., 2017). The importance of these factors in structuring sound scattering layers can vary and is dependent on the location, community dynamics, and physical setup of the oceanic system. For example, the processes that structure high-latitude systems may vary in scale relative to mid-latitude or tropical systems (Godø et al., 2012; Peña et al., 2014; Røstad et al., 2016; Aksnes et al., 2017).

Mesoscale oceanographic features (e.g., eddies, frontal boundaries) have also been identified as important in mediating the dynamics of sound scattering layers (Owen, 1981; Sabarros et al., 2009; Godø et al., 2012; Scales et al., 2014; Ternon et al., 2014; Gaube et al., 2018). These features operate across multiple spatial scales (10–100s km) and produce areas of physical and biological heterogeneity and are thought to play an important role in mediating the transport and accumulation of biological material (i.e., larvae, eggs, plankton) as well as nutrients and heat (Sabarros et al., 2009; Chelton et al., 2011). Given that these features exist across a wide range of oceanic geographies, the ubiquitous vertically migrating sound scattering layers are also likely to be influenced by these mesoscale features (Fennell and Rose, 2015).

Within the Gulf of Mexico (GoM), the dominant mesoscale features are eddies and frontal boundaries associated with the Loop Current, interspersed among larger regions of Gulf Common Water (Johnston et al., 2019). The Loop Current is formed by warm, highly saline Caribbean water entering the GoM through the Yucatan Channel. The Loop Current's position within the GoM varies and is dependent upon its retracted or extended state. When retracted, the Loop Current flows directly east from the Yucatan Channel, bypassing the GoM proper, flanking the Florida Keys, eventually forming the Gulf Stream in the North Atlantic. When extended, the Loop Current protrudes into the far north and eastern GoM as far as 28° north latitude. The Loop Current drives environmental heterogeneity in the upper 1000 m in the pelagic GoM (Cardona and Bracco, 2016) through the shedding of energetic eddies, both cyclonic and anticyclonic. Loop Current eddies are large (10–100 kms in diameter) and persistent (average lifespan of 8–9 months; Hall and Leben, 2016) anticyclonic (downwelling) features. They are characterized by elevated mean sea surface height anomalies, clockwise rotation, elevated temperatures extending to c. 1000 m water depth (Biggs, 1992; Vukovich, 2007; Herring, 2010), and low surface chlorophyll *a* concentrations. Cyclonic eddies can be formed as well, although usually on the periphery of the large anticyclones, especially when large eddies are first sloughed off the Loop Current. Cyclones are typically much more ephemeral than anticyclones. Loop Current eddies typically form in the eastern GoM and ebb westward, eventually mixing with resident GoM water to form Gulf common water. Loop Current eddies and anticyclonic regions in the GoM can be distinguished from Gulf Common Water by the presence of the Subtropical Underwater water mass, which originates in the Caribbean (Rivas et al., 2005). The boundaries between these two water types are gradients, herein termed frontal boundaries ('mixed water' of Johnston et al., 2019), exhibit intermediate characteristics. These boundaries are known as important regions that concentrate or attract prey for pelagic organisms and may affect faunal distributions from surface waters to the benthos (Richards et al., 1993).

Previous examination of micronekton through acoustic-based surveys has indicated that mesoscale features may serve to structure mesopelagic organism distribution in oceanic systems (Drazen et al., 2011; Godø et al., 2012). The intent of this study was to examine the variability in acoustic backscatter associated with mesopelagic sound scattering layers among major oceanographic features in the GoM, a dynamic, oligotrophic, oceanic bioregion. The GoM represents an excellent model system for a study such as this, as high-resolution, taxon-specific vertical distribution data exist for the numerically dominant fishes (Hopkins and Lancraft, 1984; Gartner et al., 1987; Sutton and Hopkins, 1996a; Hopkins et al., 1996; Sutton et al., 2017; Milligan and Sutton, 2020), macrocrustaceans (Heffernan and Hopkins, 1981; Flock and Hopkins, 1992; Kinsey and Hopkins, 1994; Burdett et al., 2017; Frank et al., 2020), and cephalopods (Passarella and Hopkins, 1991; Judkins et al., 2016; Judkins and Vecchione, 2020). These data, developed during

multi-decadal research programs (see references in Hopkins et al., 1996; Sutton et al., 2020), make the GoM one of the best-known deep-pelagic ecosystems in the World Ocean with respect to micronekton/nekton faunal composition and vertical distribution.

In this study, we sought to directly integrate existing biotic data, vessel-based acoustic surveys, remotely sensed oceanographic data, and predictive hydrographic ocean modeling to characterize the dominant mesoscale patterns of sound scattering layer distribution and intensity. Specifically, we examined how mesopelagic sound scattering layers respond to gradients in oceanographic conditions, light intensity, primary productivity, and temperature and salinity in order to better understand the drivers of pelagic ecosystem in a highly speciose, low-latitude pelagic ecosystem.

MATERIALS AND METHODS

Study Area

Four acoustic surveys were conducted in the northern GoM aboard the R/V *Point Sur* (**Figure 1**) during the boreal late spring (DP01: 1–7 May 2015, Boswell, 2016; DP03: 1–15 May 2016, Boswell, 2017b) and summer (DP02: 9–23 August 2015, Boswell, 2017a; DP04: 6–21 August 2016, Boswell, 2017c). Sampling sites were an offshore extension of the standard Southeast Area Monitoring and Assessment Program (SEAMAP) plankton-sampling grid, which extends from the Texas shelf to the West Florida Shelf. Grid cells that comprise the survey design are 55.6 × 55.6 km, with sampling stations located at the mid-point of each grid cell. Cruise tracks were designed during the cruises to sample multiple oceanographic features. Paired multi-frequency acoustic and biological catch (10 m^2 MOCNESS net) data were collected at each site. The acoustic methodologies are described below. Net-sampling methodologies and subsequent data are described in detail in Kupchik et al. (2018), Milligan et al. (2019), Sutton et al. (2020), and Milligan and Sutton (2020).

Acoustic Data Collection and Processing

Acoustic data were collected during the day and nighttime periods (defined by local sunrise and sunset) when the transducer was deployed, allowing for continuous surveys (∼8 h) during each transect at each station. A multiple-frequency echosounder system (Simrad EK60/Simrad EK80) was used and operated transducers at 18, 38, 70, 120 kHz. The transducers were mounted in a faring and suspended 2.5 m below the water surface. Given the limitations of using a pole-mounted system, transects were conducted at an approximate vessel speed of 2 knots. Transducers were calibrated according to the standard sphere method (Demer et al., 2015). For this paper, we examined the acoustic backscatter from the sound scattering layers using only the 38 kHz frequency due to: the widespread use of this frequency to study pelagic biomass (Davison et al., 2013; D'Elia et al., 2016; Aksnes et al., 2017; Kaartvedt et al., 2017), the complicating factor of resonance effects from gas-bearing organisms at 18 kHz, and low signal-to-noise ratios in the higher frequencies (70, 120 kHz) (Godø et al., 2009; Fennell and Rose, 2015; Davison et al., 2015). The pulse duration for 38 kHz echosounder was 4 ms with a power setting of 2000 W, and ping repetition rate of 0.2 pings s^{-1}. Sound speed profiles and absorption coefficient were computed from bin-averaged CTD data using the Ocean Toolbox (McDougall and Barker, 2011) in Matlab.

Raw acoustic backscatter data were imported and manually scrutinized in Echoview (v8, Myriax). Data from the transducer face to 15 m depth were excluded from the analysis to account for beam formation and to eliminate surface-associated interference (e.g., bubble sweep down). Data beyond 1000 m were not included in the analysis due to range dependent losses in attenuation and signal strength. Compromised data due to interference from other shipboard sonar systems (intermittent or spike noise), false bottom, and background noise were excluded from the analysis. False bottoms were manually excluded. To remove occurrences of spike noise, each sample was compared to the preceding and successive sample. If the single ping-to-ping difference was greater than 10 dB the sample was considered a spike candidate and replaced with the mean S_V of four neighboring samples (D'Elia et al., 2016). Background noise was identified and removed following a modified process described by De Robertis and Higginbottom (2007). A minimum signal-to-noise ratio of 15 dB was applied to data collected at 38 kHz. Samples that did not satisfy this threshold were considered indistinguishable from the background noise and flagged as *'no data*.' The measurements of Nautical Area Scattering Coefficient (NASC; m^2 nmi^{-2}) were derived from the echo integral in 500-m along-track x 5-m vertical bins with a −80 dB re 1 m^2 integration threshold (MacLennan et al., 2002). NASC is considered to be proportional to the abundance of biological scatterers and serves as a comparable index of organism biomass (Hazen et al., 2009; Zwolinski et al., 2010; Fennell and Rose, 2015). Integrated backscatter was further binned into three depth intervals: 15–200 m (epipelagic), 200–600 m (upper mesopelagic) and 600–1000 m (lower mesopelagic). The center of mass (m) was derived for each of the three depth intervals using the approach of Urmy et al. (2012) to describe depth of the statistical center of the backscatter within each depth interval.

Oceanographic Feature Identification Methods

Oceanographic feature classes were identified following Johnston et al. (2019); these include Loop Current-origin water (LCOW), Gulf Common Water, and frontal boundaries. These feature classes were derived from the GoM HYbrid Coordinate Ocean Model (HYCOM + NCODA Gulf of Mexico 1/25° Analysis, GoM l0.04/expt_32.5) (Chassignet et al., 2007), which is a three-dimensional, eddy-resolving circulation model that assimilates satellite- and *in situ*-derived measures to depict ocean conditions (e.g., sea surface height, zonal velocity, meridional velocity, temperature, and salinity) in near real time, from surface waters to the benthos. In the GoM, HYCOM data are available at 1/25° (c. 4 km^2) horizontal resolution, in hourly intervals from 1993 to the present day[1] (Johnston et al., 2018, 2019). Velocity fronts were calculated as the difference between the minimum and maximum

[1] Publicly available at: http://hycom.org.

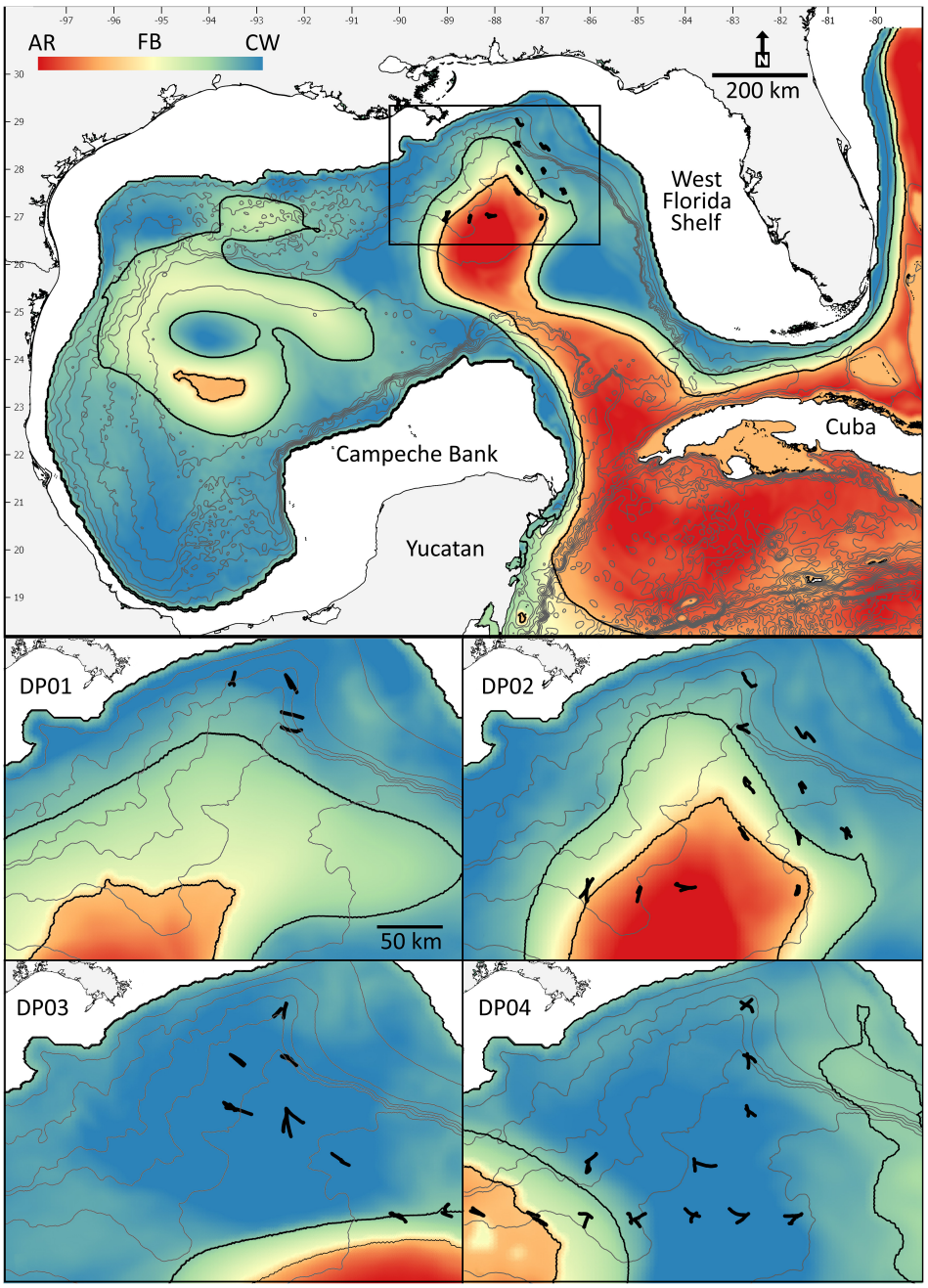

FIGURE 1 | Survey locations (filled symbols) overlaid on the feature classification map illustrating the gradients among the three primary features examined (Loop Current-origin water = red; frontal boundary = green; Gulf Common Water = blue). Lower panels represent survey tracks during each cruise (DP01–DP04). Contour lines represent 500 m depth intervals.

water speed within a 0.10 arc degree radius (~11 km) of each location, derived from the HYCOM and measured in m s^{-1}.

LCOW is generally characterized by increased SSHA, increased water temperatures (extending down to ca. 1000 m), and a reduction in surface water chlorophyll concentrations. Based on the values used in Johnston et al. (2019), we derived an index that normalized the response of the LCOW and represented a derived quantity that utilized location-specific HYCOM output, given the equation:

$$\text{LCOW index} = SSHA_i - (SSHA_{GOM} + 0.067) + T_i - 15.922 \quad (1)$$

where $SSHA_i$ represents the location-specific SSHA, $SSHA_{GOM}$ is the daily mean SSHA in the GoM and T_i represents

the location-specific temperature at 300 m. The output from Eq. 1 was scaled between 1.0 and 2.0, where 1.0 is the weakest condition and 2.0 represents the most intense condition measured for the entire GoM. The LCOW index. As such, the lower SSHA threshold for LCOW is $SSHA_{GOM} + 0.067$ m and the lower temperature threshold for the is 15.92°C, following Johnston et al. (2019).

Gulf Common Water is generally characterized by decreased SSHA and water column temperature and increased surface water chlorophyll concentrations when compared to LCOW. An index was computed for Gulf Common Water as the difference between the Johnston et al. (2019) temperature threshold at 300 m depth (13.46°C) and the location specific temperature at 300 m – i.e., the colder the water at 300 m, the greater the Gulf Common Water index value. The common water index was normalized to range from 0.0 to −1.0.

Frontal boundaries in the GoM are typically areas where significant mixing between LCOW and Common Water occur. To grade the strength of these boundaries, a frontal boundary index was calculated based on the difference between the $SSHA_i$ and the $SSHA_{GOM}$ and scaled to range from 0.0 to 1.0, with a value of 1.0 representing conditions nearest LCOW, and 0.0 being closest to Common Water (Johnston et al., 2019).

These oceanographic intensity indices were generated to span as a continuum following the classifications of Johnston et al. (2019) and then standardized and scaled to their respective ranges (i.e., LCOW: 1 to 2; frontal boundary: 0 to 1; Gulf Common Water: 0 to −1) based on the strength of the feature for the duration of the sampled period. Along-track positions for each acoustic survey were then used to extract and quantify the oceanographic conditions for each echo integration cell.

Hydrographic Properties of the Water Column

A calibrated SeaBird CTD (SBE 911+; SeaBird Electronics, Inc.) was used to characterize the water column properties. Data were collected during each night and day period as conditions allowed to characterize the diel structure of the water column. The raw instrument data were processed in the SeaBird processing software (v. 7.23), to compute 1-m bin-averaged estimates of salinity (PSU), temperature (°C), dissolved oxygen concentration (mg L^{-1}) and chl *a* (mg L^{-1}).

Approximating Surface Light Intensity and Primary Production

We examined the effect of relative light availability at 5 m depth by computing the instantaneous photosynthetically active radiation (IPAR; W m^{-2}) along each transect:

$$IPAR_{5m} = IPAR_{surf} * 2.72^{(-Kd(490)*z)} \quad (2)$$

where the surface light intensity $IPAR_{surf}$ was approximated by NOAA's Geostationary Satellite Server (GOES); *Kd(490)* represents NASA's Moderate Resolution Imaging Spectroradiometer (MODIS) derived diffuse attenuation coefficient at 490 nm, and *z* represents water depth (5 m). Observations at night have $IPAR_{surf}$ values of 0. Hourly estimates of solar elevation were derived from NOAA's Earth System Research Lab[2]. The maximum estimates of solar elevation were 71.4° at local-noon (DP02) and minimum was −65.5° (DP04) at local-midnight (**Figure 2**). Sixty-day net primary production was compiled from the MODIS observations and estimated from the Vertically Generalized Production Model (Behrenfeld and Falkowski, 1997) made available from the Oregon State Ocean Productivity standard products[3]. Integrated net primary production estimates were extracted for each cruise (**Supplementary Figure S1**).

Net Collection

Micronekton were sampled with a 10 m^2 Multiple Opening and Closing Net Sampling System (MOCNESS) conducted synchronously with acoustic data. Briefly, the MOCNESS was used to sample discrete depth intervals from 0 to 1500 m water depth at each station. The MOCNESS was configured with 9 identical nets with 333 μm mesh (see Wiebe et al., 1985 for full system description). Samples were sorted, identified to lowest taxonomic level possible, enumerated, and weighed (either individually or in groups depending on size) onboard the vessel. Organisms were preserved in formalin for long-term storage and later analyses.

Data Analysis

Patterns in acoustic backscatter at 38 kHz (NASC, m^2 nmi^{-2}) and the center of mass (m) of sound scattering layers were examined by time of day (day and night), and across the depth intervals (D'Elia et al., 2016). We investigated these patterns relative to the three oceanographic feature classes (LCOW, frontal boundary, and Common Water), using a linear mixed effects model, implemented in R (R Core Team, 2013) with the library "nlme." Since the variation in the residuals differed by day and night and across the three intervals of depth for both NASC and center of mass, a weighting option was added to the model using the varComb and varIdent structure to allow for different variances by time of day and depth domain. NASC values were $\log_{10}(x)$ transformed prior to analysis to meet the assumptions of normality. The responses in log-NASC and center of mass were examined relative to the interactions of time of day, depth interval and feature class. The cruise number was included as random effect to allow the magnitude of NASC and center of mass to vary by cruise. Tukey's *post hoc* comparisons were used to identify significant differences with respect to log mean NASC and mean center of mass.

Generalized additive mixed models (GAMMs) were used to analyze the relationships of NASC and center of mass with the environmental and oceanographic drivers for each of the three depth intervals. HYCOM-derived sea surface temperature (°C), HYCOM-derived surface salinity (PSU), CTD-derived maximum chlorophyll concentration, and an index representing the gradient of the oceanographic feature classes were included as main effects. We also examined the interactions of surface (5 m) light intensity and the feature class indices as differences in light

[2]https://www.esrl.noaa.gov/gmd/grad/solcalc/azel.html

[3]http://www.science.oregonstate.edu/ocean.productivity/

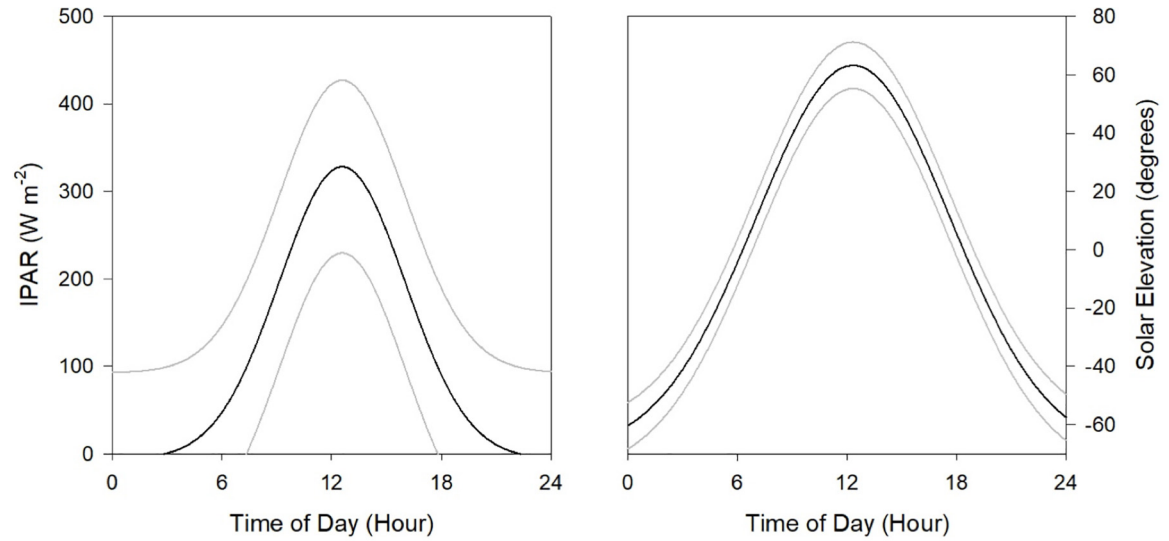

FIGURE 2 | Estimated mean (black line) and 95% confidence intervals (gray lines) of light intensity at 5 m depth ($IPAR_{5m}$, **left panel**) and solar elevation **(right panel)** across the four surveys conducted in the northern GoM during 2015 and 2016.

intensity at depth would be mediated by factors at the surface and likely reflect oceanographic differences.

Generalized additive mixed models were implemented with the "mgcv" library in R using a Gaussian distribution with an identity link function. Model selection was conducted using a null space penalization. To avoid overfitting, the spline fitting process of the main effect was restricted to 5 knots within the GAMM. We included the survey in the model as a random factor. In addition, the *varIdent* function was inserted as a weighting factor to allow for variance in fit between day and night. A Spearman's correlation matrix was calculated to determine collinearity among the environmental variables. Variables used in the model were selected by using a cut off value of 0.80. The autocorrelation of residuals was modeled using a first-order autoregressive error structure nested within each deployment.

RESULTS

Properties of Sound Scattering Layers

Acoustic backscatter intensity ($\log_{10}$ NASC) varied among the three feature classes, time of day, and across the three depth intervals. Within the epipelagic (15–200 m), acoustic backscatter intensity was significantly greater during the night among all feature types ($p < 0.001$), with values greater by a factor of 25-fold in frontal boundaries, 17-fold in LCOW, and 12-fold in Common Water, relative to daytime values (**Table 1**). During both nighttime and daytime, the lowest backscatter occurred within the LCOW (**Figure 3**). Daytime backscatter increased significantly ($p < 0.001$) from the LCOW to frontal boundaries, and from frontal boundaries to Common Water. However, at night backscatter was greatest within the frontal boundaries and slightly less, although not significantly, ($p = 0.258$), within Common Water. Similarly, within the upper mesopelagic (200–600 m), acoustic backscatter increased significantly ($p < 0.001$) from LCOW to frontal boundaries, and from frontal boundaries to Common Water during the day; however, LCOW and frontal boundary features displayed significantly greater backscatter ($p < 0.001$) at night than Common Water (**Figure 3**). In contrast to the other two depth intervals, lower mesopelagic zone (600–1000 m) LCOW waters had significantly ($p < 0.001$) greater backscatter than the same depth interval in either frontal boundary or Common Water, with nearly a 9-fold and 19-fold increase relative to the latter two features at night, respectively (**Figure 3**).

In all cases, during the day the center of mass occurred significantly deeper in frontal boundaries than in LCOW, and in Common Water than frontal boundaries ($p < 0.001$; **Figure 4**); however, at night the responses were more variable. At night the center of mass within the LCOW was consistently and significantly ($p < 0.001$) deeper than within frontal boundaries and Common Water. Within the epipelagic zone the centers of mass of frontal boundaries and Common Water were significantly shallower than within LCOW ($p < 0.001$). The centers of mass within the upper mesopelagic occurred deepened going from LCOW to frontal boundaries to Common Water, respectively ($p < 0.001$) (**Figure 4**). The location of the centers of mass within the lower mesopelagic zone was the most variable at night, with frontal boundaries having a significantly shallower center of mass (716.7 m; $p < 0.001$) than either Common Water (737.7 m) or LCOW (766.2 m) (**Figure 4**).

Effect of Environmental Drivers on Backscatter

Surface light intensity (IPAR; W m^{-2}) at 5 m water depth was not significantly different among the three oceanographic feature

TABLE 1 | Mean acoustic backscatter by time of day (TOD) and oceanographic feature class (LCOW, Loop Current-origin water; FB, Frontal boundary; CW, Common Water).

	Depth Interval	NASC (m^2 nmi^2)		MVBS (dB re $1m^{-1}$)	
TOD	**0–200 m**	**Mean**	***SD***	**Mean**	***SD***
Day	LCOW	4.85	3.35	−76.40	5.14
	FB	5.72	3.62	−75.70	4.35
	CW	8.62	3.14	−73.84	2.01
Night	LCOW	27.25	18.31	−68.92	4.99
	FB	33.57	17.38	−67.94	3.14
	CW	45.08	25.14	−66.72	3.57
	200–600 m	**Mean**	***SD***	**Mean**	***SD***
Day	LCOW	6.59	3.15	−74.86	2.52
	FB	6.05	1.46	−75.45	1.18
	CW	8.97	4.46	−73.75	2.91
Night	LCOW	6.66	3.54	−75.10	3.28
	FB	5.57	1.75	−75.88	1.64
	CW	4.64	2.89	−76.67	4.22
	600–1000 m	**Mean**	***SD***	**Mean**	***SD***
Day	LCOW	11.13	9.07	−72.87	7.35
	FB	6.70	5.18	−75.06	6.36
	CW	7.35	13.39	−74.66	0.91
Night	LCOW	13.60	11.98	−72.00	9.28
	FB	4.91	4.99	−76.41	19.18
	CW	6.20	7.47	−75.40	6.94

Acoustic data are represented as nautical area scattering coefficient (m^2 nmi^{-2}) and mean volume backscattering strength (dB re 1 m^{-1}).

classes (Kruskal–Wallis One Way ANOVA on Ranks, $p = 0.765$); although in general LCOW stations displayed greater surface light intensity, followed by frontal boundaries and Common Water (**Figure 5**). In all GAMMs light intensity and the LCOW index emerged as the most consistently significant variables (**Supplementary Table S1**) among all three depth intervals. Temperature, chlorophyll and the Common Water index were significant variables with respect to backscatter in certain cases (**Supplementary Tables S1**, **S2**). With the exception of only a few stations in cruises DP01 and DP02, transects were seaward of the coastal production plume associated with the Mississippi River, where net primary production exceeded 700 mg C m^{-2} d^{-1} (**Supplementary Figure S1**). Below we discuss the significant interactions between the oceanographic index scores and light intensity with backscatter across the three depth intervals.

Within the epipelagic, the acoustic backscatter was correlated with surface light intensity, sea surface temperature, chlorophyll concentration, and the LCOW index, as well as the interaction between light intensity and the LCOW index ($r^2 = 0.53$; **Supplementary Table S1**). The partial plots indicated an increasing trend in backscatter at light intensity values < 200 W m^{-2} (local night). As expected, backscatter decreased in the epipelagic as light levels increased beyond 200 W m^{-2}, ostensibly a function of DVM. In addition, backscatter decreased as surface temperature increased. Increased surface chlorophyll concentrations were associated with increased backscatter (**Supplementary Table S1**). As the intensity of the LCOW index increased in the epipelagic, we observed precipitous declines in backscatter, with a nearly 45% decline at night. In the epipelagic, only the LCOW index and light intensity interaction was significant ($p < 0.001$; **Figure 6**).

In the upper mesopelagic, light intensity was the most significant factor ($p < 0.001$) explaining variance in backscatter intensity, with lesser explanatory power attributed to the Common Water index ($p = 0.004$), the interaction of the Common Water index with light intensity (**Supplementary Table S1**). A decrease in backscatter was associated with increasing values of the Common Water index ($p = 0.004$) and with decreasing light intensity ($p < 0.001$) (**Supplementary Table S1**). During daytime and nighttime, a decrease in backscatter was observed with a greater LCOW index, whereas lower values of the Common Water index were associated with increased backscatter during the day (**Figure 4**). In general, the correlation of backscatter and light intensity within the upper mesopelagic was less variable than either epipelagic or lower mesopelagic depths.

Backscatter within the lower mesopelagic was significantly related to the velocity of the front, the LCOW index, and the interaction of light intensity in both LCOW and Common Water stations (**Supplementary Table S1**). The interaction of light intensity and the Common Water and LCOW indices were significant at depths greater than 600 m, with an increase in backscatter during the day at the lowest values of the Common Water index (**Figure 6**), and greater backscatter during the day and night periods for higher LCOW index (**Figure 6**).

Vertical Distribution of Backscatter

The GAM model for the center of mass indicated that within the epipelagic zone the vertical distribution of sound scattering layers were significantly related only to the maximum chlorophyll concentration ($p < 0.001$; $r^2 = 0.16$; **Supplementary Table S2**), suggesting a deepening of the center of mass as chlorophyll concentration increases.

The model for the upper mesopelagic was significant ($p < 0.001$; $r^2 = 0.33$) and selected six terms explaining variability in the center of mass: light intensity, temperature, salinity, maximum chlorophyll concentration, LCOW index and the interaction between the latter and the light intensity (**Supplementary Table S2**). The effect of light intensity on the center of mass indicated that biomass was deeper in the day and shallower at night, while an increase in sea surface temperature, salinity, and the LCOW index were associated with a deeper center of mass. In contrast, the center of mass was shallower with increases in the maximum chlorophyll concentration (**Supplementary Table S2**).

Within the lower mesopelagic, the center of mass was significantly related to the LCOW index ($p < 0.001$) in addition to the surface temperature ($p < 0.001$) and surface salinity ($p = 0.003$). A strong relationship was observed with the LCOW index, suggesting that as the LCOW index increases, the center of mass of layers gets deeper. The deepening of the center of mass occurred both during day and nighttime as indicated by the

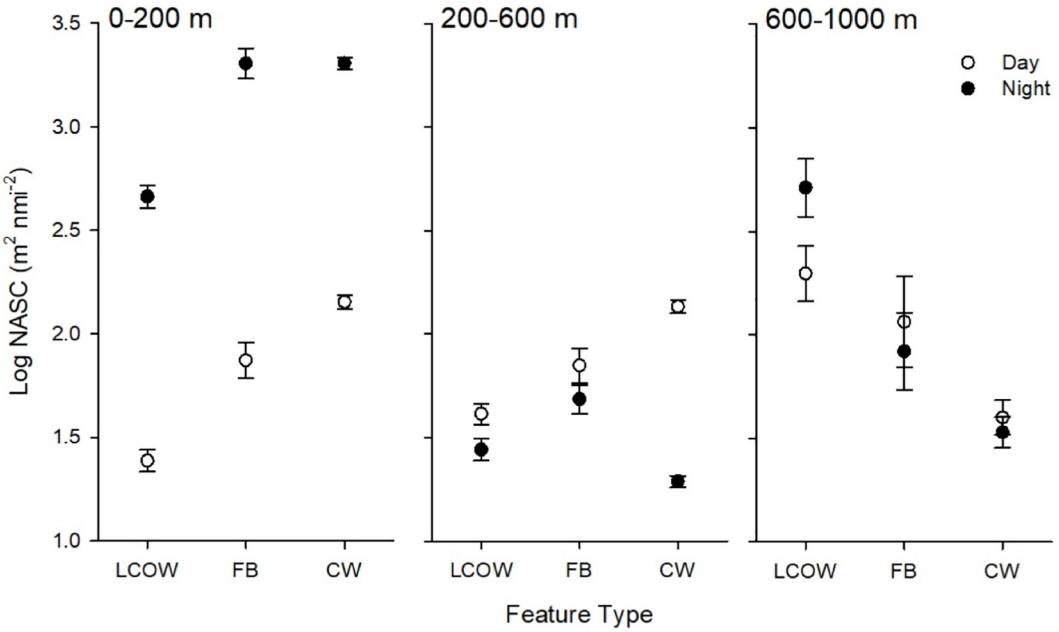

FIGURE 3 | Least-squared means of acoustic backscatter, $\log_{10}$ NASC (m^2 nmi^{-2}), by feature class, time of day (open symbols are day, filled are night) and depth interval. LCOW, Loop Current-origin water; FB, frontal boundary; and CW, Gulf Common Water. Error bars represent standard error from least-squared mean estimates.

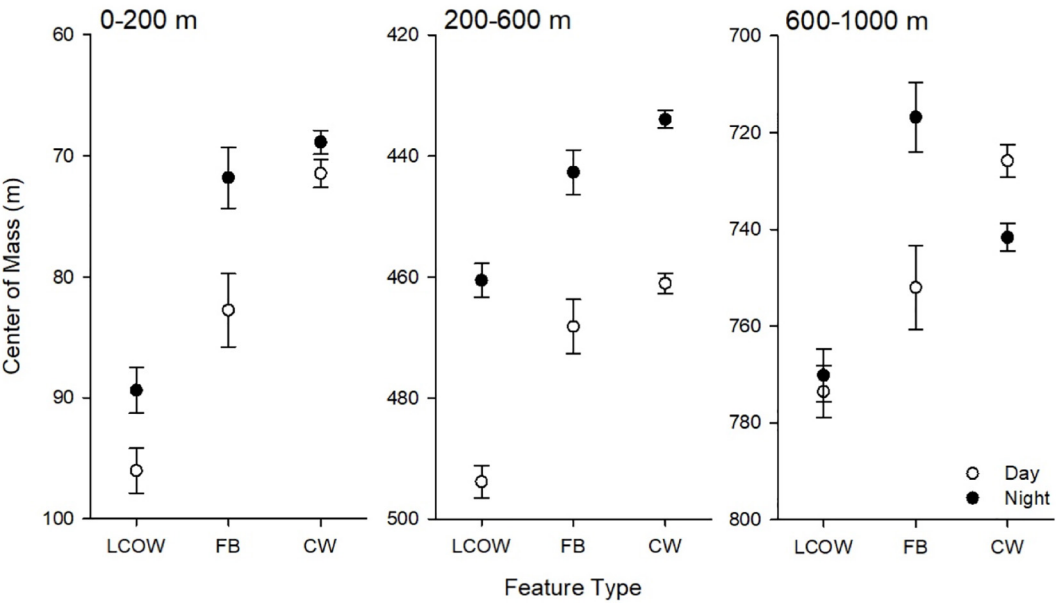

FIGURE 4 | Least-squared means of center of mass by feature class, time of day (open symbols are day, filled are night) and depth interval. LCOW, Loop Current-origin water; FB, frontal boundary; and CW, Gulf Common Water. Error bars represent standard error from least-squared mean estimates.

significant interaction between light intensity and LCOW index ($p = 0.02$) (**Supplementary Table S2**).

Biological Ground Truthing

Detailed information on the faunal composition, vertical distribution, and standing stocks of the epi- and mesopelagic fauna collected during DEEPEND surveys are reported elsewhere (Judkins et al., 2016; Burdett et al., 2017; Sutton et al., 2017; Frank et al., 2020; Judkins and Vecchione, 2020; Milligan and Sutton, 2020), but will be briefly summarized here. The two dominant taxonomic groups collected with the MOCNESS were fishes and macrocrustaceans (large euphausiids, decapod

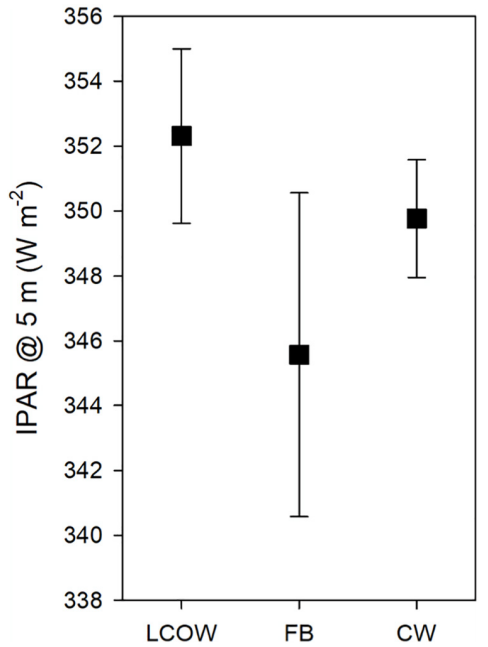

FIGURE 5 | Mean surface light intensity (IPAR) at 5 m water depth for each of the three oceanographic feature classes surveyed during DP01–DP04. LCOW, Loop Current-origin Water; FB, frontal boundary; and CW, Gulf Common Water. Error bars represent standard error of the mean.

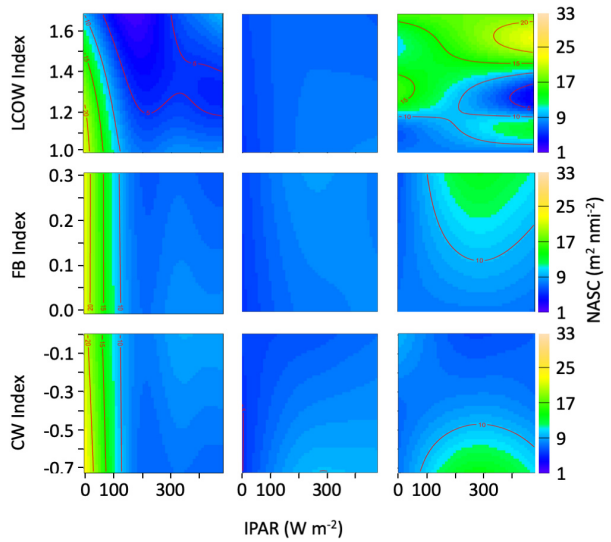

FIGURE 6 | Heatmap representing acoustic backscatter (NASC) as a function of the oceanographic index and light intensity ($IPAR_{5m}$). **(Left panels)** Represent the epipelagic (15–200 m), **(center panels)** represent upper-mesopelagic (200–600 m), and **(right panels)** represent lower mesopelagic (600–1000 m).

shrimps, mysids, lophogastrids). Macrocrustaceans were the most abundant group by number, contributing 26.5% of the total abundance of organisms collected, with euphausiids being numerically dominant (e.g., *Nematoscelis atlantica*, *Stylocheiron abbreviatum*, and *Thysanopoda obtusifrons)*. The fish assemblage was dominated by the Order Stomiiformes (75% of all fishes collected; Sutton et al., 2020), particularly species of the genus *Cyclothone* which contributed 18.7% by number of all organisms collected (fishes and invertebrates). The species *Cyclothone pallida* accounted for over half (56%) of this dominant genus. Myctophid species often dominated the numbers of upper mesopelagic layers and the epipelagic layer at night (Sutton et al., 2017, 2020; Milligan and Sutton, 2020). Other taxa commonly collected in net samples included: gelatinous zooplankton (e.g., siphonophores, medusae, and pyrosomes), shelled pteropods, cephalopods, and a wide variety of "other fishes" (Aulopiformes, Stephanoberyciformes, early life stages of coastal and benthic taxa; Sutton et al., 2017, 2020). In relation to water mass, LCOW and Common Water stations had the greatest number of individuals from net collections, with 40 and 44%, respectively. Each had similar species composition, dominated by the macrocrustaceans and fishes mentioned above.

DISCUSSION

Horizontally continuous sound scattering layers were ubiquitous in the northern GoM, throughout all periods and features surveyed in this study, occupying all three depth intervals examined. As expected, an increase in acoustic backscatter was observed during periods of low surface light intensity (<200 W m^{-2}) in the epipelagic, followed by a coincident decrease in upper mesopelagic backscatter at night due to the upwardly migrating mesopelagic assemblage. This pattern was observed consistently across all oceanographic feature classes.

Sound Scattering Layer Response to Oceanographic Features

In general, LCOW stations were characterized by the lowest backscatter intensity within the epipelagic, intermediate intensity in the upper mesopelagic, and greatest in the lower mesopelagic zone. An overall reduction in biomass within anticyclones has been reported across many systems, though the manifestations appear to be system-specific (Godø et al., 2012; Béhagle et al., 2014; Fennell and Rose, 2015; Gaube et al., 2018; but see Goldthwait and Steinberg, 2008). The reduction in lower trophic-level (e.g., zooplankton) biomass associated with anticyclonic features, which are similar in structure to LCOW (Johnston et al., 2019), has been observed previously in the northern GoM (Zimmerman and Biggs, 1999; Wormuth et al., 2000; Ressler and Jochens, 2003; Gasca, 2004) as well as in other low-latitude oceanic regions (Huggett, 2014; Lebourges-Dhaussy et al., 2014). In comparison, Godø et al. (2012) observed variation (~20 dB re 1 m^{-1}) in backscatter while transiting across oceanographic discontinuities in the Icelandic Basin, including an anticyclonic eddy. However, they noted patchiness in the biomass estimated across those features. In contrast, Fennell and Rose (2015) demonstrated increased backscatter in mesopelagic sound scattering layers in the mid-North Atlantic Ocean associated with mesoscale anticyclonic eddies and attributed the increased backscatter to transport mechanisms associated

with eddy fields. While many studies have noted that cold-core cyclonic eddies, characterized by centrally upwelled, nutrient-enriched water, promote increased primary and secondary productivity in the epipelagic (Biggs, 1992; Zimmerman and Biggs, 1999; Seki et al., 2001; Landry et al., 2008), during our survey periods we did not encounter any such biomass enhancement with respect to higher trophic levels due to the ephemeral nature and/or our undersampling of cyclonic features.

Given the pattern of reduced backscatter (and by proxy, micronekton biomass) in Loop Current and anticyclonic features, two ecological explanations can be proposed: (1) these features support less micronekton biomass as a quasi-self-contained habitat unit, or (2) these features influence avoidance behavior of vertical migrators. Of these explanations, we posit that the second is more likely. First, with respect to *in situ* production, the known generation times of micronekton are longer than the lifespans of shed Loop Current eddies (e.g., Gartner, 1991) and much longer than cyclonic eddies, which are smaller and more ephemeral than Loop Current eddies (Johnston et al., 2019). This differentiates results found for zooplankton and micronekton – the former can be "spun down" within the lifetime of an anticyclonic eddy due to lack of new production as food resources are exhausted. Second, with respect to spatial coherence of micronekton within a mesoscale feature, differential lateral advection from the surface to depth during vertical migration would be a diffusing agent (Milligan and Sutton, 2020). For micronekton to retain spatial coherence with a mesoscale feature, which is itself in motion, micronekton would have to "track" surface features during the daytime while at depth, although the extent of this effect would be dependent on how deep these features propagate at depth. The classical paradigm of daytime behavior of vertically migrating micronekton is that they are quiescent, conserving energy between feeding bouts, not actively tracking features geographically (Sutton, 2013).

Perhaps the reduction of vertical migration into the epipelagic and upper mesopelagic zones at night under LCOW results in a deep accumulation of biomass in the lower mesopelagic under anticyclonic-like conditions relative to the other two oceanographic features. This supposition would support the behavioral argument posited above. Given that the influence of anticyclonic features can be detected well into, and at times below, the 600–1000 m depth interval (Godø et al., 2012; Furey et al., 2018), it is not surprising to see a response in the sound scattering layers. In our case we detected not only an increase in biomass, but also deepening of the layers associated with LCOW.

The effects of frontal boundaries in surface waters can be highly variable with respect to spatial extent, intensity, and persistence (Belkin et al., 2009), and can therefore have variable effects on aggregating biological resources concentrated through entrainment (Owen, 1981) in addition to larger predators that exploit these hotspots (Bakun, 2006; Scales et al., 2014). The greatest acoustic backscatter was observed at night within frontal boundaries. While Loop Current eddies may be associated with reduced productivity, frontal margins of these features are known to be sites of increased faunal abundance/biomass, for example larval and juvenile fishes (Mohan et al., 2017), and may potentially offset the reduced faunal abundance/biomass observed in the adjacent LCOW.

At some sites, backscatter intensity was not conserved between day and night sampling periods. There are multiple explanations for why this may occur, including the advection of organisms into or out of the study region between sampling intervals or organisms' target strength varying as a function of depth (which is highly probable for resonant scatterers such as swim-bladders in fish). The fact that backscatter varied over diel periods at some sites and not as much at others presents a challenge in terms of interpreting acoustically measured biomass for migrating organisms, unless light cycle (or time of day) is controlled for in the analysis.

Variation in Depth Distribution

An increase in depth of the sound scattering layers as a function of anticyclonic physics is consistent with downwelling processes characteristic of these features (Carton et al., 2010; Chelton et al., 2011). The estimates of the depth of the center of mass suggest that in LCOW, the sound scattering layers are distributed at greater depths at night and that important biophysical interactions may influence the vertical distribution of the layers through either direct action (i.e., downwelling of migrators and/or their planktonic food) or through influences on individual behavior (migration choice) (Pearre, 2003). Moreover, the interaction between the LCOW index and backscatter suggests that an upper threshold in the oceanographic conditions (indicated by a high LCOW index) might mediate how organisms move into the epipelagic at night (as illustrated in **Figure 6**). This deepening of the sound scattering layers may indicate that organisms inhabiting these features may remain deeper to avoid the dynamic Loop Current waters, possibly because the current's hydrodynamics add an additional energetic burden that could contribute to a reduction in the vertical movement of the mesopelagic assemblage. Alternatively, the persistent sound scattering layer detected at depth during the day and night may be attributed in part to both asynchronous migration strategies and non-migrators that continuously remain at depth (Sutton and Hopkins, 1996a; Watanabe et al., 1999; Olivar et al., 2012; Sutton, 2013). The phenomenon of asynchronous migration has been observed across many oceanic systems (Clarke, 1974; Badcock and Merrett, 1976; Kenaley, 2008) including the GoM (Sutton and Hopkins, 1996a,b) where dragonfishes (Stomiidae), the dominant mesopelagic predatory fishes, split their time between the epipelagic and mesopelagic depth intervals at night (Sutton and Hopkins, 1996b). Summaries of MOCNESS data (Sutton et al., 2017; Milligan and Sutton, 2020) indicate that these migration strategies are commonplace among the dominant GoM fish species and that is likely to explain at least in part, the persistent sound scattering layers observed at depth.

Influence of Light Regimes

Light level consistently correlated with temporal patterns in the mesopelagic sound scattering layers. We observed predictable patterns in the way the mesopelagic assemblage responded, with consistent increases in backscatter at night in the epipelagic and mesopelagic. Other studies have demonstrated that light intensity is important for controlling the extent of vertical movement and timing (Frank and Widder, 1997; Aksnes et al., 2017; Kaartvedt et al., 2017). While we were unable to empirically

measure the light intensity at depth during this study, our results suggest that predicted light intensities from surface-derived estimates can be used as a predictor variable when direct measurements are unavailable. While others have quantitatively examined the animal response to subtle changes in light intensity (Frank and Widder, 1997; Aksnes et al., 2017; Kaartvedt et al., 2017), our estimates are appropriate to examine an integrated timescale that broadly represents the patterns observed with the DVM of the mesopelagic community. Additionally, while we were able to derive satellite-based estimates of light intensity across the three types of water masses examined, it remains unknown how variability in water transparency in LCOW, frontal boundaries and Common Water might differentially mediate light transmission to the mesopelagic region and in particular, whether the estimates we derived could result in significant differences among the three oceanographic feature classes we examined off the continental shelf.

Implications for Trophic Transfer

While we observed differences in backscatter distribution and intensity across the oceanographic conditions studied, the composition of organisms was not substantially different with net catches being dominated by crustacean macrozooplankton, namely euphausiids (e.g., *Nematoscelis atlantica*, *Stylocheiron abbreviatum*, and *Thysanopoda obtusifrons*), as well as fishes dominated by *Cyclothone* spp., dominant myctophid species (Sutton et al., 2020; Milligan and Sutton, 2020), other gonoistomatids, and hatchetfishes. An exception was noted for species composition of net hauls at frontal boundary stations, where euphausiids and pteropods were more abundant than fishes (Sutton et al., 2017). This suggests that the variation observed in backscatter is likely attributed in large part to the changes in organismal abundance and vertical distribution rather than a significant change in assemblage structure.

The differences in vertically migrating biomass among oceanographic feature types can have important implications for mediating the strength of trophic interactions and ultimately carbon transfer. Hopkins et al. (1996) estimated that 80% of all trophic exchange within the upper 1000 m of the water column in the eastern GoM (within our study area) occurs within the epipelagic zone at night. These authors determined that this consumption was driven by three dominant fish families (Myctophidae, Sternoptychidae and Gonostomatidae). Based on this study, the reduction in backscatter in LCOW suggests that the Loop Current and its associated eddies are likely areas of reduced trophic exchange, which has important implications for spatially explicit models of the GoM, and by proxy, other large marine ecosystems. Given that Loop Current eddies are persistent and dominant features within the GoM, occupying 100's of square kilometers and with lifespans exceeding a year, the systematic reduction in trophic transfer likely decreases carbon sequestration by the system as a whole (Volk and Hoffert, 1985; Irigoien et al., 2014; Davison et al., 2015). As reported by Volk and Hoffert (1985), nearly 70% of carbon transport in the upper 1000 m is mediated by the biological pump due to the vertically integrated food web, consequently transporting surface production into the deep ocean (Ducklow et al., 2001; Irigoien et al., 2014; Ariza et al., 2015; Davison et al., 2015).

CONCLUSION

We demonstrate that Loop Current-origin waters in the upper GoM are associated with decreased acoustic backscatter in comparison to the other oceanographic feature classes examined. These patterns were temporally consistent, suggesting that this oceanographic milieu dampens vertical migration by the mesopelagic assemblage. Perhaps equally important, we demonstrate that within the adjacent frontal boundaries along the margins of Loop Current eddies, increased backscatter was measured in both the epipelagic and mesopelagic at night, and we speculate that this enhancement may offset some portion of the reduced standing stocks observed within the nearby LCOW features.

Physical forcing is an important process that operates at various temporal and spatial scales and can act to structure the distribution of organisms and therefore their roles in ecosystems. In this study, we show that in addition to the previously reported relationship in sound scattering layer dynamics relative to light levels (Røstad et al., 2016; Aksnes et al., 2017), we observed a quantifiable correlation with mesoscale oceanographic features, and the nature of this latter correlation is depth-stratum-specific. Given the ubiquitous distribution, immense biomass, and critical role that migrating sound scattering layers play in the global biological pump, understanding how oceanographic processes mediate the distributional patterns of billions of tons of mesopelagic micronekton is necessary to refine global carbon models (*sensu* Proud et al., 2017). This is especially true of low-latitude, deep-pelagic ecosystems, which are by far the largest component of the World Ocean. With increases in ocean temperature, and associated ecosystem changes (e.g., expanding oxygen minimum zones; Aksnes et al., 2017), particularly in the marginal seas, approaches that leverage the benefits of large-scale observational techniques with fine-scale, process-based methods provide an efficient means to examine the physical dependencies on biological organization in oceanic systems.

DATA AVAILABILITY STATEMENT

Data are publicly available through the Gulf of Mexico Research Initiative Information and Data Cooperative (GRIIDC) at https://data.gulfresearchinitiative.org (HYCOM doi: 10.7266/N7QR4VK0; Classifications from Johnston et al. (2019) doi: 10.7266/N7QR4VK0; DP01 acoustic data: doi: 10.7289/V5WD3XJS; DP02 acoustic data: doi: 10.7289/V5RN35TF; DP03 acoustic data: doi: 10.7289/V5WD3XSX; and DP04 acoustic data: doi: 10.7289/V5RN3620).

AUTHOR CONTRIBUTIONS

KB and JW collected the data. KB, MD'E, JM, and JW performed the analysis. All authors contributed to data interpretation and manuscript writing.

FUNDING

This research was made possible by a grant from The Gulf of Mexico Research Initiative.

ACKNOWLEDGMENTS

We thank the captain and crew of the R/V *Point Sur* for their incredible support during the DEEPEND research program and at-sea operations. We appreciate the efforts of the National Centers for Environmental Information (www.ncei.noaa.gov) for assistance with archiving the acoustic data from all the DEEPEND cruises. We thank B. Penta and S. deRada at the Naval Research Lab for access to the high-resolution GoM HyCOM model output as well as C. Hu and the Optical Oceanography Laboratory at the University of South Florida for light intensity data included in the analysis. We thank S. Labua and D. Correa for assistance with data organization and processing and appreciate the comments of the two reviewers that improved this manuscript. This is contribution #176 from the Division of Coastlines and Oceans in the Institute of Environment at Florida International University.

SUPPLEMENTARY MATERIAL

The Supplementary Material for this article can be found online at: https://www.frontiersin.org/articles/10.3389/fmars.2020.00051/full#supplementary-material

REFERENCES

Aksnes, D., Dupont, N., Staby, A., Fiksen, O., Kaartvedt, S., and Aure, J. (2009). Coastal water darkening and implications for mesopelagic regime shifts in Norwegian fjord. *Mar. Ecol Press Ser.* 387, 39–49. doi: 10.3354/meps08120

Aksnes, D., Røstad, A., Kaartvedt, S., Martinez, U., Duarte, C., and Irigoien, X. (2017). Light penetration structures the deep acoustic scattering layers in the global ocean. *Sci. Adv.* 3:e160246. doi: 10.1126/sciadv.1602468

Ariza, A., Garijo, C., Landeira, J. M., Bordes, F., and Hernández-León, S. (2015). Migrant biomass and respiratory carbon flux by zooplankton and micronekton in the subtropical northeast Atlantic Ocean (Canary Islands). *Progr. Oceanogr.* 134, 330–342. doi: 10.1016/j.pocean.2015.03.003

Ariza, A., Landeira, J. M., Escánez, A., Wienerroither, R., Aguilar de Soto, N., Røstad, A., et al. (2016). Vertical distribution, composition and migratory patterns of acoustic scattering layers in the Canary Islands. *J. Mar. Syst.* 157, 82–91. doi: 10.1016/j.jmarsys.2016.01.004

Badcock, J., and Merrett, N. R. (1976). Midwater fishes in the eastern North Atlantic–I. Vertical distribution and associated biology in 30 N, 23 W, with developmental notes on certain myctophids. *Progr. Oceanogr.* 7, 3–58. doi: 10.11646/zootaxa.3895.3.1

Bakun, A. (2006). Fronts and eddies as key structures in the habitat of marine fish larvae: opportunity, adaptive response and competitive advantage. *Sci. Mar.* 70, 105–122. doi: 10.3989/scimar.2006.70s2105

Barham, E. G. (1966). Deep scattering layer migration and composition: observations from a diving saucer. *Science* 151, 1399–1403. doi: 10.1126/science.151.3716.1399

Béhagle, N., Cotté, C., Lebourges-Dhaussy, A., Roudaut, G., Duhamel, G., Brehmer, P., et al. (2017). Acoustic distribution of discriminated micronektonic organisms from a bi-frequency processing: the case study of eastern Kerguelen oceanic waters. *Progr. Oceanogr.* 156, 276–289. doi: 10.1016/j.pocean.2017.06.004

Béhagle, N., du Buisson, L., Josse, E., Lebourges-Dhaussy, A., Roudaut, G., and Ménard, F. (2014). Mesoscale features and micronekton in the Mozambique channel: an acoustic approach. *Deep Sea Res. Part IITop. Stud. Oceanogr.* 100, 164–173. doi: 10.1016/j.dsr2.2013.10.024

Behrenfeld, M. J., and Falkowski, P. G. (1997). Photosynthetic rates derived from satellite-based chlorophyll concentration. *Limnol. Oceanogr.* 42, 1–20. doi: 10.4319/lo.1997.42.1.0001

Behrenfeld, M. J., Gaube, P., Della Penna, A., O'Malley, R. T., Burt, W. J., Hu, Y., et al. (2019). Global satellite-observed daily vertical migrations of ocean animals. *Nature* 576, 257–261. doi: 10.1038/s41586-019-1796-9

Belkin, I. M., Cornillon, P. C., and Sherman, K. (2009). Fronts in large marine ecosystems. *Progr. Oceanogr.* 81, 223–236. doi: 10.1016/j.pocean.2009.04.015

Benoit-Bird, K. J., Moline, M., and Southall, B. (2017). Prey in oceanic sound scattering layers organize to get a little help from their friends. *Limnol. Oceanogr.* 62, 2788–2798. doi: 10.1002/lno.10606

Bertrand, A., Ballón, M., and Chaigneau, A. (2010). Acoustic observation of living organisms reveals the upper limit of the oxygen minimum zone. *PLoS One* 5:e10330. doi: 10.1371/journal.pone.0010330

Bianchi, D., Stock, C., Galbraith, E. D., and Sarmiento, J. L. (2013). Diel vertical migration: ecological controls and impacts on the biological pump in a one-dimensional ocean model. *Glob. Biogeochem. Cycles* 27, 478–491. doi: 10.1002/gbc.20031

Biggs, D. C. (1992). Nutrients, plankton, and productivity in a warm-core ring in the western Gulf of Mexico. *J. Geophys. Res. Oceans* 97, 2143–2154.

Boswell, K. (2016). Raw Acoustic Scattering Data Of Organisms from The Water Column, R/V Point Sur, cruise DP01- May 1-8, 2015. Distributed by: Gulf of Mexico Research Initiative Information and Data Cooperative (GRIIDC). Corpus Christi, TX: Harte Research Institute.

Boswell, K. (2017a). *Raw Acoustic Scattering Data Of Organisms From The Water Column, R/V Point Sur, cruise DP02- August 8-21, 2015. Distributed by: Gulf of Mexico Research Initiative Information and Data Cooperative (GRIIDC)*. Corpus Christi, TX: Harte Research Institute.

Boswell, K. (2017b). *Raw Acoustic Scattering Data Of Organisms From The Water Column, R/V Point Sur, Cruise DP03- April-May, 2016. Distributed by: Gulf of Mexico Research Initiative Information and Data Cooperative (GRIIDC)*. Corpus Christi, TX: Harte Research Institute.

Boswell, K. (2017c). *Raw Acoustic Scattering Data Of Organisms From The Water Column, R/V Point SUR, CRUise DP04-August 2016. Distributed by: Gulf of Mexico Research Initiative Information and Data Cooperative (GRIIDC)*. Corpus Christi, TX: Harte Research Institute.

Brierley, A. (2014). Diel Vertical Migration. *Curr. Biol.* 24, 1074–1076.

Brodeur, R. D., Seki, M. P., Pakhomov, E. A., and Suntsov, A. V. (2005). Micronekton - what are they and why are they important? North pacific marine science organization. *Pices Press* 13, 7–11.

Burdett, E. A., Fine, C. D., Sutton, T. T., Cook, A. B., and Frank, T. M. (2017). Geographic and depth distributions, ontogeny, and reproductive seasonality of decapod shrimps (Caridea: Oplophoridae) from the northeastern Gulf of Mexico. *Bull. Mar. Sci.* 93, 743–767. doi: 10.5343/bms.2016.1083

Cade, D. E., and Benoit-Bird, K. J. (2015). Depths, migration rates and environmental associations of acoustic scattering layers in the Gulf of California. *Deep Sea Res. I* 102, 78–89. doi: 10.1016/j.dsr.2015.05.001

Cardona, Y., and Bracco, A. (2016). Predictability of mesoscale circulation throughout the water column in the Gulf of Mexico. *Deep Sea Res. II Top. Stud. Oceanogr.* 129, 332–349. doi: 10.1016/j.dsr2.2014.01.008

Carton, X., Daniault, N., Alves, J., Cherubin, L., and Ambar, I. (2010). Meddy dynamics and interaction with neighboring eddies southwest of Portugal: observations and modeling. *J. Geophys. Res.* 115:C06017. doi: 10.1029/2009JC005646

Chassignet, E. P., Hurlburt, H. E., Smedstad, O. M., Halliwell, G. R., Hogan, P. J., Wallcraft, A. J., et al. (2007). The HYCOM (hybrid coordinate ocean model) data assimilative system. *J. Mar. Syst.* 65, 60–83.

Chelton, D. B., Schlax, M. G., and Samelson, R. M. (2011). Global observations of nonlinear mesoscale eddies. *Prog. Oceanogr.* 91, 167–216. doi: 10.1016/j.pocean.2011.01.002

Childress, J. J. (1983). Oceanic biology: lost in space. *Oceanogr. Present Future* 127–135. doi: 10.1007/978-1-4612-5440-9_9

Clarke, T. A. (1974). Some aspects of the ecology of stomiatoid fishes in the Pacific Ocean near Hawaii. *Fish. Bull.* 72, 337–351.

Davison, P. C., Anthony Koslow, J. A., and Kloser, R. J. (2015). Acoustic biomass estimation of mesopelagic fish: backscattering from individuals, populations, and communities. *ICES J. Mar. Sci.* 72, 1413–1424. doi: 10.1093/icesjms/fsv023

Davison, P. C., Checkley, D. M. Jr., Koslow, J. A., and Barlow, J. (2013). Carbon export mediated by mesopelagic fishes in the northeast Pacific Ocean. *Prog. Oceanogr.* 116, 14–30. doi: 10.1016/j.pocean.2013.05.013

De Robertis, A., and Higginbottom, I. (2007). A post-processing technique to estimate the signal-to-noise ratio and remove echosounder background noise. *ICES J. Mar. Sci.* 64, 1282–1291. doi: 10.1093/icesjms/fsm112

D'Elia, M., Warren, J. D., Rodriquez-Pinto, I., Sutton, T. T., Cook, A., and Boswell, K. M. (2016). Diel Variation in the vertical distribution of deep-water scattering layers in the Gulf of Mexico. *Deep Sea Res. I Oceanogr. Res. Pap.* 115, 91–102. doi: 10.1016/j.dsr.2016.05.014

Demer, D. A., Berger, L., Bernasconi, M., Bethke, E., Boswell, K. M., Chu, D., et al. (2015). *Calibration of Acoustic Instruments*. ICES Cooperative Research Report No. 326. Copenhagen: ICES, 133.

Devol, A. H. (1981). Verticaldistributionofzooplanktonrespirationinrelationtothe intense oxygen minimum zones in two British Columbia fjords. *J. Plankton Res.* 3, 593–602. doi: 10.1093/plankt/3.4.593

Drazen, D. C., de Forest, L. G., and Domokos, R. (2011). Micronekton abundance and biomass in Hawaiian waters as influenced by seamounts, eddies and the moon. *Deep Sea Res. I Oceanogr. Rese. Pap.* 58, 557–566. doi: 10.1016/j.dsr.2011.03.002

Ducklow, H. W., Steinberg, D. K., and Buesseler, K. O. (2001). Upper ocean carbon export and the biological pump. *Oceanogr. Soc.* 14, 50–58. doi: 10.5670/oceanog.2001.06

Fennell, S., and Rose, G. (2015). Oceanographic influences on deep scattering layers across the North Atlantic. *Deep Sea Res. I Oceanogr. Res. Pap.* 105, 132–141. doi: 10.1016/j.dsr.2015.09.002

Flock, M. E., and Hopkins, T. L. (1992). Species composition, vertical distribution, and food habits of the sergestid shrimp assemblage in the eastern Gulf of Mexico. *J. Crustacean Biol.* 12, 210–223. doi: 10.2307/1549076

Forward, R. B. Jr. (1976). "Light and diurnal vertical migration: photobehavior and photophysiology of plankton," in *Photochemical and Photobiological Reviews*, ed. K. C. Smith (NewYork,NY: PlenumPress), 157–210.

Frank, T., and Widder, E. (1997). The correlation of downwelling irradiance and staggered vertical migration patterns of zooplankton in Wilkinson Basin, Gulf of Maine. *J. Plankton Res.* 19, 1975–1991. doi: 10.1093/plankt/19.12.1975

Frank, T., Fine, C. D., Burdett, E. A., Cook, A. B., and Sutton, T. T. (2020). The vertical and horizontal distribution of deep-sea crustaceans in the Order Euphausiacea in the vicinity of the Deepwater Horizon oil spill. *Front. Mar. Sci.* doi: 10.3389/fmars.2020.00099

Furey, H., Bower, A., Perez-Brunius, P., Hamilton, P., and Leben, R. (2018). Deep eddies in the Gulf of Mexico observed with floats. *J. Phys. Oceanogr.* 48, 2703–2719. doi: 10.1175/jpo-d-17-0245.1

Gartner, J. V. Jr., Hopkins, T. L., Baird, R. C., and Milliken, D. M. (1987). The lanternfishes (Pisces: Myctophidae) of the eastern Gulf of Mexico. *Fish. Bull. U. S.* 85, 81–98.

Gartner, J. V. (1991). Life histories of three species of lanternfishes (Pisces: Myctophidae) from the eastern Gulf of Mexico. *Mar. Biol.* 111, 11–20. doi: 10.1007/bf01986339

Gasca, R. (2004). Distribution and abundance of hyperiid amphipods in relation to summer mesoscale features in the southern Gulf of Mexico. *J. Plankton Res.* 26, 993–1003. doi: 10.1093/plankt/fbh091

Gaube, P., Braun, C. D., Lawson, G. L., McGillicuddy, D. J., Della Penna, A., Skomal, G. B., et al. (2018). Mesoscale eddies influence the movements of mature female white sharks in the Gulf Stream and Sargasso Sea. *Sci. Rep.* 8:7363. doi: 10.1038/s41598-018-25565-8

Gjosaeter, J., and Kawaguchi, K. (1980). *A Review of the World Resources Of Mesopelagic Fish*. Rome: FAO.

Godø, O. R., Patel, R., and Pedersen, G. (2009). Diel migration and swimbladder resonance of small fish: some implications for analyses of multifrequency echo data. *ICES J. Mar. Sci.* 66, 143–148.

Godø, O. R., Samuelsen, A., Macaulay, G., Patel, R., Hjøllo, S. S., Horne, J., et al. (2012). Mesoscale eddies are oases for higher trophic marine life. *PLoS One* 7:e30161. doi: 10.1371/journal.pone.0030161

Goldthwait, S. A., and Steinberg, D. K. (2008). Elevated biomass of mesozooplankton and enhanced fecal pellet flux in cyclonic and mode-water eddies in the Sargasso Sea. *Deep Sea Res. II Top. Stud. Oceanogr.* 55, 1360–1377. doi: 10.1016/j.dsr2.2008.01.003

Hall, C. A., and Leben, R. R. (2016). Observational evidence of seasonality in the timing of loop current eddy separation. *Dyn. Atmos. Oceans* 76, 240–267. doi: 10.1016/j.dynatmoce.2016.06.002

Handegard, N. O., du Buisson, L., Brehmer, P., Chalmers, S. J., De Robertis, A., Huse, G., et al. (2013). Towards an acoustic-based coupled observation and modelling system for monitoring and predicting ecosystem dynamics of the open ocean. *Fish Fish.* 14, 605–615. doi: 10.1111/j.1467-2979.2012.00480.x

Hazen, E. L., Craig, J. K., Good, C. P., and Crowder, L. B. (2009). Vertical distribution of fish biomass in hypoxic waters on the Gulf of Mexico shelf. *Mar. Ecol. Press Ser.* 375, 195–207. doi: 10.3354/meps07791

Heffernan, J. J., and Hopkins, L. T. (1981). Vertical distribution and feeding of the shrimp genera *Gennadas* and *Bentheogennema* (Decapoda: Penaeidea) in the eastern Gulf of Mexico. *J. Crustacean Biol.* 1, 461–473.

Herring, H. J. (2010). *Gulf of Mexico Hydrographic Climatology and Method of Synthesizing Subsurface Profiles from the Satellite Sea Surface Height Anomaly*. ICES Document Report 122. Silver Spring, MD: National Oceanographic and Atmospheric Administration, 63.

Hidaka, K., Kawaguchi, K., Murakami, M., and Takahashi, M. (2001). Downward transport of organic carbon by diel migratory micronekton in the western equatorial Pacific: it's quantitative and qualitative importance. *Deep Sea Res. I Oceanogr. Res. Pap.* 48, 1923–1939. doi: 10.1016/s0967-0637(01)00003-6

Hopkins, T., Sutton, T. T., and Lancraft, T. M. (1996). The trophic structure and predation impact of a low latitude midwater fish assemblage. *Prog. Oceanogr.* 38, 205–239. doi: 10.1016/s0079-6611(97)00003-7

Hopkins, T. L., and Lancraft, T. M. (1984). The composition and standing stock of mesopelagic micronekton at 27 N 86 W in the eastern Gulf of Mexico. *Mar. Sci.* 27, 143–158.

Hudson, J. M., Steinberg, D. K., Sutton, T. T., Graves, J. E., and Latour, R. J. (2014). Myctophid feeding ecology and carbon transport along the northern Mid-Atlantic Ridge. *Deep Sea Res. I Oceanogr. Res. Pap.* 93, 104–116. doi: 10.1016/j.dsr.2014.07.002

Huggett, J. (2014). Mesoscale distribution and community composition of zooplankton in the Mozambique Channel. *Deep Sea Res. II Top. Stud. Oceanogr.* 100, 119–135. doi: 10.1016/j.dsr2.2013.10.021

Irigoien, X., Klevjer, T. A., Røstad, A., Martinez, U., Boyra, G., Acuña, J. L., et al. (2014). Large mesopelagic fishes biomass and trophic efficiency in the open ocean. *Nat. Commun.* 5:3271. doi: 10.1038/ncomms4271

Johnston, M. W., Milligan, R. J., Easson, C. G., de Rada, S., English, D., Penta, B., et al. (2019). An empirically-validated method for characterizing pelagic habitats in the Gulf of Mexico using ocean model data. *Limnol. Oceanogr. Methods* 17, 363–375.

Johnston, M. W., Milligan, R. J., Easson, C. G., deRada, S., English, D., Penta, B., et al. (2018). *Habitat classification of the Gulf of Mexico (GOM) using the HYbrid Coordinate Ocean Model (HYCOM) and salinity/temperature profiles, cruises DP01-DP04, May 2015 to August 2016. Distributed by: Gulf of Mexico Research Initiative Information and Data Cooperative (GRIIDC)*. Corpus Christi, TX: Harte Research Institute.

Judkins, H. L., Vecchione, M., and Rosario, K. (2016). Morphological and molecular evidence of *Heteroteuthis dagamensis* in the Gulf of Mexico. *Bull. Mar. Sci.* 92, 51–57. doi: 10.5343/bms.2015.1061

Judkins, H., and Vecchione, M. (2020). Vertical distribution patterns of cephalopods in the northern Gulf of Mexico. *Front. Mar. Sci.* doi: 10.3389/fmars.2020.00047

Kaartvedt, S., Røstad, A., and Aksnes, D. (2017). Changing weather causes behavioral responses in the lower mesopelagic. *Mar. Ecol. Press Ser.* 574, 259–263. doi: 10.3354/meps12185

Kenaley, C. P. (2008). Diel vertical migration of the loosejaw dragonfishes (Stomiiformes: Stomiidae: Malacosteinae): a new analysis for rare pelagic taxa. *J. Fish Biol.* 73, 888–901. doi: 10.1111/j.1095-8649.2008.01983.x

Kinsey, S. T., and Hopkins, T. L. (1994). Trophic strategies of euphausiids in a low-latitude ecosystem. *Mar. Biol.* 118, 651–661. doi: 10.1007/bf00347513

Klevjer, T. A., Irigoien, X., Røstad, A., Fraile-Nuez, E., Benítez-Barrios, V. M., and Kaartvedt, S. (2016). Large scale patterns in vertical distribution and behaviour of mesopelagic scattering layers. *Sci. Rep.* 6, 1–11. doi: 10.1038/srep19873

Kloser, R. K., Ryan, T., Sakov, P., Williams, A., and Koslow, J. A. (2002). Species identification in deep water using multiple acoustic frequencies. *Can. J. Fish. Aquat. Sci.* 59, 1065–1077. doi: 10.1139/f02-076

Kumar, P. V. H., Kumar, T. P., Sunil, T., and Gopakumar, M. (2005). Observations on the relationship between scattering layer and mixed layer. *Curr. Sci.* 88:1799.

Kupchik, M. J., Benfield, M. C., and Sutton, T. T. (2018). The first in situ encounter of *Gigantura chuni* (Giganturidae: Giganturoidei: Aulopiformes: Cyclosquamata: Teleostei), with a preliminary investigation of pair-bonding. *Copeia* 106, 641–645. doi: 10.1643/ce-18-034

Landry, M. R., Decima, M., Simmons, M. P., Hannides, C. C., and Daniels, E. (2008). Mesozooplankton biomass and grazing responses to Cyclone Opal, a subtropical mesoscale eddy. *Deep Sea Res. II Top. Stud. Oceanogr.* 55, 1378–1388. doi: 10.1016/j.dsr2.2008.01.005

Last, K. S., Hobbs, L., Berge, J., Brierley, A. S., and Cottier, F. (2016). Moonlight drives ocean-scale mass vertical migration of zooplankton during the arctic winter. *Curr. Biol.* 26, 244–251. doi: 10.1016/j.cub.2015.11.038

Lebourges-Dhaussy, A., Huggett, J., Ockhuis, S., Roudaut, G., Josse, E., and Verheye, H. (2014). Zooplankton size and distribution within mesoscale structures in the Mozambique Channel: a comparative approach using the TAPS acoustic profiler, a multiple net sampler and ZooScan image analysis. *Deep Sea Res. II Top. Stud. Oceanogr.* 100, 136–152. doi: 10.1016/j.dsr2.2013.10.022

MacLennan, D. N., Fernandes, P. G., and Dalen, J. (2002). A consistent approach to definitions and symbols in fisheries acoustics. *ICES J. Mar. Sci.* 59, 365–369. doi: 10.1006/jmsc.2001.1158

Marshall, N. B. (1954). *Aspect of Deep Sea Biology*. London: Hutchinson's Scientific.

McDougall, T. J., and Barker, P. M. (2011). *Getting Started with TEOS-10 and the Gibbs Seawater (GSW) Oceanographic Toolbox*. France: SCOR.

Merrett, N., and Roe, H. S. J. (1974). Patterns and selectivity in the feeding of certain mesopelagic fishes. *Mar. Biol.* 28, 115–126. doi: 10.1007/bf00396302

Milligan, R. J., Bernard, A. M., Boswell, K. M., Bracken-Grissom, H. D., D'Elia, M. A., DeRada, S., et al. (2019). The application of novel research technologies by the deep pelagic nekton dynamics of the Gulf of Mexico (DEEPEND) consortium. *Mar. Technol. Soc. J.* 52, 81–86. doi: 10.4031/mtsj.52.6.10

Milligan, R. J., and Sutton, T. T. (2020). Dispersion overrides environmental variability as a primary driver of the horizontal assemblage structure of the mesopelagic fish family Myctophidae in the northern Gulf of Mexico. *Front. Mar. Sci.* 7:15. doi: 10.3389/fmars.2020.00015

Mohan, J. A., Sutton, T. T., Cook, A. B., Boswell, K. M., and Wells, R. J. D. (2017). Influence of oceanographic conditions on abundance and distribution of post-larval and juvenile carangid fishes in the northern Gulf of Mexico. *Fish. Oceanogr.* 1, 1–16.

Olivar, M. P., Bernal, A., Molí, B., Peña, M., Balbín, R., Castellón, A., et al. (2012). Vertical distribution, diversity and assemblages of mesopelagic fishes in the western Mediterranean. *Deep Sea Res. I Oceanogr. Res. Pap.* 62, 53–69. doi: 10.1016/j.dsr.2011.12.014

Owen, R. (1981). Fronts and eddies in the sea: mechanisms, interactions and biological effects. *Analy. Mar. Ecosyst.* 1, 197–233. doi: 10.1371/journal.pone.0129045

Passarella, K. C., and Hopkins, T. L. (1991). Species composition and food habits of the micronektonic cephalopod assemblage in the eastern Gulf of Mexico. *Bull. Mar. Sci.* 49, 638–659.

Pearre, S. (2003). Eat and run? The hunger/satiation hypothesis in vertical migration: history, evidence and consequences. *Biol. Rev.* 78, 1–79. doi: 10.1017/s146479310200595x

Peña, M., Olivar, M. P., Balbín, R., López-Jurado, J. L., Iglesias, M., and Miquel, J. (2014). Acoustic detection of mesopelagic fishes in scattering layers of the Balearic Sea (western Mediterranean). *Can. J. Fish. Aquat. Sci.* 71, 1186–1197. doi: 10.1139/cjfas-2013-0331

Potier, M., Marsac, F., Cherel, Y., Lucas, V., Sabatié, R., Maury, O., et al. (2007). Forage fauna in the diet of three large pelagic fishes (lancetfish, swordfish and yellowfin tuna) in the western equatorial Indian Ocean. *Fish. Res.* 83, 60–72. doi: 10.1016/j.fishres.2006.08.020

Proud, R., Cox, M., Wotherspoon, S., and Brierley, A. (2017). Biogeography of the Global Ocean's Mesopelagic Zone. *Curr. Biol.* 27, 113–119. doi: 10.1016/j.cub.2016.11.003

R Core Team (2013). *R: A Language and Environment for Statistical Computing*. Vienna, Austria: R Foundation for Statistical Computing, Available at: www.R-project.org.

Ressler, P. H., and Jochens, A. E. (2003). Hydrographic and acoustic evidence for enhanced plankton stocks in a small cyclone in the northeastern Gulf of Mexico. *Continent. Shelf Res.* 23, 41–61. doi: 10.1016/s0278-4343(02)00149-8

Richards, W. J., McGowan, M. F., Leming, T., Lamkin, J. T., and Kelley, S. (1993). Larval fish assemblages at the loop current boundary in the Gulf of Mexico. *Bull. Mar. Sci.* 53, 475–537.

Rivas, D., Badan, A., and Ochoa, J. (2005). The ventilation of the deep Gulf of Mexico. *J. Phys. Oceanogr.* 35, 1763–1781. doi: 10.1175/jpo2786.1

Robertson, K. M., and Chivers, S. J. (1997). Prey occurrence in pantropical spotted dolphins, *Stenella attenuata*, from the eastern tropical Pacific. *Fish. Bull.* 95, 334–348.

Røstad, A., Kaartvedt, S., and Aksnes, D. L. (2016). Light comfort zones of mesopelagic acoustic scattering layers in two contrasting optical environments. *Deep Sea Res. I Oceanogr. Res. Pap.* 113, 1–6. doi: 10.1016/j.dsr.2016.02.020

Sabarros, P. S., Menard, S., Levenez, J., Tew-Kai, E., and Ternon, J. (2009). Mesoscale eddies influence distribution and aggregation patterns of micronekton in the mozambique channel. *Mar. Ecol. Press Ser.* 395, 101–107. doi: 10.3354/meps08087

Scales, K. L., Miller, P. I., Embling, C. B., Ingram, S. N., Pirotta, E., and Votier, S. C. (2014). Mesoscale fronts as foraging habitats: composite front mapping reveals oceanographic drivers of habitat use for a pelagic seabird. *J. R. Soc. Interf.* 11:20140679. doi: 10.1098/rsif.2014.0679

Schukat, A., Bode, M., Auel, H., Carballo, R., Martin, B., Koppelman, R., et al. (2013). Pelagic decapods in the northern Benguela upwelling system: distribution, ecophysiology and contribution to active carbon flux. *Deep Sea Res. I Oceanogr. Res. Pap.* 75, 146–156. doi: 10.1016/j.dsr.2013.02.003

Seki, M. P., Polovina, J. V., Brainard, R. E., Bidigare, R. R., Leonard, C. L., and Foley, D. G. (2001). Biological enhancement at cyclonic eddies tracked with GOES Thermal Imagery in Hawaiian waters. *Geophys. Res. Lett.* 28, 1583–1586. doi: 10.1029/2000gl012439

Spear, L. B., Ainley, D. G., and Walker, W. A. (2007). Foraging dynamics of seabirds in the eastern tropical Pacific Ocean. *Stud. Avian Biol.* 35, 1–99.

Sutton, T. T. (2013). Vertical ecology of the pelagic ocean: classical patterns and new perspectives. *J. Fish. Biol.* 83, 1508–1527. doi: 10.1111/jfb.12263

Sutton, T. T., Cook, A. B., Moore, J. A., Frank, T., Judkins, H., Vecchione, M., et al. (2017). *Inventory of Gulf Oceanic Fauna Data Including Species, Weight, And Measurements. Meg Skansi Cruises From Jan. 25–Sept. 30, 2011 in the Northern Gulf of Mexico. Distributed by: Gulf of Mexico Research Initiative Information and Data Cooperative (GRIIDC)*. Corpus Christi, TX: Harte Research Institute.

Sutton, T. T., Frank, T., Judkins, H., and Romero, I. C. (2020). "As gulf oil extraction goes deeper, who is at risk? community structure, distribution, and connectivity of the deep-pelagic fauna," in *Scenarios and Responses to Future Deep Oil Spills*, ed. S. Murawski (Cham: Springer).

Sutton, T. T., and Hopkins, T. L. (1996a). Species composition, abundance, and vertical distribution of the stomiid (Pisces: Stomiiformes) fish assemblage of the Gulf of Mexico. *Bull. Mar. Sci.* 59, 530–542.

Sutton, T. T., and Hopkins, T. L. (1996b). Trophic ecology of the stomiid (Pisces: Stomiidae) fish assemblage of the eastern Gulf of Mexico: strategies, selectivity and impact of a top mesopelagic predator group. *Mar. Biol.* 127, 179–192. doi: 10.1007/bf00942102

Ternon, J. F., Bach, P., Barlow, R., Huggett, J., Jaquemet, S., Marsac, F., et al. (2014). The Mozambique channel: from physics to upper trophic levels. *Deep Sea Res. II Top. Stud. Oceanogr.* 100, 1–9. doi: 10.1016/j.dsr2.2013.10.012

Trueman, C. N., Johnston, G., O'Hea, B., and MacKenzie, K. M. (2014). Trophic interactions of fish communities at midwater depths enhance long-term carbon storage and benthic production on continental slopes. *Proc. R. Soc. B* 281:20140669. doi: 10.1098/rspb.2014.0669

Urmy, S. S., Horne, J. K., and Barbee, D. H. (2012). Measuring the vertical distributional variability of pelagic fauna in Monterey Bay. *ICES J. Mar. Sci.* 69, 184–196. doi: 10.1093/icesjms/fsr205

Volk, T., and Hoffert, M. I. (1985). "Ocean carbon pumps: analysis of relative strengths and efficiencies in ocean-driven atmospheric CO2 changes," in *The Carbon Cycle And Atmospheric CO_2: Natural Variations Archean To Present. Geophysical Monograph*, eds E. Sundquist, and W. S. Broecker (Washington, D.C: American Geophysical Union).

Vukovich, F. M. (2007). Climatology of ocean features in the Gulf of Mexico using satellite remote sensing data. *J. Phys. Oceanogr.* 37, 689–707. doi: 10.1175/jpo2989.1

Wang, Z., DiMarco, S. F., Ingle, S., Belabbassi, L., and Al-Kharusi, L. H. (2014). Seasonal and annual variability of vertically migrating scattering layers in the northern Arabian Sea. *Deep Sea Res. I Oceanogr. Res. Pap.* 90, 152–165. doi: 10.1016/j.dsr.2014.05.008

Watanabe, H., Moku, M., Kawaguchi, K., Ishimaru, K., and Ohno, A. (1999). Diel vertical migration of myctophid fishes (Family Myctophidae) in the transitional waters of the western North Pacific. *Fish. Oceanogr.* 8, 115–127. doi: 10.1046/j.1365-2419.1999.00103.x

Webb, T. J., Vanden, B. E., and O'Dor, R. (2010). Biodiversity's big wet secret: the global distribution of marine biological records reveals chronic under-exploration of the deep pelagic ocean. *PLoS One* 5:e10223. doi: 10.1371/journal.pone.0010223

Wiebe, P. H., Morton, A. W., Bradley, A. M., Backus, R. H., Craddock, J. E., Barber, V., et al. (1985). New development in the MOCNESS, an apparatus for sampling zooplankton and micronekton. *Mar. Biol.* 87, 313–323. doi: 10.1007/bf00397811

Wormuth, J. H., Ressler, P. H., Cady, R. B., and Harris, E. J. (2000). Zooplankton and micronekton in cyclones and anticyclones in the northeast Gulf of Mexico. *Science* 18, 23–34.

Zimmerman, R. A., and Biggs, D. C. (1999). Patterns of distribution of sound-scattering zooplankton in warm- and cold-core eddies in the Gulf of Mexico, from a narrowband acoustic Doppler current profiler survey. *J. Geophys. Res.* 104, 5251–5262. doi: 10.1029/1998jc900072

Zwolinski, J. P., Oliveira, P. B., Quintino, V., and Stratoudakis, Y. (2010). Sardine potential habitat and environmental forcing off western Portugal. *ICES J. Mar. Sci.* 67, 1553–1564. doi: 10.1093/icesjms/fsq068

Conflict of Interest: The authors declare that the research was conducted in the absence of any commercial or financial relationships that could be construed as a potential conflict of interest.

frontiers in Marine Science

ORIGINAL RESEARCH
published: 21 February 2020
doi: 10.3389/fmars.2020.00099

The Vertical and Horizontal Distribution of Deep-Sea Crustaceans in the Order Euphausiacea in the Vicinity of the *DeepWater Horizon* Oil Spill

Tamara M. Frank[1], Charles D. Fine[2], Eric A. Burdett[1], April B. Cook[1] and Tracey T. Sutton[1]*

[1] *Halmos College of Natural Sciences and Oceanography, Nova Southeastern University, Dania Beach, FL, United States,*
[2] *Coral Springs Charter School, Coral Springs, FL, United States*

The vertical and horizontal distributions of Euphausiacea in the northern Gulf of Mexico (GOM), including the location of the *Deepwater Horizon* oil spill, were analyzed from 340 trawl samples collected between April and June 2011. This study is the first comprehensive survey of euphausiid distributions from depths deeper than 1000 m in the GOM and includes stratified sampling from five discrete depth ranges (0–200 m, 200–600 m, 600–1000 m, 1000–1200 m, and 1200–1500 m), and expands the depth ranges of 30 species. In addition, this study demonstrates significantly higher abundance and biomass of the euphausiid assemblage from slope vs. offshore stations, while the offshore assemblage was significantly more diverse. There is also some evidence for seasonality in reproduction amongst the seven species that had gravid females. Lastly, these data represent the first quantification of the euphausiid assemblage in the region heavily impacted by the *Deepwater Horizon* event, and as there are no pre-spill data, may serve as an impacted baseline against which to monitor changes in the euphausiid assemblage in the years following exposure to *Deepwater Horizon* oil and dispersants in the water column.

Keywords: deep-sea crustaceans, mesopelagic, Euphausiacea, Gulf of Mexico, vertical migrations

OPEN ACCESS

Edited by:
Daphne Cuvelier, Center for Marine and Environmental Sciences (MARE), Portugal

Reviewed by:
Patricia Esquete Garrote, University of Aveiro, Portugal
Travis William Washburn, University of Hawai'i at Mānoa, United States

****Correspondence:***
Tamara M. Frank
tfrank1@nova.edu

Specialty section:
This article was submitted to Deep-Sea Environments and Ecology, a section of the journal Frontiers in Marine Science

Received: *31 July 2019*
Accepted: *06 February 2020*
Published: *21 February 2020*

Citation:
Frank TM, Fine CD, Burdett EA, Cook AB and Sutton TT (2020) The Vertical and Horizontal Distribution of Deep-Sea Crustaceans in the Order Euphausiacea in the Vicinity of the DeepWater Horizon Oil Spill. Front. Mar. Sci. 7:99. doi: 10.3389/fmars.2020.00099

INTRODUCTION

Euphausiids are pelagic crustaceans that range in size from mesozooplankton (0.2 μm to 2 mm), macrozooplankton (2–20 mm), and actively swimming micronekton (20–200 mm) (Omori and Ikeda, 1984; Sutton, 2013). They are a vital part of the food web as they consume phytoplankton and zooplankton (Kinsey and Hopkins, 1994; Atkinson et al., 2009) and are in turn consumed by larger organisms including seabirds (Deagle et al., 2007), commercially important fish species such as tuna (Jayalakshmi et al., 2011), whales (Schramm, 2007), and humans (Baker et al., 1990). Euphausiacea are also important because most of them undergo diel vertical migrations, in which they remain in deeper waters during the day to avoid visual predators, and ascend 100 s of meters into shallower waters at sunset to feed under the cover of darkness (reviewed in Cohen and Forward, 2009). This behavior means that not only are they potential prey for a variety of different organisms at multiple

depth levels but are also vectors for the vertical transport of both carbon and pollutants through the water column.

The current study is unique because it utilizes samples collected simultaneously from 0 to 1500 m water depth within five discrete depth ranges. Previous studies of euphausiids in the Gulf of Mexico (GOM) did not extend past 1000 m (Kinsey and Hopkins, 1994; Gasca et al., 2001). When Burghart et al. (2007) collected samples of Decapoda, Lophogastrida and Mysida from depths greater than 1000 m in the eastern GOM, they found that the bathypelagic zone was dominated by different species than those that dominated in the mesopelagic zone. They found an additional 10 species of oplophorids present below 1000 m, that were not known to occur in the GOM. Their study also demonstrated that several species thought to be relatively rare based on collections shallower than 1000 m (Hopkins et al., 1989) were actually quite common in the deeper depths, such as the oplophorids *Acanthephyra stylorostratis* and *Hymenodora glacialis*. The Burghart et al. study emphasized the need to extend these studies to the Euphausiacea, one of the dominant groups of crustaceans in the GOM (Kinsey and Hopkins, 1994; Burdett et al., 2017).

In addition, this study sampled sites at boundary zones along the continental slope. While these boundary zones along continental margins are found in oceanic ecosystems worldwide, there are few studies on the micronektonic composition on both sides of these boundary zones, most of which focused on fish species with limited information on crustaceans (Reid et al., 1991; Aguzzi and Company, 2010; Sutton, 2013; Feagans-Bartow and Sutton, 2014). The data presented here will provide vital information needed to understand the community structure and relationships between species found at these boundary regions and adjacent oceanic systems.

The trawling sites for this study encompassed the region most heavily impacted by the *Deepwater Horizon* oil spill, resulting from the explosion on the *Deepwater Horizon* rig on April 20, 2010. This damaged rig discharged 3.19 million barrels of oil into the northeastern GOM before it was capped in July, with the deepest hydrocarbon plume occurring at 1100 m (Reddy et al., 2011; US District Court, 2015). This spill caused the crash of several local fisheries and coastal ecosystems (Gulfbase.org, 2012) and a recent study on deep-sea crustaceans in the family Oplophoridae demonstrated a significant decrease in their biomass and abundance between 2011 (1 year after the spill) and 2017 (7 years after the spill) (Nichols, 2018). The data presented here, collected 1 year after the spill, represent the first quantification of the euphausiid assemblage in this region and will serve as the initial impacted baseline against which to monitor temporal changes in the assemblage in studies conducted 5–10 years after the spill.

MATERIALS AND METHODS

Sample Collection and Processing

Samples were collected from April through June 2011 on the M/V *Meg Skansi* in the northern GOM (**Figure 1**) with a 10-m^2 mouth area, six-net MOCNESS (Multiple Opening and Closing Net and Environmental Sensing System) (Wiebe et al., 1976) with 3-mm mesh nets. Sampling was standardized at five discrete depth ranges from 0 to 1500 m, except in locations where depths did not reach 1500 m. Sampling depths were chosen based on the following rationales, developed during the NOAA-supported Offshore Nekton Sampling and Analysis Program (ONSAP): net 1 (1500–1200 m) fished below the depth at which a subsurface hydrocarbon plume was detected after the oil spill, net 2 (1200–1000 m) fished through the hydrocarbon plume (Reddy et al., 2011), net 3 (1000–600 m) fished where many of the vertical migrators reside during the day, net 4 (600–200 m) was at depths that vertical migrators pass through during their diel vertical migrations and net 5 (200–0 m) fished the epipelagic zone where strong vertical migrators are found at night. Samples were collected twice during each 24-h cycle, resulting in one "day" trawl and one "night" trawl at each station. A total of 340 discrete depth samples were collected from 45 stations. The samples were fixed in 10% buffered formalin in seawater and transported to the Deep-sea Biology lab at Nova Southeastern University, where all the euphausiids were identified to the lowest taxonomic classification possible, using the Baker et al. (1990) euphausiid key. The body lengths of up to 25 individuals (some samples contained less than 25 individuals) of each species in each sample were measured with digital calipers (CO030150 electronic digital caliper, Marathon Management). After taxonomic identification, wet weights for each species in every sample were recorded to the nearest 0.01 g (P-114 Balance, Denver Instruments). As the volume of water filtered by each net in each trawl varied, these data were standardized by dividing the combined species counts (N) or biomass (g) by the total volume filtered (m^3) for the respective net.

The stations sampled were a subset of the Southeast Area Monitoring and Assessment Program (SEAMAP) sampling grid (Eldridge, 1988), bound by the 1000-m isobath to the north and the 27°N latitudinal line to the south. Stations were divided into two groups and listed as either slope or offshore (**Figure 1**). Those stations that were on or adjacent to the 1000-m isobath, where trawls down to 1500 m were not possible, were categorized as slope stations and trawled down to their maximum depth. Stations that were located on the seaward side of the isobath where trawls down to 1500 m were possible, were categorized as offshore stations. To compare slope assemblages of euphausiids with offshore assemblages, species data from all the trawls in one area were combined; i.e., data from all slope stations (n = 13) were combined to compare with data from all offshore stations (n = 32). Standard Station (27°N, 86°W), where extensive sampling of euphausiids was conducted in the 1990s (Kinsey and Hopkins, 1994), coincided with Sampling Station SE-5.

Abundance, Biomass, and Diversity Index Calculations

Euphausiids were ranked in descending order of abundance with the most abundant species having a rank of 1, for both slope and offshore assemblages. A Spearman's rank comparison was completed to determine if there were significant differences between slope and offshore euphausiid assemblages. As the

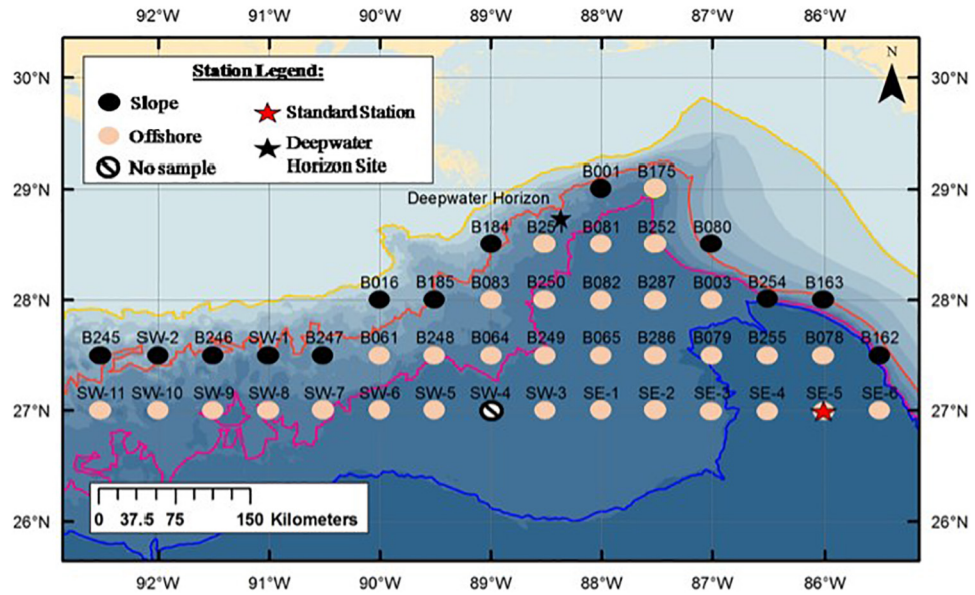

FIGURE 1 | Sampling stations of the M/V *Meg Skansi* cruise from April to June showing slope and offshore station divisions. The orange line is the 1000 m isobath. Stations on or to the landward size of this line (black circles) were considered slope stations; stations on the seaward side of this line (pink circles) were considered offshore stations. Black star indicates *Deepwater Horizon* oil rig. Red star indicates Standard Station (Kinsey and Hopkins, 1994). Figure is from Burdett et al. (2017), used with permission from the Bulletin of Marine Science.

data were not normally distributed (Shapiro-Wilk test), Mann-Whitney *U* tests were utilized to determine if there were significant differences between abundance and biomass as well as individual species' abundances for slope vs. offshore assemblages.

Species richness (*S*), evenness (*J'*), calculated with Pielou's Evenness Index equation, and diversity (*H'*), calculated with the Shannon Diversity Index equation were calculated for every depth range and time period sampled within either slope or offshore assemblages (Hill, 1973). Independent sample *t*-tests were then performed on the Shannon Diversity Indices as per Jayaraman (1999) and Aguzzi et al. (2015). All analyses and graphs were performed with the analyses package and graphing options available in Excel.

Vertical Distribution

Species whose abundance was >1% to the total euphausiid abundance were characterized as abundant species, and collectively, they made up 99% of the euphausiid abundance. Species that contributed less than 1% to the total abundance were characterized as rare species (**Figure 2**). Only the abundant species were analyzed with respect to their vertical distributions, as there were enough individuals present (over 100 per species) for meaningful analyses. The standardized abundance (N m^{-3}) was determined for each species, and the percentage of the assemblage at every depth range and time period sampled within either slope or offshore assemblages was calculated.

Gravid Female Data

The number of gravid females present was recorded for the species that had at least one gravid female, and standardized abundances (N m^{-3} of water filtered) of gravid females per depth range and per month were calculated, as was the percent of the total catch that was represented by gravid females for the specified month.

RESULTS

Temperature and salinity profiles for April–June 2011 (Burdett et al., 2017), showed that there was little variation in these physical parameters with respect to location or month – depth and range of the thermocline and halocline, as well as surface temperature/salinity and those at trawling depths – so these factors were not taken into consideration during the analyses.

Taxonomic Analyses

During the analyses, it became clear that for several groups of euphausiids collected at these sites, the species description did not match known species. The characteristic distinguishing *Nematoscelis atlantica* and *Nematoscelis microps* (James, 1970; Roger, 1978; Mikkelsen, 1987; Baker et al., 1990) is the number of setae on the propodus of the first thoracic leg, which should be 5–6 for *N. atlantica*, and 8–9 for *N. microps*. In addition, the dactylus should be straight and evenly tapering in *N. atlantica*, while it is described as being strongly recurved in *N. microps*. Of the first two hundred individuals that were examined, 91% of them possessed seven setae, while the dactylus was between the diagrams in the keys (Baker et al., 1990; Gibbons et al., 1999; Brinton et al., 2000). Dr. Martha Nizinski, Curator of Decapods at the National Museum of Natural History, could also not determine which species

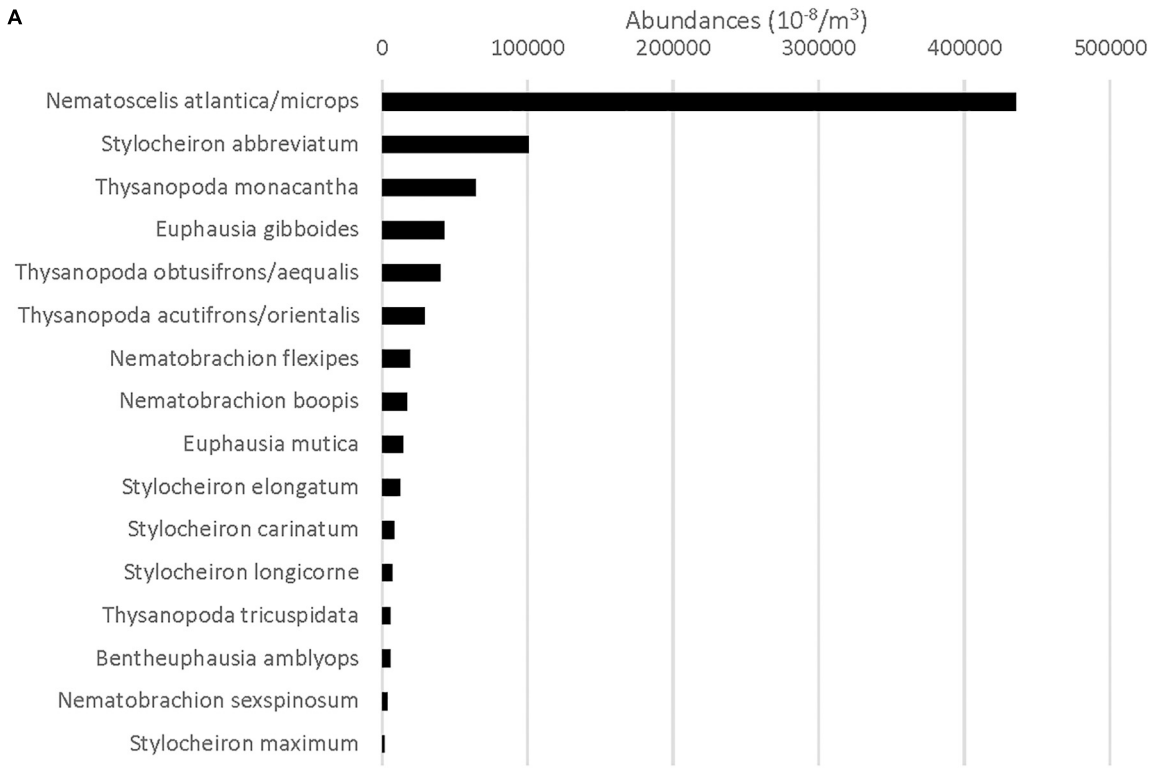

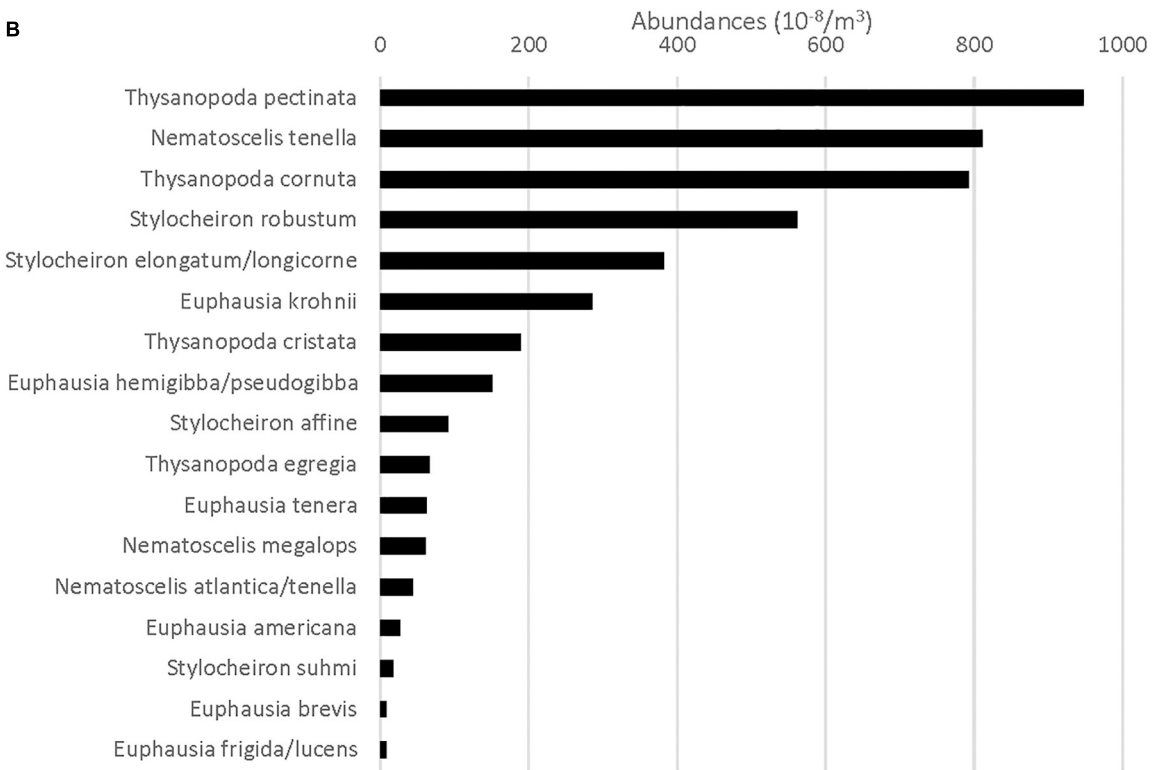

FIGURE 2 | (A) Total standardized abundance (N m^{-3}) for the species that comprise the top 99% of all Euphausiacea caught (categorized as abundant species) at all stations. **(B)** Total standardized abundance for the species that comprise the remaining 1% of all Euphausiacea caught (categorized as rare). *X*-axis maximum value is different from that in **(A)**.

group these aberrant individuals belonged to, so, while ∼ 10% of the 25000 individuals examined did have the "correct" number of setae, they were all grouped together as *Nematoscelis atlantica/Nematoscelis microps*. Ongoing molecular analyses will determine if this is a new species, or if the original separation was a misidentification of a single species. Furthermore, *Thysanopoda obtusifrons* and *Thysanopoda aequalis* (James, 1970; Mikkelsen, 1987; Baker et al., 1990) are reportedly distinguishable by the structure of their antennular lappets. *T. obtusifrons* should have an antennular lappet that covers a third to half of the width of the base of the second segment of the antennular peduncle, while *T. aequalis* should have an antennular lappet that covers the full width of the base of the second segment. This difference was not readily apparent in the samples analyzed in this study, so the two species were grouped together as *T. obtusifrons* and *T. aequalis*. Lastly, *T. acutifrons* and *T. orientalis* are two very closely related species and cannot be differentiated unless they are sexually mature adults with petasmae or thelyca (Baker et al., 1990). The individuals in these samples were small with very few sexually mature individuals, so these two species were grouped together as *T. acutifrons* and *T. orientalis*.

Slope Assemblage vs. Offshore Assemblage Comparison

In total, 51,559 euphausiids belonging to 31 species were collected. Numerically, 16 species made up 99% of the total (slope + offshore stations) euphausiid assemblage and were categorized as abundant, while 15 species made up the remaining 1% and were categorized as rare. *N. atlantica/N. microps* was by far the most abundant euphausiid taxon, accounting for 51.2% of all euphausiids present, with *Stylocheiron abbreviatum* (12.4%) being the only other species to account for more than 10% of the total assemblage (**Figure 2A**). Each of the rare species included in the bottom 1% accounted for 0.2% or less of the total euphausiid assemblage (**Figure 2B**).

The total number of individuals caught per m^3 was significantly greater (Mann Whitney *U*, $p = 0.004$) in slope samples than it was in offshore samples (**Figure 3A**). However, in terms of individual species' contributions to the total abundance, the relative abundance of each species (i.e., the percent contribution to the total abundance) remained consistent (less than a 2% difference in relative abundance) for the species categorized as abundant in both locations (**Figure 4**), with the exception of *N. atlantica/N. microps* and *Euphausia mutica*. *N. atlantica/N. microps* accounted for 56.1% of the total abundance for slope samples vs. 49.4% of the total abundance for offshore samples. *E. mutica* accounted for 0.1% of the total abundance for slope samples vs. 2.6% of the total abundance for offshore samples. While *N. atlantica/N. microps* was the most abundant species in both slope and offshore samples, *E. mutica* was the 7th most abundant species in offshore samples and the 16th most abundant in slope samples (**Figure 4**).

While there were more offshore stations, station variance was very low for both slope ($1.19 \times 10^{-5} m^{-3}$) and offshore ($6.41 \times 10^{-6}$ m^{-3}) stations, indicating that the greater abundance of euphausiids in slope waters vs. offshore waters was not due to skewed data resulting from more trawling offshore. Of the ten rare species that were present only in the offshore samples, four of them (*N. tenella, S. robustum, E. krohnii*, and *E. hemigibba/E. pseudogibba)* were collected in substantial numbers (91, 63, 32, and 17) and distributed across multiple stations. The remaining six species were collected in much lower numbers (one to seven) and additional slope sampling is needed before drawing any conclusions about their geographical restrictions.

A Spearman's Rank correlation demonstrated a significant ($\rho = 0.90$, DF = 31 $p < 0.001$) monotonic relationship, meaning that as slope abundances increased, each abundant species' respective offshore abundance also increased. Eight of the 16 abundant euphausiid species were significantly more abundant in the slope samples than offshore (all $p < 0.01$; Mann Whitney *U*), while one species (*E. mutica*) was significantly ($p < 0.01$) more abundant in offshore samples than in slope samples (**Figure 4**).

With respect to the rare euphausiid species, 10 species were found in offshore samples that were not found in slope samples (**Figure 5**), with *Nematoscelis tenella* ($n = 91$), *Stylocheiron robustum* ($n = 63$), *Euphausia krohnii* ($n = 32$), and *Euphausia hemigibba/Euphausia pseudogibba* ($n = 17$) occurring in abundances of over 10 individuals. The abundance of the remaining six species ranged from one to seven. There were no species found in slope samples that were not found in offshore samples.

The biomass for the euphausiid assemblage reflected the abundance trends, with biomass for the slope assemblage being significantly higher (Mann-Whitney *U*, $p = 0.0004$) than it was for the offshore assemblage (**Figure 3B**). The biomass trends for individual species also reflected abundance trends, with the biomass of the majority of abundant euphausiid species higher at slope stations than at offshore stations (**Figure 6**). *N. atlantica/N. microps* had the highest biomass for both slope and offshore locations. The same eight species that were significantly more abundant in the slope stations also had significantly (Mann-Whitney *U*, all $p < 0.01$) higher biomasses than in the offshore stations; the same species (*E. mutica*) that was significantly more abundant in the offshore stations also had a significantly (Mann-Whitney *U*, $p < 0.01$) higher biomass in offshore stations. Euphausiids made up 15.8% of the total biomass of all the crustaceans collected during this study (1.837 kg), making it the 3rd highest ranking crustacean family in terms of biomass in this region, with *N. atlantica/N. microps*, the most abundant euphausiid, making up 44% of the total euphausiid biomass. *Thysanopoda acutifrons/Thysanopoda orientalis* was the 6th-most abundant euphausiid, but due to its larger size compared to the more abundant species, it ranked 2nd in terms of biomass, making up 12.7% of the total euphausiid biomass.

Slope and offshore euphausiid assemblages were compared using the Shannon Diversity (*H'*) and Pielou's #Evenness (*J'*) indices, but these analyses did not include the bathypelagic zone because bathypelagic samples were not available for the slope stations. Diversity was significantly higher ($p < 0.001$) in the slope samples than the offshore samples in the epipelagic zone during the day (**Table 1**) but was significantly higher (<0.001) in the offshore samples than the slope samples during the night (**Table 2**). In the mesopelagic zone (200–1000 m),

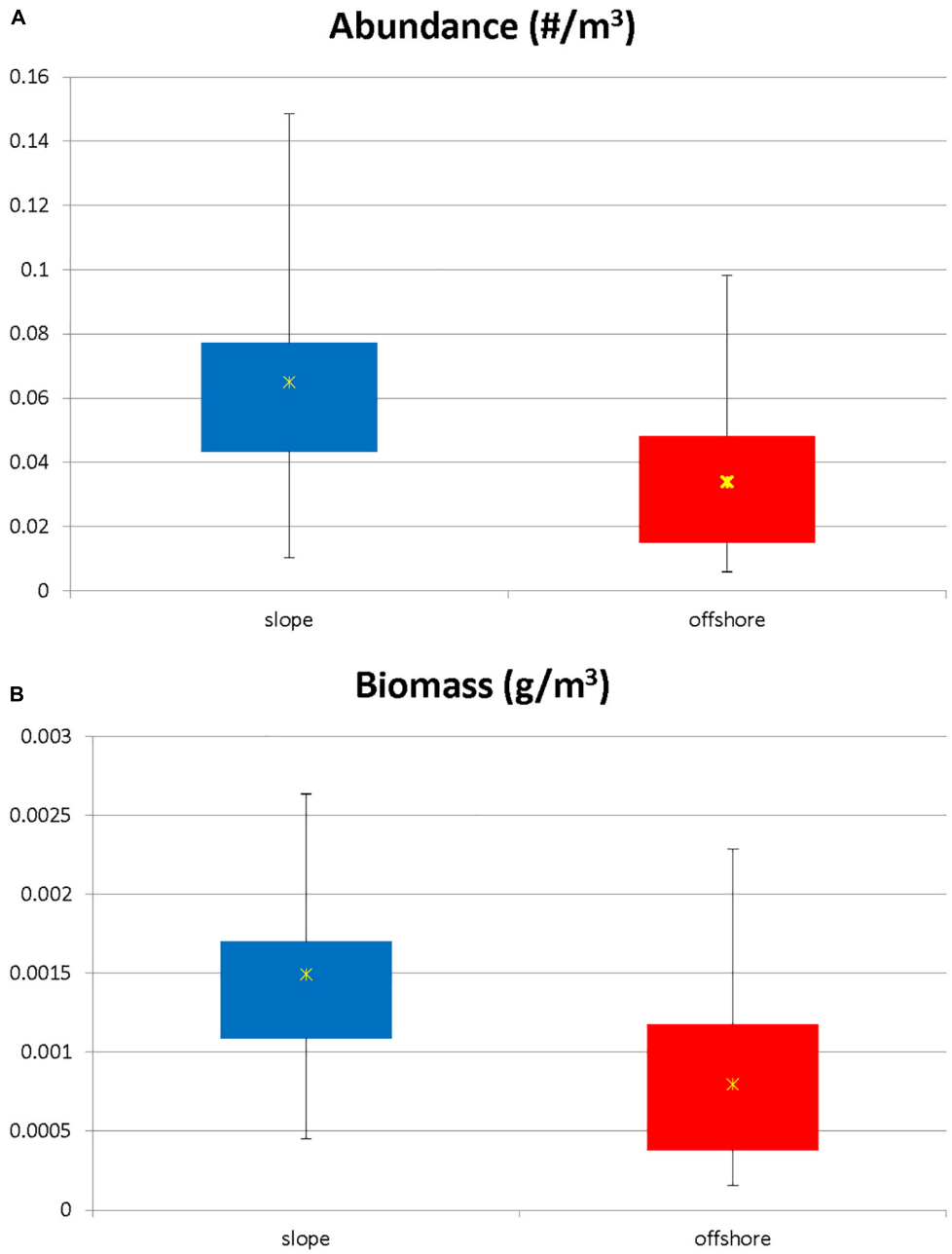

FIGURE 3 | (A) Standardized abundance (N m^{-3}) for slope vs. offshore euphausiid assemblage. Abundance was significantly higher in the slope stations (Kruskal Wallis, $p = 0.005$). Stars represent mean values. **(B)** Standardized biomass for slope vs. offshore euphausiid assemblage. Biomass was significantly higher in the slope stations (Kruskal Wallis, $p = 0.0009$). Stars represent mean values.

both day and night, the diversity was significantly higher ($p < 0.05$) in the offshore samples. The upper and lower mesopelagic assemblages were more evenly distributed offshore during the day, whereas the epipelagic assemblage was more evenly distributed over the slope.

Vertical Distribution

Vertical distribution patterns were determined for the 16 most abundant species (those that made up 99% of the euphausiid assemblage). These species could be separated into three distinct groups based on their vertical distributions: (1) species in which over 50% of the population migrated to a shallower depth range at night, and were thus categorized as strong vertical migrators (SVM – **Figure 7A**); (2) species in which 19.5–41.3% of the population migrated to a shallower depth range at night and thus categorized as weak vertical migrators (WVM – **Figure 7B**); and (3) species where less than 2% of the population moved to a shallower depth

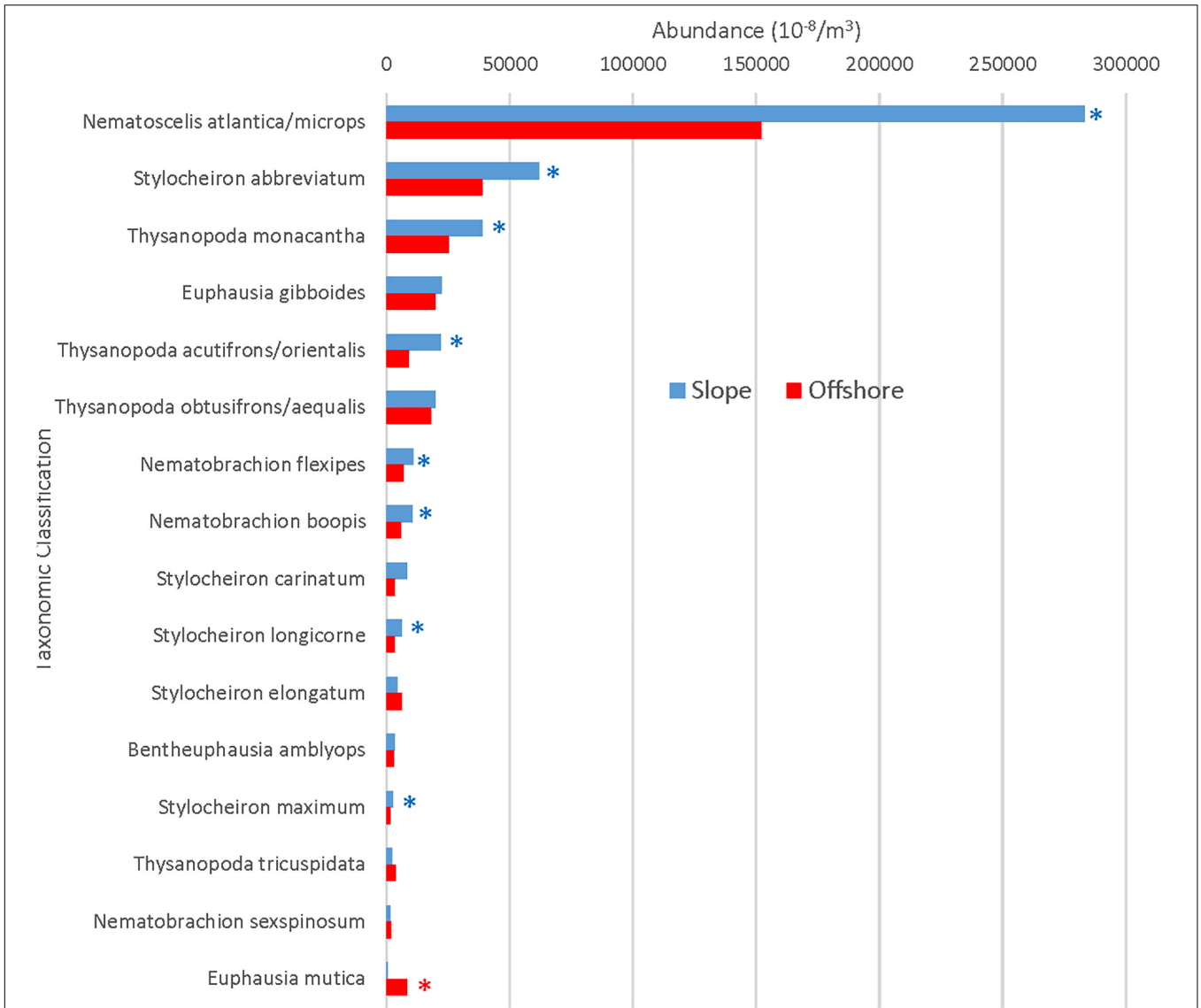

FIGURE 4 | Slope and offshore standardized abundances for abundant species. Asterisks indicate significantly greater abundances for slope (blue) or offshore (red) locations. Species are arranged from maximum to minimum abundances at slope stations.

range at night, and thus categorized as non-vertical migrators (NVM- **Figure 7C**).

A total of 6 of the 16 abundant species were strong vertical migrators, five species were weak vertical migrators, and five species showed no discernable vertical migrations. All six of the species that were considered strong vertical migrators had over 50% of their respective day populations caught at depths of between 200 and 600 m during the day. Four of the five species that showed a weak vertical migration pattern had over 50% of their respective day populations caught between 200 and 600 m, while the other weak migrator, *Bentheuphausia amblyops*, was found primarily between 600 and 1200 m (40.4% between 600 and 1000 m and 46.1% between 1000 and 1200 m) during the day, with a small portion (11.8%) migrating up to 200–600 m at night. Of the five species that showed no vertical migration, more than 50% of the *S. abbreviatum* and *Stylocheiron carinatum* individuals were caught between 0 and 200 m during both the day and the night. The remaining three species (*Stylocheiron longicorne*, *Stylocheiron elongatum*, and *Nematobrachion boopis*) were caught primarily between 200 and 600 m during both the day and night.

The 15 species that accounted for the remaining 1% of total euphausiid abundance were not caught in sufficient quantities to create meaningful vertical distribution graphs. **Supplementary Table S1** shows the depth distribution of these rare species.

Gravid Female Data

Gravid females were found in seven species. *N. atlantica/N. microps* had the highest number of gravid females, and

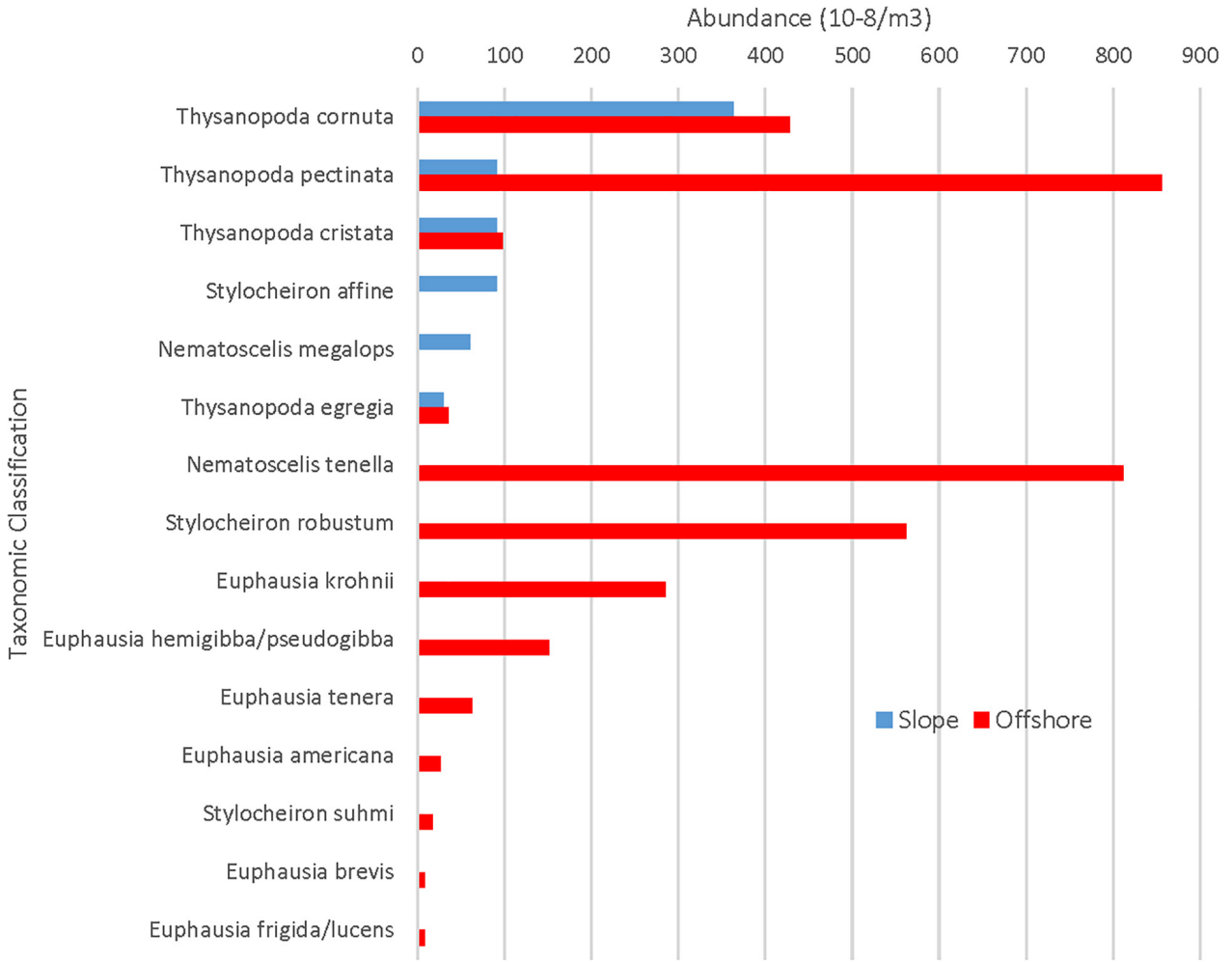

FIGURE 5 | Slope and offshore abundances for rare euphausiids. *X*-axis maximum value is substantially lower than that of **Figure 4**.

Euphausia tenera had the highest percentage of gravid females. *N. atlantica/N. microps* was the only species in which gravid females were caught in all five depth ranges (**Table 3**). **Table 4** shows monthly representation of gravid female abundance and what percent of that species' population the gravid abundance represents. Only one species had gravid females in April (*N. atlantica/N. microps*), while five species had gravid females in May and six species had gravid females in June. *N. atlantica/N. microps* is the only species in which gravid females were caught in all 3 months of sampling with the greatest abundance ($2925 \times 10^{-7} m^{-3}$) and percent (10.0%) of population gravid occurring in May.

DISCUSSION

Assemblage Structure

Sixteen species of euphausiids made up 99% of the euphausiid abundance, with the most abundant species being the combined species group *N. atlantica/N. microps,* in both slope and offshore stations. The only previous study in this region was by Kinsey and Hopkins (1994), conducted at their Standard Station, which overlapped with Station SE-5 in the current study. Combined values of *N. atlantica* and *N. microps* from the Hopkins and Kinsey study puts them as the 5th most abundant species in their study while the three most abundant species in their study were *E. tenera*, *S. carinatum*, and *Euphausia americana.* More recent studies by Castellanos and Gasca (1999) and Gasca et al. (2001) collected Euphausiacea from the southern GOM, and although they only trawled in the epipelagic zone (0–200 m), their night trawls would have collected most of the vertical migrating species. They found 17 species of euphausiids and determined that three species, *S. carinatum, Stylocheiron suhmi*, and *E. tenera* (in decreasing order of abundance) contributed to the majority of the euphausiid abundance in both spring and summer. This means that two of the top three most abundant species in these two studies (*S. carinatum* and *E. tenera),* separated by location (southern GOM vs. northern GOM) and time (7 years) were the same. In the current study, *E. tenera* was extremely rare, with only six collected in 340 samples from all depths, while *S. carinatum*

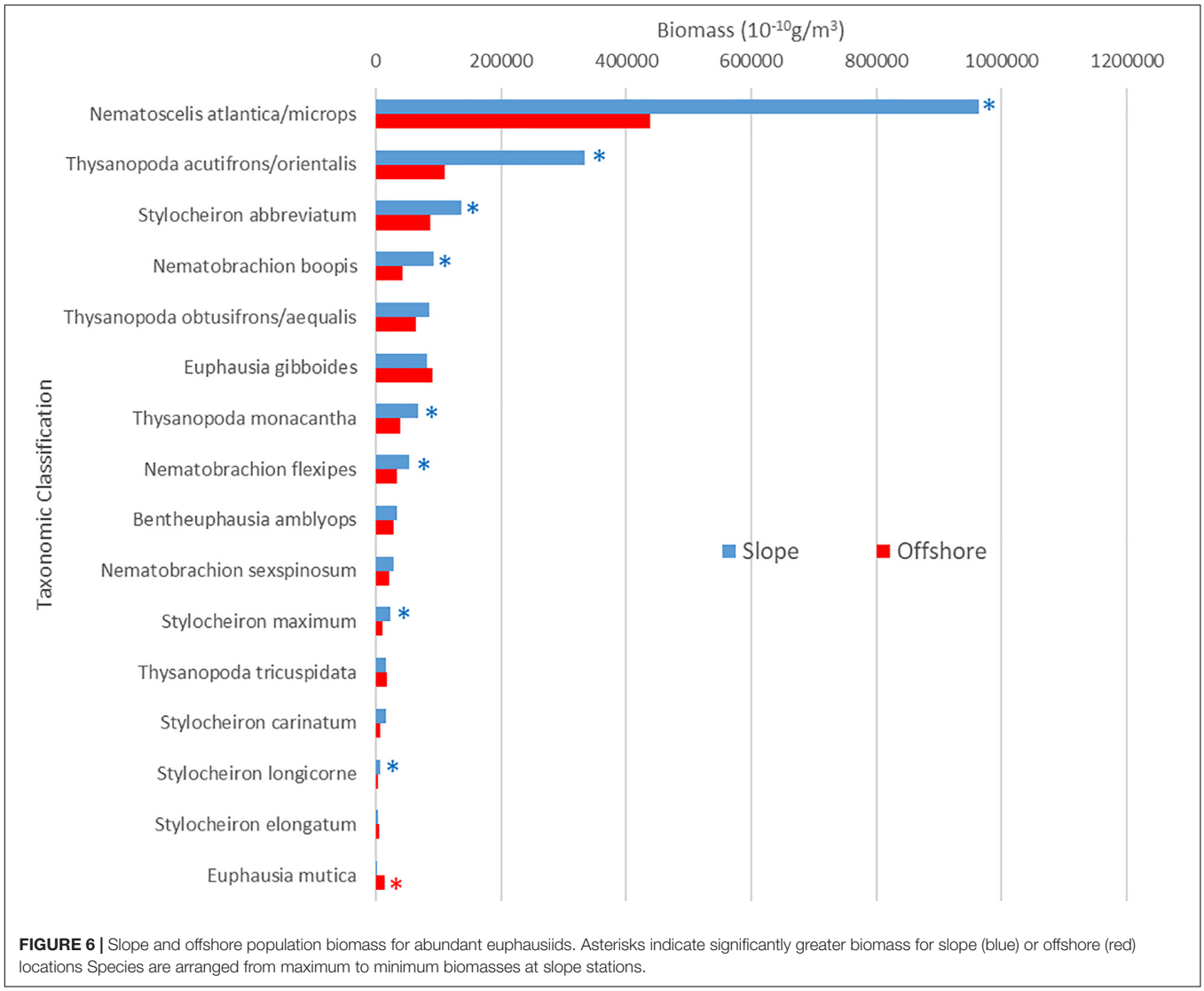

FIGURE 6 | Slope and offshore population biomass for abundant euphausiids. Asterisks indicate significantly greater biomass for slope (blue) or offshore (red) locations Species are arranged from maximum to minimum biomasses at slope stations.

ranked 11th in abundance for the abundant species. *E. americana*, the 3rd most abundant species in the Hopkins and Kinsey study, and *S. suhmi*, the 2nd most abundant species in the Gasca studies, were was also extremely rare in the current study, with only four and two collected in all samples.

Interestingly, the species that were most abundant in the Gasca et al. and Kinsey and Hopkins studies *E. americana* (mean body length = 11.15 mm), *E. tenera* (mean body length = 10.86 mm), *S. carinatum* (mean body length = 12.01 mm), and *S. suhmi* (mean body length = 5.77 mm) are all substantially smaller species than this study's three most abundant species – *N. atlantica/N. microps* (mean body length = 16.36 mm), *S. abbreviatum* (mean body length = 13.80 mm), and *Thysanopoda monacantha* (mean body length = 13.08 mm). With the most recent unimpacted baseline data more than 15 years old, it is impossible to determine if the change in the assemblage rank from smaller species to larger species was due to protracted slow change in the assemblage due to spatial and temporal changes in oceanographic conditions (temperature, nutrient availability, and runoff) or a more acute shift resulting in response to the *DWH* oil spill. The possibility that this shift may be due to the oil spill arises from the fact that oil droplets in the

TABLE 1 | Evenness and diversity indices for daytime slope and offshore assemblages of euphausiids.

Depth range (m)	*S*	*n*	*J'*	*H'*
Slope assemblage				
0–200	10	12.5	0.67	1.39*
200–600	17	87.1	0.51	1.32
600–1000	20	25.5	0.35	1.06
Offshore assemblage				
0–200	10	3.9	0.52	0.73
200–600	21	64.0	0.53	1.68*
600–1000	21	9.7	0.52	1.60*

*S, species richness; n, total number of individuals × 10^{-4} m^{-3}; J', Pielou's evenness index; H', Shannon diversity index. *Signifies significantly higher diversity.*

TABLE 2 | Evenness and diversity indices for nighttime slope and offshore assemblages of euphausiids.

Depth range (m)	*S*	*n*	*J'*	*H'*
Slope assemblage				
0–200	16	134.1	0.65	1.76
200–600	17	65.1	0.53	1.45
600–1000	12	14.2	0.67	1.64
Offshore assemblage				
0–200	21	85.5	0.62	1.93*
200–600	26	70.0	0.52	1.70*
600–1000	22	9.2	0.57	1.83*

S, species richness; n, total number of individuals $\times$ $10^{-4}m^{-3}$*; J', Pielou's evenness index; H, Shannon diversity index. *Signifies significantly higher diversity.*

water could have a greater impact on smaller species due to their larger surface area to volume ratios; as animals increase in size, their surface area doubles, but their volume triples (Schmidt-Nielsen, 1984). The relatively larger surface area means a larger area for contaminants to diffuse into the body, and the smaller volume means less internal components to dilute the contaminants, giving rise to the possibility that oil/dispersants might have a greater impact on smaller individuals. This has been experimentally demonstrated in copepods (Jiang et al., 2012), where smaller individuals were more sensitive to oil WAF (water associated fraction) than larger ones, and in the amphipod *Gammarus oceanicus,* where larvae were hundreds of times more sensitive to oils than adults (Lindén, 1976). Further decadal long studies are required in this region to determine if this is an acute shift in the assemblage that may show recovery over time or is simply part of a persistent decadal pattern.

Slope vs. Offshore

The abundance and biomass of euphausiids were significantly greater in slope than in offshore stations (**Figure 3**), but the vast majority of the euphausiid assemblage was found between 0 and 600 m in both regions, which was also reported by Kinsey and Hopkins (1994) and Castellanos and Gasca (1996) at their study sites. These data indicate that deeper depths offshore cannot account for the distribution differences, and the reason remains to be determined.

The offshore assemblage was significantly more diverse than the slope assemblage at all depths and times of day, with the exception of the epipelagic assemblage sampled during the day, which was significantly more diverse over the slope (**Tables 1**, **2**). Diversity values incorporate species richness and evenness within a population and since species richness was the same for both locations in the epipelagic zone (10 species), the lower number of individuals offshore (5×10^{-4} m^{-3}) compared to those over the slope (11×10^{-4} m^{-3}) might explain the observed differences.

While studies comparing slope and offshore fauna are relatively rare, Reid et al., 1991 described a mesopelagic-boundary community for micronekton off the coast of Hawaii, that occupied a narrow boundary zone over the upper slope. The faunal composition of this boundary community differed substantially from the neighboring oceanic community for fishes, squids, and crustaceans. In addition, there were higher concentrations of boundary species closer to shore, with rapid seaward reduction in abundances, similar to what we report here for Euphausiidae, and what Burdett et al. (2017) reported for the Oplophoridae. However, although Burdett et al. (2017) sampled many of the same Oplophoridae species sampled in the Reid et al., 1991 study, they found several species with significantly different distributions. For example, *Janicella spinacauda* was primarily an offshore species in the NE GOM, while the Reid study found them to be equally abundant in both inshore and offshore samples, indicating that there may be considerable local differences in species compositions and diversity. The data reported here, together with the Burdett and Reid studies (and earlier studies referenced therein) emphasize the idea that boundary communities are globally distributed, and that slope communities are unique to their regions, with local geography, currents and even seasonality contributing to these differences. Future studies need to take into account that there may be significant differences in species composition and biomass between slope and. neritic stations, and how these boundary communities impact the neritic ecosystem.

Species richness in night assemblages increased in the epipelagic zone for both offshore and slope samples compared to their respective day assemblages. The greatest increase occurred in the offshore epipelagic samples (10 species during the day, 20 species at night), due to the nighttime vertical migrations of these species. These findings are supported by Biggs et al. (1977) and Castellanos and Gasca (1999), who also noted species richness increased during the night in the epipelagic zone. This huge increase in species richness in the epipelagic zone due to vertical migrations at night underscores of importance of conducting a full spatial and temporal sampling series when attempting to assess the impact of human activities on deep-sea species.

Gravid Female Data

At least one gravid female was found in seven species of Euphausiacea. Six of these species were categorized as abundant, while one (*E. tenera*) was a rare species. Gravid females were found at all depth ranges with the majority found between 200 and 600 m (**Table 3**). *N. atlantica/N. microps* gravid females (total of 1683 gravid females, 9.3% of the sampled population) were present in all depth ranges, with the vast majority occurring between 0 and 600 m depth. The total number of gravid *N. atlantica/N. microps* females (the only species for which large numbers of gravid females were found) varied from April to June, but the total number of individuals varied as well, so there were no substantial differences in the percent of gravid females collected each month. Four of the seven species that had at least one gravid female, had the largest percent of their population gravid in the month of June. In addition, the number of species with gravid females increased from one in April, to five in May, to six in June (**Table 4**). Previous studies suggest that euphausiids reproduce seasonally (Cuzin-Roudy, 2000; Gómez-Gutiérrez and Robinson, 2005), and data from the current study point towards a seasonal aspect to their reproduction as well. Further data are needed on reproductive seasonality in euphausiids, as the timing

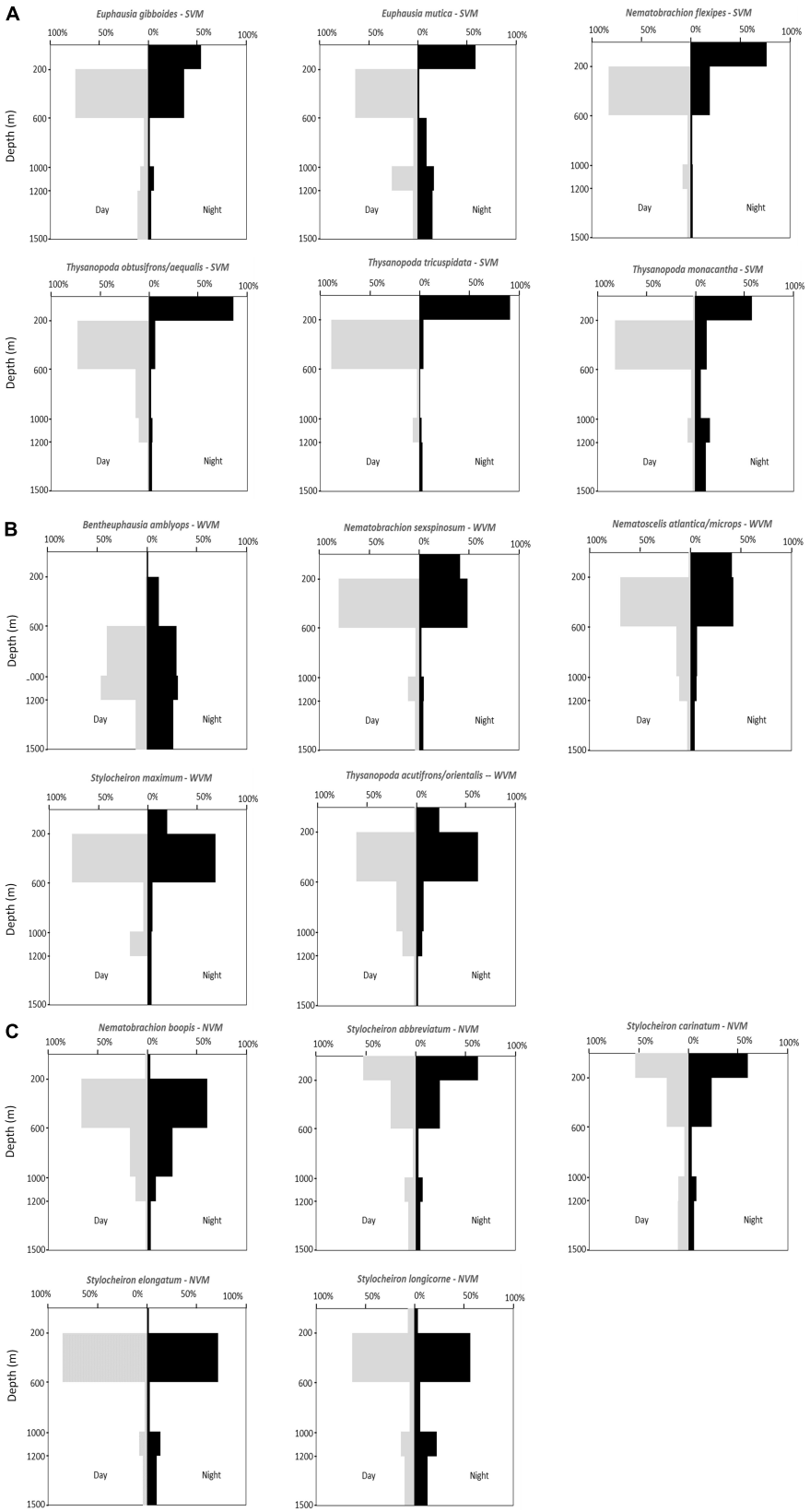

FIGURE 7 | Vertical distribution patterns of abundant euphausiid species. **(A)** Strong vertical migrators (SVM). **(B)** Weak vertical migrators (WVM). **(C)** Non-vertical migrators (NVM).

TABLE 3 | Abundances ($\times 10^{-7} m^{-3}$) of gravid euphausiid species for each depth range and the percent of the population that gravid females represent.

Species	Abundance ($\times 10^{-7} m^{-3}$)					% of species' population
	0–200 m	200–600 m	600–1000 m	1000–1200 m	1200–1500 m	
Euphausia gibboides	0	6	0	0	0	0.1
Euphausia tenera	0	0	0	12	0	28.6
Nematoscelis atlantica/microps	1165	3936	739	324	194	9.3
Stylocheiron abbreviatum	0	0	5	18	9	0.1
Stylocheiron carinatum	11	6	0	0	4	0.9
Stylocheiron elongatum	0	6	2	0	4	0.6
Stylocheiron maximum	0	6	0	0	0	1.2

of events like an oil spill in the GOM would have significantly greater impacts if they occur during the reproductive season.

Vertical Distribution

The data for most species in the current study support the conclusions of Kinsey and Hopkins (1994) in terms of whether species are strong, weak or non-vertical migrators. Based on the data reported in the current study, *T. tricuspidata*, whose sample size was too small for Kinsey and Hopkins (1994) to categorize, can now also be added to the list of strong vertical migrators in the GOM, with more than 50% of the daytime population ascending to shallower depths at night. *N. atlantica/N. microps* and *Stylocheiron maximum* were considered to be vertical migrators by Kinsey and Hopkins (1994), but their sample size was not large enough for them to distinguish between strong and weak vertical migrators. Based on the large sample sizes in the current study, these species can be identified as weak vertical migrators, as are *Nematobrachion sexspinosum, Bentheuphausia amblyops*, and *T. acutifrons/T. orientalis*.

However, their conclusion that *S. longicorne* was a vertical migrator are not supported by the results of the current study. Their conclusion was based on a small sample size and apparent movements from 200 to 300 m during the day, to 125 to 200 m during the night. These depth ranges encompass two of the depth ranges in the current study, so if vertical migrations were occurring, they should have been apparent. Based on the large sample size in the current study and the fact that the percentage of the population at night in the epipelagic zone (2.3%) was lower than during the day (7.4%), this species should be considered a non-vertical migrator.

Bergstrom and Stromberg (1997), studying the euphausiid assemblage off the Swedish west coast, found that *Meganyctiphanes norvegica* did not vertically migrate through a thermocline that was present between 50 and 60 m, although *Thysanoessa raschii* did. This suggests that some euphausiid species may be limited by thermoclines with respect to their vertical distribution, but others are not. At the time of the current study, a thermocline was present between 25 and 600 m and a halocline was present between 125 and 500 m at both slope and offshore locations (Burdett et al., 2017). As shown by Burdett et al., there were no significant differences between temperature or salinity at similar depths between slope and offshore stations. Since the thermocline in the present study extended for hundreds of meters and all the vertically migrating species of euphausiids traversed these depths, it does not appear that the presence of a thermocline inhibited the vertical activity of euphausiids in this study. In addition, the lack of differences in this parameter between offshore and slope stations indicates that differences in distribution patterns for these species cannot be attributed to this factor.

Supplementary Table S2 shows depth ranges for all euphausiids caught in the GOM from previous studies. Due to the deeper depths included in the current study, the depth ranges of 30 species have been expanded – 25 down to 1500 m. two down to 1200 m, and three to shallower depths where they were not reported before.

There is one species of weak vertical migrator, *Bentheuphausia amblyops,* with a deeper daytime depth distribution than the other 15 abundant species, with more than 50% of the daytime population found at the depth of the subsurface plume (1000 to 1200 m) that initially resulted from the *DWHOS* [e.g., Camilli et al., 2010; Hazen et al., 2010; Ryan et al., 2011)]. One might anticipate that this species would be more profoundly affected by the oil spill that the shallower living species. However, extensive sampling of the water column in 2010 from the surface to just above the seafloor showed PAH concentrations higher than 0.3 μ/L in (Murawski et al., 2016; Romero et al., 2018), levels which are toxic to marine organisms (Whitehead et al., 2012).

TABLE 4 | Gravid female abundance ($\times 10^{-7} m^{-3}$) by month for each species of Euphausiacea.

Species	Abundance ($\times 10^{-7} m^{-3}$)		
	April	May	June
Euphausia gibboides	0	8 (0.2%)	0
Euphausia tenera	*NA	0	2 (33.3%)
Nematoscelis atlantica/microps	2381 (8.4%)	2925 (10.0%)	1132 (8.8%)
Stylocheiron abbreviatum	*NA	5 (0.1%)	5 (0.1%)
Stylocheiron carinatum	0	8 (1%)	3 (3.2%)
Stylocheiron elongatum	*NA	0	5 (0.6%)
Stylocheiron maximum	0	3 (1.0%)	2 (1.4%)

**NA indicates no individuals of that species were collected. "0" indicates that individuals of that species were collected but none of them were gravid. Numbers in parentheses are the percent of that species population that gravid females represent for that month.*

Therefore, it is unlikely that any species specific effects would be present. In addition, these types of analyses require comparisons with samples collected before the oil spill, and these samples do not exist, with the exception of the 15-year old Kinsey and Hopkins study, which did not mention quantify *B. amblyops* in their study.

However, the fact that 11 of the 16 most abundant species are vertical migrators can substantially increase the impact of an anthropogenic event such as an oil spill. Vertical migrators serve as vectors of oil released in deeper waters, such as the *DWHOS*, to surface waters, as well as vectors of oil spilled at the surface, to deeper waters. Being primary prey for a variety of species – stomiid deep-sea fish, tuna, whales, seabirds (Sutton and Hopkins, 1996; Deagle et al., 2007; Schramm, 2007; Jayalakshmi et al., 2011) – they would serve as mechanisms of trophic transport of contaminants through the food web.

CONCLUSION

In conclusion, the results of this study indicate that there are significant differences between offshore and slope assemblages of euphausiids, with both biomass and abundance being significantly higher at the slope stations, indicating that these location factors need to be taken into account when describing the assemblages in regions when sampling includes stations close to the continental slope. In addition, this study also supports suggestions from earlier studies that seasonality in reproduction is present in euphausiids, data that are vital for modeling potential effects of anthropomorphic disturbances in this region. While no conclusions can be drawn about the impact of the *DWHOS*, it is interesting that there has been a shift in the assemblage from domination by smaller species to domination by larger species between a study that occurred 15 years ago, and the current study, that occurred 1 year after the oil spill. Finally, the large number of vertical migrators, the extent of their migrations, and the significant effect of this behavior on species richness in shallow waters, emphasizes the need to conduct studies of this type throughout the water column, both during the day and at night. These data will also serve as an impacted baseline against which to monitor future assemblage shifts as the region recovers from any changes that may have resulted from the *Deepwater Horizon* oil spill.

DATA AVAILABILITY STATEMENT

The datasets generated for this study can be found in the https://data.gulfresearchinitiative.org (doi: 10.7266/N7VX0DK2).

AUTHOR CONTRIBUTIONS

TS and AC did all the cruise planning, led the cruises, and provided the samples for analysis. TF, CF, and EB completed all the taxonomic analysis. TF and CF completed the majority of the statistical analyses, wrote the manuscript, and produced the figures and tables.

FUNDING

This project was funded in part by the NOAA Office of Response and Restoration and in part from a grant from the Gulf of Mexico Research Initiative (GoMRI) to the Deep Pelagic Nekton Dynamics of the Gulf of Mexico (DEEPEND) Consortium. Data are publicly available through the Gulf of Mexico Research Initiative Information and Data Cooperative (GRIIDC) at https://data.gulfresearchinitiative.org (doi: 10.7266/N7VX0DK2).

ACKNOWLEDGMENTS

We thank the crew of the M/V *Meg Skansi* for collecting the samples used in this study. We also thank Martha Nizinski for her aid in validating specimen identification, Lacey Malarky for her contributions to the statistical analysis of this report, and D. Hahn and N. Thompson for the manuscript review.

SUPPLEMENTARY MATERIAL

The Supplementary Material for this article can be found online at: https://www.frontiersin.org/articles/10.3389/fmars.2020.00099/full#supplementary-material

REFERENCES

Aguzzi, J., and Company, J. B. (2010). Chronobiology of deep-water decapod crustaceans on continental margins. *Adv. Mar. Biol.* 58, 55–225. doi: 10.1016/B978-0-12-381015-1.00003-4

Aguzzi, J., Sbragaglia, V., Tecchio, S., Navarro, J., and Company, J. B. (2015). Rhythmic behaviour of marine benthopelagic species and the synchronous dynamics of benthic communities. *Deep Sea Res. Part 1 Oceanog. Res. Pap.* 95, 1–11. doi: 10.1016/j.dsr.2014.10.003

Atkinson, A., Siegel, V., Pakhomov, E. A., Jessopp, M. J., and Loeb, V. (2009). A re-appraisal of the total biomass and annual production of Antarctic krill. *Deep Sea Res. I* 56, 727–740. doi: 10.1016/j.dsr.2008.12.007

Baker, A. de, C., Boden, B. P., and Brinton, E. (1990). *A Practical Guide to the Euphausiids of the World*. London: Natural History Museum, 1–96.

Bergstrom, B., and Stromberg, J. O. (1997). Behavioral differences in relation to pycnoclines during vertical migration of the euphausiids *Meganyctiphanes norvegica* (M. Sars) and *Thysanoessa raschii* (M. Sars). *J. Plankton Res.* 19, 255–261. doi: 10.1093/plankt/19.2.255

Biggs, D. C., Zimmerman, R. A., Gasca, R., Suarez-Morales, E., Castellanos, I. A., and Leben, R. R. (1977). Note on plankton and cold-core rings in the Gulf of Mexico. *Fish. Bull.* 95, 369–375.

Brinton, E., Ohman, M. C., Townsend, A. W., Knight, M. D., and Bridgeman, A. L. (2000). Euphausiids of the World Ocean. Leiden: ETI BioInformatics.

Burdett, E., Fine, C., Sutton, T., Cook, A., and Frank, T. (2017). Geographic and depth distributions, ontogeny, and reproductive seasonality of decapod shrimps (Caridea: Oplophoridae) from the northeastern Gulf of Mexico. *Bull. Mar. Sci.* 93, 743–767. doi: 10.5343/bms.2016.1083

Burghart, S. E., Hopkins, T. L., and Torres, J. J. (2007). The bathypelagic decapoda, lophogastrida, and Mysida of the eastern Gulf of Mexico. *Mar. Biol.* 152, 315–327. doi: 10.1007/s00227-007-0691-3

Camilli, R., Reddy, C. M., Yoerger, D. R., Van Mooy, B. A. S., Jakuba, M. V., Kinsey, J. C., et al. (2010). Tracking hydrocarbon plume transport and biodegradation at Deepwater Horizon. *Science* 330, 201–204. doi: 10.1126/science.1195223

Castellanos, I. A., and Gasca, R. (1996). Eufáusidos (Crustacea: Euphausiacea) de aguas superficiales del sur del Golfo de Mexico. *Caribb. J. Sci.* 32, 187–194.

Castellanos, I. A., and Gasca, R. (1999). Epipelagic euphausiids (Euphausiacea) and spring mesoscale features in the Gulf of Mexico. *Crustaceana* 72, 391–404. doi: 10.1163/156854099503456

Cohen, J. H., and Forward, R. B. Jr. (2009). Zooplankton diel vertical migration-a review of proximate control. *Oceanogr. Mar. Biol.* 47, 77–110.

Cuzin-Roudy, J. (2000). Seasonal reproduction, multiple spawning, and fecundity in northern krill, *Meganyctiphanes norvegica*, and Antarctic krill, *Euphausia superba*. *Can. J. Fish. Aquat. Sci.* 57, 6–15. doi: 10.1139/f00-165

Deagle, B. E., Gales, N. J., Evans, K., Jarman, S. N., Robinson, S., Trebilco, R., et al. (2007). Studying seabird diet through genetic analysis of faeces: a case study on macaroni penguins (*Eudyptes chrysolophus*). *PLoS One* 2:831. doi: 10.1371/journal.pone.0000831

Eldridge, P. J. (1988). The southeast area monitoring and assessment program (SEAMAP): a state federal-university program for collection, management, and dissemination of fishery-independent data and information in the southeastern United States. *Mar. Fish Rev.* 50, 29–39.

Feagans-Bartow, J. N., and Sutton, T. T. (2014). Ecology of the oceanic rim: pelagic eels as key ecosystem components. *Mar. Ecol. Prog. Ser.* 502, 257–266. doi: 10.3354/meps10707

Felder, D. L., and Camp, D. K., (2010). *Gulf of Mexico Origin, Waters, and Biota: Biodiversity*. College Station, TX: Texas A&M University Press.

Gasca, R., Castellanos, I., and Biggs, D. C. (2001). Euphausiids (Crustacea Euphausiacea) and summer mesoscale features in the Gulf of Mexico. *Bull. Mar. Sci.* 68, 397–408.

Gibbons, M. J., Spiridonov, V. A., and Tarling, G. A., (1999). "Euphausiacea," in *South Atlantic Zooplankton*, Vol. 2, ed. D. Boltovskoy, (Leiden: Backhuys Publishers)

Gómez-Gutiérrez, J., and Robinson, C. J. (2005). Embryonic, early larval development time, hatching mechanism and interbrood period of the sac-spawning euphausiid *Nyctiphanes simplex* Hansen. *J. Plankton Res.* 27, 279–295. doi: 10.1093/plankt/fbi003

Gulfbase.org (2012). *Resource Database for Gulf of Mexico Research*. Available at: http://www.gulfbase.org/facts.php

Hazen, T. C., Dubinsky, E. A., DeSantis, T. Z., Andersen, G. L., Piceno, Y. M., Singh, N., et al., (2010). Deep-sea oil plume enriches indigenous oil-degrading bacteria. *Science* 330, 204–208. doi: 10.1126/science.1195979

Hill, M. O. (1973). Diversity and evenness: a unifying notation and its consequences. *Ecology* 54, 427–432. doi: 10.2307/1934352

Hopkins, T. L., Gartner, J. V. Jr., and Flock, M. E. (1989). The caridean shrimp (Decapoda: Natantia) assemblage in the mesopelagic zone of the eastern Gulf of Mexico. *Bull. Mar. Sci.* 45, 1–14.

James, B. M., (1970). "Euphausiacean crustacea," in *Contributions on the Biology of the Gulf of Mexico*, eds W. E. Pequegnat, and F. A. Chase, Jr.(Houston: Gulf Publishing), 205–229.

Jayalakshmi, K. J., Jasmine, P., Muraleedharan, K. R., Prabhakaran, M. P., Habeebrehman, H., Jacob, J., et al. (2011). Aggregation of *Euphausia sibogae* during summer monsoon along the southwest coast of India. *J. Mar. Biol.* 10:945734. doi: 10.1155/2011/945734

Jayaraman, K. (1999). *A Statistical Manual for Forestry Research*. Bangkok: Food and Agricultural Organization of the United Nations, Regional Office for Asia and the Pacific, 1–231.

Jiang, Z., Huang, Y., Chen, Q., Zeng, J., and Xu, X. (2012). Acute toxicity of crude oil water accommodated fraction on marine copepods: the relative importance of acclimatization temperature and body size. *Mar. Environ. Res.* 81, 12–17. doi: 10.1016/j.marenvres.2012.08.003

Kinsey, S. T., and Hopkins, T. L. (1994). Trophic strategies of euphausiids in a low-latitude ecosystem. *Mar. Biol.* 118, 651–661. doi: 10.1007/bf00347513

Lindén, O. (1976). Effects of oil on the amphipod *Gammarus oceanicus*. *Environ. Pollut. (1970)* 10, 239–250. doi: 10.1016/j.toxicon.2013.11.015

Mikkelsen, P. (1987). The Euphausiacea of eastern Florida (Crustacea: Malacostraca). *Proc. Biol. Soc.* 100, 275–295.

Moore, H. B. (1950). The relation between the scattering layer and the Euphausiacea. *Biol. Bull.* 99, 181–212. doi: 10.2307/1538738

Murawski, S. A., Fleeger, J. W., Patterson, W. F., Hu, C., Daly, K., Romero, I., et al. (2016). How did the Deepwater Horizon oil spill affect coastal and continental shelf ecosystems of the Gulfof Mexico? *Oceanography* 29, 160–173. doi: 10.5670/oceanog.2016.80

Nichols, D. (2018). A Temporal Analysis of a Deep-Pelagic Crustacean Assemblage (Decapoda: Caridea: Oplophoridae and Pandalidae) in the Gulf of Mexico After the Deep Water Horizon Oil Spill. Ph.D. thesis, Nova Southeastern University, Fort Lauderdale, FL. doi: 10.2307/1538738

Omori, M., and Ikeda, T. (1984). Methods in marine zooplankton ecology. *J. Mar. Biol. Assoc. U. K.* 65, 562–894.

Reddy, C. M., Arey, J. S., Seewald, J. S., Sylva, S. P., Lemkau, K. L., Nelson, R. K., et al. (2011). Composition and fate of gas and oil released to the water column during the Deepwater Horizon oil spill. *Proc. Nat. Acad. Sci. U.S.A.* 109, 20229–20234. doi: 10.1073/pnas.1101242108

Reid, S. B., Hirota, J., Young, R. E., and Hallacher, L. E. (1991). Mesopelagic-boundary community in Hawaii: micronekton at the interface between neritic and oceanic ecosystems. *Mar. Biol.* 109, 427–440. doi: 10.1007/BF01313508

Roger, C. (1978). *Bioecological Sheets on Tropical Pacific Euphausiids.* Initiations – Documentations Techniques, Paris (ORSTOM) 36. Paris: IRD Editions, 1–81.

Romero, I. C., Sutton, T., Carr, B., Quintana-Rizzo, E., Ross, S. W., Hollander, D. J., et al. (2018). Decadal assessment of polycyclic aromatic hydrocarbons in mesopelagic fishes from the Gulf of Mexico reveals exposure to oil-derived sources. *Environ. Sci. Technol.* 52, 10985–10996. doi: 10.1021/acs.est.8b02243

Ryan, J. P., Zhang, Y., Thomas, H., Rienecker, E. V., Nelson, R. K., and Cummings, S. R. (1'2011). "A high-resolution survey of a deep hydrocarbon plume in the Gulf of Mexico during the 2010 Macondo blowout," in *Monitoring and Modeling the Deepwater Horizon Oil Spill: A Record-Breaking Enterprise. Geophysical Monograph Series*, Vol. 195, eds Y. Liu, A. Macfadyen, Z.-G. Ji, and R. H. Weisberg, 63–75. doi: 10.1029/2011GM001106

Schmidt-Nielsen, K. (1984). *Scaling: Why is Animal Size so Important?* Cambridge: Cambridge University Press.

Schramm, M. J. (2007). *Tiny Krill: Giants in Marine Food Chain. NOAA National Marine Sanctuary Program*. Available at: http://sanctuaries.noaa.gov/news/pdfs/sanctuarywatch/sw8_3.pdf (accessed December 12, 2013).

Springer, S., and Bullis, H. R. Jr. (1956). *Collections by the Oregon in the Gulf of Mexico. List of Crustaceans, Mollusks, and Fishes Identified From Collections Made by the Exploratory Fishing Vessel Oregon in the Gulf of Mexico and Adjacent Seas 1950 Through 1955*. United States Department of the Interior, Special Scientific Report, Fisheries, 196. Washington, DC: U.S. Department of the Interior, Bureau of Commercial Fisheries, 1–134.

Sutton, T. T. (2013). Vertical ecology of the pelagic ocean: classical patterns and new perspectives. *J. Fish. Biol.* 83, 1508–1527. doi: 10.1111/jfb.12263

Sutton, T. T., and Hopkins, T. L. (1996). Trophic ecology of the stomiid (Pisces: Stomiidae) fish assemblage of the eastern Gulf of Mexico: strategies, selectivity and impact of a top mesopelagic predator group. *Mar. Biol.* 127, 179–192. doi: 10.1007/bf00942102

Whitehead, A., Dubansky, B., Bodinier, C., Garcia, T.I, Miles, S., Pilley, C., et al. (2012). Genomic and physiological footprint of the Deepwater Horizon oil spill on resident marsh fishes. *Proc. Natl. Acad. Sci. U.S.A.* 109, 20298–20302. doi: 10.1073/pnas.1109545108

Wiebe, P. H., Burk, K. H., Boyd, S. H., and Morton, A. W. (1976). A multiple opening-closing net and environmental sensing system for sampling zooplankton. *J. Mar. Res.* 34, 313–326.

Conflict of Interest: The authors declare that the research was conducted in the absence of any commercial or financial relationships that could be construed as a potential conflict of interest.

frontiers in Marine Science

ORIGINAL RESEARCH
published: 21 February 2020
doi: 10.3389/fmars.2020.00047

Vertical Distribution Patterns of Cephalopods in the Northern Gulf of Mexico

Heather Judkins[1] and Michael Vecchione[2]*

[1] Department of Biological Sciences, University of South Florida St. Petersburg, St. Petersburg, FL, United States, [2] NMFS National Systematics Laboratory, National Museum of Natural History, Smithsonian Institution, Washington, DC, United States

Cephalopods are important in midwater ecosystems of the Gulf of Mexico (GOM) as both predator and prey. Vertical distribution and migration patterns (both diel and ontogenic) are not known for the majority of deep-water cephalopods. These varying patterns are of interest as they have the potential to contribute to the movement of large amounts of nutrients and contaminants through the water column during diel migrations. This can be of particular importance if the migration traverses a discrete layer with particular properties, as happened with the deep-water oil plume located between 1000 and 1400 m during the Deepwater Horizon (DWH) oil spill. Two recent studies focusing on the deep-water column of the GOM [2011 Offshore Nekton Sampling and Analysis Program (ONSAP) and 2015–2018 Deep Pelagic Nekton Dynamics of the Gulf of Mexico (DEEPEND)] program, produced a combined dataset of over 12,500 midwater cephalopod records for the northern GOM region. We summarize vertical distribution patterns of cephalopods from the cruises that utilized a 10 m^2 Multiple Opening/Closing Net and Environmental Sensing System (MOC10). About 95% of the cephalopods analyzed here either move through or live within 1000–1400 m zone. Species accounts include those with synchronous (e.g., *Pterygioteuthis* sp.) and asynchronous (e.g., *Stigmatoteuthis arcturi*) vertical migration. Non-migration patterns of some midwater cephalopods (e.g., *Vampyroteuthis infernalis*) are also highlighted. Ontogenic shifts are noted for some species examined.

Keywords: squid, octopod, vertical migration, DEEPEND, Deepwater Horizon, deep-sea, development

OPEN ACCESS

Edited by:
Jose Angel Alvarez Perez, Universidade do Vale do Itajaí, Brazil

Reviewed by:
Helena Passeri Lavrado, Federal University of Rio de Janeiro, Brazil
Richard Schwarz, GEOMAR Helmholtz Centre for Ocean Research Kiel, Germany

****Correspondence:***
Heather Judkins
Judkins@mail.usf.edu

Specialty section:
This article was submitted to Deep-Sea Environments and Ecology, a section of the journal Frontiers in Marine Science

Received: *17 August 2019*
Accepted: *24 January 2020*
Published: *21 February 2020*

Citation:
Judkins H and Vecchione M (2020) Vertical Distribution Patterns of Cephalopods in the Northern Gulf of Mexico. Front. Mar. Sci. 7:47. doi: 10.3389/fmars.2020.00047

INTRODUCTION

The Deepwater Horizon (DWH) oil spill generated one of the largest oil spill responses to date, including millions of dollars allocated to scientific research to examine the impacts of this devastating event (i.e., Gulf of Mexico Research Initiative, NAS Gulf Research Program). It was not only a blowout that affected the seafloor immediately surrounding the wellhead, the surface, and coastline, but also a midwater event. One of the questions post-spill was "Where has all the oil gone"? Passow and Hetland (2016) determined that a deep plume of trapped oil formed between 1000 and 1400 m depth (Socolofsky et al., 2011) due to the petrocarbons that became neutrally buoyant in seawater at that depth. This contaminated layer dispersed from the site via subsurface

currents that impinged on the continental slope of the region, leaving extensive oiled sediment (Romero et al., 2015).

Two comprehensive, long-term programs established post-spill have examined the faunal groups found within the water column (0–1500 m) in the northern Gulf of Mexico (GOM). The Offshore Nekton Sampling and Analysis Program (ONSAP) and the Deep Pelagic Nekton Dynamics of the Gulf of Mexico (DEEPEND) consortium have compiled an immense dataset for midwater fauna over a period of 8 years (2011–2018) examining biodiversity and contaminant questions about multiple deep-water pelagic faunal groups (Judkins et al., 2016; Burdett et al., 2017; Richards et al., 2018; Romero et al., 2018).

Historically, the oceanic midwater environment has received little attention (Webb et al., 2010), as it is very difficult to study. However, it is the largest biome on Earth (Robison, 2004; Sutton, 2013). Past deep-sea cephalopod inventories include work conducted using various methods such as closing-net systems as well as large, open trawl nets (Nesis, 1972, 1993; Lu and Clarke, 1975a,b; Young, 1978; Vecchione and Pohle, 2002; Judkins et al., 2016). Recently, remotely operated vehicles have been used to collect precise observations on vertical distribution and other properties (Vecchione et al., 2001; Widder et al., 2005; Robison et al., 2017).

Another, less direct technique that has been utilized to assess cephalopod biodiversity and distributional patterns is the examination of stomach contents from predators. Cephalopods are major prey items for many vertebrates, including seabirds, large tunas and billfishes, and marine mammals (Summers, 1983; Williams, 1995; Lansdell and Young, 2003; Xavier et al., 2018). These studies have examined gut contents and through knowledge of the predators and their migrations and feeding grounds, inferred cephalopod distributions, both spatially as well as vertically.

While faunal inventories and indirect methods to assess deep-sea cephalopod diversity and distribution are important, few vertical distribution patterns have been compiled. Efforts in the 1970s reported vertical distribution of cephalopods in various regions (Clarke and Lu, 1975; Lu and Clarke, 1975a,b; Roper and Young, 1975; Young, 1978). Since that time, vertical distribution patterns have been documented for various zooplankton groups such as fish larvae and cephalopod paralarvae (Hopkins, 1982; Ropke et al., 1993; Salman et al., 2003) but larger specimens have not been included. There are approximately 700 species of cephalopods worldwide (Young et al., 2019) with great morphological and genetic variation among the families, especially those of oceanic habitats. Vertical distribution patterns vary among cephalopod taxa and developmental stages.

The deep oil plume of the DWH oil spill was detected in May, 2010 (Dierks et al., 2010) and persisted for months after that (Camilli et al., 2010; Joye et al., 2011; Reddy et al., 2014) as a horizontal plume that moved toward the southwest with deep-water currents (Melvin et al., 2016). There was also an anomaly of low dissolved oxygen observed at depths of 1100–1200 m below the surface (Kessler et al., 2011). This deep-water oil plume exposed any meso- and/or bathypelagic organisms living in or moving through this plume to potential toxicity.

In light of the need to know which cephalopods may have been exposed to the deep oil plume, as well as a need for comprehensive accounts on deep-sea species, this study reports on 39 cephalopod species from the northern GOM, examining the following questions: (1) How many species move through or are found within the deep oil plume located between 1000 and 1400 m? (2) What are the vertical distribution patterns of deep-sea cephalopods in water column of the northern GOM and how does this relate to past accounts of these species? (3) Are there developmental shifts in vertical distribution of these cephalopods?

MATERIALS AND METHODS

Two midwater sampling programs provided all material for this analysis. ONSAP (2011) and the DEEPEND (2015–2018) programs sampled in the northern GOM (**Figure 1**). A 10 m^2 Multiple Opening and Closing Net and Environmental Sensing System (MOC10) (Wiebe et al., 1976) with 3 mm mesh was used by both programs (as described in DEEPEND, 2015). The following depths were targeted on each MOC10 tow during both cruise programs: 1200–1500, 1000–1200, 600–1000, 200–600, and 0–200 m at all 169 stations where cephalopods were collected and tows quantified. Sampling depths were chosen based on the following premise: 1200–1500 m was a depth range below where a subsurface hydrocarbon plume was detected during the initial spill; 1000–1200 m fished through the hydrocarbon plume (Reddy et al., 2012); 600–1000 m fished where the vertically migrating species are known to reside during the day; 200–400 m fished where vertical migrators are known to move through during daily migrations; and 0–200 m fished the epipelagic zone where vertical migrators gather at night (Burdett et al., 2017). Sampling was conducted twice at each station per cruise (∼solar noon and ∼midnight).

Three thousand seven hundred and thirty cephalopods were documented using the MOC10 from both programs. Flow metering on the trawls allowed inference of the amount of water filtered through each net and these were used to standardize abundance per volume of water per tow. The 2150 specimens included in the analyses here were those individuals collected in quantifiable trawl tows. Specimens were measured and identified to species level when possible at sea and either sampled for molecular projects (i.e., Sosnowski, 2017; Timm et al., 2020), frozen, or preserved (10% formalin). Identifications were verified or corrected post-cruise. Non-parametric Kruskal–Wallis analyses were conducted to compare the standardized abundances of the six most abundant species (**Table 1**) among depth bins, day vs. night.

The vertical distribution plots (VDP) include 2150 individuals while the ontogenic shift plots (OSP) include 1820 individuals. The numbers vary between the two analyses due to the lack of measurable size (dorsal mantle length) for the ontogenic shift analyses because of collecting damage to some specimens. Plots of vertical migration and ontogenic shifts were created using the R program (**Figures 3–10** and **Supplementary Materials A, B**)

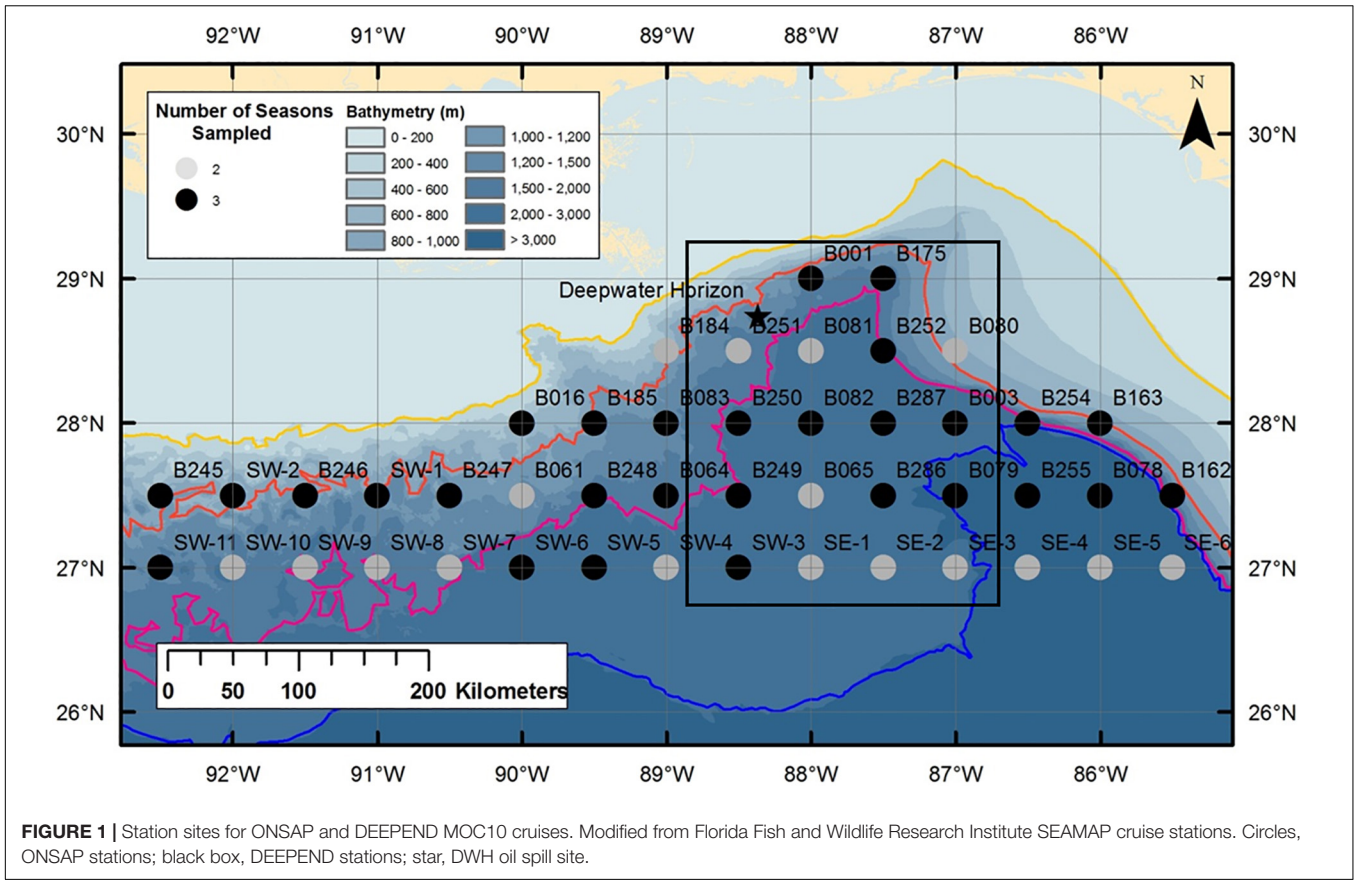

FIGURE 1 | Station sites for ONSAP and DEEPEND MOC10 cruises. Modified from Florida Fish and Wildlife Research Institute SEAMAP cruise stations. Circles, ONSAP stations; black box, DEEPEND stations; star, DWH oil spill site.

(R Core Team, 2013). VDP's were created for cephalopod species where possible and species were grouped according to their VDP patterns (**Figures 3–7** and **Supplementary Material A**). These groups are based on patterns identified for deep-water fishes of the GOM by T. Sutton (unpublished).

We felt it important to include rare species as **Supplementary Material** because reports from multiple projects will eventually allow enough published information to accumulate for ecological patterns to be discerned (Vecchione and Pohle, 2002). We arbitrarily chose 20 individuals as an adequate number of individuals to include in VDP and OSP descriptions.

RESULTS

Cephalopods are found throughout the water column with the mesopelagic zone containing more individuals than the epipelagic or the upper bathypelagic zones (**Figure 2**). Of the 39 species examined for this analysis, 37 species (95%) are found to either live within or move through the 1000–1400 m depth zone (**Table 1**). Occupancy of this zone varied among species (i.e., 2 of 70 *Abralia redfieldi* individuals vs. 21 of 39 *Bathyteuthis* sp. individuals, **Table 1**).

The DEEPEND team is in the process of analyzing vertical distribution patterns for multiple faunal groups including fishes, crustaceans, gelatinous organisms, and cephalopod, pteropod, and heteropod mollusks[1]. T. Sutton et al. (unpublished) examined distributional data for oceanic fishes and the results revealed seven major diel vertical patterns for the 151 fish taxa examined. Based on plots of diel vertical distribution, we grouped cephalopods into six of the seven possible vertical-distributional patterns following T. Sutton et al. (unpublished). Although these patterns were visually obvious in the pooled samples presented in the figures, the Kruskal–Wallis analyses of the underlying data failed to reject the null hypothesis of no statistically significant differences in diel patterns in vertical distribution even for the six most abundant species (**Table 2**). This is likely because of high within-group variance (i.e., variance in abundance among samples within day and night depth bins) not obvious in the pooled figures.

Based on visual assessment of pooled samples, six species were holoepipelagic non-migrators with centers of abundance the upper 200 m day and night (**Figure 3** and **Supplementary Material A**). The seven nyctoepipelagic synchronous vertically migrating species inhabit the meso- and/or the bathypelagic zones during the day and migrate to the epipelagic zone nightly (**Figure 4**). The 14 species of mesopelagic asynchronous vertical migrators are found primarily in the mesopelagic during the day and move into or between the epi- or the upper mesopelagic at night (**Figures 5**, **7** and **Supplementary**

[1]http://www.deependconsortium.org/images/documents/publications_1-12-18.pdf

TABLE 1 | Midwater cephalopods ordered by abundance; total individuals examined; mantle length range; evidence of vertical migration; evidence of ontogenic shift; percent of species that was found between 1000 and 1400 m.

Species	Total # individuals	Mantle length range (mm ML)	Vertical migration Y/N/weak	Ontogenic shift Y/N/weak	% total located between 1000 and 1400 m
Cranchia scabra	353	4–115	N	N	11
Vampyroteuthis infernalis	157	4–135	N	N	44
Japetella diaphana	153	5–92	N	Y	37
Leachia atlantica	110	7–80	N	N	38
Pyroteuthis margaritifera	106	8–33	Y	Y	17
Stigmatoteuthis arcturi	102	2–69	Y	N	13
Mastigoteuthis agassizii	82	13–110	N	Weak	48
Bolitaena pygmaea	77	6–64	N	Y	43
Abralia redfieldi	70	5–13	Y	N	1
Onychoteuthis banksii	61	4–326	W	Y	13
Grimalditeuthis bonplandi	53	6–84	N	Weak	49
Histioteuthis corona	50	6–46	Y	N	28
Pterygioteuthis gemmata	45	6–28	Y	N	<1
Chiroteuthis sp.	42	6–121	Y/W	N	19
Pterygioteuthis giardi	40	6–37	Y	N	<1
Octopoteuthis sp.	40	5–100	Y	W	<1
Ornithoteuthis antillarum	39	5–40	Y	W	18
Bathyteuthis sp.	39	6–72	N	N	54
Selenoteuthis scintillans	37	8–29	Y	Y	<1
Abraliopsis atlantica	35	6–27	Y	N	<1
Argonauta argo	35	3–7	N	N	1
Brachioteuthis sp.	35	6–47	N	N	11
Helicocranchia pfefferi	32	10–59	N	Y	20
Helicocranchia sp. *A*	31	6–44	N	Y	35
Haliphron atlanticus	29	4–32	N	Y	10
Heteroteuthis dagamensis	27	3–15	Y	N	11
Discoteuthis discus	22	6–50	Y	N	<1
Sandalops melancholicus	20	7–46	N	Y	15
Joubiniteuthis portieri	19	5–159	N	N	21
Cycloteuthis sirventi	18	9–28	N	N	22
Sthenoteuthis pteropus	18	5–25	N	W	11
Macrotritopus defilippi	17	4–12	N	N	18
Walvisteuthis jeremiahi	17	5–24	N	Y	N/A
Bathothauma lyromma	16	5–82	N	W	31
Taningia danae	12	7–34	W	W	N/A
Galiteuthis armata	11	12–53	N	Y	82
Chtenopteryx sicula	10	7–15	Y	W	10
Hyaloteuthis pelagica	9	4–8	N/A	N	22
Ancistrocheirus lesueurii	7	4–18	N/A	N/A	29

Material A). *Chtenopteryx sicula* is placed as a mesopelagic non-migrator (**Supplementary Material A**). There is one species, *Joubiniteuthis portieri*, that falls into the deep meso-/bathypelagic asynchronous migrator category (**Supplementary Material A**). The seven deep-meso/bathypelagic non-migrating species are found between 600 and >1000 m depth during the day and night (**Figure 6** and **Supplementary Material A**). Two squid species (*Leachia atlantica*, *Sandalops melancholicus*) do not fit into a described pattern and are labeled as "unclassified" here (**Figure 7**). The nine species with less than 20 individuals are found in the **Supplementary Material**.

Ontogenic shift plots' were created (**Figures 8–10** and **Supplementary Material B**) and patterns reveal that seven cephalopod species descend deeper as they develop (**Figure 8**). Sixteen species show no evidence of ontogenic shift (**Figures 9A,B**). There are three species for which it appears that the adults live closer to the surface whereas smaller individuals inhabit a deeper zone (**Figure 10**). Those OSP's with less than 20 individuals examined can be found in **Supplementary Material B** (13 species).

Table 1 summarizes the number of individuals included for each VDP, OSP, mantle length (ML) range, whether a species

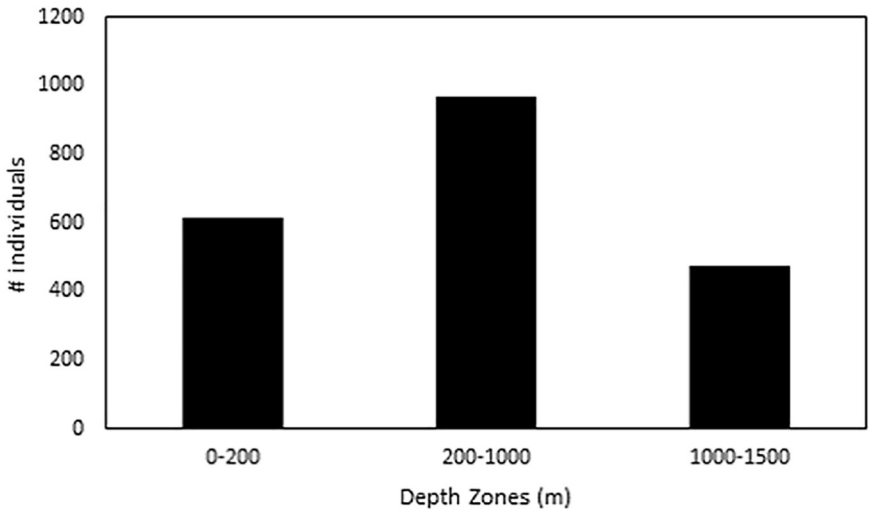

FIGURE 2 | Total cephalopod distribution divided into ocean zones from 0 to 1500 m depth.

is considered a vertical migrator and the percentage of the species that was found between 1000 and 1400 m. Caution is important when using this analysis because the sample sets in some cases are small. Kruskal–Wallis analyses did not reveal any statistically significant results with regard to distributional differences between day and night even for the six most abundant species (**Table 2**).

Family Accounts

Vampyroteuthidae

Among 157 *Vampyroteuthis infernalis* individuals, the majority were below 600 m both day and night (4–135 mm ML). Two individuals (ML = 5 mm, 7 mm) were found between 200 and 600 m. We do not believe that this depth layer is characteristic of juveniles as over 30 individuals of similar MLs found between 600 and 1500 m. Vampires are non-migrators and do not appear to exhibit an ontogenic shift during their life history (**Figures 6**, **9**).

Alloposidae

Twenty-nine *Haliphron atlanticus* were collected from the surface layer down to 1200 m. Mantle lengths ranged from 4 to 32 mm with no evidence of diel vertical migration. Larger *H. atlanticus* were found in the upper layers (**Figures 5**, **10**).

Argonautidae

Thirty-five individuals (3–7 mm ML) were examined for the VDP (**Figures 3**, **9**). Nine were collected during day tows and 26 collected at night. *Argonauta argo* were found in the surface layer both day and night but also down to 1500 m deep. They are classified as holoepipelagic non-migrators here but it should be noted with more sampling, a vertical migration pattern may become apparent. There is no evidence of ontogenic shift.

Octopodidae

Only 5 of 17 *Macrotritopus defilippi* paralarvae (4–12 mm ML) were collected in day tows at the surface (0–200 m) while during the night tows, 12 specimens were collected from 0 to 1500 m. They appear to be holoepipelagic non-migrators (**Figure 3**). Additional material needs to be collected to make firm conclusions on vertical migration and any possible ontogenic shift (**Supplementary Material B**).

Amphitretidae

Seventy-seven *Bolitaena pygmaea* (6–64 mm ML) are distributed from 0 to 1500 m with no diel migration pattern observed. They do shift to deeper water as they develop with all individuals larger than 20 mm ML caught below 600 m (**Figures 6**, **8**). One hundred fifty-three *Japetella diaphana* (5–92 mm ML) follow a similar pattern, with no obvious diel migration pattern, and those larger than 26 mm ML living below 600 m, with one exception where a 44 mm ML specimen was collected between 0 and 200 m (**Figures 6**, **8**). For both species, the peak abundance both day and night was in the 600–1000 m depth zone.

Brachioteuthidae

Thirty-five *Brachioteuthis* sp. (6–47 mm ML) were available for examination of vertical migration and possible ontogenic shifts. Brachioteuthids were found throughout the water column (0–1500 m) during day and night. There is no

TABLE 2 | Results of Kruskal–Wallis test comparing day/night standardized abundances per species per depth bin.

Species	Kruskal–Wallis H	df	Significance
Cranchia scabra	5.782	4	0.216
Japetella diaphana	8.400	4	0.078
Leachia atlantica	4.473	4	0.346
Pyroteuthis margaritifera	5.782	4	0.216
Stigmatoteuthis arcturi	6.545	4	0.162
Vampyroteuthis infernalis	7.354	4	0.118

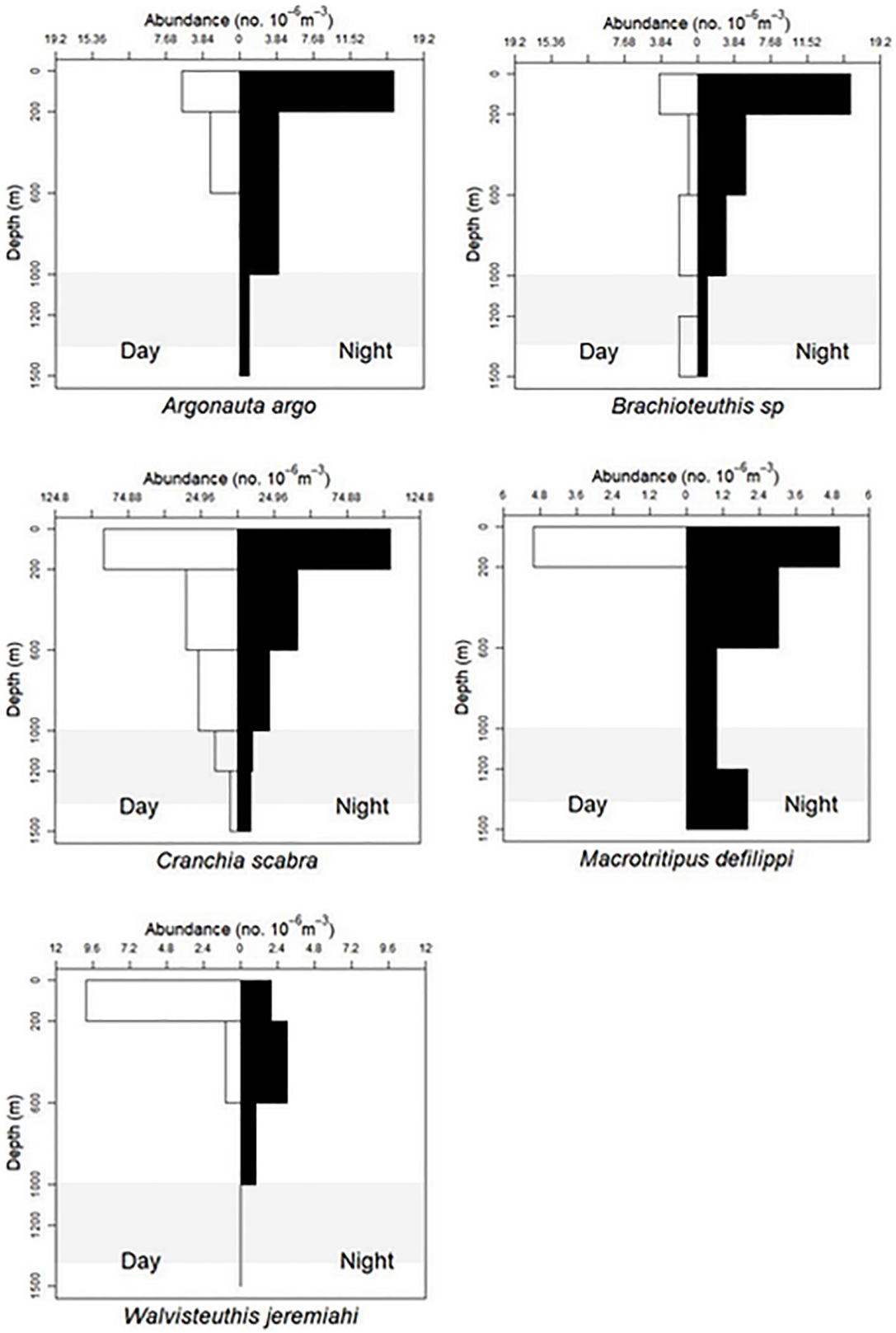

FIGURE 3 | Vertical distribution patterns of five cephalopods. Holoepipelagic non-migration pattern described by T. Sutton et al. (unpublished). *A. argo*, *n* = 35; *Brachioteuthis* sp., *n* = 35; *C. scabra*, *n* = 353; *M. defilippi*, *n* = 17; *W. jeremiahi*, *n* = 17; shaded region indicates the deep oil plume zone.

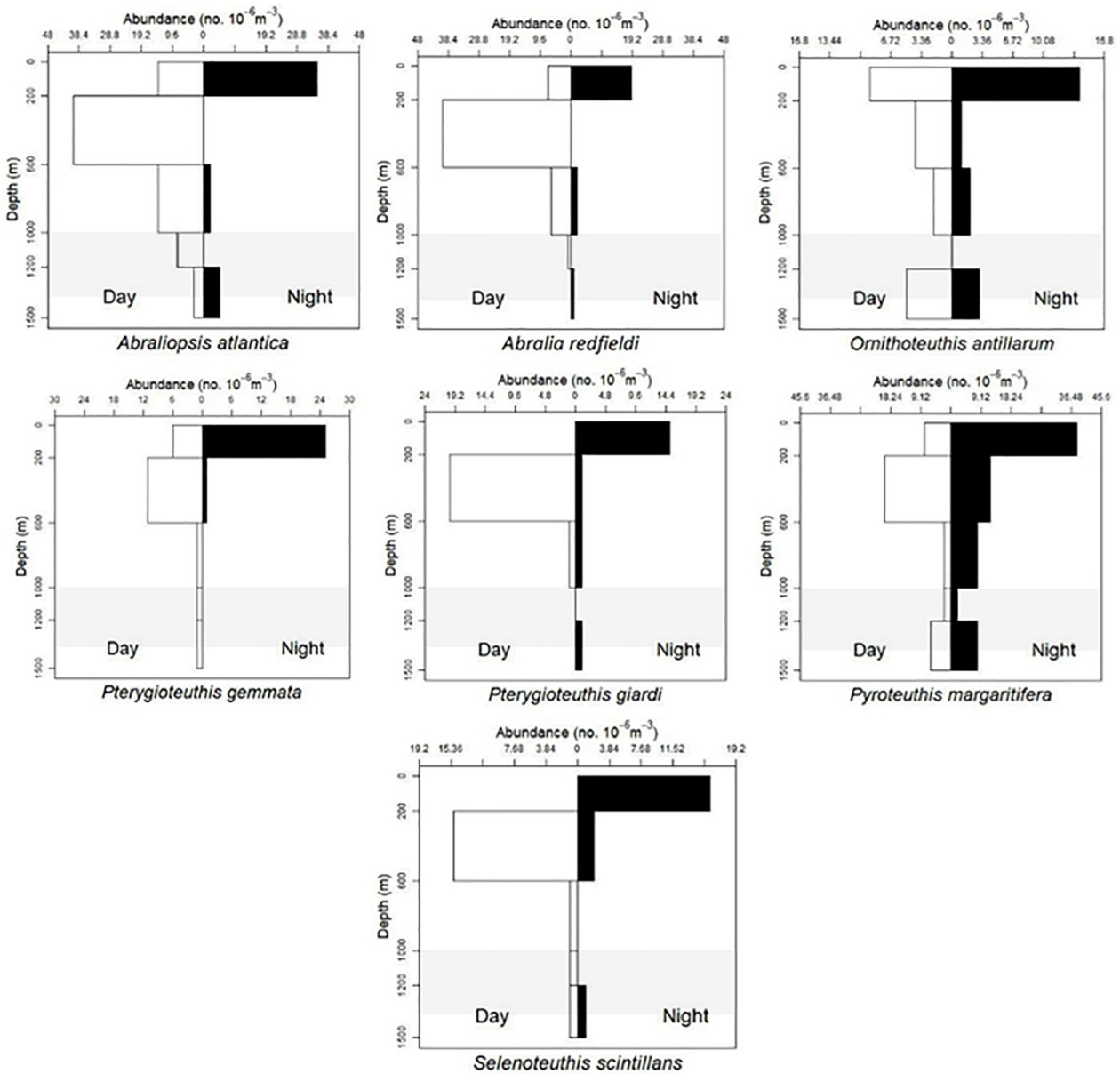

FIGURE 4 | Vertical distribution patterns of seven cephalopods. Nyctoepipelagic synchronous diel migration described by T. Sutton et al. (unpublished). *A. atlantica*, $n = 32$; *A. redfieldi*, $n = 70$; *O. antillarum*, $n = 39$; *P. gemmata*, $n = 45$; *P. giardi*, $n = 40$; *P. margaritifera*, $n = 106$; *S. scintillans*, $n = 37$; shaded region indicates the deep oil plume zone.

evidence in this analysis of vertical migration or ontogenic shift (**Figures 3**, **9**).

Chiroteuthidae

Forty-two *Chiroteuthis* sp. (6–121 mm ML) showed that individuals were caught from 0 to 1500 m during the day and from 0 to 1200 m during the night (**Figure 5**). There is some evidence of diel vertical migration but plots would need to be broken out by species for further clarification. We found no evidence of ontogenic shift for this genus (**Supplementary Material B**). Fifty-three *Grimalditeuthis bonplandi* (6–84 mm ML) were analyzed. They were found from the surface to 1500 m during day and night with the majority of individuals found between 600 and 1500 m. We found no evidence of vertical migration but an ontogenic shift for this species is evident, with larger individuals found in the lower meso- and upper bathypelagic zones (**Figures 6**, **8**).

Joubiniteuthidae

Nineteen *J. portieri* (5–159 mm ML) documented the species living throughout the water column; six were found

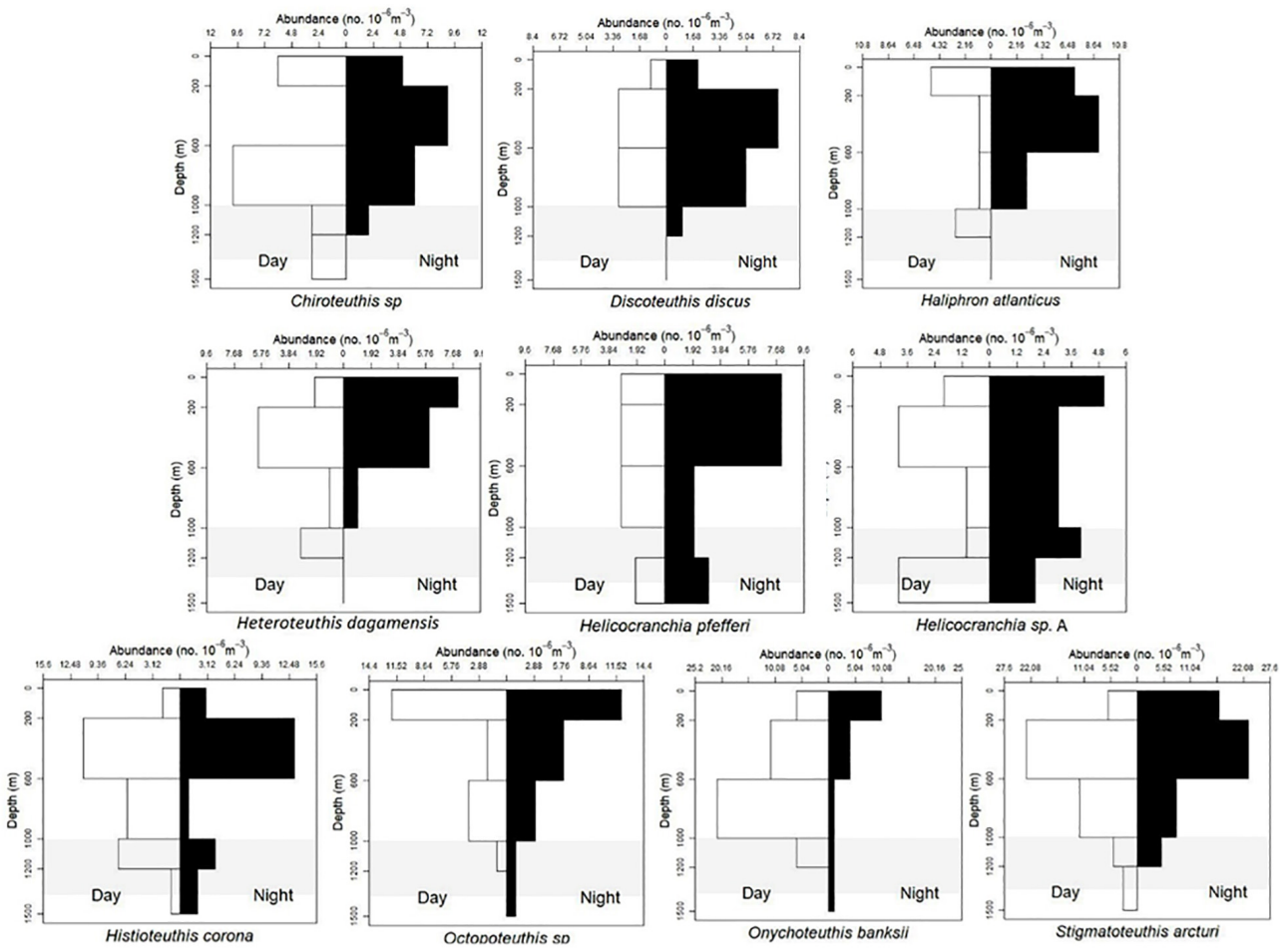

FIGURE 5 | Vertical distribution patterns of 10 cephalopods. Mesopelagic asynchronous migrators as described by T. Sutton et al. (unpublished). *Chiroteuthis* sp., $n = 42$; *Discoteuthis* sp., $n = 22$; *H. atlanticus*, $n = 29$; *H. dagamensis*, $n = 27$; *Helicocranchia* sp. A, $n = 31$; *H. pfefferi*, $n = 32$; *H. corona*, $n = 50$; *O. banksii*, $n = 61$; *S. arcturi*, $n = 102$; *S. melancholicus*, $n = 20$; *Cycloteuthis sirventi*, $n = 18$; *Sthenoteuthis pteropus*, $n = 18$; *Octopoteuthis* sp., $n = 40$; shaded region indicates the deep oil plume zone.

in day tows inhabiting the upper and lower mesopelagic zone while thirteen individuals were collected at night from the surface to 1500 m. There is some evidence of vertical migration but no ontogenic shift for this species (**Supplementary Materials A, B**).

Mastigoteuthidae

The majority of *Mastigoteuthis agassizii* (13–110 mm ML) were found below 600 m. They are deep meso-/bathypelagic non-migrators. There appears to be a weak ontogenic shift to deeper water as this species becomes larger (**Figures 6**, **8**).

Cranchiidae

Three hundred fifty-three *Cranchia scabra* (4–115 mm ML) were used for the VDP and the ontogenic shift analysis. They are found distributed between 0 and 1500 m. There is no evidence of vertical migration or ontogenic shift for this species (**Figures 3**, **9**).

Leachia atlantica (7–80 mm ML) demonstrate a non-migration vertical pattern ($n = 110$) as they are found at all depths (**Figure 7**). They are currently placed as "unclassified" here. There is no evidence of ontogenic shift (**Figures 9A,B**).

Thirty-two *Helicocranchia pfefferi* (10–59 mm ML) were included in the VDP, which showed individuals distributed throughout the water column both day and night with some weak diel vertical migration occurring at the deeper depths (**Figure 5**). There does not appear to be an ontogenic shift for this species (**Figures 9A,B**). The VDP and ontogenic shift patterns for a currently undescribed *Helicocranchia* species, *Helicocranchia* sp. A (6–44 mm ML) show the same diel vertical distribution pattern but the species does appear to move deeper in the water column as it develops (**Figures 5**, **8**).

The diel vertical distribution of sixteen *Bathothauma lyromma* (5–82 mm ML) was skewed, as there were 12 collected during day tows but only four individuals captured at night. This species was found throughout the water column during the day and deeper depths (below

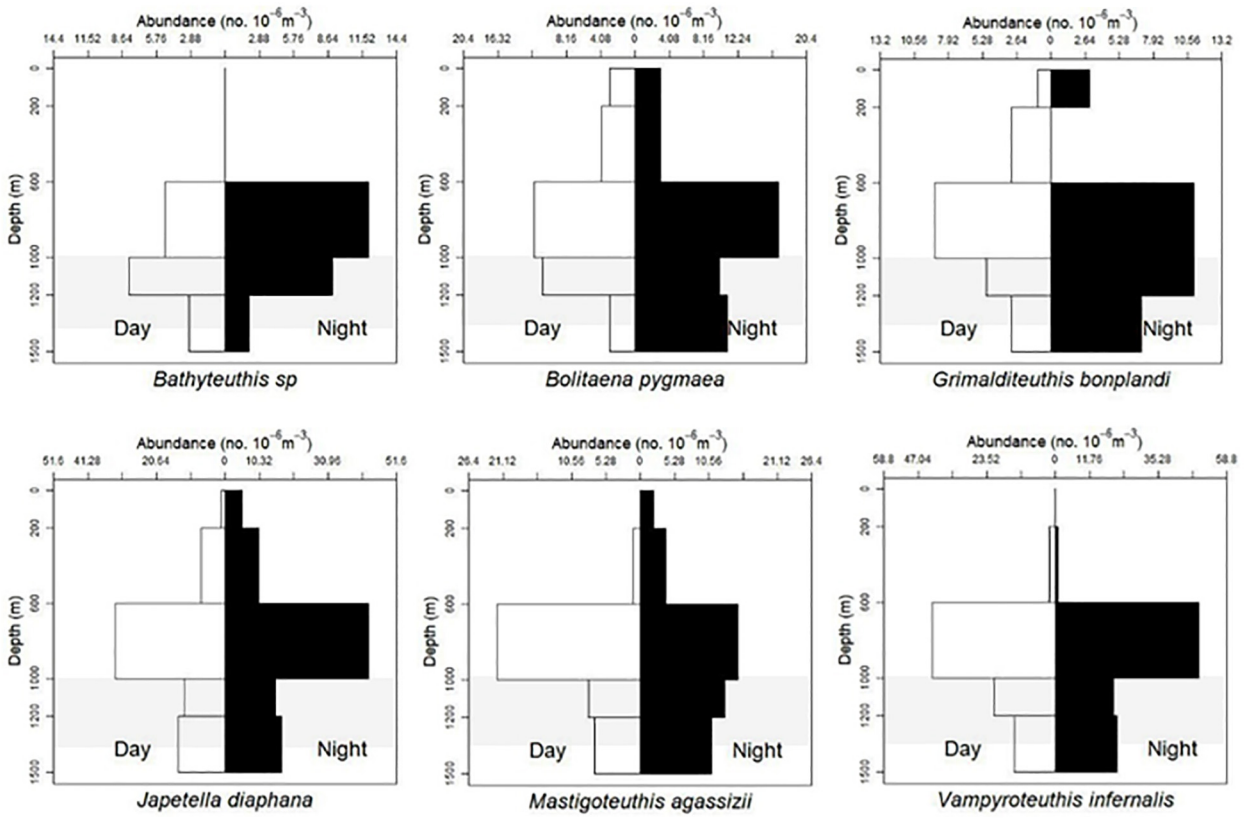

FIGURE 6 | Vertical distribution of six cephalopods. Deep-meso/bathypelagic non-migration as described by T. Sutton et al. (unpublished). *Bathyteuthis* sp., *n* = 39; *B. pygmaea*, *n* = 77; *G. bonplandi*, *n* = 53; *J. diaphana*, *n* = 153; *M. agassizii*, *n* = 82; *V. infernalis*, *n* = 157; shaded region indicates the deep oil plume zone.

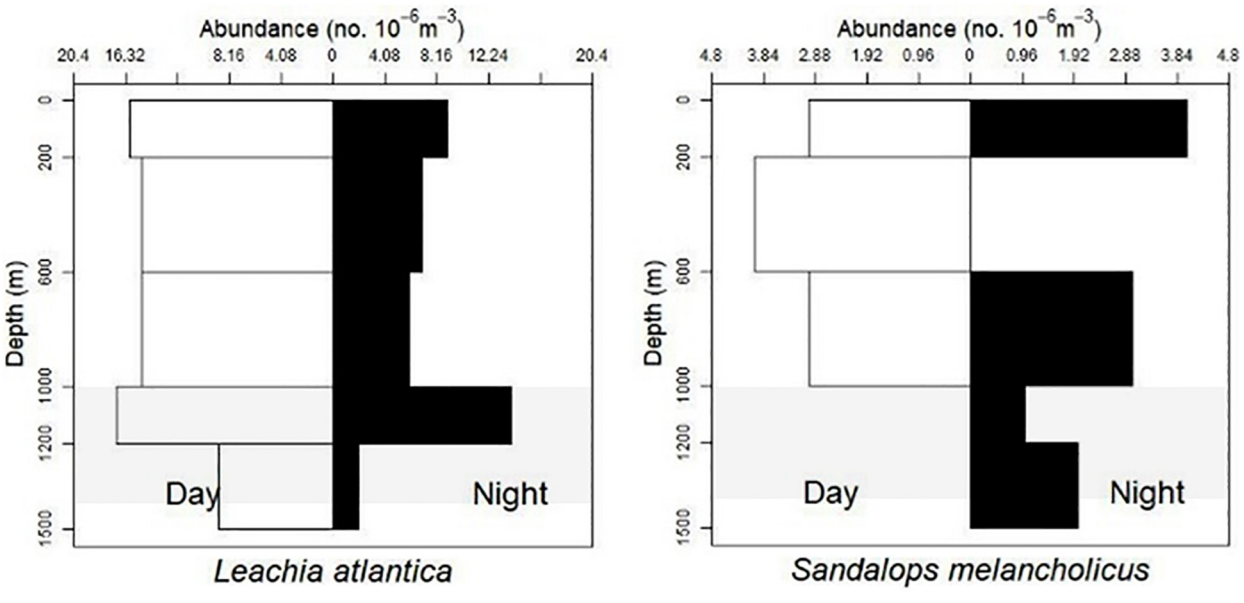

FIGURE 7 | Vertical distribution patterns unclassified. *L. atlantica*, *n* = 110; *S. melancholicus*, *n* = 20; shaded region indicates the deep oil plume zone.

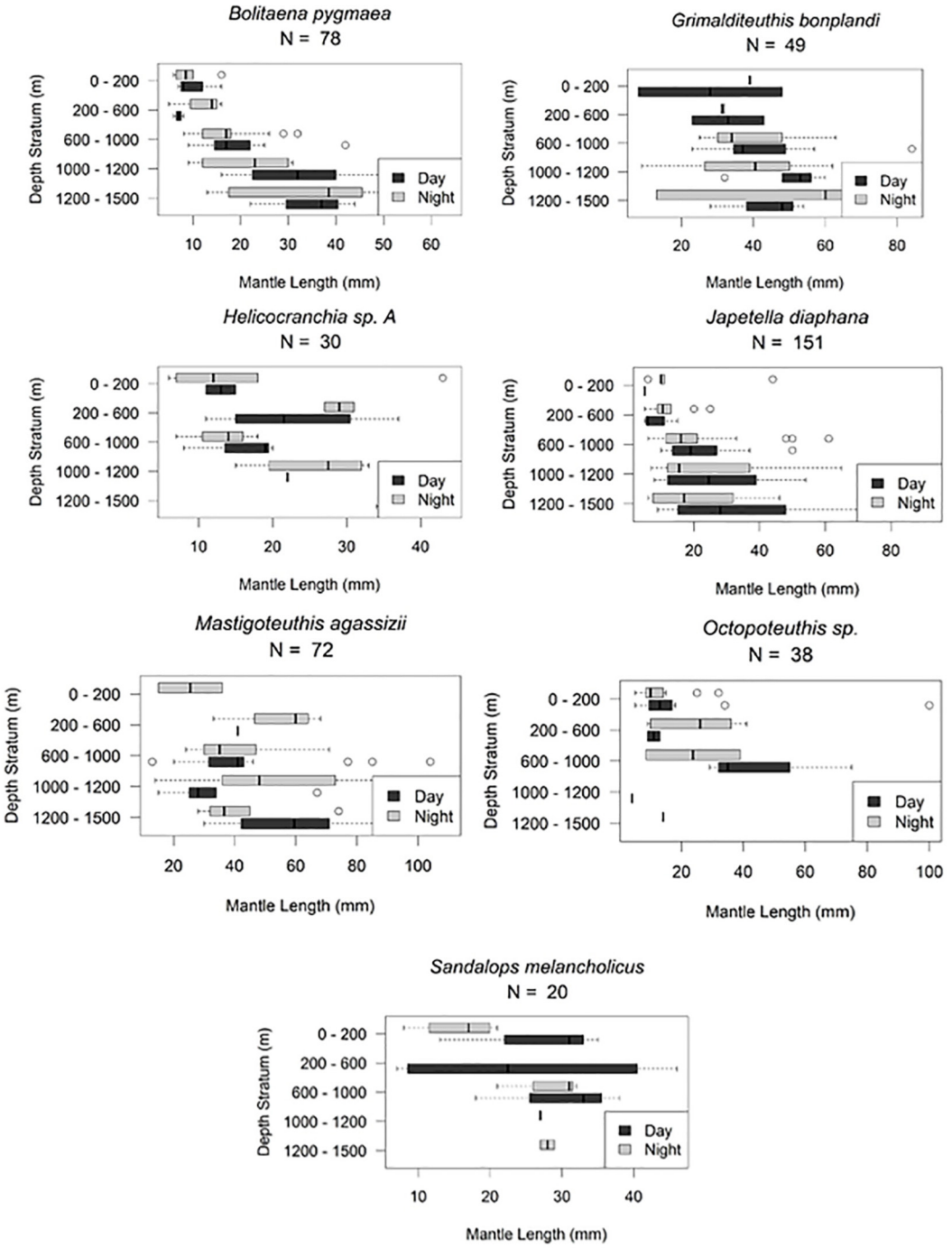

FIGURE 8 | Cephalopod ontogenic shift patterns demonstrating a shift deeper as these species develop. Horizontal line, median; box limits, 1st and 3rd quartiles; circles, outliers.

600 m) at night. A weak ontogenic shift was noted for this species but more material is required to confirm this pattern (**Supplementary Materials A, B**).

The distribution of 20 *S. melancholicus* (7–46 mm ML) encompasses the water column from 0 and 1500 m with no evidence of diel vertical pattern within this small sample set. There appears to be an ontogenic shift with larger animals found at deeper depths (**Figures 7**, **8**).

Eleven *Galiteuthis armata* (12–53 mm ML) were considered for this analysis. All individuals were found between 600 and 1500 m with no evidence of vertical migration. There appears to be an ontogenic shift by this species

(>12 mm ML) but additional material is needed to confirm this (**Supplementary Materials A, B**).

Cycloteuthidae

Cycloteuthis sirventi (*n* = 18) are distributed throughout the water column from 0 to 1500 m depth with more collected during night tows than day tows (9–28 mm ML) (**Supplementary Materials A, B**). *Discoteuthis discus* (*n* = 22) was also documented from the surface to 1200 m and is a mesopelagic asynchronous migrator (6–50 mm ML). No ontogenic shift was apparent for either taxon (**Figure 5** and **Supplementary Material B**).

Ancistrocheiridae

Preliminary findings indicate that *Ancistrocheirus lesueurii* (4–18 mm ML) is found throughout the water column from 0 to 1500 m. Additional records are needed to confirm any pattern of vertical distribution or ontogenic shift as there are only seven specimens available for analysis (**Supplementary Materials A, B**).

Enoploteuthidae

Thirty-five *Abraliopsis atlantica* (6–27 mm ML) and 70 *A. redfieldi* (5–13 mm ML) were plotted and both species are found from 0 to 1500 m. Both are nyctoepipelagic synchronous vertical migrators, living primarily at mesopelagic depths during the day and moving up to the epipelagic zone nightly (**Figure 4**). However, there is no evidence of ontogenic shift for either species (**Figures 9A,B**).

Lycoteuthidae

Selenoteuthis scintillans (8–29 mm ML) are nyctoepipelagic synchronous vertical migrators, moving from mainly the upper mesopelagic zone to the epipelagic zone nightly (*n* = 37). Larger individuals are found in the upper mesopelagic zone (**Figures 4**, **9**).

Pyroteuthidae

One hundred and six *Pyroteuthis margaritifera* (8–33 mm ML) were distributed throughout the water column (0–1500 m) both day and night but overall they are nyctoepipelagic synchronous migrators, with the majority of the population found in the upper mesopelagic zone during daytime and moving to the epipelagic zone nightly (**Figure 4**). Smaller individuals were living at depth whereas larger individuals were shallower (**Figure 10**).

Pterygioteuthis gemmata (6–28 mm ML) were also found mainly in the upper mesopelagic zone in daytime, migrating nightly to the epipelagic zone (**Figure 4**). *Pterygioteuthis giardi* (6–37 mm ML) is also a nyctoepipelagic synchronous migrator (**Figure 4**). Neither of these species appear to undergo an ontogenic shift during development (**Figures 9A,B**) within the limits of our methods.

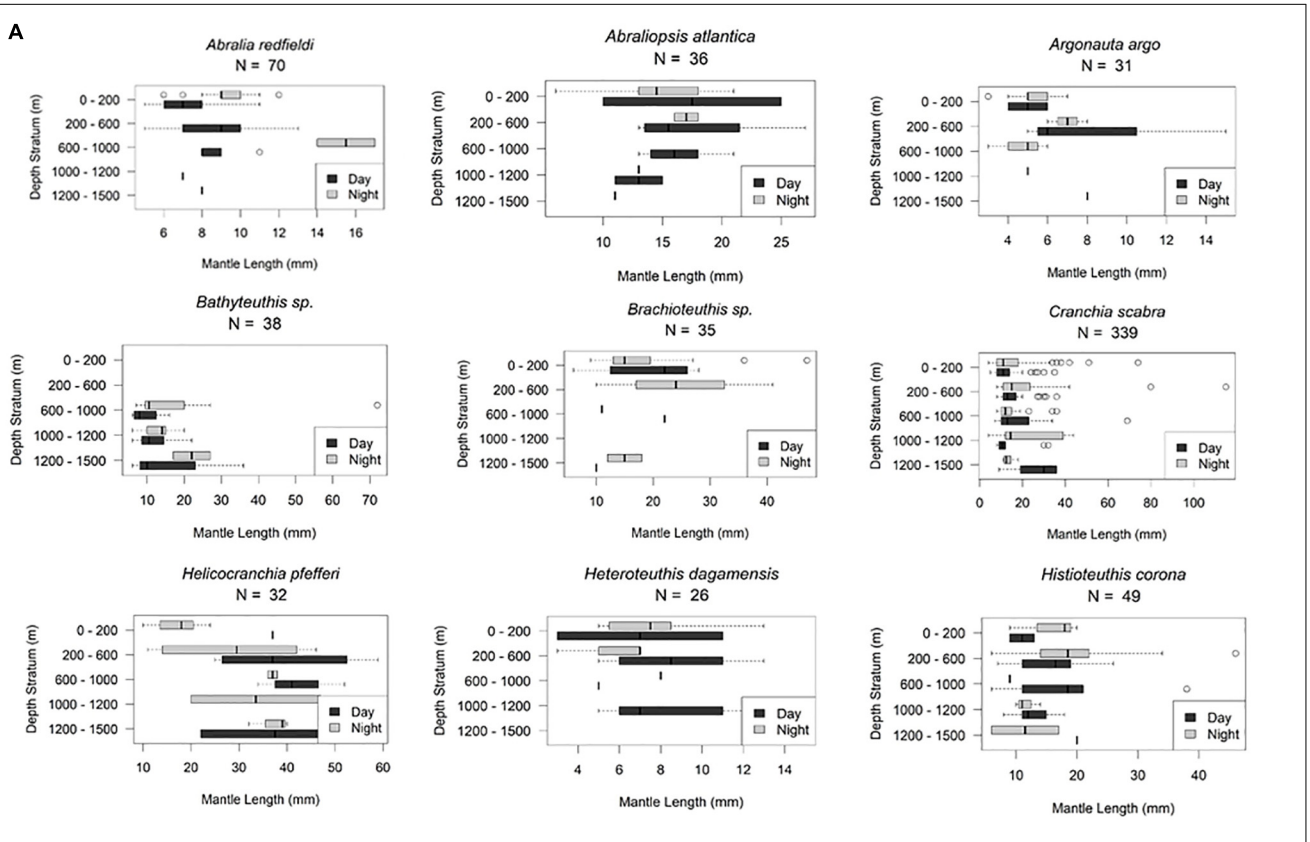

FIGURE 9 | Continued

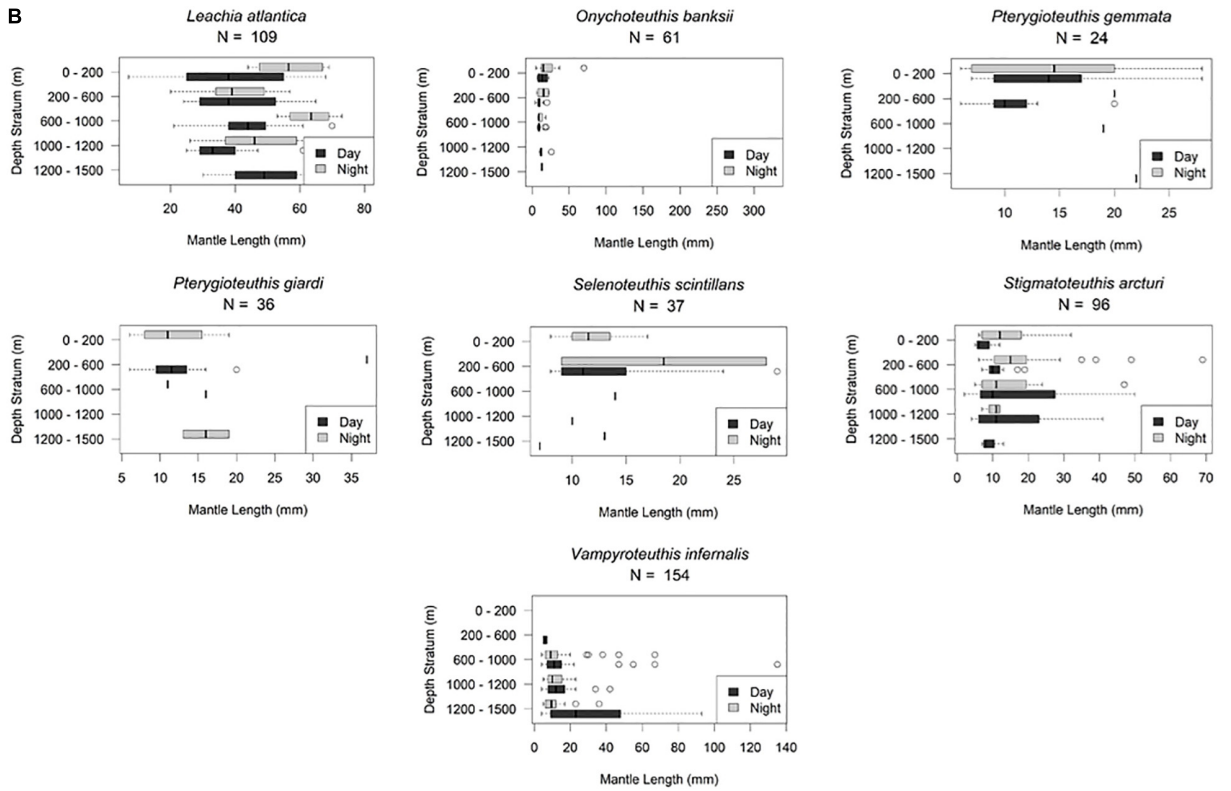

FIGURE 9 | (A,B) Cephalopods showing no evidence of ontogenic shift. Horizontal line, median; box limits, 1st and 3rd quartiles; circles, outliers.

Histioteuthidae

Histioteuthis corona (6–46 mm ML) and *Stigmatoteuthis arcturi* (2–69 mm ML) are found throughout the water column with high concentrations found in the upper mesopelagic zone. They are mesopelagic asynchronous migrators, living primarily from the lower to upper mesopelagic zone at night. We found no evidence of ontogenic shift for either species (**Figures 5**, **9**).

Octopoteuthidae

The two *Octopoteuthis* species (*O. sicula*, *O. megaptera*) found in the northern GOM were combined into one VDP due to the difficulty of identifying specimens confidently to species because many were badly damaged (5–100 mm ML). Forty *Octopoteuthis* sp. display a mesopelagic asynchronous migration pattern (**Figures 5**, **8**).

Twelve *Taningia danae* (7–34 mm ML) were included in a VDP (**Supplementary Materials A, B**) as there is little distribution information in past literature about this species. They were caught from 0 to 1000 m deep with the majority living above 600 m, and indicated a weak vertical migration pattern. Additional material is needed to confirm this assessment (**Supplementary Materials A, B**).

Ommastrephidae

Ornithoteuthis antillarum (5–40 mm ML) follows the nyctoepipelagic synchronous diel migration pattern with some vertical migration from the meso- to the epipelagic zone. Smaller individuals were found throughout the water column (<15 mm ML) while larger individuals (>23 mm ML) were above 600 m (**Figures 4**, **10**). This could be evidence of a weak ontogenic shift for this species moving upwards as they get larger. Eighteen *Sthenoteuthis pteropus* (5–25 mm ML) display a uniform distribution from 0–1500 m (**Supplementary Material A**) with a weak ontogenic shift (**Supplementary Material B**). We include a VDP for *Hyaloteuthis pelagica* (4–8 mm ML) in spite of its rarity because of scarce historical records. Nine specimens show a vertical distribution from 0 to 1200 m. No ontogenic pattern is documented at this time (**Supplementary Materials A, B**).

Onychoteuthidae

Sixty-one *Onychoteuthis banksii* (4–326 mm ML) showed that the species is found from the surface to 1500 m, with more collected during daytime hours than at night. We found evidence of a mesopelagic asynchronous migration for this species (**Figure 5**). There is no strong evidence of ontogenic shift as this species grows (**Figures 9A,B**). *Walvisteuthis jeremiahi* (5–24 mm ML) were documented from 0 to 1000 m as holoepipelagic non-migrators with a similar ontogenic shift pattern (**Supplementary Materials A, B**).

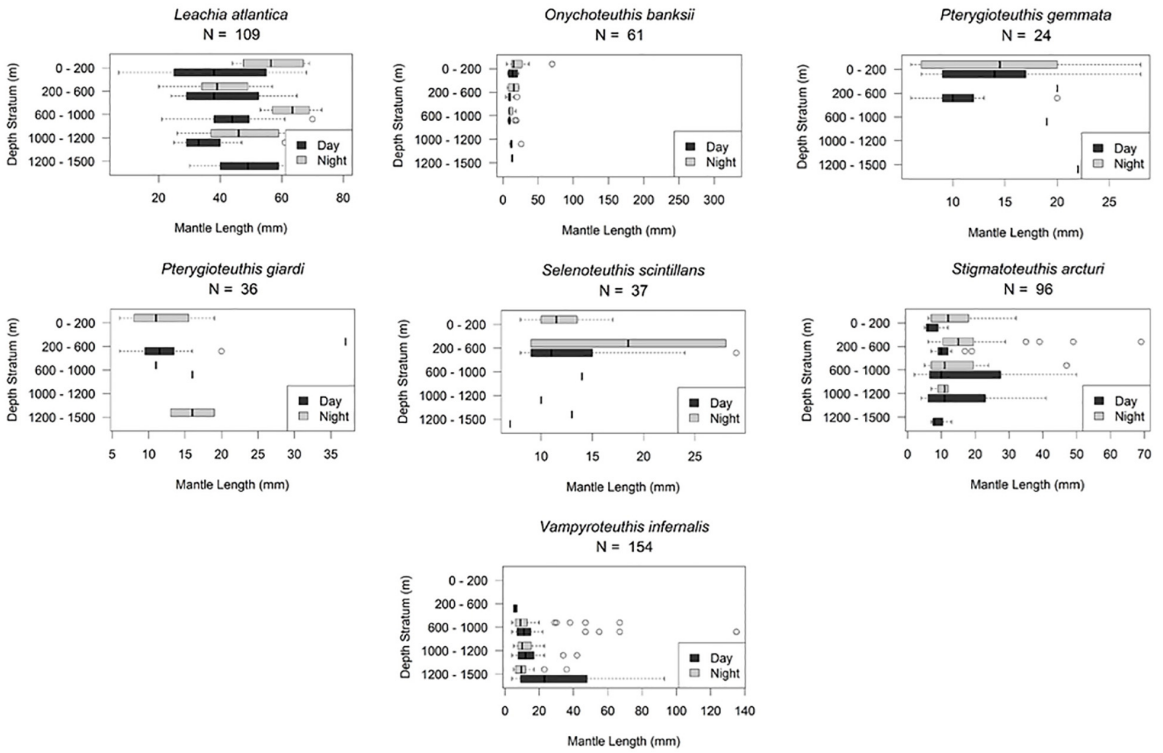

FIGURE 10 | Cephalopods displaying an ontogenic shift from deeper zones to shallow zones as they develop. Horizontal line, median; box limits, 1st and 3rd quartiles; circles, outliers.

Sepiolidae

Heteroteuthis dagamensis (3–15 mm ML) are found from 0 to 1200 m in the northern GOM with evidence of the species being mesopelagic asynchronous vertical migrators. Six larger individuals (>9 mm ML) were found above 600 m while only one was found in the 1000–1200 m depth zone. There is no evidence of ontogenic shift (**Figures 5**, **9**).

Bathyteuthidae

Thirty-nine *Bathyteuthis* sp. (6–72 mm ML) were used to create a VDP that shows they live solely in the lower meso- and upper bathypelagic zones at all sizes. They are considered deep meso-/bathypelagic non-vertical migrators with no evidence of ontogenic shift (**Figures 6**, **9**).

Chtenopterygidae

Although only 10 specimens of *C. sicula* (7–15 mm ML) were collected, a VDP is included due to the scarcity of available literature. They occupy depths from the surface to 1200 m with many inhabiting the upper mesopelagic zone. From the plot, they appear to move down the water column at night but this is likely a product of a low sample size (**Supplementary Material A**). They also exhibit a weak ontogenic shift, as they get larger, they move deeper into the water column (**Supplementary Material B**). More material is needed for a robust assessment.

DISCUSSION

The DWH spill was an ecological disaster from the surface to the seafloor. The midwater plume lasted for months (Camilli et al., 2010; Melvin et al., 2016) and numerous taxa interacted with it as they either lived within it or moved vertically through it on their nightly migrations (Burdett et al., 2017; Romero et al., 2018). Multiple faunal groups are found within the upper bathypelagic zone including fishes, cephalopods, crustaceans, and gelatinous organisms (Pond et al., 2000; Robison et al., 2010; Sutton et al., 2010; Letessier et al., 2011; Cook et al., 2013; Judkins et al., 2016; Hosia et al., 2017). All of these taxa play a role in the carbon flux from the surface to benthic habitats. This biological carbon pump becomes vulnerable as oil drilling moves farther off the coast into deeper waters. When another spill occurs, knowing the migrating and non-migrating populations that may interact with any contamination will provide a baseline of sorts for species that may be impacted in the upper bathypelagic zone.

We found that 95% of oceanic cephalopod species of the northern GOM spend time in the upper bathypelagic zone for some portion of their lives (1000–1500 m), either migrating through or living within it (**Figure 2** and **Table 3**). Past records support these 37 cephalopod species having been collected from similar depths in various regions around the world (Lu and Clarke, 1975a; Roper and Young, 1975; Young, 1978; Lu and Roper, 1979; Vecchione and Pohle, 2002; Shea et al., 2017). Although the Kruskal–Wallis results reveal no significance for

TABLE 3 | Current study species and our placement of cephalopods within the vertical migration pattern categories according to T. Sutton et al. (unpublished) and Roper and Young (1975).

Species	Sutton et al. classification	Roper and Young classification
Cranchia scabra	Holoepipelagic non-migrator	Non-migrator
Argonauta argo	Holoepipelagic non-migrator	Does not fit well by definition
Brachioteuthis sp.	Holoepipelagic non-migrator	First order diel vertical migrator
Macrotritopus defilippi	Holoepipelagic non-migrator	Non-migrator
Walvisteuthis jeremiahi	Holoepipelagic non-migrator	Non-migrator
Bathothauma lyromma	Holoepipelagic non-migrator	Non-migrator
Abraliopsis atlantica	Nyctoepipelagic synchronous diel migrator	First order diel vertical migrator
Abralia redfieldi	Nyctoepipelagic synchronous diel migrator	First order diel vertical migrator
Pyroteuthis margaritifera	Nyctoepipelagic synchronous diel migrator	First order diel vertical migrator
Pterygioteuthis gemmata	Nyctoepipelagic synchronous diel migrator	First order diel vertical migrator
Pterygioteuthis giardi	Nyctoepipelagic synchronous diel migrator	First order diel vertical migrator
Selenoteuthis scintillans	Nyctoepipelagic synchronous diel migrator	First order diel vertical migrator
Ornithoteuthis antillarum	Nyctoepipelagic synchronous diel migrator	Non-migrator
Haliphron atlanticus	Mesopelagic asynchronous migrator	Second order diel vertical migrator
Chiroteuthis sp.	Mesopelagic asynchronous migrator	Second order diel vertical migrator
Helicocranchia pfefferi	Mesopelagic asynchronous migrator	Second order diel vertical migrator
Helicocranchia sp. *A*	Mesopelagic asynchronous migrator	Second order diel vertical migrator
Sandalops melancholicus	Mesopelagic asynchronous migrator	Non-migrator
Histioteuthis corona	Mesopelagic asynchronous migrator	Second order diel vertical migrator
Stigmatoteuthis arcturi	Mesopelagic asynchronous migrator	Second order diel vertical migrator
Cycloteuthis sirventi	Mesopelagic asynchronous migrator	Diel vertical spreader
Discoteuthis discus	Mesopelagic asynchronous migrator	Non-migrator
Sthenoteuthis pteropus	Mesopelagic asynchronous migrator	Non-migrator
Octopoteuthis sp.	Mesopelagic asynchronous migrator	Non-migrator
Heteroteuthis dagamensis	Mesopelagic asynchronous migrator	Second order diel vertical migrator
Onychoteuthis banksii	Mesopelagic asynchronous migrator	Second order diel vertical migrator
Joubiniteuthis portieri	Deep meso-/bathypelagic asynchronous migrator	Diel vertical spreader
Vampyroteuthis infernalis	Deep meso-/bathy non-migrator	Non-migrator
Grimalditeuthis bonplandi	Deep meso-/bathy non-migrator	Non-migrator
Mastigoteuthis agassizii	Deep meso-/bathy non-migrator	Non-migrator
Bolitaena pygmaea	Deep meso-/bathy non-migrator	Non-migrator
Japetella diaphana	Deep meso-/bathy non-migrator	Non-migrator
Bathyteuthis sp.	Deep meso-/bathy non-migrator	Non-migrator
Leachia atlantica	Does not fit well by definition	Non-migrator

any of the six species examined, this is most likely due to small sample sizes and large within-group variation. Erickson et al. (2017) showed that sampling variability is very high in young pelagic cephalopods. Large sample sizes are needed for a robust statistical analysis.

Cephalopods are important links among various components of marine ecosystems. The contribution of nektonic squids to the coupling of energy flows among marine ecosystems during their ontogenic migrations is poorly understood (Arkhipkin, 2013). It is often neglected in ecosystem models despite their capacity to move significant amounts of resources between ecosystems (Arkhipkin, 2013). The vertically migrating squids contribute to this resource flux throughout the water column.

The bathypelagic zone is part of the largest unexplored realm on Earth (Webb et al., 2010). There have been multiple programs to close the gap of deep-sea exploration such as MAR-ECO and CMarZ, both supported by the Census of Marine Life as well as the DEEPEND consortium supported by the Gulf of Mexico Research Initiative (GoMRI). These programs have scratched the surface of the bathypelagic zone which continues to require focused, collaborative sampling efforts. The dataset created here is currently the largest of its kind for midwater cephalopods.

Vertical Migration Patterns

Past studies of cephalopod vertical migration have been conducted using a modified Isaac-Kid midwater trawl (IKMT) or rectangular midwater trawls (RMT 8) (Lu and Clarke, 1975b; Lu and Roper, 1979; Salman et al., 2003; Shea and Vecchione, 2010). One caution using these types of nets, fished either open or with a closing cod-end, is the possibility of organisms being captured during descent or ascent to the desired discreet depth. The RMT8 and MOC10 are opening/closing net systems, which can descend closed to the desired depth and then open, so we have higher confidence in inferred vertical distribution patterns using this type of gear. Roper and Young (1975)

TABLE 4 | Cephalopod species found living between (10% or more of abundance) or moving through 1000–1400 m.

Living between 1000 and 1400 m	Moving through 1000–1400 m
Ancistrocheirus lesueurii	*Abralia redfieldi*
Bathothauma lyromma	*Abraliopsis atlantica*
Bathyteuthis sp.	*Histioteuthis corona*
Bolitaena pygmaea	*Onychoteuthis banksii*
Brachioteuthis sp.	*Ornithoteuthis antillarum*
Chtenopteryx sicula	*Pterygioteuthis gemmata*
Chiroteuthis sp.	*Pterygioteuthis giardi*
Cranchia scabra	*Selenoteuthis scintillans*
Cycloteuthis sirventi	*Stigmatoteuthis arcturi*
Galiteuthis armata	
Grimalditeuthis bonplandi	
Haliphron atlanticus	
Helicocranchia pfefferi	
Helicocranchia sp. A	
Heteroteuthis dagamensis	
Hyaloteuthis pelagica	
Japetella diaphana	
Joubiniteuthis portieri	
Leachia atlantica	
Macrotritipus defillipi	
Mastigoteuthis agassizii	
Pyroteuthis margaritifera	
Sandalops melancholicus	
Sthenoteuthis pteropus	
Vampyroteuthis infernalis	

examined three programs that documented cephalopod vertical migration patterns using IKMTs. They created categories for the cephalopods based on the vertical migration patterns noting that these are not mutually exclusive; some species may exhibit a combination of patterns and that all patterns are not sharply defined (Roper and Young, 1975).

Many of the plots in the current study reinforce the patterns defined by Roper and Young (1975). Some plots (i.e., *P. margaritifera*, *Octopoteuthis* sp., *O. banksii*, *H. pfefferi*, *A. argo*) extend the known depth range for the species. This is likely due to our deeper trawling efforts. The current study found that while some cephalopod species fit within the Roper and Young (1975) categories, others did not because there was not a clear pattern or few individuals included in their original analysis (**Table 4**). We used the categories created by T. Sutton et al. (unpublished) to compare with those of Roper and Young (1975) as they align better with our observations regarding cephalopods. The categories are more specific by depth zones than those reported by Roper and Young (1975) used due to the capability of the MOC10 to collect discreet depth zone samples in this study (**Table 4**). Examples of this can be found when looking at certain species (i.e., *S. melancholicus*, *D. discus*, *S. pteropus*) as Roper and Young (1975) classified them as non-migrators but the patterns exhibited with the current plots demonstrate a nightly upward movement into the upper mesopelagic or epipelagic which places these species into the asynchronous migrator category.

It should be noted that some groups need additional material to strengthen the patterns inferred here (i.e., *Chiroteuthis*, *Brachioteuthis*, and *Octopoteuthis*) because they are grouped by genus and not compared at the species level. As more material becomes available, clearer conclusions can be made.

Ontogenic Shifts

Past studies have focused on ontogenic shifts of various cephalopod groups, notably the ommastrephids (Shigeno et al., 2001; Shea, 2005). Ontogenic examination of deep-water cephalopods is less available; some work has been presented by Villanueva (1992), Quetglas et al. (2010), and Shea and Vecchione (2010). Developmental strategies such as anti-predator behavior changes through ontogeny have been examined as well (York and Bartol, 2016).

Shea and Vecchione (2010) examined paralarvae of three mesopelagic cephalopod species from the North Atlantic Ocean and compared allometric changes with ontogenic changes in their diel vertical migration patterns. They found that the brachioteuthids were caught primarily during the day while we recorded the opposite pattern (**Figure 3**). We examined 35 brachioteuthids ranging in size from 6 to 47 mm ML and found them in the upper 600 m during the day and from 0 to 1500 m at night. This aligns with a holoepipelagic vertical distribution pattern where the majority of the species spends time in the upper 200 m but can be found deeper as well. There does not appear to be an ontogenic shift within the specimens we examined. These findings do not align closely with what Shea and Vecchione (2010) report but this could be due to differences in sampling depths, specimen sizes, or species considered (**Figures 3**, **9**).

Shea and Vecchione (2010) also documented that *C. sicula* paralarvae were found between 0 and 300 m when <6.5 mm ML as well as allometric changes that occur once they are below the euphotic zone. We find that *C. sicula* (7–15 mm ML) are found from 0 to 600 m during the day and from 0 to 1200 m at night. This could align with Shea and Vecchiones' (2010) thought that there is an ecological change that corresponds with allometric change for this group. However, note that our study has only 10 specimens to examine for this comparison (**Supplementary Materials A, B**).

The ontogenic migration of *Histioteuthis reversa* to deeper waters has been observed in the Mediterranean Sea (Quetglas et al., 2010). They concluded that adult females ascend the water column to spawn because spent females have been collected at the surface, as reported elsewhere (Voss et al., 1998). The two histioteuthid species studied here (*H. corona* and *S. arcturi*) were found throughout the water column when smaller than 20 mm ML and the larger animals (>20 mm ML) were found at shallower depths both day and night indicating that the pattern inferred for *H. reversa* may be consistent for the family.

CONCLUSION

Cephalopods are widely distributed throughout the water column down to 1500 m with the mesopelagic zone containing the largest number of individuals. This study reveals that 95% of the species

examined spent all or part of their lives in the upper bathypelagic zone which is where the deep oil plume was located during the DWH oil spill. This study provides new details, as there were no baseline data for midwater cephalopods of the GOM prior to the spill. The VDP and ontogenic shifts analyzed with a reliable collection method contribute additional evidence and include large sample sizes for many species, providing reference data for midwater cephalopods in the GOM.

DATA AVAILABILITY STATEMENT

The datasets generated for this study are available on request to the corresponding author.

ETHICS STATEMENT

Ethical review and approval was not required for the animal study because this is not required for cephalopods in the United States at this time.

AUTHOR CONTRIBUTIONS

HJ and MV were responsible for cephalopod collection and identification as well as writing and reviewing the manuscript.

FUNDING

This research was made possible by a grant from the Gulf of Mexico Research Initiative. GOM data are publicly available through the Gulf of Mexico Research Initiative Information and Data Cooperative (GRIIDC) at https://data.gulfresearchinitiative.org, doi: 10.7266/N70P0X3T and doi: 10.7266/N7XP7385.

ACKNOWLEDGMENTS

We would like to thank the crews of the NOAA Ship *Pisces* and the R/V *Point Sur* during the sampling process. We thank Tracey Sutton for the use of his vertical migration pattern definitions he is creating for fishes. We would also like to acknowledge April Cook and Rosanna Milligan for their assistance with data and graphs.

SUPPLEMENTARY MATERIAL

The Supplementary Material for this article can be found online at: https://www.frontiersin.org/articles/10.3389/fmars.2020.00047/full#supplementary-material

MATERIAL A | Cephalopod vertical distribution plots for species with fewer than 20 individuals for analysis.

MATERIAL B | Ontogenic shift plots of cephalopods with fewer than 20 individuals for analysis.

REFERENCES

Arkhipkin, A. (2013). Squid as nutrient vectors linking South-west Atlantic marine ecosystems. *Deep Sea Res. II* 95, 7–20. doi: 10.1016/j.dsr2.2012.07.003

Burdett, E. A., Fine, C. D., Sutton, T. T., Cook, A. C., and Frank, T. M. (2017). Geographic and depth distributions, ontogeny, and reproductive seasonality of decapod shrimps (Caridea: Oplophoridae) from the northeastern Gulf of Mexico. *Bull. Mar. Sci.* 93, 743–767. doi: 10.5343/bms.2016.1083

Camilli, R., Reddy, C. M., Yoerger, D. R., Van Mooy, B. A. S., Jakuba, M. V., Kinsey, J. C., et al. (2010). Tracking hydrocarbon plume transport and biodegradation at deepwater horizon. *Science* 330, 201–204. doi: 10.1126/science.1195223

Clarke, M. R., and Lu, C. C. (1975). Vertical distribution of cephalopods at 18°N 25°W in the North Atlantic. *J. Mar. Biol. Assoc. U.K.* 55, 165–182. doi: 10.1017/s0025315400015812

Cook, A. B., Sutton, T. T., Galbraith, J. K., and Vecchione, M. (2013). Deep-pelagic (0-3000m) fish assemblage structure over the Mid-Atlantic Ridge in the area of the Charlie-Gibbs Fracture Zone. *Deep Sea Res. II* 98, 279–291. doi: 10.1016/j.dsr2.2012.09.003

DEEPEND, (2015). *DEEPEND Cruise Report DP01*. Available at: http://www.deependconsortium.org/images/documents/DP01_report.pdf (accessed October 4, 2019).

Dierks, A. R., Highsmith, R. C., Asper, V. L., Joung, D., Zhou, Z., Guo, L., et al. (2010). Characterization of subsurface polycyclic aromatic hydrocarbons at the Deepwater Horizon site. *Geophys. Res. Lett.* 37:L20602. doi: 10.1029/2010GL045046

Erickson, C. A., Roper, C. F. E., and Vecchione, M. (2017). Variability of paralarval-squid occurrence in meter-net tows from east of Florida, USA. *Southeastern Naturalist.* 16, 629–642. doi: 10.1656/058.016.0411

Hopkins, T. L. (1982). The vertical distribution of zooplankton in the eastern Gulf of Mexico. *Deep Sea Res. I* 29, 1069–1083. doi: 10.1016/0198-0149(82)90028-0

Hosia, A., Falkenhaug, T., Baxter, E. J., and Pagès, F. (2017). Abundance, distribution and diversity of gelatinous predators along the northern Mid-Atlantic Ridge: a comparison of different sampling methodologies. *PLoS One* 12:e0187491. doi: 10.1371/journal.pone.0187491

Joye, S. B., MacDonald, I. R., Leifer, I., and Asper, V. (2011). Magnitude and oxidation potential of hydrocarbon gases released from the BP oil well blowout. *Nat. Geosci.* 4, 160–164. doi: 10.1038/ngeo1067

Judkins, H., Vecchione, M., Cook, A., and Sutton, T. (2016). Diversity of midwater cephalopods in the northern Gulf of Mexico: comparison of two collecting methods. *Mar. Biodivers.* 47, 647–657. doi: 10.1007/s12526-016-0597-598

Kessler, J. D., Valentine, D. L., Redmond, M. C., Du, M., Chan, E. W., Mendes, S. D., et al. (2011). A persistent oxygen anomaly reveals the fate of spilled methane in the deep Gulf of Mexico. *Science* 331, 312–315. doi: 10.1126/science.1199697

Lansdell, M., and Young, H. (2003). Pelagic cephalopods from eastern Australia: species composition, horizontal and vertical distribution determined from the diets of pelagic fishes. *Rev. Fish. Biol. Fish.* 17, 125–138. doi: 10.1007/s11160-006-9024-8

Letessier, T. B., Falkenhaug, T., Debes, H., Bergstad, O. A., and Brierly, A. S. (2011). Abundance patterns and species assemblages of euphausiids associated with the Mid-Atlantic Ridge. North Atlantic. *J. Plank. Res.* 33, 1510–1525. doi: 10.1093/plankt/fbr056

Lu, C. C., and Clarke, M. R. (1975a). Vertical distribution of cephalopods at 11°N 20°W in the North Atlantic. *J. Mar. Biol. Assoc. U.K.* 55, 369–389.

Lu, C. C., and Clarke, M. R. (1975b). Vertical distribution of cephalopods at 40°N 53°W in the North Atlantic. *J. Mar. Biol. Assoc. U.K.* 55, 143–163. doi: 10.1017/s0025315400015800

Lu, C. C., and Roper, C. F. E. (1979). *Cephalopods from Deepwater Dumpsite 106 (Western Atlantic): Vertical Distribution and Seasonal Abundance. Smithsonian Contributions to Zoology; #288*. Washington, DC: Smithsonian Institution Press.

Melvin, A. T., Thibodeaux, L. J., Parsons, A. R., Overton, E., Valsaraj, K. T., and Nandakumar, K. (2016). Oil-material fractionation in Gulf deep water

horizontal intrusion later: field data analysis with chemodynamic fate model for Macondo 252 oil spill. *Mar. Pol. Bull.* 105, 110–119. doi: 10.1016/j.marpolbul.2016.02.043

Nesis, K. (1972). Oceanic cephalopods of the Peru Current: horizontal and vertical distribution. *Okeanologiya* 12, 506–519.

Nesis, K. (1993). Vertical migration of the micronektonic squids *Pyroteuthis margaritifera* (Ruppell) and *Pterygioteuthis gemmata* (Chun) from catches with a non-closing net. *Okeanologiya* 33, 110–115.

Passow, U., and Hetland, R. D. (2016). What happened to all of the oil? *Oceanography* 29, 88–95. doi: 10.5670/oceanog.2016.73

Pond, D. W., Sargent, J. R., Fallick, A. E., Allen, C., Bell, M. V., and Dixon, D. R. (2000). δ13C values of lipids from phototropic zone microplankton and bathypelagic shrimps at the Azores sector of the Mid-Atlantic Ridge. *Deep Sea Res. I* 47, 121–136. doi: 10.1016/s0967-0637(99)00050-3

Quetglas, A., de Mesa, A., Ordines, F., and Grau, A. (2010). Life history of the deep-sea cephalopod family Histioteuthidae in the western Mediterranean. *Deep sea Res. I* 57, 999–1008. doi: 10.1016/j.dsr.2010.04.008

R Core Team (2013). *R: A Language and Environment for Statistical Computing*. Vienna: R Foundation for Statistical Computing.

Reddy, C. M., Arey, J. S., Seewald, J. S., Sylva, S. P., Lemkau, K. L., Nelson, R. K., et al. (2012). Composition and fate of gas and oil released to the water column during the Deepwater Horizon oil spill. *Proc. Matl. Acad. Sci. U.S.A.* 109, 20229–20234. doi: 10.1073/pnas.1101242108

Reddy, R. K., Rao, A., Yu, Z., Wu, X., Nandakumar, K., Thibodeaus, L., et al. (2014). *Challenges in and Approaches to Modeling the Complexities of Deepwataer Oil and Gas Release. Oil Spill Remediation: Colloid Chemistry-Based Principles and Solutions*, 1st Edn, Chap. 4. Hoboken, NJ: John Wiley & Sons, Inc, 89–126.

Richards, T. M., Gipson, E. E., Cook, A., Sutton, T. T., and Wells, R. J. D. (2018). Trophic ecology of meso- and bathypelagic predatory fishes in the Gulf of Mexico. *ICES J. Mar. Sci.* 76, 662–672. doi: 10.1093/icesjms/fsy074

Robison, B. (2004). Deep pelagic biology. *J. Exp. Mar. Bio. Ecol.* 300, 253–272. doi: 10.1016/j.jembe.2004.01.012

Robison, B. H., Reisbichler, K. R., and Sherlock, R. E. (2017). The coevolution of midwater research and ROV technology at MBARI. *Oceanography* 30, 26–37. doi: 10.5670/oceanog.2017.421

Robison, B. H., Sherlock, R. E., and Reisenbichler, K. R. (2010). The bathypelagic community of Monterey Canyon. *Deep Sea Res. II* 57, 1551–1556. doi: 10.1016/j.dsr2.2010.02.021

Romero, I. C., Schwing, P. T., Brooks, G. R., Larson, R. A., Hastings, D. W., Ellis, G., et al. (2015). Hydrocarbons in deep-sea sediments following the 2010 Deepwater Horizon blowout in the northeast Gulf of Mexico. *PLoS One* 10:e0128371. doi: 10.137/journal.pone.0128371

Romero, I. C., Sutton, T., Carr, B., Quintana-Rizzo, E., Ross, S. W., Hollander, D. J., et al. (2018). Mesopelagic fishes from the Gulf of Mexico reveals exposure to oil-derived sources. *Environ. Sci. Tech.* 52, 10985–10996. doi: 10.1021/acs.est.8b02243

Roper, C. F. E., and Young, R. E. (1975). *Vertical distribution of pelagic cephalopods; Smithsonian Contributions to Zoology, #209*. Washington, DC: Smithsonian Institution Press.

Ropke, A., Nellen, W., and Piatkowski, U. (1993). A comparative study on the influence of the pycnocline on the vertical distribution of fish larvae and cephalopod paralarvae in three ecologically different areas of the Arabian Sea. *Deep Sea Res. II* 40, 801–819. doi: 10.1016/0967-0645(93)90059-v

Salman, A., Katagan, T., and Benli, H. A. (2003). Vertical distribution and abundance of juvenile cephalopods in the Aegean Sea. *Sci. Mar.* 67, 167–176. doi: 10.3989/scimar.2003.67n2167

Shea, E., Judkins, H., Staudinger, M. D., Hartigan, V., Lindgren, A., and Vecchione, M. (2017). Cephalopod biodiversity in the vicinity of Bear Seamount, western North Atlantic. *Mar. Biodivers.* 47:699. doi: 10.1007/s12526-017-0633-633

Shea, E. K. (2005). Ontongeny of the fused tentacles in three species of Ommastrephid squids (Cephalopoda, Ommastrephidae). *Invert. Biol.* 124, 25–38. doi: 10.1111/j.1744-7410.2005.1241-04.x

Shea, E. K., and Vecchione, M. (2010). Ontogenic changes in diel vertical migration patterns compared with known allometric changes in three mesopelagic squid species suggest an expanded definition of paralarva. *ICES J. Mar. Sci.* 67, 1436–1443. doi: 10.1093/icesjms/fsq104

Shigeno, S., Kidokoro, H., Goto, T., Tsuchiya, K., and Segawa, S. (2001). Early ontogeny of the Japanese Common squid *Todarodes pacificus* (Cephalopoda, Ommastrephidae) with special reference to its characteristic morphology and ecological significance. *Zool. Sci.* 18, 1011–1026. doi: 10.2108/zsj.18.1011

Socolofsky, S. A., Adams, E. E., and Sherwood, C. R. (2011). Formation dynamics of subsurface hydrocarbon intrusions following the Deepwater Horizon blowout. *Geophys. Res. Let.* 38:L09602. doi: 10.1029/2011GL047174

Sosnowski, A. (2017). *Genetic Identification and Population Characteristics of Deep-Sea Cephalopod Species in the Gulf of Mexico and Northwestern Atlantic Ocean*. Master's Thesis, University of South Florida, Florida.

Summers, W. C. (1983). Physiological and trophic ecology of cephalopods. The Mollusca. *Ecology* 6, 261–279. doi: 10.1016/b978-0-12-751406-2.50013-1

Sutton, T. T. (2013). Vertical ecology of the pelagic ocean: classical patterns and new perspectives. *J. Fish. Biol.* 83, 1508–1527. doi: 10.1111/jfb.12263

Sutton, T. T., Wiebe, P. H., Madin, L., and Bucklin, A. (2010). Diversity and community structure of pelagic fishes to 5000 m depth in the Sargasso Sea. *Deep Sea Res. II* 57, 2220–2233. doi: 10.1016/j.dsr2.2010.09.024

Timm, L., Bracken- Grissom, H., Sosnowski, A., Breitbart, M., Vecchione, M., and Judkins, H. (2020). Population genomics of three deep-sea cephalopod species reveals connectivity between the Gulf of Mexico and northwestern Atlantic Ocean. *Deep Sea Res. I* (in press). doi: 10.1016/j.dsr.2020.103222

Vecchione, M., and Pohle, G. (2002). Midwater cephalopods in the western North Atlantic Ocean off Nova Scotia. *Bull. Mar. Sci.* 71, 883–892.

Vecchione, M., Young, R. E., Guerra, A., Lindsay, D. J., Clague, D. A., Bernhad, J. M., et al. (2001). Worldwide observations of remarkable deep-sea squids. *Science* 294:2505. doi: 10.1126/science.294.5551.2505

Villanueva, R. (1992). Deep-sea cephalopods of the northwestern Mediterranean: implications of up-slope ontogenetic migration in two bathybenthic species. *J. Zool. Lond.* 227, 267–276. doi: 10.1111/j.1469-7998.1992.tb04822.x

Voss, N. A., Nesis, K. N., and Rodhouse, P. G. (1998). "The cephalopod family Histioteuthidae (Oegopsida): systematics, biology, and biogeography," in *Systematics and Biogeography of Cephalopods*, eds N. A. Voss, M. Vecchione, R. B. Toll, and M. Sweeney, (Washington D.C: Smithsonian Contributions to Zoology).

Webb, T. J., Vanden Berghe, E., and O'Dor, R. (2010). Biodiversity's "big wet secret" the global distribution of marine biological records reveals chronic under-exploration of the deep pelagic ocean. *PLoS One* 5:e10223. doi: 10.1371/journal.pone.0010223

Widder, E., Robison, B. E., Reisenbichler, K., and Haddock, S. (2005). Using red light for in situ observations of deep-sea fishes. *Deep Sea Res. I* 52, 2077–2085. doi: 10.1016/j.dsr.2005.06.007

Wiebe, P. H., Burt, K. H., Boyd, S. H., and Morton, A. W. (1976). A multiple opening/closing net and environmental sensing system for sapling zooplankton. *J. Mar. Res.* 34:326.

Williams, T. D. (1995). *The Penguins: Spheniscidae*. Oxford: Oxford University Press.

Xavier, J. C., Cherel, Y., Allcock, L., Rosa, R., Sabirov, R. M., and Blicher, M. E. (2018). A review on the biodiversity, distribution, and trophic roles of cephalopods in the Arctic and Antarctic marine ecosystems under a changing ocean. *Mar. Biol.* 165:93. doi: 10.1007/s00227-018-3352-3359

York, C. A., and Bartol, I. K. (2016). Anti-predatory behavior of squid throughout ontogeny. *J. Exp. Mar. Biol. Ecol.* 480, 26–35. doi: 10.1016/j.jembe.2016.03.011

Young, R. E. (1978). Vertical distribution and photosensitive vesicles of pelagic cephalopods from Hawaiian waters. *Fish. Bull.* 76, 583–614.

Young, R. E., Vecchione, M., and Mangold, K. M. (1922–2003). *2019. Cephalopoda Cuvier 1797. Octopods, Squids, Nautiluses, etc.* Available at: http://tolweb.org/Cephalopoda/19386/2019.03.26 (accessed March 26, 2019).

Conflict of Interest: The authors declare that the research was conducted in the absence of any commercial or financial relationships that could be construed as a potential conflict of interest.

frontiers in Marine Science

ORIGINAL RESEARCH
published: 28 February 2020
doi: 10.3389/fmars.2020.00054

Temporal Variability of Polycyclic Aromatic Hydrocarbons in Deep-Sea Cephalopods of the Northern Gulf of Mexico

Isabel C. Romero[1], Heather Judkins[2] and Michael Vecchione[3]*

[1] College of Marine Science, University of South Florida, Tampa, FL, United States, [2] Biological Sciences Department, University of South Florida St. Petersburg, St. Petersburg, FL, United States, [3] NMFS National Systematics Laboratory, National Museum of Natural History, Washington, DC, United States

As part of the effort to understand the effects of the Deepwater Horizon Oil Spill (DWHOS), we analyzed tissue from five species of midwater oceanic cephalopods in the northern Gulf of Mexico (GoM) during three time periods, including one period sampled fortuitously just before the spill (2010), and two periods sampled after the spill (2011 and 2015–2016). The species, *Japetella diaphana*, *Abralia redfieldi*, *Histioteuthis corona*, *Leachia atlantica*, and *Onychoteuthis banksii* were collected in three geographic areas in the GoM (east, south and southeast of the Macondo wellhead). Results indicate a shift in the composition of polycyclic aromatic hydrocarbons (PAHs) in the tissue of all cephalopods after 2010, with a more petrogenic source in 2011 that weathered and mixed with other sources in 2015–2016. Overall, PAH concentrations, as well as lipid content, were lower in 2011 relative to 2010 and 2015–2016, suggesting secondary effects to oil-residues exposure from the DWHOS. Collectively, PAHs in the tissues of deep-sea cephalopods indicate an episodic exposure to petrogenic PAHs that occurred between 2010 (pre-spill) and 2011, and continued through 2015–2016.

Keywords: oil spills, exposure to oil contamination, oil-residues, long-term effects, deepwater horizon spill

OPEN ACCESS

Edited by:
Erik Cordes,
Temple University, United States

Reviewed by:
Helen K. White,
Haverford College, United States
Eduardo Carlos Meduna Hajdu,
Federal University of Rio de Janeiro, Brazil
Ian MacDonald,
Florida State University, United States

****Correspondence:***
Isabel C. Romero
isabelromero@mail.usf.edu

Specialty section:
This article was submitted to Deep-Sea Environments and Ecology, a section of the journal Frontiers in Marine Science

Received: *29 August 2019*
Accepted: *27 January 2020*
Published: *28 February 2020*

Citation:
Romero IC, Judkins H and Vecchione M (2020) Temporal Variability of Polycyclic Aromatic Hydrocarbons in Deep-Sea Cephalopods of the Northern Gulf of Mexico. Front. Mar. Sci. 7:54. doi: 10.3389/fmars.2020.00054

INTRODUCTION

Ecosystem-based management of the oceans relies heavily on continuous observations, essential for distinguishing natural variability from anthropogenic changes. However, epi-, meso-, and bathy-pelagic environments generally lack such studies. This was highlighted in 2010 by the absence of baseline data during the Deepwater Horizon oil spill (DWHOS) in the Gulf of Mexico (GoM). The DWHOS occurred at a depth of 1500 m, releasing approximately 4000000 barrels of oil that contaminated vast areas of the water column (e.g., oil residues rose to form surface slicks contaminating the water column, subsurface plumes concentrated at 900–1300 m) and coastal environments (e.g., marshes, beaches), as well as an extensive area of the seafloor (about 76000 km^2 by sinking of oil residues from the water column) (Dietrich et al., 2012; Brooks et al., 2015; MacDonald et al., 2015; Romero et al., 2015, 2017; Daly et al., 2016; Harding et al., 2016; Murawski et al., 2016; Yan et al., 2016). The deep-pelagic habitat in the GoM was among the environments most affected by the DWHOS, as indicated by multiple studies detecting high concentration of contaminants and shifts in the composition of microbial communities (Hazen et al., 2010;

Fisher et al., 2016; Wade et al., 2016; Yan et al., 2016). Effects to marine communities were observed as carbon from the DWHOS entered the planktonic and mesopelagic food webs, and oil-derived toxic compounds were found to correlate with elevated skin lesions in bottom-dwelling offshore fishes (Graham et al., 2010; Chanton et al., 2012; Murawski et al., 2014; Quintana-Rizzo et al., 2015). Oil residues from the DWHOS have persisted in the deep-pelagic habitat of the GoM longer than anticipated. For example, 4–6 years after the DWHOS as found in the water column and in deep-pelagic fishes (Walker et al., 2017; Chanton et al., 2018; Romero et al., 2018). The potential consequences of the DWHOS on deep-pelagic invertebrates are yet to be determined, as exposure to oil-derived toxic compounds has not been previously studied in invertebrates from the pelagic domain of the GoM.

Many deep-sea pelagic organisms undergo diel vertical migrations, playing an important role in the flux of organic carbon between the surface and bathypelagic depths, including the water column and benthic ecosystems (Steinberg et al., 2008; Davison et al., 2013; Hudson et al., 2014; Irigoien et al., 2014; Steinberg and Landry, 2017; Taucher et al., 2018). Deep-sea cephalopod species are of particular interest due to their role in the diets of large fishes and marine mammals (Davis et al., 2007; Young et al., 2010; Romeo et al., 2012; Logan et al., 2013; Lalas and Webster, 2014; Salman and Karakulak, 2019; Southall et al., 2019). They are also voracious predators (Stewart et al., 2014; Corrales et al., 2015; Hoving and Robison, 2017) and are therefore potential vectors for contaminants through the water column (Unger et al., 2008).

Exposure to toxic compounds, such as polycyclic aromatic hydrocarbons (PAHs), is of specific concern in deep-pelagic cephalopods. These toxic compounds are highly lipid-soluble and therefore can cross lipid membranes and bioaccumulate in marine organisms. Mollusks, including cephalopods, have a reduced capacity to metabolize PAHs with higher bioaccumulation potential than other aquatic organisms (Lacoue-Labarthe et al., 2016; Rodrigo and Costa, 2017). In addition, cephalopods have high growth rates, short life spans, and high sensitivity to environmental changes (Rodrigo and Costa, 2017). Cephalopods have a high capacity to bioaccumulate and concentrate contaminants at higher levels than other aquatic groups, thus are potentially useful bioindicators of aquatic contamination over short periods (Gomes et al., 2013; Semedo et al., 2014). During the DWHOS, an unprecedented amount of PAHs was released, with PAHs remaining mostly offshore and contaminating the deep-pelagic domain of the northern GoM (U.S. District Court, 2015; Wade et al., 2016; Romero et al., 2017, 2018). However, comprehensive studies of PAHs in cephalopod tissues are scarce, with little understanding of the influence of natural and biological factors (e.g., diet, migratory behavior, habitat) affecting their storage after major events like the DWHOS.

This study investigated, for the first time, the composition and concentration of PAHs in deep-sea cephalopods of the GoM over a long period, to better understand levels of contamination, interspecies variability, exposure to natural sources, and potential consequences to the deep-pelagic environment. Specifically, samples were collected before and up to 6 years after the DWHOS (pre-spill: 2010, post-spill: 2011, long-term period: 2015–2016). The samples collected before the DWHOS (January to March, 2010), provided an exceptional opportunity to study uptake and persistence of petrogenic PAHs under multiple natural and anthropogenic sources present in the GoM (Mitra et al., 2002; Mitra and Bianchi, 2003; Romero et al., 2016). Overall, this study provides a time-series analysis of PAH composition and concentrations generating trends in PAH signatures for baseline and chronic conditions in deep-sea cephalopods.

MATERIALS AND METHODS

Collection of Samples

Samples were collected during three different studies conducted between 2010 and 2016. In all studies, trawl samples were collected within the upper 1500 m of the water column. In 2010, sampling was conducted from January to March aboard the NOAA Ship R/V *Pisces* for the Sperm Whale Acoustic Prey Survey (SWAPS; see Judkins et al., 2015) using a large midwater trawl. In 2011, sampling was conducted from March to September aboard the R/V *Meg Skansi* as part of the Offshore Nekton Sampling and Analysis Program (ONSAP) using a 10-m^2 MOCNESS (MOC10) with 3-mm mesh (Judkins et al., 2017). In 2015 and 2016, sampling was conducted in May and August aboard the R/V *Point Sur* as part of the Deep Pelagic Nekton Dynamics of the Gulf of Mexico (DEEPEND), also using a MOC10. All studies covered similar sites in the northern GoM (**Figure 1**). The spatial range of these studies extended from 24.4 to 29.3° N latitude and 86.5 to 90.9° W longitude (**Figure 1**). Sampling stations were located in three areas in the northern GoM relative to the Macondo wellhead, similar to previous studies in the region (Judkins et al., 2017; Romero et al., 2018). In the east area, four stations were sampled, located between ∼41 and ∼ 123 km east of the wellhead. In the south area, ten stations were sampled, located between ∼88 and ∼312 km south of the wellhead. In the southeast area, eight stations were sampled, located between ∼120 and ∼297 km southeast of the wellhead. All areas were sampled between 2010 and 2016, except for the southeast area (only during 2010 and 2015–2016).

Taxonomic identification of all samples was highly consistent among studies. All specimens were identified to the lowest taxonomic level possible, by either H. Judkins or M. Vecchione while at sea. Deep-sea cephalopod species that were available for chemical analysis and included in this study are *Japetella diaphana* (n = 18), *Abralia redfieldi* (n = 11), *Histioteuthis corona* (n = 11), *Leachia atlantica* (n = 21), and *Onychoteuthis banksii* (n = 13) (**Figure 2**). PAH exposure and accumulation was studied as PAH concentrations in the mantle tissue. A small piece of mantle tissue was taken from the anterior portion of the mantle and samples were kept frozen at −20°C until freeze-dried.

Lipid Extraction

Frozen mantle tissue was freeze-dried (Labonco® 7754040 vacuum freeze-drier and 7806020 bulk tray) following guidance from previous studies (Beriro et al., 2014; Romero et al., 2018).

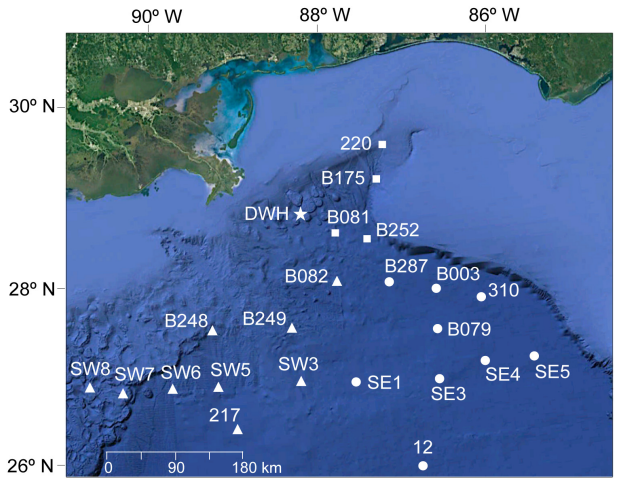

FIGURE 1 | Map showing the location of 22 stations across three areas in the northern Gulf of Mexico relative to the Deepwater Horizon wellhead site (shown as a star). Areas include: north (shown as squares), south (triangles), and southeast (circles). Background map: Google Earth (version 7.3, 2019).

FIGURE 2 | Deep-sea cephalopod species analyzed in this study: **(A)** *Histioteuthis corona*, **(B)** *Japetella diaphana*, **(C)** *Onychoteuthis banksii*, **(D)** *Leachia atlantica*, and **(E)** *Abralia redfieldi*. Photo credit: D. Fenolio **(A–D)** and M. Vecchione **(E)**.

Freeze-dried samples were ground to homogenize the tissue, which was then extracted using an Accelerated Solvent Extraction system (ASE 200®, Dionex) under high temperature (100°C) and pressure (1500 psi) with a solvent mixture of 9:1 (v:v) hexane:dichloromethane. Deuterated PAHs (d_{10}-acenaphthene, d_{10}-phenanthrene, d_{10}-fluoranthene, d_{12}-benz(a)anthracene, d_{12}-benzo(a)pyrene, d_{14}-dibenz(ah)anthracene; Ultra Scientific ISM-750-1) were added to samples prior to extraction as surrogate standards. A one-step extraction and clean-up procedure was applied using 11 ml extraction cells with glass fiber filters (pre-combusted at 450°C for 4 h), 5 g silica gel (high purity grade, 100–200 mesh, pore size 30A, Sigma Aldrich, United States; pre-combusted at 450°C for 4 h, and deactivated 2%), sand (pre-combusted at 450°C for 4 h), and 0.01–0.1 g freeze-dried homogenized sample (Romero et al., 2018). Tissue extracts were concentrated to ∼100–200 µl using a RapidVap (LABONCO RapidVap® Vertex™ evaporator model 73200 series) and a gentle stream of nitrogen. Two extraction control blanks were included with each set of samples (10–14 samples). An internal standard was added (d14-terphenyl; Ultra Scientific ATS-160-1) to all samples prior to GC/MS analysis. All solvents used were at the highest purity available.

Total lipid content (TLC; %lipids) in tissue was calculated gravimetrically from ASE extracts using 100% dichloromethane (Sloan et al., 2004) in samples with sufficient mass available (∼0.5 g) after PAH analysis. For samples with limited mass after PAH extraction, we followed modified gas chromatography method (Hooper and Parrish, 2009) to calculate the %lipid as the total lipid-equivalent fraction by calculating the sum of individual lipids to generate an estimate of total lipids (see Romero et al., 2018, for details).

Analytical Method and Quality Control

We followed modified EPA methods 8270D and 8015C, and QA/QC protocols for the analysis of PAHs. Analyses were carried out on an Agilent 7680B gas chromatograph interfaced with an Agilent 7010 triple quadrupole mass spectrometer (GC/MS/MS). A 30 m RXi-5sil (Restek Corporation, PA, United States) was used with GC liners in the injector in splitless injection mode. UHP helium was used as the carrier gas, while UHP argon gas was used to facilitate the dissociation of the precursor ions (CID) in the collision cell (at 1 mTorr pressure). Inlet temperature was 295°C, constant flow rate was 1 ml/min, and MS detector temperature was 250°C. GC oven temperature program was 60°C for 2 min, 60°C to 200°C at a rate of 8°C/min, 200°C to 300°C at a rate of 4°C/min and held for 4 min, and 300°C to 325°C at a rate of 10°C/min and held for 5 min.

The GC/MS/MS was operated in Multiple Reaction Monitoring mode (MRM) to characterize parent and alkyl PAHs at a high resolution without interferences in the chromatograms. Molecular ion masses for PAHs (precursor and product ions) were selected based on previous studies using GC-MS/MS-MRM (Sorensen et al., 2016; Adhikari et al., 2017; Romero et al., 2018; van Eenennaam et al., 2018). Selected target compounds were 2-ring PAHs: naphthalene (N) and alkylated homologs (N C1-C4); 3-ring: acenaphthylene (ACL), acenaphthene (ACE), fluorene (F), dibenzothiophene (D), phenanthrene (P), anthracene (AN), and their alkylated homologs (P/AN C1-C4, D C1-C2); 4-ring: fluoranthene (FL), pyrene (PY), benz[a]anthracene (BAA), chrysene (C), and their alkylated homologs (FL/PY C1-C4, BAA/C C1-C4); 5-ring: benzo[b]fluoranthene (BBF), benzo[k]fluoranthene (BKF), benzo[a]pyrene (BAP), dibenz[a,h]anthracene (DA), and alkylated homologs (BP/PER C1-C4); and 6-ring: indeno[1,2,3-cd]pyrene (ID), benzo[ghi]perylene (BGP).

For accuracy and precision of analyses we included laboratory blanks for every 10–14 samples, spiked controls for every 14–18 samples, tuned MS/MS to PFTBA (perfluorotributylamine) daily, checked samples with a standard reference material (NIST 2779) daily, and reanalyzed sample batches when replicated standards exceeded ±20% of relative standard deviation (RSD), and/or when recoveries were low. Recovery of individual PAHs ranged within QA/QC criteria of 50–120%. PAH concentrations are reported as recovery corrected. Each PAH analyte was identified using certified standards (Chiron S-4083-K-T, Chiron S-4406-200-T) and performance was checked using a 5-point calibration curve (0.04, 0.08, 0.31, 1.0 ppm). Quantitative determination of PAHs was conducted using response factors (RFs) calculated from the certified standard NIST2779. The limits of quantification and detection (N = 10) ranged from 0.01 to 0.9 ng/g and 0.001 to 0.3 ng/g, respectively.

Data Analysis

Polycyclic aromatic hydrocarbons concentrations reported in this study are expressed as tissue lipid weight concentrations, and average values are shown as arithmetic mean ± standard error. Total PAH concentrations were calculated as the sum of 2-ring to 6-ring PAHs and their alkylated homologs. Low molecular weight (LMW) PAHs are the sum of all 2–3 ring PAHs (including alkylated homologs), and high molecular weight (HMW) PAHs are the sum of 4–6 ring PAHs (including alkylated homologs). To assess sources of PAHs in the tissue samples, selected diagnostic ratios were calculated: (1) FL/Pyr ratio; (2) % Retene; and (3) pyrogenic index [PI; Σ (other 3–6 ring EPA priority PAHs)/Σ(5 alkylated PAHs)]. For the pyrogenic index, the five alkylated PAHs are the alkylated compounds of: N, P, D, F, and C. The "other" 3–6 ring EPA priority PAHs are: ACL, ACE, AN, FL, PY, BAA, BBF, BKF, BAP, ID, DA, and BGP (Wang and Fingas, 2003; Fitzgerald and Gohlke, 2014; Romero et al., 2015, 2018). These PAH ratios include isomer pairs with similar adsorption and dissolution properties abundant in different sources.

Statistical analyses were conducted on log-transformed data to approach normal distribution. Differences in mean concentrations with respect to years and species were tested by one-way ANOVA followed by Tukey's HSD test. Significance was set at $p < 0.05$. We used JMP 12.1 for Mac (SAS Institute Inc., Cary, NC, United Sates, 1989–2007).

RESULTS

Species Variability

Large variability among cephalopod species was found for %lipid content and PAH concentrations over the studied period (**Figure 3**). For example, %lipid content varied significantly among the species studied, although a similar temporal trend was observed with lower %lipid content in 2011 (post-spill) for all species sampled in this year ($p < 0.05$; *J. diaphana*: 4.0 ± 0.8%; *A. redfieldi*: 7.2 ± 1.6%; *H. corona*: 11.8 ± 1.3%; *L. atlantica*: 5.6 ± 0.6%; and *O. banksii*: 6.1 ± 0.5%; **Figure 3**). Lipid loss in 2011 relative to 2010 (pre-spill) was about 50% in *J. diaphana* and *L. atlantica*, and about 25% in *A. redfieldi* and *H. corona*.

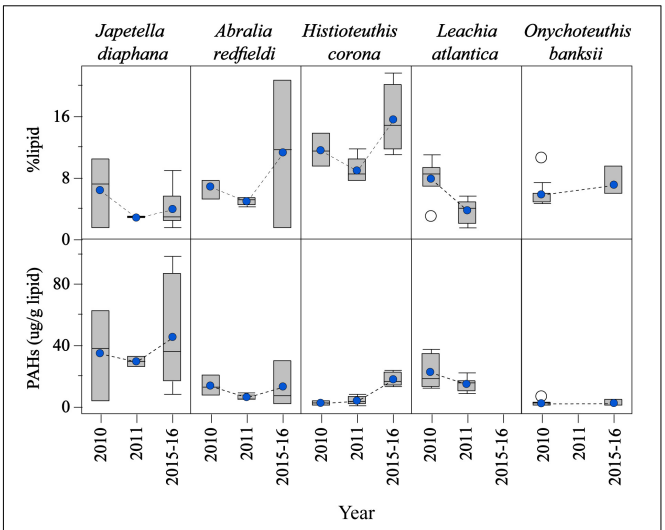

FIGURE 3 | Temporal variability of lipid contents and PAH concentrations in the mantle tissue of deep-sea cephalopod species collected in the northern Gulf of Mexico. Sampling years: pre-spill: 2010, and post-spill: 2011, and long-term: 2015–2016. PAHs refer to the sum of 2–6 ring including alkylated homologs. Graph shows shaded boxes as the interquartile ranges, with horizontal lines indicating median values and whiskers representing 10th and 90th percentile. Blue circles denote mean values, and white circles denote outliers.

An increase in %lipid content was observed in 2015–2016 for all species sampled in the long-term period (**Figure 3**).

Due to the differences found in %lipid content among the species studied, PAH concentrations were calculated as lipid-normalized concentrations (μg PAH/g lipid weight). PAH concentrations were lower post-spill for *J. diaphana*, *A. redfieldi*, and *L. atlantica*, with 16%, 56%, 34% decrease in PAH concentration in 2011 relative to 2010, respectively (**Figure 3**). *Histioteuthis corona* showed lower PAH concentrations in 2010 (pre-spill) and 2011 (post-spill), with a ∼84% increase in concentration during 2015–2016 (long-term period; **Figure 3**). In contrast, *O. banksii* showed similar PAH concentrations between the pre-spill and long-term periods (**Figure 3**). The temporal trend in PAH concentration observed in most species is not explained by %lipid content because lipid-normalized PAH data removes the influence of interspecies %lipid content. Also, we found that PAH concentrations were not correlated with mantle length in all cephalopod species ($p > 0.05$), except *H. corona* ($R^2 = 0.011$; $p < 0.01$; **Table 1**). However, significant differences of PAH concentrations between cephalopod life stages were not found in any studied year for any species, including for *H. corona* ($p > 0.05$; **Table 1**). Therefore, the temporal trend in PAH concentration for *H. corona* is not explained by the different lengths of animals collected among the years.

A similar abundance of 3-ring (76 – 81% phenanthrene compounds, including alkyl homologs) and 4-ring (11 – 17% pyrene and fluoranthene compounds, including alkyl homologs) PAHs were observed among the species studied (**Figure 4**). However, small changes in the composition of PAHs were detected between the periods covered in this study (**Figure 4** and

TABLE 1 | Temporal variability of PAH concentrations (μg/g lipid weight) in mantle tissue of mature and immature deep-sea cephalopods from the northern GoM.

Species	Life stages	*n*	Collection period		
			2010	2011	2015–2016
Japetella diaphana	Immature	4	37.7	32.1	30.1 ± 13.9
	Mature	14	32.9 ± 29.6	26.2	48.4 ± 12.0
Histioteuthis corona	Immature	5	N.A.	4.2	17.5 ± 2.2
	Mature	6	2.0 ± 1.0	3.0 ± 1.6	N.A.
Abralia redfieldi	Immature	2	N.A.	N.A.	15.5 ± 13.9
	Mature	9	13.3 ± 3.9	5.8 ± 0.9	7.2
Leachia atlantica	Mature	21	22.2 ± 3.4	14.4 ± 1.4	N.A.
Onychoteuthis banksii	Immature	1	N.A.	N.A.	4.4
	Mature	12	1.8 ± 0.6	N.A.	0.7 ± 0.4

Studied periods: pre-pill (2010), post-spill (2011), long-term (2015–2016). Data are shown as mean ±SE.

Supplementary Figure S1). In 2010 (pre-spill), PAH composition indicates a dominant petrogenic source in all species except *O. banksii* with a strong signature of pyrogenic PAHs (from probable combustion products). In 2011 (post-spill), a small change was observed with an increase in the abundance of 2–3 ring and alkyl PAHs (up to ∼20%). The small shift in the composition of PAHs indicates a larger source of low molecular weight PAHs post-spill (2011) for *A. redfieldi*, *L. atlantica* and *O. banksii* (typical distribution of %lipid abundance in the order of C0 < C1 < C2 > C3 > C4). Species like *H. corona* and *J. diaphana* showed a decrease in low molecular weight PAHs and an increase in alkyl PAHs post-spill, that may be related to their different behavior in the water column (see section "Discussion"). Altogether, the changes observed in the composition of PAHs indicate a different source after the spill that mixed with other sources over time (e.g., pyrogenic, seeps), like indicated by the composition of PAHs during the long-term period (2015–2016; **Figure 4**, **Supplementary Figure S1**).

Spatial Variability of PAHs

In 2010 (pre-spill), significantly lower PAH concentrations were observed in the south area relative to the other areas ($p < 0.001$; east: 15.9 ± 6.4 μg/g lipid; south: 4.5 ± 3.7 μg/g lipid; southeast: 18.9 ± 4.7 μg/g lipid). In contrast, in 2015–2016 (long-term period), PAH concentrations were not significantly different among the areas studied ($p > 0.05$). Only the south area showed significant differences in PAH concentrations in the tissue samples among years ($p < 0.001$), with an increase of PAHs over time (**Supplementary Figure S2**). The composition of PAHs changed post-spill (2011) and returned during the long-term period to conditions similar to pre-spill (**Supplementary Figure S3**). These results indicate that the temporal trend observed in the concentration and composition of PAHs is independent of the area sampled in each time period.

General Temporal Trends in PAH Levels and Composition

Even though a large variability was observed among the cephalopod species studied, all species indicate a higher exposure to 2–3 ring PAHs after 2010 (**Figure 4**). By integrating the PAH data from all species together, the general temporal trend observed indicates a ∼2-fold increase in PAH concentrations during the long-term period relative to samples collected pre-spill for the deep-sea cephalopod assemblage in the northern GoM (2010: 13.5 ± 3.0 μg/g lipid weight; 2011: 11.5 ± 1.7 μg/g lipid weight; and 2015–2016: 29.0 ± 6.6 μg/g lipid weight). Significantly higher concentrations were consistently observed in the long-term period relative to the pre-spill and post-spill periods ($p < 0.01$; **Figure 5**). Collectively, the trends observed in PAH composition and calculated ratios suggest an episodic exposure to petrogenic PAHs that occurred after the post-spill period (2011) and continue through 2016 ($p < 0.01$; **Figures 6**, **7**). In 2010 (pre-spill), higher ratios denote a more pyrogenic origin for PAHs (higher combustion sources) (HMW: 19.3 ± 2.0%; FL/Pyr: 1.5 ± 0.3; PI: 0.4 ± 0.1). In contrast, lower PAH ratios in 2011 (post-spill), indicate a petrogenic source (HMW: 11.5 ± 0.9%; FL/Pyr: 0.9 ± 0.1; PI: 0.1 ± 0.01). A slight increase in PAH ratios during the long-term period (2015–2016) indicate weathered oil-residues (more alkyl PAH compounds), as expected 5–6 years after the DWHOS (HMW: 15.9 ± 1.7%; FL/Pyr: 1.1 ± 0.2; PI: 0.3 ± 0.01). A similar %lipid abundance of retene (a 3-ring PAH) among sampling periods ($p > 0.05$) indicates a consistently low source of natural PAHs to the deep-pelagic environment during this study (2010–2016).

DISCUSSION

Interspecies differences were observed in lipid content and PAH concentrations, suggesting biological factors (e.g., diet, habitat, life span, behavior, and lipid metabolism) play an important role in the bioaccumulation of PAHs in the mantle tissues (**Table 1**). The species examined in this study are different from one another in many physical and ecological aspects (**Supplementary Table S1**). *Abralia redfieldi* is a small muscular squid (collected sizes: 9–35 mm ML), living primarily in the mesopelagic and migrating to the epipelagic zone nightly (Judkins and Vecchione, this vol). *Onychoteuthis banksii* is also a muscular squid, but larger (collected sizes: 14–326 mm ML) and found at depth during the day and migrating to the upper mesopelagic and epipelagic zones nightly. In contrast, *J. diaphana* is a gelatinous octopod (collected sizes: 9–105 mm ML), found throughout the water column from the epi- to the bathy-pelagic zones; it exhibits ontogenic descent (i.e., larger individuals tend to live deeper in the water column than smaller ones). *Leachia atlantica* is a glass squid species (collected sizes: 36–111 mm ML) that uses an ammonia-filled chamber to achieve neutral buoyancy and it is found throughout the water column with no evidence of ontogenic descent (Judkins and Vecchione, this vol). Very different from the other species studied, *H. corona* is a large squid with ammoniacal muscle tissue (collected sizes: 17–71 mm ML; max known size: ∼190 mm ML) that does not vertically migrate daily, primarily inhabiting the mesopelagic zone. Altogether, these multiple ecological differences might affect lipid content and PAH concentrations among the species studied (**Figure 3**), as species are exposed to different environments in the water

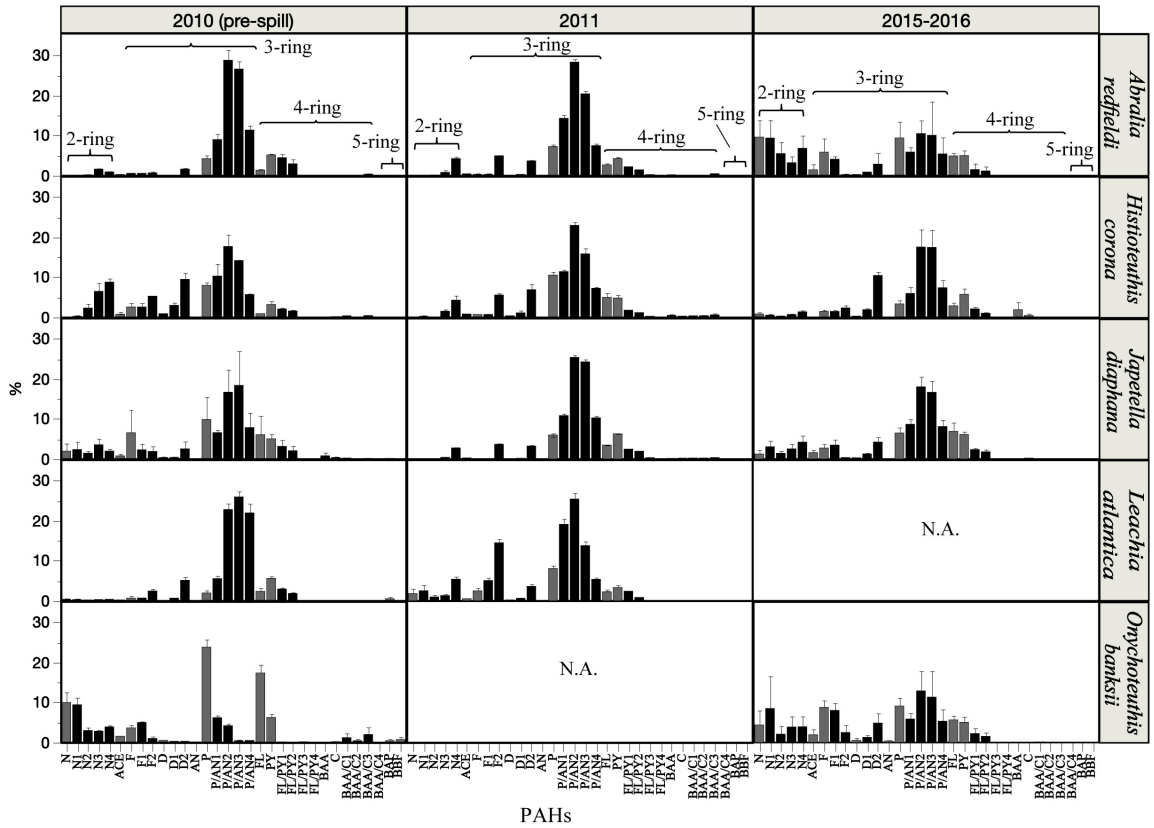

FIGURE 4 | Relative abundance (%) of PAH compounds in the mantle tissue of deep-sea cephalopod species collected in the northern Gulf of Mexico. Sampling years: pre-spill: 2010, post-spill: 2011, and long-term: 2015–2016. Graphs shows gray bars as parent PAHs, and black bars as alkylated PAHs. Data are shown as mean ±SE.

column. For example, *H. corona* and *J. diaphana* do not migrate vertically every day to the surface (∼50 m). Therefore, they may have been exposed to different hydrocarbon mixtures formed in the water column after released at ∼1500 m depth containing distinct chemical compositions (Ryerson et al., 2012). Also, biological parameters such as lipid metabolism may have an essential role in the variability of PAH bioaccumulation among cephalopod species. It seems that in some shallower-living cephalopod species, the digestive gland has an important role in detoxification of organic pollutants, including PAHs (Rodrigo and Costa, 2017). The physiological and molecular mechanisms involved in detoxification processes for organic pollutants in deep-sea cephalopod species are not known. It seems likely that the pathways for detoxification of organic pollutants may be different among the deep-sea cephalopod species studied as shown by the PAH concentrations in the mantle tissues (**Figure 3**).

Interestingly, the temporal trends observed in this study were all similar among the deep-sea cephalopod species studied. For example, our results indicate a shift in the composition of PAHs in all cephalopod species in 2011 (post-spill) relative to 2010 (January to March; pre-spill) that continue to 2015–2016 (long-term period; **Figures 4**, **6**), supporting previous studies that suggest exposure and uptake of oil-derived PAHs from the DWHOS occurred in offshore organisms (Murawski et al., 2014; Snyder et al., 2015; Romero et al., 2018). There are multiple sources of PAHs in the northern GoM (seeps, riverine discharges, continental runoff, coastal erosion, atmospheric deposition, and oil and gas exploration) (Park et al., 2001, 2002; Mitra and Bianchi, 2003; Tansel et al., 2011), with seeps as the most abundant among those sources (Ocean Studies Board and Marine Board, 2003). However, the DWHOS released an amount over seven times the average annual input of oil into the GoM, becoming the most important source of PAHs in summer to fall of 2010 (Murawski et al., 2014). As expected, most of the change in the composition of PAHs occurred for the low-molecular weight compounds (2–3 rings), abundant in oil that weathered and mixed over time with other sources (e.g., Mississippi river, natural seeps), as observed in 2015–2016. This inference is supported by similar abundances of retene between pre-pill and post-spill periods (**Figure 7**) indicating that natural sources of PAHs in the GoM do not explain the temporal trend observed in the composition of PAHs in the deep-sea cephalopod species studied.

The temporal trend for lipid content and PAH concentrations were also similar among the cephalopod species with significant changes over the 6-years of this study (**Figure 3**). However, the temporal trends observed in **Figure 3**, were not as expected for a one point-source contamination event, like the DWHOS

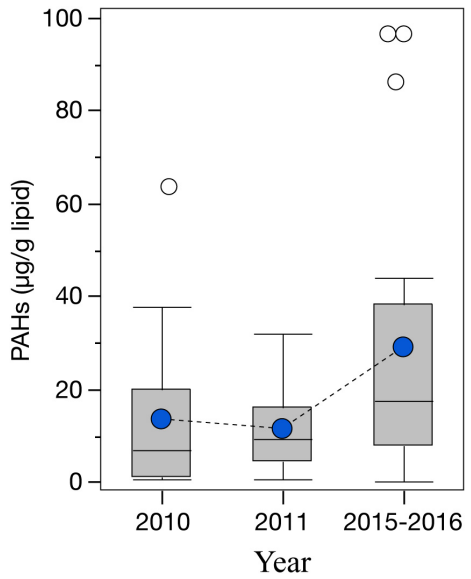

FIGURE 5 | Temporal variability of PAH concentrations in the mantle tissue of deep-sea cephalopods (species combined) collected in the northern Gulf of Mexico. Sampling years: pre-spill: 2010, post-spill: 2011, and long-term: 2015–2016. PAHs refer to the sum of 2–6 ring including alkylated homologs. Graph shows shaded boxes as the interquartile ranges, with horizontal lines indicating median values and whiskers representing 10th and 90th percentile. Blue circles denote mean values, and white circles denote outliers.

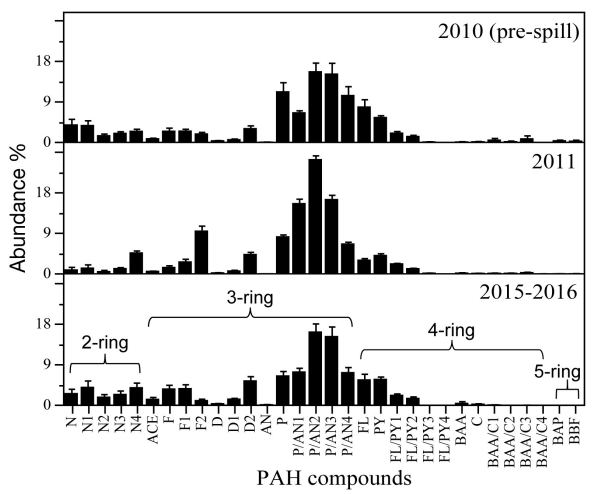

FIGURE 6 | Relative abundance (%) of PAH compounds in the mantle tissue of deep-sea cephalopods collected in the northern Gulf of Mexico. Sampling years: pre-spill: 2010, post-spill: 2011, and long-term: 2015–2016. Data are shown as mean ±SE.

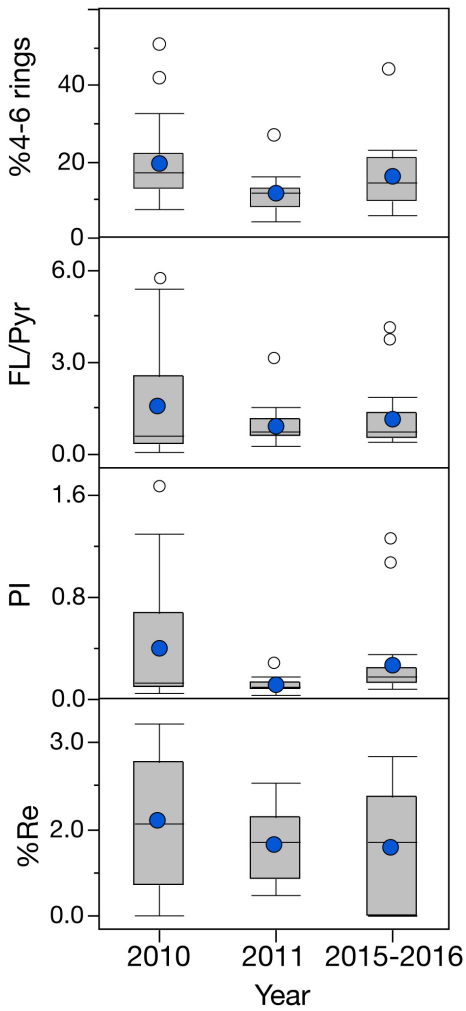

FIGURE 7 | Temporal variation of PAH ratios in the mantle tissue of deep-sea cephalopods collected in the northern Gulf of Mexico. Sampling years: pre-spill: 2010, post-spill: 2011, and long-term: 2015–2016. Graph shows shaded boxes as the interquartile ranges, with horizontal lines indicating median values and whiskers representing 10th and 90th percentile. Blue circles denote mean values, and white circles denote outliers. Data are shown as mean ±SE.

in the summer of 2010. Lipid content was lower in 2011 (post-spill) relative to 2010 (pre-spill) for all species with samples collected in this year. Similarly, lipid-normalized PAH concentrations were lower in 2011 relative to 2010 for all species with samples collected in this year, except for *H. corona* (with similar concentrations for 2010 and 2011). The fact that in 2011 PAH composition shows a shift in the source of PAHs but concentrations decreased, as well as lipid content, indicates that the temporal trends observed are secondary effects of the exposure to oil-residues from the DWHOS. We hypothesize that the lower lipid content in the cephalopod species observed in 2011 (post-spill) may be due to a change in dietary intake (decrease in prey availability) and/or dietary quality (e.g., fatty acids decrease in prey). Stable-isotope analysis of *J. diaphana*, *H. corona*, *O. banksii* and *L. atlantica* (Staudinger et al., in press, Richards et al., unpublished data) indicate that these species occupy multiple trophic positions, inhabiting a variety of ecological niches within the water column, all potentially affected by the DWHOS. Several studies demonstrated carbon from the DWHOS entered the planktonic and mesopelagic

food web after the spill (Chanton et al., 2012; Quintana-Rizzo et al., 2015) supporting the idea that potential prey species from different trophic levels were affected by oil-residues, which may have influenced the dietary intake of cephalopods. Moreover, several studies in shallower species, showed that dietary inputs can severely affect lipids, which are critical in cephalopod development (Navarro and Villanueva, 2003; Almansa et al., 2006; Guinot et al., 2013; Reis et al., 2016). Due to the hydrophobic properties of PAHs, significant changes in lipid content may also affect bioaccumulation of PAHs. The exception observed in the temporal trend for PAH concentrations in *H. corona* suggests other factors are important for bioaccumulation of PAHs in cephalopods. In this species, lower lipid content was observed post-spill (2011), albeit similar PAH concentrations pre- and post-spill (2010 and 2011), and 84% higher concentrations in the long-term period (2015–2016). Of all the species studied, *H. corona* is the only one that lives in the mesopelagic zone and does not migrate to the surface to feed (**Supplementary Table S1**). Oil-residues have been observed in the water column years after the spill (Walker et al., 2017), probably from resuspension of contaminated sediments (Romero et al., 2017; Diercks et al., 2018). It is possible that the dietary intake for *H. corona* was affected like the other species studied (**Figure 3**), but with an extended period of exposure to oil-residues persistent at depth. This is supported by elevated PAH concentrations observed in the long-term period (2015–2016).

Collectively, PAH composition trends in the deep-sea cephalopod species studied suggest an episodic exposure to petrogenic PAHs that occurred after the pre-spill sampling campaign in 2010 and continued through 2015–2016. Exposure to oil-derived PAHs occurred after the DWHOS, but secondary effects, including potential trophic-web effects, may have influenced the lipid content and PAH levels post-spill (2011). It appears that exposure to oil-derived residues is longer than expected in the pelagic deep-sea environment, as observed from the same event in mesopelagic fishes (Romero et al., 2018). This phenomenon may have disturbed the deep-sea environment via the food web, as indicated by the temporal trend observed in cephalopod species. Due to the important role of lipids on the physiology of cephalopods (Reis et al., 2016), future studies should evaluate lipid composition in relation to dietary intake and organic contaminants. Also, studies should cover longer periods for a better understating of the persistence of organic pollutants at depth and impacts to pelagic communities from different trophic levels.

DATA AVAILABILITY STATEMENT

Data are publicly available through the Gulf of Mexico Research Initiative and Data Cooperative (GRIIDC) at https://data.gulfresearchinitiative.org (doi: 10.7266/XN8NE9DW).

ETHICS STATEMENT

The animal study was reviewed and approved by the IACUC USF.

AUTHOR CONTRIBUTIONS

IR carried out the laboratory and data analyses, and wrote the manuscript including figures and tables. HJ and MV collected the samples and identified specimens to species levels, as well as contributing to the manuscript by revising, editing, and adding references and comments.

FUNDING

This research was supported by the Gulf of Mexico Research Initiative (GOMRI) through the programs DEEPEND (Deep Pelagic Nekton Dynamics of the Gulf of Mexico). Also, it includes work that was conducted by the National Marine Fisheries Service (SWAPS) and as part of the Deepwater Horizon Natural Resource Damage Assessment (ONSAP) being conducted cooperatively among NOAA, academic institutions (e.g., USF St. Petersburg, NSU), and other federal and state trustees.

ACKNOWLEDGMENTS

The authors would like to thank the crew of the R/V *Pisces*, R/V *Meg Skansi*, and R/V *Point Sur* for their help during the field program, T. Sutton for support and information about ONSAP and DEEPEND programs, D. Fenolio for images, and the technicians Thea Barlett, Hannah Hamontree, and Olivia Traenkle for laboratory support.

SUPPLEMENTARY MATERIAL

The Supplementary Material for this article can be found online at: https://www.frontiersin.org/articles/10.3389/fmars.2020.00054/full#supplementary-material

FIGURE S1 | % change in the composition of PAHs in 2011 (post-spill) and 2015–2016 (long-term period) relative to 2010 (pre-spill) in the mantle tissue of deep-sea cephalopods collected in the northern Gulf of Mexico. Graph shows bars as the % difference of normalized concentrations by total PAHs between sampling periods (2011 minus 2010; 2015–2016 minus 2010). Values >0 indicate an increase in the abundance of individual PAHs, while values <0 indicate a decrease in the abundance of individual PAHs.

FIGURE S2 | Temporal variability of PAH concentrations in the mantle tissue of deep-sea cephalopods (species combined) collected in the northern Gulf of Mexico. Sampling years: pre-spill: 2010, post-spill: 2011, and long-term: 2015–2016. PAHs refer to the sum of 2–6 ring including alkylated homologs. Graph shows shaded boxes as the interquartile ranges, with horizontal lines indicating median values and whiskers representing 10th and 90th percentile. Blue circles denote mean values, and white circles denote outliers.

FIGURE S3 | Relative abundance (%) of PAH compounds in the mantle tissue of deep-sea cephalopods collected in three areas in northern Gulf of Mexico. Sampling years: pre-spill: 2010, post-spill: 2011, and long-term: 2015–2016. Data are shown as mean ±SE.

TABLE S1 | Ecological characteristics of deep-sea cephalopod species from the northern GoM.

REFERENCES

Adhikari, P. L., Wong, R. L., and Overton, E. B. (2017). Application of enhanced gas chromatography/triple quadrupole mass spectrometry for monitoring petroleum weathering and forensic source fingerprinting in samples impacted by the deepwater Horizon oil spill. *Chemosphere* 184, 939–950. doi: 10.1016/j.chemosphere.2017.06.077

Almansa, E., Domingues, P., Sykes, A., Tejera, N., Lorenzo, A., and Andrade, J. P. (2006). The effects of feeding with shrimp or fish fry on growth and mantle lipid composition of juvenile and adult cuttlefish (*Sepia officinalis*). *Aquaculture* 256, 403–413. doi: 10.1016/j.aquaculture.2006.02.025

Beriro, D. J., Vane, C. H., Cave, M. R., and Nathanail, C. P. (2014). Effects of drying and comminution type on the quantification of polycyclic aromatic hydrocarbons (PAH) in a homogenised gasworks soil and the implications for human health risk assessment. *Chemosphere* 111, 396–404. doi: 10.1016/j.chemosphere.2014.03.077

Brooks, G. R., Larson, R. A., Schwing, P. T., Romero, I., Moore, C., Reichart, G. J., et al. (2015). Sedimentation pulse in the NE Gulf of Mexico following the 2010 DWH blowout. *PLoS One* 10:132341. doi: 10.1371/journal.pone.0132341

Chanton, J. P., Cherrier, J., Wilson, R. M., Sarkodee-Adoo, J., Bosman, S., Mickle, A., et al. (2012). Radiocarbon evidence that carbon from the Deepwater Horizon Spill entered the planktonic food web of the Gulf of Mexico. *Environ. Res. Lett.* 7, 1–4. doi: 10.1088/1748-9326/7/4/045303

Chanton, J. P., Giering, S. L. C., Bosman, S. H., Rogers, K. L., Sweet, J., Asper, V. L., et al. (2018). Isotopic composition of sinking particles : oil effects, recovery and baselines in the Gulf of Mexico, 2010-2015. *Elem. Sci. Anthr.* 6, 2010–2015. doi: 10.1525/elementa.298

Corrales, X., Coll, M., Tecchio, S., María, J., Mario, A., and Palomera, I. (2015). Ecosystem structure and fishing impacts in the northwestern Mediterranean Sea using a food web model within a comparative approach. *J. Mar. Syst.* 148, 183–199. doi: 10.1016/j.jmarsys.2015.03.006

Daly, K. L., Passow, U., Chanton, J., and Hollander, D. (2016). Assessing the impacts of oil-associated marine snow formation and sedimentation during and after the Deepwater Horizon oil spill. *Biochem. Pharmacol.* 13, 18–33. doi: 10.1016/j.ancene.2016.01.006

Davis, R. W., Jaquet, N., Gendron, D., Markaida, U., Bazzino, G., and Gilly, W. (2007). Diving behavior of sperm whales in relation to behavior of a major prey species, the jumbo squid, in the Gulf of California, Mexico. *Mar. Ecol. Prog. Ser.* 333, 291–302. doi: 10.3354/meps333291

Davison, P. C. Jr., Koslow, J. A., and Barlow, J. (2013). Carbon export mediated by mesopelagic fishes in the northeast Pacific Ocean. *Prog. Oceanogr.* 116, 14–30. doi: 10.1016/j.pocean.2013.05.013

Diercks, A., Dike, C., Asper, V. L., Dimarco, S. F., and Jeffrey, P. (2018). Scales of seafloor sediment resuspension in the northern Gulf of Mexico. *Elem. Sci. Anthr.* 1, 1–28. doi: 10.1525/elementa.285

Dietrich, J. C., Trahan, C. J., Howard, M. T., Fleming, J. G., Weaver, R. J., Tanaka, S., et al. (2012). Surface trajectories of oil transport along the Northern Coastline of the Gulf of Mexico. *Cont. Shelf Res.* 41, 17–47. doi: 10.1016/j.csr.2012.03.015

Fisher, C. R., Montagna, P. A., and Sutton, T. T. (2016). How did the Deepwater Horizon oil spill impact deep-sea ecosystems? *Oceanography* 29, 182–195. doi: 10.5670/oceanog.2016.82

Fitzgerald, T. P., and Gohlke, J. M. (2014). Contaminant levels in gulf of Mexico reef fish after the deepwater horizon oil spill as measured by a fishermen-led testing program. *Environ. Sci. Technol.* 48, 1993–2000. doi: 10.1021/es405 1555

Gomes, F., Oliveira, M., Ramalhosa, M. J., Delerue-matos, C., and Morais, S. (2013). Polycyclic aromatic hydrocarbons in commercial squids from different geographical origins : levels and risks for human consumption. *Food Chem. Toxicol.* 59, 46–54. doi: 10.1016/j.fct.2013.05.034

Graham, W. M., Condon, R. H., Carmichael, R. H., D'Ambra, I., Patterson, H. K., Linn, L. J., et al. (2010). Oil carbon entered the coastal planktonic food web during the Deepwater Horizon oil spill. *Environ. Res. Lett.* 5:045301. doi: 10.1088/1748-9326/5/4/045301

Guinot, D., Monroig, O., Navarro, J. C., Varo, I., Amat, F., and Hontoria, F. (2013). Enrichment of *Artemia metanauplii* in phospholipids and essential fatty acids as a diet for common octopus (Octopus vulgaris) paralarvae. *Aquac. Nutr.* 19, 837–844. doi: 10.1111/anu.12048

Harding, V., Camp, J., Morgan, L. J., and Gryko, J. (2016). Oil residue contamination of continental shelf sediments of the Gulf of Mexico. *Mar. Pollut. Bull.* 113, 488–495. doi: 10.1016/j.marpolbul.2016.07.032

Hazen, T. C., Dubinsky, E. A., DeSantis, T. Z., Andersen, G. L., Piceno, Y. M., Singh, N., et al. (2010). Deep-sea oil plume enriches indigenous oil-degrading bacteria. *Science* 330, 204–208. doi: 10.1126/science.1195979

Hooper, T., and Parrish, C. C. (2009). Profiling neutral lipids in individual fish larvae by using shortcolumn gas chromatography with flame ionization detection. *Limnol. Oceanogr. Methods* 7, 411–418. doi: 10.4319/lom.2009.7.411

Hoving, H. J. T., and Robison, B. H. (2017). The pace of life in deep-dwelling squids. *Deep Res. I* 126, 40–49. doi: 10.1016/j.dsr.2017.05.005

Hudson, J. M., Steinberg, D. K., Sutton, T. T., Graves, J. E., and Latour, R. J. (2014). Myctophid feeding ecology and carbon transport along the northern Mid-Atlantic Ridge. *Deep Res. I* 93, 104–116. doi: 10.1016/j.dsr.2014.07.002

Irigoien, X., Klevjer, T. A., Rostad, A., Martinez, U., Boyra, G., Acuna, J. L., et al. (2014). Large mesopelagic fishes biomass and trophic efficiency in the open ocean. *Nat. Commun.* 5:4271. doi: 10.1038/ncomms4271

Judkins, H., Arbuckle, S., Vecchione, M., and Martinez, A. (2015). Cephalopods in the potential prey field of sperm whales (Physeter macrocephalus) (Cetacea : Physeteridae) in the northern Gulf of Mexico. *J. Nat. Hist.* 49, 37–41. doi: 10.1080/00222933.2013.802045

Judkins, H., Vecchione, M., Cook, A., and Sutton, T. (2017). Diversity of midwater cephalopods in the northern Gulf of Mexico : comparison of two collecting methods. *Mar. Biodivers.* 47, 647–657. doi: 10.1007/s12526-016-0597-8

Lacoue-Labarthe, T., Le PAbic, C., and Bustamante, P. (2016). Ecotoxicology of early-life stages in the common cuttlefish. *Vie Milieu* 66, 65–79.

Lalas, C., and Webster, T. (2014). Contrast in the importance of arrow squid as prey of male New Zealand sea lions and New Zealand fur seals at The Snares, subantarctic New Zealand. *Mar. Biol.* 161, 631–643. doi: 10.1007/s00227-013-2366-6

Logan, J. M., Toppin, R., Smith, S., Galuardi, B., Porter, J., and Lutcavage, M. (2013). Contribution of cephalopod prey to the diet of large pelagic fish predators in the central North Atlantic Ocean. *Deep Res. II* 95, 74–82. doi: 10.1016/j.dsr2.2012.06.003

MacDonald, I. R., Garcia-Pineda, O., Beet, A., Daneshgar, A., Feng, L., Graettinger, G., et al. (2015). Natural and unnatural oil slicks in the Gulf of Mexico. *J. Geophys. Res. Ocean* 120, 3896–3912.

Mitra, S., and Bianchi, T. (2003). A preliminary assessment of polycyclic aromatic hydrocarbon distributions in the lower Mississippi River and Gulf of Mexico. *Mar. Chem.* 82, 273–288. doi: 10.1016/S0304-4203(03)00074-4

Mitra, S., Bianchi, T. S., Mckee, B. A., and Sutula, M. (2002). Black carbon from the mississippi river: quantities, sources, and potential implications for the global carbon cycle. *Environ. Sci. Technol.* 36, 2296–2302. doi: 10.1021/es015834b

Murawski, S. A., Fleeger, J. W., Patterson, W. F., Hu, C., Daly, K., Romero, I., et al. (2016). How did the Deepwater Horizon oil spill affect coastal and continental shelf ecosystems of the Gulf of Mexico? *Oceanography* 29, 160–173. doi: 10.5670/oceanog.2016.80

Murawski, S. A., Hogarth, W. T., Peebles, E. B., and Barbeiri, L. (2014). Prevalence of external skin lesions and polycyclic aromatic hydrocarbon concentrations in Gulf of Mexico fishes, post-Deepwater Horizon. *Trans. Am. Fish. Soc.* 143, 37–41. doi: 10.1080/00028487.2014.911205

Navarro, J. C., and Villanueva, R. (2003). The fatty acid composition of Octopus vulgaris paralarvae reared with live and inert food : deviation from their natural fatty acid profile. *Aquaculture* 219, 613–631. doi: 10.1016/s0044-8486(02)00311-3

Ocean Studies Board and Marine Board (2003). *Oil in the Sea III. Inputs, Fates, and Effects*. Washington, D.C: National Academies Press.

Park, J., Wade, T. L., and Sweet, S. (2001). Atmospheric distribution of polycyclic aromatic hydrocarbons and deposition to Galveston Bay, Texas, USA. *Atmos. Environ.* 35, 3241–3249. doi: 10.1016/s1352-2310(01)00080-2

Park, J., Wade, T. L., and Sweet, S. T. (2002). Atmospheric deposition of PAHs, PCBs, and organochlorine pesticides to Corpus Christi Bay, Texas. *Atmos. Environ.* 36, 1707–1720. doi: 10.1016/s1352-2310(01)00586-6

Quintana-Rizzo, E., Torres, J. J., Ross, S. W., Romero, I., Watson, K., Goddard, E., et al. (2015). δ13C and δ15N in deep-living fishes and shrimps after the Deepwater Horizon oil spill Gulf of Mexico. *Mar. Pollut. Bull.* 94, 241–250. doi: 10.1016/j.marpolbul.2015.02.002

Reis, D. B., Acosta, N. G., Almansa, E., Tocher, D. R., Andrade, J. P., Sykes, A. V., et al. (2016). Composition and metabolism of phospholipids in Octopus vulgaris and *Sepia officinalis* hatchlings. *Comp. Biochem. Physiol. B Biochem. Mol. Biol.* 200, 62–68. doi: 10.1016/j.cbpb.2016.06.001

Rodrigo, A. P., and Costa, P. M. (2017). The Role of the cephalopod digestive gland in the storage and detoxification of marine pollutants. *Front. Physiol.* 8:232. doi: 10.3389/fphys.2017.00232

Romeo, T., Battaglia, P., and Peda, C. (2012). Pelagic cephalopods of the central Mediterranean Sea determined by the analysis of the stomach content of large fish predators. *Helgo. Mar. Res.* 66, 295–306. doi: 10.1007/s10152-011-0270-3

Romero, I. C., Özgökmen, T., Snyder, S., Schwing, P., O'Malley, B. J., Beron-Vera, F. J., et al. (2016). Tracking the hercules 265 marine gas well blowout in the Gulf of Mexico. *J. Geophys. Res. Ocean* 121, 706–724. doi: 10.1002/2015JC011037

Romero, I. C., Schwing, P. T., Brooks, G. R., Larson, R. A., Hastings, D. W., Flower, B. P., et al. (2015). Hydrocarbons in deep-sea sediments following the 2010 Deepwater Horizon Blowout in the Northeast Gulf of Mexico. *PLoS One* 10:128371. doi: 10.1371/journal.pone.0128371

Romero, I. C., Sutton, T., Carr, B., Quintana-Rizzo, E., Ross, S. W., Hollander, D. J., et al. (2018). A decadal assessment of polycyclic aromatic hydrocarbons in mesopelagic fishes from the Gulf of Mexico reveals exposure to oil-derived sources. *Environ. Sci. Technol.* 52, 10985–10996. doi: 10.1021/acs.est.8b02243

Romero, I. C., Toro-farmer, G., Diercks, A., Schwing, P., Muller-Karger, F., Murawski, S., et al. (2017). Large-scale deposition of weathered oil in the Gulf of Mexico following a deep-water oil spill. *Environ. Pollut.* 228, 179–189. doi: 10.1016/j.envpol.2017.05.019

Ryerson, T. B., Camilli, R., Kessler, J. D., Kujawinski, E. B., Reddy, C. M., Valentine, D. L., et al. (2012). Chemical data quantify Deepwater Horizon hydrocarbon flow rate and environmental distribution. *Proc. Natl. Acad. Sci. U.S.A.* 109, 20246–20253. doi: 10.1073/pnas.1110564109

Salman, A., and Karakulak, F. S. (2019). Cephalopods in the diet of albacore, *Thunnus alalunga*, from the eastern mediterranean. *J. Mar. Biol. Assoc. U. K.* 89, 635–640. doi: 10.1017/S0025315408002555

Semedo, M., Oliveira, M., Gomes, F., Reis-henriques, M. A., Delerue-matos, C., Morais, S., et al. (2014). Seasonal patterns of polycyclic aromatic hydrocarbons in digestive gland and arm of octopus (Octopus vulgaris) from the Northwest Atlantic. *Sci. Total Environ.* 481, 488–497. doi: 10.1016/j.scitotenv.2014.02.088

Sloan, C. A., Brown, D. W., Pearce, R. W., Boyer, R. H. Bolton, J. L., Burrows, D. G., et al. (2004). Extraction, cleanup, and gas chromatography/mass spectrometry analysis of sediments and tissues for organic contaminants. *U.S. Dept. Commer. NOAA Tech. Memo. NMFS-NWFSC-59*, 47.

Snyder, S. M., Pulster, E. L., Wetzel, D. L., and Murawski, S. A. (2015). PAH exposure in Gulf of Mexico demersal fishes, post-deepwater horizon. *Environ. Sci. Technol.* 49, 8786–8795. doi: 10.1021/acs.est.5b01870

Sorensen, L., Meier, S., and Mjos, S. A. (2016). Application of gas chromatography/tandem mass spectrometry to determine a wide range of petrogenic alkylated polycyclic aromatic hydrocarbons in biotic samples. *Rapid Commun. Mass Spectr.* 30, 2052–2058. doi: 10.1002/rcm.7688

Southall, B. L., Benoit-bird, K. J., Moline, M. A., and Moretti, D. (2019). Quantifying deep-sea predator– prey dynamics: implications of biological heterogeneity for beaked whale conservation. *J. Appl. Ecol.* 56, 1040–1049. doi: 10.1111/1365-2664.13334

Steinberg, D. K., Cope, J. S., Wilson, S. E., and Kobari, T. (2008). A comparison of mesopelagic mesozooplankton community structure in the subtropical and subarctic North Pacific Ocean. *Deep Res. II* 55, 1615–1635. doi: 10.1016/j.dsr2.2008.04.025

Steinberg, D. K., and Landry, M. R. (2017). Zooplankton and the ocean carbon cycle. *Annu. Rev. Earth Planet. Sci.* 9, 413–444. doi: 10.1146/annurev-marine-010814-015924

Stewart, J. S., Hazen, E. L., Bograd, S. J., Jarrett, E. K., Gilly, W. F., and Robison, B. H. (2014). Combined climate- and prey-mediated range expansion of humboldt squid (Dosidicus gigas), a large marine predator in the California Current System. *Glob. Chang. Biol.* 20, 1832–1843. doi: 10.1111/gcb.12502

Tansel, B., Fuentes, C., Sanchez, M., Predoi, K., and Acevedo, M. (2011). Persistence profile of polyaromatic hydrocarbons in shallow and deep Gulf waters and sediments: effect of water temperature and sediment-water partitioning characteristics. *Mar. Pollut. Bull.* 62, 2659–2665. doi: 10.1016/j.marpolbul.2011.09.026

Taucher, J., Stange, P., Algueró-muñiz, M., Bach, L. T., Nauendorf, A., Kolzenburg, R., et al. (2018). In situ camera observations reveal major role of zooplankton in modulating marine snow formation during an upwelling-induced plankton bloom. *Prog. Oceanogr.* 164, 75–88. doi: 10.1016/j.pocean.2018.01.004

U.S. District Court, (2015). *Findings of Facts and Conclusions of Law - Phase 2 Trial*. Coffeyville, KS: U.S. District Court.

Unger, M. A., Harvey, E., Vadas, G. G., and Vecchione, M. (2008). Persistent pollutants in nine species of deep-sea cephalopods. *Mar. Pollut. Bull.* 56, 2003–2005.

van Eenennaam, J. S., Rahsepar, S., Radoviæ, J. R., Oldenburg, T. B. P., Wonink, J., Langenhoff, A. A. M., et al. (2018). Marine snow increases the adverse effects of oil on benthic invertebrates. *Mar. Pollut. Bull.* 126, 339–348. doi: 10.1016/j.marpolbul.2017.11.028

Wade, T. L., Sericano, J. L., Sweet, S. T., Knap, A. H., and Guinasso, N. L. (2016). Spatial and temporal distribution of water column total polycyclic aromatic hydrocarbons (PAH) and total petroleum hydrocarbons (TPH) from the Deepwater Horizon (Macondo) incident. *Mar. Pollut. Bull.* 103, 286–293. doi: 10.1016/j.marpolbul.2015.12.002

Walker, B. D., Druffel, E. R. M., Kolasinski, J., Roberts, B. J., Xu, X., and Rosenheim, B. E. (2017). Stable and radiocarbon isotopic composition of dissolved organic matter in the Gulf of Mexico. *Geophys. Res. Lett.* 44, 8424–8434. doi: 10.1002/2017GL074155

Wang, Z., and Fingas, M. F. (2003). Development of oil hydrocarbon fingerprinting and identification techniques. *Mar. Pollut. Bull.* 47, 423–452. doi: 10.1016/S0025-326X(03)00215-7

Yan, B., Passow, U., Chanton, J. P., Nöthig, E.-M., Asper, V., Sweet, J., et al. (2016). Sustained deposition of contaminants from the Deepwater Horizon spill. *Proc. Natl. Acad. Sci. U.S.A.* 113, E3332–E3340. doi: 10.1073/pnas.1513156113

Young, J. W., Guest, M. A., Lansdell, M., Phleger, C. F., and Nichols, P. D. (2010). Discrimination of prey species of juvenile swordfish *Xiphias gladius* (Linnaeus, 1758) using signature fatty acid analyses. *Prog. Oceanogr.* 86, 139–151. doi: 10.1016/j.pocean.2010.04.028

Conflict of Interest: The authors declare that the research was conducted in the absence of any commercial or financial relationships that could be construed as a potential conflict of interest.

frontiers in Marine Science

ORIGINAL RESEARCH
published: 03 March 2020
doi: 10.3389/fmars.2020.00101

Reproductive Ecology of Dragonfishes (Stomiiformes: Stomiidae) in the Gulf of Mexico

Alex D. Marks[1]*, *David W. Kerstetter*[1], *David M. Wyanski*[2] and *Tracey T. Sutton*[1]

[1] Halmos College of Natural Sciences and Oceanography, Nova Southeastern University, Dania Beach, FL, United States,
[2] South Carolina Department of Natural Resources, Marine Resources Research Institute, Charleston, SC, United States

The most abundant fishes on Earth live in the meso- and bathypelagic (deep-pelagic, collectively) zones of the open ocean, where they play a key role in deep-sea food webs by mediating energy flow from surface waters to great depth. Of these fishes, the most speciose taxon is the family Stomiidae (dragonfishes). Despite being the numerically dominant predators of the global mesopelagic zone, stomiid reproductive ecology is poorly known. Research surveys rarely catch larger adults, impeding reproductive ecology studies. Between 2010 and 2011, the Offshore Nekton Sampling and Analysis Program sampled the Gulf of Mexico using a research-sized, opening/closing trawl (10-m^2 MOCNESS) and a commercial-sized, high-speed rope trawl (HSRT). Size-distribution analysis by gear type revealed: the HSRT caught more specimens per species, and the HSRT caught significantly larger specimens, whereas the MOCNESS sampled more juveniles. Gonads were dissected from 714 individuals representing 47 species, and the 12 dominant species were analyzed in further detail. Gonadal histology assessment indicated that stomiids are gonochoristic and exhibit asynchronous oocyte development and batch spawning. A total of 11 of the 12 species had sex ratios that did not significantly differ from a 1:1 (male:female) ratio ($P < 0.05$). Histological analysis indicated that females mature at larger sizes than males. Given the lack of age and growth data for this family, these data are critical for estimating stomiid production rates, a key element for quantifying the role of stomiids in the transfer of organic matter within the deep-pelagic zone, the planet's largest cumulative ecosystem.

Keywords: Stomiidae, reproduction, mesopelagic, sex ratio, gonad histology, maturity, size distributions

OPEN ACCESS

Edited by:
Michael Vecchione, National Oceanic and Atmospheric Administration (NOAA), United States

Reviewed by:
Shannon Colleen DeVaney, Pierce College, United States
Mackenzie E. Gerringer, The State University of New York College Geneseo, United States

***Correspondence:**
Alex D. Marks
am2919@nova.edu

Specialty section:
This article was submitted to Deep-Sea Environments and Ecology, a section of the journal Frontiers in Marine Science

Received: *30 August 2019*
Accepted: *07 February 2020*
Published: *03 March 2020*

Citation:
Marks AD, Kerstetter DW, Wyanski DM and Sutton TT (2020) Reproductive Ecology of Dragonfishes (Stomiiformes: Stomiidae) in the Gulf of Mexico. Front. Mar. Sci. 7:101. doi: 10.3389/fmars.2020.00101

INTRODUCTION

Mesopelagic (200–1,000 m depth) fishes comprise the majority of Earth's fish biomass (Irigoien et al., 2014; Nelson et al., 2016). A study by Gjøsaeter and Kawaguchi (1980) used trawl catch data to estimate the global aggregate biomass of mesopelagic fishes to be 1×10^9 tons. However, the authors also indicated that this number was likely an underestimate due to trawl avoidance (most research-sized nets are relatively small compared to commercial nets) and extrusion (specimens passing through the meshes of larger, commercial-sized trawls) (Kashkin and Parin, 1983). More recent studies based on modeling and acoustic data (Koslow et al., 1997; Kaartvedt et al., 2012) suggest the global biomass to be significantly higher than earlier estimates; for example, the biomass of mesopelagic fishes between 40°N and 40°S alone is estimated to be at least an order of magnitude

higher, between 7 and 10 billion metric tons (Koslow et al., 1997; Kaartvedt et al., 2012; Irigoien et al., 2014). Given their high abundance and biomass, mesopelagic fishes likely play a significant role in global, deep-pelagic food webs.

The most speciose family of mesopelagic fishes (305 valid species; Fricke et al., 2018a) is the Stomiidae (*sensu* Fink, 1985), collectively including the snaggletooths (Astronesthinae), viperfishes (Chauliodontinae), black dragonfishes (Idiacanthinae), loosejaws (Malacosteinae), scaleless black dragonfishes (Melanostomiinae), and scaly dragonfishes (Stomiinae). These predatory fishes inhabit all oceans, including the Southern Ocean (Gibbs, 1969; Fink, 1985; Kenaley, 2007), and while they predominantly occupy the mesopelagic zone, evidence indicates that some species thrive in the deeper waters of the bathypelagic (1,000–4,000 m depth) zone (Gibbs, 1969; Childress et al., 1980). Ecologically, stomiids play an important role in deep-sea ecosystems because they are trophic mediators and link surface waters to those of the deep-pelagic. Most stomiids are vertical migrators and migrate to the epipelagic (0–200 m depth) zone at night to feed on the heightened influx of lanternfishes (Myctophidae), the primary fish zooplanktivores in most oceanic food webs (Clarke, 1974; Hopkins and Gartner, 1992). By bringing carbon fixed in the surface waters to their deeper daytime depth ranges, stomiids regulate deep-sea energy flow and play a vital role in the interzonal transfer of energy between the epipelagic, mesopelagic, and bathypelagic zones (Sutton and Hopkins, 1996a).

Quantifying carbon flow through mesopelagic systems requires an estimate of fish biomass and production, which in turn requires data on reproduction. Although aspects of stomiid feeding ecology have been quantified (Clarke, 1982; Sutton and Hopkins, 1996a; Butler et al., 2001; Kenaley, 2012), the data gap regarding their reproductive ecology remains, a consequence of insufficient sample sizes of adults due to the type of gear commonly used to collect specimens. Larger, sexually mature stomiids are likely more adept at net avoidance than smaller juveniles (Clarke, 1974; Fisher and Pearcy, 1983; Sutton and Hopkins, 1996b), thereby impeding synoptic studies of reproductive biology. However, hermaphroditism is known to occur in Gonostomatidae, a sister taxon in the Stomiiformes. Reproductive information is a key component of bioenergetics modeling, which takes into account the productivity of species and is frequently applied to several areas of study such as predator-prey interactions and ecosystem modeling (Hansen et al., 1993). Each of these areas requires knowledge about the reproduction of its component species. In this paper, we utilize one of the largest sets of deep-pelagic samples, one that utilized two complementary gear types to sample both juveniles and large adults. By using samples obtained with a Multiple Opening/Closing Net and Environmental Sensing System (MOCNESS) midwater trawl, as well as a high-speed rope trawl (HSRT), we had an unprecedented opportunity to investigate stomiid reproductive ecology.

Anthropogenic events may significantly hinder the capacity for mesopelagic fishes to regulate energy flow in the deep sea because such events can create unfavorable conditions for growth and survival. For example, repurcussions of hydrocarbon toxicity on larval fishes due to catastrophes such as oil spills have been widely documented, including declines in productivity at the population level due to decreases in reproductive health (Brown et al., 1996; Short, 2003). The Gulf of Mexico is particularly relevant in this regard given the location, size, and duration of the *Deepwater Horizon* oil spill (DWHOS), which lasted from April–September 2010. In order to understand the impact of the DWHOS on deep-pelagic fishes and expand our knowledge base of important predators, the focus of this study was to quantify reproductive parameters and investigate reproductive life history characteristics of stomiids in the Gulf of Mexico. The following questions relating to stomiid reproductive ecology were investigated: (1) Are stomiids gonochoristic, like most teleosts, or hermaphroditic, like sister taxa in the order Stomiiformes? (2) What type of oocyte development and spawning pattern is exhibited by stomiids? (3) What are the sex ratios of stomiid species? and (4) What are the sizes at maturity for stomiids in the Gulf of Mexico? These results can be used to further investigations of the impact of anthropogenic events to deep-pelagic assemblages, as well as general studies on mesopelagic ecosystems and carbon flow.

MATERIALS AND METHODS

Sample Collection

A series of seven cruises was conducted in the Gulf of Mexico between 2010 and 2011 as part of the DWHOS Offshore Nekton Sampling and Analysis Program. A total of 1,600 trawl samples were collected at stations arranged in a grid pattern across the northern gulf, most of which were seaward of the 1,000-m isobath (**Figure 1**). All sampling occurred both day and night from the surface to 1,500 m depth using two gear types in order to catch a broad assortment of individual sizes and species.

During three cruise series, sampling was conducted with a six-net, 10-m^2 mouth area MOCNESS midwater trawl (Wiebe et al., 1985), with each net having a uniform mesh size of 3 mm (stretched). Each deployment produced up to five discrete-depth, quantitative samples; the sixth net was an oblique tow from the surface to 1,500 m and catches in this net were not processed quantitatively. Sampling occurred in each month from January–September 2011, and a total of 46 stations were sampled either twice (17 stations) or three times (29 stations) (**Figure 1A**). Additional sampling details can be found in Burdett et al. (2017) and (Sutton et al., 2020). On four additional cruises, specimens were collected using a HSRT (Dotson and Griffith, 1996) with an effective mouth area of 165.47 m^2 (Sutton & Mercier unpubl. data) and a graded mesh size (stretched) of 3.2 m at the mouth which tapered to 19 mm at the cod end. A total of 17 stations were sampled one to four times (**Figure 1B**), with each cruise lasting 3 weeks, between December 2010 and September 2011. Specimens used in this study were opportunistically selected from both gears to increase the size spectrum from juveniles to spawning-sized adults.

After capture and subsequent identification and data logging, all stomiid specimens were fixed in a 10% (v:v) formalin:seawater solution. Specimens were stored in formalin until sample

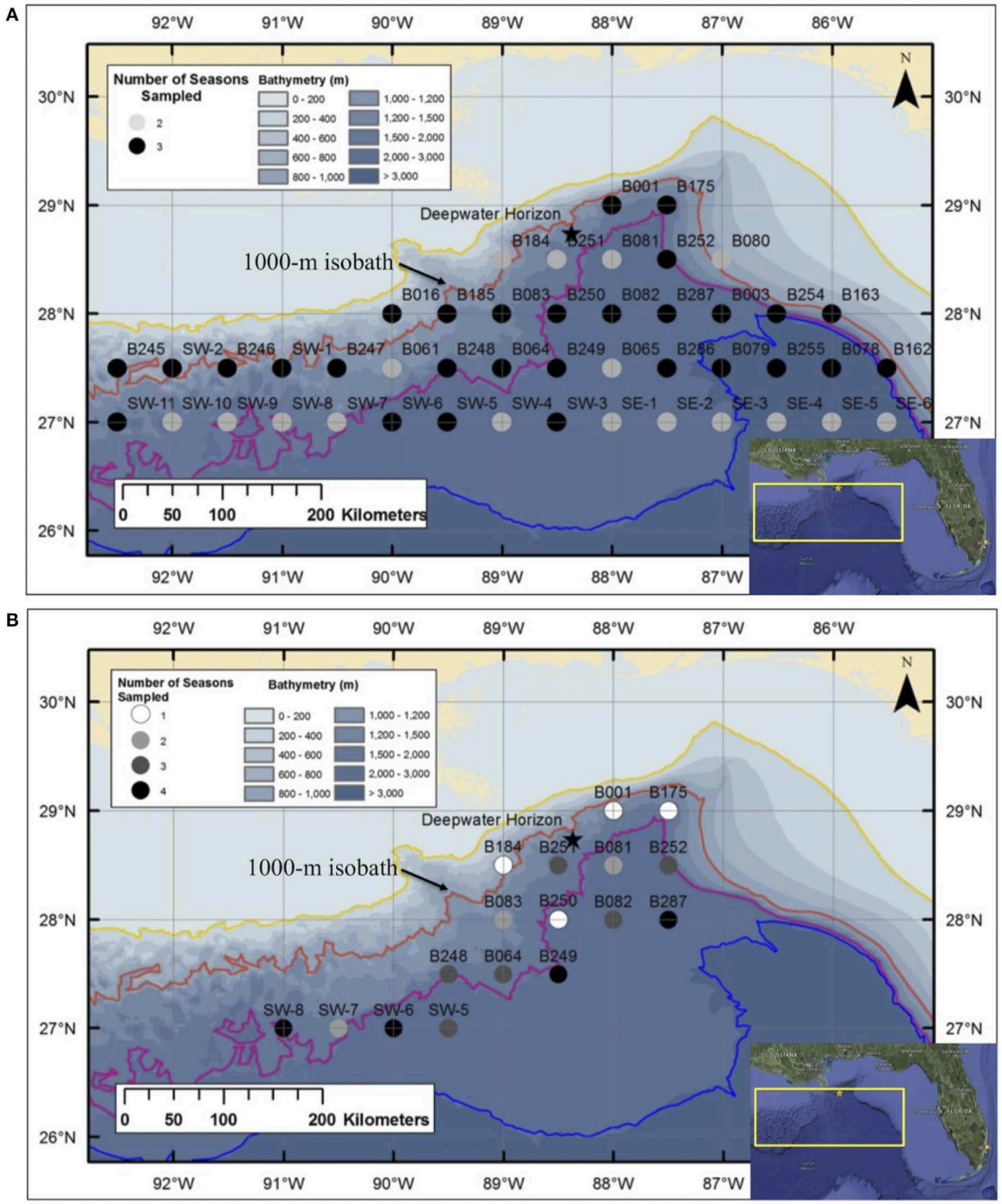

FIGURE 1 | Deepwater stations sampled in the Gulf of Mexico during: **(A)** *Meg Skansi* 6, *Meg Skansi* 7, and *Meg Skansi* 8 cruises between January and September 2011; and **(B)** *Pisces* 8, *Pisces* 9, *Pisces* 10, and *Pisces* 12 cruises between December 2010 and September 2011. All adjacent sampling stations were equidistant from each other by 30 nautical miles (55.6 km). Isobaths, from top to bottom, indicate depths of 200, 1,000, 2,000, and 3,000 m, respectively. The 1,000-m isobath is individually labeled for reference. The black star marks the site of the *Deepwater Horizon* oil spill that occurred between April and September 2010.

processing began back in the laboratory and were never transferred to alcohol after fixation. Just before they were processed, specimens were transferred to water to de-gas under a fume hood. Specimens for this study were selected during sequential processing of trawl samples at the Nova Southeastern University Oceanic Ecology Laboratory. When practical, all

TABLE 1 | Cruise details from the 2010 to 2011 expeditions in the Gulf of Mexico and the total number of stomiid specimens from each cruise used in this study (N_{study}).

Cruise	Date	Sampling gear	N_{tows}	$N_{samples}$	Total stomiids	N_{study}
Pisces 8	1–20 Dec 2010	HSRT	37	37	2,915	75
Meg Skansi 6	27 Jan–31 Mar 2011	MOCNESS	65	270	901	19
Pisces 9	22 Mar–11 Apr 2011	HSRT	36	36	2,093	20
Meg Skansi 7	14 Apr–30 Jun 2011	MOCNESS	92	373	905	7
Pisces 10	21 Jun–14 Jul 2011	HSRT	48	48	4,510	61
Meg Skansi 8	18 Jul–30 Sep 2011	MOCNESS	95	445	765	95
Pisces 12	7–29 Sep 2011	HSRT	50	50	6,103	437
SUMMARY						
7 cruises	Dec 2010–Sep 2011		423	1,259	18,192	714

The total number of samples processed quantitatively (one tow yielded up to five samples on MOCNESS cruises, and one sample on HSRT cruises) is denoted by "$N_{samples}$". HSRT, High-Speed Rope Trawl; MOCNESS, Multiple Opening/Closing Net and Environmental Sensing System.

specimens for each species collected on the seven cruises (**Table 1**) were used in this study. In cases of superfluous specimens, a subsample spanning the available size spectrum was chosen for the species.

Specimen Processing

Stomiid specimens were selected for reproductive analysis as they became available during a large-scale, quantitative taxonomic analysis program. Specimens were identified using the keys of Gibbs (1964a,b, 1969), Morrow (1964a,b,c), Morrow and Gibbs (1964), Barnett and Gibbs (1968), Goodyear and Gibbs (1969), Gibbs et al. (1983), Gomon and Gibbs (1985), Gibbs and McKinney (1988), Sutton and Hartel (2004), Kenaley and Hartel (2005), Kenaley (2007), and Flynn and Klepadlo (2012). Species were measured to the nearest 0.1 mm standard length (SL) and total wet weights were recorded to the nearest 0.01 g. Entire gonads were removed and the wet weight recorded to the nearest 0.001 g. All gonads were stored in 70% ethanol for at least 1 week prior to histological preparation.

Histology

Transverse subsections of 1–2 cm were removed from the middle of one lobe of the preserved gonads and dehydrated using an automated tissue processor before being embedded in paraffin. Gonadal tissue was cross-sectioned twice at 5 μm using a microtome, then mounted on glass microscope slides, rehydrated, stained with Harris's hematoxylin, and counterstained with eosin-y with phloxine following routine histological procedures (Avwioro, 2011).

Histological sections were examined with a compound microscope as an aid in determining sex, as well as one of five reproductive phases. Without reference to body length or date of capture, tissue sections were classified as "immature," "developing," "spawning capable," "regressing," or "regenerating," following the criteria of Brown-Peterson et al. (2011). Based on key histological markers (type of spermatogenic cells present in males, type and size of oocytes in females), samples were classified as "mature" if they were in one of the four latter reproductive phases. Gonads that were underdeveloped and unable to be identified as male or female with certainty were classified as "undifferentiated." Photomicrographs were taken of demonstrative samples to show key structures involved in the reproductive development of males (**Figure 2**) and females (**Figure 3**). Specimens ($N = 41$) in which the reproductive phase could not be determined unequivocally were not assigned a maturity phase and were excluded from analyses.

Statistical Analysis

All statistical analysis was performed using R 0.98.1062 (R Development Core Team, 2013) for the 12 dominant ($N \geq 19$ individuals) species, and results were considered significant at $P < 0.05$. Sex ratios were calculated using the total number of males to females, both immature and mature. Sex ratios were also calculated for only the mature males and females of each species. A Chi-Square Goodness of Fit Test was performed using the chisq.test() function to determine if the sex ratio of each species diverged from the expected ratio of 1:1 (male: female). All specimens identified as "undifferentiated" were incorporated only in size distribution analyses.

The size at 50% maturity (L_{50}) was estimated using the "MASS" package (Venables and Ripley, 2002) glm() and dose.p() functions for binomial regression to show the percentage of mature specimens as a function of 10-mm size class. In cases where complete model separation occurred (i.e., each size class had *only* immature specimens, or *only* mature specimens), size at maturity was determined to be the smallest mature specimen. Size at maturity, based on histological results, was used in conjunction with size distributions by gear type to extrapolate what portion of all measured specimens of each species caught during the seven cruises was immature or mature. Additionally, a *t*-test was used to assess gear selectivity by comparing the mean sizes of specimens collected with the MOCNESS and HSRT.

RESULTS

Sampling

In total, 714 specimens representing 47 stomiid species were examined, the majority of which (61%) were collected in the fall of 2011. Of the 714 specimens, 364 females, 318 males, and 32 undifferentiated specimens were identified. For the 12

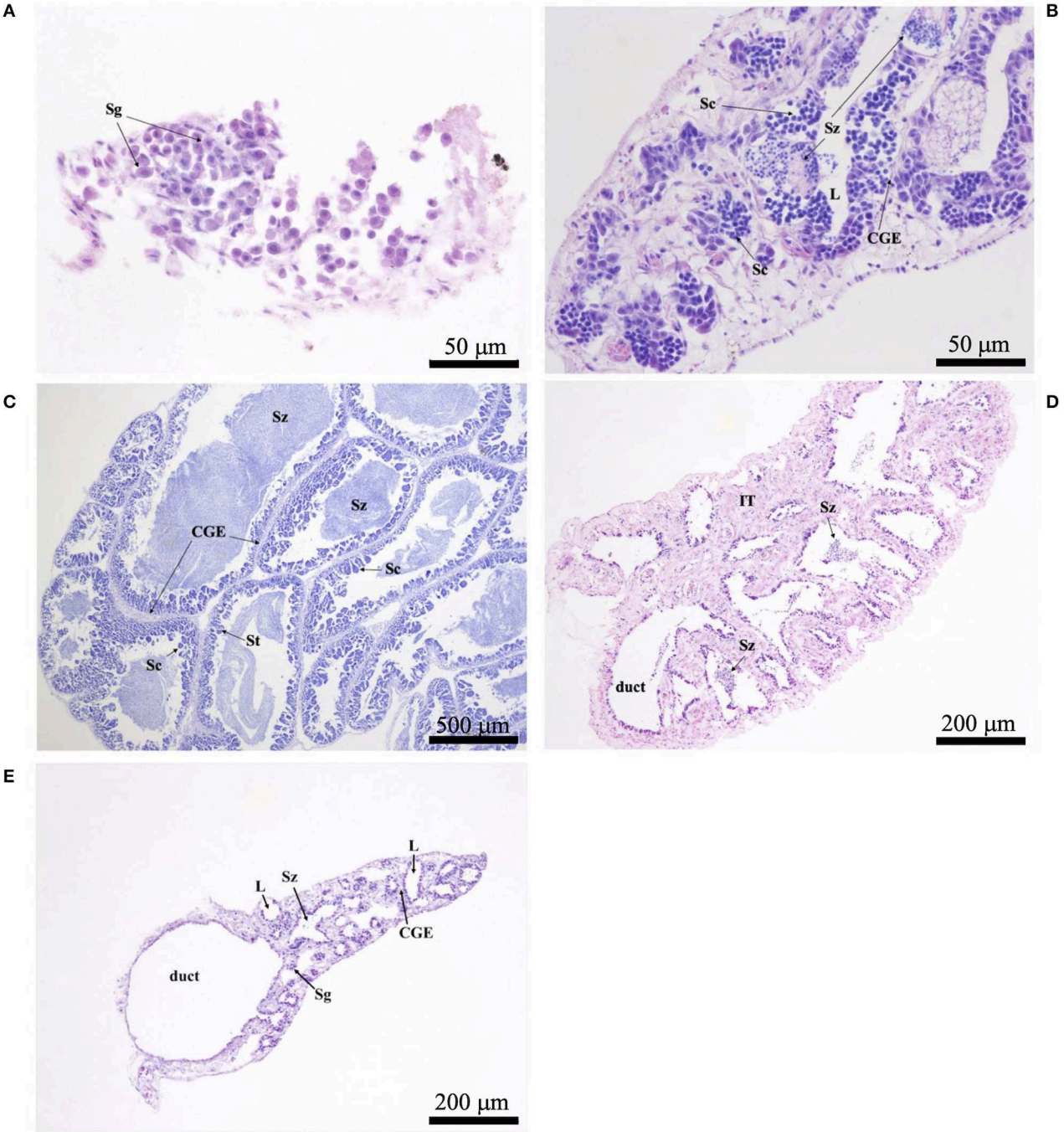

FIGURE 2 | Photomicrographs of testicular histology, depicting: **(A)** *Astronesthes atlanticus* in the immature phase, with only spermatogonia (Sg) in the testes; scale bar = 50 µm; **(B)** *Melanostomias melanops* in the developing phase, with spermatocysts of spermatocytes (Sc), and cysts of spermatozoa (Sz) that have not yet entered the lobular lumina (L). Continuous germinal epithelium (CGE) present; scale bar = 50 µm; **(C)** peripheral tissue of *Echiostoma barbatum* in the spawning capable phase, with Sc, spermatids (St), Sz, and CGE; scale bar = 500 µm; **(D)** *Melanostomias melanops* in the regressing phase, with residual Sz in the lumina and duct; note the expanded interstitial (connective) tissue (IT); scale bar = 200 µm; **(E)** *Echiostoma barbatum* in the regenerating phase, with residual Sz in some lobules, empty lumina (L), CGE, and Sg proliferation; scale bar = 200 µm.

dominant species, the size and weight compositions of female, male, and undifferentiated specimens sampled are shown in **Table 2**. Morphometric data for the less-abundant 35 species are presented in **Supplementary Table 1**.

Reproductive Strategy

No histological evidence of testicular and ovarian tissue was observed simultaneously in any stomiid gonad, indicating that stomiids are gonochoristic. Following the terminology of Grier

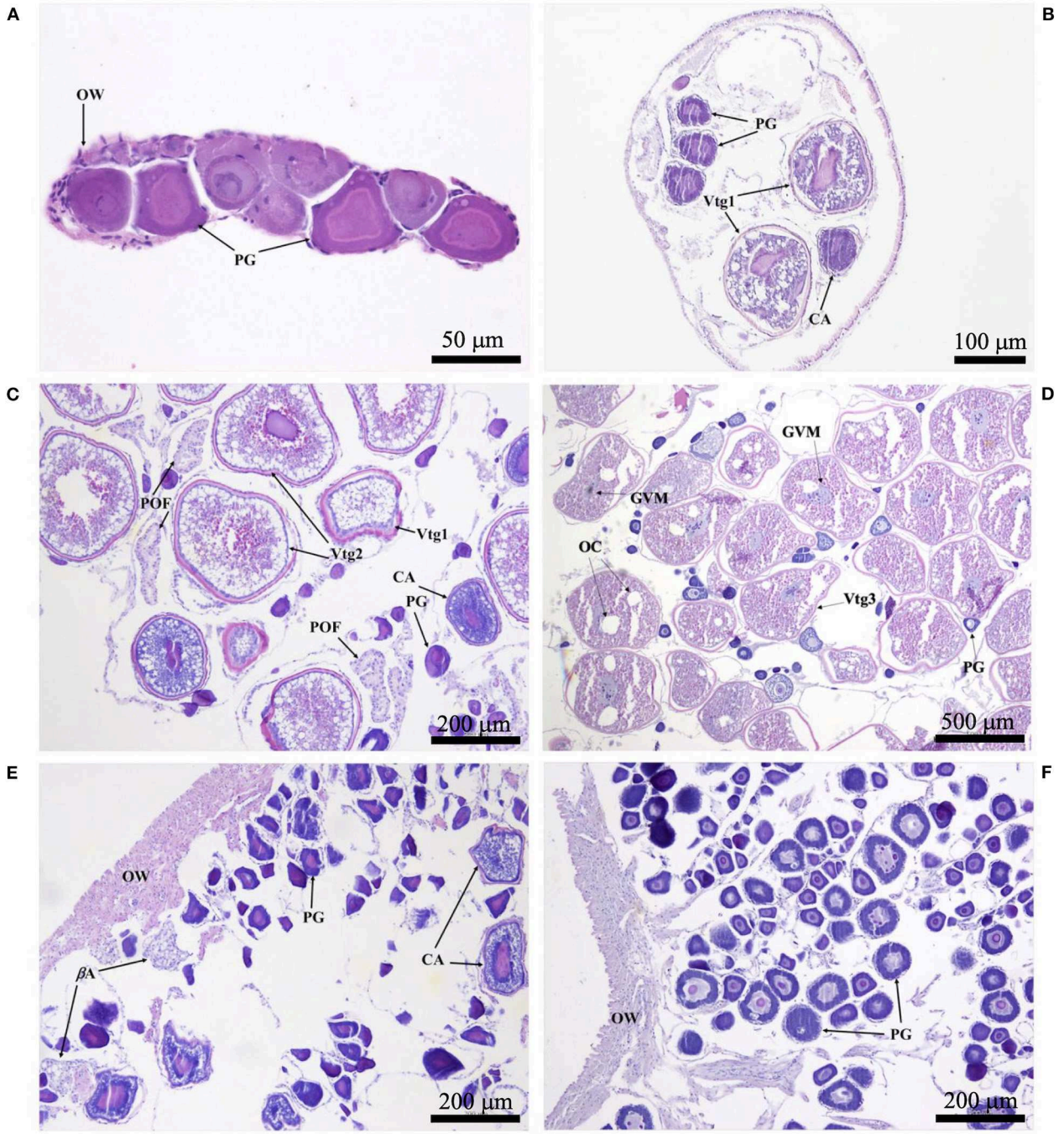

FIGURE 3 | Photomicrographs of ovarian histology, depicting: **(A)** *Photostomias guernei* in the immature phase, with only primary growth oocytes (PG) and a thin ovarian wall (OW); scale bar = 50 µm; **(B)** *Eustomias hypopsilus* in the developing phase, with PG, cortical alveolar oocytes (CA), and primary vitellogenic oocytes (Vtg1); scale bar = 100 µm; **(C)** *Aristostomias xenostoma* in the spawning capable phase, with PG, CA, primary and secondary vitellogenic oocytes (Vtg1 & Vtg2), and postovulatory follicles (POF); scale bar = 200 µm; **(D)** *Echiostoma barbatum* in the actively spawning subphase undergoing oocyte maturation, with PG, tertiary vitellogenic oocytes (Vtg3), oil coalescence (OC), and germinal vesicle migration (GVM); scale bar = 500 µm; **(E)** *Aristostomias xenostoma* in the regressing phase, with beta atresia (*β*A), PG, and few CA; scale bar = 200 µm; **(F)** *Eustomias schmidti* in the regenerating phase, with larger PG and a thicker OW; scale bar = 200 µm.

and Uribe (2009), male stomiids possess an unrestricted, lobular testicular structure. Histological assessment of the testes also indicates that males are able to spawn continuously, as evidenced by the preponderance of spawning capable individuals (83%) and scarcity of individuals in the regressing and regenerating phases. In females, 25% of all specimens were spawning capable. Oocytes

TABLE 2 | Count, size range, mean standard length (SL), and standard deviation, range of wet weight, and mean wet weight and standard deviation of 12 dominant stomiid species collected in the Gulf of Mexico between 2010 and 2011.

Taxon	*N*	SL Range (mm)	Mean SL (mm)	Weight Range (g)	Mean Weight (g)
ASTRONESTHINAE					
Astronesthes atlanticus (Parin and Borodulina, 1996)	**19**				
Female	10	55.9–169.7	121.6 ± 31.0	1.31–28.74	15.26 ± 8.40
Male	9	95.3–149.8	122.7 ± 17.9	7.33–26.26	15.92 ± 6.57
Astronesthes richardsoni (Poey, 1852)	**24**				
Female	13	59.9–181.1	123.8 ± 41.6	1.00–40.09	15.37 ± 12.99
Male	8	72.7–154.5	122.1 ± 33.3	1.00–29.21	14.67 ± 10.30
Undifferentiated	3	63.0–83.5	70.0 ± 11.7	1.07–3.09	1.82 ± 1.11
Astronesthes similus (Parr, 1927)	**22**				
Female	12	57.6–121.1	79.0 ± 21.9	1.09–13.00	4.34 ± 4.42
Male	8	67.8–121.9	92.3 ± 21.1	2.03–10.68	6.08 ± 3.92
Undifferentiated	2	59.2–68.0	63.6 ± 6.2	1.24–1.78	1.51 ± 0.38
CHAULIODONTINAE					
Chauliodus sloani (Bloch and Schneider, 1801)	**75**				
Female	50	55.3–250.0	165.9 ± 58.4	0.40–47.24	15.00 ± 11.60
Male	24	68.1–200.0	160.6 ± 39.0	0.82–21.42	10.32 ± 6.11
Undifferentiated	1	69.9	69.9	0.59	0.59
MALACOSTEINAE					
Aristostomias xenostoma (Regan and Trewavas, 1930)	**36**				
Female	14	44.9–120.5	81.7 ± 19.9	0.50–14.73	4.45 ± 3.78
Male	22	48.5–117.3	85.5 ± 21.7	0.62–13.56	5.75 ± 4.39
Malacosteus niger (Ayres, 1848)	**89**				
Female	47	46.8–178.9	102.6 ± 34.5	0.45–53.40	9.02 ± 12.24
Male	41	51.8–117.3	87.9 ± 14.6	0.47–12.23	3.49 ± 2.24
Undifferentiated	1	48.8	48.8	0.33	0.33
Photostomias guernei (Collett, 1889)	**73**				
Female	39	46.0–116.4	85.8 ± 22.8	0.24–6.61	2.65 ± 1.93
Male	33	64.1–116.9	100.6 ± 13.6	0.92–5.87	3.39 ± 1.48
Undifferentiated	1	58.7	58.7	0.49	0.49
MELANOSTOMIINAE					
Echiostoma barbatum (Lowe, 1843)	**72**				
Female	33	86.0–312.3	224.3 ± 74.2	4.01–240.54	95.16 ± 70.67
Male	35	83.2–276.5	224.1 ± 51.1	3.37–126.88	72.50 ± 36.18
Undifferentiated	4	77.6–92.7	84.7 ± 6.2	1.95–3.81	2.66 ± 0.82
Eustomias fissibarbis (Pappenheim, 1914)	**21**				
Female	11	66.7–170.0	112.7 ± 31.5	0.46–11.09	3.85 ± 3.28
Male	10	80.8–119.8	100.7 ± 10.7	0.88–3.85	1.95 ± 0.90
Eustomias hypopsilus (Gomon and Gibbs, 1985)	**30**				
Female	20	86.0–140.9	125.4 ± 13.3	0.59–3.50	1.79 ± 0.67
Male	10	109.3–119.6	115.2 ± 3.3	0.78–1.91	1.35 ± 0.37
Eustomias schmidti (Regan and Trewavas, 1930)	**75**				
Female	41	82.5–281.6	134.9 ± 56.6	0.67–123.33	12.77 ± 23.52
Male	27	77.0–152.4	114.1 ± 21.9	0.62–7.06	2.74 ± 1.86
Undifferentiated	7	77.5–92.0	83.7 ± 4.8	0.78–1.36	0.95 ± 0.20
Melanostomias melanops (Brauer, 1902)	**26**				
Female	14	92.3–206.9	159.5 ± 37.6	1.14–39.03	16.66 ± 13.45
Male	12	127.0–189.6	163.5 ± 20.3	5.37–22.28	13.66 ± 5.34

Species listed by subfamily and sex. Taxonomic authorities provided by Fricke et al. (2018b).

in all developmental stages, without dominant populations, were observed to be simultaneously present in the ovary, indicative of asynchronous oocyte development and batch spawning. Through this type of oocyte development, stomiids either spawn more than once during each spawning season, or continuously throughout the year with no discrete spawning season.

TABLE 3 | Overall and mature sex ratios of 12 dominant stomiids in the Gulf of Mexico, listed by subfamily.

	Overall				Mature			
Taxon	***N***	**Sex ratio (M:F)**	χ^2	***P***	***N***	**Sex ratio (M:F)**	χ^2	***P***
ASTRONESTHINAE								
Astronesthes atlanticus		1:1.11	0.05	0.819		1:1	0	1
Female	10				8			
Male	9				8			
Astronesthes richardsoni		1:1.63	1.19	0.275		1:1.17	0.08	0.781
Female	13				7			
Male	8				6			
Astronesthes similus		1:1.5	0.80	0.371		1:0.43	1.60	0.206
Female	12				3			
Male	8				7			
CHAULIODONTINAE								
Chauliodus sloani		1:2.08	9.14	**0.003**		1:1.35	1.19	0.276
Female	50				31			
Male	24				23			
MALACOSTEINAE								
Aristostomias xenostoma		1:0.64	1.78	0.182		1:0.27	9.14	**0.002**
Female	14				6			
Male	22				22			
Malacosteus niger		1:1.15	0.41	0.522		1:0.44	8.64	**0.003**
Female	47				17			
Male	41				39			
Photostomias guernei		1:1.18	0.50	0.480		1:0.82	0.60	0.439
Female	39				27			
Male	33				33			
MELANOSTOMIINAE								
Echiostoma barbatum		1:0.94	0.06	0.808		1:0.67	2.0	0.157
Female	33				20			
Male	35				30			
Eustomias fissibarbis		1:1.1	0.05	0.827		1:0.20	5.33	**0.021**
Female	11				2			
Male	10				10			
Eustomias hypopsilus		1:2	3.33	0.068		1:1.60	1.38	0.239
Female	20				16			
Male	10				10			
Eustomias schmidti		1:1.52	2.88	0.090		1:0.42	6.08	**0.014**
Female	41				11			
Male	27				26			
Melanostomias melanops		1:1.17	0.15	0.695		1:0.58	1.32	0.251
Female	14				7			
Male	12				12			

Calculated chi-square value (χ^2) and P-value (P) also presented, with degrees of freedom = 1.
Bolded values indicate species with sex ratios of statistical significance.

Sex Ratio

Chauliodus sloani was the only species in which the overall sex ratio (juveniles included) significantly differed from the expected 1:1 ratio; this species exhibited a sex ratio of 1:2.08, indicating a significant female bias ($P = 0.003$) (**Table 3**). When considering mature (adult) fish only, the observed sex ratio significantly favored males in the species *Aristostomias xenostoma, Eustomias fissibarbis, Eustomias schmidti,* and *Malacosteus niger,* presumably because males mature earlier than females (**Table 3**).

Size at Maturity

Maturity data were sufficient to estimate size at 50% maturity of five species using binomial regression. In increasing order, female size (SL) at 50% maturity was 106.4 mm in *Eustomias hypopsilus,* 110.9 mm in *Malacosteus niger*, 151.9 mm in *Chauliodus sloani,*

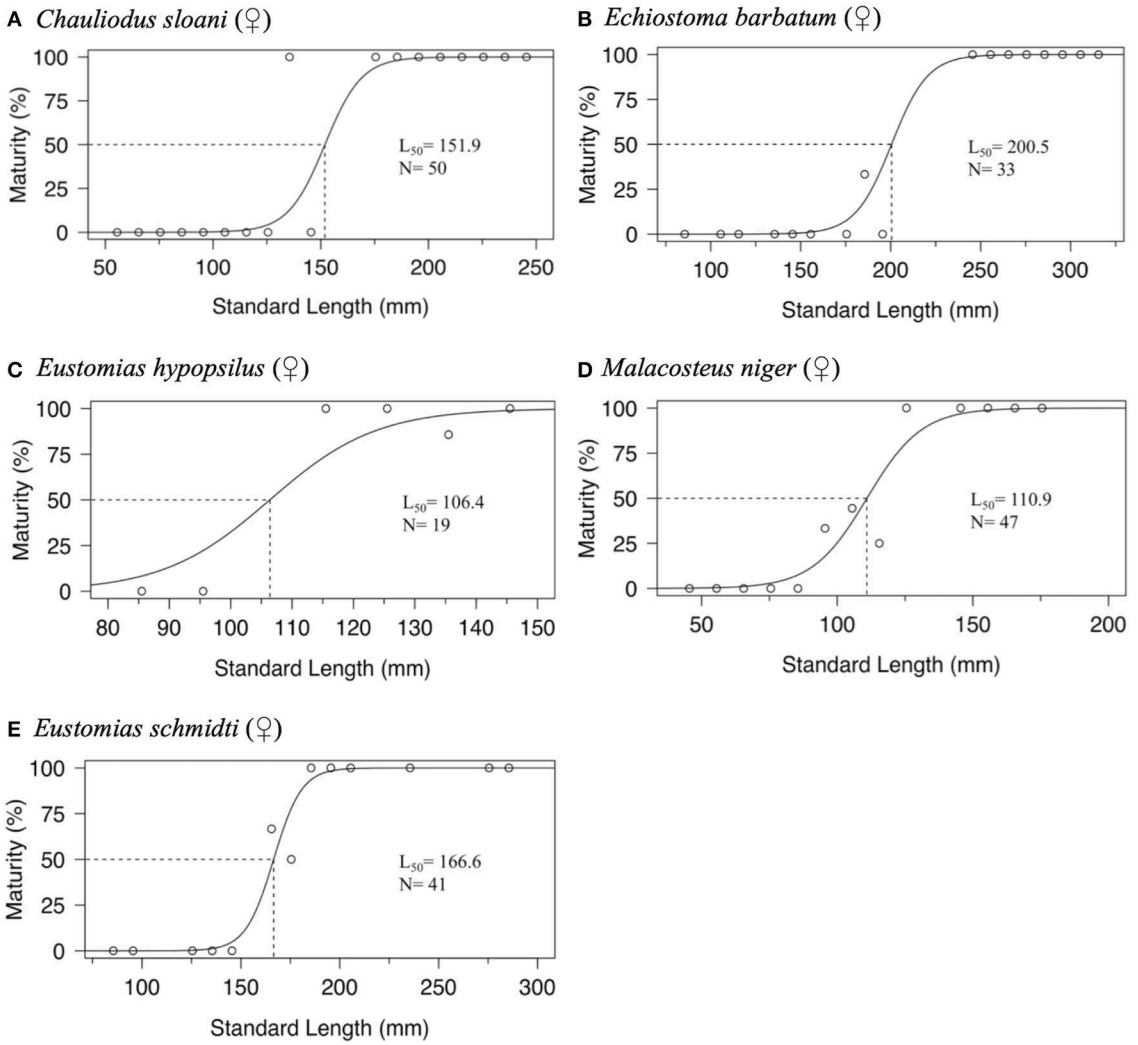

FIGURE 4 | Binomial regression of size at maturity of: **(A)** female *Chauliodus sloani*, **(B)** female *Echiostoma barbatum,* **(C)** female *Eustomias hypopsilus*, **(D)** female *Malacosteus niger*, and **(E)** female *Eustomias schmidti*. Dotted lines indicate standard length at median sexual maturity (L_{50}). *N* = sample size.

166.6 mm in *Eustomias schmidti*, and 200.5 mm in *Echiostoma barbatum* (**Figure 4**). In females of *E. hypopsilus,* the smallest mature specimen was larger than the estimated size at 50% maturity (**Table 4**) due to small sample size, especially in intermediate size classes.

Binomial regression was not appropriate for the remaining species either because there was not enough variation in the ratio of immature to mature specimens per size class, or because size classes were perfect predictors of maturity state (all specimens were either immature or mature in a given size class). No immature males of *Aristostomias xenostoma, Eustomias fissibarbis, Eustomias hypopsilus*, *Melanostomias melanops*, and *Photostomias guernei* were identified, and less than four specimens were classified as immature for *Astronesthes atlanticus*, *Astronesthes richardsoni, Astronesthes similus*, *Chauliodus sloani,* and *Malacosteus niger*. The length of the smallest mature specimen of each sex was considered the size at maturity in species for which L_{50} could not be estimated. Specimen size at which the smallest mature individual was identified, as well as L_{50} and L_{99}, is presented in **Table 4**. Males reached maturity at smaller lengths than their female conspecifics in all 12 species.

Size Distributions

Size-frequency distributions are shown in **Figure 5** for each of the 12 dominant species. Distributions were separated by gear type to demonstrate the differing size selectivity of the MOCNESS and HSRT. Two patterns emerged, both of which were observed for every species: the MOCNESS captured smaller juveniles more effectively than the HSRT (**Figure 6**; two sample *t*-test, $t = 42.3$, $P << 0.001$), and the HSRT caught more specimens per species. Superimposing the size at maturity based on histological data revealed a third pattern: the majority of specimens collected with the HSRT were mature.

TABLE 4 | Smallest size (standard length) at maturity, length at 50% maturity (L_{50}), and length at 99% maturity (L_{99}) of 12 dominant stomiids in the Gulf of Mexico, listed by subfamily, and sex.

Taxon	Sex	Smallest Mature (mm)	L_{50} (mm)	L_{99} (mm)
ASTRONESTHINAE				
Astronesthes atlanticus	Female	109.1	–	–
	Male	106.7	–	–
Astronesthes richardsoni	Female	121.8	–	–
	Male	115.7	–	–
Astronesthes similus	Female	106.9	–	–
	Male	73.4	–	–
CHAULIODONTINAE				
Chauliodus sloani	Female	133.7	151.9	191.1
	Male	95.5	–	–
MALACOSTEINAE				
Aristostomias xenostoma	Female	83.5	–	–
	Male	48.5	–	–
Malacosteus niger	Female	92.4	110.9	157.5
	Male	66.3	–	–
Photostomias guernei	Female	71.4	–	–
	Male	64.1	–	–
MELANOSTOMIINAE				
Echiostoma barbatum	Female	189.9	200.5	246.7
	Male	158.0	–	–
Eustomias fissibarbis	Female	147.8	–	–
	Male	81.0	–	–
Eustomias hypopsilus	Female	119.9	106.4	146.3
	Male	109.3	-	–
Eustomias schmidti	Female	165.1	166.6	199.1
	Male	77.0	–	–
Melanostomias melanops	Female	161.0	–	–
	Male	127.0	–	–

Empty cells indicate L_{50} and L_{99} were not calculated using binomial regression due to the lack of size overlap between immature and mature specimens, or lack of immature males and females for some species.

DISCUSSION

Histology and Reproductive Strategy

This study is the first extensive examination of the reproductive ecology of stomiids, the top predators of the mesopelagic zone, collected using multiple gear types that sample the full known size range of the taxa. No histological evidence of testicular and ovarian tissue was observed simultaneously in the gonad, indicating that stomiids are gonochoristic, unlike other species within the Stomiiformes. For example, protandric hermaphroditism has been documented in species of the family Gonostomatidae, including *Cyclothone atraria* (Gilbert, 1905); *Sigmops bathyphilus* [*sensu* Miya and Nishida (2000), formerly *Gonostoma bathyphilum* (Vaillant, 1884)]; *S. elongatus* [*sensu* Miya and Nishida (2000), formerly *Gonostoma elongatum* (Günther, 1878)]; and *S. gracilis* [*sensu* Miya and Nishida (2000), formerly *Gonostoma gracile* (Günther, 1878)] (Kawaguchi and Marumo, 1967; Fisher, 1983; Miya and Nemoto, 1985; Badcock, 1986). Considering that the deep-pelagic habitat harbors a lower abundance (per volume) of fishes and larger nearest-neighbor distances between conspecifics than coastal seas (Marshall, 1954), the chance of finding a mate is lower, and thus hermaphroditism could confer benefits through population-level "bet-hedging." Typically, the terminal sex is female, meaning the bulk of the biomass of these species is found within the egg-producing component. However, maintaining separate sexes can increase reproductive fitness relative to hermaphroditism in two ways: energy can be focused on gamete production instead of reconfiguring the reproductive system, and reproductive opportunities will not be forfeited while undergoing the change (Warner, 1975; Helfman et al., 2009).

Gonochorism may benefit longer-lived predators during large-scale disturbances by preserving genetic diversity. If stomiids were protandrous hermaphrodites like other hermaphroditic stomiiform fishes, a sudden decline in smaller fishes due to a large-scale disturbance (DWHOS) could hypothetically cause a large-scale cohort loss of spawning females some length of time after the event. Smaller fishes may be more vulnerable to oil toxicity than larger fishes (Barron et al., 2004), so the loss of this cohort, which would never have been able to spawn, could result in a loss of genetic diversity at the population level. As genetic diversity is a primary attribute of resilience to disturbance, the finding of gonochorism in this keystone predator group (Sutton and Hopkins, 1996a) is significant.

Sex Ratio

Departure from the expected 1:1 sex ratio is not common in most fishes (Conover and Van Voorhees, 1990). For *Chauliodus sloani*, we found there was a significant bias in favor of females among juveniles. One hypothesis that can explain this is that females reach maturity at a larger size than males (**Table 4**). Overall, we found the higher ratio of females to males to be the exception; in most cases where sex ratio significantly favored one sex over the other, males were favored. This pattern held for *Aristostomias xenostoma, Malacosteus niger, Eustomias fissibarbis,* and *Eustomias schmidti*. One possible explanation for this pattern is that males mature faster because development of spermatozoa is energetically less costly than development of ova. If the assemblage of these species actually favors males, having a higher ratio of males to females would increase the probability of females finding mates. We believe that female location of a mate may be facilitated by dimorphisms in light organs; many stomiids have males that possess enlarged postorbital photophores in contrast to those of females, which are smaller or absent (Gibbs, 1964a; Morrow and Gibbs, 1964; Krueger and Gibbs, 1966; Borodulina, 1994, 2009). The benefit of larger postorbital photophores in males may be to aid females in finding a mate by increasing male detectability over greater distances in an environment with diminished light levels (Herring, 2000). The larger postorbital photophore in males can be seen as an evolutionary trade-off to small size, and thus restricted mobility, in male stomiids. Alternatively, divergence from a 1:1 sex ratio can be attributed to other factors such as differential growth rates

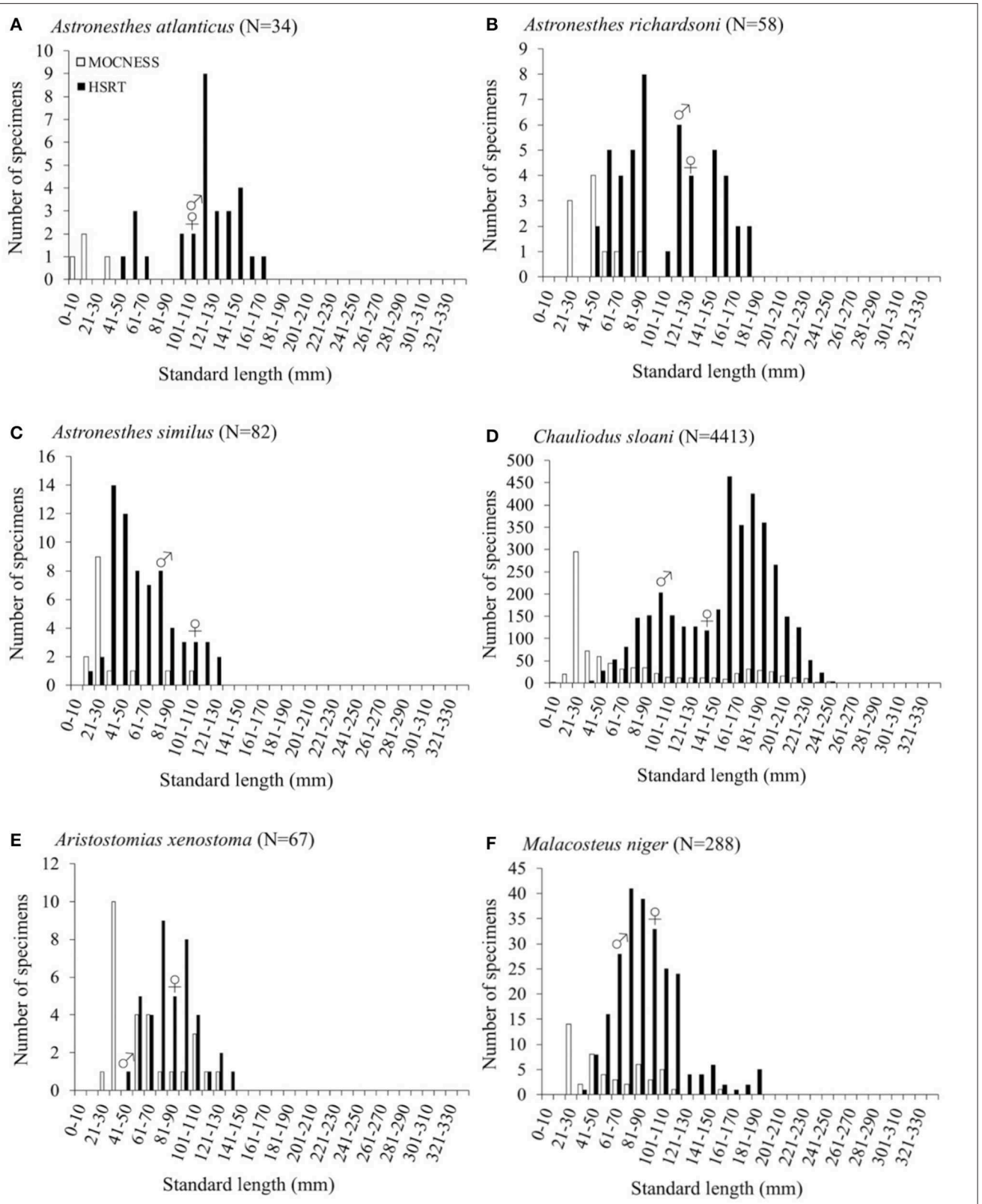

FIGURE 5 | Continued

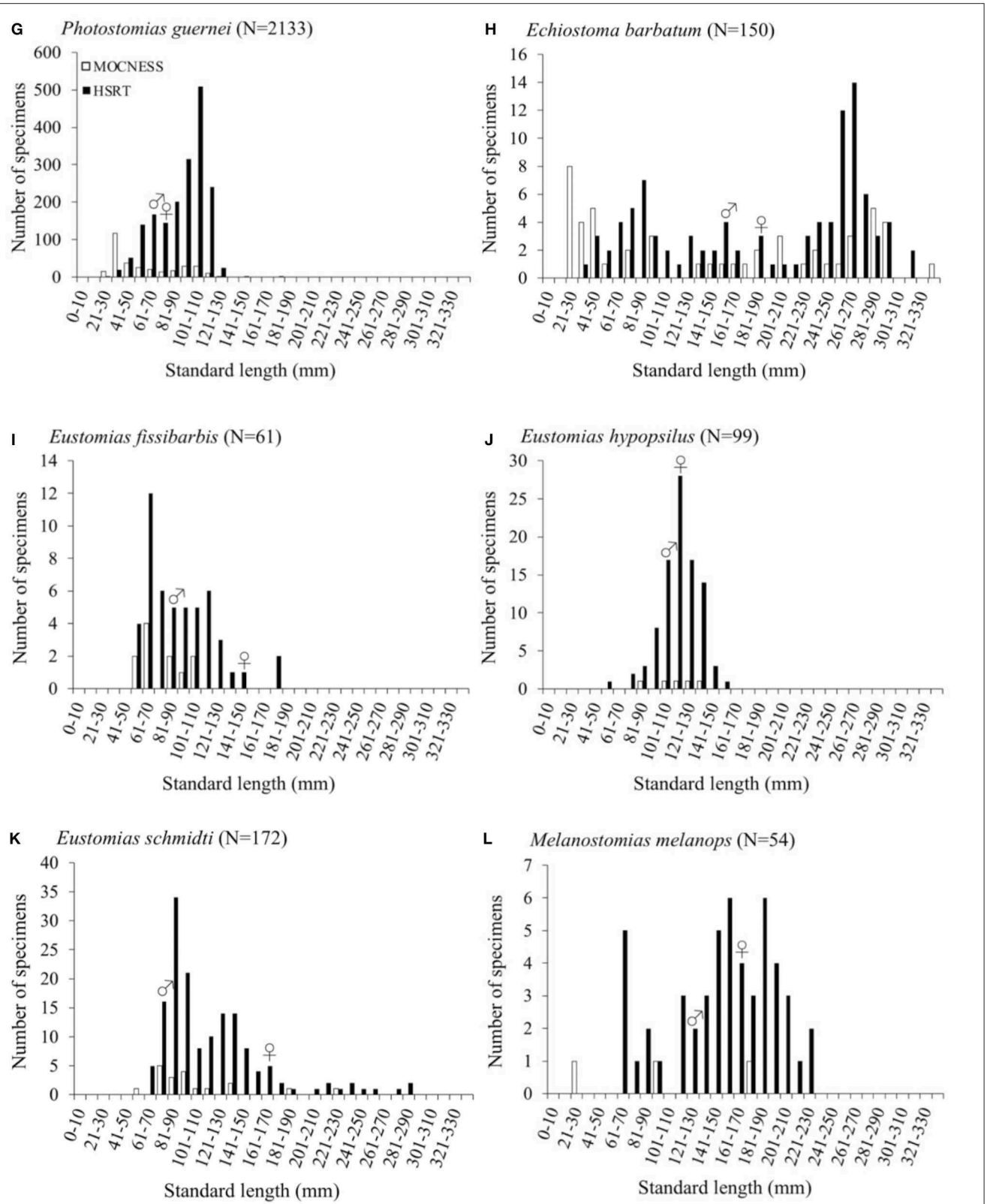

FIGURE 5 | Size distributions as a function of gear type of **(A)** *Astronesthes atlanticus*, **(B)** *Astronesthes richardsoni*, **(C)** *Astronesthes similus*, **(D)** *Chauliodus sloani*, **(E)** *Aristostomias xenostoma*, **(F)** *Malacosteus niger*, **(G)** *Photostomias guernei*, **(H)** *Echiostoma barbatum*, **(I)** *Eustomias fissibarbis*, **(J)** *Eustomias hypopsilus*, **(K)** *Eustomias schmidti*, and **(L)** *Melanostomias melanops* from the northern Gulf of Mexico.

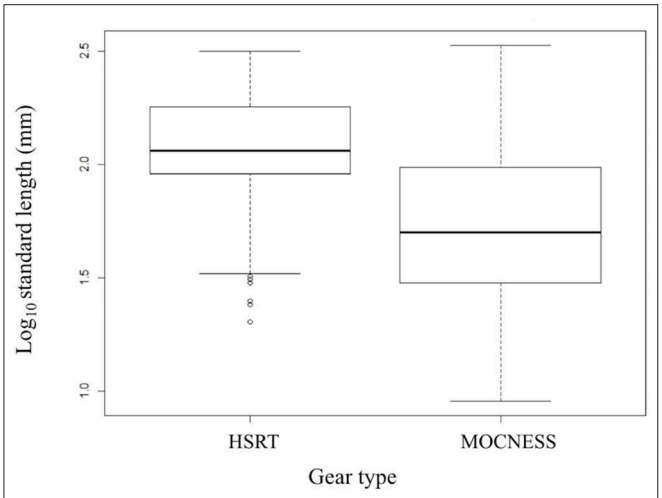

FIGURE 6 | Boxplot comparing the size distributions of the 12 dominant stomiid species collected with the HSRT and MOCNESS in the Gulf of Mexico. Bolded horizontal lines indicate the median, and boxes represent the interquartile range (IQR), with the top and bottom lines indicating the 75th and 25th percentile, respectively. Whiskers represent minimum and maximum values no more than 1.5 times the IQR (upper value = 75th percentile + 1.5 × IQR, lower value = 25th percentile − 1.5 × IQR). Open circles represent outliers and indicate smaller fish were caught. HSRT, High-Speed Rope Trawl; MOCNESS, Multiple Opening/Closing Net and Environmental Sensing System.

and differences in spatial distributions between sexes (Trindade-Santos and Freire, 2015), or a genetic basis for sex determination. Little is known about the mechanism of sex determination in stomiids, but Chen (1969) presented evidence of heterogamety in the form of the XO sex type in *Sternoptyx diaphana* (Family Sternoptychidae), a family in the same order as the stomiids.

Previous studies on stomiid sex ratios are limited, so comparisons are not possible for most of the species studied. Based on 100 specimens taken with 40 and 60-ft midwater trawls, Krueger and Gibbs (1966) found the overall sex ratio of *Echiostoma barbatum* from the Mississippi Delta to be significantly female-biased, at 2:1, which differed from this study. Specimens ranged in size from 51.0 to 291.0 mm SL, with the largest male being 252 mm SL and the largest female at 291 mm. Krueger and Gibbs (1966) indicated that *E. barbatum* has dimorphic postorbital photophores and suggested that high male mortality is responsible for a female-biased sex ratio. While larger photophores may increase detection by females, the reasoned drawback is the simultaneous attraction of potential predators due to a more conspicuous display signal. Stomiids have been found in the diets of epipelagic fishes and mammals (Robison and Craddock, 1983; Flynn and Paxton, 2013), but no sex determination was made of those predated-upon individuals. If males experience higher rates of mortality due to increased detection by predators, sex ratios might favor females. However, the data presented in this study do not support this hypothesis.

Size at Maturity

The current data support the conclusion that, in general, female stomiids mature at larger sizes than males, which is a common life-history pattern in deep-sea fishes (Herring, 2002). In this study, *Echiostoma barbatum* was found to reach 50% maturity at much smaller lengths (158.0 mm SL for males, 189.9 mm SL for females) than those determined by Krueger and Gibbs (1966); they reported that males and females were mature at 220 and 271 mm SL, respectively. Differences in size at maturity of *E. barbatum* may be attributed to contrasting methodologies between studies. While we used histology to classify maturity state, Krueger and Gibbs (1966) relied upon oocyte size and macroscopic observations of gonads. Histology is a more accurate method to classify internal gonadal development and ultimately reveals more information on the reproductive development of fishes (West, 1990).

Size at maturity has also been reported in studies from other waters. For example, two species of *Photostomias* collected near Hawaii are reported to mature at 60 and 120 mm SL (Clarke, 1982), which is similar to the minimum length at maturity found in our study. However, Clarke did not report the species due to taxonomic uncertainty of the genus. Kenaley (2009) clarified the taxonomy of the unidentified *Photostomias* species collected by Clarke (1982). Clarke (2000) mentioned that female *Eustomias fissibarbis* and *Eustomias schmidti* from the North Atlantic Ocean mature at larger sizes than males, but no specific lengths were provided for comparison. The differences in size at maturity of *E. barbatum* and *Photostomias guernei* between this study and previous studies may be a result of the number and size of specimens available for histological analysis, or differences in environmental conditions, or gear types between the studies. For *P. guernei*, this difference may even be attributed to species; Kenaley (2009) described the two unidentified species from Clarke (1982) as new to science.

Binomial regression was not used to estimate minimum size at maturity in males and females of most species due to complete separation of maturity state. Small sample size, especially for male stomiids, likely contributed to complete separation. Only 11 (4%) of 239 male specimens were identified as immature. In males of *Aristostomias xenostoma, Eustomias fissibarbis, Eustomias hypopsilus, Eustomias schmidti,* and *Melanostomias melanops,* the smallest mature individual identified was also the smallest individual overall, suggesting that males of these species may mature at even smaller sizes. Alternatively, it could also suggest that immaturity is a relatively short-lived phase in the reproductive cycle of male stomiids, and reaching maturity is a rapid process. The example of the ribbon sawtail fish *Idiacanthus fasciola* Peters 1877, a species of barbeled stomiid, lends credence to this hypothesis. Males are no more than 10–20% the standard length of mature females, and are mature immediately following transformation from the larval stage (Marshall, 1954; Clarke, 1983). A larger sample of specimens representative of smaller size classes would likely improve the estimate of size of maturity in stomiids.

Size Distributions

While an advantage to using individual gear types for sampling midwater fishes is the targeting of specific sizes (Kashkin and Parin, 1983; Millar, 1992), it is also a potential hindrance, especially when assessing the size distributions of species

assemblages. Using one type of gear can bias results and produce spurious conclusions because of size-specific selectivity (Willis et al., 2000). Gear selectivity in trawls is largely related to mesh size. In this study, the MOCNESS had a 3-mm mesh size and primarily caught smaller specimens. MacLennan (1992) reported that with smaller mesh sizes, the chance of smaller fishes escaping through the net is reduced. Larger nets, such as the rope trawl, effectively collect larger fishes, and yield a larger catch per unit effort (e.g., time) (Kashkin and Parin, 1983). Larger, mature stomiids would have been greatly underrepresented from the sample set and true size distributions would be poorly reflected if the only specimens used in this study were collected with the 10-m^2 MOCNESS. The reproductive component of the assemblage would have been missed. From a sampling standpoint, the benefits of using a large rope trawl only apply to larger predatory species, not for smaller taxa. Using the larger gear was crucial to effectively sample the reproductive component of stomiid assemblages, and, in conjunction with the MOCNESS, depict a more accurate representation of stomiid size distributions in the Gulf of Mexico.

The Link Between Reproductive Ecology and Oil Contamination in Pelagic Ecosystems

A recent paper by Romero et al. (2018) chronicled the exposure and contamination of mesopelagic fishes by the DWHOS, using polycyclic aromatic hydrocarbon (PAH) signatures as a proxy to identify DWHOS hydrocarbons. These authors presented baseline (pre-spill) PAH levels, along with levels shortly after (2010–2011) and 5–7 years after the DWHOS. The authors reported a dramatic increase in PAH levels in muscle tissues of vertically migrating fishes from the families Gonostomatidae, Sternoptychidae, and Myctophidae (all primary prey of Stomiidae) in 2010–2011, then a reduction in PAH muscle tissue loads in 2015–2017 (but still above pre-spill levels). The primary pathway of incorporation of PAHs was identified as contaminated prey consumption. The findings most relevant to this study, however, were the heightened levels of PAHs in ovaries of fishes collected between 2015 and 2017, with eggs containing 13× more PAHs than other tissues. Furthermore, PAH levels from the eggs of fishes collected during this period were above levels known to cause abnormalities in developing fishes (Sundberg et al., 2006; Sørhus et al., 2017). An explanation for the differences in PAH concentration between eggs and somatic tissue is the maternal transfer of contaminants to offspring. Lipophilic contaminants such as PAHs are transferred to the egg during vitellogenesis, when maternal resources for embryo development are stored in the yolk (Lubzens et al., 2017). This mechanism of oil contaminant retention is important for future risk assessment and monitoring studies in the deep-pelagic ocean, where biological (e.g., egg production), chemical (e.g., oil composition), physical (e.g., animal and oil dispersion), and behavioral (e.g., vertical migration) factors are key processes with respect to exposure to contaminants, with bioaccumulation of organic chemicals in mesopelagic fishes potentially higher than their shallower counterparts (Romero et al., 2018).

Continued threats of major contamination events in the Gulf of Mexico are likely, given the trajectory of oil extraction going deeper (Sutton et al., 2020) and the increased likelihood of accidents with greater platform depth (8.5% for every 30 m; Muehlenbachs et al., 2013). The average depth of ultra-deep drilling in the Gulf of Mexico is now over 500 m deeper than *Deepwater Horizon* (Murawski et al., 2020). Therefore, given the link between oil contamination, egg production, and bioaccumulation, it is becoming increasingly important to understand the dynamics of deep-pelagic fish reproduction to understand the full effects of oil spills in the deep-pelagic environment.

In conclusion, given the link between increasing petrogenic contamination of the deep ocean and fish reproduction, the key questions for which we have urgent need for information include: (1) how often do fishes spawn (e.g., iteroparous vs. semelparous, total vs. batch spawning); (2) what proportion of the fish population spawns; and (3) when do females produce eggs. In this study, the first extensive study on the reproductive ecology of stomiids in the Atlantic Ocean, as well as the largest study on the reproductive ecology of this family globally, we provide evidence that the 12 stomiids investigated maintain separate sexes, exhibit asynchronous oocyte development and batch spawning, and generally have even sex ratios, with females reaching maturity at larger sizes than males. Further studies of the deep-pelagic domain in other regions will allow comparisons of stomiid reproduction on a global basis, though future investigators must carefully consider gear type due to the inherent avoidance capacity of larger fishes. Our findings provide critical keystone predator data for oceanic ecosystem and bioenergetics modeling and suggest that stomiid reproductive tactics enhance the taxon's resilience to point-source disturbances such as DWHOS, which ideally would serve to maintain carbon flow and the reproductive health of the deep-pelagic Gulf of Mexico.

DATA AVAILABILITY STATEMENT

The datasets generated for this study are available on request to the corresponding author.

ETHICS STATEMENT

Ethical review and approval was not required for the animal study because the vertebrate animals we worked with for this study were all dead before research began.

AUTHOR CONTRIBUTIONS

AM conducted the research, analyzed the data, and wrote the manuscript with input from DK, DW, and TS. DK also provided statistical guidance and DW assisted in reading histology slides and analyzing histological data. TS oversaw all aspects of this research, including the collection, and identification of specimens. All authors have agreed to being listed as such and approve of the submitted version of this manuscript.

FUNDING

This research was made possible in part by a grant from The Gulf of Mexico Research Initiative. Data are publicly available through the Gulf of Mexico Research Initiative Information & Data Cooperative (GRIIDC) at https://data.gulfresearchinitiative.org (doi: 10.7266/N7ZS2V04).

ACKNOWLEDGMENTS

We are indebted to the captains and crews of the M/V *Meg Skansi* and NOAA FRV *Pisces,* as well as the scientific team for their shiptime services during sample collection and processing. Similarly, we thank Katie Bowen, Kendall Lord, Lacey Malarky, Michael Novotny, and Nina Pruzinsky of the Oceanic Ecology Laboratory at Nova Southeastern University for their assistance with quantitative sample processing. We especially thank April Cook for her assistance with database management and Rosanna Milligan for statistical support. This is contribution number 820 of the South Carolina Marine Resources Center.

SUPPLEMENTARY MATERIAL

The Supplementary Material for this article can be found online at: https://www.frontiersin.org/articles/10.3389/fmars.2020.00101/full#supplementary-material

REFERENCES

Avwioro, G. (2011). Histochemical uses of haematoxylin - a review. *J. Pharm. Clin. Sci.* 1, 24–34.

Ayres, W. O. (1848). Description of a new genus of fishes, Malacosteus. *Proc. Boston. Soc. Nat. Hist.* 3, 69–70.

Badcock, J. (1986). Aspects of the reproductive biology of *Gonostoma bathyphilum* (*Gonostomatidae*). *J. Fish. Biol.* 29, 589–603. doi: 10.1111/j.1095-8649.1986.tb04975.x

Barnett, M. A., and Gibbs, R. H. (1968). Four new stomiatoid fishes of the genus *Bathophilus* with a revised key to the species of *Bathophilus*. *Copeia* 1968, 826–832. doi: 10.2307/1441850

Barron, M. G., Carls, M. G., Heintz, R., and Rice, S. D. (2004). Evaluation of fish early life-stage toxicity models of chronic embryonic exposures to complex polycyclic aromatic hydrocarbon mixtures. *Toxicol. Sci.* 78, 60–67. doi: 10.1093/toxsci/kfh051

Bloch, M. E., and Schneider, J. G. (1801). *Systema Ichthyologiae: Iconibus CX Ilustratum*, Vol. 1. Berolini: Sumtibus Auctoris Impressum et Bibliopolio Sanderiano Commissum.

Borodulina, O. (1994). The external structure of the postorbital organ in species of the genus *Astronesthes* (Astronesthidae). *J. Ichthyol.* 34, 142–150.

Borodulina, O. (2009). External structure of the postorbital organ in some representatives of the family Melanostomiidae (*Stomiiformes*). *J. Ichthyol.* 49, 698–701. doi: 10.1134/S0032945209080165

Brauer, A. (1902). Diagnosen von neuen Tiefseefischen welche von der Valdivia-Expedition gesammelt sind. *Zool. Anz.* 25, 277–298.

Brown, E. D., Baker, T., Hose, J., Kocan, R., Marty, G., McGurk, M., et al. (1996). "Injury to the early life history stages of Pacific herring in Prince William Sound after the Exxon Valdez oil spill," in *Proc 18 Am Fish Soc Symp* (Anchorage, AK), 448–462.

Brown-Peterson, N. J., Wyanski, D. M., Saborido-Rey, F., Macewicz, B. J., and Lowerre-Barbieri, S. K. (2011). A standardized terminology for describing reproductive development in fishes. *Mar. Coast. Fish.* 3, 52–70. doi: 10.1080/19425120.2011.555724

Burdett, E. A., Fine, C. D., Sutton, T. T., Cook, A. B., and Frank, T. M. (2017). Geographic and depth distributions, ontogeny, and reproductive seasonality of decapod shrimps (*Caridea: Oplophoridae*) from the northeastern Gulf of Mexico. *Bull. Mar. Sci.* 93, 743–767. doi: 10.5343/bms.2016.1083

Butler, M., Bollens, S. M., Burkhalter, B., Madin, L. P., and Horgan, E. (2001). Mesopelagic fishes of the Arabian Sea: distribution, abundance and diet of *Chauliodus pammelas, Chauliodus sloani, Stomias Affinis,* and *Stomias Nebulosus*. *Deep Sea Res. Topical Stud. Oceanogr.* 48, 1369–1383. doi: 10.1016/S0967-0645(00)00143-0

Chen, T. (1969). Karyological heterogamety of deep-sea fishes. *Postilla* 130, 1–29.

Childress, J., Taylor, S., Cailliet, G. M., and Price, M. (1980). Patterns of growth, energy utilization and reproduction in some meso-and bathypelagic fishes off southern California. *Mar. Biol.* 61, 27–40. doi: 10.1007/BF00410339

Clarke, T. A. (1974). Some aspects of the ecology of stomiatoid fishes in the Pacific Ocean near Hawaii. *Fish. Bull.* 72, 337–351.

Clarke, T. A. (1982). Feeding habits of stomiatoid fishes from Hawaiian waters. *Fish. Bull.* 80, 287–304.

Clarke, T. A. (1983). Sex ratios and sexual differences in size among mesopelagic fishes from the central Pacific Ocean. *Mar. Biol.* 73, 203–209. doi: 10.1007/BF00406889

Clarke, T. A. (2000). Review of nine species of North Atlantic *Eustomias*, subgenus *Dinematochirus* (Pisces: Stomiidae), with the description of two new species. *Copeia* 2000, 96–111. doi: 10.1643/0045-8511(2000)2000[0096:RONSON]2.0.CO;2

Collett, R. (1889). Diagnoses de poissons nouveaux provenant des campagnes de "L'Hirondelle." II. Sur un genre nouveau de la famille des Stomiatidae. *Bull. Soc. Zool. Fr.* 14, 291–293.

Conover, D. O., and Van Voorhees, D. A. (1990). Evolution of a balanced sex ratio by frequency-dependent selection in a fish. *Science* 250, 1556–1558. doi: 10.1126/science.250.4987.1556

Dotson, R. C., and Griffith, D. A. (1996). A high-speed midwater rope trawl for collecting coastal pelagic fishes. *CalCOFI Rep.* 37, 134–139.

Fink, W. L. (1985). Phylogenetic interrelationships of the stomiid fishes (*Teleostei*: *Stomiiformes*). *Misc. Publ. Mus. Zool. Univ. Mich.* 171, 1–127.

Fisher, J. P., and Pearcy, W. G. (1983). Reproduction, growth and feeding of the mesopelagic fish *Tactostoma macropus* (Melanostomiatidae). *Mar. Biol.* 74, 257–267. doi: 10.1007/BF00403449

Fisher, R. A. (1983). Protrandric sex reversal in *Gonostoma elongatum* (Pisces: *Gonostomatidae*) from the eastern Gulf of Mexico. *Copeia* 1983, 554–557. doi: 10.2307/1444411

Flynn, A., and Klepadlo, C. (2012). Two new species of *Photonectes* (*Teleostei*: *Stomiidae*) from the Indo-Pacific, and a re-examination of P *Achirus. Mem. Mus. Victoria* 69, 259–267. doi: 10.24199/j.mmv.2012.69.04

Flynn, A. J., and Paxton, J. R. (2013). Spawning aggregation of the lanternfish *Diaphus danae* (family *Myctophidae*) in the north-western Coral Sea and associations with tuna aggregations. *Mar. Freshw. Res.* 63, 1255–1271. doi: 10.1071/MF12185

Fricke, R., Eschmeyer, W. N., and Fong, J. D. (2018a). *Species by Family/Subfamily*. Available online at: http://researcharchive.calacademy.org/research/ichthyology/catalog/SpeciesByFamily.asp (accessed Jun 12, 2018).

Fricke, R., Eschmeyer, W. N., and van der Laan, R. (2018b). *Catalog of Fishes: Genera, Species, References*. Avaliable online at: http://researcharchive.calacademy.org/research/ichthyology/catalog/fishcatmain.asp (accessed Nov 19, 2018).

Gibbs, R. H. (1964a). "Family Astronesthidae," in *Fishes of the Western North Atlantic*, eds H. B. Bigelow, D. M. Cohen, M. M. Dick, R. H. Gibbs, M. Grey, J. E. Morrow, L. P. Schultz, and V. Walters (New Haven, CT: Yale University Press), 311–350. doi: 10.2307/j.ctvbcd0k1.11

Gibbs, R. H. (1964b). "Family Idiacanthidae," in *Fishes of the Western North Atlantic*, Vol. 4, eds H. B. Bigelow, C. M. Breder, D. M. Cohen, G. W. Mead, D. Merriman, Y. H. Olsen, et al. (New Haven, CT: Yale University Press), 512–522. doi: 10.2307/j.ctvbcd0k1.13

Gibbs, R. H. (1969). Taxonomy, sexual dimorphism, vertical distribution, and evolutionary zoogeography of the bathypelagic fish genus *Stomias*

(*Stomiatidae*). *Smithson Contrib. Zool.* 31, 1–25. doi: 10.5479/si.00810282.31

Gibbs, R. H., Clarke, T. A., and Gomon, J. R. (1983). *Taxonomy and Distribution of the Stomioid Fish Genus Eustomias (Melanostomiidae), I: Subgenus Nominostomias*. Washington, DC: Smithsonian Institution Press.

Gibbs, R. H., and McKinney, J. F. (1988). High-count species of the stomiid fish genus *Astronesthes* from Southern subtropical convergence region: two new species and redescription of *Cryptostomias* (*Astronesthes*) *psychrolutes*. *Smithson Contrib. Zool.* 460, 1–25. doi: 10.5479/si.00810282.460

Gilbert, C. H. (1905). The deep-sea fishes of the Hawaiian Islands. *U.S. Fish. Comm. Bull.* 23, 577–713.

Gjøsaeter, J., and Kawaguchi, K. (1980). A review of the world resources of mesopelagic fish. *FAO Fish. Tech. Pap.* 193, 1–151.

Gomon, J. R., and Gibbs, R. H. (1985). Taxonomy and distribution of the stomioid fish genus *Eustomias* (Melanostomiidae), II: *Biradiostomias*, new subgenus. *Smithson Contrib. Zool.* 409, 1–58. doi: 10.5479/si.00810282.409

Goodyear, R. H., and Gibbs, R. H. (1969). Systematics and zoogeography of stomiatoid fishes of the *Astronesthes cyaneus* species group (Family Astronesthidae) with descriptions of three new species. *Arch. Fischereiwiss* 20, 107–131.

Grier, H. J., and Uribe, M. C. (2009). "The testes and spermatogenesis in teleosts," in *Reproductive Biology and Phylogeny of Fishes (Agnathans and Bony Fishes)*, ed B. G. Jamieson (Enfield, NH: Science Publishers), 119–142.

Günther, A. (1878). II.-Preliminary notices of deep-sea fishes collected during the voyage of H.M.S 'Challenger'. *J. Nat. Hist.* 2, 17–28.

Hansen, M. J., Boisclair, D., Brandt, S. B., Hewett, S. W., Kitchell, J. F., Lucas, M. C., et al. (1993). Applications of bioenergetics models to fish ecology and management: where do we go from here? *Trans. Am. Fish. Soc.* 122, 1019–1030. doi: 10.1577/1548-8659(1993)122<1019:AOBMTF>2.3.CO;2

Helfman, G., Collette, B. B., Facey, D. E., and Bowen, B. W. (2009). *The Diversity of Fishes: Biology, Evolution, and Ecology*. Sussex: John Wiley & Sons.

Herring, P. J. (2000). Species abundance, sexual encounter and bioluminescent signalling in the deep sea. *Philos. Trans. R. Soc.* 355, 1273–1276. doi: 10.1098/rstb.2000.0682

Herring, P. J. (2002). *The Biology of the Deep Ocean*. New York: Oxford University Press.

Hopkins, T. L., and Gartner, J. V. (1992). Resource-partitioning and predation impact of a low-latitude myctophid community. *Mar. Biol.* 114, 185–197. doi: 10.1007/BF00349518

Irigoien, X., Klevjer, T. A., Røstad, A., Martinez, U., Boyra, G., Acuña, J., et al. (2014). Large mesopelagic fishes biomass and trophic efficiency in the open ocean. *Nat. Commun.* 5:3271. doi: 10.1038/ncomms4271

Kaartvedt, S., Staby, A., and Aksnes, D. L. (2012). Efficient trawl avoidance by mesopelagic fishes causes large underestimation of their biomass. *Mar. Ecol. Prog. Ser.* 456, 1–6. doi: 10.3354/meps09785

Kashkin, N. I., and Parin, N. V. (1983). Quantitative assessment of micronektonic fishes by nonclosing gear (a review). *Biol. Oceanogr.* 2, 263–287.

Kawaguchi, K., and Marumo, R. (1967). Biology of *Gonostoma gracile* (Gonostomatidae). I. Morphology, life history and sex reversal. *Inform. Bull. Plankt. Jpn.* 1967, 53–69.

Kenaley, C. P. (2007). Revision of the stoplight loosejaw genus *Malacosteus* (Teleostei: Stomiidae: Malacosteinae), with description of a new species from the temperate southern hemisphere and Indian Ocean. *Copeia* 2007, 886–900. doi: 10.1643/0045-8511(2007)7[886:ROTSLG]2.0.CO;2

Kenaley, C. P. (2009). Revision of indo-pacific species of the loosejaw dragonfish genus *Photostomias* (Teleostei: *Stomiidae*: Malacosteinae). *Copeia* 2009, 175–189. doi: 10.1643/CI-07-224

Kenaley, C. P. (2012). Exploring feeding behaviour in deep-sea dragonfishes (Teleostei: Stomiidae): jaw biomechanics and functional significance of a loosejaw. *Biol. J. Linn. Soc.* 106, 224–240. doi: 10.1111/j.1095-8312.2012.01854.x

Kenaley, C. P., and Hartel, K. E. (2005). A revision of Atlantic species of *Photostomias* (Teleostei: Stomiidae: Malacosteinae), with a description of a new species. *Ichthyol. Res.* 52, 251–263. doi: 10.1007/s10228-005-0281-7

Koslow, J. A., Kloser, R. J., and Williams, A. (1997). Pelagic biomass and community structure over the mid-continental slope off southeastern Australia based upon acoustic and midwater trawl sampling. *Mar. Ecol. Prog. Ser.* 30, 21–35. doi: 10.3354/meps146021

Krueger, W. H., and Gibbs, R. H. (1966). Growth changes and sexual dimorphism in the stomiatoid fish *Echiostoma barbatum*. *Copeia* 1966, 43–49. doi: 10.2307/1440759

Lowe, R. (1843). Notices of fishes newly observed or discovered in Madeira during the years 1840, 1841, and 1842. *Proc. Zool. Soc. Lond.* 11, 81–95.

Lubzens, E., Bobe, J., Young, G., and Sullivan, C. V. (2017). Maternal investment in fish oocytes and eggs: the molecular cargo and its contributions to fertility and early development. *Aquaculture* 472, 107–143. doi: 10.1016/j.aquaculture.2016.10.029

MacLennan, D. N. (1992). Fishing gear selectivity: an overview. *Fish. Res.* 13, 201–204. doi: 10.1016/0165-7836(92)90076-6

Marshall, N. B. (1954). *Aspects of Deep Sea Biology*. New York, NY: Philosophical Library.

Millar, R. B. (1992). Estimating the size-selectivity of fishing gear by conditioning on the total catch. *J. Am. Stat. Assoc.* 87, 962–968. doi: 10.1080/01621459.1992.10476250

Miya, M., and Nemoto, T. (1985). Protandrous sex reversal in *Cyclothone atraria* (Family *Gonostomatidae*). *Jpn. J. Ichthyol.* 31, 438–440.

Miya, M., and Nishida, M. (2000). Molecular systematics of the deep-sea fish genus *Gonostoma* (*Stomiiformes*: *Gonostomatidae*): two paraphyletic clades and resurrection of *Sigmops*. *Copeia* 2000, 378–389. doi: 10.1643/0045-8511(2000)000[0378:MSOTDS]2.0.CO;2

Morrow, J. E. (1964a). "Family Chauliodontidae," in *Fishes of the Western North Atlantic*, eds H. B. Bigelow, D. M. Cohen, M. M. Dick, R. H. Gibbs, M. Grey, J. E. Morrow, L. P. Schultz, and V. Walters (New Haven, CT: Yale University Press), 274–289. doi: 10.2307/j.ctvbcd0k1.9

Morrow, J. E. (1964b). "Family Stomiatidae," in *Fishes of the Western North Atlantic*, eds H. B. Bigelow, D. M. Cohen, M. M. Dick, R. H. Gibbs, M. Grey, J. E. Morrow, L. P. Schultz, and V. Walters (New Haven, CT: Yale University Press), 290–310. doi: 10.2307/j.ctvbcd0k1.10

Morrow, J. E. (1964c). "Family Malacosteidae," in *Fishes of the Western North Atlantic*, eds H. B. Bigelow, C. M. Breder, D. M. Cohen, G. W. Mead, D. Merriman, Y. H. Olsen, et al. (New Haven, CT: Yale University Press), 523–549. doi: 10.2307/j.ctvbcd0k1.14

Morrow, J. E., and Gibbs, R. H. (1964). "Family Melanostomiatidae," in *Fishes of the Western North Atlantic*, eds H. B. Bigelow, C. M. Breder, D. M. Cohen, G. W. Mead, D. Merriman, Y. H. Olsen, et al. (New Haven, CT: Yale University Press), 351–511. doi: 10.2307/j.ctvbcd0k1.12

Muehlenbachs, L., Cohen, M. A., and Gerarden, T. (2013). The impact of water depth on safety and environmental performance in offshore oil and gas production. *Energy Policy* 55, 699–705. doi: 10.1016/j.enpol.2012.12.074

Murawski, S., Hollander, D. J., Gilbert, S., and Gracia, A. (2020) "Deep-water oil and gas production in the Gulf of Mexico, and related global trends," in *Scenarios and Responses to Future Deep Oil Spills*, eds S. Murawski, C. Ainsworth, S. Gilbert, D. Hollander, C. Paris, and M. Schlüter (Cham: Springer), 16–32. doi: 10.1007/978-3-030-12963-7_2

Nelson, J. S., Grande, T. C., and Wilson, M. V. (2016). *Fishes of the World*. Hoboken, NJ: John Wiley & Sons.

Pappenheim, P. (1914). Die Fische der Deutschen Südpolar-Expedition 1901–1903. II. Die Tiefseefische. *Deutschen Südpolar-Expedition*. 15, 161–200.

Parin, N., and Borodulina, O. (1996). Revision of the *Astronesthes indicus* species group (Astronesthidae), with descriptions of five new species. *J. Ichthyol.* 36, 551–565.

Parr, A. E. (1927). The stomiatoid fishes of the suborder Gymnophotodermi (Astronesthidae, Melanostomiatidae, Idiacanthidae) with a complete review of the species. *Bull. Bingham Oceanogr. Coll.* 3, 1–123.

Poey, F. (1852). *Memorias sobre la Historia Natural de la Isla de Cuba: Accompañadas de Sumarios Latinos y Extractos en Frances*, Vol. 1. La Habana: Barcina.

R Development Core Team (2013). *A Language and Environment for Statistical Computing*. Vienna: R Foundation for Statistical Computing.

Regan, C. T., and Trewavas, E. (1930). The fishes of the families Stomiatidae and Malacosteidae. *Danish Dana Expedition 1920–22*. 6, 1–143.

Robison, B. H., and Craddock, J. E. (1983). Mesopelagic fishes eaten by Fraser's dolphin, *Lagenodelphis hosei*. *Fish. Bull.* 81, 283–289.

Romero, I. C., Sutton, T., Carr, B., Quintana-Rizzo, E., Ross, S. W., Hollander, D. J., et al. (2018). Decadal assessment of polycyclic aromatic hydrocarbons

in mesopelagic fishes from the Gulf of Mexico reveals exposure to oil-derived sources. *Environ. Sci. Technol.* 52, 10985–10996. doi: 10.1021/acs.est.8b02243

Short, J. (2003). Long-term effects of crude oil on developing fish: lessons from the Exxon Valdez oil spill. *Energy Sources* 25, 509–517. doi: 10.1080/00908310390195589

Sørhus, E., Incardona, J. P., Furmanek, T., Goetz, G. W., Scholz, N. L., Meier, S., et al. (2017). Novel adverse outcome pathways revealed by chemical genetics in a developing marine fish. *Elife* 6, 1–30. doi: 10.7554/eLife.20707

Sundberg, H., Ishaq, R., Tjärnlund, U., Åkerman, G., Grunder, K., Bandh, C., et al. (2006). Contribution of commonly analyzed polycyclic aromatic hydrocarbons (PAHs) to potential toxicity in early life stages of rainbow trout (*Oncorhynchus mykiss*). *Can. J. Fish. Aquat. Sci.* 63, 1320–1333. doi: 10.1139/f06-034

Sutton, T. T., Frank, T., Judkins, H., and Romero, I. C. (2020) "As oil extraction goes deeper, who is at risk? community structure, distribution and connectivity of the deep-pelagic fauna," in *Scenarios and Responses to Future Deep Oil Spills*, eds S. Murawski, C. Ainsworth, S. Gilbert, D. Hollander, C. Paris, and M. Schlüter (Cham: Springer), 403–418. doi: 10.1007/978-3-030-12963-7_24

Sutton, T. T., and Hartel, K. E. (2004). New species of *Eustomias* (Teleostei: *Stomiidae*) from the western North Atlantic, with a review of the subgenus *Neostomias*. *Copeia* 2004, 116–121. doi: 10.1643/CI-03-120R1

Sutton, T. T., and Hopkins, T. L. (1996a). Trophic ecology of the stomiid (Pisces: *Stomiidae*) fish assemblage of the eastern Gulf of Mexico: strategies, selectivity and impact of a top mesopelagic predator group. *Mar. Biol.* 127, 179–192. doi: 10.1007/BF00942102

Sutton, T. T., and Hopkins, T. L. (1996b). Species composition, abundance, and vertical distribution of the stomiid (Pisces: *Stomiiformes*) fish assemblage of the Gulf of Mexico. *Bull. Mar. Sci.* 59, 530–542.

Trindade-Santos, I., and Freire, K. M. F. (2015). Analysis of reproductive patterns of fishes from three large marine ecosystems. *Front. Mar. Sci.* 2:38. doi: 10.3389/fmars.2015.00038

Vaillant, L. L. (1884). In Filhol, H. Explorations sous-marines. Voyage du "Talisman". *La Nat*. 559. 182–186.

Venables, W. N., and Ripley, B. D. (2002). *Modern Applied Statistics With S, 4th Edn*. Berlin, Heidelberg: Springer-Verlag.

Warner, R. R. (1975). The adaptive significance of sequential hermaphroditism in animals. *Am. Nat.* 109, 61–82. doi: 10.1086/282974

West, G. (1990). Methods of assessing ovarian development in fishes: a review. *Mar. Freshw. Res.* 41, 199–222. doi: 10.1071/MF9900199

Wiebe, P. H., Morton, A. W., Bradley, A. M., Backus, R. H., Craddock, J. E., Barber, V., et al. (1985). New development in the MOCNESS, an apparatus for sampling zooplankton and micronekton. *Mar. Biol.* 87, 313–323. doi: 10.1007/BF00397811

Willis, T. J., Millar, R. B., and Babcock, R. C. (2000). Detection of spatial variability in relative density of fishes: comparison of visual census, angling, and baited underwater video. *Mar. Ecol. Prog. Ser.* 198, 249–260. doi: 10.3354/meps198249

Conflict of Interest: TS, one of the editors for the research topic in which this manuscript will be submitted, is also a coauthor on this manuscript. However, he did not review this paper.

The remaining authors declare that the research was conducted in the absence of any commercial or financial relationships that could be construed as a potential conflict of interest.

frontiers in Marine Science

ORIGINAL RESEARCH
published: 24 April 2020
doi: 10.3389/fmars.2020.00257

Pelagic Habitat Partitioning of Late-Larval and Juvenile Tunas in the Oceanic Gulf of Mexico

Nina M. Pruzinsky[1], Rosanna J. Milligan[2] and Tracey T. Sutton[1]*

[1] Oceanic Ecology Laboratory, Nova Southeastern University, Halmos College of Natural Sciences and Oceanography, DEEPEND Consortium, Dania Beach, FL, United States, [2] Seascape Ecology Laboratory, Nova Southeastern University, Halmos College of Natural Sciences and Oceanography, DEEPEND Consortium, Dania Beach, FL, United States

Tunas are ecologically important in pelagic ecosystems, but due to their high economic value, large-bodied species are overfished. Declines in fishery landings of large-bodied tuna species in the Gulf of Mexico (GoM) are expected to increase fishing pressures on unmanaged, small-bodied tuna species, whose life history traits are less known. While predicting spawning stocks and recruitment success typically focuses on estimates of larval abundances, juveniles may provide a better estimate of future adult stock sizes, as they are more likely to survive to adulthood because mortality rates scale inversely with body size. However, distributional studies on juveniles are rare, leading to a gap in our understanding of tuna ecology. In the present study, tuna early life stages were collected across the GoM from January–September 2011. The size class examined in this study, representing large larvae and small juveniles, is larger than that of previous larval tuna studies in the GoM. Faunal composition, abundance, frequency of occurrence, and diel catchability were investigated. Generalized additive models (GAMs) were used to examine spatiotemporal distributions of the family Scombridae and the three most-abundant tuna species in the GoM's epipelagic waters with respect to location, oceanographic features, and temporal change. In total, 11 of the 16 scombrid species inhabiting the GoM were collected, with small-bodied tuna species (*Euthynnus alletteratus*, *Thunnus atlanticus*, *Auxis thazard*) dominating the assemblage. Overall, scombrids were caught at higher abundances and frequencies at night than during the day, demonstrating that nighttime sampling generates a more accurate representation of faunal abundance and distribution. Abundance and presence–absence GAMs identified a coastal group (*E. alletteratus* and *A. thazard*) associated with productive continental shelf/slope environments (low salinity, higher chlorophyll *a* concentrations, nearer to shelf break) and an oceanic group (represented by *T. atlanticus*) associated with offshore, oligotrophic habitats (high salinity, lower chlorophyll *a* concentrations, further from shelf break). These results demonstrate that over a broad spatiotemporal domain, large larvae and juvenile tunas partition pelagic habitat on the mesoscale in addition to the temporal partitioning of adult spawning. These factors are important for spatially and temporally explicit modeling aimed at predicting tuna stock sizes.

Keywords: tuna early life stages, Gulf of Mexico, tuna ecology, little tunny, blackfin tuna, frigate tuna, spatial dynamics, assemblage drivers

OPEN ACCESS

Edited by:
Heather Bracken-Grissom, Florida International University, United States

Reviewed by:
Bruce Collette, Smithsonian National Museum of Natural History (SI), United States
Guillaume Rieucau, Louisiana Universities Marine Consortium, United States

****Correspondence:***
Nina M. Pruzinsky
npruzinsky@gmail.com

Specialty section:
This article was submitted to Deep-Sea Environments and Ecology, a section of the journal Frontiers in Marine Science

Received: *28 August 2019*
Accepted: *31 March 2020*
Published: *24 April 2020*

Citation:
Pruzinsky NM, Milligan RJ and Sutton TT (2020) Pelagic Habitat Partitioning of Late-Larval and Juvenile Tunas in the Oceanic Gulf of Mexico. Front. Mar. Sci. 7:257. doi: 10.3389/fmars.2020.00257

INTRODUCTION

Scombridae (i.e., the tunas, mackerels, and bonitos) are of high ecological and economic importance in pelagic ecosystems. While they are top-level predators that contribute to the pelagic food web and ecosystem structure, function, and stability (Matthews et al., 1977; Collette and Graves, 2019), they also support valuable commercial and recreational fisheries worldwide. Fisheries management and conservation efforts require information on the population dynamics of tuna early life stages in addition to spawning adults. Larval abundance indices and distribution data are used to predict spawning stock biomass, spawning patterns (location and time), spawning habitat quality, and recruitment success (Scott et al., 1993; Hsieh et al., 2006; Richardson et al., 2010). Moreover, information on larval spatiotemporal distribution and abundance provides insight into the factors that influence survival, growth, and recruitment.

Mortality rates are inversely related to body size in bony fishes; thus, the mortality rate is much higher for larvae than for juveniles (and adults; Hendriks, 1999; ICCAT, 2016a). Therefore, it is important to survey the abundance and distribution of juvenile fishes, as they represent the members of the surviving year class. High taxonomic uncertainty and limited knowledge regarding the distributional patterns of late-larval and juvenile tunas have led to an "operational taxonomic unit" gap in our understanding of tuna ecology. Thus, understanding the biological, ecological, and spatiotemporal distribution information of juvenile tunas can provide new data for fisheries management efforts and will increase our understanding of critical juvenile habitat. The lack of data on these important life history stages (larger larvae and smaller juveniles) limits adult population prediction and management.

The Gulf of Mexico (GoM) has been recognized as a spawning and nursery habitat for highly mobile pelagic fish species, including scombrids (Lindo-Atichati et al., 2012; Rooker et al., 2013). A total of 16 scombrid species inhabit the GoM, with nine tuna species from four genera: *Auxis, Euthynnus*, *Katsuwonus*, and *Thunnus*. Due to overfishing, large-bodied tunas (e.g., *Thunnus albacares, Thunnus obesus,* and *Thunnus thynnus*) populations are depleted or fully exploited in the GoM (Majkowski, 2007; Juan-Jordá et al., 2011). Declines in large-bodied tuna fisheries are expected to directly increase fishing pressures on small-bodied tunas (ICCAT, 2016a,b), which are essential components of this pelagic ecosystem (ICCAT, 2016b).

Despite their prevalence in the GoM, small-bodied tuna species (e.g., *Euthynnus alletteratus* and *Thunnus atlanticus*) are relatively understudied (Cornic and Rooker, 2018), and as a result, there are currently no federal management plans or stock assessments for these fishes (ICCAT, 2016b). Limited knowledge regarding their basic ecology, biology, and distribution and abundance patterns has hindered our ability to manage small-bodied tuna species that may be heavily fished in the future and/or subjected to future large-scale anthropogenic disturbances, such as oil spills from increasingly deeper oil and gas extraction activities. Thus, it is essential to study late-larval and juvenile size classes in order to enhance our knowledge on these small-bodied species and their future populations in the GoM.

The GoM's highly dynamic and complex pelagic ecosystem contains hydrographic features (e.g., Loop Current, fronts, and mesoscale eddies) that can influence the development and survival of early life stages. The GoM is a semi-enclosed oceanic system that connects the Caribbean Sea to the Atlantic Ocean by the Loop Current, which transports warm water into the Gulf through the Yucatan Channel and makes an anticyclonic turn before exiting through the Straits of Florida to become the Florida Current and then the Gulf Stream (McEachran and Fechhelm, 1998). The extensions of the Loop Current have strong seasonal and annual variability, which alter the current's location, flow patterns, temperature, and hydrographic features (Molinari, 1980; Nakata et al., 2000), and in turn, affects organismal behaviors and distributions. The boundary of the Loop Current is a highly dynamic region with meanders and strong convergence and divergence zones that can generate cyclonic and anticyclonic eddies (Olson and Backus, 1985). In the northern GoM, the Mississippi River empties large quantities of nutrients into the GoM, creating a zone of high primary productivity near the river's mouth (Le Fevre, 1986; Grimes and Kingsford, 1996) that is sometimes transported offshore by interacting eddies.

Previous studies showed that specific oceanographic features provide favorable conditions for larval *T. thynnus* survival and recruitment success, such as moderately warm, offshore oligotrophic waters that are outside the Loop Current and corresponding eddies (Muhling et al., 2010). While most studies have focused on larval *T. thynnus*, mesoscale features and the freshwater inflow from the Mississippi River have also been associated with the distributions of *Auxis* spp., *Thunnus* spp., and *Katsuwonus pelamis* (Lang et al., 1994; Richardson et al., 2010; Lindo-Atichati et al., 2012; Habtes et al., 2014; Cornic and Rooker, 2018). However, species-specific analyses remain incomplete for these taxa, as most studies only describe distributions and abundances based on genus level (e.g., *Auxis* spp. and *Thunnus* spp.). Therefore, understanding the influence of habitat parameters on the spatiotemporal dynamics of small-bodied tuna early life stages is essential for assessing their population status within the GoM.

The objectives of this study were to determine the faunal composition and assemblage structure of scombrids throughout the oceanic domain of the northern GoM and to characterize the spatiotemporal distributions of the most-abundant larval and juvenile scombrids in the GoM's epipelagic waters with respect to location, oceanographic features, and temporal change using generalized additive models (GAMs).

MATERIALS AND METHODS

Sample Collection and Processing

Late-larval and juvenile scombrids were collected across the GoM during three research cruises from January to September 2011,

Abbreviations: CW, Gulf Common Water classification; LCOW, Loop Current Origin Water classification; MIX, Intermediate Water classification; ONSAP, Offshore Nekton Sampling and Analysis Program; S_{EPI}, minimum salinity in the epipelagic zone; T_{EPI}, maximum temperature (°C) recorded in the epipelagic zone.

as part of the NOAA-supported Offshore Nekton Sampling and Analysis Program (ONSAP). The ONSAP was created to assess the composition, abundance and distribution of deep-water invertebrates and fishes in the oceanic GoM that could have been impacted by the *Deepwater Horizon* oil spill (April–September 2010). Scombrids were collected using a 10-m^2 mouth area, 3-mm mesh Multiple Opening/Closing Net and Environmental Sensing System (MOCNESS; Wiebe et al., 1985) at a subset of established Southeast Area Monitoring and Assessment Program (SEAMAP) stations (Sutton et al., 2016; Cook et al., Unpublished).

Full details of the sampling methodology are provided in Cook et al. (Unpublished), but a brief description is as follows: the MOCNESS, a six-net, discrete-depth sampling system, surveyed specific depth strata in the water column from the surface down to 1500 m depth, with deployments centered around solar noon (day sampling) and midnight (night sampling). The depth strata were: 0–200 m (epipelagic), 200–600 m (upper mesopelagic), 600–1000 m (lower mesopelagic), 1000–1200 m (upper bathypelagic), and 1200–1500 m (upper bathypelagic). A Tsurumi-Seiki-Kosakusho (T.S.K.) magnetically sensed flowmeter was used to calculate the water volume filtered by each net; this value was then used to standardize abundances per unit effort (presented as no. individuals 10^{-5} m^{-3}). Samples were fixed in 10% buffered formalin:seawater at sea and later transferred to 70% ethanol:water in the laboratory.

Larval and juvenile scombrids were identified to the lowest taxonomic level possible using morphological characteristics, body shape, myomere counts, and pigmentation patterns (Richards, 2005; Pruzinsky, 2018). Late-larval and juvenile *Auxis thazard* were identified by the presence of a distinct lateral midline of pigmentation along the tail. In cases of taxonomic uncertainty due to the lack of larval pigmentation or the juvenile stage being morphologically undescribed (e.g., *Thunnus albacares*), specimens were identified to genus level only. Quality assurance/quality control were conducted with leading scombrid taxonomic experts John Lamkin (NOAA NMFS, Miami) and Aki Shiroza, M.S. (NOAA NMFS, Miami), in order to ensure the accuracy of larval identifications. Standard length (SL) measurements to the nearest 0.01 mm were taken for all specimens.

Data Analysis

Catch Data

Although the water column was sampled from the surface to 1500 m depth, scombrid early life stages primarily inhabit epipelagic depths (Richards, 2005); therefore, statistical analyses were conducted with quantitative samples collected in the upper 200 m of the water column. Standardized abundances and percent frequency of occurrence (F_o) were calculated for each species. Standardized abundances were derived by dividing the sum of the raw count of individuals by the sum of the volume of water filtered, and F_o was determined by dividing the total number of trawls in which a taxon occurred by the total number of trawls in the epipelagic. Scombrid size-frequency plots were examined to investigate variation in size classes.

Spatiotemporal Distributions in the Epipelagic: GAMs

Scombrid abundance and presence–absence GAMs were fitted using the gamlss package (Rigby and Stasinopoulos, 2005) R software (R Core Team, 2019) to examine the distributions of the family Scombridae and the three most-abundant species (*Euthynnus alletteratus, Thunnus atlanticus, Auxis thazard*) in relation to a suite of oceanographic, spatial, and temporal variables. GAMs allow for non-linear relationships between response and multiple explanatory variables using additive smoothing functions (Zuur et al., 2009). The variables considered for the full models were: water mass type (following Johnston et al., 2019), sea surface height anomaly (SSHA), minimum salinity in the epipelagic zone (S_{EPI}), sea surface chlorophyll *a* concentrations (Chl *a*), distance to the nearest 200-m isobath, maximum temperature recorded in the epipelagic (T_{EPI}), Julian date (since January 1, 2011), and diel cycle (day or night sampling). Water masses were identified as Gulf Common Water (CW), Loop Current Origin Water (LCOW) or an intermediate type (MIX) based on the mean recorded temperature between 200 and 600 m depth collected by *in situ* MOCNESS sensors (Johnston et al., 2019). S_{EPI} and T_{EPI} were also collected from *in situ* MOCNESS sensors. SSHA was derived from E.U. Copernicus Marine Service Information (CMEMS[1]), and Chl *a* data were downloaded from NASA Ocean Color Group's Moderate Resolution Imaging Spectroradiometer (MODIS Aqua[2]; Nasa Goddard Space Flight Center, Ocean Ecology Laboratory, Ocean Biology Processing Group, 2018). Distance to the nearest 200-m isobath was calculated using the *marmap* package in R (Pante and Simon-Bouhet, 2013) and were derived from the General Bathymetric Chart of the Oceans (GEBCO[3]).

Prior to each analysis, collinearity of the explanatory variables was examined using a pair-plot or pairwise scatterplot. The inclusion of variables that appeared to covary in the pair-plots were verified using variance inflation factors (VIF > 5 reflected highly correlated variables) (Zuur et al., 2010). Because the survey period covered January to September only, T_{EPI} and Julian date were linearly correlated (**Supplementary Figure 1**; tau = 0.73); thus, one of the collinear variables (i.e., T_{EPI}) was dropped in order to create the "full model." The model did not converge when including Chl *a*, so it was removed from the full model as well. SSHA was also dropped from the full model, as the water mass classifications were used for simplicity.

The full model contained five explanatory variables: water mass, S_{EPI}, distance to the nearest 200-m isobath, Julian date (2011), and diel cycle. Water masses denoted where an individual scombrid was collected based on water type classification (LCOW, CW, MIX water). S_{EPI} was indicative of coastal runoff and riverine input. Distance to the nearest 200-m isobath (km) was considered indicative of coastal influence and geographic location. Julian date denoted intra-annual temporal change by indicating when the specimen was collected in 2011, and diel cycle was used to investigate differential catch patterns exhibited during the day and at night.

[1]http://marine.copernicus.eu/

[2]https://oceancolor.gsfc.nasa.gov/

[3]https://www.gebco.net/

Scombrid abundance data were modeled using the negative binomial distribution (NBI; Rigby and Stasinopoulos, 2005) and presence–absence data were modeled using the binomial distribution. Smoothers were fitted for distance to the nearest 200-m isobath, Julian date, and S_{EPI} using a penalized Beta-splines (pb) smoother. In each case ≤50 iterations of the Rigby and Stasinopoulos algorithm (RS method) and ≤200 iterations of the Cole and Green algorithm (CG method; Rigby and Stasinopoulos, 2005) were used to fit the models. Log_e volume filtered was included in each model as an offset term to allow for differences in catch effort.

Term selection for each model was conducted by backward-selection using AICc scores. If the difference between the full model and reduced models AICc scores (dAICc) was <2, the models were considered to be equivalent and the removed variable did not affect scombrid abundance or occurrence. If the dAICc was from 2 to 4, the explanatory variable was considered to have marginally affected scombrid abundance or occurrence, and if the dAICc was >4, the explanatory variable was considered an important determinant of scombrid abundance or occurrence (Burnham and Anderson, 2002). The resulting fitted models were validated by visual examination of the quantile residuals and plotted against the observed data and against each explanatory term included in the full model.

Abundance data can be affected by encountering random, large aggregations or patches of fishes, which can skew the results, while presence–absence data comes with the cost of losing information about the actual, observed abundances. Thus, modeling both abundance and presence–absence data provided validation for the observed patterns in both models and highlighted where the models agree or disagree.

RESULTS

Catch Summary

A total of 326 larval and juvenile scombrids were collected from 890 quantitative tows (net fished correct depth strata with valid flow data) from the surface to 1500 m (**Table 1**). The majority of scombrids (75%, n = 245) were collected in the epipelagic zone during both day (n = 100) and night (n = 107) quantitative tows (**Table 2**). Scombrids were collected in 35.8% of all epipelagic trawl samples, which was more frequent than the pelagic trawl samples from the surface to 1500 m (15%).

Overall, 85.0% of individuals were identified to species, 13.5% to genus only, and 1.5% to family only. The larval and juvenile scombrid assemblage in this survey comprised 11 of the 16 scombrid species previously reported from the GoM (Richards, 2005). Only four specimens of the endangered *T. thynnus* were collected, all of which were caught below the epipelagic zone (>200 m depth). One *T. thynnus* larva (6.4 mm SL) was collected on August 25, 2011, outside of their known spawning time period.

Scombrid specimens ranged in size from 3.0 to 111.4 mm SL, with an average size of 11.8 mm SL (**Table 1** and **Figure 1**). The smallest identifiable larval scombrid was *Katsuwonus pelamis* (3.2 mm SL) and the largest was a juvenile *Auxis* sp. (111.4 mm SL). Most specimens were collected in the late-larval phase (81.3%), with 18.7% of individuals in the juvenile stage.

TABLE 1 | Counts and size range of scombrid specimens caught in quantitative tows from the surface to 1500 m depth.

Species	Larvae	Juvenile	Total	Size range (mm SL)
Euthynnus alletteratus	89	32	121	4.9–44.5
Thunnus atlanticus	61	1	62	4.0–16.0
Auxis thazard	33	9	42	5.7–21.0
Thunnus spp.	33	1	34	4.3–47.0
Katsuwonus pelamis	23	3	26	3.2–16.0
Auxis spp. juv.	0	10	10	15.2–111.4
Auxis rochei	5	1	6	5.4–86.7
Scombridae UNID.	5	0	5	3.0–9.0
Sarda sarda	5	0	5	5.0–9.0
Acanthocybium solandri	4	0	4	7.5–13.0
*Thunnus thynnus**	4	0	4	5.3–7.0
Scomber colias	0	3	3	11.4–51.9
Scomberomorus cavalla	1	1	2	6.3–16.2
Thunnus albacares	2	0	2	5.0–8.5
Total	265	61	326	3.0–111.4

An asterisk (*) indicates that all individuals were collected below the epipelagic zone (>200 m depth).

Epipelagic Abundances and F_o

The most-abundant species collected in epipelagic zone from January to September 2011 were *Euthynnus alletteratus, Thunnus atlanticus,* and *Auxis thazard*, comprising approximately 72% of the total abundance of scombrids captured (**Table 2**). *Euthynnus alletteratus* was the most-abundant species caught (n = 97; 1.87 ind. 10^{-5} m^{-3}), accounting for c. 40% of the total scombrids captured. *Thunnus atlanticus*, the most common true tuna species (*Thunnus* spp.) in our samples, was the second-most abundant species overall (n = 42; 0.81 ind. 10^{-5} m^{-3}), comprising c. 17% of the captured scombrids. *Thunnus atlanticus*, along with the other *Thunnus* species, comprised c. 29% of the scombrid abundance (n = 70; 1.35 ind. 10^{-5} m^{-3}). *Auxis thazard* was the third-most abundant species collected (n = 38; 0.73 ind. 10^{-5} m^{-3}) in this study.

Scombrids collected in the epipelagic zone were collected in higher abundances at night (6.98 ind. 10^{-5} m^{-3}) than during the day (2.31 ind. 10^{-5} m^{-3}; **Table 2**). The abundance estimate of *E. alletteratus* derived from night samples (2.50 ind. 10^{-5} m^{-3}) was twice that from day samples (1.19 ind. 10^{-5} m^{-3}), while *T. atlanticus* abundance estimates exhibited a four-fold increase from day (0.32 ind. 10^{-5} m^{-3}) to night sampling (1.27 ind. 10^{-5} m^{-3}). *Auxis thazard* and *Katsuwonus pelamis* were also caught at higher rates at night (1.34 and 0.52 ind. 10^{-5} m^{-3}, respectively) than during the day (both 0.08 ind. 10^{-5} m^{-3}).

The most-abundant species were also collected at higher F_o at night than during the day in the epipelagic zone (**Table 2**). There was 27.0% F_o during the day and 43.9% at night for the family Scombridae. *Euthynnus alletteratus* had a higher F_o at night, occurring in 11.0% of the day trawls and 15.0% of the night trawls. *Thunnus atlanticus* exhibited a F_o in 7.0% of the day trawls and 14.0% of the night trawls. *Auxis thazard* F_o increased between

TABLE 2 | Total standardized abundance (no. ind. 10^{-5} m^{-3}) and F_o (%) of scombrid larvae and juveniles collected in the epipelagic zone.

Species	Counts			Standardized abundance			F_o		
	Day	Night	Total	Day	Night	Total	Day	Night	Total
Euthynnus alletteratus	30	67	97	1.19	2.50	1.87	11.0	15.0	13.0
*Thunnus atlanticus**	8	34	42	0.32	1.27	0.81	7.0	14.0	10.6
*Auxis thazard***	2	36	38	0.08	1.34	0.73	2.0	10.3	6.3
Thunnus spp.	10	17	27	0.40	0.63	0.52	7.0	9.4	8.22
Katsuwonus pelamis	2	14	16	0.08	0.52	0.31	2.0	8.4	5.3
Auxis spp.	0	10	10	0.00	0.37	0.19	0	5.6	2.9
Acanthocybium solandri	2	2	4	0.08	0.07	0.08	2.0	1.9	1.9
Unidentified Scombridae	0	3	3	0.00	0.11	0.06	0	1.9	1.0
Auxis rochei	0	2	2	0.00	0.07	0.04	0	0.9	0.5
Sarda sarda	2	0	2	0.08	0.00	0.04	2.0	0	1.0
Scomber colias	0	2	2	0.00	0.07	0.04	0	2.8	1.5
Scomberomorus cavalla	1	0	1	0.04	0.00	0.02	1.0	0	0.5
Thunnus albacares	1	0	1	0.04	0.00	0.02	1.0	0	0.5
Thunnus thynnus	0	0	0	0.00	0.00	0.00	0	0	0
Family Scombridae**	58	187	245	2.31	6.98	4.72	27.0	43.9	35.8

Day refers to tows sampled around solar noon and night refers to tows sampled around midnight. Diel cycle (day vs. night sampling) retained as important (**) or marginally important (*) variable in the abundance GAMs.

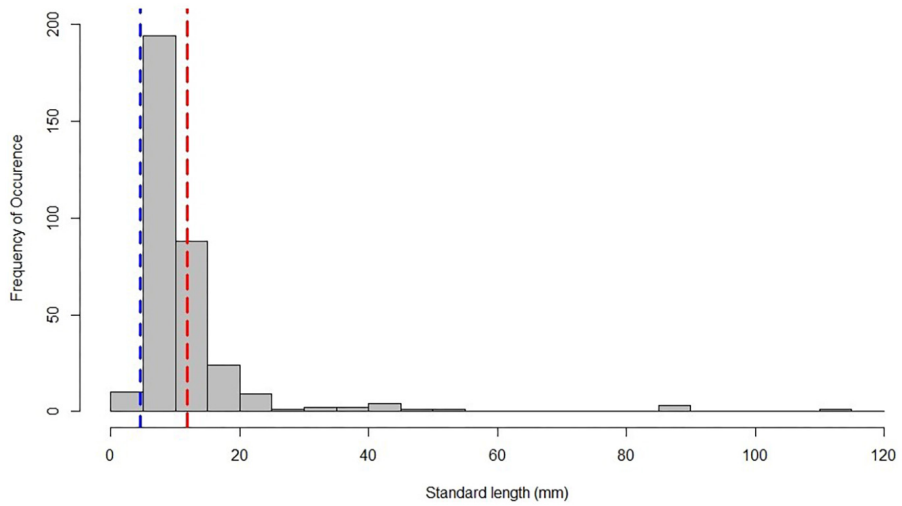

FIGURE 1 | Size-frequency plot of larval and juvenile scombrids collected from January to September in 2011, with the average-sized specimen indicated by the red dashed line. The blue dashed line signifies the average-sized specimen collected on DEEPEND's complementary ichthyoplankton cruises (4.6 mm SL; Cornic et al., 2018).

day and night samples, with 2.0% of the day trawls and 10.3% of the night trawls. *Katsuwonus pelamis* exhibited a F_o in 2.0% of day trawls and 8.4% of night trawls. The remaining, rare-event species and taxa did not exhibit higher nighttime abundances or occurrences, though less than five individuals were collected from each of these species in the epipelagic zone (**Table 2**).

Spatiotemporal Distributions: Generalized Additive Models

The fitted GAM modeling the total abundance of Scombridae included Julian date, water mass, diel cycle, and distance to the nearest 200-m isobath as important explanatory variables (**Table 3**). Overall, abundances began to increase in April and May and peaked in August (**Figures 2A,C**). More individuals were caught in CW (**Figures 2D,F**), further from the shelf break (**Figures 2G,H**), and at nighttime (**Figures 2I,J**). The fitted GAM modeling Scombridae occurrences included Julian date as an important variable, and water mass as a marginally important variable (**Table 3**). Results aligned with the abundance GAMs, in which there was a higher probability of catching scombrids later in the year (**Figures 2B,C**) and in CW (**Figures 2E,F**).

Euthynnus alletteratus was only captured in CW; therefore, *E. alletteratus* GAMs were only fitted to samples collected

TABLE 3 | dAICc values of abundance and presence–absence GAMs after dropping each explanatory variable for Scombridae, *Euthynnus alletteratus*, *Thunnus atlanticus*, and *Auxis thazard*.

Taxon:	Scombridae		*E. alletteratus* (CW only)		*T. atlanticus* (LCOW/CW only)		*A. thazard* (CW only)	
Data modeled:	**Abundance**	**Presence–absence**	**Abundance**	**Presence–absence**	**Abundance**	**Presence–absence**	**Abundance**	**Presence–absence**
Julian date	**30.7**	**13.2**	**21.4**	**11.0**	**16.7**	**20.8**	−1.7	−2.1
Water mass	**10.5**	***2.1***	NA	NA	−2.2	−1.2	NA	NA
Diel cycle	**8.4**	1.8	0.6	−2.2	***2.3***	0.5	**4.1**	**6.2**
Distance to 200-m isobath	**7.0**	0.9	**7.6**	***3.4***	−4.3	−0.5	0.2	***2.7***
S_{EPI}	−2.2	−0.6	**7.8**	**6.2**	**11.3**	***3.8***	−2.1	−1.8

Important explanatory variables (dAICc > 4) are bolded and marginally important variables (2 < dAICc < 4) are italicized and bolded. "CW only" and "LCOW/CW only" indicate when water mass types were excluded from analyses.

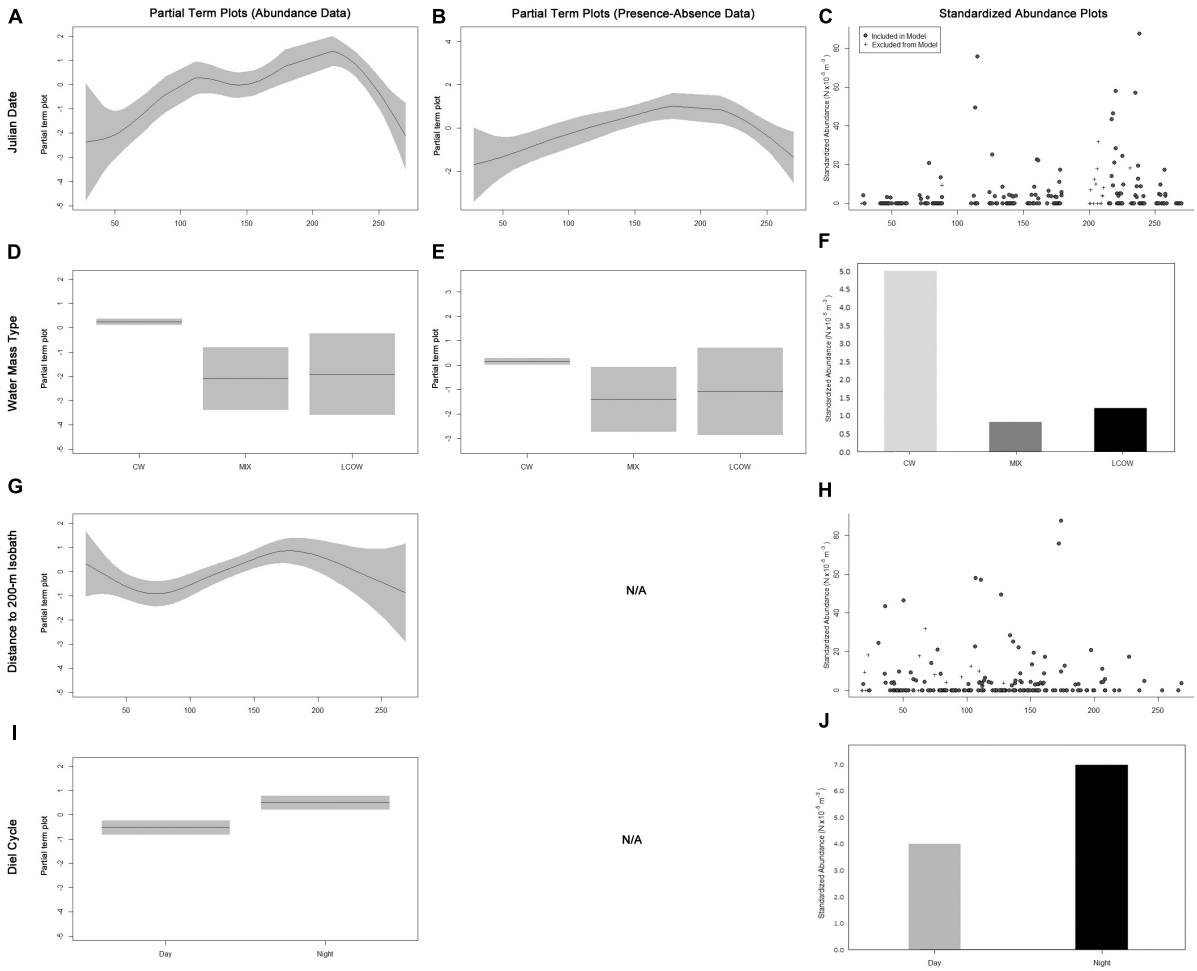

FIGURE 2 | Term plots for the best-fitting models for Scombridae data fitted to the abundance data **(A,D,G,I)** and presence–absence data **(B,E)**. Standardized abundance plots **(C,F,H,J)** are also presented for all important and marginally important variables. Data that had to be excluded from the model due to missing MOCNESS sensor data are indicated by crosses.

from CW, and water mass was removed as a variable from the full models. The fitted GAM modeling the abundance of *E. alletteratus* contained Julian date, S_{EPI}, and distance to the nearest 200-m isobath as important explanatory variables (**Table 3**). *Euthynnus alletteratus* abundances increased throughout the year, with the highest peak occurring around August (**Figures 3A,C**). Higher abundances were associated with lower S_{EPI} (**Figures 3D,F**), in which catches occurred in waters as fresh as 29.47 and most specimens ($n = 59$) were collected in $S_{EPI} < 34$. More individuals were also collected nearer to the shelf break

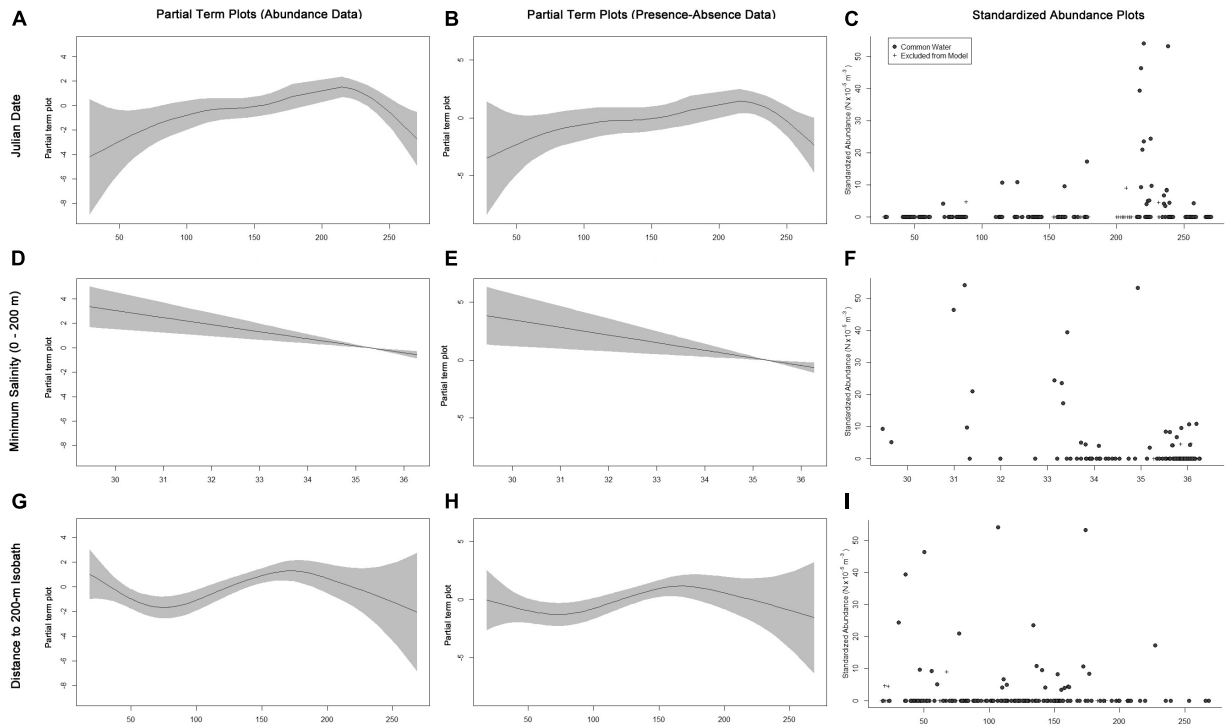

FIGURE 3 | Term plots for the best-fitting models for *Euthynnus alletteratus* data fitted to the abundance data **(A,D,G)** and presence–absence data **(B,E,H)**. Standardized abundance plots **(C,F,I)** are also presented for all important and marginally important variables. Data that had to be excluded from the model due to missing MOCNESS sensor data are indicated by crosses.

(19.79 to 227.31 km from the shelf break), with the majority of specimens within 180 km of the isobath (n = 62, **Figures 3G,I**). The fitted GAM modeling *E. alletteratus* occurrences identified Julian date and S_{EPI} as important, and distance to the nearest 200-m isobath as marginally important variables (**Table 3**). The presence–absence model results were similar to the abundance GAMs, in which individuals were more likely to be caught later in the year (**Figures 3B,C**), in low S_{EPI} (**Figures 3E,F**), and nearer to the shelf break (**Figures 3H,I**).

Only one *Thunnus atlanticus* specimen was collected in MIX water; thus, the GAMs fitted to *T. atlanticus* only included samples from LCOW and CW. The fitted GAM modeling the total abundance of *T. atlanticus* included Julian date and S_{EPI} as important and diel cycle as marginally important variables (**Table 3**). *Thunnus atlanticus* abundances showed higher abundances beginning in June and continuing through September (**Figures 4A,C**). High abundances were positively correlated with higher S_{EPI} (**Figures 4D,F**), with catches occurring only in S_{EPI} between 33.82 and 36.13. The majority of specimens (n = 37, 88%) were caught in water with $S_{EPI} > 35$. More individuals were collected at nighttime (**Figures 4G,H**). The fitted GAM modeling *T. atlanticus* occurrences included Julian date as important and S_{EPI} as marginally important variables (**Table 3**). The presence–absence model results were similar to the abundance GAMs, in which there was a higher probability of catching *T. atlanticus* from June to September (**Figures 4B,C**) and in higher S_{EPI} (**Figures 4E,F**).

Auxis thazard was only collected in CW; therefore, only samples from CW were included, and the water mass variable was removed from the full models. The fitted GAM modeling the total *A. thazard* abundance included diel cycle as an important variable (**Table 3**), with more individuals collected at night (**Figures 5A,C**). The fitted GAM modeling *A. thazard* occurrences included diel cycle as important (**Table 3**) and distance to the nearest 200-m isobath as marginally important variables (**Table 3**). The presence–absence model results were similar to the abundance GAMs, in which there was a higher probability of catching *A. thazard* at night (**Figures 5B,C**) and mid-shelf as an outer neritic species (**Figures 5D,E**).

DISCUSSION

Assemblage Structure and Spatiotemporal Distributions

The present study identified the faunal composition and assemblage structure of late-larval and juvenile scombrids throughout the northern GoM and characterized the spatiotemporal distributions of the most-abundant species in epipelagic waters with respect to geographic location, oceanographic features, and temporal change.

Of the 16 scombrid species that inhabit the GoM, 11 species were collected in the present study. The collection of a high proportion of the species that occur in the GoM

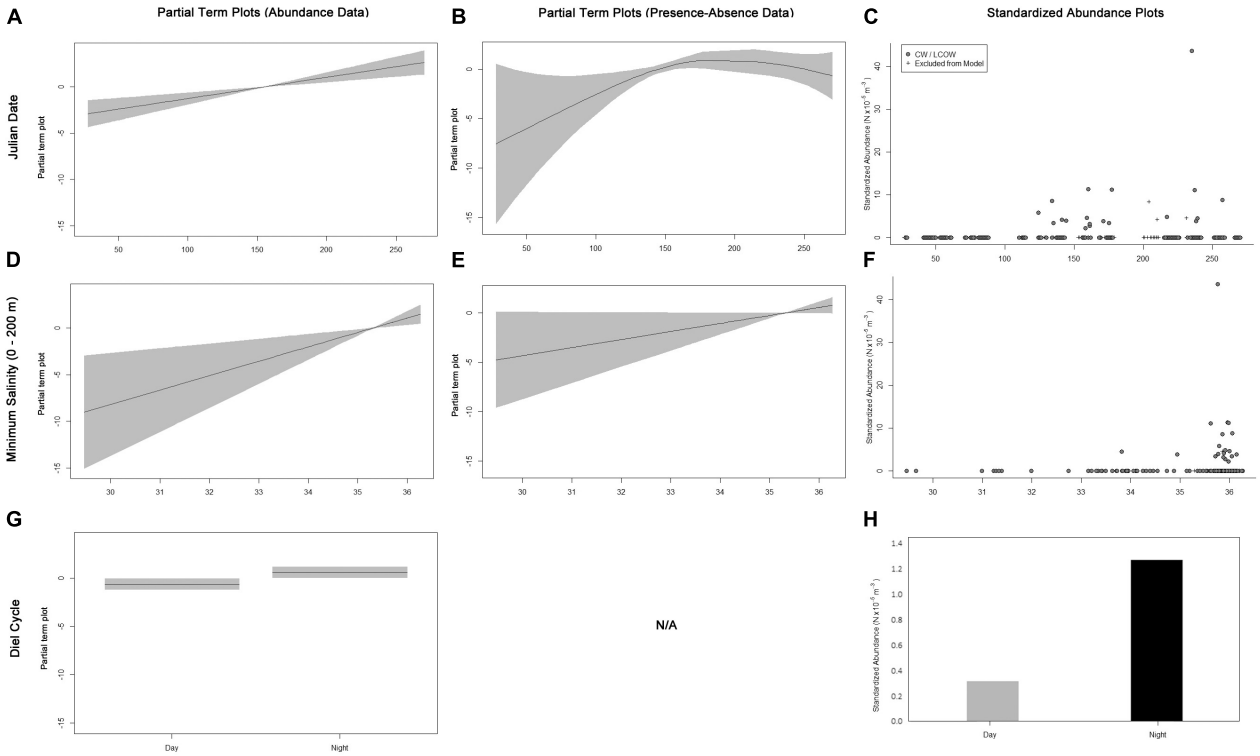

FIGURE 4 | Term plots for the best-fitting models for *Thunnus atlanticus* data fitted to the abundance data **(A,D,G)** and presence–absence data **(B,E)**. Standardized abundance plots **(C,F,H)** are also presented for all important and marginally important variables. Data that had to be excluded from the model due to missing MOCNESS sensor data are indicated by crosses.

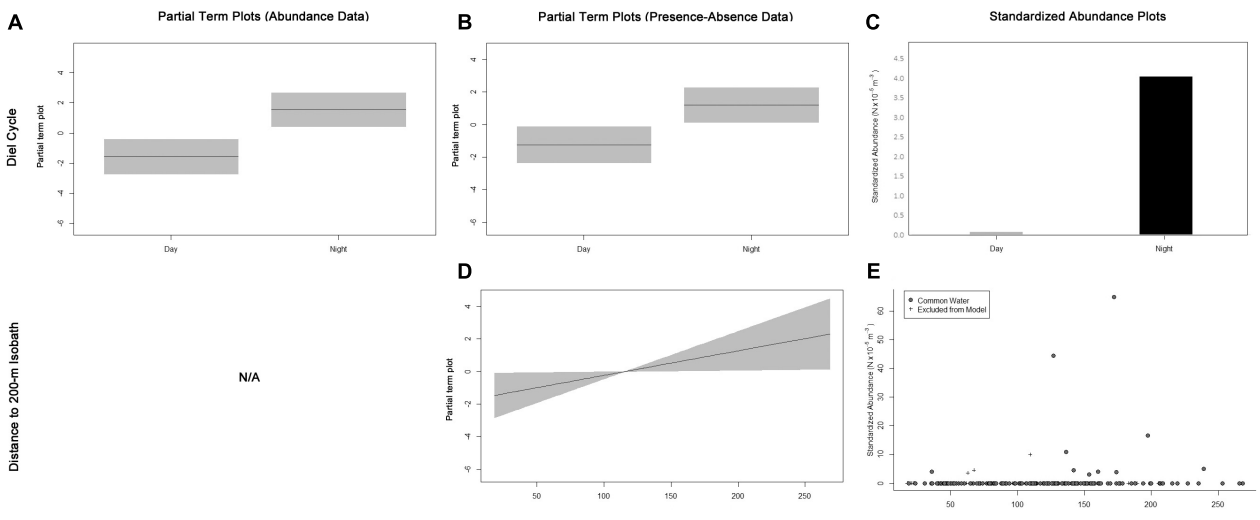

FIGURE 5 | Term plots for the best-fitting models for *Auxis thazard* data fitted to the abundance data **(A)** and presence–absence data **(B,D)**. Standardized abundance plots **(C,E)** are also presented for all important and marginally important variables. Data that had to be excluded from the model due to missing MOCNESS sensor data are indicated by crosses.

is likely a function of the continuous surveying method, the longevity of sampling (9-month uninterrupted sampling period, January–September 2011), and the day/night sampling during these cruise series. The advantage of continuously sampling a large spatial area and environmental conditions over a relatively long time period (9 months) increases the likelihood of collecting a variety of species. These large-scale faunal surveys remain extremely rare in

pelagic research; thus, the data presented here are both robust and unique.

The dominant tunas of the Tribe Thunnini that occur in the GoM, primarily *Thunnus* spp., but also *Auxis* spp., *Euthynnus alletteratus,* and *Katsuwonus pelamis* (Richards et al., 1993; Richardson et al., 2010; Habtes et al., 2014; Cornic et al., 2018), were collected in the present study. *Thunnus* spp. have consistently been reported as the dominant tuna taxon in ichthyoplankton surveys during the GoM's spring and summer months (Richards et al., 1993; Lindo-Atichati et al., 2012; Cornic et al., 2018), although, the most-abundant taxa captured in this study were small-bodied tuna species: *E. alletteratus, T. atlanticus*, and *Auxis thazard*. It is possible that the preponderance of small-bodied taxa in our study relative to previous studies reflects higher survivorship of their early life history stages than larger-bodied tunas, the latter showing a more r-selected reproductive strategy (*sensu* Pianka, 1970).

Scombrids collectively preferred CW conditions over the warmer and high SSHA waters within the MIX water and LCOW. Of the three most-abundant species, *T. atlanticus* was the only species collected in LCOW in addition to CW. Lindo-Atichati et al. (2012) found that larval *E. alletteratus* had similar abundances between CW and LCOW in the GoM, larval *Auxis* spp. (i.e., *A. thazard* and *A. rochei*) were found along the boundaries of anticyclonic features and within the GoM's CW, and *Thunnus* spp. and *T. thynnus* larvae were more abundant in the boundaries of anticyclonic features in the GoM. It has been proposed that year-round inhabitant species (e.g., *T. atlanticus*) have broader habitat preferences in the GoM than *T. thynnus* and are better able to tolerate warm features, such as the Loop Current and warm eddies (Muhling et al., 2010; Teo and Block, 2010; Lindo-Atichati et al., 2012). Variability in the abundances within CW can also relate to smaller-scale oceanographic features (e.g., cyclonic eddies) in addition to changes in environmental variables that were investigated in this study (i.e., S_{EPI}, Chl *a*).

Abundance and presence–absence GAMs additionally identified a coastal group (*E. alletteratus* and *A. thazard*) and an oceanic group, represented by *T. atlanticus*. The coastal group was associated with more productive continental shelf and slope environments (low S_{EPI}, high Chl *a*, nearer to shelf break), while the oceanic group was associated with offshore, oligotrophic habitats (high S_{EPI}, low Chl *a*, further from shelf break).

Nearshore environments and areas with high terrestrial runoff are associated with low S_{EPI} and high Chl *a*, which relates to the coastal life history traits of *E. alletteratus* and *A. thazard*. *Euthynnus alletteratus* preferred nearshore environments with lower S_{EPI} (<34), and *A. thazard* was characterized as an outer neritic species, as it preferred areas along the outer shelf break. Maximum freshwater discharge into the GoM from the Mississippi River occurs in the spring. The plume is characterized by lower S_{EPI} and higher Chl *a*. Their preference of nearshore environments with lower S_{EPI} suggests that areas with high freshwater inflow are suitable habitats for the larvae and small-bodied juvenile size classes of coastal tunas. As nutrients increase from runoff, primary and secondary production increase, and in turn provide food for larvae along the continental shelf regions (Le Fevre, 1986; Grimes and Finucane, 1991; Grimes and Kingsford, 1996). Thus, riverine discharge likely maximizes growth and survival of *E. alletteratus* and *A. thazard* early life stages.

The GoM experienced a highly productive year in 2011 (Muller-Karger et al., 2015), with high Chl *a* waters and low S_{EPI}, especially along the coast due to increased runoff from the Mississippi River. These favorable and highly productive conditions in the nearshore environment could contribute to the numerical dominance of *E. alletteratus* and *A. thazard* observed in this study.

Offshore waters typically exhibit higher S_{EPI} and low to moderate Chl *a*. Larval and juvenile *T. atlanticus* were collected in offshore waters, with higher S_{EPI}. Spawning in these open-ocean environments increases the initial survival of their eggs and larvae due to the reduction in ichthyoplankton predators compared to the coastal waters, though this may be offset at exogenous feeding by lower food supply. Similar to adult *T. atlanticus*, adult *T. thynnus* also spawn in waters with lower surface Chl *a* (0.10–0.16 mg m^{-3}) and higher S_{EPI} (35.5–37.0; Teo et al., 2007). Other pelagic fishes (e.g., swordfish, *Xiphias gladius*) also utilize warm, oligotrophic waters for spawning (Teo et al., 2007). Some tuna species have larvae adapted to living in these nutrient-poor environments, utilizing appendicularians for food at the beginning of their piscivorous early life stages (Llopiz et al., 2010). It appears that *T. atlanticus* early life stages prefer to remain in, and have adapted to, living in areas with increased S_{EPI} and decreased Chl *a*.

Cornic et al. (2018) also found that *T. atlanticus* larvae preferred intermediate to high salinities, ranging from 31 to 36, and identified *T. atlanticus* as the most common true tuna from surveys conducted in the northern GoM (June and July, 2007 to 2010), accounting for 81% of the *Thunnus* larvae. High abundances of *T. atlanticus* also observed in the present study suggest that *T. atlanticus* is the most-abundant true tuna species inhabiting the GoM.

Temporal changes in scombrid abundances were associated with species-specific spawning preferences, in which high peaks in abundances in April, June, and August were influenced by *A. thazard, E. alletteratus,* and *T. atlanticus*, respectively.

An increase in abundance in April (around day 115) was dominated by *A. thazard* specimens. *Auxis thazard* spawns at sea surface temperatures (SSTs) of 21.6 to 30.5°C, with mass spawning between 25.0 and 26.0°C (Rudomiotkina, 1984; ICCAT, 2016a). The SSTs in April reached the massive spawning temperature range for *A. thazard*, which provides an explanation for the high observed abundances of this species.

Euthynnus alletteratus produces several spawning batches per reproductive season (Chur, 1973; Rudomiotkina, 1986; ICCAT, 2016a), which explains the numerous peaks in abundances throughout the year (increasing from March to September and a large peak in August). Additionally, spawning occurs when waters are the warmest in the GoM (preferably greater than 25°C), from April to November. Surface temperatures reached about 25°C in April, when spawning begins to occur for this species (Chur, 1973; Rudomiotkina, 1986; ICCAT, 2016a). Thus, the temporal changes observed through this 9-month survey influenced the high abundance of *E. alletteratus* in the GoM.

For *T. atlanticus,* spawning in the GoM typically occurs between June and September (Collette, 2010), particularly when SSTs reach 27°C (Juarez and Frías, 1986). Water temperatures reached 27°C in June when abundances strongly increased (with highest catches in August), aligning with the previously reported spawning preferences. A few specimens were collected in September, as temperatures began to drop. These patterns relate to the high abundances noted in the ichthyoplankton surveys conducted by Cornic and Rooker (2018) in June and July in 2011.

In addition to the three most-abundant taxa, *Katsuwonus pelamis*, *Auxis rochei, Sarda sarda, Acanthocybium solandri, Thunnus thynnus, Scomber colias,* and *Thunnus albacares* were collected in the present study. Some species, such as the non-resident *T. thynnus*, were rare in these collections, most likely due to their restricted and shorter spawning seasons in the GoM compared to other resident spawners (ICCAT, 2016a). However, it is interesting to note the collection of a 6.4 mm SL *T. thynnus* specimen in late August. A comparison with estimated growth rates suggests that the specimen was approximately 9 days old (Malca et al., 2017), indicating that this specimen was spawned in mid-August. While this is an observation of only a single specimen, our findings suggest that the spawning period for *T. thynnus,* which is currently estimated as occurring between April and June in the GoM, may extend through to August in a limited fashion. Moreover, all *T. thynnus* larvae were collected below 200 m depth, which indicates a level of connectivity between 'classic' epipelagic fishes and deeper pelagic waters over the course of development. Conducting additional larval surveys outside of the "typical" spawning period would help elucidate the extent to which spawning occurs at other times of year in this highly valuable species.

This study highlights the value of large-spatiotemporal scale surveys of oceanic ecosystems such as the GoM, given that scombrid species spawn at different times throughout the year and under different environmental conditions. These large-scale and long-term surveys provide information on the variance in the ecology of species that inhabit an area, can identify commonalities among the faunal assemblage overtime (among years and/or months), and can highlight typical and rare species occurrences in a region.

Size Classes

The 10-m^2 MOCNESS (3-mm mesh) primarily caught large larval and small juvenile scombrids. The average size specimen collected in this study (11.8 mm SL) was greater than other ichthyoplankton surveys in the GoM, such as Muhling et al. (2012) that collected larvae between 2.5 and 5.0 mm SL and DEEPEND's complementary ichthyoplankton cruises that collected an average-sized specimen of 4.6 mm SL (Cornic and Rooker, 2018).

The MOCNESS is a larger gear type compared to bongo and neuston nets (with mesh sizes ranging from 335 to 1200 μm) that are typically used in ichthyoplankton surveys to catch small larvae (Richards et al., 1984; Lindo-Atichati et al., 2012; Habtes et al., 2014; Cornic et al., 2018). All else being equal, avoidance is a function of mouth size and extrusion is a function of mesh size (MacLennan, 1992). The larger mouth area, mesh sizes, and faster tow speeds of the MOCNESS ostensibly reduce the ability of these larger larvae and small juveniles to avoid the gear, and in turn, these larger nets are more effective at capturing larger fishes (Kashkin and Parin, 1983). Thus, this study collected fewer planktonic larvae compared to other ichthyoplankton surveys, as smaller individuals were extruded through the MOCNESS's larger mesh, and in turn, the assemblages of larger larvae and small juveniles were represented.

The larger individuals collected in this study, existing in a higher Reynold's number environment than small larvae, have increased swimming abilities and mobility due to the development of locomotive features and the need to sustain their high energetic needs and high metabolic costs. More mobile individuals can actively locate and capture prey more easily, adjust their distributions within the water column (horizontally and vertically), and, in turn, increase their growth and survival rates (Werner and Gilliam, 1984). Understanding the assemblage structure and distributional patterns of these larger larvae and small juvenile size classes are critical for fisheries management and conservation efforts as these size classes represent the cohort that has survived the high-mortality "gauntlet" experienced by small larvae (Anonymous, 1984; ICCAT, 2016a).

Comparison of the relative dominance between sampling strategies in the same place and at similar times of year can also potentially inform taxon-specific mortality rates at different size classes. While larval assemblages are used as a proxy for predicting spawning stock biomass, late-larval and juvenile assemblages should also be used to predict future stocks, as these individuals provide a more accurate representation of the surviving year classes of scombrids in the GoM, and subsequently, those individuals (and genetic lineages) that have a higher chance of persisting to adulthood. It is an advantage to use multiple sampling methods (e.g., neuston nets, bongos, MOCNESS) in order to gain a more complete analysis of scombrid ecology and size class assemblages.

Diel Catchability in the Epipelagial

It is important to understand diel differences in day and night catch rates during surveying, as quantitative data are used in scombrid stock assessments. In this study, scombrid early life stages were collected at higher abundances and higher frequencies at night than during the daytime in the epipelagic zone. Increased catches at night are most likely a result of net detection and avoidance during the daytime (Davis et al., 1990). Diel differences in feeding activity also influence catch rates. Most larval and juvenile scombrids feed during the day (Young and Davis, 1990; Tanabe, 2001; Morote et al., 2008), when they are more active. Sensing the nets, and swimming away from them, is more likely to occur during the day when early life stages are more active. Thus, higher catches at night may be related to lower activity levels, decreased swimming activity, and reduced ability to visually detect and avoid nets (Takashi et al., 2006).

While daytime sampling may be appropriate for smaller larvae, it is evident that for the size classes collected in this study (larger larvae and smaller juveniles) it is more beneficial to sample at night in order to collect a more accurate representation of abundance in the epipelagic. These larger individuals are able to

actively move across larger spatial scales, and their distributions are more likely to be behavioral compared to a planktonic existence exhibited by larvae.

There is additional supporting evidence of higher capture rates of larval tuna at night. Cornic and Rooker (2018) noted an increase in abundances of *T. atlanticus* prior to sunset and after dawn in the northern GoM, though their sampling protocol did not include night (midnight) sampling, obfuscating comparison to the present study. In the vicinity of Puerto Rico and the Virgin Islands, Hare et al. (2001) collected more *K. pelamis* larvae at night, but larval *T. atlanticus* and *E. alletteratus* abundances were similar between day and night tows. Previous studies involving larval *Auxis* spp. also observed higher catches at night in the Philippines, Atlantic Ocean, and Pacific Ocean (Wade and Bravo, 1951; Matsumoto, 1959; Strasburg, 1960; Klawe, 1963).

Recognizing catch differences between day and night sampling is important for fisheries management. Results from this study indicate that it is more appropriate to sample the epipelagic zone at night in order to collect quantitative abundance data that more accurately reflect the true abundance of large larvae and smaller juvenile scombrids in an area.

CONCLUSION

Bongo nets have proven effective at catching smaller larvae, neuston nets effectively catch slightly larger larvae, and hook-and-line sampling catches adults. However, an effective sampling method does not currently exist for sampling these large larvae and small juveniles, and traditional gear types undersample these size classes. Utilizing multiple sampling methods to target tuna early life stages can improve long-term assessments of recruitment, spawning, and stock biomass of tunas. Such large-scale surveys taken over seasonal cycles provide invaluable information regarding spawning, recruitment, and survivorship rates throughout a year. This study provided a cumulative quantitative analysis and more accurate representation of the scombrid cohort that survived the high mortality that is typically experienced by small larvae. It is important to continue exploring additional modifications of sampling methods for these size classes in order to gather ecological data on these poorly studied, small-bodied tuna species.

Scombrids have a wide variety of life history strategies and spatiotemporal distributions that are often dictated by adult spawning and migratory behaviors. Through spawning, adults establish the initial broad distribution of eggs and small larvae, and the larger larvae and small juveniles modify these distributions through their own behavior. Different seasonal and horizontal distributional patterns existed among the species examined in this study. Horizontal distributions were closely linked with physical characteristics of the water column and mesoscale oceanographic features. Oceanic species (*Thunnus atlanticus*) preferred more oligotrophic habitats (high S_{EPI}, low Chl *a*, further distance from shelf break), while coastal species (*Euthynnus alletteratus* and *Auxis thazard*) preferred more productive continental shelf and slope environments (low S_{EPI}, high Chl *a*, nearer to shelf break).

Overall, this study quantified the habitat preferences of late-larval and juvenile scombrids in the northern GoM. Results from this study demonstrate the partitioning of pelagic habitat by tunas, from late larvae to adults, particularly for small-bodied tuna species (e.g., *E. alletteratus* and *T. atlanticus*) that do not have any current stock assessments or management plans in place. By understanding habitat preferences of tuna early life stages, we can protect critical spawning grounds and nursery habitats and aim to improve management and conservation efforts regarding scombrid populations in the GoM.

DATA AVAILABILITY STATEMENT

Data are publicly available through the Gulf of Mexico Research Initiative Information & Data Cooperative (GRIIDC) at https://data.gulfresearchinitiative.org (doi: 10.7266/N7VX0DK2). Additional data were sourced from the E.U. Copernicus Marine Service (GLOBAL_ANALYSIS_FORECAST_PHY_001_024), the GEBO_2014 Grid (version 20141103) and NASA's Ocean Biology Processing Group (doi: 10.5067/AQUA/MODIS/L3M/CHL/2018).

AUTHOR CONTRIBUTIONS

NP and TS designed the study; NP analyzed the samples and organized the database; NP and RM performed the statistical analysis and prepared the figures. All authors contributed to manuscript preparation and revision, and read and approved the submitted version.

FUNDING

This research was funded in part by the NOAA Office of Response and Restoration and in part by a grant from The Gulf of Mexico Research Initiative (GoMRI).

ACKNOWLEDGMENTS

The authors would like to thank both the science staff and the crew aboard the *R/V Meg Skansi*. Additional thanks go to Dr. John Lamkin and Aki Shiroza from NOAA NMFS, Miami, FL, for assisting in the larval identifications. This manuscript includes work that was conducted and samples that were collected as part of the *Deepwater Horizon* Natural Resource Damage Assessment being conducted cooperatively among academic partners, NOAA, other Federal and State Trustees, and BP.

SUPPLEMENTARY MATERIAL

The Supplementary Material for this article can be found online at: https://www.frontiersin.org/articles/10.3389/fmars.2020.00257/full#supplementary-material

REFERENCES

Anonymous, (1984). Meeting of the working group on juveniles tropical tunas. *Coll. Vol. Sci. Pap.* 21, 1–289.

Burnham, K., and Anderson, D. (2002). "Model selection and multimodel inference: a practical information-theoretic approach," in *Prediction and the Power Transformation Family*, eds R. J. Carroll, and D. Ruppert, (New York, NY: Springer-Verlag).

Chur, V. (1973). Some biological characteristics of little tuna (Euthynnus alletteratus, Rafinesque, 1810) in the eastern part of the tropical Atlantic. *Coll. Vol. Sci. Pap*. 1, 489–500.

Collette, B., and Graves, J. (2019). *Tunas and Billfishes of the World*. Baltimore: Johns Hopkins University Press.

Collette, B. B. (2010). "Reproduction and development in epipelagic fishes," in *Reproduction and Sexuality in Marine Fishes: Patterns and Processes*, ed. K. S. Cole, (Berkeley: University of California Press).

Cornic, M., and Rooker, J. R. (2018). Influence of oceanographic conditions on the distribution and abundance of blackfin tuna (*Thunnus atlanticus*) larvae in the Gulf of Mexico. *Fish Res.* 201, 1–10. doi: 10.1016/j.fishres.2017.12.015

Cornic, M., Smith, B. L., Kitchens, L. L., Bremer, J. R. A., and Rooker, J. R. (2018). Abundance and habitat associations of tuna larvae in the surface water of the Gulf of Mexico. *Hydrobiologia* 806, 29–46. doi: 10.1007/s10750-017-3330-0

Davis, T. L., Jenkins, G. P., and Young, J. W. (1990). Diel patterns of vertical distribution in larvae of southern bluefin, *Thunnus maccoyii*, and other tuna in the East Indian Ocean. *Mar. Ecol. Prog. Ser.* 59, 63–74. doi: 10.3354/meps059063

Grimes, C. B., and Finucane, J. H. (1991). Spatial distribution and abundance of larval and juvenile fish, chlorophyll and macrozooplankton around the Mississippi River discharge plume, and the role of the plume in fish recruitment. *Mar. Ecol. Prog. Ser.* 75, 109–119. doi: 10.3354/meps075109

Grimes, C. B., and Kingsford, M. J. (1996). How do riverine plumes of different sizes influence fish larvae: do they enhance recruitment? *Mar. Freshw. Res.* 47, 191–208.

Habtes, S., Muller-Karger, F. E., Roffer, M. A., Lamkin, J. T., and Muhling, B. A. (2014). A comparison of sampling methods for larvae of medium and large epipelagic fish species during spring SEAMAP ichthyoplankton surveys in the Gulf of Mexico. *Limnol. Oceanogr.-Methods* 12, 86–101. doi: 10.4319/lom.2014.12.86

Hare, J. A., Hoss, D. E., Powell, A. B., Konieczna, M., Peters, D. S., Cummings, S. R., et al. (2001). Larval distribution and abundance of the family Scombridae and Scombrolabracidae in the vicinity of Puerto Rico and the Virgin Islands. *Bull. Sea Fish Inst.* 2, 13–29.

Hendriks, A. J. (1999). Allometric scaling of rate, age and density parameters in ecological models. *Oikos* 86, 293–310.

Hsieh C-h, Reiss, C. S., Hunter, J. R., Beddington, J. R., May, R. M., and Sugihara, G. (2006). Fishing elevates variability in the abundance of exploited species. *Nature* 443:859. doi: 10.1038/nature05232

ICCAT, (2016a). *ICCAT Manual. International Commission for the Conservation of Atlantic Tuna*. Madrid: ICCAT Publications.

ICCAT, (2016b). *Report of the Standing Committee on Research and Statistics (SCRS)*. Madrid: ICCAT Publications, 1–426.

Johnston, M., Milligan, R., Easson, C., DeRada, S., Penta, B., and Sutton, T. (2019). An empirically-validated method for characterizing pelagic habitats in the gulf of mexico using ocean model data. *Limnol Oceanogr.-Methods* 17, 362–375.

Juan-Jordá, M. J., Mosqueira, I., Cooper, A. B., Freire, J., and Dulvy, N. K. (2011). Global population trajectories of tunas and their relatives. *Proc. Natl. Acad. Sci. U.S.A.* 108, 20650–20655. doi: 10.1073/pnas.1107743108

Juarez, M., and Frías, P. (1986). "Distribución de las larvas de bonito (*Kasuwonus pelamis*) y falsa albacora (*Thunnus atlanticus*)(Pisces: Scombridae) en la zona económica de Cuba," in *Actas de la Conferencia ICCAT Sobre el Programa del Año Internacional del Listado*, eds P. E. K. Symons, M. Miyake, and G. T. Sakagawa, (Madrid: International Commission for the Conservation of Atlantic Tunas).

Kashkin, N. I., and Parin, N. V. (1983). Quantitative assessment of micronektonic fishes by nonclosing gear (a review). *Biol. Oceanogr.* 2, 263–287.

Klawe, W. L. (1963). Observations on the spawning of four species on tuna (*Neothunnus macropterus*, *Katsuwonus pelamis, Auxis thazard* and *Euthynnus lineatus*) in the Eastern Pacific Ocean, based on the distribution of their larvae and juveniles. *Inter.-Am. Trop. Tuna Commun. Bull.* 6, 447–540.

Lang, K. L., Grimes, C. B., and Shaw, R. F. (1994). Variations in the age and growth of yellowfin tuna larvae, *Thunnus albacares*, collected about the Mississippi River plume. *Environ. Biol. Fish* 39, 259–270. doi: 10.1007/bf00005128

Le Fevre, J. (1986). Aspects of the biology of frontal systems. *Adv. Mar. Biol.* 23, 163–299. doi: 10.1016/s0065-2881(08)60109-1

Lindo-Atichati, D., Bringas, F., Goni, G., Muhling, B., Muller-Karger, F. E., and Habtes, S. (2012). Varying mesoscale structures influence larval fish distribution in the northern Gulf of Mexico. *Mar. Ecol. Prog. Ser.* 463, 245–257. doi: 10.3354/meps09860

Llopiz, J. K., Richardson, D. E., Shiroza, A., Smith, S. L., and Cowen, R. K. (2010). Distinctions in the diets and distributions of larval tunas and the important role of appendicularians. *Limnol. Oceanogr.* 55, 983–996. doi: 10.4319/lo.2010.55.3.0983

MacLennan, D. N. (1992). Fishing gear selectivity: an overview. *Fish. Res.* 13, 201–204. doi: 10.1016/0165-7836(92)90076-6

Majkowski, J. (2007). *Global Fishery Resource of Tuna and Tuna-like Species: FAO Fish Tech Pap 54*. Rome: FAO.

Malca, E., Muhling, B., Franks, J., García, A., Tilley, J., Gerard, T., et al. (2017). The first larval age and growth curve for bluefin tuna (Thunnus thynnus) from the Gulf of Mexico: comparisons to the Straits of Florida, and the Balearic Sea (Mediterranean). *Fish. Res.* 190, 24–33. doi: 10.1016/j.fishres.2017.01.019

Matsumoto, W. M. (1959). *Descriptions of Euthynnus and Auxis Larvae from the Pacific and Atlantic Oceans and adjacent seas: Fish Bull, Book* 50. Copenhagen: Carlsberg Foundation.

Matthews, F. D., Damaker, D. M., Knapp, L. W., and Collette, B. (1977). *Food of Western North Atlantic tunas* (*Thunnus*) and *Lancetfishes* (*Alepisaurus*). Silver Spring: Department of Commerce, National Oceanic and Atmospheric Administration, National Marine Fisheries Service.

McEachran, J. D., and Fechhelm, J. D. (1998). *Fishes of the Gulf of Mexico, Myxiniformes to Gasterosteiformes*, Vol. 1. Austin: University of Texas Press.

Molinari, R. L. (1980). Current variability and its relation to sea-surface topography in the Caribbean Sea and Gulf of Mexico. *Mar. Geod* 3, 409–436. doi: 10.1080/01490418009388006

Morote, E., Olivar, M. P., Pankhurst, P. M., Villate, F., and Uriarte, I. (2008). Trophic ecology of bullet tuna *Auxis roche*i larvae and ontogeny of feeding-related organs. *Mar. Ecol. Prog. Ser.* 353, 243–254. doi: 10.3354/meps07206

Muhling, B., Roffer, M., Lamkin, J., Ingram, G., Upton, M., Gawlikowski, G., et al. (2012). Overlap between Atlantic bluefin tuna spawning grounds and observed Deepwater Horizon surface oil in the northern Gulf of Mexico. *Mar. Pollut. Bull.* 64, 679–687. doi: 10.1016/j.marpolbul.2012.01.034

Muhling, B. A., Lamkin, J. T., and Roffer, M. A. (2010). Predicting the occurrence of Atlantic bluefin tuna (*Thunnus thynnus*) larvae in the northern Gulf of Mexico: building a classification model from archival data. *Fish. Oceanogr.* 19, 526–539. doi: 10.1111/j.1365-2419.2010.00562.x

Muller-Karger, F. E., Smith, J. P., Werner, S., Chen, R., Roffer, M., Liu, Y., et al. (2015). Natural variability of surface oceanographic conditions in the offshore Gulf of Mexico. *Prog. Oceanogr.* 134, 54–76. doi: 10.1016/j.pocean.2014.12.007

Nakata, H., Kimura, S., Okazaki, Y., and Kasai, A. (2000). Implications of meso-scale eddies caused by frontal disturbances of the Kuroshio Current for anchovy recruitment. *ICES J. Mar. Sci.* 57, 143–152. doi: 10.1006/jmsc.1999.0565

Nasa Goddard Space Flight Center, Ocean Ecology Laboratory, Ocean Biology Processing Group (2018). *Moderate-Resolution Imaging Spectroradiometer (MODIS) Aqua Chlorophyll Data; Reprocessing*. Greenbelt, MD: NASA OB. DAAC.

Olson, D. B., and Backus, R. H. (1985). The concentrating of organisms at fronts: a cold-water fish and a warm-core Gulf Stream ring. *J. Mar. Res.* 43, 113–137. doi: 10.1357/002224085788437325

Pante, E., and Simon-Bouhet, B. (2013). marmap: a package for importing, plotting and analyzing bathymetric and topographic data in R. *PLoS ONE* 8:e73051. doi: 10.1371/journal.pone.0073051

Pianka, E. R. (1970). On r-and K-selection. *Am. Nat.* 104, 592–597.

Pruzinsky, N. (2018). *Identification and Spatiotemporal Dynamics of Tuna (Family: Scombridae; Tribe: Thunnini) Early Life Stages in the Oceanic Gulf of Mexico*. Masters Thesis. Dania, FL: Nova Southeastern University.

R Core Team, (2019). *R: A Language and Environment for Statistical Computing*. Vienna: R Foundation for Statistical Computing.

Richards, W. J. (2005). *Early Stages of Atlantic Fishes: An Identification Guide for the Western Central North Atlantic, Two*, Vol. 2. Boca Raton, FL: CRC Press.

Richards, W. J., McGowan, M. F., Leming, T., Lamkin, J. T., and Kelley, S. (1993). Larval fish assemblages at the loop current boundary in the gulf of Mexico. *Bull. Mar. Sci.* 53, 475–537.

Richards, W. J., Potthoff, T., Kelley, S., McGowan, M. F., Ejsymont, L., Power, J. H., et al. (1984). Larval distribution and abundance of engraulidae, carangidae, clupeidae, lutjanidae, serranidae, coryphaenidae, istiophoridae, xiphiidae and scombridae in the Gulf of Mexico. *NOAA Tech. Mem. NMFS SEFC* 144, 1–51.

Richardson, D. E., Llopiz, J. K., Guigand, C. M., and Cowen, R. K. (2010). Larval assemblages of large and medium-sized pelagic species in the Straits of Florida. *Prog. Oceanogr.* 86, 8–20. doi: 10.1016/j.pocean.2010.04.005

Rigby, R. A., and Stasinopoulos, D. M. (2005). Generalized additive models for location, scale and shape. *J. R. Stat. Soc. Ser. C (Appl. Stat.)* 54, 507–554.

Rooker, J. R., Kitchens, L. L., Dance, M. A., Wells, R. D., Falterman, B., and Cornic, M. (2013). Spatial, temporal, and habitat-related variation in abundance of pelagic fishes in the Gulf of Mexico: potential implications of the Deepwater Horizon Oil Spill. *PLoS ONE* 8:e76080. doi: 10.1371/journal.pone.0076080

Rudomiotkina, G. (1984). New data on reproduction of *Auxis* spp. In the Gulf of Guinea. *Collect. Vol. Sci. Pap.* 20, 465–468.

Rudomiotkina, G. (1986). Data on reproduction of Atlantic black skipjack in the tropical West African water. *Collect Vol. Sci. Pap. ICCAT* 25, 258–261.

Scott, G. P., Turner, S. C., Churchill, G. B., Richards, W. J., and Brothers, E. B. (1993). Indices of larval bluefin tuna, *Thunnus thynnus*, abundance in the Gulf of Mexico; modelling variability in growth, mortality, and gear selectivity. *Bull. Mar. Sci.* 53, 912–929.

Strasburg, D. W. (1960). Estimates of larval tuna abundance in the central Pacific. *Fish. Bull.* 60, 231–255.

Sutton, T. T., Cook, A. B., Moore, J., Frank, T., Judkins, H., Vecchione, M., et al. (2016). *Inventory of Gulf Oceanic Fauna Data Including Species, Weight, and Measurements. Meg Skansi cruises from Jan.* 25 – *Sept. 30, 2011 in the Northern Gulf of Mexico. Distributed by: Gulf of Mexico Research Initiative Information and Data Cooperative (GRIIDC).* Christi: Harte Research Institute, Texas A&M University-Corpus.

Takashi, T., Kohno, H., Sakamoto, W., Miyashita, S., Murata, O., and Sawada, Y. (2006). Diel and ontogenetic body density change in Pacific bluefin tuna, *Thunnus orientalis* (Temminck and Schlegel), larvae. *Aquacult. Res.* 37, 1172–1179. doi: 10.1111/j.1365-2109.2006.01544.x

Tanabe, T. (2001). Feeding habits of skipjack tuna *Katsuwonus pelamis* and other tuna *Thunnus* spp. juveniles in the tropical western Pacific. *Fish. Sci.* 67, 563–570. doi: 10.1046/j.1444-2906.2001.00291.x

Teo, S. L., and Block, B. A. (2010). Comparative influence of ocean conditions on yellowfin and Atlantic bluefin tuna catch from longlines in the Gulf of Mexico. *PLoS ONE* 5:e10756. doi: 10.1371/journal.pone.0010756

Teo, S. L., Boustany, A. M., and Block, B. A. (2007). Oceanographic preferences of Atlantic bluefin tuna, *Thunnus thynnus*, on their Gulf of Mexico breeding grounds. *Mar. Biol.* 152, 1105–1119. doi: 10.1007/s00227-007-0758-1

Wade, C. B., and Bravo, P. (1951). Larvae of tuna and tuna-like fishes from Philippine waters. *Fish Bull* 51, 455–485.

Werner, E. E., and Gilliam, J. F. (1984). The ontogenetic niche and species interactions in size-structured populations. *Annu. Rev. Ecol. Syst.* 15, 393–425. doi: 10.1146/annurev.es.15.110184.002141

Wiebe, P., Morton, A., Bradley, A., Backus, R., Craddock, J., Barber, V., et al. (1985). New development in the MOCNESS, an apparatus for sampling zooplankton and micronekton. *Mar. Biol.* 87, 313–323. doi: 10.1007/bf00397811

Young, J. W., and Davis, T. L. (1990). Feeding ecology of larvae of southern bluefin, albacore and skipjack tunas (Pisces: Scombridae) in the eastern Indian Ocean. *Mar. Ecol. Prog. Ser.* 61, 17–29. doi: 10.3354/meps061017

Zuur, A. F., Ieno, E. N., and Elphick, C. S. (2010). A protocol for data exploration to avoid common statistical problems. *Methods Ecol. Evol.* 1, 3–14. doi: 10.1111/j.2041-210x.2009.00001.x

Zuur, A. F., Ieno, E. N., Walker, N., Saveliev, A. A., and Smith, G. M. (2009). *Mixed Effects Models and Extensions in Ecology with R*. Berlin: Springer Science & Business Media.

Conflict of Interest: The authors declare that the research was conducted in the absence of any commercial or financial relationships that could be construed as a potential conflict of interest.

frontiers in Marine Science

ORIGINAL RESEARCH
published: 29 April 2020
doi: 10.3389/fmars.2020.00169

Hiding in Plain Sight: Elopomorph Larvae Are Important Contributors to Fish Biodiversity in a Low-Latitude Oceanic Ecosystem

Jon A. Moore[1,2], Dante B. Fenolio[3], April B. Cook[4] and Tracey T. Sutton[4]*

[1] Harriet L. Wilkes Honors College, Florida Atlantic University, Jupiter, FL, United States, [2] Harbor Branch Oceanographic Institute, Florida Atlantic University, Fort Pierce, FL, United States, [3] Center for Conservation and Research, San Antonio Zoo, San Antonio, TX, United States, [4] Halmos College of Natural Sciences and Oceanography, Nova Southeastern University, Dania Beach, FL, United States

Leptocephalus larvae of elopomorph fishes are a cryptic component of fish diversity in nearshore and oceanic habitats. However, identifying those leptocephali can be important in illuminating species richness in a region. Since the *Deepwater Horizon* oil spill in 2010, sampling of offshore fishes in the epi-, meso-, and upper bathypelagic depth strata of the northern Gulf of Mexico resulted in 8989 identifiable specimens of leptocephalus larvae or transforming juveniles, in 118 taxa representing 83 recognized and established species and an additional 35 distinctive leptocephalus morphotypes not yet linked to a known described species. Leptocephali account for ∼13% of the total species richness of fishes collected in the offshore region. A new morphotype of Muraenidae leptocephalus is also described. We compare this study with other leptocephalus diversity studies in the western Atlantic.

Keywords: leptocephali, leptocephalus, MOCNESS, DEEPEND, ONSAP, Gulf of Mexico

OPEN ACCESS

Edited by:
Michael Vecchione, National Oceanic and Atmospheric Administration (NOAA), United States

Reviewed by:
Mackenzie E. Gerringer, SUNY Geneseo, United States
Dave Johnson, National Museum of Natural History (SI), United States
David G. Smith, Smithsonian Institution, United States

****Correspondence:***
Jon A. Moore
jmoore@fau.edu

Specialty section:
This article was submitted to Deep-Sea Environments and Ecology, a section of the journal Frontiers in Marine Science

Received: *09 August 2019*
Accepted: *03 March 2020*
Published: *29 April 2020*

Citation:
Moore JA, Fenolio DB, Cook AB and Sutton TT (2020) Hiding in Plain Sight: Elopomorph Larvae Are Important Contributors to Fish Biodiversity in a Low-Latitude Oceanic Ecosystem. Front. Mar. Sci. 7:169. doi: 10.3389/fmars.2020.00169

INTRODUCTION

Elopomorph fishes are basal teleosts, comprising the Elopiformes (tarpon and ladyfishes), Albuliformes (bonefishes), Notacanthiformes (spiny eels and halosaurs), and Anguilliformes (true eels, including the formerly separate Saccopharyngiformes) (Forey, 1973; Arratia, 1999; Dornburg et al., 2015; Poulsen et al., 2018). One unique characteristic of elopomorph fishes is a larval stage known as the leptocephalus (Greenwood et al., 1966; Pfeiler, 1986; Wiley and Johnson, 2010). This stage features an extended planktonic phase, allowing the larva to stay in the water column from a few months to several years before metamorphosis to a juvenile, depending on the species (Hulet, 1978; Smith, 1979, 1989a; Miller, 2009). The head is small, the body is transparent (**Figure 1**) and laterally compressed, with thin sheets of musculature on either side of the body subdivided into V- or W-shaped myomeres (Smith, 1979, 1989a) and large amounts of gelatinous glycosaminoglycans (GAGs) as an extracellular matrix sandwiched between the sheets of musculature (Miller, 2009). Leptocephali lack hemoglobin, and most species have sparse or no pigmentation (Pfeiler, 1991; Bishop et al., 2000; Miller, 2009). Because the head is small, and therefore the gills as well, and erythrocytes with hemoglobin do not develop until the latter part of metamorphosis, much of the respiration is via cutaneous exchange across the surface of the leaf-shaped body (Pfeiler, 1991). The high surface area to volume ratio allows for gas exchange and also possibly uptake of

FIGURE 1 | A sample of morphological diversity in leptocephalus larvae and a transforming juvenile. Top to bottom: transforming Congridae? juvenile eel, congrid *Rhynchoconger flavus*, unidentified muraenid similar to *Gymnothorax miliaris*, ophichthid *Myrichthys breviceps*, synaphobranchid Ilyophinae sp. D_3 from Straits of Florida, congrid *Ariosoma anale*, chlopsid *Chlopsis bicolor*, and elopid *Elops smithii*. Images are not to scale and are provided to show a sample of the diversity of leptocephalus morphology and pigmentation. All photos by Dante Fenolio.

dissolved organic matter (Pfeiler and Govoni, 1993). Besides uptake of dissolved organic matter, leptocephali are reported to feed on larvacean houses, fecal pellets, marine snow, bacteria, and protists (Mochioka and Iwamizu, 1996; Govoni, 2010; Miller et al., 2013; Liénart et al., 2016).

Understanding larval fishes and their ecology is very important for gaining insights into recruitment for fisheries management (Blaxter, 1984; Sammons and Bettoli, 1998; Valdez-Moreno et al., 2010). Larval fishes can also elucidate regional biodiversity (Limouzy-Paris et al., 1994; Richardson and Cowen, 2004a; Miller et al., 2006, 2016; Miller and McCleave, 2007). Distinctive larvae were recognized as representing cryptic species before the adults were distinguished; for example, Smith (1989b) recognized a unique larva of an unknown *Elops* sp. in the western North Atlantic and McBride et al. (2010) described adults as a new species, *Elops smithi*. However, many distinctive morphotypes are still not linked to the adults of described species.

While many leptocephali are smaller than 10 cm total length (TL), some are large enough to get caught in standard larger-mesh fishing nets. Some anguilliform leptocephali can reach more than 30 cm TL (Miller et al., 2013; Kurogi et al., 2016) and notacanthiform leptocephali from the families Halosauridae and Notocanthidae, in particular, grow to 1.8 m TL (Nielsen and Larsen, 1970). During various trawling expeditions to Bear Seamount, it was not unusual to find leptocephali in the cod end and wrapped around the mesh of the wings of high-speed rope trawls, Yankee 36 bottom trawls, and IGYPT midwater nets (Moore et al., 2003, 2004). Similarly, Miller et al. (2013) compared leptocephali caught with an IKMT vs. a large pelagic trawl. They show that net avoidance does occur given that the larger pelagic trawl caught more species and larger leptocephali than the IKMT. However, the larger pelagic trawl had larger mesh in the cod end and therefore failed to capture smaller leptocephali. Castonguay and McCleave (1987) indicated that net avoidance may be an issue resulting in differential day vs. night catches of at least some leptocephali. They also showed very little vertical migration in most species examined; however, there did appear to be some vertical differences in size classes of particular species. Other investigators have also noted diel vertical migrations in leptocephali on small vertical scales of 50–150 m within the epipelagic and in a few cases the upper mesopelagic zones (Kajihara et al., 1988; Smith, 1989a; Otake et al., 1998; Miller, 2015).

One issue hindering biodiversity studies in low latitude oceanic ecosystems is the difficulty in identification of some leptocephali. Even though leptocephali have a basic body plan with a transparent, compressed, leaf-like body, there is variation in many features that allow for identification to family, genus, or species for many of the elopomorphs in the western Atlantic (**Figures 1**, **2**). Leptocephali of major clades are distinguished based on features such as tail type and presence of pelvic fins (forked tail and pelvic fins in Elopiformes and Albuliformes, long fleshy post-caudal streamer and pelvic fins in Notacanthiformes, terminal pointed or rounded caudal fin with pelvic fins absent in Anguilliformes). Other features that distinguish leptocephali include myomere counts, which correspond with vertebral counts in juveniles and adults (Fahay and Obenchain, 1978; Smith, 1989a; Miller and Tsukamoto, 2004), gut length and swellings or loops in the gut (Fahay, 2007), morphology of the liver along the gut (Leiby, 1989), location of the last vertical blood vessel coming off the posterior most portion of the larval kidney (Castle, 1970), pigmentation patterns (Smith, 1989a; Baldwin, 2013), morphology of teeth (Smith, 1989a), body and body shape (Fahay, 1983; Miller, 2009), and relative positions of the dorsal and anal fin origins (Smith, 1989a).

One difficulty with using these features is that they are often modified or lost during metamorphosis. Many leptocephali undergo transformations that are as profound as the metamorphosis of a tadpole to a frog. This has made it difficult to link the larva with the adult using morphological features. For example, species of the genus *Ariosoma* are distinguished by pigmented lines resembling angled slash marks in the myosepta along the lateral midline and both the dorsal and anal fin origins are positioned very far back, close to the caudal fin. However, before the leptocephali begin other signs of metamorphosis, such as loss of teeth, loss of transparency, and a thickening of the body, *Ariosoma* leptocephali initiating metamorphosis lose the lateral

FIGURE 2 | A sample of morphological diversity in the heads of leptocephalus larvae, showing differences in shape, dentition, pigmentation, eye shape, and rostral projections. Clockwise from top center: halosaurid "Tiluropsis," nettastomatid *Nettenchelys pygnaea*, nettastomatid *Facciolella* sp. C FWNA, synaphobranchid Ilyophinae sp. D_3 FWNA from Straits of Florida, nettastomatid *Saurenchelys stylura* from Straits of Florida, ophichthid *Stictorhinus potamius*, congrid *Xenomystax congroides*, nettastomatid *Facciolella* sp., ophichthid *Ophichthus puncticeps* from Straits of Florida, and congrid *Bathycongrus* sp. A FWNA. All photos by Dante Fenolio.

pigmentation and both median fins begin extending anteriorly. This can result in leptocephali with transitional morphologies that are unlike the typical leptocephalus for that species and yet distinct from juveniles and adults. Individuals caught in the midst of transformation to the juvenile stage can have a mix of features (**Figure 1**, top).

One traditional method for identification of leptocephali relied on growing out specimens to a point past metamorphosis so the morphology of the leptocephalus larva could be linked with the juvenile or adult morphology (Kuroki et al., 2010). Another method was assembling a series of leptocephalus specimens that bridged that same transformation (Castle, 1970). The metamorphosis of leptocephali to juveniles can occur quickly; in several species where this is known, the majority of the metamorphosis occurs over a period of several days to a very few weeks (Ochiai and Nozawa, 1980; Kuroki et al., 2010; Huang et al., 2018). This rapidity of metamorphosis means there are even fewer specimens of individuals caught in the midst of this transformation, making assembling a series of specimens difficult. These methods are even more likely to fail for rare or deep-sea species, where their numbers may be greatly reduced and their duration as epipelagic plankton may be brief or non-existent (some deep-sea eel larva may rarely rise to the epipelagic, for example, *Saccopharynx* spp., *Monognathus* spp., or cyematids; Poulsen et al., 2018).

There are more than 1058 known species of elopomorph fishes worldwide, with the true eels (Anguilliformes) making up the vast majority (1009 species; Fricke et al., 2019). Within the western Central Atlantic (e.g., the Gulf of Mexico, Caribbean Sea, and the adjacent portions of northern South America, Central America, and southern North America) there are 188 described species of elopomorphs recorded (Carpenter, 2002; McBride et al., 2010), and 127 species have been recorded from the Gulf of Mexico (Leiby, 1989; Smith, 1989c,d; McEachran and Fechhelm, 1998; McEachran, 2009). Unfortunately, the distributions of many eel species are not well known because adults may be cryptic, burrowing in soft sediments or living deep in hard structures and therefore difficult to capture. Leptocephali may prove helpful in demonstrating the wider distributions for some of these species. However, there are a number of distinctive leptocephalus larvae known from the Gulf of Mexico that have not yet been linked to a known adult species (Böhlke, 1989b). Table 1 in Miller and McCleave (1994) shows how relatively few research cruises focused on leptocephali were conducted in the Gulf of Mexico from the 1950s to the 1980s.

This paper describes the elopomorph fauna, based on leptocephali collected from the oceanic waters of the northern and eastern Gulf of Mexico following the *Deepwater Horizon* oil spill and subsequent surveys, and further discusses the contribution of these larvae to the overall species richness observed in the offshore Gulf environment.

MATERIALS AND METHODS

Following the *Deepwater Horizon* oil spill, the NOAA Office of Response and Restoration provided support for the creation of the Offshore Nekton Sampling and Analysis Program (ONSAP) to generate biological information on the fauna potentially impacted by the spill (Cook et al., unpublished). The goal of this program was to provide independent data for use during the Natural Resource Damage Assessment (NRDA) process. During ONSAP, the R/V *Pisces* conducted four cruises in the Gulf of Mexico during late 2010 and 2011, with cruises identified as PC8 (Dec 2010), PC9 (Mar–Apr 2011), PC10 (Jun–Jul 2011), and PC12 (Aug–Sep 2011). All sampling on the *Pisces* used a modified Irish Herring/High-Speed Rope Trawl (HSRT). The station grid chosen for sampling aligned with SEAMAP stations, with the designation of station names retained in this study (**Figure 3**; modified from Eldridge, 1988), with stations occurring at every half degree latitude–longitude crossing, stations were approximately 30 nautical miles (nm) apart. Sampling at each station was conducted day and night to capture diel migration dynamics, with deployments centered around solar noon and midnight, respectively. Due to the nature of the *Pisces* modified trawling net, which had no closing mechanism, discrete depth bins were restricted to "shallow" and "deep," with trawls reaching depths between 0–700 and 0–1500 m, respectively.

Additional sampling for ONSAP was conducted in 2011 on the merchant vessel *Meg Skansi*, with the same sampling grid as the *Pisces*, but instead using a 10-m^2 mouth area, 3-mm mesh, 6-net Multiple Opening Closing Net and Environmental Sensing System (MOCNESS) midwater trawl. A flowmeter attached to the frame recorded the volume filtered by each net, and a ship-board

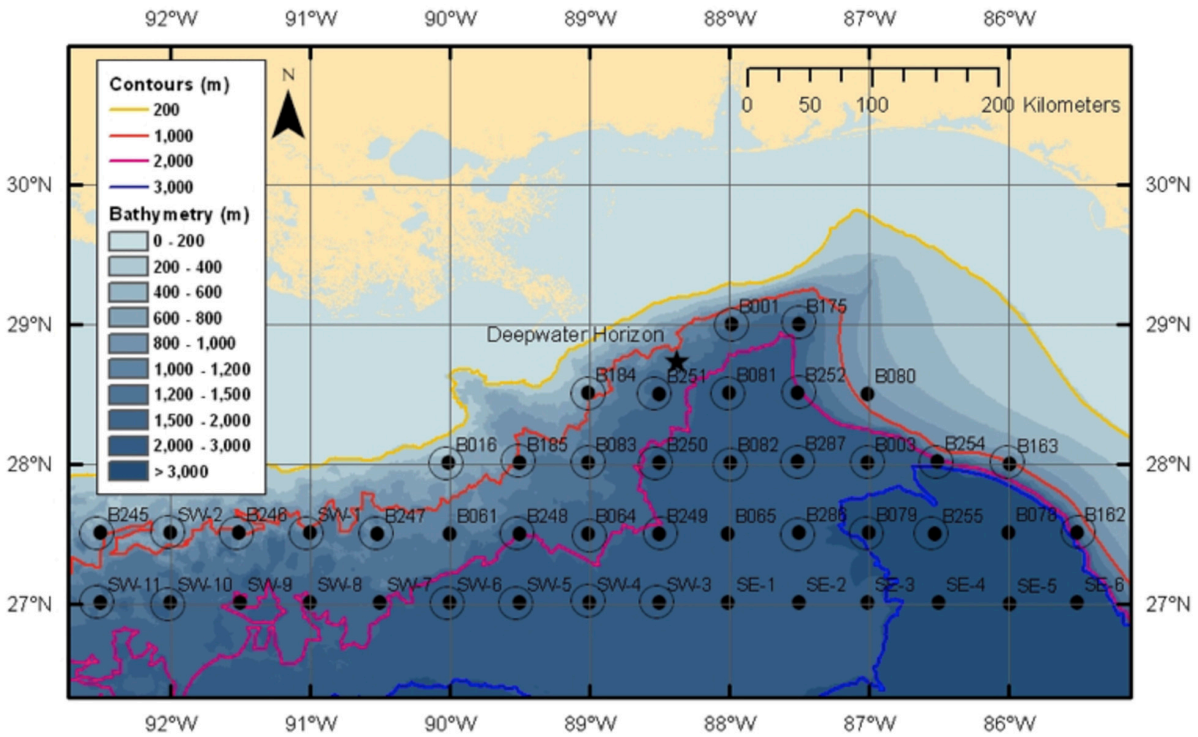

FIGURE 3 | SEAMAP sampling grid used by both ONSAP and DEEPEND cruises (Eldridge, 1988). Note the location of the DWH marked by a star. Yellow line marks the 200 m isobath, orange the 1000 m isobath, pink the 2000 m isobath, and blue the 3000 m isobath.

computer operated the opening and closing of the respective nets based on real-time depth information (see Weibe et al., 1985 for detailed description of unit). The MOCNESS sampling protocol was standardized at all locations: net 0 fished from the surface to the maximum depth (usually 1500 m, bottom depth permitting); net 1 fished from 1500–1200 m depth; net 2 fished from 1200–1000 m; net 3 fished from 1000–600 m; net 4 fished from 600–200 m; and net 5 fished from 200–0 m. The rationale for sampling these depth strata was to characterize the fauna below, within, and above the depth range of a large hydrocarbon plume reported at 1000–1200 m depth (Camilli et al., 2010), as well as to characterize potential trends in the vertical distributions of migrating and non-migrating taxa as reported by Sutton (2013). The M/V *Meg Skansi* trawling surveys were divided into three major cruise series: MS6 (25 Jan–1 Apr 2011), MS7 (19 Apr–30 Jun 2011), and MS8 (18 Jul–30 Sep 2011).

More recently, the Deep Pelagic Nekton Dynamics of the Gulf of Mexico (DEEPEND) consortium continued the MOCNESS time-series of trawl sampling at the same stations on the R/V *Point Sur*. There were six DEEPEND cruises: DP01 (1–8 May 2015), DP02 (8–22 Aug 2015), DP03 (1–16 May 2016), DP04 (5–20 Aug 2016) and DP05 (29 Apr–12 May 2017), and DP06 (18 Jul–2 Aug 2018). While the DEEPEND sampling cruises were shorter than those conducted during the *Meg Skansi* cruises, efforts were made to standardize sampling methodologies. Attention was also given to sampling mesoscale oceanographic features associated with the Loop Current and its eddies, and combined CTD, satellite, and AUV information was collated to inform and define key oceanographic features. More detailed information on the various sampling programs can be found in the paper by Cook et al. (unpublished).

The leptocephali were identified following Böhlke (1989b) and their standard lengths measured to the nearest 0.1 mm using digital calipers. Only distinctive species and morphotypes are included here; damaged leptocephalus specimens, specimens only identifiable to family, transforming juveniles that could not be identified to a species or distinctive morphotype, or juveniles/adults over 2.0 g weight were excluded from the results. Distributional information on elopomorphs used in this study came from Böhlke (1989a,b) and Carpenter (2002), with information on Gulf of Mexico occurrences from McEachran and Fechhelm (1998) and McEachran (2009).

The methodology for the vertical profiles is found in Cook et al. (unpublished). The depth profiles illustrated were calculated from just DEEPEND cruise samples.

The DEEPEND specimens were collected under the Florida Atlantic University IACUC protocols A15-06 and A18-12.

RESULTS

A total of 8989 elopomorph leptocephali were collected, measured, weighed, identified, and included in this study from the research area in the northern Gulf of Mexico (**Table 1**). A total of 118 taxa representing known species or distinctive morphotypes of leptocephali were collected

TABLE 1 | Size range and number of specimens captured for ONSAP (2010–2011, including R/V *Pisces* and M/V *Meg Skansi* cruises) and DEEPEND (2015–2018, all six R/V *Point Sur* cruises) cruises by species or morphotype.

Taxa	SL range (mm)	ONSAP *Pisces*	ONSAP *Meg Skansi*	DEEPEND	Total
Elopomorpha (118 taxa)					
Elopiformes (three taxa)					
Elopidae (two taxa)					
Elops saurus	19	0	1	0	1
Elops smithi	26–32	0	2	1	3
Megalopidae (one taxon)					
Megalops atlanticus	18–25	0	2	2	4
Albuliformes (one taxon)					
Albulidae (one taxon)					
Albula vulpes	30–67	0	2	4	6
Notacanthiformes (seven taxa)					
Halosauridae (seven taxa)					
Aldrovandia sp.	78–320	3	1	0	4
Aldrovandia gracilis	80	0	1	0	1
Aldrovandia oleosa	121	0	0	1	1
Aldrovandia phalacra	100	1	1	0	2
Halosaurus guentheri	126	1	0	0	1
Leptocephalus giganteus	135–377	1	6	1	8
"Tiluropsis"	136–320	4	4	6	14
Anguilliformes (107 taxa)					
Anguillidae (one taxon)					
Anguilla rostrata	30–54	0	28	3	31
Chlopsidae (six taxa)					
Chilorhinus suensonii	17–47	1	19	10	30
Chlopsis bicolor	22–50	0	13	2	15
Chlopsis dentatus	17–45	0	9	2	11
Kaupichthys hyoproroides	9–53	0	30	23	53
Kaupichthys nuchalis	17–45	0	4	4	8
Robinsia catherinae	33–55	0	3	3	6
Congridae (24 taxa)					
Acromycter perturbator	105	0	0	2	2
Ariosoma anale	50–256	36	3	12	51
Ariosoma balearicum	17–217	583	443	255	1281
Ariosoma selenops	62–103	1	0	5	6
Ariosoma sp. FWNA	149	0	1	0	1
Bathycongrus dubius	35–96	0	8	2	10
Bathycongrus sp. A FWNA	28–156	1	1	3	5
Bathycongrus sp. B FWNA	–	0	0	1	1
Bathycongrus sp. C FWNA	46	0	1	0	1
Conger oceanicus	43–92	1	3	5	9
Conger triporiceps	43–90	0	6	0	6
Genus C sp. B FWNA	50–66	0	2	0	2
Gnathophis sp. FWNA	24–102	5	63	53	121
Heteroconger longissimus	15–110	0	11	6	17
Heteroconger luteolus	15–132	5	83	134	222
Parabathymyrus oregoni	135–195	0	1	3	4
Paraconger sp. FWNA	17–110	168	1069	486	1723
Pseudophichthys splendens	19–128	10	12	7	29
Rhynchoconger flavus	15–189	17	697	566	1280
Rhynchoconger gracilior/guppyi FWNA	13–112	1	71	28	100
Uroconger syringinus	24–169	4	62	89	155
Xenomystax congroides	23–229	28	26	21	75

(Continued)

TABLE 1 | Continued

Taxa	SL range (mm)	ONSAP *Pisces*	ONSAP *Meg Skansi*	DEEPEND	Total
Derichthyidae (one taxon)					
Derichchtys serpentinus	127	1	1	0	2
Eurypharyngidae (one taxon)					
Eurypharynx pelecanoides	21–21	0	2	1	3
Moringuidae (three taxa)					
Moringua edwardsi	23–51	0	15	17	32
Neoconger mucronatus	14–46	0	18	1	19
Neoconger sp. FWNA	31	0	1	0	1
Muraenidae (16 taxa)					
Anarchias similis	24–51	0	20	1	21
Channomuraena vittata	55–80	1	1	0	2
Gymnothorax conspersus	51–86	0	4	0	4
Gymnothorax conspersus/kolpos FWNA	83–98	0	2	11	13
Gymnothorax kolpos	46–95	0	2	4	6
Gymnothorax miliaris	20–75	0	7	7	14
Gymnothorax moringa	23–72	2	56	28	86
Gymnothorax nigromarginatus/ocellatus/saxicola FWNA	21–80	8	132	116	256
Gymnothorax sp. 1 JAM	51–85	3	5	6	14
Gymnothorax sp. A FWNA	44–59	0	0	2	2
Gymnothorax sp. B FWNA	53	0	1	0	1
Gymnothorax sp. C FWNA	50–62	0	1	2	3
Gymnothorax sp. D FWNA	46	0	0	1	1
Gymnothorax vicinus	30–82	1	27	12	40
Monopenchelys acuta	44–45	0	2	0	2
Uropterygius macularius	27–57	0	3	4	7
Nemichthyidae (four taxa)					
Avocettina infans	10–180	811	77	96	984
Labichthys carinatus	21–146	1	1	3	5
Nemichthys curvirostris	29–325	252	56	72	380
Nemichthys scolopaceus	180–273	58	3	0	61
Nettastomatidae (nine taxa)					
Facciolella sp. B FWNA	55–105	0	3	6	9
Facciolella sp. C FWNA	78–99	0	2	3	5
Hoplunnis diomedianus	30	1	1	0	2
Hoplunnis macrura	21–107	1	219	155	375
Hoplunnis similis	65–99	0	1	1	2
Hoplunnis sp. C FWNA	78	0	1	0	1
Hoplunnis tenuis	11–150	4	169	112	285
Nettastoma melanura	17–74	0	14	2	16
Nettenchelys pygmaea	19–88	2	53	67	122
Ophichthidae (32 taxa)					
Ahlia egmontis	33–91	0	62	21	83
Aplatophis chauliodus	25–59	0	6	3	9
Aprognathodon platyventris	–	0	0	1	1
Apterichthus kendalli	69	1	0	0	1
Bascanichthyini sp. FWNA	20	0	1	0	1
Bascanichthys bascanium	26–91	0	2	16	18
Bascanichthys scuticaris	68	0	0	1	1
Callechelyini sp. FWNA	87	0	0	1	1
Callechelys guineensis	27	0	1	0	1
Callechelys muraena	31–71	0	15	5	20
Echiophis punctifer	17–61	0	2	0	2

(Continued)

TABLE 1 | Continued

Taxa	SL range (mm)	ONSAP *Pisces*	ONSAP *Meg Skansi*	DEEPEND	Total
Gordiichthys irretitus	64–69	0	0	2	2
Gordiichthys randalli	52–101	0	2	9	11
Letharchus aliculatus	42–115	1	3	2	6
Letharchus velifer	24–49	0	1	1	2
Myrichthys breviceps	77–125	2	4	7	13
Myrichthys ocellatus	118	0	0	1	1
Myrophis platyrhynchus	44–68	0	5	8	13
Myrophis punctatus	13–107	0	250	27	277
Ophichthini sp. 1 FWNA	19–68	0	2	1	3
Ophichthini sp. 2 FWNA	23–60	1	6	0	7
Ophichthini sp. 3 FWNA	55	1	0	0	1
Ophichthini sp. 5 FWNA	71	0	1	0	1
Ophichthini sp. 7 FWNA	53–89	0	2	10	12
Ophichthus gomesii	23–102	76	137	84	297
Ophichthus melanoporus	32–105	0	2	1	3
Ophichthus puncticeps	74	0	1	0	1
Ophichthus rex	39–55	0	0	5	5
Pseudomyrophis frio	44–79	0	1	1	2
Pseudomyrophis fugesae	52–62	0	2	2	4
Quassiremus ascensionis	28–69	0	2	0	2
Stictorhinus potamius	100	0	0	1	1
Serrivomeridae (one taxon)					
Serrivomer beanii	34–89	3	0	0	3
Synaphobranchidae (eight taxa)					
Dysomma anguillare	22–59	0	57	31	88
Dysommina proboscideus	26–78	0	3	0	3
Ilyophinae sp. A_5 FWNA	99	0	1	0	1
Ilyophinae sp. B_5 FWNA	33	0	1	0	1
Ilyophinae sp. C_1 FWNA	38–49	0	3	0	3
Ilyophinae sp. D_4 FWNA	63	0	0	1	1
Synaphobranchus oregoni	89–93	0	3	0	3
Synaphobranchus sp. FWNA	83–96	0	2	0	2
Unknown family (two taxa)					
Type I sp. B FWNA	19–53	0	3	0	3
Type II FWNA	56	0	1	0	1
Totals		2104	4173	2712	8989

The list includes transforming juveniles. FWNA indicates a specific morphotype described in Böhlke (1989b).

by the ONSAP and DEEPEND projects. Of those 118 taxa, leptocephali of 83 are currently recognized as larvae or transforming juveniles of established species. Roughly half of the taxa collected were rare, represented by four or fewer individuals. Several leptocephalus larval morphotypes represent multiple species (*Paraconger* sp., *Gnathophis* sp., *Rhynchoconger gracilior/guppyi*, *Gymnothorax conspersus/kolpos*, *Gymnothorax ocellatus/nigromarginatus/saxicola*) because features of the leptocephalus morphology overlap or are indistinguishable between the species. This study also found one new morphotype that is distinctive from those already known.

That new morphotype, here designated as *Gymnothorax* sp. 1 JAM (**Figure 4**), has a leptocephalus very similar to that of *Gymnothorax vicinus*, in that the dorsal fin origin is at midbody and there is an interrupted line of pigment spots on the ventral midline of the esophagus; however, this new morphotype has 153–169 total myomeres (131–142 in *G. vicinus*, Smith, 1989e), 95–105 preanal myomeres (60–68 in *G. vicinus*), 42–59 predorsal myomeres (53–63 in *G. vicinus*), and a last vertical blood vessel at 86–92 myomeres (60–67 in *G. vicinus*). There are no lateral pigments, no band of pigments through the eye, and very few melanophores over the brain, one melanophore lateral to the heart, and three to five at the base of the pectoral fin bud.

Leptocephali account for 13% of the total species richness of fishes collected in the ONSAP and DEEPEND projects (Cook and Sutton, 2018a,b,c; Sutton et al., 2018a,b; Cook and Sutton, 2019). Leptocephali of the families Congridae (5600 specimens), Nemichthyidae (1430), Nettastomatidae (819), Ophichthidae (800), and Muraenidae (473) were especially abundant in the northern Gulf of Mexico. The most abundant

FIGURE 4 | Muraenidae leptocephalus morphotype *Gymnothorax* sp.1 JAM. Collected 11 May 2017 at station B175D in the 0–200 m stratum. Specimen was 51 mm SL. Photo by Dante Fenolio.

species were *Paraconger* sp. (1698 individuals), *Ariosoma balearicum* (1281), *Rhynchoconger flavus* (1280), *Avocettina infans* (984), *Nemichthys curvirostris* (380), *Hoplunnis macrura* (375), *Ophichthus gomesii* (297), *Hoplunnis tenuis* (285), and *Myrophis punctatus* (277).

A number of the leptocephali identifiable to established species represent new records for the Gulf of Mexico based on the complete list of fishes in McEachran (2009) and chapters in Böhlke (1989a,b). Taxa that represent new records of occurrence for the Gulf of Mexico include: *Dysommina proboscideus*, *Quassiremus ascensionis*, *Derichchtys serpentinus*, *Hoplunnis similis*, and *Serrivomer beanii*. Several other taxa were not reported in either McEachran and Fechhelm (1998) or McEachran (2009), but were listed as leptocephali occurring in the Gulf of Mexico by Leiby (1989) and Smith (1989c) (e.g., *Chilorhinus suensoni*, *Chlopsis bicolor*, *Chlopsis dentatus*, *Kaupichthys hyoproroides*, *Robinsia catherinae*, *Gordiichthys randalli*, *Pseudomyrophis frio*, *Pseudomyrophis fugesae*, and *Stictorhinus potamius*).

There is some evidence for net avoidance in certain taxa, as determined by higher catches at night for species found almost exclusively in the epipelagic (**Figure 5**). For example, abundance estimates of *Gnathophis* sp. were almost four times greater at night than during the day. Likewise, *Heteroconger luteolus* leptocephali were collected in more than seven times greater abundance at night. Other taxa seemed to show little difference in day vs. night catch rates (**Figure 6**), which may indicate less ability to swim out of the way of the net. Those species that show net avoidance had firmer, more muscular leptocephali when freshly caught, compared to other taxa, such as most muraenids, which had flimsier bodies when fresh out of the net. Species caught in the high-speed rope trawl, but not in slower MOCNESS nets may also reflect taxa that are capable of net avoidance. *Hoplunnis tenuis*, *Ahlia egmontis*, and some other taxa showed evidence of diel vertical migration (**Figure 7**). Not all leptocephali were confined to the epipelagic; some were found in moderate abundances in the 200–600 m depth stratum and some species were collected as deep as 1500 m. A few species, particularly members of the Synaphobranchidae, spanned the water column, down to bathypelagic depths (**Figure 8**). These deep specimens were often still in the larval stage (not metamorphosing juveniles in the process of settling out).

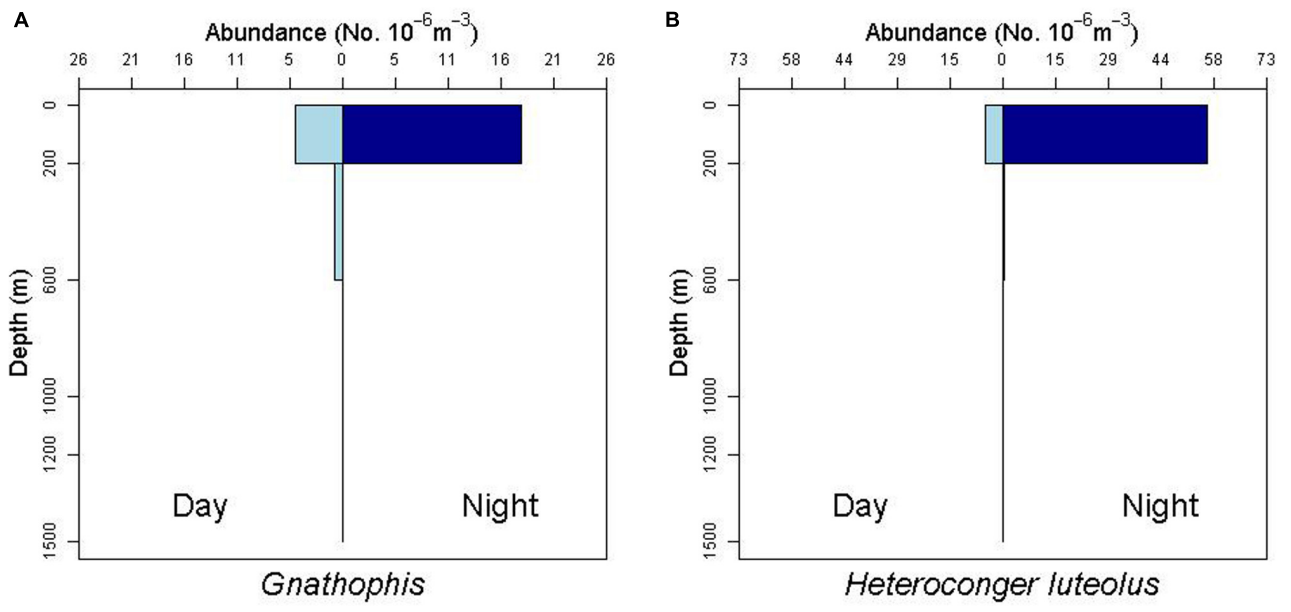

FIGURE 5 | Depth profiles for the congrid leptocephalus morphotype *Gnathophis* sp. and the congrid species *Heterconger luteolus*. Note the greater abundances at night in the surface stratum (0–200 m) as an indication of possible net avoidance by these taxa during the day.

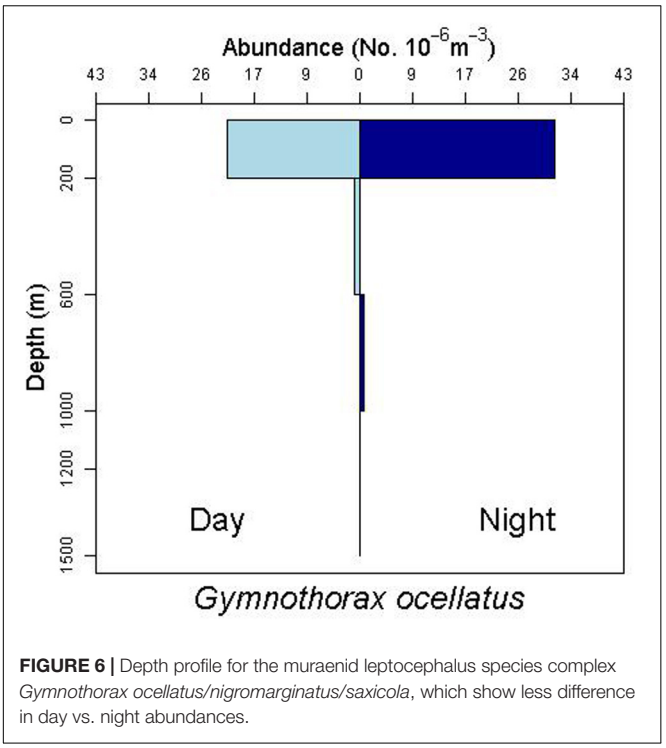

FIGURE 6 | Depth profile for the muraenid leptocephalus species complex *Gymnothorax ocellatus/nigromarginatus/saxicola*, which show less difference in day vs. night abundances.

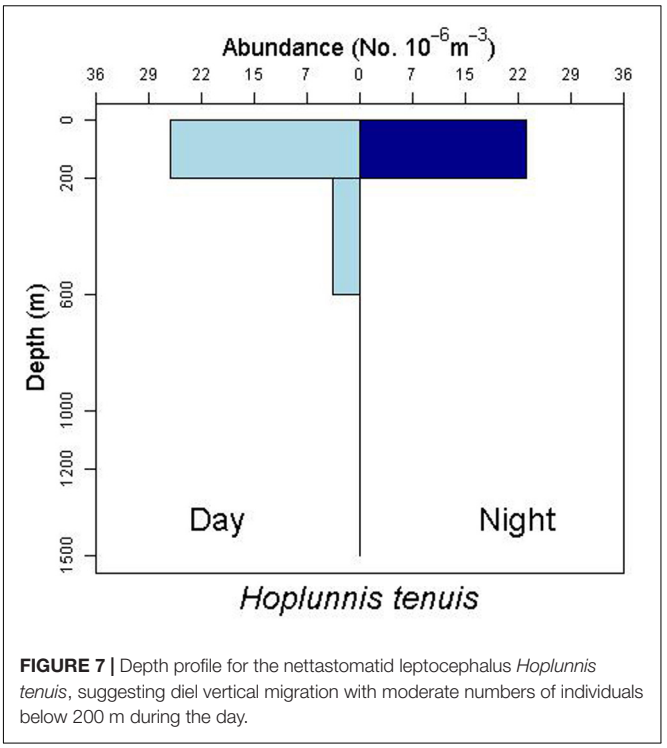

FIGURE 7 | Depth profile for the nettastomatid leptocephalus *Hoplunnis tenuis*, suggesting diel vertical migration with moderate numbers of individuals below 200 m during the day.

DISCUSSION

Given that the number of leptocephali species and morphotypes collected in the oceanic Gulf of Mexico is close to the number of adult species known from the Gulf (McEachran, 2009), leptocephali can serve as an important indicator of eel biodiversity and represent potential distributional range extensions and undiscovered species. Any ichthyofaunal biodiversity survey that does not include an analysis of leptocephali runs the risk of greatly undercounting the species richness in a given region. However, it should be acknowledged that capture of a larval species is not unequivocal evidence that the adults also occur in the Gulf of Mexico. Richardson and Cowen (2004b) stated that knowledge of both adult and larval diversity is necessary to understand the full species richness of some eel groups, such as the family Ophichthidae. Unfortunately, leptocephali are often lumped into a common "leptocephalus" category in ichthyoplankton surveys, and are also frequently omitted or minimally included in identification guides to larval fishes (Richards et al., 1993; Leis and Carson-Ewart, 2000; Richards, 2005; Lyczkowski-Shultz et al., 2013). The latter is another reason that leptocephali are "hiding in plain sight"; if students do not see them in guides and surveys, elopomorph larvae will be further overlooked.

In this study, distinctive leptocephali account for 13% of the overall species richness found in the pelagic realm of the northern and eastern Gulf of Mexico by the ONSAP and DEEPEND investigations. It is likely that some larval morphotypes will eventually be linked to adult specimens of already-known species, but in some cases, distinctive larvae could also point to undiscovered species, as was the case with *E. smithi* (McBride et al., 2010).

Comparing our results with those of previous investigations from other areas in the low-latitude western North Atlantic, three things become clear. First, the sampling gear used makes a big difference in results (Habtes et al., 2014). Our use of a highspeed rope trawl on the R/V *Pisces* added several large specimens and examples of faster swimming species not collected in our MOCNESS cruises. Limouzy-Paris et al. (1994) sampled with a 1-m^2 mouth MOCNESS system for a series of trawls in the Florida Straits. Their leptocephalus diversity represents a smaller subset of what we found, and this may reflect the smaller MOCNESS gear with resulting greater net avoidance, compared to our study. Of the 28 species of elopomorphs listed in their table, our study collected 25 of those (89%). The species (Limouzy-Paris et al., 1994) captured at the greatest number of stations correspond with many of our most abundant species. Second, differences in the eel fauna in different studies also reflect smaller scale faunal differences within the tropical/subtropical western North Atlantic. Leptocephali collected from the West Florida shelf break near our sampling area shared 18 out of 21 species (86%) with our study (Crabtree et al., 1992). Miller and McCleave (2007) studied leptocephali in the Sargasso Sea and found at least 61 taxa, of those 44 (72%) were also in our collections. Interestingly, many of the dominant taxa in our study (*Paraconger* sp., *R. flavus*, *A. infans*, *H. macrura*, *N. curvirostris*) are relatively minor in abundance or completely absent from Miller and McCleave's study. They also found several taxa not represented in our collections (e.g., *Conger escuelentus*, *Mixomyrophis pusillapinna*, *Ichthyapus ophioneus*).

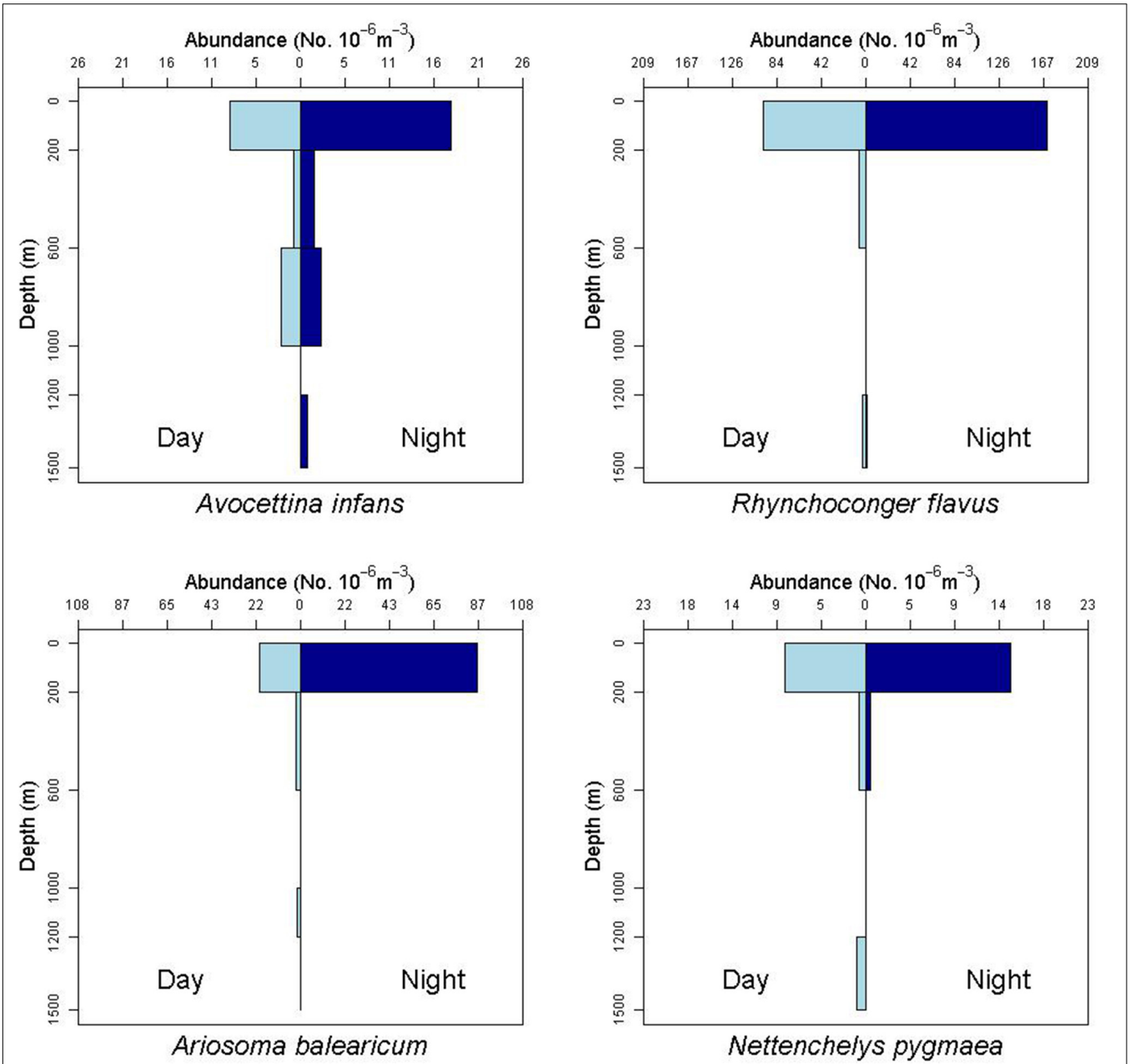

FIGURE 8 | Depth profile of the leptocephalus for the nemichthyid species *Avocettina infans*, showing a distribution down to 1500 m depth and possible net avoidance at the surface. The profile of the congrid leptocephalus of *Rhynchoconger flavus* also shows captures at 1200–1500 m. The profile of the congrid *Ariosoma balearicum* shows captures down to 1200 m during the day. The profile for the synaphobranchid species *Nettenchelys pygmaea* also shows daytime captures down to 1500 m.

Richardson and Cowen (2004a) examined leptocephalus diversity around Barbados where they found 68 taxa, and 49 of those (72% of their taxa) were also collected in our study. The taxa unique to their study were either newly described by them (Richardson and Cowen, 2004b) and not found in our collections or taxa known from the southeastern Caribbean. Third, several leptocephalus larvae are very rare and only collected in studies with larger sample sizes. Our study shared many rare species/morphotypes (for example, Ophichthini sp.1, *Gymnothorax* sp. A and sp. C, *Aprognathodon platyventris*, and *Ophichthus puncticeps*) with that of Richardson and Cowen (2004a), who examined over 4500 specimens. To our knowledge, several of the morphotypes we report here have not been listed in the literature since Böhlke (1989b), such as Type I sp. B, Type II, Ilyophinae sp. A_5, *Facciolella* sp. B, congrid Genus C sp. B, and Ophichthini sp. 5.

While Richards et al. (1993) did not explicitly identify many species of leptocephali in their study, instead grouping them as "leptocephali," they did point out that the reason for the high diversity of larval fishes associated with the Loop Current in the northern Gulf of Mexico was due to mixing of tropical and warm temperate oceanic, mesopelagic, coastal demersal, and pelagic species in the region. This appears to explain the high species richness we found in our study, although we would also add bathypelagic and deep-demersal taxa to the faunal components mixed in this region.

Leptocephali show diel vertical migration in some species (Castonguay and McCleave, 1987; Kajihara et al., 1988; Otake et al., 1998; Miller, 2015). Most studies of vertical migration in leptocephali subdivide the upper 200 m of water into several distinct strata. Our collection methods integrated the entire epipelagic stratum into one net, so we were not able to discern finer-scale diel migration within that zone. However, we do have evidence of larger scale migrations, where some species move from the upper mesopelagic (200–600 m) during daytime to the epipelagic at night (**Figure 7**, see also *Gnathophis* sp. in **Figure 5**, and *R. flavus* and *A. balearicum* in **Figure 8**).

A number of leptocephali were collected in deep-water strata. For example, specimens of *A. infans*, *R. flavus*, and *A. balearicum* were found in reduced abundances below the epipelagic zone (**Figure 8**), but throughout the sampled water column to 1500 m and possibly deeper. All of the relatively rare *Synaphobranchus oregoni* and *Synaphobranchus* sp. specimens came from the 600–1200 m strata. The rarity of some leptocephalus types may be an indication that these larvae do not generally come to the surface. For example, halosaurs are ubiquitous and relatively abundant demersal fishes on the continental slope to abyssal plains, but their larvae ("Tiluropsis" and *Leptocephalus giganteus*) are very rarely captured, indicating that they most likely stay in the deeper layers. *Leptocephalus giganteus* was only collected in the MOCNESS from nets fished between 1000–1200, 600–1000, and 200–600 m depth. Leptocephali remaining at depth may help explain the absence in this study of larvae of *Saccopharynx* and *Monognathus*, and the absence or rarity of other bathypelagic species (Poulsen et al., 2018).

DATA AVAILABILITY STATEMENT

The datasets generated for this study can be found in the Gulf of Mexico Research Initiative Information and Data Cooperative (GRIIDC) at https://data.gulfresearchinitiative.org (doi:10.7266/N7R49NTN, 10.7266/N7VX0DK2, 10.7266/N70P03T, 10.7266/N7XP7385, 10.7266/N7902234, and 10.7266/n7-ac8e-0240.

ETHICS STATEMENT

The animal study was reviewed and approved by the Florida Atlantic University IACUC Committee.

AUTHOR CONTRIBUTIONS

TS and JM conceptualized the study. JM, DF, AC, and TS participated in the research cruises and collected samples. JM identified the specimens. DF took the photographic images. AC managed the specimen database and analyzed the vertical distribution data. JM wrote the manuscript with contributions from DF, AC, and TS.

FUNDING

This research was funded in part by the NOAA Office of Response and Restoration and in part by a grant from The Gulf of Mexico Research Initiative (GoMRI).

ACKNOWLEDGMENTS

We thank the captains, crews, and other scientists who participated in the cruises of the R/V *Pisces*, M/V *Meg Skansi*, and R/V *Point Sur* for their assistance in collecting the leptocephalus specimens. Our heartfelt appreciation goes particularly to David Smith for his longstanding and comprehensive work on Atlantic leptocephalus larvae and their identification. Thanks also go to Rich Jones for his help in identifying some leptocephali in this study. Finally, we strongly value the feedback from four reviewers who helped improve this manuscript. The data are publicly available through the Gulf of Mexico Research Initiative Information and Data Cooperative (GRIIDC) at https://data.gulfresearchinitiative.org (doi:10.7266/N7R49NTN, 10.7266/N7VX0DK2, 10.7266/N70P03T, 10.7266/N7XP7385, 10.7266/N7902234, and 10.7266/n7-ac8e-0240).

REFERENCES

Arratia, G. (1999). "The monophyly of teleostei and stem-group teleosts," in *Mesozoic Fishes 2, Systematics and Fossil Record*, eds G. Arratia and H.-P. Schultze (Munich: Verlag Dr. Friedrich Pfeil), 265–334.

Baldwin, C. C. (2013). The phylogenetic significance of colour patterns in marine teleost larvae. *Zool. J. Linn. Soc.* 168, 496–563. doi: 10.1111/zoj.12033

Bishop, R. E., Torres, J. J., and Crabtree, R. E. (2000). Chemical composition and growth indices in leptocephalus larvae. *Mar. Biol.* 137, 205–214. doi: 10.1007/s002270000362

Blaxter, J.H.S. (1984). "Ontogeny, systematics and fisheries," in *Ontogeny and Systematics of Fishes*, eds H.G. Moser, W.J. Richards, D.M. Cohen, M.P. Fahay, A.W. Kendall, S.L. Richardson, Vol. 1 (ASIH Spec. Publ.), 1–6.

Böhlke, E. B. (eds.) (1989a). Fishes of the Western North Atlantic: Anguilliformes and Saccopharyngiformes. *Mem. Sears Found. Mar. Res.* 9, 1–655.

Böhlke, E. B. (eds.) (1989b). Fishes of the Western North Atlantic: Leptocephali. *Mem. Sears Found. Mar. Res.* 2, 656–1055.

Camilli, R., Reddy, C. M., Yoerger, D. R., Van Moov, B. A., Jakuba, M. V., Kinsey, J. C., et al. (2010). Tracking hydrocarbon plume transport and biodegradation at Deepwater Horizon. *Science* 330, 201–204. doi: 10.1126/science.1195223

Carpenter, K. E. (eds.) (2002). *The Living Marine Resources of the Western Central Atlantic: Bony Fishes Part 1 (Acipenseridae to Grammatidae)*, Vol. 2. Rome: Food and Agriculture Organization of the United Nations.

Castle, P. H. J. (1970). Distribution, larval growth, and metamorphosis of the eel *Derichthys serpentinus* Gill, 1884 (Pisces: Derichthyidae). *Copeia* 1970, 444–452.

Castonguay, M., and McCleave, J. D. (1987). Vertical distributions, diel and ontogenetic vertical migrations and net avoidance of leptocephali of *Anguilla* and other common species in the Sargasso Sea. *J. Plankton Res.* 9, 195–214. doi: 10.1093/plankt/9.1.195

Cook, A., and Sutton, T. T. (2018a). *Inventory of Gulf oceanic Fauna Data Including Species, Weight, and Measurements. Cruises DP01 May 1-8, 2015 and DP02 August 9-21, 2015 R/V on the Point Sur in the Northern Gulf of Mexico (Distributed by: Gulf of Mexico Research Initiative Information and Data Cooperative (GRIIDC))*. Corpus Christi, TX: Harte Research Institute, Texas A&M University, doi: 10.7266/N70P0X3T

Cook, A., and Sutton, T. T. (2018b). *Inventory of Gulf of Mexico Oceanic Fauna data Including Species, Weight, and Measurements from R/V Point Sur (Cruises DP03 and DP04) May-August, 2016. Distributed by: Gulf of Mexico Research Initiative Information and Data Cooperative (GRIIDC)*. Harte Research Institute, Texas A&M University: Corpus Christi, doi: 10.7266/N7XP7385

Cook, A., and Sutton, T. T. (2018c). *Inventory of Oceanic Fauna Data Including Species, Weight, and Measurements from R/V Point Sur (Cruise DP05) in the Gulf of Mexico from 2017-05-01 to 2017-05-11. Distributed by: Gulf of Mexico Research Initiative Information and Data Cooperative (GRIIDC)*. Corpus Christi, TX: Harte Research Institute, Texas A&M University, doi: 10.7266/N7902234

Cook, A., and Sutton, T. T. (2019). *Inventory of Oceanic Fauna Data Including Species, Weight, and Measurements from R/V Point Sur cruise PS19-04 (DP06) in the Gulf of Mexico from 2018-07-19 to 2018-08-01. Distributed by: Gulf of Mexico Research Initiative Information and Data Cooperative (GRIIDC)*. Corpus Christi: Harte Research Institute, Texas A&M University. doi: 10.7266/n7-ac8e-0240

Crabtree, R. E., Cyr, E. C., Bishop, R. E., Falkenstein, L. M., and Dean, J. M. (1992). Age and growth of tarpon, *Megalops atlanticus*, larvae in the eastern Gulf of Mexico, with notes on relative abundance and probable spawning areas. *Environ. Biol. Fishes* 35, 361–370. doi: 10.1007/bf00004988

Dornburg, A., Friedman, M., and Near, T. J. (2015). Phylogenetic analysis of molecular and morphological data highlights uncertainty in the relationships of fossil and living species of Elopomorpha (Actinopterygii: Teleostei). *Mol. Phylog. Evol.* 89, 205–218. doi: 10.1016/j.ympev.2015.04.004

Eldridge, P. J. (1988). The southeast area monitoring and assessment program (SEAMAP): a state federal university program for collection, management, and dissemination of fishery independent data and information in the southeastern United States. *Mar. Fish. Rev.* 50, 29–39.

Fahay, M. P. (1983). Guide to the early stages of marine fishes occurring in the western North Atlantic Ocean, Cape Hatteras to the southern Scotian Shelf. *J. Northwest Atl. Fish. Sci.* 4, 1–1992.

Fahay, M. P. (2007). *Early Stages of Fishes in the Western North Atlantic Ocean:(Davis Strait, Southern Greenland and Flemish Cap to Cape Hatteras)*. Dartmouth: Northwest Atlantic Fisheries Organization.

Fahay, M. P., and Obenchain, C. L. (1978). Leptocephali of the ophichthid genera ahlia, myrophis, ophichthus, pisodonophis, callechelys, letharchus, and apterichtus on the atlantic continental shelf of the United States. *Bull. Mar. Sci.* 28, 442–486.

Forey, P. L. (1973). A revision of the Elopiformes fishes, fossil and recent. *Bull. Br. Mus. Nat. Hist. (Geol.)* 10, 1–222.

Fricke, R., Eschmeyer, W. N., and Fong, J. D. (2019). *Eschmeyer's Catalog of Fishes, Species by Family/Subfamily (Last Updated 1 July 2019)*. Available at http://researcharchive.calacademy.org/research/ichthyology/catalog/SpeciesByFamily.asp.

Govoni, J. J. (2010). Feeding on protists and particulates by the leptocephali of the worm eels *Myrophis* spp. (Teleostei: Anguilliformes: Ophichthidae), and the potential energy contribution of large aloricate protozoa. *Sci. Mar.* 74, 339–344. doi: 10.3989/scimar.2010.74n2339

Greenwood, P. H., Rosen, D. E., Weitzman, S. H., and Myers, G. S. (1966). Phyletic studies of teleostean fishes, with a provisional classification of living forms. *Bull. Am. Mus. Nat. Hist.* 131, 341–455.

Habtes, S., Muller-Karger, F. E., Roffer, M. A., Lamkin, J. T., and Muhling, B. A. (2014). A comparison of sampling methods for larvae of medium and large epipelagic fish species during spring SEAMAP ichthyoplankton surveys in the Gulf of Mexico. *Limnol. Oceanogr. Methods* 12, 86–101. doi: 10.4319/lom.2014.12.86

Huang, W. C., Chang, J. T., Liao, C., Tawa, A., Iizuka, Y., Liao, T. Y., et al. (2018). Pelagic larval duration, growth rate, and population genetic structure of the tidepool snake moray *Uropterygius micropterus* around the southern Ryukyu Islands, Taiwan, and the central Philippines. *PeerJ* 6:e4741. doi: 10.7717/peerj.4741

Hulet, W. H. (1978). Structure and functional development of the eel leptocephalus *Ariosoma balearicum* (De La Roche, 1809). *Philos. Trans. Roy. Soc. Lond. B Biol. Sci.* 282, 107–138. doi: 10.1098/rstb.1978.0010

Kajihara, T., Tsukamoto, K., Otake, T., Mochioka, N., Hasumoto, H., Oya, M., et al. (1988). Sampling leptocephali with reference to the diel vertical migration and the gears. *Nippon Suisan Gakkaishi* 54, 941–946. doi: 10.2331/suisan.54.941

Kurogi, H., Chow, S., Yanagimoto, T., Konishi, K., Nakamichi, R., Sakai, K., et al. (2016). Adult form of a giant anguilliform leptocephalus *Thalassenchelys coheni* Castle and Raju 1975 is *Congriscus megastomus* (Günther 1877). *Ichthyol. Res.* 63, 239–246. doi: 10.1007/s10228-015-0492-5

Kuroki, M., Fukuda, N., Yamada, Y., Okamura, A., and Tsukamoto, K. (2010). Morphological changes and otolith growth during metamorphosis of Japanese eel leptocephali in captivity. *Coast. Mar. Sci.* 34, 31–38.

Leiby, M. M. (1989). Family Ophichthidae. *Mem. Sears. Found. Mar. Res.* 9, 764–897. doi: 10.2307/j.ctvbcd0jj.10

Leis, J. M., and Carson-Ewart, B. M. (eds.) (2000). *The Larvae of Indo-Pacific Coastal Fishes: An Identification Guide to Marine Fish Larvae*. Leiden: Brill.

Liénart, C., Feunteun, E., Miller, M. J., Aoyama, J., Mortillaro, J. M., Hubas, C., et al. (2016). Geographic variation in stable isotopic and fatty acid composition of anguilliform leptocephali and particulate organic matter in the South Pacific. *Mar. Ecol. Prog. Ser.* 544, 225–241. doi: 10.3354/meps11575

Limouzy-Paris, C., McGowan, M. F., Richards, W. J., Umaran, J. P., and Cha, S. S. (1994). Diversity of fish larvae in the Florida Keys: results from SEFCAR. *Bull. Mar. Sci.* 54, 857–870.

Lyczkowski-Shultz, J., Hanisko, D. S., Sulak, K. J., Konieczna, M., and Bond, P. J. (2013). Characterization of ichthyoplankton in the northeastern Gulf of Mexico from SEAMAP plankton surveys, 1982-1999. *Gulf Carib. Res.* 25, 43–98.

McBride, R. S., Rocha, C. R., Ruiz-Carus, R., and Bowen, B. W. (2010). A new species of ladyfish, of the genus *Elops* (Elopiformes: Elopidae), from the western Atlantic Ocean. *Zootaxa* 2346, 29–41.

McEachran, J. D., and Fechhelm, J. D. (1998). *Fishes of the Gulf of Mexico*. Vol. 1. Austin, TX: University of Texas Press.

McEachran, J. D. (2009). "Fishes (Vertebrata: Pisces) of the Gulf of Mexico," in *Gulf of Mexico Origins, Waters, and Biota. Biodiversity*, eds D. L. Felder and D. K. Camp (College Station, TX: Texas A&M Press), 1223–1316.

Miller, M. J. (2009). Ecology of anguilliform leptocephali: remarkable transparent fish larvae of the ocean surface layer. *Aqua-BioSci. Monogr.* 2, 1–94.

Miller, M. J. (2015). Nighttime vertical distribution and regional species composition of eel larvae in the western Sargasso Sea. *Region. Stud. Mar. Sci.* 1, 34–46. doi: 10.1016/j.rsma.2015.03.003

Miller, M. J., Aoyama, J., Mochioka, N., Otake, T., Castle, P. H., Minagawa, G., et al. (2006). Geographic variation in the assemblages of leptocephali in the western South Pacific. *Deep Sea Res. Part I: Oceanogr. Res. Pap.* 53, 776–794. doi: 10.1016/j.dsr.2006.01.008

Miller, M. J., Chikaraishi, Y., Ogawa, N. O., Yamada, Y., Tsukamoto, K., and Ohkouchi, N. (2013). A low trophic position of Japanese eel larvae indicates feeding on marine snow. *Biol. Lett.* 9:20120826. doi: 10.1098/rsbl.2012.0826

Miller, M. J., and McCleave, J. D. (1994). Species assemblages of leptocephali in the subtropical convergence zone of the Sargasso Sea. *J. Mar. Res.* 52, 743–772. doi: 10.1357/0022240943076948

Miller, M. J., and McCleave, J. D. (2007). Species assemblages of leptocephali in the southwestern Sargasso Sea. *Mar. Ecol. Prog. Series* 344, 197–212. doi: 10.3354/meps06923

Miller, M. J., Wouthuyzen, S., Sugeha, H. Y., Kuroki, M., Tawa, A., Watanabe, S., et al. (2016). High biodiversity of leptocephali in Tomini Bay Indonesia in the center of the Coral Triangle. *Reg. Stud. Mar. Sci.* 8, 99–113. doi: 10.1016/j.rsma.2016.09.006

Miller, M. J., and Tsukamoto, K. (2004). *An Introduction to Leptocephali: Biology and Identification*, 1st Edn. Tokyo: Ocean Research Institute, University of Tokyo.

Mochioka, N., and Iwamizu, M. (1996). Diet of anguilloid larvae: leptocephali feed selectively on larvacean houses and fecal pellets. *Mar. Biol.* 125, 447–452.

Moore, J. A., Vecchione, M., Collette, B. B., Gibbons, R., and Hartel, K. E. (2004). Selected fauna of Bear Seamount (New England Seamount chain), and the presence of "natural invader" species. *Arch. Fish. Mar. Res.* 51, 241–250.

Moore, J. A., Vecchione, M., Collette, B. B., Gibbons, R., Hartel, K. E., Galbraith, J. K., et al. (2003). Biodiversity of Bear Seamount, New England seamount chain: results of exploratory trawling. *J. Northwest Atl. Fish. Sci.* 31, 363–372. doi: 10.2960/j.v31.a28

Nielsen, J. G., and Larsen, V. (1970). Remarks on the identity of the giant Dana eel-larva. *Vidensk. Medd. Dan. Naturhist. Foren. Kbh.* 133, 149–157.

Ochiai, A., and Nozawa, Y. (1980). On the metamorphosis and burrowing habits of the snake eel, *Muraenichthys gymnotus*. *Jpn. J. Ichthyol.* 27, 237–242.

Otake, T., Inagaki, T., Hasumoto, H., Mochioka, N., and Tsukamoto, K. (1998). Diel vertical distribution of *Anguilla japonica* leptocephali. *Ichthyol. Res.* 45, 208–211. doi: 10.1007/bf02678565

Pfeiler, E. (1986). Towards an explanation of the developmental strategy in leptocephalous larvae of marine teleost fishes. *Environ. Biol. Fish.* 15, 3–13. doi: 10.1007/bf00005385

Pfeiler, E. (1991). Glycosaminoglycan composition of anguilliform and elopiform leptocephali. *J. Fish Biol.* 38, 533–540. doi: 10.1111/j.1095-8649.1991.tb03140.x

Pfeiler, E., and Govoni, J. J. (1993). Metabolic rates in early life history stages of elopomorph fishes. *Biol. Bull.* 185, 277–283. doi: 10.2307/1542007

Poulsen, J. Y., Miller, M. J., Sado, T., Hanel, R., Tsukamoto, K., and Miya, M. (2018). Resolving deep-sea pelagic saccopharyngiform eel mysteries: identification of Neocyema and Monognathidae leptocephali and establishment of a new fish family "Neocyematidae" based on larvae, adults and mitogenomic gene orders. *PLoS ONE* 13:e0199982. doi: 10.1371/journal.pone.0199982

Richards, W. J., McGowan, M. F., Leming, T., Lamkin, J. T., and Kelley, S. (1993). Larval fish assemblages at the Loop Current boundary in the Gulf of Mexico. *Bull. Mar. Sci.* 53, 475–537.

Richards, W. J. (eds) (2005). *Early Stages of Atlantic Fishes: An Identification Guide for the Western Central North Atlantic, Two Volume Set*. Boca Raton, FL: CRC Press.

Richardson, D. E., and Cowen, R. K. (2004a). Diversity of leptocephalus larvae around the island of Barbados (West Indies): relevance to regional distributions. *Mar. Ecol. Prog. Ser.* 282, 271–284. doi: 10.3354/meps282271

Richardson, D. E., and Cowen, R. K. (2004b). New leptocephalus types collected around the island of Barbados (West Indies). *Copeia* 2004, 888–895. doi: 10.1643/ci-04-073r1

Sammons, S. M., and Bettoli, P. W. (1998). Larval sampling as a fisheries management tool: early detection of year-class strength. *N. Am. J. Fish. Manage.* 18, 137–143. doi: 10.1577/1548-8675(1998)018<0137:lsaafm>2.0.co;2

Smith, D. G. (1979). Guide to the leptocephali (Elopiformes, Anguilliformes, and Notacanthiformes). *NOAA Tech. Rept. NMFS Circular* 424, 1–43.

Smith, D. G. (1989a). Introduction to leptocephali. Fishes of the Western North Atlantic. *Mem. Sears Found. Mar. Res.* 9, 657–668.

Smith, D. G. (1989b). Order elopiformes; families Elopidae, Megalopidae, and Albulidae: leptocephali. Fishes of the Western North Atlantic. *Mem. Sears Found. Mar. Res.* 9, 961–972. doi: 10.2307/j.ctvbcd0jj.21

Smith, D. G. (1989c). Family Chlopsidae: leptocephali. Fishes of the Western North Atlantic. *Mem. Sears Found. Mar. Res.* 9, 933–942. doi: 10.2307/j.ctvbcd0jj.16

Smith, D. G. (1989d). Family Derichthyidae: leptocephali. Fishes of the Western North Atlantic. *Mem. Sears Found. Mar. Res.* 9, 917–920. doi: 10.2307/j.ctvbcd0jj.13

Smith, D. G. (1989e). Family Muraenidae: leptocephali. Fishes of the Western North Atlantic. *Mem. Sears Found. Mar. Res.* 9, 900–916. doi: 10.2307/j.ctvbcd0jj.12

Sutton, T. T., Cook, A., Moore, J. A., Frank, T., Judkins, H., Vecchione, M., et al. (2018a). *Inventory of Gulf Oceanic Fauna Data Including Species, Weight, and Measurements, Pisces cruises from Dec. 1 2010 – Sept. 29, 2011 in the Northern Gulf of Mexico (Distributed by: Gulf of Mexico Research Initiative Information and Data Cooperative (GRIIDC))*. Corpus Christi, TX: Harte Research Institute, Texas A&M University, doi: 10.7266/N7R49NTN

Sutton, T. T., Cook, A., Moore, J. A., Frank, T., Judkins, H., Vecchione, M., et al. (2018b). *Inventory of Gulf Oceanic Fauna Data Including Species, Weight, and Measurements. Meg Skansi cruises from Jan. 25 – Sept. 30, 2011 in the Northern Gulf of Mexico (Distributed by: Gulf of Mexico Research Initiative Information and Data Cooperative (GRIIDC))*. Corpus Christi, TX: Harte Research Institute, Texas A&M University, doi: 10.7266/N7VX0DK2

Sutton, T. T. (2013). Vertical ecology of the pelagic ocean: classical patterns and new perspectives. *J. Fish Biol.* 83, 1508–1527. doi: 10.1111/jfb.12263

Valdez-Moreno, M., Vásquez-Yeomans, L., Elías-Gutiérrez, M., Ivanova, N. V., and Hebert, P. D. (2010). Using DNA barcodes to connect adults and early life stages of marine fishes from the Yucatan Peninsula, Mexico: potential in fisheries management. *Mar. Freshw. Res.* 61, 655–671. doi: 10.1071/MF09222

Weibe, P. H., Morton, A. W., Bradley, A. M., Backus, R. H., Craddock, J. E., Barber, C., et al. (1985). New development in the MOCNESS, an apparatus for sampling zooplankton and micronekton. *Mar. Biol.* 87, 313–323. doi: 10.1007/bf00397811

Wiley, E. O., and Johnson, G. D. (2010). "A teleost classification based on monophyletic groups," in *Origin and Phylogenetic Interrelationships of Teleosts*, eds J. S. Nelson, H.-P. Schultze, and M. V. H. Wilson (Munich: Verlag Dr. Friedrich Pfeil), 123–182.

Conflict of Interest: The authors declare that the research was conducted in the absence of any commercial or financial relationships that could be construed as a potential conflict of interest.

frontiers in Marine Science

ORIGINAL RESEARCH
published: 08 July 2020
doi: 10.3389/fmars.2020.00552

Combined eDNA and Acoustic Analysis Reflects Diel Vertical Migration of Mixed Consortia in the Gulf of Mexico

Cole G. Easson[1,2], Kevin M. Boswell[3], Nicholas Tucker[3], Joseph D. Warren[4] and Jose V. Lopez[2]*

[1] Biology Department, Middle Tennessee State University, Murfreesboro, TN, United States, [2] Department of Biological Sciences, Nova Southeastern University, Dania Beach, FL, United States, [3] Department of Biological Sciences, Biscayne Bay Campus, Florida International University, North Miami, FL, United States, [4] School of Marine and Atmospheric Sciences, Stony Brook University, Southampton, NY, United States

Oceanic diel vertical migration (DVM) constitutes the daily movement of various mesopelagic organisms migrating vertically from depth to feed in shallower waters and return to deeper water during the day. Accurate classification of taxa that participate in DVM remains non-trivial, and there can be discrepancies between methods. DEEPEND consortium (www.deependconsortium.org) scientists have been characterizing the diversity and trophic structure of pelagic communities in the northern Gulf of Mexico (nGoM). Profiling has included scientific echosounders to provide accurate and quantitative estimates of organismal density and timing as well as quantitative net sampling of micronekton. The use of environmental DNA (eDNA) can detect uncultured microbial taxa and the remnants that larger organisms leave behind in the environment. eDNA offers the potential to increase understanding of the DVM and the organisms that participate. Here we used real-time shipboard echosounder data to direct the sampling of eDNA in seawater at various time-points during the ascending and descending DVM. This approach allowed the observation of shifts in eDNA profiles concurrent with the movement of organisms in the DVM as measured by acoustic sensors. Seawater eDNA was sequenced using a high-throughput metabarcoding approach. Additionally, fine-scale acoustic data using an autonomous multifrequency echosounder was collected simultaneously with the eDNA samples and changes in organism density in the water column were compared with changes in eDNA profiles. Our results show distinct shifts in eukaryotic taxa such as copepods, cnidarians, and tunicates, over short timeframes during the DVM. These shifts in eDNA track changes in the depth of sound scattering layers (SSLs) of organisms and the density of organisms around the CTD during eDNA sampling. Dominant taxa in eDNA samples were mostly smaller organisms that may be below the size limit for acoustic detection, while taxa such as teleost fish were much less abundant in eDNA data compared to acoustic data. Overall, these data suggest that eDNA, may be a powerful new tool for understanding the dynamics and composition of the DVM, yet challenges remain to reconcile differences among sampling methodologies.

Keywords: pelagic, Gulf of Mexico, eDNA, acoustics, DEEPEND

OPEN ACCESS

Edited by:
Øyvind Fiksen, University of Bergen, Norway

Reviewed by:
Luis Manuel Bolaños, Oregon State University, United States
Thor Aleksander Klevjer, Norwegian Institute of Marine Research (IMR), Norway

****Correspondence:***
Cole G. Easson
cgeasson86@gmail.com

Specialty section:
This article was submitted to Deep-Sea Environments and Ecology, a section of the journal Frontiers in Marine Science

Received: *30 August 2019*
Accepted: *16 June 2020*
Published: *08 July 2020*

Citation:
Easson CG, Boswell KM, Tucker N, Warren JD and Lopez JV (2020) Combined eDNA and Acoustic Analysis Reflects Diel Vertical Migration of Mixed Consortia in the Gulf of Mexico. Front. Mar. Sci. 7:552. doi: 10.3389/fmars.2020.00552

INTRODUCTION

Diel vertical migration (DVM) is a well-recognized phenomenon among the world's oceans where large numbers of fish, decapods, cephalopods, and many other species migrate vertically through the water column during crepuscular periods (Hays, 2003; Sutton et al., 2017). Generally, the animals participating in this migration will transit from deep ocean habitats (500–1000 meters) up into the epipelagic depths (0–200 meters) at night and return to the depths at dawn. Many micronekton (actively swimming organisms ∼2–20 cm length; Kloser et al., 2009) perform this daily migration in search of prey, but these migrating organisms are also important food resources for larger predators in the pelagic ecosystem. This striking vertical movement of organisms across different pelagic depths provides opportunities to study unique ecological interactions in the pelagic environment including predator-prey interactions and energy transfer between the surface and deep ocean.

Often, the DVM process is measured using echosounders to detect sound scattering layers (SSLs) in the water column. The SSLs are ubiquitous features throughout the world's oceans and are mainly comprised of vertically migrating taxa that serve as primary prey resources for larger predators, like marine mammals (Proud et al., 2017, 2019). The SSLs are dominant biological features of these vast ecosystems and contribute importantly to the global process of carbon transport and sequestration (Irigoien et al., 2014). The depths at which SSLs occur are dynamic and often dependent on the geographic location, depth of the water column and time of day, which gives rise to well-recognized and remarkable DVM patterns (Klevjer et al., 2016).

While acoustic techniques can provide information about the dynamics of the DVM, they have a limited ability to discern the specific composition of migrating layers of organism. This gap in knowledge can be filled with towed net sampling, though a single net sampling method often cannot adequately capture all types of pelagic organisms (Milligan et al., 2018). For example, gelatinous zooplankton are not well represented in MOCHNESS sampling gear and thus may be underestimated with net sampling. One promising potential solution is the use of environmental DNA (eDNA) to detect the organisms present in the environment (Thomsen and Willerslev, 2015; Ruppert et al., 2019). eDNA consists of genetic material sampled from an environmental source rather than directly from a biological source (Thomsen and Willerslev, 2015). This sampling technique can capture all the cells that are present in the environment, which may allow for the detection and identification of larger organisms through shed biological trace remnants (cells, feces, mucus etc.). This technique when coupled with next-generation metabarcoding sequencing techniques can provide a census of the organisms present in the environment (Bucklin et al., 2016). To date, eDNA has been leveraged to profile a wide variety of environments including freshwater lakes and streams, terrestrial soils, and marine seawater and sediment (e.g., Bista et al., 2017; Cowart et al., 2018). Studies that have utilized eDNA methods in the marine environment have shown the ability to detect a variety of multicellular vertebrate and invertebrate taxa (Foote et al., 2012; Thomsen and Willerslev, 2015; Cowart et al., 2018), and complement more traditional faunal survey techniques.

In the current study, we sampled eDNA during the DVM in the northern Gulf of Mexico (nGoM) to assess whether this technique captures the dynamics of this daily migration and the composition of SSLs. Sampling of eDNA was directed by shipboard acoustic sensors to sample seawater at different time-points during the DVM, and eDNA data was compared to *in-situ* and shipboard acoustic data to assess whether changes in eDNA communities were related to changes observed by the acoustic sensors.

MATERIALS AND METHODS

Sampling of environmental DNA (eDNA) was directed by real-time multifrequency acoustic data to identify the dominant SSLs and estimate the depth of the vertically migrating organisms (micronekton). All observations described in this study were collected from a drifting research vessel (*R/V Pt. Sur*) during one DEEPEND cruise (DP05) where a ship-board multifrequency echosounder system characterized the depth profiles of the SSLs and directed in-situ sampling of CTD rosette outfitted with water samplers and an acoustic probe. For the cast at night, CTD 83 (Sea-Bird 911plus), was deployed within the mesopelagic zone just above the rising SSL (**Table 1**). It was held in that position while the SSL rose and migrated past the CTD. Seawater samples were collected throughout the DVM process. During the morning CTD cast, the SSL migrated from the surface to deeper, so CTD 84 was placed below the SSL and then held in position while the SSL moved to the same depth and then below the CTD. Water samples were taken at each time-point, similar to night casts. We also sampled in the epipelagic zone (∼90 m), but these samples were not taken during the DVM. The sampling scheme is detailed in **Table 1**.

Acoustic Data Collection

Multifrequency acoustic backscatter data was collected with a calibrated pole-mounted echosounder system (Simrad EK60 and EK80). The transducers were mounted in an enclosed housing and suspended 2.5 m below the water surface (see Boswell et al., 2020 for additional details). Backscatter data were collected simultaneously at four frequencies (18, 38, 70, and 120 kHz). The 18, 38, and 70 kHz echosounders had sufficient power and signal to noise to permit examination of the migrating layers, however, effects of attenuation limited data quality beyond 350 m for the 120 kHz. The dominant acoustic features detected from the shipboard echosounder were examined in more detail with an autonomous echosounder (Simrad EK80 WBAT) mounted onto the bottom of the CTD rosette frame and deployed as an acoustic probe (Kubilius et al., 2015; Kloser et al., 2016). The WBAT was configured with a 70 kHz and 120 kHz transducer and was programmed to alternate in 100 ping sequences between the two transducers. The hardware limitations of the echosounder prevented simultaneous collection at both frequencies. The on-axis gain was measured by suspending a 38.1 mm tungsten carbide sphere (∼6% cobalt binder) 7 m below the CTD while

TABLE 1 | Seawater collection metadata for DEEPEND cruise DP05 which had CTD casts (nos. 83 and 84) representing collection times for eDNA.

Ascending VM	Date	Site	CTD	Depth (m)	Collection time description
83-320-3-x	5/10/2017	B175N	CTD_083	320	Above SSL at 16:40
83-320-4-x	5/10/2017	B175N	CTD_083	320	Within SSL at 19:00
83-320-5-x	5/10/2017	B175N	CTD_083	320	Within SSL at 19:26
83-320-6-x	5/10/2017	B175N	CTD_083	320	Within SSL at 19:41
83-92-7-x	5/10/2017	B175N	CTD_083	92	Post SSL at 20:06
83-92-12	5/10/2017	B175N	CTD_083	92	Post SSL
Descending VM					
84-320-1-x	5/11/2017	B175D	CTD_084	320	Below SSL at 05:12
84-326-4-x	5/11/2017	B175D	CTD_084	320	Within SSL at 06:11
84-326-5-x	5/11/2017	B175D	CTD_084	320	Within SSL at 06:29
84-326-6-x	5/11/2017	B175D	CTD_084	320	Within SSL at 06:51
84-326-7-x	5/11/2017	B175D	CTD_084	320	Post SSL at 07:29
84-93-8-x	5/11/2017	B175D	CTD_084	93	Post SSL at 07:43
84-93-11-x	5/11/2017	B175D	CTD_084	93	Post SSL at 08:05

eDNA samples were collected at specific times corresponding to the position of the sound scattering layers (SSL) relative to the CTD. Further information available for the DP05 cruise can be found as ***Supplementary Data*** *or at the DEEPENDconsortium.org website.*

probing through the water column. Calibration was performed using the Simrad Lobe program within the EK80 software (Demer et al., 2015). Sound speed profiles and absorption coefficient were computed from bin-averaged CTD data using the Ocean Toolbox (McDougall and Barker, 2011).

Raw acoustic backscatter data collected from the shipboard echosounder were imported and scrutinized in Echoview (v9) and processed following methods described by D'Elia et al. (2016) and Boswell et al. (2020). Briefly, data from the transducer face to 15 m depth were excluded from the analysis to account for nearfield effects and to eliminate surface-associated interference (e.g., bubble sweep down). Data were examined for interference from other shipboard sonar systems (intermittent or spike noise), false bottom, and background noise. False bottoms were manually excluded. Background noise was identified and removed following a modified process described by De Robertis and Higginbottom (2007). The measurements of Nautical Area Scattering Coefficient (NASC; m^2 nmi^{-2}) were derived from the echo integral in 500-m along-track x 5-m vertical bins (MacLennan et al., 2002). NASC is generally understood to be proportional to the abundance of biological scatterers and serves as a comparable index of organism biomass (Hazen et al., 2009; Zwolinski et al., 2010; Fennell and Rose, 2015). Integrated backscatter was further binned into three depth intervals: 15–200 m (epipelagic), 200–600 m (upper mesopelagic) and 600–1000 m (lower mesopelagic). We then compared the maximum NASC (m^2 nmi^{-2}) values with depth as a function of time from the 18 and 38 kHz transducer by applying a dB- difference (ΔdB_{18-38} = dB_{18}–dB_{38}) operation to highlight two categories of scatterers within the scattering layer: (1) swim bladdered fish (SBF) and (2) non-swim bladdered fish/crustaceans (NSBFC) following D'Elia et al. (2016). Swim bladdered fish targets were classified as having a ΔdB_{18-38} range between +3 and +12 dB while the non-swim bladdered fish/crustaceans were classified as having a ΔdB_{18-38} range between -14 and 0 dB. Backscatter from these two classes were integrated into 20 m (vertical) by 3 min (horizontal) cells and exported from Echoview for additional analysis.

Acoustic backscatter data from the WBAT were examined in Echoview. Given that the emphasis was to enumerate the individual scatterers within the migrating layer, we focused the analysis on the detected point targets using a single target detection algorithm in Echoview. Sequential targets which satisfied the criteria for the algorithm were tracked and identified as an individual if they had more than 3 targets across 5 consecutive pings. For point target recognition, we used a minimum uncompensated TS threshold of −75 dB and an echo length ranging from a minimum 0.7 ms to a maximum 1.50 ms. The maximum gain compensation was set to 6.0 dB with a maximum phase deviation of 0.6 degrees for both major and minor axes. Point targets within 2 to 75 m of the WBAT were included for use in analysis. During the deployment, the WBAT remained stationary at two depths during the migration of the scattering layer: ∼92 and 320 m. The acoustic data were divided into two periods and were related to the depth of the CTD during the profiling activity. The first period occurred between 16:45 and 20:00 and targeted single targets at ∼320 m depth. Data collected during this period were divided into 10-min time intervals for processing. The second period occurred between 20:00 and 20:24 and corresponded to when the CTD was positioned at ∼90 m. Data collected during this period were divided into 3-min time intervals to capture single targets at higher temporal resolution. Target strength (dB re 1 m^2) distributions were derived from each interval and analyzed to examine the temporal changes in the size of detected point targets (Lurton, 2002). We conducted a Kruskal-Wallis Chi-squared test to test for significant changes among depths.

Seawater Collections for eDNA

Seawater samples were collected according to the position of the CTD relative to the SSLs and at specific times using the 12 L Niskin bottle array also mounted on the CTD (**Table 1**). Seawater was collected to sample the eDNA for potential

changes in composition of prokaryotic and eukaryotic organisms. Collections and filtering have been described by Easson and Lopez (2019). Immediately after the CTD arrived back on the surface, replicate two-liter samples ($N = 3$) were taken from each Niskin bottle and were filtered through sterile 0.45 υm filter membranes to remove all cells from the seawater. No organisms were directly sampled, and filters were visually inspected to ensure no organisms were visible on the filter. Filter membranes were placed in sterile tubes and frozen until analysis at NSU.

eDNA Sequencing and Statistical Analyses

DNA was extracted using the PowerLyzer PowerSoil DNA Isolation Kit (QIAGEN) following the manufacturer's protocol. Polymerase chain reaction (PCR) was performed following the 18S Illumina Amplicon protocol of the Earth Microbiome Project[1]. Sample preparation and sequencing followed the methods outlined in Easson and Lopez (2019), except that a 300 cycle Illumina MiSeq kit was used to generate paired-end 150 bp amplicons.

Bioinformatics processing was conducted in R using the DADA2 pipeline (Callahan et al., 2016; R Core Team, 2018). Initially, sequences were trimmed to remove ambiguous bases (max $N = 0$), sequences longer than 150 bp and shorter than 90 bp. The default ASV2 parametric error model was used to calculate sequence error rates. Next, sequences were dereplicated to infer sequence variants, paired-end reads were combined, and chimeras were removed. Once these processes finished, a sequence table of amplicon sequence variants (ASVs) was constructed. ASVs were taxonomically classified using the Silva database (release 128; Quast et al., 2015).

Statistical analysis was done in R (R Core Team, 2018) using the R packages vegan and picante (Kembel et al., 2010; Oksanen et al., 2017). Analysis was conducted separately on CTD 83 (ascending DVM at night) and CTD 84 (descending DVM descending DVM during day). ASV abundance was transformed to relative abundance so each ASV is represented as a proportion in the whole dataset for a specific sample. Initial analysis assessed eDNA community diversity (Inverse Simpson's index) and richness (total number of unique ASVs) and compared these metrics across sampling time-points in each CTD. Beta diversity was then assessed by calculating Bray-Curtis dissimilarity among samples and a permuted multivariate analysis of variance (PERMANOVA) was used to compare beta diversity among sampling time points in each CTD.

RESULTS

Acoustic Analyses of nGoM Migrating Organisms

Shipboard Acoustic Data

During the day, the depth of the maximum backscatter (NASC, m^2 nmi^{-2}) occurred at a depth of ∼440 m (NASC = 58.86 m^2 nmi^{-2}) (**Figure 5**). The scattering layer began migrating upwards at ∼17:30 and completed the migration at 20:23, with a large amount of backscatter filling the upper 150 m of the water column (CTD 83). The downward migration began around 04:00 with the descent completing at ∼08:30 where the scattering layer settled at ∼460 m (NASC = 55.33 m^2 nmi^{-2}) (CTD 84).

Two distinct scattering layers were identified which contributed significantly to the measured water column backscatter. When the CTD was in the upper mesopelagic zone (16:45 to 20:00), the center of mass of the SBF was ∼325 m (± 97.9 m). In contrast, the center of mass for NSBFC were located an average of 407 m (± 114.3 m). When the CTD was raised to the epipelagic zone (20:00 to 20:25), the center of mass of SBF was 155 m (± 43.6 m), while NSBFC were at ∼292 m (± 217 m). Variability in the depth of the NASC maxima between SBF and NSBFC was consistent during both depth profiles.

We observed significant variability when examining the temporal patterns of target strength distributions collected at the two depths from the probe positioned within the ascending DVM. Additionally, the target strength distributions varied significantly in the distribution of scatterers within the mesopelagic layer at 320 m ($p < 0.001$; $\chi^2 = 830.8$, $df = 17$) but not within the epipelagic layer ($p = 0.629$; $\chi^2 = 5.253$, $df = 7$) (**Figure 1**).

eDNA Profiles of nGoM Organisms

A total of 3,033,134 sequence reads were recovered for the 40 samples in CTD83 and CTD84. Taxonomic classification using the Silva database (Release 128) identified 10,185 unique ASVs. Since the goal of this study was to assess detection of micronekton that are potentially vertically migrating, taxa that did not fit into this category based on taxonomic classification or had an unknown classification were excluded. Most taxa in the dataset were either unicellular (3,634 taxa) or could only be definitively classified as eukaryotes (6,326 taxa) and were thus excluded from analysis (**Supplementary Table S1**). The final analyzed dataset contained 92 taxa for mesopelagic CTD 83 (**Supplementary Table S2**), 74 taxa for mesopelagic CTD 84 (**Supplementary Table S3**), and 62 taxa in the epipelagic samples from both CTDs.

An exception to unicellular taxa not being involved in the DVM may be those unicellular taxa that are parasitic to vertically migrating taxa such as in the order Syndiniales, which were abundant in the current dataset (Guillou et al., 2008). Taxonomic classification of eDNA for most ASVs was only to order due to a short amplicon length (∼150 bp), limited taxonomic resolution in the Silva database, and a lack of many deep-sea organisms in taxonomic databases. In many cases, unique ASVs were detected, but these ASVs could only be classified to a higher taxonomic group. Henceforth, when individual taxa are referenced, these are unique ASVs that may be only broadly taxonomically classified.

CTD 83 – Ascending DVM

For the ascending phase of the DVM in the mesopelagic, we observed significant shifts in eDNA diversity and composition over time (**Supplementary File 1**) with several groups of organisms exhibiting temporal shifts in relative abundance, suggesting variability in the structure of eukaryotic communities

[1] earthmicrobiome.org

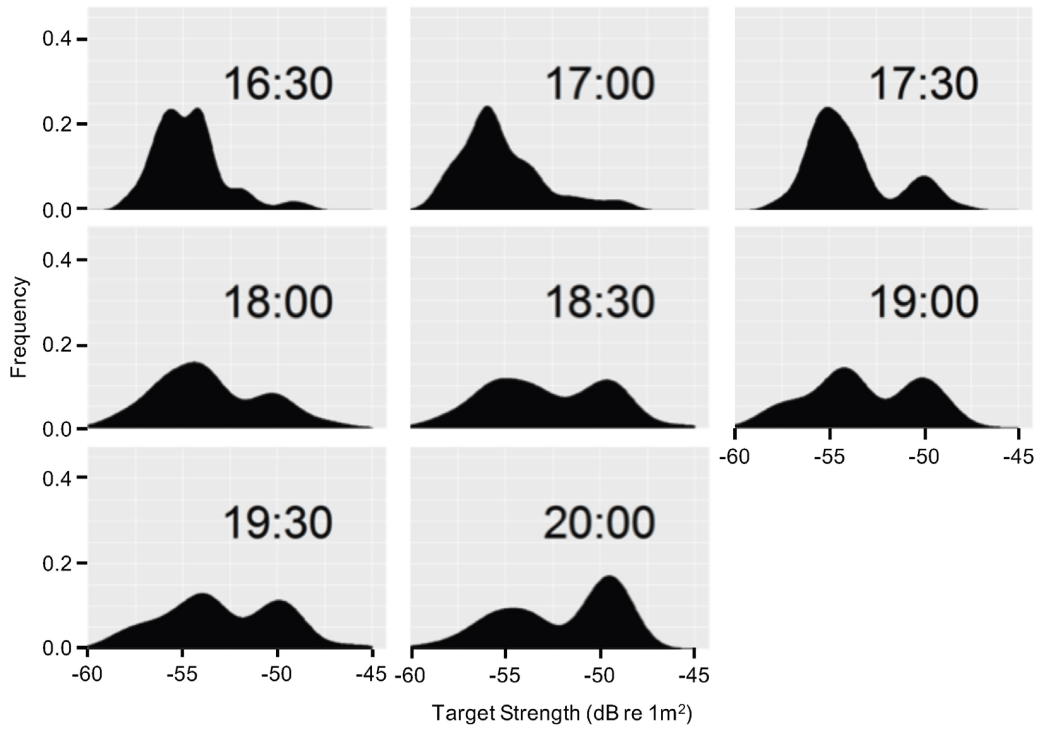

FIGURE 1 | Target strength (dB re 1 m^2) density distributions during CTD cast 83 derived from the WBAT deployed at 320 m. Each distribution is approximately representative of a 12 min period where the WBAT was deployed. The asterisks indicate intervals where the water was sampled for eDNA.

over time. Broad taxonomic groups such as arthropods, tunicates, annelids, cnidarians, ctenophores, and teleost fish were variable over the course of the DVM (**Figure 2**). Interestingly, different groups of organisms displayed peak relative abundance at different times during the DVM. For example, copepods in the class Maxillopoda appeared most abundant within the earliest sampled time-points of the DVM (at 19:00) whereas other taxa such as tunicates, ctenophores, and cnidarians appeared most abundant in the subsequent sample taken 26 min later. Teleost fish (Class Actinopterygii), which are typically considered to comprise much of the vertically migrating taxa biomass, did not display a high relative abundance in the eDNA dataset though they were consistently present (**Figure 2**). During the ascending DVM, gelatinous zooplankton (tunicates, ctenophores, and cnidarians) all exhibited the highest relative abundance within the middle time point of the vertically migrating band (at 19:26), however, since these organisms tend to only weakly scatter sound unless occurring in swarms (Ressler, 2002; D'Elia et al., 2016), it may be difficult to discern them in the acoustic dataset. Conversely, there is another group of gelatinous zooplankton, physonect siphonophores, that do scatter significant amounts of acoustic backscatter due to their gas-containing pneumatophore (Warren et al., 2001; Lavery et al., 2007). It is often not possible to acoustically differentiate scattering contributions from siphonophores and some swim-bladdered fish (Proud et al., 2019) which further complicates the analysis. Lastly, Annelids (Phylum Annelida) represented an abundant group in the eDNA dataset (**Figure 2**). Annelids in the class Clitellata exhibited an increase in relative abundance late in the ascending DVM (**Supplementary Table S2**).

The eDNA dataset allows us to breakdown each of these broad taxonomic groups to determine how many potential species are driving the observed dynamics (**Supplementary Table S2**). Previous research has noted variable vertical migration behavior within broader taxonomic groups, and eDNA techniques could help refine our understanding of these behaviors. Within our current dataset, we observed that in most cases, the main drivers of the DVM patterns (**Figure 3**) were due to only a few taxa in each group. For example, in Arthropoda, we observed 14 total taxa (**Table 2**), but only three of these taxa had much impact on the temporal variation of the group (**Figure 3**). Two of these taxa (ASV18, ASV19) exhibited a peak relative abundance early in the DVM, while the third taxon, ASV20, was most abundant late in the DVM. Each of these three taxa were copepods belonging to the order Calanoida. Similar to the results in Arthropoda, relatively few taxa were observed driving temporal variation in Cnidaria (3 dominant members from the order Siphonophorae), Ctenophora (1 dominant member), Tunicata (10 taxa with 2 main drivers from the family Oikopleuridae), teleost fishes (1 dominant member), and Annelids (1 dominant member).

CTD84 – Descending DVM

In the mesopelagic zone during the descending vertical migration of organisms, we also observed significant shifts in eDNA diversity and composition over short temporal scales (**Supplementary Results**). Similar to the ascending DVM in

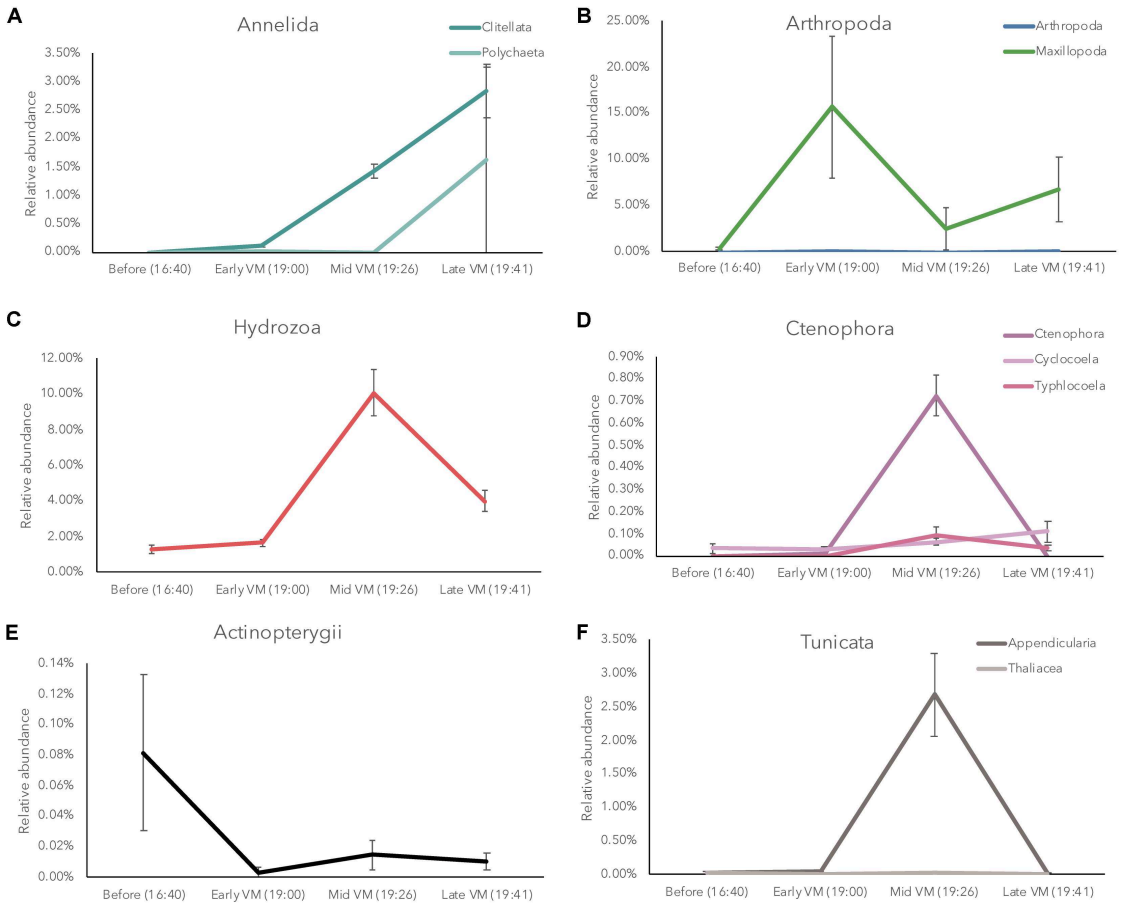

FIGURE 2 | Relative abundance of Annelida **(A)**, Arthropoda **(B)**, Hydrozoa **(C)**, Ctenophora **(D)**, Actinopterygii **(E)**, and Tunicata, **(F)** in the eDNA community during the ascending diel vertical migration (CTD 83). Note different y-axis scales between each group.

CTD 83, several broad groups of organisms were dynamic over the course of our sampling, however, the patterns were somewhat different in CTD 84. Tunicates in class Appendicularia showed a slight increase early in the vertical migration and then a gradual decrease in relative abundance over time (**Figure 4**). Arthropods in the class Maxillopoda (likely copepods) decreased in relative abundance until the middle of the vertical migration and then gradually increased in relative abundance. Ctenophore and Cnidarian relative abundance both peaked during the middle of the DVM. Teleost fish displayed low relative abundance in this dataset, but they were consistently present with high variability among samples. Annelids in the class Clitellata displayed a higher relative abundance late in the descending DVM (**Figure 4**), similar to the observed pattern in the ascending DVM (**Figure 3**).

The taxonomic composition for the descending DVM was somewhat different compared to the ascending DVM (**Supplementary Table S3**). In Arthropoda (18 taxa total), only ASV20, which appeared later in the DVM in the ascending phase of the DVM (CTD 83), was abundant in the descending DVM (**Figure 5**). Two other taxa (ASV 24 & ASV 27) in the order Calanoida and one taxon (ASV66) in the order Harpacticoida, were abundant in the descending DVM eDNA dataset. Fewer tunicate taxa were detected in the descending DVM, and we observed an absence of the two most abundant taxa from the ascending DVM. Annelids and teleost fish (Class Actinoptergii) exhibited lower richness compared to CTD83 and were comprised of only two and one unique taxa, respectively. Within the phyla Cnidaria and Ctenophora, we detected 15 and 8 unique taxa, respectively, though both were generally less abundant compared to CTD83, and were dominated by only a few taxa (**Figure 5**). The majority of Cnidarian taxa belonged to the order Siphonophorae (9 taxa), which includes taxa with gas inclusions (in suborder Physonectae), but taxonomic identification was only possible to order with the current sequence data.

Epipelagic eDNA Communities

Our samples in the epipelagic zone, which occurred during the DVM, represent post-migration samples for both CTD 83 (night) and CTD84 (day). The eDNA in these samples were composed of similar groups of taxa to those in mesopelagic including copepods (Class Maxillopoda), tunicates (Class Appendicularia), Annelids (Class Clitellata), and hydrozoans (Class Hydrozoa; **Supplementary Figure S1**). Of these six groups, Maxillopoda

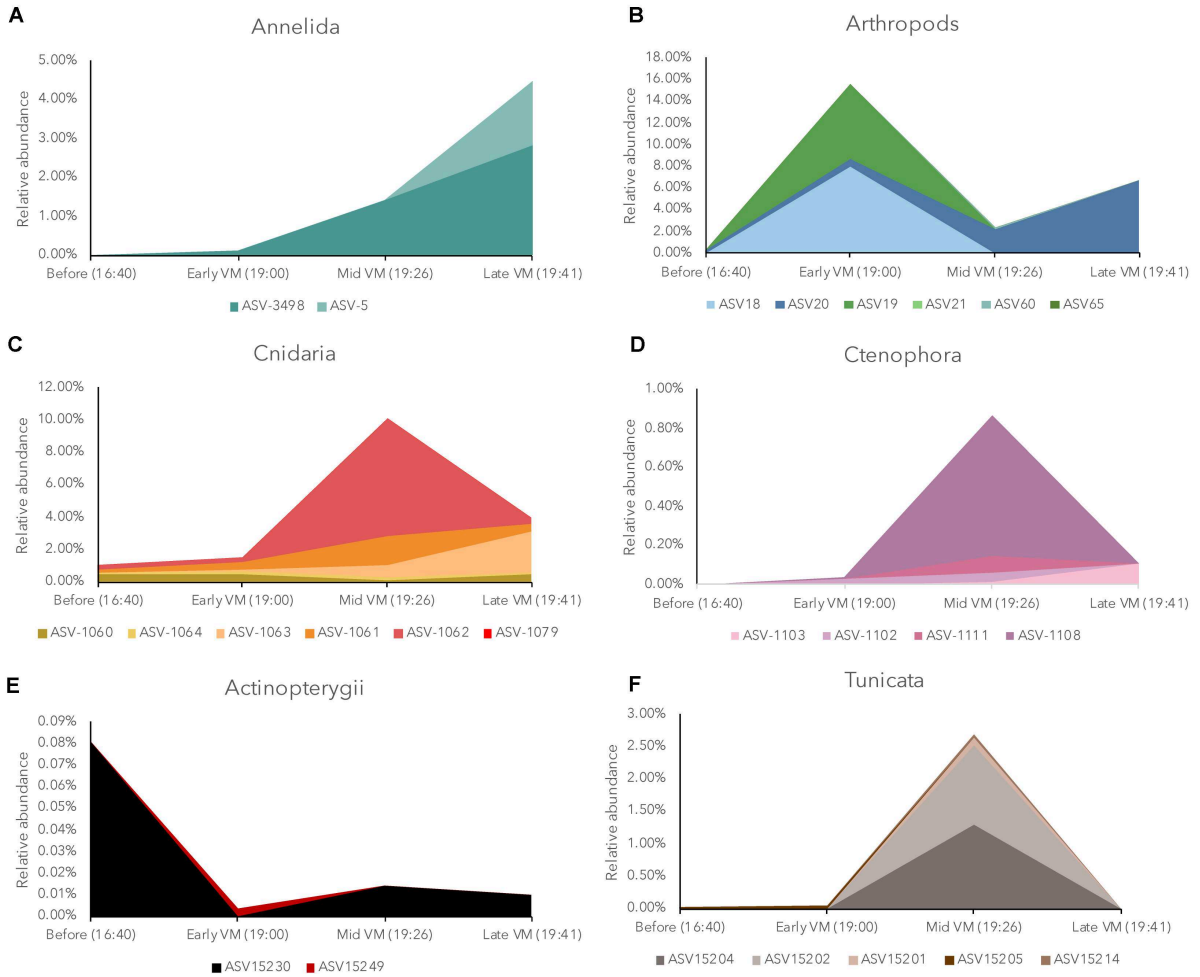

FIGURE 3 | Relative abundance of Annelida **(A)**, Arthropoda **(B)**, Hydrozoa **(C)**, Ctenophora **(D)**, Actinopterygii **(E)**, and Tunicata, **(F)** in the eDNA community during the ascending diel vertical migration (CTD 83) broken down into individual amplicon sequence variants (ASVs) as identified by the Silva database. The dynamics of most groups were dominated by relatively few ASVs. Individual ASVs are represented by different colors in each panel and each legend lists the unique taxonomic identifier in the current dataset. ASVs with a maximum relative abundance less than 0.05% were not plotted. Note different y-axis scales between each group.

was the richest, containing 33 unique ASVs. Within this group, some of the same taxa were dominant (e.g., ASV18), but overall, there appeared to be more copepods in the orders Cyclopoida and Harpacticoida compared to samples from the mesopelagic zone. Cnidarians in the class Hydrozoa were less prevalent and less rich in our epipelagic samples, though some similar taxa were detected. The full results for the epipelagic taxa are summarized in **Supplementary Table S4**.

DISCUSSION

Studying the oceanic pelagic environment is challenging due to remoteness, depth, and the vast expanse of ocean that this zone covers. Given these fundamental challenges, cost-effective, yet comprehensive tools are needed to capture the biodiversity and dynamics of this understudied environment. Remote sensing tools such as echosounders have been utilized to capture the placement and movement (i.e., DVM) of organisms in the pelagic environment (Milligan et al., 2018), but the ability of this technology to resolve the identities of organisms is limited (D'Elia et al., 2016). The current study suggests that eDNA has the potential to fill in some of these gaps in our knowledge through its ability to resolve finer scale taxonomic identities of the organisms in this environment. Our results show that during the DVM, we are able to detect changes in the eDNA community that are concurrent with shifts in the depth of the SSLs through the migration process. The eDNA results show a complex community of arthropods, tunicates, cnidarians, ctenophores, annelids, and fish, which are all known members of the pelagic environment and in some cases are known diel vertical migrators.

eDNA Faunal Assessment

Our eDNA dataset detected many resident fauna of the pelagic environment, and while we had more resolution on organism identity compared to acoustics, we were often not able to

TABLE 2 | Taxonomic summary of eDNA fauna in the mesopelagic samples of CTD 83 and CTD 84.

Phylum	No. ASV orders		No. unique ASVs		No. shared ASVs	Total unique ASVs	Taxonomic orders detected
	CTD83	CTD84	CTD83	CTD84			
Annelida	3	2	2	1	1	4	CTD83: Clitellata, Scolecida, Spionida CTD84: Clitellata, Phyllodocida
Arthropoda	4	4	7	8	5	20	CTD83: Collembola, Calanoida, Cyclopoida, Harpacticoida CTD84: Collembola, Calanoida, Cyclopoida, Harpacticoida
Actinopterygii (Class)	1	1	2	0	1	3	CTD83: unclassified CTD84: unclassified
Cnidaria	3	3	5	3	12	20	CTD83: Anthoathecata, Siphonophorae, Trachymedusae CTD84: Anthoathecata, Siphonophorae, Trachymedusae, unclassified
Ctenophora	3	4	3	4	4	11	CTD83: Lobata, Cydippida, unclassified CTD84: Cyclocoela, Lobata, Cydippida, Typhlocoela, unclassified
Tunicata	3	2	6	2	4	12	CTD83: Copelata, Pyrosomata, Salpida CTD84: Copelata, Pyrosomata

Individual amplicon sequence variant (ASV) classifications for CTD 83 and CTD 84 are located in ***Supplementary Tables S1, S2****, respectively.*

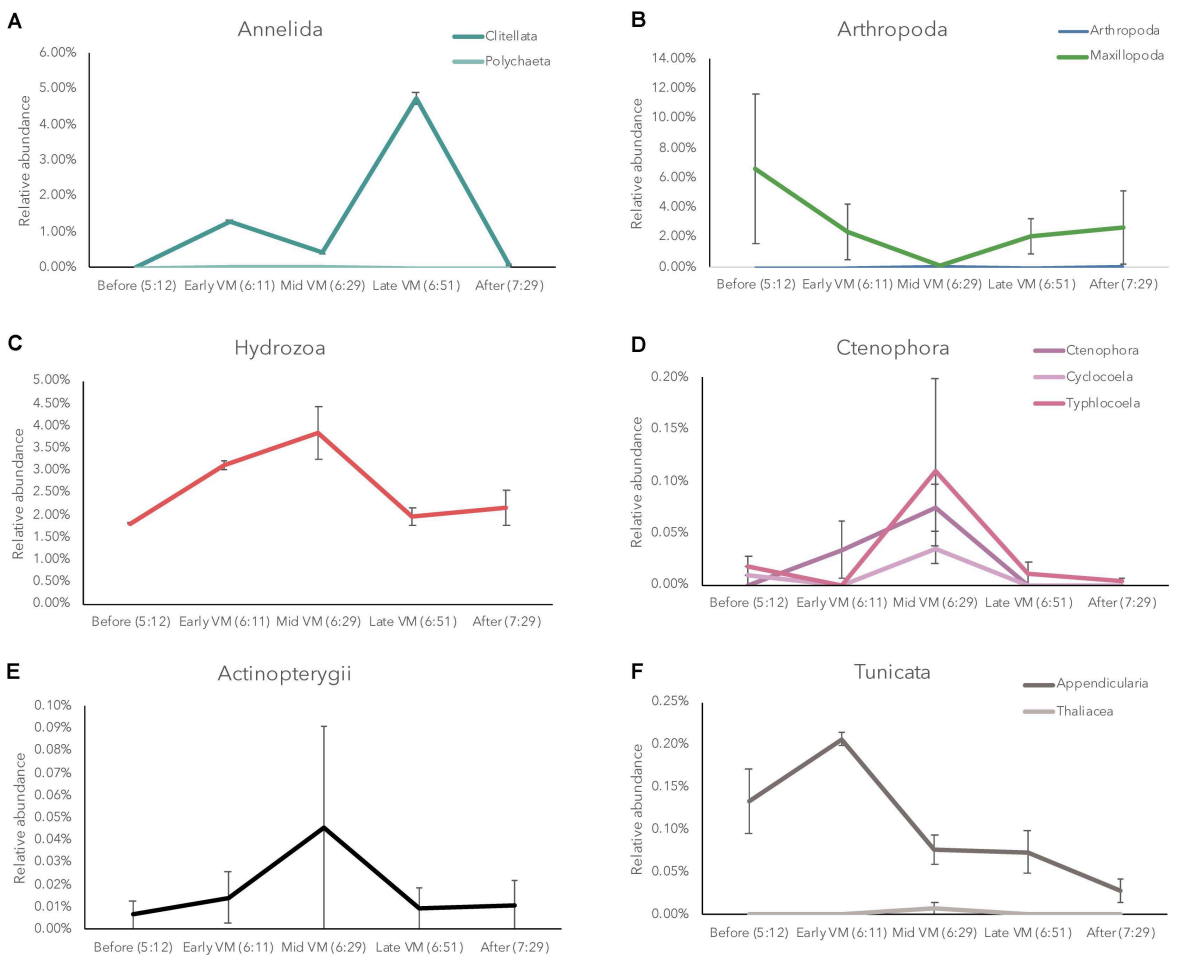

FIGURE 4 | Relative abundance of Annelida **(A)**, Arthropoda **(B)**, Hydrozoa **(C)**, Ctenophora **(D)**, Actinopterygii **(E)**, and Tunicata, **(F)** in the eDNA community during the descending diel vertical migration (CTD 84).

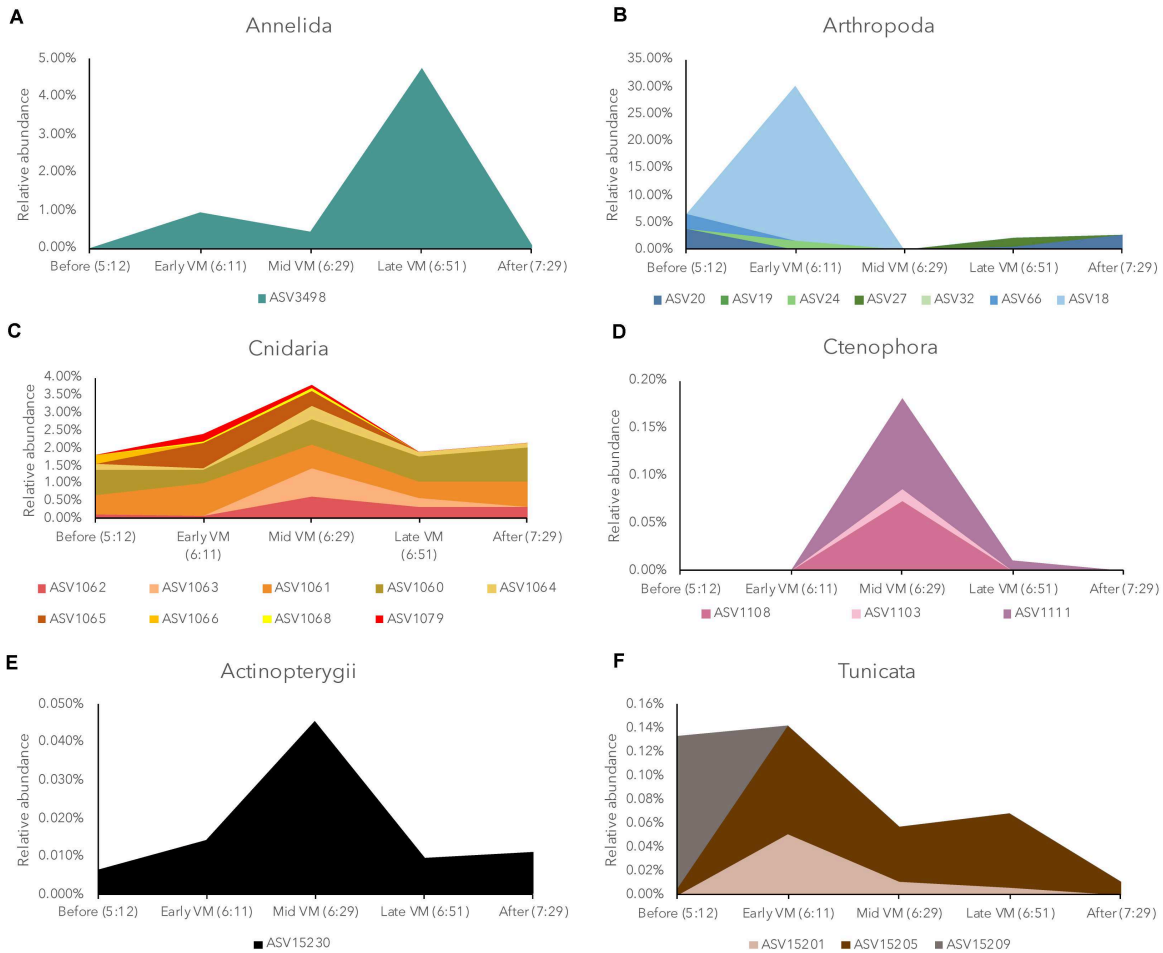

FIGURE 5 | Relative abundance of Annelida **(A)**, Arthropoda **(B)**, Hydrozoa **(C)**, Ctenophora **(D)**, Actinopterygii **(E)**, and Tunicata, **(F)** in the eDNA community during the descending diel vertical migration (CTD 84) broken down into individual amplicon sequence variants (ASVs) as identified by the Silva database. Individual ASVs are represented by different colors in each panel and each legend lists the unique taxonomic identifier in the current dataset. ASVs with a maximum relative abundance less than 0.05% were not plotted.

resolve fine-scale taxonomic identities. With our short 18S rRNA fragment, we were only able to identify ∼31% of our sequences further than a kingdom classification. The presence of many unidentified sequences may represent additional biodiversity in key pelagic groups that we were unable to classify here. Although efforts have been growing, the pelagic environment is understudied relative to many other habitats (Sutton, 2013; de Vargas et al., 2015; Sieracki et al., 2019). The poor classification of many of our sequences may be due to a lack of representation of whole faunal groups or at least an absence of closely related taxa in the Silva database. These instances would lead to low taxonomic resolution in our dataset despite being able to parse individual taxa via our sequence-clustering algorithm. In addition to our classification issues, we also observed the absence or low abundance of some faunal groups that we expected to be more abundant. For example, teleost fish (Class Actinopterygii) were present, but only in low abundance in our dataset. We hypothesized that much of the biomass observed in the acoustic data was attributed to teleost fish, but this dominance is not reflected in the eDNA dataset. We also expected to observe other groups of crustaceans such as decapods in our eDNA dataset (Thomsen and Willerslev, 2015; D'Elia et al., 2016), but surprisingly these groups were absent. Potential explanations for these findings include: (1) low concentrations of eDNA from these organisms present in the environment during the short timeframe we sampled (low rate of eDNA production) or the actual low abundance of these organisms, (2) a lack of resolution in the taxonomic database to identify organisms in these taxonomic groups (organisms are present in dataset but unidentified), (3) organisms like physonect siphonophores were contributing to acoustic backscatter ascribed to teleost fish (Proud et al., 2019), and (4) issues with sequence processing methodology or the presence of inhibitors in certain cells that prevented proper sequencing of taxa in these groups. Previous studies have noted the lack of coverage of many key pelagic taxonomic

groups in major databases such as NCBI and Barcode of Life Data System (BoLD) (Kvist, 2013; Cowart et al., 2018), and at present, these limitations likely limit the overall ability of 18S eDNA to finely resolve biodiversity in these hard to study environments.

We identified a diverse array of taxa in the pelagic environment that corresponds with previous faunal assemblage characterizations (**Table 2**). In our present dataset, sequences matching several groups of tunicates were identified, and taxonomic classification of these sequences indicated that they belonged to the groups Appendicularia (Larvaceans) and Thaliacea (Salps & Pyrosomes). Previous research has shown that members of each of these groups can alter biogeochemical cycling in the pelagic environment, through carbon export to deeper depths (Andersen, 1998). For Appendicularia, the dominant members of our eDNA dataset, this is through their contributions to marine snow via their discarded mucus houses (Barham, 1979), which can be a food source for other pelagic organisms such as copepods (Steinberg, 1995). Representative taxa such as *Pyrosoma atlantica* have been observed and collected via MOCNESS sampling at depth in the nGoM during DEEPEND cruises (Cook and Sutton, 2018), and this species has been identified in DVM elsewhere (Henschke et al., 2019). In addition, our eDNA dataset revealed as many as 17 Cnidarian taxa belonging to the class Hydrozoa. These hydrozoans were classified into three different orders, with Siphonophorae being the most abundant and species rich. These taxa are broadly distributed in all oceans forming crucial trophic links in the deep sea (Robison, 2004; Mapstone, 2014). Several members of this order contain gas-inclusions (sub-order Physonectae) and are therefore detectable by our acoustic sensors. Our current eDNA dataset cannot determine what proportion of the community is physonect siphonophores, but previous studies in the GoM have shown this group can be prevalent among siphonophore assemblages (Sanvicente-Añorve et al., 2007). Ctenophores (phylum Ctenophora), while generally less abundant in the eDNA dataset than tunicates or cnidarians, were consistently detected in both the ascending and descending DVM samples. Ctenophores in four orders were present in our dataset along with three taxa that could not be classified past phylum. Some species of ctenophores and siphonophores have been observed to vertically migrate when strong physical stratification of the water column is absent, thus some taxa present in our dataset may represent active migrators over the course of our experimental timeframe (Júnior et al., 2015). Copepods (Class Maxillopoda) appear as the most dominant potential migrator in our eDNA dataset, comprising nearly 20% of eDNA sequences at some time points. Copepods are abundant zooplankton members in many ocean basins, and previous research has observed variable DVM patterns within this group (Bollens and Frost, 1991; Hays et al., 2001). Across our eDNA dataset, we identified at least 20 copepod taxa, of which 13 were classified as Calanoida. The dominance of calanoid copepods is consistent with other research showing that this group is the most successful of all copepods and able to colonize all depths in the water column (e.g., Huys and Boxshall, 1991; Fosshagen et al., 2001).

Signatures of Copepods: Actual Dynamics of the DVM?

The acoustic data in the present study capture the movement of mostly fish and other strong scatterers that form the dominant members of SSLs (> -60 dB). A clear migration signal can be seen for these organisms rising toward the surface displaying the characteristic DVM behavior, which co-occurs with a gradual increase in the size of organisms around the CTD (**Figure 5**). While our eDNA dataset does not necessarily capture an increase in these large migrators, we do see an increase in the relative abundance of copepod sequences (**Figure 6**) that precedes the arrival of larger acoustic targets (i.e., micronekton). Previous research has shown that calanoid copepods, the dominant copepod in our eDNA dataset, are often numerically dominant in these habitats and will migrate vertically to avoid predation (Bollens and Frost, 1989, 1991; Proud et al., 2019). While we lack direct evidence for predation avoidance in the current study, the pattern of relative abundance for two calanoid taxa (ASV18 & ASV19) in CTD 83 may suggest that these taxa are ascending to avoid vertically migrating micronekton predators. Further investigation of these dynamics is warranted, including direct sampling of these organisms, to derive any causality for the observed copepod dynamics, since other research has shown copepod vertical migration can be related to body condition (Hays et al., 2001) or environmental cues (Batchelder et al., 2002).

There are a few points of uncertainty in the current study that prevent us from drawing a direct relationship between the eDNA and acoustic datasets. The 18S eDNA dataset estimates a relative abundance of sequences in a volume of water, which can be difficult to relate to absolute abundances captured in the acoustic data. Additionally, we have some uncertainty as to whether our eDNA samples encompass a definitive time frame given the potential for differential residence time (i.e., how quickly DNA degrades in the pelagic environment; Rees et al., 2014; Thomsen and Willerslev, 2015) and how the presence of an organism in the environment relates to the timing of its presence in the eDNA dataset. Previous research has indicated a relatively low residence time for DNA in seawater (Dell'Anno and Corinaldesi, 2004), which would support that our eDNA dataset dynamics are capturing recent shifts in organism abundance. Despite these limitations, our data show the potential for eDNA to be widely used as a tool for monitoring pelagic biodiversity and the dynamics of the DVM. Several aspects of this study could be improved in future studies to increase the impact and resolution of eDNA data, and here we have made a few recommendations. Since the eDNA dataset captured many smaller pelagic organisms, coupling future eDNA samples with net sampling or a higher acoustic frequency that could discern smaller organisms such as copepods, would help calibrate eDNA results. These comparisons could help answer some key questions in eDNA research such as providing estimates of spatial and temporal distributions and more precise links between the presence of organisms in the environment and the presence of their DNA. Using multiple primer sets [e.g., 18S – current study, COI (fish and molluscs), 16S (crustaceans); Bernard et al., 2017; Bracken-Grissom, 2017] in order to minimize primer bias

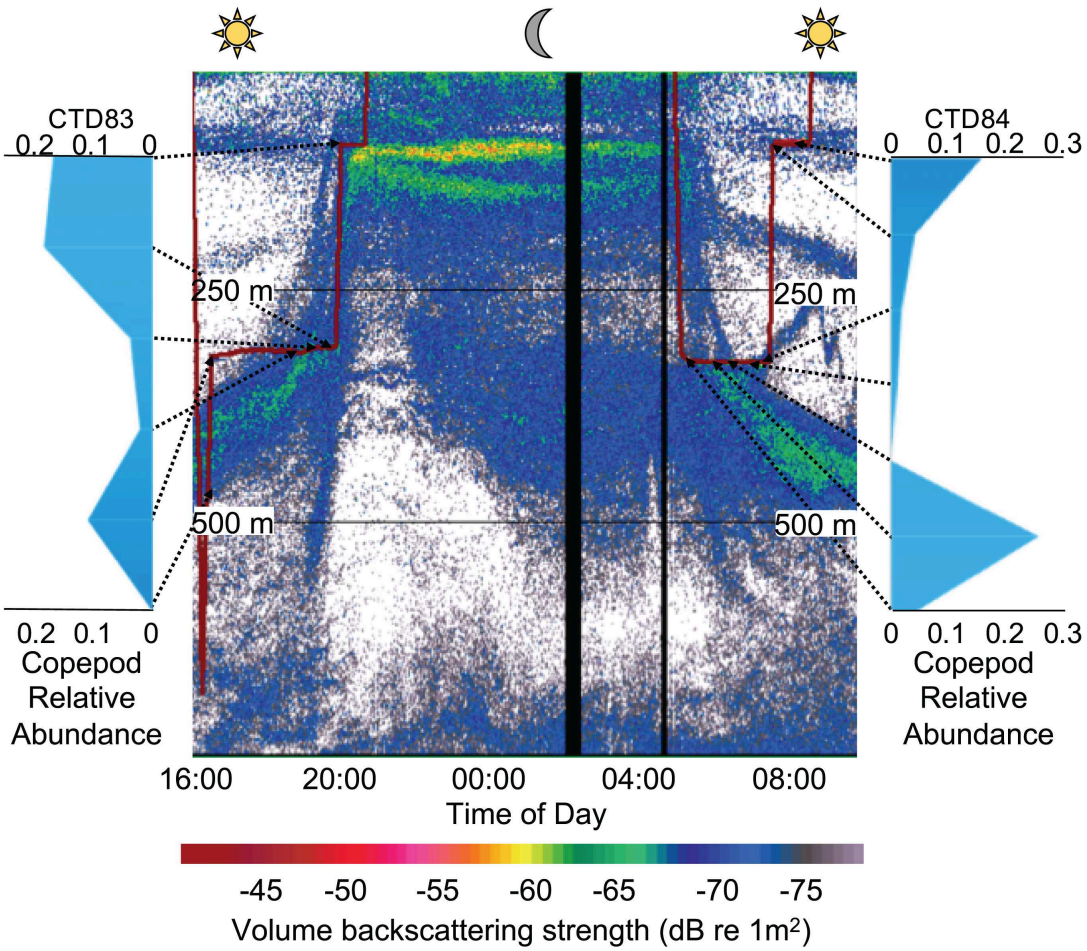

FIGURE 6 | Relative abundance of copepods detected with eDNA from water samples collected at depth (arrows) relative to the deep scattering layer observed at 38 kHz. Two water collection events are displayed (red line, CTD 83 and 84) during the ascending and descending phase of the migration, respectively. The WBAT was deployed on the CTD during the ascending migration phase at 320 m and 93 m depth). The two black vertical regions in the echogram represent periods where the echosounder was not operational.

in PCR reactions and generating longer sequencing amplicons would likely help capture additional diversity in the pelagic environment. Alternatively, a non-PCR metagenomics approach would eliminate all PCR bias but would require greatly increased sequencing depth.

CONCLUSION

In conclusion, we have expanded the application of an established molecular ecology method (eDNA sequencing) to an important global phenomenon (DVM). We demonstrate the identification of a diverse marine community within our eDNA dataset that for certain groups may capture additional biodiversity compared to more traditional sampling methods. Our data indicate that the taxa present before the DVM (outside the SSL) differ from those present within the SSLs and after the DVM. Some dynamics within our dataset appear to mirror changes in the acoustic data suggesting eDNA metabarcoding is capturing real shifts in the composition of vertically migrating organisms, however, additional effort is needed to resolve the source of backscatter data collected at depth and the identity of organisms that are being detected in eDNA profiles during DVM activities.

DATA AVAILABILITY STATEMENT

Data are publicly available through the Gulf of Mexico Research Initiative Information and Data Cooperative (GRIIDC) at https://data.gulfresearchinitiative.org [CTD Data DP05: doi: 10.7266/N7GM85P1 (English et al., 2018); raw acoustic data for DP05: doi: 10.7266/N7474871 (Boswell et al., 2018; Easson, 2020); eDNA sequence data DP05: doi: 10.7266/n7-awwx-4g13].

AUTHOR CONTRIBUTIONS

CE, KB, and JW contributed to the conception and design of the study. JL and KB collected acoustic and seawater samples.

CE generated genetic data, organized datasets, performed eDNA analysis, and constructed the initial design for the manuscript. KB, NT, and JW processed acoustic and CTD data for analysis. All authors contributed to the article and approved the submitted version.

FUNDING

This research was made possible by a grant from The Gulf of Mexico Research Initiative to support the consortium research entitled "Deep Pelagic Nekton Dynamics of the Gulf of Mexico" administered by Nova Southeastern University. This was contribution #200 from the Center for Coastal Oceans Research in the Institute of Water and Environment at Florida International University.

SUPPLEMENTARY MATERIAL

The Supplementary Material for this article can be found online at: https://www.frontiersin.org/articles/10.3389/fmars.2020.00552/full#supplementary-material

REFERENCES

Andersen, V. (1998). "Salp and pyrosomid blooms and their importance in biogeochemical cycles," in *The Biology of Pelagic Tunicates*, ed. Q. Bone (New York, NY: Oxford University Press), 125–137.

Barham, E. G. (1979). Giant larvacean houses: observations from deep submersibles. *Science* 205, 1129–1131. doi: 10.1126/science.205.4411.1129

Batchelder, H. P., Edwards, C. A., and Powell, T. M. (2002). Individual-based models of copepod populations in coastal upwelling regions: implications of physiologically and environmentally influenced diel vertical migration on demographic success and nearshore retention. *Prog. Oceanogr.* 53, 307–333. doi: 10.1016/s0079-6611(02)00035-6

Bernard, A., Weber, M., Finnegan, K., Shivji, M., and Eytan, R. (2017). *DNA Sequences of the Mitochondrial Cytochrome C Oxidase I (COI) Genes From Deep Sea Fishes. Cruises DP01 and DP02 from May 2015 - August 2015*. Texas, TX: Gulf of Mexico Research Initiative Information and Data Cooperative (GRIIDC).

Bista, I., Carvalho, G. R., Walsh, K., Seymour, M., Hajibabaei, M., Lallias, D., et al. (2017). Annual time-series analysis of aqueous eDNA reveals ecologically relevant dynamics of lake ecosystem biodiversity. *Nat. Comm.* 8:14087.

Bollens, S. M., and Frost, B. W. (1989). Zooplanktivorous fish and variable diel vertical migration in the marine planktonic copepod Calanus pacificus. *Limnol. Oceanogr.* 34, 1072–1083. doi: 10.4319/lo.1989.34.6.1072

Bollens, S. M., and Frost, B. W. (1991). Diel vertical migration in zooplankton: rapid individual response to predators. *J. Plankton Res.* 13, 1359–1365. doi: 10.1093/plankt/13.6.1359

Boswell, K., Sutton, T. T., and LaBua, S. (2018). *Raw Acoustic Scattering Data of Organisms From the Water Column, Cruise DP05, April 2017 – May 2017*. Texas, TX: Gulf of Mexico Research Initiative Information and Data Cooperative (GRIIDC).

Boswell, K. M., D'Elia, M., Johnston, M. W., Mohan, J. A., Warren, J. D., Wells, R. J., et al. (2020). Oceanographic structure and light levels drive patterns of sound scattering layers in a low-latitude oceanic system. *Front. Mar. Sci.* 7:51. doi: 10.3389/fmars.2020.00051

Bracken-Grissom, H. (2017). *16S and COI Barcoding Sequences for Crustaceans and Cephalopods in the Gulf of Mexico and Florida Straits From 2015-2016*. Texas, TX: Gulf of Mexico Research Initiative Information and Data Cooperative (GRIIDC).

Bucklin, A., Lindeque, P. K., Rodriguez-Ezpeleta, N., Albaina, A., and Lehtiniemi, M. (2016). Metabarcoding of marine zooplankton: prospects, progress and pitfalls. *J. Plankton Res.* 38, 393–400. doi: 10.1093/plankt/fbw023

Callahan, B. J., McMurdie, P. J., Rosen, M. J., Han, A. W., Johnson, A. J. A., and Holmes, S. P. (2016). DADA2: high-resolution sample inference from illumina amplicon data. *Nat. Methods* 13:581. doi: 10.1038/nmeth.3869

Cook, A., and Sutton, T. (2018). *Inventory of Oceanic Fauna Data Including Species, Weight, and Measurements From R/V Point Sur (Cruise DP05) in the Gulf of Mexico From 2017-05-01 to 2017-05-11*. Texas, TX: Gulf of Mexico Research Initiative Information and Data Cooperative (GRIIDC).

Cowart, D. A., Murphy, K. R., and Cheng, C. H. C. (2018). Metagenomic sequencing of environmental DNA reveals marine faunal assemblages from the West Antarctic Peninsula. *Mar. Genom.* 37, 148–160. doi: 10.1016/j.margen.2017.11.003

De Robertis, A., and Higginbottom, I. (2007). A post-processing technique to estimate the signal-to-noise ratio and remove echosounder background noise. *ICES J. Mar. Sci.* 64, 1282–1291. doi: 10.1093/icesjms/fsm112

de Vargas, C., Audic, S., Henry, N., Decelle, J., Mahé, F., Logares, R., et al. (2015). Eukaryotic plankton diversity in the sunlit ocean. *Science* 348:126 1605.

D'Elia, M., Warren, J. D., Rodriguez-Pinto, I., Sutton, T. T., Cook, A., and Boswell, K. M. (2016). Diel variation in the vertical distribution of deep-water scattering layers in the Gulf of Mexico. *Deep Sea Res. Part I Oceanogr. Res. Pap.* 115, 91–102. doi: 10.1016/j.dsr.2016.05.014

Dell'Anno, A., and Corinaldesi, C. (2004). Degradation and turnover of extracellular DNA in marine sediments: ecological and methodological considerations. *Appl. Environ. Microbiol.* 70, 4384–4386. doi: 10.1128/aem.70.7.4384-4386.2004

Demer, D. A., Berger, L., Bernasconi, M., Bethke, E., Boswell, K., Chu, D., et al. (2015). *Calibration of Acoustic Instruments*. ICES Cooperative Research Report No. 326.

Easson, C. (2020). "Eukaryotic 18S rRNA Sequences as part of eDNA analyses of Diel Vertical Migration of Mixed Consortia in the Gulf of Mexico from 2016-05-03 to 2017-05-11," in *Distributed by: Gulf of Mexico Research Initiative Information and Data Cooperative (GRIIDC), Harte Research Institute* (Texas A&M University–Corpus Christi). doi: 10.7266/n7-awwx-4g13

Easson, C. G., and Lopez, J. V. (2019). Environmental drivers of bacterioplankton community structure in the northern Gulf of Mexico. *Front. Microb.* 9:3175. doi: 10.3389/fmicb.2018.03175

English, D., Hu, C., Cook, A., and Sutton, T. (2018). *Conductivity, Temperature, and Depth (CTD) Data for DEEPEND Stations, Cruise DP05, May 2017*. Texas, TX: Gulf of Mexico Research Initiative Information and Data Cooperative (GRIIDC).

Fennell, S., and Rose, G. (2015). Oceanographic influences on deep scattering layers across the North Atlantic. *Deep Sea Res. Part I Oceanogr. Res. Pap.* 105, 132–141. doi: 10.1016/j.dsr.2015.09.002

Foote, A. D., Thomsen, P. F., Sveegaard, S., Wahlberg, M., Kielgast, J., Kyhn, L. A., et al. (2012). Investigating the potential use of environmental DNA (eDNA) for genetic monitoring of marine mammals. *PLoS One* 7:e41781. doi: 10.1371/journal.pone.0041781

Fosshagen, A., Boxshall, G. A., and Iliffe, T. M. (2001). The epacteriscidae, a cave-living family of calanoid copepods. *Sarsia* 86, 245–318. doi: 10.1080/00364827.2001.10425520

Guillou, L., Viprey, M., Chambouvet, A., Welsh, R. M., Kirkham, A. R., Massana, R., et al. (2008). Widespread occurrence and genetic diversity of marine parasitoids belonging to Syndiniales (Alveolata). *Environ. Microbiol.* 10, 3349–3365. doi: 10.1111/j.1462-2920.2008.01731.x

Hays, G. C. (2003). "A review of the adaptive significance and ecosystem consequences of zooplankton diel vertical migrations," in *Migrations and Dispersal of Marine Organisms*, (Dordrecht: Springer), 163–170. doi: 10.1023/b:hydr.0000008476.23617.b0

Hays, G. C., Kennedy, H., and Frost, B. W. (2001). Individual variability in diel vertical migration of a marine copepod: why some individuals remain at depth when others migrate. *Limnol. Oceanogr.* 46, 2050–2054. doi: 10.4319/lo.2001.46.8.2050

Hazen, E. L., Friedlaender, A. S., Thompson, M. A., Ware, C. R., Weinrich, M. T., Halpin, P. N., et al. (2009). Fine-scale prey aggregations and foraging ecology of humpback whales Megaptera novaeangliae. *Mar. Ecol. Prog. Ser.* 395, 75–89. doi: 10.3354/meps08108

Henschke, N., Pakhomov, E. A., Kwong, L. E., Everett, J. D., Laiolo, L., Coghlan, A. R., et al. (2019). Large vertical migrations of Pyrosoma atlanticum play an important role in active carbon transport. *J. Geophys. Res. Biogeo*. 124, 1056–1070. doi: 10.1029/2018jg004918

Huys, R., and Boxshall, G. A. (1991). *Copepod Evolution: 1-468*. London: The Ray Society, 159.

Irigoien, X., Klevjer, T. A., Røstad, A., Martinez, U., Boyra, G., Acuña, J. L., et al. (2014). Large mesopelagic fishes biomass and trophic efficiency in the open ocean. *Nat. Comm.* 5:3271.

Júnior, M. N., Brandini, F. P., and Codina, J. C. U. (2015). Diel vertical dynamics of gelatinous zooplankton (Cnidaria, Ctenophora and Thaliacea) in a subtropical stratified ecosystem (South Brazilian Bight). *PLoS One* 10:e0144161. doi: 10.1371/journal.pone.0144161

Kembel, S. W., Cowan, P. D., Helmus, M. R., Cornwell, W. K., Morlon, H., Ackerly, D. D., et al. (2010). Picante: R tools for integrating phylogenies and ecology. *Bioinformatics* 26, 1463–1464. doi: 10.1093/bioinformatics/btq166

Klevjer, T. A., Irigoien, X., Røstad, A., Fraile-Nuez, E., Benítez-Barrios, V. M., and Kaartvedt, S. (2016). Large scale patterns in vertical distribution and behaviour of mesopelagic scattering layers. *Sci. Rep.* 6:19873.

Kloser, R. J., Ryan, T. E., Keith, G., and Gershwin, L. (2016). Deep-scattering layer, gas-bladder density, and size estimates using a two-frequency acoustic and optical probe. *ICES J. Mar. Sci.* 73, 2037–2048. doi: 10.1093/icesjms/fsv257

Kloser, R. J., Ryan, T. E., Young, J. W., and Lewis, M. E. (2009). Acoustic observations of micronekton fish on the scale of an ocean basin: potential and challenges. *ICES J. Mar. Sci.* 66, 998–1006. doi: 10.1093/icesjms/fsp077

Kubilius, R., Ona, E., and Calise, L. (2015). Measuring in situ krill tilt orientation by stereo photogrammetry: examples for *Euphausia superba* and *Meganyctiphanes norvegica*. *ICES J. Mar. Sci.* 72, 2494–2505. doi: 10.1093/icesjms/fsv077

Kvist, S. (2013). Barcoding in the dark: a critical view of the sufficiency of zoological DNA barcoding databases and a plea for broader integration of taxonomic knowledge. *Mol. Phylogenet. Evol.* 69, 39–45. doi: 10.1016/j.ympev.2013.05.012

Lavery, A. C., Wiebe, P. H., Stanton, T. K., Lawson, G. L., Benfield, M. C., and Copley, N. (2007). Determining dominant scatterers of sound in mixed zooplankton populations. *J. Acoust. Soc. Am.* 122, 3304–3326. doi: 10.1121/1.2793613

Lurton, X. (2002). *An Introduction to Underwater Acoustics: Principles and Applications*. Berlin: Springer Science & Business Media.

MacLennan, D. N., Fernandes, P. G., and Dalen, J. (2002). A consistent approach to definitions and symbols in fisheries acoustics. *ICES J. Mar. Sci.* 59, 365–369. doi: 10.1006/jmsc.2001.1158

Mapstone, G. M. (2014). Global diversity and review of Siphonophorae (Cnidaria: Hydrozoa). *PLoS One* 9:e87737. doi: 10.1371/journal.pone.0087737

McDougall, T. J., and Barker, P. M. (2011). Getting started with TEOS-10 and the Gibbs Seawater (GSW) oceanographic toolbox. *SCOR/IAPSO WG* 127, 1–28.

Milligan, R. J., Bernard, A. M., Boswell, K. M., Bracken-Grissom, H. D., D'Elia, M. A., DeRada, S., et al. (2018). The application of novel research technologies by the deep pelagic nekton dynamics of the Gulf of Mexico (DEEPEND) Consortium. *Mar. Technol. Soc. J.* 52, 81–86. doi: 10.4031/mtsj.52.6.10

Oksanen, J., Blanchet, F. G., Friendly, M., Kindt, R., Legendre, P., McGlinn, D., et al. (2017). *Vegan: Community Ecology Package*. R package version 2.4–5.

Proud, R., Cox, M. J., and Brierley, A. S. (2017). Biogeography of the global ocean's mesopelagic zone. *Curr. Biol.* 27, 113–119. doi: 10.1016/j.cub.2016.11.003

Proud, R., Handegard, N. O., Kloser, R. J., Cox, M. J., and Brierley, A. S. (2019). From siphonophores to deep scattering layers: uncertainty ranges for the estimation of global mesopelagic fish biomass. *ICES J. Mar. Sci.* 76, 718–733. doi: 10.1093/icesjms/fsy037

Quast, C., Pruesse, E., Gerken, J., Schweer, T., Yilmaz, P., Peplies, J., et al. (2015). "SILVA databases," in *Encyclopedia of Metagenomics: Genes, Genomes and Metagenomes: Basics, Methods, Databases and Tools*, ed. K. E. Nelson (Berlin: Springer). 626–635.

R Core Team (2018). *R: A Language and Environment for Statistical Computing*. Vienna: R Foundation for Statistical Computing.

Rees, H. C., Maddison, B. C., Middleditch, D. J., Patmore, J. R., and Gough, K. C. (2014). The detection of aquatic animal species using environmental DNA–a review of eDNA as a survey tool in ecology. *J. Appl. Ecol.* 51, 1450–1459. doi: 10.1111/1365-2664.12306

Ressler, P. H. (2002). Acoustic backscatter measurements with a 153 kHz ADCP in the northeastern Gulf of Mexico: determination of dominant zooplankton and micronekton scatterers. *Deep Sea Res. Part I Oceanogr. Res. Pap.* 49, 2035–2051. doi: 10.1016/S0967-0637(02)00117-6

Robison, B. H. (2004). Deep pelagic biology. *J. Exp. Mar. Biol. Ecol.* 300, 253–272. doi: 10.1016/j.jembe.2004.01.012

Ruppert, K. M., Kline, R. J., and Rahman, M. S. (2019). Past, present, and future perspectives of environmental DNA (eDNA) metabarcoding: a systematic review in methods, monitoring, and applications of global eDNA. *Glob. Ecol. Conserv.* 17: e00547. doi: 10.1016/j.gecco.2019.e00547

Sanvicente-Añorve, L., Alba, C., Alatorre, M. A., and Flores-Coto, C. (2007). Cross-shelf and vertical distribution of siphonophore assemblages under the influence of freshwater outflows in the southern Gulf of Mexico. *Hydrobiologia* 586, 69–78. doi: 10.1007/s10750-006-0492-6

Sieracki, M. E., Poulton, N. J., Jaillon, O., Wincker, P., de Vargas, C., Rubinat-Ripoll, L., et al. (2019). Single cell genomics yields a wide diversity of small planktonic protists across major ocean ecosystems. *Sci. Rep.* 9, 1–11.

Steinberg, D. K. (1995). Diet of copepods (Scopalatum vorax) associated with mesopelagic detritus (giant larvacean houses) in Monterey Bay, California. *Mar. Biol.* 122, 571–584. doi: 10.1007/bf00350679

Sutton, T. T. (2013). Vertical ecology of the pelagic ocean: classical patterns and new perspectives. *J. Fish. Biol.* 83, 1508–1527. doi: 10.1111/jfb.12263

Sutton, T. T., Clark, M. R., Dunn, D. C., Halpin, P. N., Rogers, A. D., Guinotte, J., et al. (2017). A global biogeographic classification of the mesopelagic zone. *Deep Sea Res. Part I Oceanog. Res. Pap.* 126, 85–102. doi: 10.1016/j.dsr.2017.05.006

Thomsen, P. F., and Willerslev, E. (2015). Environmental DNA–An emerging tool in conservation for monitoring past and present biodiversity. *Biol. Conserv.* 183, 4–18. doi: 10.1016/j.biocon.2014.11.019

Warren, J. D., Stanton, T. K., Benfield, M. C., Wiebe, P. H., Chu, D., and Sutor, M. (2001). In situ measurements of acoustic target strengths of gas-bearing siphonophores. *ICES J. Mar. Sci.* 58, 740–749. doi: 10.1006/jmsc.2001.1047

Zwolinski, J. P., Oliveira, P. B., Quintino, V., and Stratoudakis, Y. (2010). Sardine potential habitat and environmental forcing off western Portugal. *ICES J. Mar. Sci.* 67, 1553–1564. doi: 10.1093/icesjms/fsq068

Conflict of Interest: The authors declare that the research was conducted in the absence of any commercial or financial relationships that could be construed as a potential conflict of interest.

frontiers in Marine Science

ORIGINAL RESEARCH
published: 10 July 2020
doi: 10.3389/fmars.2020.00579

Taxonomic Richness and Diversity of Larval Fish Assemblages in the Oceanic Gulf of Mexico: Links to Oceanographic Conditions

Corinne R. Meinert[1], Kimberly Clausen-Sparks[1], Maëlle Cornic[1], Tracey T. Sutton[2] and Jay R. Rooker[1,3]*

[1] Department of Marine Biology, Texas A&M University, Galveston, TX, United States, [2] Department of Marine and Environmental Sciences, Nova Southeastern University, Dania Beach, FL, United States, [3] Department of Wildlife and Fisheries Sciences, Texas A&M University, College Station, TX, United States

Biodiversity enhances the productivity and stability of marine ecosystems and provides important ecosystem services. The aim of this study was to characterize larval fish assemblages in pelagic waters of the northern Gulf of Mexico (NGoM) and identify oceanographic conditions associated with areas of increased taxonomic richness (T_F) and Shannon diversity (H'). Summer ichthyoplankton surveys were conducted in the NGoM in 2015 and 2016 using neuston net (surface layer; upper 1 m) and oblique bongo net (mixed layer; 0–100 m) tows. Over 17,000 fish larvae were collected over the two-year study, and 99 families of fish larvae were present. Catch composition in the surface layer was relatively similar to the mixed-layer catch, with carangids (jacks), scombrids (mackerels, tunas), and exocoetids (flyingfishes) being numerically dominant, while deep-pelagic species, including myctophids (lanternfishes), gonostomatids (bristlemouths), and sternoptychids (marine hatchetfishes), were present almost exclusively in the mixed layer samples. Generalized additive models were used to evaluate the effect of oceanographic conditions on ichthyoplankton abundance and biodiversity. Salinity and sea surface height (SSH) were the most influential oceanographic conditions, with higher occurrence, higher T_F, and higher H' all present in areas of lower salinity, and lower SSH. This study highlights the ecological importance of cyclonic mesoscale features and areas of upwelling as areas of increased biodiversity for larval fishes, and also indicates that the mixed layer in the NGoM is essential habitat for deep-pelagic fishes during the early life interval.

Keywords: pelagic fishes, ichthyoplankton, mesopelagic, epipelagic, biodiversity, open ocean, Loop Current, Gulf of Mexico

OPEN ACCESS

Edited by:
Michael Vecchione, National Oceanic and Atmospheric Administration (NOAA), United States

Reviewed by:
Andrew Corso, College of William & Mary, United States
Andrew Richard Thompson, National Oceanic and Atmospheric Administration (NOAA), United States

****Correspondence:***
Corinne R. Meinert
corinneraem@gmail.com; meinert.8@tamu.edu

Specialty section:
This article was submitted to Deep-Sea Environments and Ecology, a section of the journal Frontiers in Marine Science

Received: *30 July 2019*
Accepted: *22 June 2020*
Published: *10 July 2020*

Citation:
Meinert CR, Clausen-Sparks K, Cornic M, Sutton TT and Rooker JR (2020) Taxonomic Richness and Diversity of Larval Fish Assemblages in the Oceanic Gulf of Mexico: Links to Oceanographic Conditions. Front. Mar. Sci. 7:579. doi: 10.3389/fmars.2020.00579

INTRODUCTION

Pelagic fishes play an important role in open ocean ecosystems, and changes in their abundances can impact community structure and ecosystem stability (Cury, 2000; Myers, 2003; Myers and Worm, 2003). Declines in the abundances of pelagic fishes are often attributed to overfishing (Ward and Myers, 2005) but other types of anthropogenic disturbance (e.g., habitat loss or degradation)

and climate change also influence their distribution and abundance (Lehodey et al., 2006; Rijnsdorp et al., 2009). New management approaches that focus on ecosystem-level processes rather than single stocks or species are necessary to effectively mitigate past overexploitation and better understand the drivers of community change in pelagic ecosystems (Pikitch et al., 2004).

Research on the early life stages of pelagic fishes is important because it can provide information on spawning locations, spawning stock biomass, and population-level processes (Houde, 2002). Unfortunately, studies on larvae and juvenile fishes during the first few months of life are limited or non-existent for many open ocean species despite the fact that biological data on these stages are needed to better assess and monitor recruitment variability. Temporal and spatial trends in the distribution and abundance of fish larvae can be used to identify environmental factors that affect early life survival (Nonaka et al., 2000). Moreover, changes in the distribution, abundance, and assemblage composition can also be indicative of changing oceanographic conditions (Hernandez et al., 2010; Carassou, 2012), including anthropogenic disturbances such as the *Deepwater Horizon* oil spill (Rooker et al., 2013; Kitchens and Rooker, 2014). To date, information on the early life ecology and the environmental drivers of abundance of pelagic fishes in the Northern Gulf of Mexico (NGoM) is incomplete for most taxa. This is particularly true when considering the numerically dominant deep-pelagic taxa, and such information is needed to fill in data gaps regarding factors that influence the distribution, abundance, and population dynamics of pelagic species (Richardson, 2008).

The pelagic environment in particular provides unique challenges for locating areas of high biodiversity because the geographic location of mesoscale features and associated conditions are dynamic in time and space (Marchese, 2015). As a result, management of pelagic ecosystems requires multifaceted approaches that couple ecology and oceanography (Game et al., 2009; Lewison et al., 2015). Despite increased awareness of the importance of biodiversity, our understanding of biological communities in pelagic ecosystems is incomplete (Mittermeier et al., 2011). Identifying areas of high taxonomic richness (T_F) and diversity and the oceanographic conditions that create or maintain areas of elevated biodiversity are critical because species-rich ecosystems are considered more stable and less likely to collapse compared to species-poor ecosystems (Bakun, 2006; Worm et al., 2006). Increased biodiversity also has a positive impact on ecosystem services and functions, such as resource use efficiency, nutrient cycling, and higher fisheries yields, and can stabilize ecosystems against regime shifts (Gamfeldt et al., 2014; Rocha et al., 2015).

As a model system, the NGoM offers many advantages for evaluating the biodiversity and structure of larval fish assemblages. Most notably, the oceanic component of this region is generally considered oligotrophic, but gets occasional injections of nutrient discharges from the Mississippi-Atchafalaya River System (MARS) that lead to higher productivity (Dagg and Breed, 2003). This supports primary and secondary production and high fishery yields of "coastal pelagic" taxa (Browder, 1993). Surrounding the MARS plume, densities of fish larvae may reach up to 20 times higher than reported for other areas of the GoM (Grimes and Finucane, 1991; Richards, 1993). In addition, the Loop Current and associated mesoscale features in the NGoM can concentrate fish eggs and larvae, particularly along fronts associated with divergent (cyclonic), and convergent (anticyclonic) eddies (Richards, 1993; Shulzitski et al., 2015). These mesoscale features play an important role in regulating the spatial distribution of ichthyoplankton (Karnauskas et al., 2013), and a higher northern intrusion of the Loop Current has been shown to increase the abundance of fish larvae in the NGoM (Lindo-Atichati, 2012). The Loop Current is generally associated with higher salinity and warmer waters. In particular, cyclonic features (cold core) often enhance production through upwelling, leading to increased foraging opportunities for fish larvae, and are thus assumed to serve as critical nursery habitat for several taxa of pelagic fishes (Richardson et al., 2010).

Here, we assess the attributes of the NGoM as early life habitat of pelagic fishes, including deep-pelagic taxa, with a special emphasis on identifying areas, and oceanographic conditions that support larval fish assemblages with high T_F and Shannon diversity (H'). When determining biodiversity of the pelagic environment, it is well recognized that mesopelagic fauna (depth range: 200 to 1000 m) of both invertebrates and fishes, frequent the upper 200 m of the water column, or epipelagic zone during all life stages through diel vertical migration (Richards, 1993). In response, deep-pelagic fish taxa may be important determinants of T_F and H' in the epipelagic zone, and an objective of this study was to quantify linkages between fishes typically associated with these two different zones of the water column. We also coupled T_F and H' with physicochemical and biological factors using generalized additive models (GAMs) to evaluate the relative importance of oceanographic conditions on biodiversity, which provides a means for identifying regions and conditions that support species-rich assemblages of fish larvae in the NGoM. We hypothesize that biodiversity hotspots for larval fishes (high T_F and H') in the NGoM will occur primarily in convergence zones (frontal features).

MATERIALS AND METHODS

Sample Design

Ichthyoplankton surveys were conducted in June and July over two consecutive years (2015, 2016) in a sampling corridor that ranged from 27.0–28.0°N and 88.0–91.0°W. The sampling corridor contained 48 stations located on transects at both 27.0°N and 28.0°N, with stations along each transect approximately 15 km apart (**Figure 1**), which represents an area sampled continuously for the past decade to assess larval recruitment variability of pelagic fishes, including billfishes, tunas, dolphinfishes, and swordfish (e.g., Rooker et al., 2012, 2013; Kitchens and Rooker, 2014; Cornic et al., 2018). Near-surface sampling was conducted with a 1 × 2 m neuston net rigged with a 1200 μm mesh. Neuston net tows were conducted in the upper 1 m of the water column (surface layer) at each station, and each tow was approximately 10 min in duration. In addition, oblique bongo net tows were conducted from between

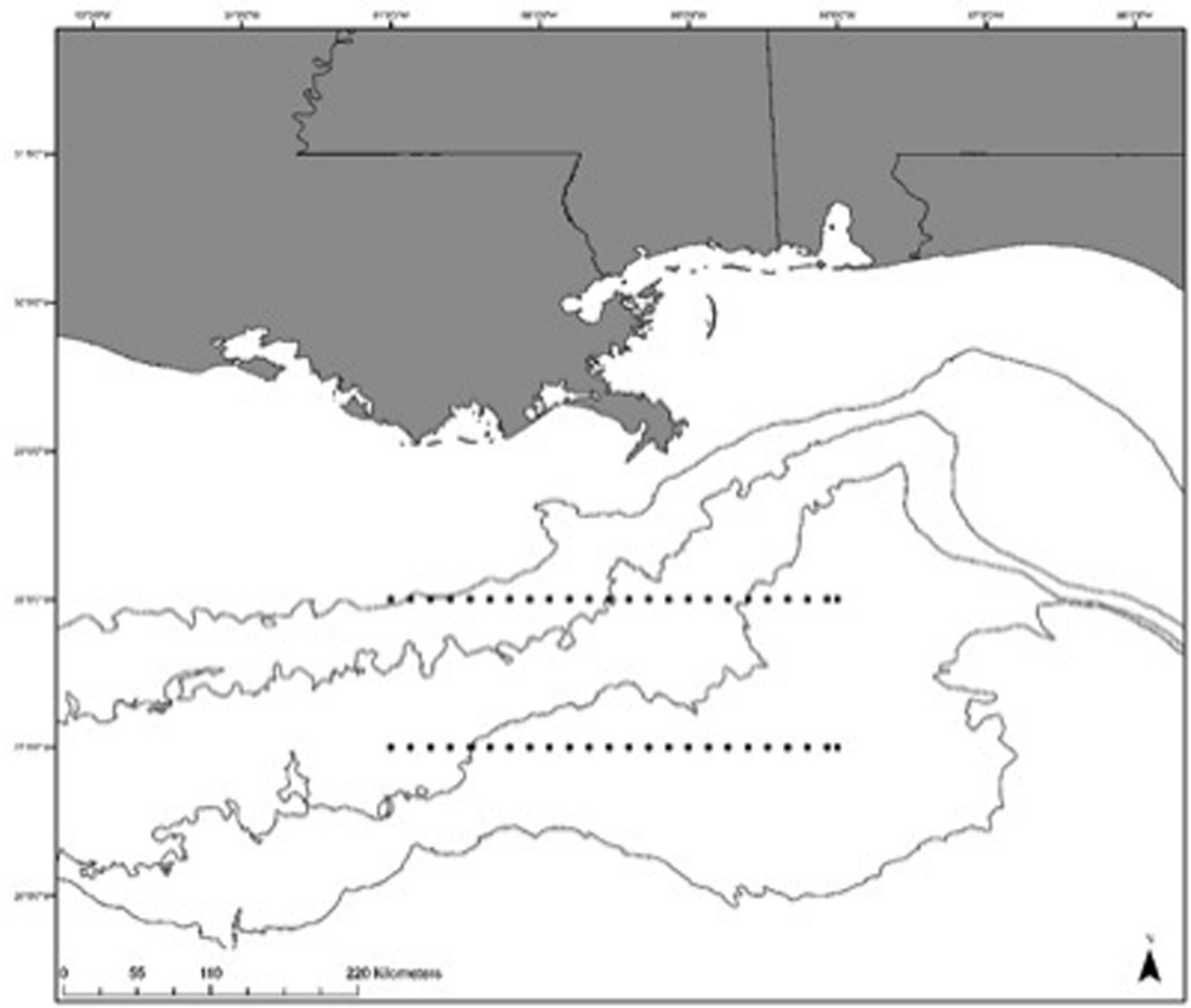

FIGURE 1 | Sampling sites (black dots) of the June and July ichthyoplankton cruises performed in 2015 and 2016 in the Northern Gulf of Mexico.

0–100 + m of the water column (mixed layer) at each station; paired bongo nets were rigged with 333-μm mesh and 500-μm mesh nets. Although different mesh sizes were used for surface and mixed layer sampling, catch composition is known to be similar between the mesh sizes and gears with similar tow profiles (Richards, 1993; Randall et al., 2015), which allows for general comparisons of assemblage structure and diversity between the two distinct regions of the water column. All tows were performed at a vessel speed of approximately 2.5 knots, and the volume of water sampled during each tow was determined by equipping nets with General Oceanics flowmeters (Model 2030R, Miami, FL, United States).

Sargassum (kg/m^3) collected in the neuston nets and invertebrates in the neuston and combined bongo nets (kg/m^3) were separated, weighed, and recorded. Samples from neuston and combined 333-μm mesh and 500-μm bongo tows were preserved in a 100% ethanol solution for transport back to the lab. Sea surface temperature (SST, °C), salinity, and dissolved oxygen (mg/L) were measured at the surface of each station using a Sonde 6920 Environmental Monitoring System (YSI Inc., Yellow Springs, Ohio, United States). Other oceanographic parameters at each station were determined using remotely sensed data accessed through Copernicus Marine Environmental Monitoring Service[1] and the marine geospatial ecology toolbox (version 0.8a44) in ArcGIS (version 10.0). Sea surface height (SSH, m) data were calculated weekly at a resolution of 1/4 degree using satellite altimetry measurements (GLOBAL_ANALYSIS_PHYS_001_020) from Copernicus[2]. Distance to the Loop Current was estimated by measuring the linear distance from the edge of the feature (km), based on the 20-cm SSH contour following Randall et al. (2015) using the

[1]http://marine.copernicus.eu/

[2]http://marine.copernicus.eu/services-portfolio/access-to-products/

Spatial Analyst toolbox in ArcGIS. Water depth at each station was estimated from NOAA National Geophysical Data Center using the GEODAS US Coastal Relief Model Grid with a grid cell size of 3 arc-s[3].

Samples from each station were sorted under Leica MZ stereomicroscope in the laboratory and fish larvae were isolated and preserved in 70% ethanol solution. All fish larvae were identified to family through visual identification following keys in Richards (2006), with family used as the taxonomic level for assessing biodiversity (Hernandez et al., 2013). Although T_F and H' were estimated from identification to family level, genetic approaches such as High resolution Melting Analysis and Polymerase chain reaction were often used to determine species identification for certain taxa, which provided confirmation of assignments to the family level for all individuals assayed (Smith et al., 2009). Issues that led to identification of unknown specimens included trawl damage to the specimen and/or individuals too small to accurately identify. Damaged samples had either a significant amount of tissue missing or only part of the body was found. Individuals with a total standard length of less than 2 mm were too small to accurately identify in some cases.

Data Analysis

Two diversity measures were applied to the larval fish assemblages. Species richness (S) is commonly used to represent total number of species per sample but here we estimated T_F as the number of families present in each sample. Similarly, Shannon diversity (H') was based on diversity at the family level following the equation

$$H^{'} = \frac{n \log n - \Sigma\, fi \log fi}{n}$$

where n is the total number of individuals and f_i is the number of individuals for each family.

Diversity measures T_F and H' were used for statistical testing, with each station consisting of both surface layer and mixed layer samples. A two-way analysis of variance (ANOVA) was used to examine effects of station location and month-year date with separate models developed using TF and H' as dependent variables. A Bonferroni adjustment was used to account for multiple testing to decrease chances for a Type I error. Two-way ANOVAs were also used to examine inter- and intra-annual differences in both TF and H' for surface layer, mixed layer, and combined samples. Tukey's honestly significant difference (HSD) test was used to test for *post hoc* differences among means. All statistical analyses were run using R (version 3.4.2) with alpha set at 0.05 (Wood, 2011; Oksanen et al., 2017).

Generalized additive models were used to examine the influence of oceanographic factors for varying time periods (month, year) on T_F and H'. Explanatory variables used in GAMs were month, year, SST, SSH, distance to Loop Current boundary, salinity (SAL), dissolved oxygen (DO), depth, invertebrate biomass, and *Sargassum* biomass. GAMs are extensions of general linear models and allow fixed effects to be modeled by using a smoothing function (Guisan et al., 2002). General GAM construction follows the equation:

$$E\,[y] = g^{-1}\left(\beta_O + \sum_k S_k\,(x_k)\right)$$

Where $E[y]$ equals the expected values of the response variable (T_F or H'), g represents the link function, β_0 equals the intercept, x represents one of k explanatory variables, and S_k represents the smoothing function of each respective explanatory variable. In addition to oceanographic data collected at each station described earlier, remotely sensed data (SSH, distance to Loop Current) were included as explanatory variables in GAMs. Spatial autocorrelation was not deemed to be an issue for fixed stations given the dynamic nature of oceanographic conditions across our sampling corridor. A manual procedure was used to identify influential variables on TF and H', and the final model for each diversity measure was based on minimizing the Akaike information criterion (AIC). Collinearity among variables was examined using Spearman's test and variance inflation factor (VIF), ($\rho > 0.60$ and VIF > 5); collinearity was not found to be an issue thus all environmental variables were tested. A manual backward stepwise selection process was used to remove explanatory variables that did not influence T_F or H' based models. Stepwise selection ended when all remaining variables were significant ($p > 0.05$) or the AIC value started to increase when non-significant variables were removed. Percent deviance explained (DE) was calculated for each model to examine overall fit. Once the final model was selected, each variable was removed individually to see the response in ΔAIC, and ΔDE in order to assess the relative importance of each predictor variable following Rooker et al. (2012).

RESULTS

Assemblage Composition

A total of 17,091 larvae (N = 9,551 in 2015 and N = 7,540 in 2016) comprising 99 families were collected over 2 years of sampling in the NGoM (**Table 1**). The top five families by percent composition in 2015 from the surface layer accounted for over 70% of the larvae collected: carangids (jacks), clupeids (herrings), exocoetids (flyingfishes), scombrids (mackerels and tunas), and istiophorids (billfishes). For the mixed layer in 2015, myctophids (lanternfishes), scombrids, carangids, gonostomatids (bristlemouths), and gobiids (gobies) were the dominant families by percent composition (**Table 1**). General trends in catch percent composition persisted in 2016 and numerically dominant families in the surface layer were carangids, exocoetids, scombrids, istiophorids, and hermiramphids (halfbeaks), with carangids alone accounting for nearly 40% of the larvae collected. Deep-pelagic taxa again dominated the mixed layer from 2016 with 41% of the catch comprised of myctophids, gonostomatids, and bregmacerotids (codlets) larvae. A small percentage of the fish larvae collected (~6%) could not be positively identified because of damage or the larvae were too small.

[3]http://www.ngdc.noaa.gov/mgg/gdas/gd_designagrid.html

TABLE 1 | Catch data of larvae in the northern Gulf of Mexico in 2015 and 2016 from surface (0–1 m with neuston tows) and mixed layer (0–100 + m with oblique bongo tows).

Family	2015 Surface density	2015 Surface % occurrence	2015 Mixed layer density	2015 Mixed % occurrence	2016 Surface density	2016 Surface % occurrence	2016 Mixed layer Density	2016 Mixed layer % occurrence
Acanthuridae (surgeonfishes)			0.3	9.4				
Acropomatidae (lanternbellies)	1.6	1.4	1.1	27.8			0.7	12.8
Alepisauridae (lancetfish)			0.1	3.1			0.9	2.3
Anguillidae (freshwater eels)			0.3	8.3			0.4	7.0
Antennariidae (frogfishes)	0.7	28.1	0.7	18.8	0.1	1.7	0.5	13.0
Atherinopsidae (New World silversides)	0.4	5.3						
Apogonidae (cardinalfishes)			0.7	2.8			0.4	1.2
Ariommatidae (ariommatids)			0.4	8.3			0.1	2.3
Balistidae (triggerfishes)	1.0	38.0	0.2	5.3	0.2	21.4	0.2	3.5
Bathylagidae (deep-sea smelts)			0.7	2.8			0.5	1.5
Belonidae (needlefishes)			0.7	2.8				
Blenniidae (combtooth blennies)	0.6	9.4						
Bothidae (lefteye flounders)			2.3	36.5	0.3	4.8	1.8	25.6
Bramidae (pomfrets)			0.3	7.3			0.7	2.3
Bregmacerotidae (codlets)	0.2	1.4	9.9	58.3			16.9	75.6
Callionymidae (dragonets)			0.9	19.8			0.2	4.7
Caproidae (boarfishes)	0.2	2.8			0.1	1.2	0.4	1.2
Carangidae (jacks)	13.2	71.9	2.5	75.0	6.5	6.7	19.9	62.8
Carapidae (pearlfishes)	0.3	1.4	0.1	3.1			0.4	1.2
Ceratiidae (seadevils)							0.1	3.5
Centrophrynidae (prickly seadevils)			0.3	1.4				
Cetomimidae (flabby whalefishes)			0.1	3.1			0.4	1.2
Chaetodontidae (butterflyfishes)			0.3	1.4				
Chiasmodontidae (swallowers)			0.1	4.2			0.3	7.0
Chlorophthalmidae (greeneyes)	0.2	1.4	1.6	21.9	0.3	1.2	0.2	4.7
Clupeidae (herrings)	7.9	1.4	8.5	1.4	0.3	14.0	2.6	17.4
Congridae (conger eels)			0.5	1.4	0.7	3.6	0.9	14.0
Coryphaenidae (dolphinfishes)	0.4	1.4	0.3	3.1	0.2	17.9	0.4	23.3
Cynoglossidae (tonguefishes)	0.2	22.9	0.8	17.8			4.5	7.0
Dactylopteridae (flying gurnards)	0.5	4.2	0.4	12.5	0.1	2.4		
Diodontidae (porcupinefishes)			0.3	1.4				
Diretmidae (spinyfins)			0.3	1.4				
Echeneidae (remoras)	0.2	2.8	0.2	5.3	0.7	1.2	0.1	3.5
Ephippidae (spadefishes)					0.7	1.2		
Epigonidae (deepwater cardinalfishes)							0.9	2.3
Evermannellidae (sabertoothfishes)			0.1	5.3			0.1	3.5

(Continued)

TABLE 1 | Continued

Family	2015 Surface density	2015 Surface % occurrence	2015 Mixed layer density	2015 Mixed % occurrence	2016 Surface density	2016 Surface % occurrence	2016 Mixed layer Density	2016 Mixed layer % occurrence
Exocoetidae (flyingfishes)	7.0	93.8	0.6	11.5	3.5	65.5	0.3	4.7
Fistulariidae (cornetfishes)			0.3	1.4				
Gadidae (cods)	0.2	1.4	0.3	1.4				
Gempylidae (snake mackerels)	0.2	2.8	2.7	47.9	0.2	3.6	3.2	44.2
Gerreidae (mojarras)	0.6	9.4			0.2	12.0	0.4	2.3
Gigantactinidae (whipnose anglerfishes)			0.7	2.8				
Giganturidae (telescopefishes)			0.7	2.8				
Gobiidae (gobies)			12.4	52.8			13.0	51.2
Gonostomatidae (bristlemouths)	0.2	1.4	14.2	8.3	0.4	6.0	17.8	8.2
Hemiramphidae (halfbeaks)	1.6	38.5	0.3	1.4	0.4	25.0		
Holocentridae (squirrelfishes)	0.3	2.8	0.4	9.4				
Howellidae (oceanic basslets)			0.4	13.5			1.0	18.7
Istiophoridae (billfishes)	1.3	3.3	0.4	9.4	0.7	27.4		
Kyphosidae (sea chubs)	0.6	22.9	0.1	2.8	0.3	23.9		
Labridae (wrasses and parrotfishes)			2.6	24.0	0.7	1.2	0.2	5.8
Lamprididae (opahs)			0.3	1.4				
Lobotidae (tripletails)	0.9	7.3	0.3	2.8	0.2	3.6		
Lutjanidae (snappers)	0.4	1.4	6.0	42.8	0.7	1.2	5.0	23.3
Malacanthidae (tilefishes)			0.1	3.1				
Melamphaidae (ridgeheads)			0.3	7.3			0.8	15.1
Megalopidae (tarpons)					0.7	1.2		
Melanostomiidae (scaleless black dragonfishes)			0.3	1.4				
Microdesmidae (wormfishes)	0.2	2.8	1.7	13.5			1.2	17.4
Monacanthidae (filefishes)	1.0	38.5	0.3	7.3	0.2	4.8		
Moridae (codlings)			0.1	3.1				
Mugilidae (mullets)	0.1	6.3	0.7	1.4	0.7	1.2		
Mullidae (goatfishes)	1.7	36.5	0.7	1.4	0.2	1.7		
Muraenesocidae (pike congers)							0.4	1.2
Myctophidae (lanternfishes)	1.0	6.3	30.6	95.8	0.1	9.5	55.9	95.4
Nettastomatidae (duckbill eels)			0.4	8.3			0.3	7.0
Nomeidae (driftfishes)	0.2	1.4	1.6	63.5	0.4	25.0	14.6	6.5
Notosudidae (waryfishes)			0.3	1.4			0.4	1.2

(Continued)

TABLE 1 | Continued

Family	2015 Surface density	2015 Surface % occurrence	2015 Mixed layer density	2015 Mixed % occurrence	2016 Surface density	2016 Surface % occurrence	2016 Mixed layer Density	2016 Mixed layer % occurrence
Ogcocephalidae (batfishes)							0.4	1.2
Ophichthidae (snake eels)			0.2	2.8			0.9	2.3
Ophidiidae (cusk-eels)	0.2	2.8	0.3	11.5	0.7	1.2	0.7	12.8
Ostraciidae (boxfishes)			0.3	1.4				
Paralepididae (barracudinas and daggertooths)			1.0	2.8			4	37.3
Paralichthyidae (sand flounders)			2.3	25.0	0.7	1.2	4.3	25.6
Percophidae (flatheads)			0.7	2.8			0.4	1.2
Phosichthyidae (lightfishes)			0.5	15.6			2.2	29.7
Phycidae (phycid hakes)							0.4	1.2
Polymixiidae (beardfishes)			0.2	1.4			0.4	1.2
Pomacanthidae (angelfishes)	0.2	1.4	0.7	2.8				
Pomacentridae (damselfishes)	0.2	14.6	0.6	9.4	0.9	14.0	0.3	7.0
Priacanthidae (bigeyes)	0.2	2.8	0.2	5.3				
Scaridae (parrotfishes)	0.2	1.4	1.1	18.8			0.4	1.2
Sciaenidae (drums and croakers)			0.3	2.8			0.2	3.5
Scombridae (tunas and mackerels)	4.3	62.5	24.3	9.6	3.3	53.6	26.0	82.6
Scopelarchidae (pearleyes)			0.2	5.3				
Scorpaenidae (scorpionfishes)			0.6	15.6	0.7	1.2	0.2	3.5
Serranidae (sea basses)			3.3	37.5	0.7	1.2	0.9	15.1
Sparidae (porgies)			0.3	1.4				
Sphyraenidae (barracudas)	0.2	11.5	0.9	21.9	0.2	15.5	0.9	2.3
Sternoptychidae (marine hatchetfishes)			3.6	1.4			1.4	25.6
Stomiidae (dragonfishes)			0.1	5.3			0.4	11.6
Syngnathidae (pipefishes and seahorses)	0.9	7.3					0.2	3.5
Synodontidae (lizardfishes)	0.2	1.4	1.6	14.6			0.6	8.1
Tetraodontidae (puffers)	0.2	9.4	0.6	14.6	0.2	2.4	0.4	8.1
Trachipteridae (ribbonfishes)			0.7	2.8				
Trichiuridae (cutlassfishes)			0.2	4.2			0.9	2.3
Uranoscopidae (stargazers)			0.3	1.4				
Xiphiidae (swordfish)	0.6	4.2	0.3	1.4	0.4	7.1		
Zeidae (dories)			0.3	1.4				
Unknown/Damaged	0.2		11.6		0.4		13.2	

Total families collected, densities of larvae caught by net type per 1000 m^{-3}, and percent frequency of occurrence by stations by net type are presented.

Distinct differences in the percent composition of certain families were observed between months for both surface and mixed layer samples; albeit certain taxa were consistently high in both June and July (**Table 1**). In the surface layer, exocoetids accounted for the largest percentage of the total catch in June 2015 and June 2016 compared to July 2015 and July 2016, whereas carangids were most common in the surface layer in July 2015 and July 2016 as compared to June 2015 and June 2016. July 2015 had a high percent composition of clupeids compared to June 2015 and June and July of 2016. Myctophids dominated the mixed layer for both months and years sampled except July 2015, when scombrids were the dominant taxa in the mixed layer. Scombrids were abundant for other years and months sampled. Carangids were consistently in the top three families based on percent composition and consistently caught in all months and years in both surface and mixed layer samples (**Table 2**).

Of the 99 families collected, the percent frequency of occurrence by station of 44 families was greater than 10% in either surface or mixed layer samples in 2015 or 2016 (**Table 1**), representing high diversity across stations. In the surface layer, exoceotids, carangids, scombrids, and hemiramphids were relatively common and present at the majority of stations sampled across both years (**Table 1**). Several families were also common to the mixed layer with percent frequency of occurrence from combined years being over 50%, including myctophids, bregmacerotids, and scombrids. Certain taxa were common in 1 year but conspicuously less common in the other year sampled, in particular scombrids and carangids.

Biodiversity: T_F and H'

Taxonomic richness in the surface layer and mixed layer varied between the 2 years surveyed (ANOVA, $p < 0.001$), with mean T_F per station being higher in 2015 (6.3 ± 2.8) than 2016 (4.6 ± 3.2) for the surface station, and similarly, with mean T_F per station being higher for the mixed layer in 2015 (12.4 ± 4.6) than 2016 (10.7 ± 4.7; **Figure 2**). Mean T_F per station was similar between June (5.9 ± 2.6) and July (5.2 ± 3.5) surveys (ANOVA, $p > 0.05$) for surface stations. Mean T_F per station in the mixed layer was significantly higher in June (12.9 ± 4.2) than July (10.4 ± 4.9) surveys (ANOVA, $p < 0.001$).

Shannon diversity (H') in the surface layer and mixed layer (**Figure 2**) was different between years (ANOVA, $p < 0.001$), with mean H' per station being higher in 2015 (1.4 ± 0.4 surface, 2.0 ± 0.4 mixed) than 2016 (1.2 ± 0.6 surface, 1.7 ± 0.5 mixed). Mean H' was significantly different between months as well for both layers (ANOVA, $p < 0.05$), with June (1.3 ± 0.4 surface, 2.0 ± 0.3 mixed) being higher than July (1.0 ± 0.6 surface, 1.8 ± 0.5 mixed).

Both T_F and H' varied spatially in the NGoM, with the most pronounced horizontal trend occurring between the north and south sampling transects and in areas impacted by MARS (**Figure 3**), where salinity was lower. In general, mean T_F and H' was higher along the northern transect (28.0°N) across all months and years sampled (**Figure 2**). In both 2015 and 2016, the northern transect had higher mean T_F (10.5 and 9.1) and

TABLE 2 | Catch data of top eight larval families in the northern Gulf of Mexico in 2015 and 2016 from surface (0–1 m with neuston tows) and mixed layer (0–100 + m with oblique bongo tows).

Year	Month	Exocoetidae	Carangidae	Scombridae	Mullidae	Clupeidae	Istiophoridae	Hemiramphidae	Nomeidae	Unknown	Other
Surface											
2015	June	44.3	12.1	11.9	5.3	0.1	3.4	2.4	0.9	0.3	19.3
	July	6.6	37.5	9.2	1.5	24.9	2.8	2.5	0.3	0.4	14.3
2016	June	30.9	27.6	16.7	1.1	2.6	0.9	3.5	3.7	0.5	12.6
	July	9.6	49.7	21.9	0.7	0.3	6.4	1.4	0.7	0.0	9.5
Year	**Month**	**Myctophidae**	**Carangidae**	**Scombridae**	**Bregmacerotidae**	**Gonostomidae**	**Gobiidae**	**Nomeidae**	**Lutjanidae**	**Unknown**	**Other**
Mixed Layer											
2015	June	22.6	9.6	8.0	8.9	6.3	2.8	8.2	3.0	6.6	24.1
	July	10.0	12.2	17.9	1.6	8.9	10.5	2.4	3.3	5.7	27.5
2016	June	31.6	6.8	6.3	9.8	6.7	6.2	9.2	0.5	5.0	18.0
	July	17.7	12.1	11.9	5.0	10.0	4.6	3.4	4.5	7.3	23.5

Percent total of top families of the raw data by net type, year, and month are presented.

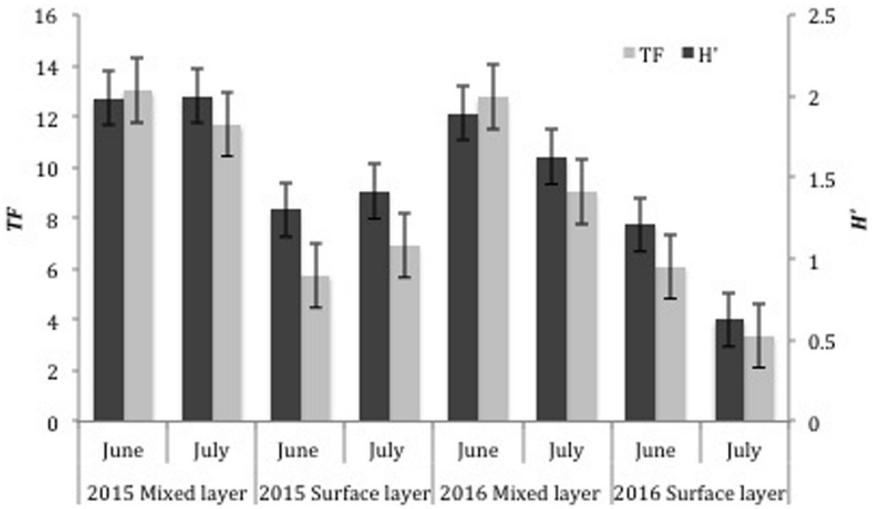

FIGURE 2 | Comparison of taxonomic richness (T_F) and Shannon diversity (H') of all ichthyoplankton collected in the surface (0–1 m with neuston tows) and mixed layer samples (0–100 + m with oblique bongo tows) in 2015 and 2016 in the Northern Gulf of Mexico. Error bars represent standard error of the mean.

mean H' (1.8 and 1.4), compared to T_F (8.2 and 6.4), and H' (1.6 and 1.2) for the southern transect (27.0°N). Marked differences were observed in both indices between surface and mixed layer samples (**Figure 2**). In 2015 and 2016, mean T_F (12.4 and 10.9), and H' (2.0 and 1.8) were higher in the mixed layer compared to mean T_F (6.3 and 4.8) and H' (1.4 and 0.9) in the surface layer, which is not surprising given that oblique bongo tows in the mixed layer sample a significantly larger fraction of the water column. In 2015, areas of high T_F were associated with the Loop Current boundary. June and July of 2015 had the highest northern intrusion of the Loop Current, while the 2016 July Loop Current had already detached into a large, anticyclonic Loop Current eddy. In 2015, areas of high T_F and H' were located near the Loop Current boundary.

Fish Habitat Modeling

Final T_F–based (AIC = 835.0, DE = 37.8%) and H'-based (AIC = 224.5, DE = 40.9%) GAMs for collections from the surface layer included all environmental variables tested: SST, SSH, salinity, dissolved oxygen, invertebrate biomass, and distance to Loop Current, while *Sargassum* biomass was additionally included in the neuston net samples (**Table 3**). Based on ΔAIC and ΔDE (%), salinity (ΔAIC = 13.0, ΔDE = 5.0%), *Sargasum* biomass (ΔAIC = 4.6, ΔDE = 4.1%), and invertebrate biomass (ΔAIC = 8.2, ΔDE = 3.7%) were the most influential explanatory variables in the T_F-based GAM. Dissolved oxygen (ΔAIC = 21.2, ΔDE = 7.8%) was again influential in the H'-based GAM along with SST (ΔAIC = 5.8, ΔDE = 4.1%) and SSH (ΔAIC = 5.0, ΔDE = 2.3%), albeit to a lesser degree. Responses plots from GAMs indicated that T_F and H' for fish larvae in the surface layer were higher at high sea surface temperatures (>28°C), lower sea surface heights (0.3–0.5 m), lower salinity, higher invertebrate biomass, farther from the Loop Current, and at lower *Sargassum* biomass (**Figures 4**, **5**).

Final T_F- (AIC = 995.9, DE = 41.8%) and H' – (AIC = 131.6, DE = 42.6%) based GAMs for collections from the mixed layer also included all environmental variables tested (**Table 3**). Based on ΔAIC and ΔDE (%), salinity (ΔAIC = 12.8, ΔDE = 3.5%), invertebrate biomass (ΔAIC = 10.5, ΔDE = 2.4%), and SST (ΔAIC = 6.2, ΔDE = 2.1%) were the most influential explanatory variables in the T_F-based GAM. SST (ΔAIC = 15.8, ΔDE = 6.3%) in the H'-based GAM along with SSH (ΔAIC = 12.3, ΔDE = 6.1%) and invertebrate biomass (ΔAIC = 4.4, ΔDE = 2.0%) were the most influential variables (**Table 3**). Responses plots from GAMs indicated that T_F and H' for fish larvae in the mixed layer were higher at SSTs above 28°C, lower sea surface heights (0.3–0.5 m), lower salinity, higher invertebrate biomass, and farther from the Loop Current (**Figures 6**, **7**).

DISCUSSION

Larvae of epipelagic and mesopelagic species were collected throughout our sampling corridor in both surface and mixed layer samples. Common epipelagic fishes (e.g., carangids, exocoetids, and scombrids) accounted for almost half of the fish percent composition assemblage in surface waters, and the dominance of larval taxa that inhabit the epipelagic zone as adults has also been reported in ichthyoplankton surveys of the Straits of Florida (Richardson et al., 2010), tropical Atlantic Ocean (Katsuragawa et al., 2014), and the Pacific Ocean (Vilchis et al., 2009). Densities of these taxa were markedly higher than any mesopelagic taxon collected (e.g., myctophids∼ 0.1 larvae 1000 m^{-3}) in the surface layer. In contrast, mesopelagic fishes, most notably myctophids, bregmacerotids, and gonostomatids, dominated percent composition collections in the mixed layer, with myctophids alone accounting for nearly one quarter of the larval fish assemblage in the upper

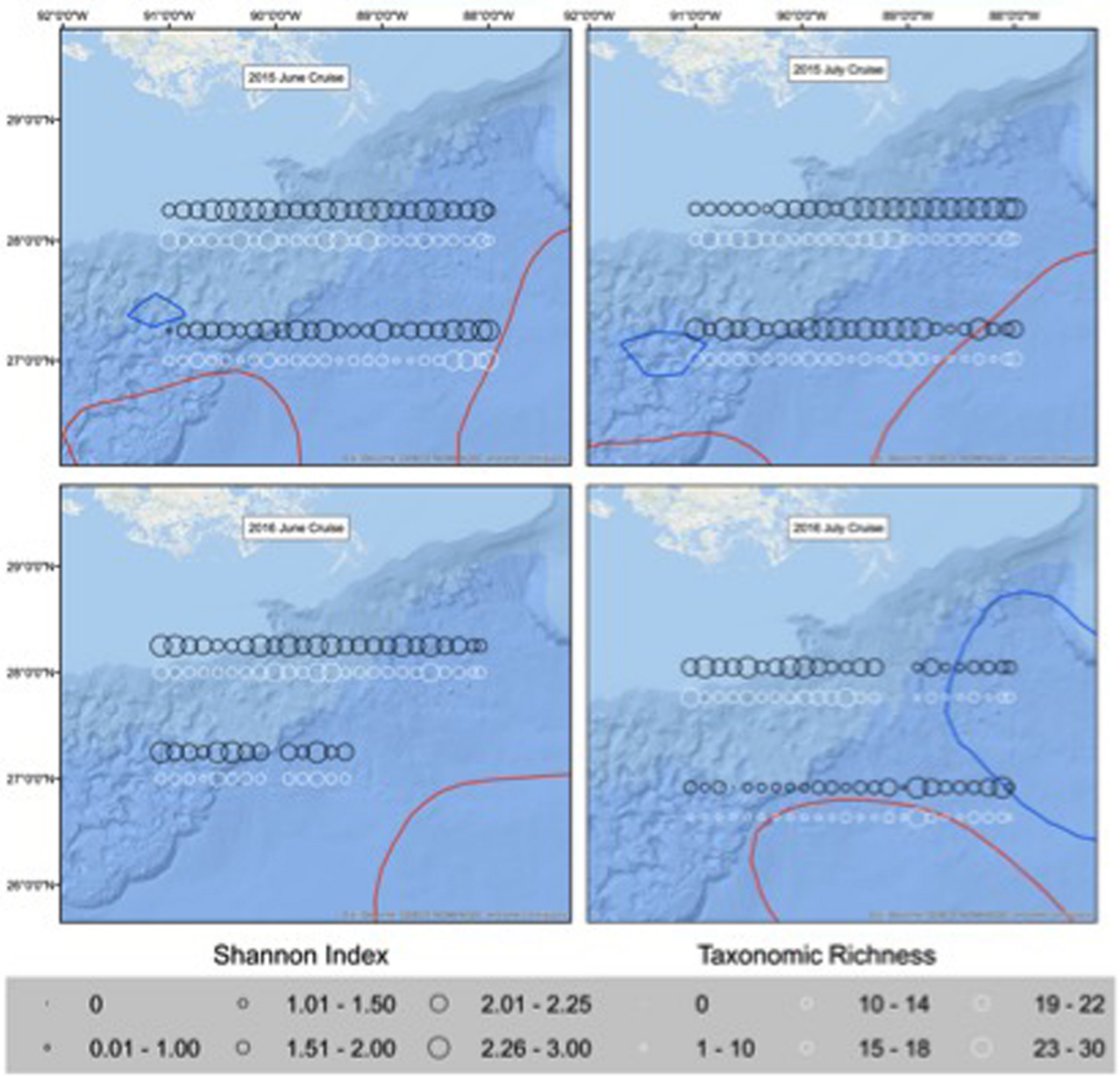

FIGURE 3 | Shannon index (*H'*; black) and taxonomic richness (T_F; white) of larvae collected in June and July of 2015 and 2016 in the Northern Gulf of Mexico. Circles represent diversity of larvae per station. Location of the Loop Current and warm eddies is represented in red and cold core eddies are represented in blue.

100 m and present at high densities (>40 larvae 1000 m^{-3}). These results are consistent with the findings that mesopelagic larval fishes dominated the catch composition in the mixed layer of other regions in the Atlantic Ocean, including the Mediterranean Sea (Alemany et al., 2010; Torres et al., 2011). Direct comparisons with other studies are limited because the majority of surveys using comparable sampling gears focused on specific taxa rather than the entire family level ichthyoplankton assemblage (e.g., Rooker et al., 2013; Kitchens and Rooker, 2014; Randall et al., 2015); however, an earlier study by Richards (1993) characterized the ichthyoplankton assemblage in the NGoM using bongo net tows to 200 m with an observed T_F of 100, of which our study is highly similar (T_F = 99). They also reported that myctophids, carangids, and gonostomatids were commonly collected in the upper 200 m, supporting our observation that the mixed layer represents important habitat of mesopelagic fishes during the early life period.

Mesopelagic fish larvae, particularly myctophids, bregmacerotids, and gonostomatids, were numerically dominant by percent composition in samples from the mixed layer. At night, juveniles and adults of these taxa are known to

TABLE 3 | Akaike information criterion (AIC), deviance explained (DE), and variables retained in the final GAMs based on taxonomic richness (T_F), and Shannon diversity (H') for surface samples (0–1 m with neuston tows), and mixed layer samples (0–100 + m with oblique bongo tows) collected in 2015 and 2016.

Surface samples (0–1 m with neuston tows)					Mixed Layer Samples (0–100 + m with oblique bongo tows)				
	Model	**Variables**	**Δ AIC**	**Δ DE**		**Model**	**Variables**	**Δ AIC**	**Δ DE**
T_F	Final AIC: 835.0	SST	0.4	0.8	T_F	Final AIC: 995.9	SST**	6.2	2.1
	Final DE: 37.8%	SSH*	4.6	2.1		Final DE: 41.8%	SSH*	5.3	1.8
		Salinity**	13	5			Salinity**	12.8	3.5
		DO	12.8	2.2			DO	9	0.9
		Invert Biomass*	8.2	3.7			Invert Biomass***	10.5	2.4
		Distance to LC	0.5	0.6			Distance to LC	1.8	0
		Sargasum Biomass*	4.6	4.1					
H'	Final AIC: 224.5	SST*	5.8	4.1	H'	Final AIC: 131.6	SST***	15.8	6.3
	Final DE: 40.9%	SSH*	5	2.3		Final DE: 42.6%	SSH**	12.3	6.1
		Salinity	0.2	0.9			Salinity*	2.4	1.3
		DO**	21.2	7.8			DO	1.6	2.2
		Invert Biomass	0.2	0.6			Invert Biomass*	4.4	2
		Distance to LC	1.3	0.3			Distance to LC	2	0
		Sargasum Biomass	0.9	0.2					

*Variation in AIC (Δ AIC), DE (Δ DE), and p values (***p < 0.001, **p < 0.01, and *p < 0.05) are also presented to evaluate the importance of each variable. SST, Sea surface temperature; SSH, sea surface height; DO, dissolved oxygen, and Distance to LC, Distance to the Loop Current.*

migrate from the mesopelagic zone to the epipelagic zone (D'Elia et al., 2016); Rodriguez et al. (2006) also reported high catches of mesopelagic fishes in the epipelagic zone of the Canaries-African Coastal Transition Zone. All samples were collected during the day and their presence in the upper 100 m of the water column suggests that the earliest life stages remain in the epipelagic zone in the daytime hours, and diel vertical migration between the zones commences later (Moku et al., 2003). Several midwater taxa, including species within these three families, hatch in the epipelagic zone and begin migration as they transition from larvae to juveniles (Watanabe et al., 2002). A large fraction of the individuals collected in our surveys from these families were relatively small (<5 mm SL) with many specimens appearing to be recently hatched, likely accounting for the high numbers of mesopelagic taxa in our bongo net collections from the mixed layer.

Taxonomic richness and Shannon diversity (H') varied across the sampling corridor, with estimates of both diversity measures generally higher along the northern transect (28.0°N). It is possible, even likely, that T_F and H' were higher along the northern transect because this region borders the outer continental shelf, and thus both continental shelf and oceanic species are likely present in this region, with mixed communities leading to higher diversity. Many of the families of fish larvae collected along the northern transect in this study were indicative of continental shelf assemblages (McEachran and Fechhelm, 2010), and a greater presence of continental shelf species was often found at stations impacted by freshwater inflow (green water, lower salinity, and higher turbidity). That said, the northern transect stations were seaward of the continental shelf in slope waters where fish larvae of oceanic taxa (e.g., exocoetids, istiophorids, and scombrids) are known to occur. While the northern transect was essentially a mixed assemblage of both continental shelf and oceanic taxa, nearly all of the stations in the southern transect (27.0°N) were in oceanic waters, which explains the high abundances of exocoetids and scombrids. As a result, the larval fish assemblage was primarily comprised of oceanic species with limited contribution of continental shelf species, leading to lower overall diversity or reduced T_F and H' relative to stations in the northern transect.

Assemblage diversity also varied temporally and both T_F and H' were generally higher in June than July in both sampling years. In the surface layer, exocoetids, mullids, and clupeids comprised a significantly higher percentage of the assemblage in June for both years, while carangids and scombrids were higher in July. In the mixed layer, myctophids and bregmacerotids dominated the June assemblage while carangids and scombrids comprised a greater proportion of the catch in July. Temporal shifts in the abundance and assemblage composition of larval fishes are often attributed to seasonal patterns of spawning in the Gulf of Mexico (Sanvicente-Añorve et al., 1998), equatorial Atlantic Ocean (Mourato et al., 2014), and inland waters off Australia (King et al., 2016), but other factors such as the position of mesoscale features or oceanographic conditions are also known to influence presence and spatial distribution of fish larvae (Cowen et al., 2000; Randall et al., 2015; Cornic et al., 2018). Results of the present study are consistent with other studies conducted in the NGoM that indicate higher numbers of exocoetids in June (Randall et al., 2015) and higher numbers of scombrids in July (Cornic et al., 2018), with both studies attributing seasonal patterns in larval abundance to temporal variation in spawning activity. Carangids, myctophids, and bregmacerotids are known to display variable spawning throughout the year (Moku et al., 2003; Ditty et al., 2004;

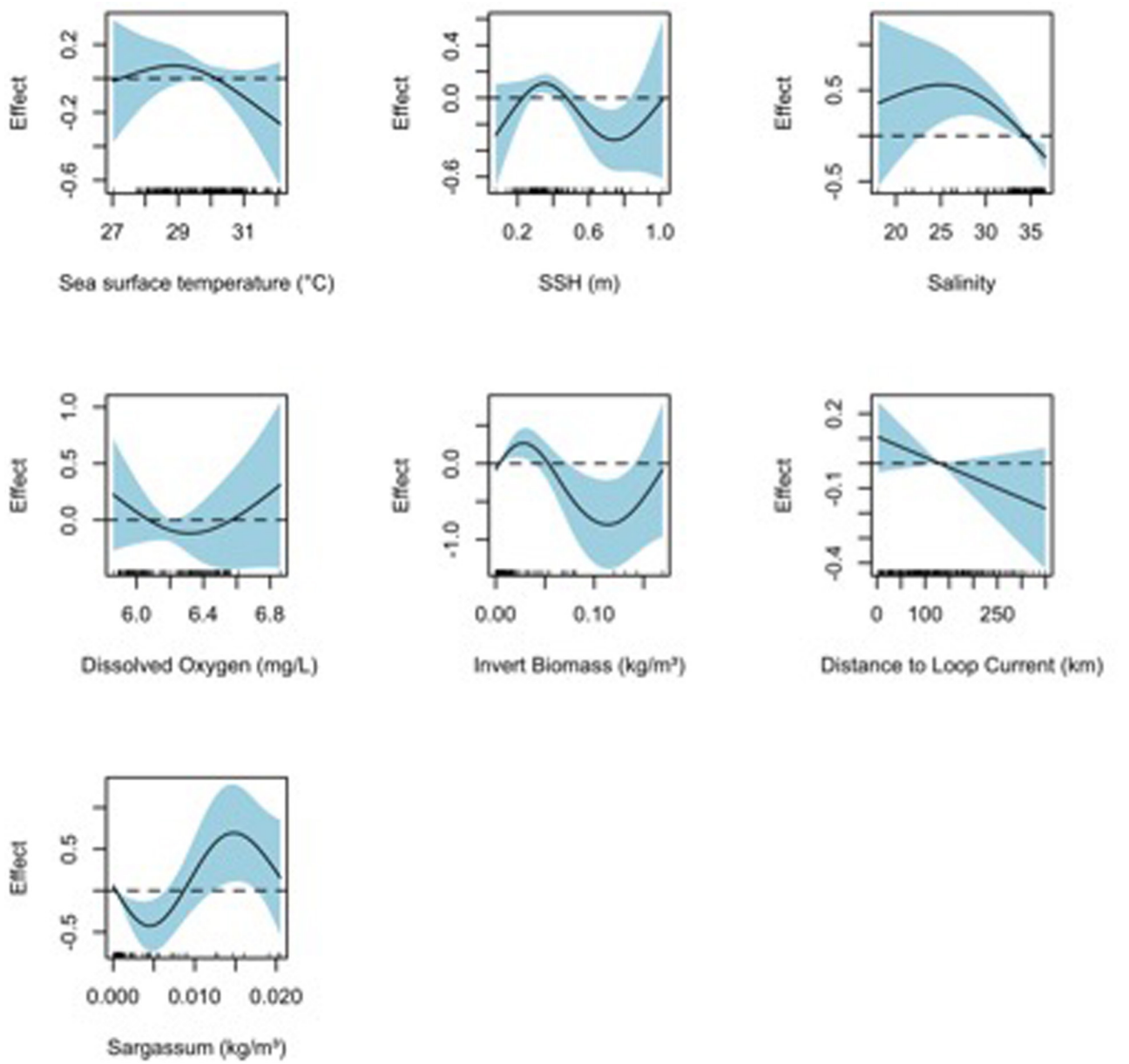

FIGURE 4 | Response plots for 2015 oceanographic variable of the surface sample (0–1 m with neuston tows) taxonomic richness (T_F) from full generalized additive model (GAM). Plots include sea surface temperature (°C), sea surface height (m), salinity, dissolved oxygen (mg/L), invertebrate biomass (kg m^{-3}), distance to Loop Current (km), and *Sargassum* density (kg m^{-3}). Solid lines represent smoothed values and the shaded area represents 95% confidence intervals. Dashed line displayed at $y = 0$ on response plots.

Namiki et al., 2007), and this may have contributed to observed temporal shifts in the presence of certain taxa in our collections. Inter-annual variability in the abundance and diversity of larval fishes are common and often associated with temporal shifts in the location of mesoscale features (Richardson et al., 2010; Rooker et al., 2013). In 2015, a higher northward penetration of the Loop Current corresponded with higher T_F and H', while the northward penetration of the Loop Current was reduced in 2016 and lower T_F and H' were observed. This suggests that diversity of the larval fish assemblage in this region is related to the northward extension of the Loop Current, perhaps due to physical convergence, as the Loop Current water itself is highly oligitrophic, and these results are consistent with previous studies (Rooker et al., 2012; Cornic et al., 2018).

The intrusion of the MARS also affects the distribution and abundance of fish larvae in the NGoM (Govoni et al., 1989; Grimes and Finucane, 1991), and a primary physicochemical indicator of MARS intrusion is salinity. In the present study, salinity was an important explanatory variable in both T_F and H'

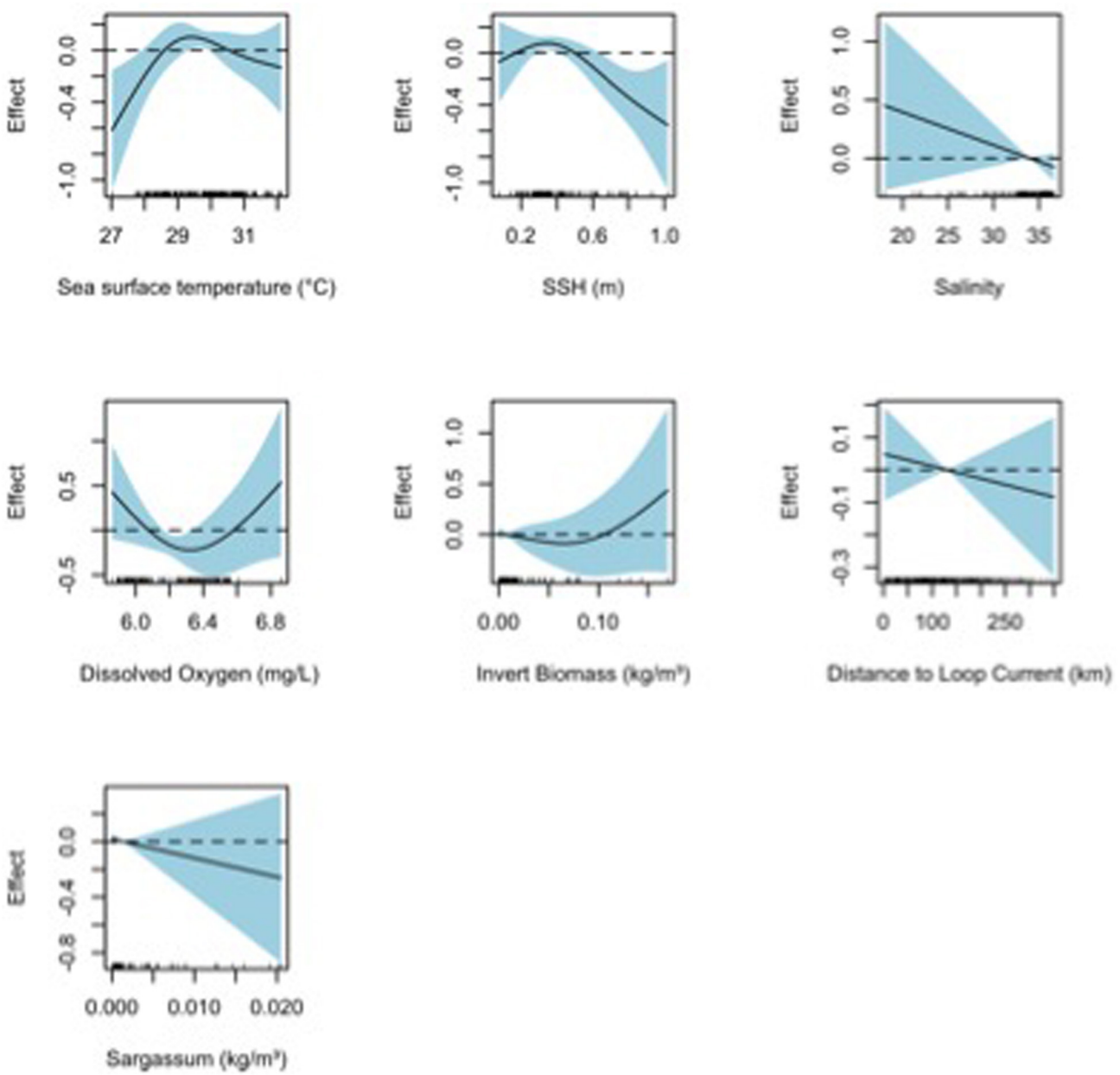

FIGURE 5 | Response plots for 2015 oceanographic variable of the surface sample (0–1 m with neuston tows) Shannon diversity (*H'*) from full generalized additive model (GAM). Plots include sea surface temperature (°C), sea surface height (m), salinity, dissolved oxygen (mg L^{-1}), invertebrate biomass (kg m^{-3}), distance to Loop Current (km), and *Sargassum* density (kg m^{-3}). Solid lines represent smoothed values and the shaded area represents 95% confidence intervals. Dashed line displayed at $y = 0$ on response plots.

GAMs, indicating that assemblage diversity for larval fishes may be highly dependent on the spatial configuration of lower salinity intrusions from MARS. Freshwater discharge from MARS in the spring creates a salinity gradient in the NGoM that ranges from the river delta to the continental shelf over the summer months (Schiller et al., 2011; O'Connor et al., 2016). Stations with highest diversity of larval fishes were often found in areas with lower salinity, suggesting that areas impacted by freshwater inflow may serve as habitat for a wider range of taxa, including both continental shelf and oceanic species. We observed that both T_F and *H'* were higher in low salinity areas because both continental shelf taxa (serranids, lutjanids, and sciaenids) and oceanic taxa (exocoetids, scombrids, and istiophorids) were often present in collections, leading to higher diversity. Generally, the MARS plume is larger in area and outflow in June relative to July as the greatest amount of freshwater is discharged in the spring (Aulenbach et al., 2007). Results from this study showed higher diversity of larval fishes in our June surveys for both 2015 and

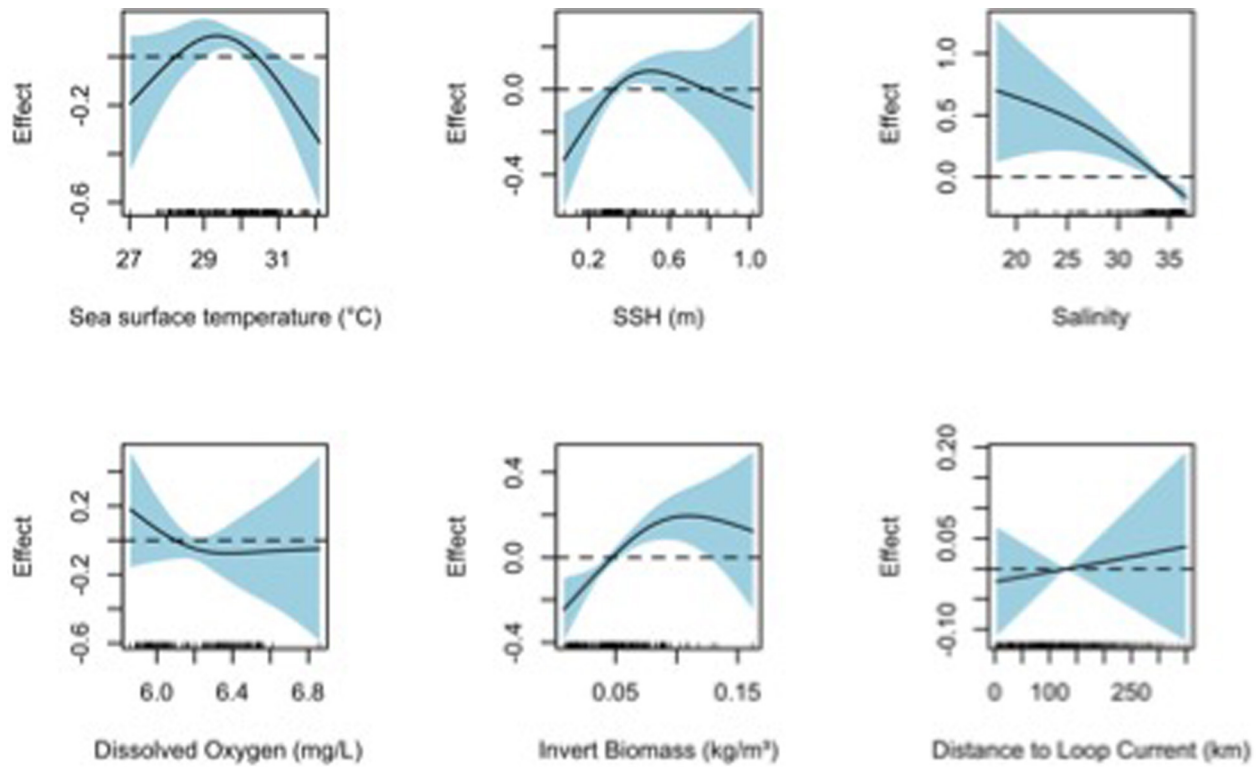

FIGURE 6 | Response plots for 2016 oceanographic variable of the bongo net taxonomic richness (T_F) from full generalized additive model (GAM). Plots include sea surface temperature (°C), sea surface height (m), salinity, dissolved oxygen (mg L^{-1}), invertebrate biomass (kg m^{-3}), and distance to Loop Current (km). Solid lines represent smoothed values and the shaded area represents 95% confidence intervals. Dashed line displayed at $y = 0$ on response plots.

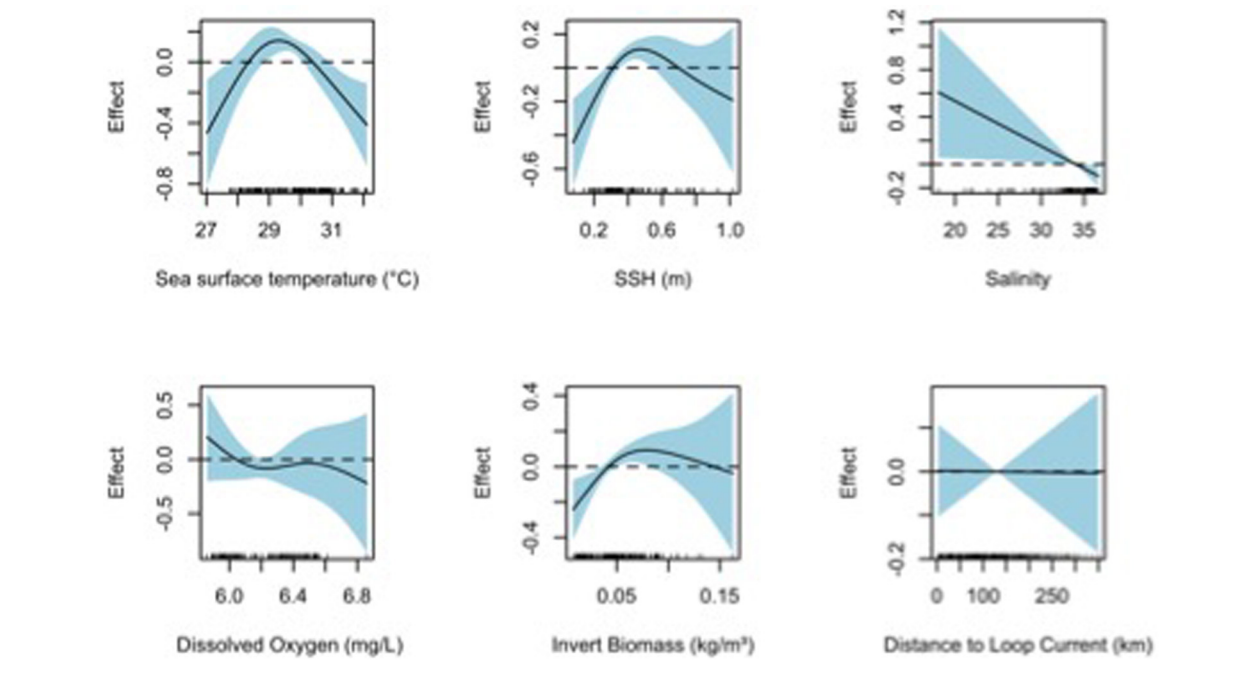

FIGURE 7 | Response plots for 2016 oceanographic variable of the bongo net Shannon diversity (H') from full generalized additive model (GAM). Plots include sea surface temperature (°C), sea surface height (m), salinity, dissolved oxygen (mg L^{-1}), invertebrate biomass (kg m^{-3}), and distance to Loop Current (km). Solid lines represent smoothed values and the shaded area represents 95% confidence intervals. Dashed line displayed at $y = 0$ on response plots.

2016, suggesting that the influx of freshwater from the MARS impacted the assemblage composition and the location of areas with higher T_F and H'. Moreover, 2015 had significantly higher diversity measures than 2016, which also appears associated with the MARS plume, as there was a greater freshwater discharge in 2015 (896,600 $ft^3\ s^{-1}$) than in 2016 (539,150 $ft^3\ s^{-1}$)[4]. MARS freshwater inflow into the oceanic ecosystem is also associated with an influx of nutrients that increase primary and secondary productivity (Lohrenz et al., 1997; O'Connor et al., 2016) and likely increases food opportunities for larval fishes. Thus, areas impacted by MARS may represent favorable habitat that supports growth and survival during early life (Grimes and Finucane, 1991), which may have also contributed to higher T_F and H' observed at stations influenced by MARS. This is consistent with findings that show physiochemical processes, such as salinity, have been shown to influence larval fish distribution and the interaction between larval fish and the surrounding environment ultimately determines survival and recruitment success (Fogarty et al., 1991; Bruce et al., 2001).

Spatial variability in SSH and SST were also important drivers of T_F and H' in this study. GAMs indicated that diversity increased in areas with lower SSH (cold-core eddies) and mid-level water temperatures (28–30°C). Cold-core eddies are associated with upwelling, as cold, nutrient-rich waters in these features support higher primary productivity (Biggs et al., 1997), and assemblage diversity has been shown to increase in areas of elevated productivity in both marine and terrestrial ecosystems (Waide et al., 1999; Cardinale et al., 2002). Convergent zones where two mesoscale features meet are also responsible for aggregating plankton and are therefore favorable conditions for the survival of fish larvae in the GoM (Bakun, 2006) as well as several other marginals seas including the Mediterranean Sea (Alemany et al., 2010), Caribbean Sea (Erisman et al., 2017), and Gulf of California (Avendaño-Ibarra et al., 2013), potentially leading to the increased diversity of larval fishes along these features. In addition to the fronts physically transporting larvae to convergent zones, these zones also increase feeding opportunities for larvae, leading to higher survival rates (Bakun, 2006; Acha et al., 2018; Sato et al., 2018). Results from recent studies in the NGoM of pelagic larval fishes yield similar results, with billfishes, dolphinfishes, and tunas being associated with frontal features and convergent zones (Rooker et al., 2013; Kitchens and Rooker, 2014; Cornic et al., 2018).

CONCLUSION

Baseline estimates of biodiversity and assemblage structure are critical understanding the impacts of anthropogenic stressors on marine ecosystem, and this study serves as reference point for assessing the impacts of changing conditions onlarval fish assemblages in oceanic waters of the NGoM. Biodiversity hotspots of fish larvae in the NGoM were located in areas where continental shelf and oceanic communities coalesced, with T_F and H' highest along the northern transect due to the influence of both MARS and mesoscale oceanographic features (Loop Current), confirming that biodiversity hotspots for larval fishes (high T_F and H') in the NGoM will occur primarily in convergence zones (frontal features). As a result, factors that alter physicochemical conditions (i.e., freshwater inflow linked to MARS), or the geographic position of these oceanographic features (shifts in western boundary currents due to climate change; Chen et al., 2019) will ultimately influence assemblage diversity in the NGoM, possibly leading to broader changes in ecosystem structure and stability. Additionally, our assumption that fish larvae of numerically dominant families that use the epipelagic zone as adults (istiophorids, carangids, scombrids, and exocoetids, etc.) account for the majority of ichthyoplankton in the surface layer, while the mixed layer will have a significant contribution of mesopelagic taxa, was also supported. Mesopelagic families, particularly myctophids and gonostomatids were an important component of the mixed layer assemblage, and this finding highlights the ecological connectivity that occurs between epipelagic and deep pelagic zones.

[4]https://waterdata.usgs.gov/

DATA AVAILABILITY STATEMENT

The data are publicly available through the Gulf of Mexico Research Initiative Information and Data Cooperative (GRIIDC) at https://data.gulfresearchinitiative.org (doi: 10.7266/N7PZ576R, doi: 10.7266/N72B8W3M, doi: 10.7266/N76M356C, and doi: 10.7266/N76W98G7).

ETHICS STATEMENT

The animal study was reviewed and approved by Institutional Animal Care and Use Committee.

AUTHOR CONTRIBUTIONS

CM, KC-S, MC, TS, and JR contributed to the design, collection, identification, and analysis of biological samples. CM and JR wrote the manuscript. All authors contributed to the article and approved the submitted version.

FUNDING

This research was made possible by a grant from The Gulf of Mexico Research Initiative.

ACKNOWLEDGMENTS

We thank all the scientists and crew who participated in the surveys and laboratory work conducted over the course of this project. In particular, a special thanks to M. Dance, J. Ditty, D. Johnson, J. Lee, L. Podsim, J. Plumlee, L. Randall, T. Richards, B. Saurez, C. Steffen, and D. Wells.

REFERENCES

Acha, E. M., Ehrlich, M. D., Muelbert, J. H., Pájaro, M., Bruno, D., Machinandiarena, L., et al. (2018). "Ichthyoplankton associated to the frontal regions of the southwestern atlantic," in *Plankton Ecology of the Southwestern Atlantic: From the Subtropical to the Subantarctic Realm*, eds M. S. Hoffmeyer, M. E. Sabatini, F. P. Brandini, D. L. Calliari, and N. H. Santinelli (Berlin: Springer International Publishing), 219–246. doi: 10.1007/978-3-319-77869-3_11

Alemany, F., Quintanilla, L., Velez-Belchi, P., Garcia, A., Corte's, D., Rodríguez, J. M., et al. (2010). Characterization of the spawning habitat of Atlantic bluefin tuna and related species in the Balearic Sea (western Mediterranean). *Prog. Oceanogr.* 86, 21–38. doi: 10.1016/j.pocean.2010.04.014

Aulenbach, B. T., Buxton, H. T., Battaglin, W. T., and Coupe, R. H. (2007). *Streamflow and Nutrient Fluxes of the Mississippi-Atchafalaya River Basin and Sub Basins for the Period of Record Through 2005*. Open-File Report. 2007–1080. Reston, VA: U.S. Geological Survey.

Avendaño-Ibarra, R., Godínez-Domínguez, E., Aceves-Medina, G., González-Rodríguez, E., and Trasviña, A. (2013). Fish larve response to biophysical changes in the gulf of California, Mexico (Winter-Summer). *J. Mar. Sci.* 2013, 1–17. doi: 10.1155/2013/176760

Bakun, A. (2006). Fronts and eddies as key structures in the habitat of marine fish larvae: opportunity, adaptive response and competitive advantage. *Sci. Mari.* 70(Suppl. 2), 105–122. doi: 10.3989/scimar.2006.70s2105

Biggs, D. C., Zimmerman, R. A., Gasca, R., Suarez-Morales, E., Castellanos, I., and Leben, R. R. (1997). Note on plankton and cold-core rings in the Gulf of Mexico. *Fish. Bull.* 95, 369–375.

Browder, J. (1993). A pilot model of the Gulf of Mexico continental shelf. Paper presented at the Trophic models of aquatic ecosystems. *ICLARM Conf. Proc.* 26, 279–284.

Bruce, B. D., Evans, K., Sutton, C. A., Young, J. W., and Furlani, D. M. (2001). Influence of mesoscale occeanographic processes on larval distribution and stock structure in jackass morwong (*Nemadactylus macropterus*: *Cheilodactylidae*). *ICES J. Mar. Sci.* 58, 1072–1080. doi: 10.1006/jmsc.2001.1099

Carassou, L. (2012). Cross-shore, seasonal, and depth-related structure of ichthyoplankton assemblages in coastal Alabama. *Trans. Am. Fish. Soc.* 141:1137. doi: 10.1080/00028487.2012.675920

Cardinale, B. J., Palmer, M. A., and Collins, S. L. (2002). Species diversity enhances ecosystem functioning through interspecific facilitation. *Nature* 415, 426–429. doi: 10.1038/415426a

Chen, C., Wang, G., Xie, S., and Liu, W. (2019). Why Does Global Warming Weaken the gulf Stream but Intensify in Kuroshio? *J. Clim.* 32, 7437–7451. doi: 10.1175/jcli-d-18-0895.1

Cornic, M., Smith, B. L., Kitchens, L. L., Bremer, J. R. A., and Rooker, J. R. (2018). Abundance and habitat associations of tuna larvae in the surface water of the Gulf of Mexico. *Hydrobiologia* 806, 29–46. doi: 10.1007/s10750-017-3330-0

Cowen, R. K., Lwiza, K. M., Sponaugle, S., Paris, C. B., and Olson, D. B. (2000). Connectivity of marine populations: open or closed? *Science* 287, 857–859. doi: 10.1126/science.287.5454.857

Cury, P. (2000). Small pelagics in upwelling systems: patterns of interaction and structural changes in "wasp-waist" ecosystems. *ICES J. Mar. Sci.* 57, 603–618. doi: 10.1006/jmsc.2000.0712

Dagg, M. J., and Breed, G. A. (2003). Biological effects of Mississippi River nitrogen on the northern Gulf of Mexico-a review and synthesis. *J. Mar. Syst.* 43, 133–152. doi: 10.1016/j.jmarsys.2003.09.002

D'Elia, M., Warren, J. D., Rodriguez-Pinto, I., Sutton, T. T., Cook, A., and Boswell, K. M. (2016). Diel variation in the vertical distribution of deep-water scattering layers in the Gulf of Mexico. *Deep Sea Res. Part I-Oceanogr. Res. Pap.* 115, 91–102. doi: 10.1016/j.dsr.2016.05.014

Ditty, J. G., Shaw, R. F., and Cope, J. S. (2004). Distribution of carangid larvae (*Teleostei*: *Carangidae*) and concentrations of zooplankton in the northern Gulf of Mexico, with illustrations of early *Hemicaranx amblyrhynchus* and *Caranx* spp. larvae. *Mar. Biol.* 145, 1001–1014. doi: 10.1007/s00227-004-1381-z

Erisman, B., Heyman, W., Kobara, S., Ezer, T., Pittman, S., Aburto-Oropeza, O., et al. (2017). Fish spawning aggregations: where well-placed management actions can yield big benefits for fisheries and conservation. *Fish Fish.* 18, 128–144. doi: 10.1111/faf.12132

Fogarty, M. J., Sissenwine, M. P., and Cohen, E. B. (1991). Recruitment variability and the dynamics of exploited marine populations. *Trends Ecol. Evol.* 6, 241–246. doi: 10.1016/0169-5347(91)90069-a

Game, E. T., Grantham, H. S., Hobday, A. J., Pressey, R. L., Lombard, A. T., and Beckley, L. E. (2009). Pelagic protected areas: the missing dimension in ocean conservation. *Trends Ecol. Evol.* 24, 360–369.

Gamfeldt, L., Lefcheck, J. S., Byrnes, J. E., Cardinale, B. J., Duffy, J. E., and Griffin, J. N. (2014). Marine biodiversity and ecosystem functioning: what's known and what's next? *Oikos* 124, 252–265. doi: 10.1111/oik.01549

Govoni, J. J., Hoss, D. E., and Colby, D. R. (1989). The spatial-distribution of larval fishes about the Mississippi River plume. *Limnol. Oceanogr.* 34, 178–187. doi: 10.4319/lo.1989.34.1.0178

Grimes, C. B., and Finucane, J. H. (1991). Spatial distribution and abundance of larval and juvenile fish, chlorophyll and macrozooplankton around the Mississippi River discharge plume, and the role of the plume in fish recruitment. *Mar. Ecol. Prog. Ser.* 75, 109–119. doi: 10.3354/meps075109

Guisan, A., Edwards, T. C., and Hastie, T. (2002). Generalized linear and generalized additive models in studies of species distributions: setting the scene. *Ecol. Model.* 157, 89–100. doi: 10.1016/s0304-3800(02)00204-1

Hernandez, F. J. Jr., Carassou, L., Graham, W. M., and Powers, S. P. (2013). Evaluation of the taxonomic sufficiency approach for ichthyoplankton community analysis. *Mar. Ecol. Prog. Ser.* 491, 77–90. doi: 10.3354/meps10475

Hernandez, F. J. Jr., Powers, S. P., and Graham, W. M. (2010). Seasonal variability in ichthyoplankton abundance and assemblage composition in the northern Gulf of Mexico off Alabama. *Fish. Bull.* 108, 193–207.

Houde, E. (2002). "Mortality," in *Fishery Science, the Unique Contributions of Early Life Stages*, eds L. A. Fuiman and R. G. Werner (Oxford: Blackwell Science), 64–87.

Karnauskas, M., Schirripa, M. J., Kelble, C. R., Cook, G. S., and Craig, J. K. (2013). Ecosystem status report for the Gulf of Mexico. *NOAA Tech. Mem. NMFS-SEFSC.* 653:52.

Katsuragawa, M., Dias, J. F., Harari, C., Namiki, C., and Zani-Teixeira, M. L. (2014). Patetrns in larval fish assemblaged under the influence of the Brazil Current. *Cont. Shelf Res.* 89, 103–117. doi: 10.1016/j.csr.2014.04.024

King, A. J., Gwinn, D. C., Tonkin, Z., Mahoney, J., Raymond, S., Beesley, L., et al. (2016). Using abiotic drivers of fish spawning to inform environmental flow management. *J. Appl. Ecol.* 53, 34–43. doi: 10.1111/1365-2664.12542

Kitchens, L. L., and Rooker, J. R. (2014). Habitat associations of dolphinfish larvae in the Gulf of Mexico. *Fish. Oceanogr.* 23, 460–471. doi: 10.1111/fog.12081

Lehodey, P., Alheit, J., Barange, M., Baumgartner, T., Beaugrand, G., Drinkwater, K., et al. (2006). Climate variability, fish, and fisheries. *J. Clim.* 19, 5009–5030.

Lewison, R., Hobday, A. J., Maxwell, S., Hazen, E., Hartog, J. R., Dunn, D. C., et al. (2015). Dynamic ocean management: identifying the critical ingredients of dynamic approaches to ocean resource management. *BioScience* 65, 486–498. doi: 10.1093/biosci/biv018

Lindo-Atichati, D. (2012). Varying mesoscale structures influence larval fish distribution in the northern Gulf of Mexico. *Mar. Ecol. Prog. Ser.* 463, 245–257. doi: 10.3354/meps09860

Lohrenz, S. E., Fahnenstiel, G. L., Redalje, D. J., Lang, G. A., Chen, X., and Dagg, M. J. (1997). Variations in primary production of northern Gulf of Mexico continental shelf waters linked to nutrient inputs from the Mississippi River. *Mar. Ecol. Prog. Ser.* 155, 45–54. doi: 10.3354/meps155045

Marchese, C. (2015). Biodiversity hotspots: a shortcut for a more complicated concept. *Global Ecol. Conserv.* 3, 297–309. doi: 10.1016/j.gecco.2014.12.008

McEachran, J. D., and Fechhelm, J. D. (2010). *Fishes of the Gulf of Mexico, Volume 2: Scorpaeniformes to Tetraodontiformes*. Austin, Tx: University of Texas Press.

Mittermeier, R. A., Turner, W. R., Larsen, F. W., Brooks, T. M., and Gascon, C. (2011). "Global biodiversity conservation: the critical role of hotspots," in *Biodiversity Hotspots*, eds F. Zachos and J. Habel (Berlin: Springer). doi: 10.1016/j.gecco.2014.12.008

Moku, M., Tsuda, A., and Kawaguchi, K. (2003). Spawning season and migration of the myctophid fish *Diaphus theta* in the western North Pacific. *Ichthyol. Res.* 50, 52–58. doi: 10.1007/s102280300007

Mourato, B. L., Hazin, F., Bigelow, K., Musyl, M., Carvalho, F., and Hazin, H. (2014). Spatio-temporal trends of sailfish, *Istiophorus platypterus* catch rates in relation to spawning ground and environmental factors in the equatorial and southwestern Atlantic Ocean. *Fish. Oceanogr.* 23, 32–44. doi: 10.1111/fog.12040

Myers, R. A. (2003). Rapid worldwide depletion of predatory fish communities. *Nature* 423, 280–283.

Myers, R. A., and Worm, B. (2003). Rapid worldwide depletion of predatory fish communities. *Nature* 423, 280–283. doi: 10.1038/nature01610

Namiki, C., Bonecker, A. C. T., and De Castro, M. S. (2007). Occurrence and abundance of three larval codlet species (*Bregmacerotidae*, *Teleostei*) in the Southwest Atlantic Ocean (12-22 degrees S). *J. Appl. Ichthyol.* 23, 136–141. doi: 10.1111/j.1439-0426.2006.00818.x

Nonaka, R. H., Matsuura, Y., and Suzuki, K. (2000). Seasonal variation in larval fish assemblages in relation to oceanographic conditions in the Abrolhos Bank region off eastern Brazil. *Fish. Bull.* 98, 767–784.

O'Connor, B. S., Muller-Karger, F. E., Nero, R. W., Hu, C. M., and Peebles, E. B. (2016). The role of Mississippi river discharge in offshore phytoplankton blooming in the northeastern Gulf of Mexico during August 2010. *Remote Sens. Environ.* 173, 133–144. doi: 10.1016/j.rse.2015.11.004

Oksanen, J., Guillaume, F., Blanchet, F., Friendly, M., Kindt, R., Legendre, P., et al. (2017). *vegan: Community Ecology Package. R Package Version 2.4-4*. Avaliable online at: https://CRAN.R-project.org/package=vegan (accessed July, 2019).

Pikitch, E. K., Santora, C., Babcock, E. A., Bakun, A., Bonfil, R., Conover, D. O., et al. (2004). Ecology. Ecosystem-based fishery management. *Science* 305, 346–347. doi: 10.1126/science.1098222

Randall, L. L., Smith, B. L., Cowan, J. H., and Rooker, J. R. (2015). Habitat characteristics of bluntnose flyingfish Prognichthys occidentalis (*Actinopterygii*. *Exocoetidae*), across mesoscale features in the Gulf of Mexico. *Hydrobiologia* 749, 97–111. doi: 10.1007/s10750-014-2151-7

Richards, W. J. (1993). Larval fish assemblages at the Loop Current boundary in the Gulf of Mexico. *Bull. Mar. Sci.* 53:475.

Richards, W. J. (2006). *Early Stages of Atlantic Fishes; an Identification Guide for the Western Central North Atlantic*. Boca Raton, FL: Taylor & Francis.

Richardson, D. E. (2008). *Physical and Biological Characteristics of Billfish Spawning Habitat in the Straits of Florida*. Dissertation, University of Miami, Miami, FL.

Richardson, D. E., Llopiz, J. K., Guigand, C. M., and Cowen, R. K. (2010). Larval assemblages of large and medium-sized pelagic species in the Straits of Florida. *Prog. Oceanogr.* 86, 8–20. doi: 10.1016/j.pocean.2010.04.005

Rijnsdorp, A. D., Peck, M. A., Engelhard, G. H., Mollmann, C., and Pinnegar, J. K. (2009). Resolving the effect of climate change on fish populations. *ICES J. Mar. Sci.* 66, 1570–1583. doi: 10.1093/icesjms/fsp056

Rocha, J., Yletyinen, J., Biggs, R., Blenckner, T., and Peterson, G. (2015). Marine regime shifts: drivers and impacts on ecosystems services. *Philos. Trans. R. Soc. B Biol. Sci.* 370:20130273.

Rodriguez, J. M., Hernandez- Leon, S., and Barton, E. D. (2006). Vertical distriv=bution of fish larvae in the Canaries-African coastal transition zone in the summer. *Mar. Biol.* 149, 885–897. doi: 10.1007/s00227-006-0270-z

Rooker, J. R., Kitchens, L. L., Dance, M. A., Wells, R. J., Falterman, B., and Cornic, M. (2013). Spatial, temporal, and habitat-related variation in abundance of pelagic fishes in the Gulf of Mexico: potential implications of the deepwater horizon oil spill. *PLoS One* 8:e76080. doi: 10.1371/journal.pone.0076080

Rooker, J. R., Simms, J. R., Wells, R. J. D., Holt, S. A., Holt, G. J., Graves, J. E., et al. (2012). Distribution and habitat associations of billfish and swordfish larvae across mesoscale features in the Gulf of Mexico. *PLoS One.* 7:e34180. doi: 10.1371/journal.pone.0034180

Sanvicente-Añorve, L., Flores-Coto, C., and Sánchez-Velasco, L. (1998). Spatial and seasonal patterns of larval fish assemblages in the southern Gulf of Mexico. *Bull. Mar. Sci.* 62, 17–30.

Sato, M., Barth, J. A., Benoit-Bird, K. J., Pierce, S. D., Cowles, T. J., Brodeur, R. D., et al. (2018). Coastal upwelling fronts as a boundary for planktivorous fish distributions. *Mar. Ecol. Prog. Ser.* 595, 171–186. doi: 10.3354/meps12553

Schiller, R. V., Kourafalou, V. H., Hogan, P., and Walker, N. D. (2011). The dynamics of the Mississippi River plume: Impact of topography, wind and offshore forcing on the fate of plume waters. *J. Geophys. Res. Oceans* 116:C06029.

Shulzitski, K., Sponaugle, S., Hauff, M., Walter, K., D'Alessandro, E. K., and Cowen, R. K. (2015). Close encounters with eddies: oceanographic features increase growth of larval reef fishes during their journey to the reef. *Biol. Lett.* 11:20140746. doi: 10.1098/rsbl.2014.0746

Smith, B. L., Lu, C.-P., and Alvarado Bremer, J. R. (2009). High-resolution melting analysis (HRMA): a highly sensitive inexpensive genotyping alternative for population studies. *Mol. Ecol. Resour.* 10, 193–196. doi: 10.1111/j.1755-0998.2009.02726.x

Torres, A. P., Reglero, P., Balbin, R., Urtizberea, A., and Alemany, F. (2011). Coexistence of larvae of tuna species and other fish in the surface mixed layer in the NW Mediterranean. *J. Plankton Res.* 33, 1793–1812. doi: 10.1093/plankt/fbr078

Vilchis, L. I., Balance, L. T., and Watson, W. (2009). Temporal variability of neustonic ichthyoplankton assemblages of the eastern Pacific warm pool: can community structure be linked to climate variability? *Deep Sea Res. I* 56, 125–140. doi: 10.1016/j.dsr.2008.08.004

Waide, R. B., Willig, M. R., Steiner, C. F., Mittelbach, G., Gough, L., Dodson, S. I., et al. (1999). The relationship Between Productivity and Species Richness. *Annu. Rev. Ecol. Systemat.* 30, 257–300.

Ward, P., and Myers, R. A. (2005). Shifts in open-ocean fish communities coinciding with the commencement of commercial fishing. *Ecology* 86, 835–847. doi: 10.1890/03-0746

Watanabe, H., Kawaguchi, K., and Hayashi, A. (2002). Feeding habits of juvenile surface-migratory myctophid fishes (family Myctophidae) in the Kuroshio region of the western North Pacific. *Mar. Ecol. Prog. Ser.* 236, 263–272. doi: 10.3354/meps236263

Wood, S. N. (2011). Fast stable restricted maximum likelihood and marginal likelihood estimation of semiparametric generalized linear models. *J. R. Stat. Soc.* 73, 3–36. doi: 10.1111/j.1467-9868.2010.00749.x

Worm, B., Barbier, E. B., Beaumont, N., Duffy, J. E., Folke, C., Halpern, B. S., et al. (2006). Impacts of biodiversity loss on ocean ecosystem services. *Science* 314, 787–790.

Conflict of Interest: The authors declare that the research was conducted in the absence of any commercial or financial relationships that could be construed as a potential conflict of interest.

frontiers in Marine Science

ORIGINAL RESEARCH
published: 05 November 2020
doi: 10.3389/fmars.2020.507992

Trophic Structure and Sources of Variation Influencing the Stable Isotope Signatures of Meso- and Bathypelagic Micronekton Fishes

Travis M. Richards[1], Tracey T. Sutton[2] and R. J. David Wells[1,3]*

[1] Department of Marine Biology, Texas A&M University at Galveston, Galveston, TX, United States, [2] Halmos College of Natural Sciences and Oceanography, Nova Southeastern University, Dania Beach, FL, United States, [3] Department of Wildlife and Fisheries Sciences, Texas A&M University, College Station, TX, United States

To better understand spatiotemporal variation in the trophic structure of deep-pelagic species, we examined the isotope values of particulate organic matter (POM) (isotopic baseline) and seven deep-pelagic fishes with similar diet compositions but contrasting vertical distributions across mesoscale features in the Gulf of Mexico using stable isotope and amino acid compound-specific isotope analyses. Species examined included four migratory (*Benthosema suborbitale*, *Lepidophanes guentheri*, *Melamphaes simus*, *Sigmops elongatus*) and three non-migratory zooplanktivorous fishes (*Argyropelecus hemigymnus*, *Cyclothone obscura*, *Sternoptyx pseudobscura*). Isotopic values of POM increased with depth, with meso- and bathypelagic samples characterized by higher $\delta^{13}C$ and $\delta^{15}N$ values relative to epipelagic samples. Despite similar diet compositions, mean $\delta^{15}N$ values of fishes spanned 3.43‰ resulting in mean trophic position estimates among species varying by 1.09 trophic levels. Interspecific differences in $\delta^{15}N$ were driven by higher $\delta^{15}N$ values in the non-migratory and deepest dwelling *C. obscura* (10.61‰) and lower $\delta^{15}N$ values in the migratory and shallowest dwelling *L. guentheri* (7.18‰) and *B. suborbitale* (8.11‰). Similarly, fish $\delta^{15}N_{sourceAA}$ values were correlated with depth, with the lowest values occurring in the migratory *L. guentheri* and *B. suborbitale* and highest values occurring in the non-migratory *C. obscura*. Our data suggest that depth-related trends in fish $\delta^{15}N$ and $\delta^{15}N_{sourceAA}$ values are driven by shallower dwelling species feeding within epipelagic food webs supported by POM with lower $\delta^{15}N$ values, while deeper dwelling, non-migratory species increasingly use food webs at depth supported by POM with elevated $\delta^{15}N$ values. Horizontal isotopic variation was observed across a large mesoscale oceanographic feature (Loop Current), with POM, three migratory, and one non-migratory species characterized by higher $\delta^{13}C$ and lower $\delta^{15}N$ values in the anticyclonic Loop Current relative to surrounding water masses. Our results demonstrate that isotopic values of POM can vary significantly over relatively small horizontal and vertical scales and that baseline variation can be conserved in the signatures of higher-order

OPEN ACCESS

Edited by:
Luis Cardona, University of Barcelona, Spain

Reviewed by:
Jeffrey C. Drazen, University of Hawai'i at Mânoa, United States
Ainhoa Bernal Bajo, Institute of Marine Sciences, Spanish National Research Council, Spain

***Correspondence:**
Travis M. Richards
Travis.Richards3@gmail.com

Specialty section:
This article was submitted to Deep-Sea Environments and Ecology, a section of the journal Frontiers in Marine Science

Received: *28 October 2019*
Accepted: *28 September 2020*
Published: *05 November 2020*

Citation:
Richards TM, Sutton TT and Wells RJD (2020) Trophic Structure and Sources of Variation Influencing the Stable Isotope Signatures of Meso- and Bathypelagic Micronekton Fishes. Front. Mar. Sci. 7:507992. doi: 10.3389/fmars.2020.507992

consumers. By gaining a more thorough understanding of the sources contributing to isotopic variation of deep-pelagic fishes, this paper will inform the design and interpretation of future feeding studies in the pelagic realm and advances our knowledge of deep-pelagic food web structure.

Keywords: micronekton, stable isotope analysis, mesopelagic, bathypelagic, Gulf of Mexico, lanternfish, hatchetfish, bristlemouths

INTRODUCTION

The deep-pelagic ocean provides a suite of ecosystem services, including carbon sequestration, nutrient regeneration, and waste absorption, which are vital to ocean health (Mengerink et al., 2014; Thurber et al., 2014). Although its importance is well established, the deep pelagic is chronically understudied, with knowledge of ecosystem function lagging behind coastal and shelf systems (Webb et al., 2010). Currently, natural resource extraction and fisheries are expanding into the deep ocean before management strategies can be developed, resulting in a concerted effort to characterize deep-pelagic ecosystems so that the effects of anthropogenic activities can be assessed (Ramirez-Llodra et al., 2011; Mengerink et al., 2014; Murawski et al., 2020). In particular, recent research has centered on understanding deep-pelagic food webs, as trophic interactions regulate animal populations (especially in ecosystems with no physical refuge), determine energy pathways, and influence the resilience of communities to perturbation (Winemiller and Polis, 1996; Chipps and Garvey, 2007).

A thorough understanding of deep-pelagic food webs necessitates detailed trophic information of micronekton, small (2–10 cm) swimming fishes, crustaceans, and cephalopods that represent a dominant proportion of the global nekton biomass (Irigoien et al., 2014; Vereshchaka et al., 2019). Ubiquitous throughout the world's oceans, micronekton play important roles in ecological and biogeochemical processes that underpin ecosystem services including carbon sequestration and fisheries production (Angel, 1989; Longhurst et al., 1990). Many micronekton undergo diel vertical migrations (DVM) through the water column to feed within the epipelagic zone (0–200 m) at night before returning to daytime depths in the meso- (200–1,000 m) or bathypelagic zones (1,000–4,000 m). Through DVM, micronekton represent an important source of connectivity between the epi-, meso-, and bathypelagic zones and have been shown to be important prey of consumers throughout the water column (Sutton and Hopkins, 1996; Moteki et al., 2001; Choy et al., 2013). Additionally, by feeding heavily on zooplankton, micronekton link higher-order consumers with primary and secondary production (Hopkins and Gartner, 1992; Hopkins et al., 1996). Considering their high global abundance and importance to pelagic food webs, describing micronekton trophic structure is critical to increasing our understanding of deep-pelagic ecosystem structure and function.

Stable isotope analysis (SIA) is a tool commonly used to describe trophic structure in pelagic systems (Peterson and Fry, 1987; Vander Zanden and Rasmussen, 2001). Stable isotopes of carbon undergo small levels of fractionation during trophic transfer and can be used to delineate energy pathways from primary producers to consumers (DeNiro and Epstein, 1978; Wada et al., 1991). Nitrogen stable isotopes undergo larger levels of fractionation during trophic transfer and can be used to make estimations of trophic position and food chain length (Minagawa and Wada, 1984; Post, 2002). While the utility of SIA in ecology is well established, correct interpretation of SIA data is difficult, as numerous sources of variation unrelated to an organism's diet can contribute to the isotopic signatures of consumers (Boecklen et al., 2011). For instance, because a consumer's isotopic signature is determined by both its trophic position and the isotope value of basal carbon sources, high isotopic variability in primary producers over fine spatiotemporal scales can result in isotopic variation in consumers not reflective of a change in trophic status (Popp et al., 2007). Traditionally, variation at the base of the food web has been accounted for via comprehensive sampling of primary producers, which can be logistically challenging in pelagic systems. Amino acid compound-specific isotope analysis (AA-CSIA) allows for changes in trophic status to be distinguished from isotopic variation at the base of the food web (Popp et al., 2007; Bradley et al., 2015). The method uses two groups of individual amino acids that undergo differing levels of ^{15}N enrichment during trophic transfer. "Source" amino acids undergo minimal ^{15}N enrichment with each trophic step (<1‰) (e.g., phenylalanine, serine, glycine, lysine, tyrosine) and have been shown to accurately reflect the δ^{15}N values of primary producers at the base of food webs (McClelland and Montoya, 2002; Popp et al., 2007; Chikaraishi et al., 2009). Comparatively, "trophic" amino acids (e.g., alanine, aspartic acid, glutamic acid, isoleucine, proline, valine) undergo larger, predictable levels of ^{15}N enrichment and can be used to estimate trophic position (McClelland and Montoya, 2002; Chikaraishi et al., 2009). Because AA-CSIA incorporates both baseline and trophic information within a single sample, trophic position estimates can be made without having to characterize the isotopic values of primary producers (Popp et al., 2007; Bradley et al., 2015).

Delineations of energy pathways and trophic position estimations are critical to understanding deep-pelagic food webs and are uncommon for the Gulf of Mexico (GOM) and many pelagic systems (McClain-Counts et al., 2017; Richards et al., 2018). However, for SIA data to be interpreted correctly, a thorough understanding of how biological and environmental sources of variation affect isotope values of consumers is needed. Using SIA and AA-CSIA, we examined the isotope values of particulate organic matter (POM) and seven deep-pelagic fishes with similar diet compositions but contrasting vertical distributions over two sampling years and across a large mesoscale feature in the GOM. By selecting species with

similar diet compositions and contrasting depth distributions, we aimed to highlight isotopic variation related to spatial and temporal factors while keeping variation related to diet at a minimum. The species selected included four vertical migrators (Myctophiformes: *Benthosema suborbitale*, *Lepidophanes guentheri*; Beryciformes: *Melamphaes simus*; Stomiiformes: *Sigmops elongatus*) and three non-migratory species (Stomiiformes: *Argyropelecus hemigymnus*, *Cyclothone obscura*, *Sternoptyx pseudobscura*). Vertically migrating species exhibited daytime depth distributions ranging from the upper mesopelagic zone (*B. suborbitale*) to the lower meso- and upper bathypelagic zones (*M. simus*) and nighttime distributions concentrated within the epi- and upper mesopelagic zones (**Figure 1** and **Table 1**). Non-migratory species exhibited contrasting depth distributions ranging from the upper mesopelagic zone (*A. hemigymnus*) to the bathypelagic zone (*C. obscura*) (**Figure 1** and **Table 1**). All species are zooplanktivorous and feed primarily on copepods (*B. suborbitale*, *C. obscura*, *M. simus*), a mixture of copepods and small euphausiids (*L. guentheri*, *S. elongatus*), copepods and ostracods (*A. hemigymnus*), and copepods and polychaetes (*S. pseudobscura*) (Hopkins and Baird, 1985; Hopkins and Gartner, 1992; Hopkins et al., 1996; Burghart et al., 2010).

Using these seven species of micronekton as model taxa, we ask the following questions: Does depth of occurrence and vertical migration type affect the stable isotope values of micronekton with similar diet compositions? Are differences among species driven by differences in diet or by variation at the base of the food web? Finally, how spatially (horizontal and vertical) variable are the isotopic values of primary producers and deep-pelagic micronekton in the GOM?

MATERIALS AND METHODS

Study Design and Sample Collection

Sample collections for this study took place during four oceanographic cruises in 2015–2016, with cruises conducted in May (spring) and August (summer) of each year. While sampling stations for each cruise fell within the same geographic area, the stations visited varied due to the changing position of the Loop Current (**Figure 2**). Circulation in the eastern GOM is dominated by the anticyclonic Loop Current, which brings warm, oligotrophic water northward into the GOM before deflecting eastward and then exiting through the Florida Straits. Northward extension into the GOM by the Loop Current is highly variable and introduces significant spatial heterogeneity to the pelagic GOM (Vukovich and Crissman, 1986; Davis et al., 2002). Previous studies have shown that currents associated with the Loop Current and mesoscale eddies can act to concentrate primary and secondary production and in turn can alter the spatial distribution of higher-order consumers such as tunas, billfishes, and marine mammals (Davis et al., 2002; Rooker et al., 2013). In order to examine the influence of the Loop Current on deep-pelagic trophic structure, sampling sites were classified as either falling within Loop Current water (LCW) or within the surrounding water mass, hereafter referred to as Gulf common water (GCW), following designations described by Johnston et al. (2019). In addition to LCW and GCW sites, Johnston et al. (2019) identified sampling sites along the fronts between the Loop Current and Gulf common water that exhibited characteristics intermediate to the two water masses. These sites, classified as "mixed" by Johnston et al. (2019), did not yield SIA samples for this study.

Micronekton were collected using a Multiple Opening and Closing Net with Environmental Sensing System (MOCNESS), which sampled discrete depth strata from the surface to 1,500 m depth. The depth strata sampled included 0–200 m (epipelagic), 200–600 m (upper mesopelagic), 600–1,000 m (lower mesopelagic), 1,000–1,200 m (bathypelagic), and 1,200–1,500 m (bathypelagic) (Milligan et al., 2018; Cook et al., unpublished data). Micronekton samples selected for SIA were measured to the nearest millimeter for standard length (SL) and frozen at −20°C. Samples selected for AA-CSIA, which were only collected during 2016, were stored in liquid nitrogen at sea before long-term storage at −80°C. In order to characterize the isotopic baseline, samples of particulate organic matter (POM) were collected from the surface, epi-, meso-, and bathypelagic zones at each station. Epi- and mesopelagic samples were collected from the deep chlorophyll maximum (mean depth, 76.6 m) and oxygen minimum zone (mean depth, 426.6 m), respectively, while bathypelagic samples were collected from maximum trawl depth (∼1,500 m). Exact depths for the deep chlorophyll maximum and oxygen minimum varied by station and were visually identified during the downcast of a CTD sensor conducted prior to MOCNESS deployment (Cook et al., unpublished data). Water collections for POM samples were made using 12-L Niskin bottles attached to the CTD rosette and filtered across pre-combusted (2 h at 450°C) 47-mm glass microfiber filters (GF/F) with a 0.7 μm pore size and frozen at −20°C.

Stable Isotope Analysis

Following collection at sea, white muscle tissue was dissected from the lateral musculature of micronekton, rinsed with deionized water, and examined under a microscope for the presence of bones. Cleaned samples were then lyophilized, homogenized, weighed (∼1 mg sample), and wrapped in tin capsules. Prior to SIA, samples of POM were placed in a drying oven at 60°C until a constant weight was achieved (∼24 h) and then folded and wrapped into tin capsules. The C:N of fishes in the present study were low (species mean C:N range, 3.32–3.53), suggesting lipids would not significantly confound the interpretation of $\delta^{13}C$ values. Thus, all statistical analyses were performed on uncorrected $\delta^{13}C$ values. Samples for SIA were analyzed at the University of California at Davis Stable Isotope Facility (UC Davis SIF) using an elemental analyzer (PDZ Europa ANCA-GSL) interfaced with an isotope ratio mass spectrometer (PDZ Europa 20–20). The long-term standard deviation for instrumentation precision at the UC Davis SIF for SIA is 0.2 and 0.3‰ for $\delta^{13}C$ and $\delta^{15}N$, respectively. Isotopic ratios are presented in delta notation relative to the international standards Vienna PeeDee Belemnite (VPDB) and air for carbon and nitrogen, respectively.

Sample preparation for AA-CSIA followed a similar protocol to SIA except a larger amount of tissue (∼3 mg) was dissected,

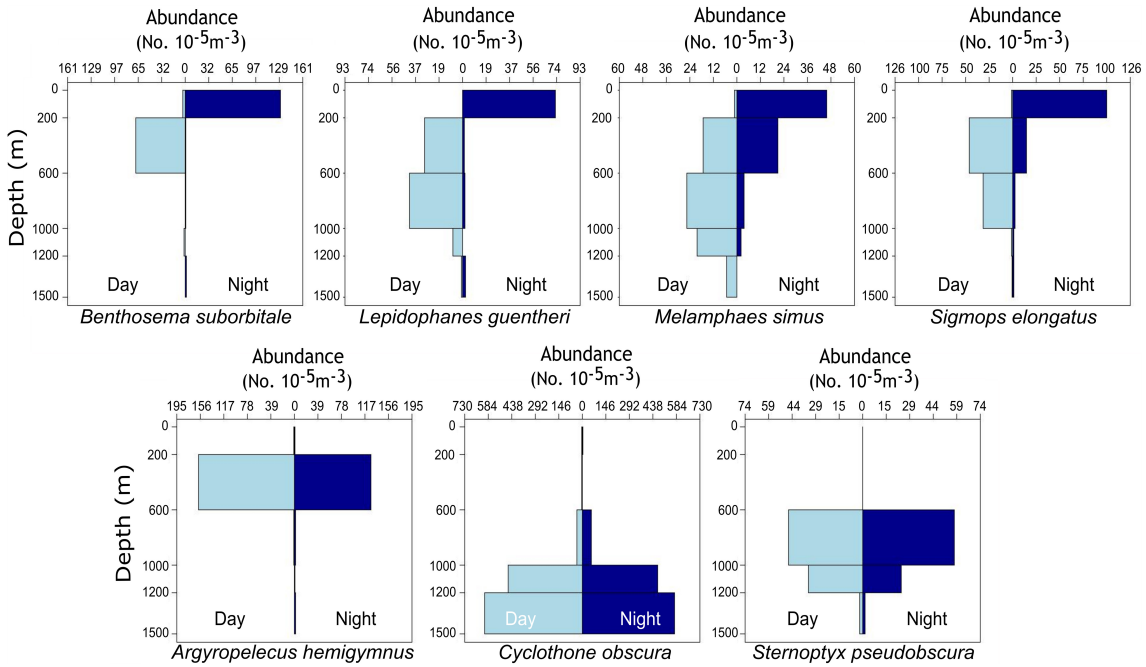

FIGURE 1 | Vertical bar plots representing the standardized abundance of migratory (top row) and non-migratory (bottom row) species collected with day and night MOCNESS tows from 2015 to 2016. Plots represent catch data for each species combined across four oceanographic cruises and not data solely from individuals used for stable isotope analysis. Abundances were standardized by the volume of water filtered during MOCNESS tows as described in Cook et al. (unpublished data).

lyophilized, homogenized, and stored in 2-ml glass dram vials prior to submission. Sample preparation for AA-CSIA at UC Davis SIF followed protocols outlined in Yarnes and Herszage (2017). Briefly, samples were hydrolyzed with 6 M HCl to isolate amino acids before derivatization using esterification-acetylation to yield N-acetyl isopropyl esters. The nitrogen isotope compositions of the resulting N-acetyl amino acid isopropyl esters were determined using a gas chromatograph (Thermo Trace GC 1310) linked to an isotope-ratio mass spectrometer (Thermo Scientific Delta V Advantage IRMS) via a GC IsoLink II combustion interface. Samples were injected into a DB-1301 (Agilent Technologies) column (60 m × 0.25 mm × 1.0 μm film) at a temperature of 255°C (splitless, 1 min) under a constant flow rate of 1.2 ml/min. During analysis, all samples were analyzed in duplicate with triplicate measurements made if values exceeded expected measurement error ± 1‰ (Yarnes and Herszage, 2017). Norleucine was used as an internal standard during analysis, while two amino acid compounds developed by the UC Davis SIF were comeasured during analysis of fish samples and were used for calibration and normalization of amino acid data. Standard deviation for all amino acids averaged ± 0.38‰. The $\delta^{15}N_{sourceAA}$ values for each species are presented as the weighted mean of the four source amino acids phenylalanine, lysine, glycine, and serine, while $\delta^{15}N_{TrophicAA}$ represents the weighted mean of the three trophic amino acids alanine, leucine, and glutamic acid (Bradley et al., 2015; Gloeckler et al., 2018). Both source and trophic amino acids were weighted by the standard deviation of each amino acid (Bradley et al., 2015; Gloeckler et al., 2018).

Data Analysis

Interspecific differences in the $\delta^{13}C$ and $\delta^{15}N$ values of POM and fishes were examined using a three-factor multivariate analysis of variance (MANOVA), with $\delta^{13}C$ and $\delta^{15}N$ included as dependent variables and species, sampling year (2015, 2016), and water type (LCW, GCW) as independent variables. Following MANOVA, analysis of variance (ANOVA) was used to explore interspecific differences in $\delta^{13}C$ and $\delta^{15}N$. Intraspecific variation in $\delta^{13}C$ and $\delta^{15}N$ was explored using ordinary least squares regression to characterize the relationship between standard length (SL) and $\delta^{13}C$ and $\delta^{15}N$. For species with statistically significant relationships between length and $\delta^{13}C$ or $\delta^{15}N$, length was used as a covariate in two-factor analysis of covariance (ANCOVA) to assess the effects of sampling year and water type on each isotope for each species. Similarly, variation in POM $\delta^{13}C$ and $\delta^{15}N$ within each depth zone was assessed using two-factor ANCOVA, with sampling year and water type included as independent variables and depth of water collection included as a covariate. Following ANOVA/ANCOVA, *a posteriori* differences among means were analyzed using Shaffer's multiple comparison procedure (Shaffer's MCP), as it is less affected by unbalanced sample sizes relative to other *post hoc* tests and adjusts to control for type I error during multiple comparisons (Shaffer, 1986; Bretz et al., 2016). ANOVA/ANCOVA tests met assumptions of normality and homoscedasticity, which were checked through visual inspection of residual plots and normal qq plots. All statistical analyses were performed in R (R version 3.6.0) using the car and

TABLE 1 | Summary table depicting sample totals of deep-pelagic fishes for each sampling year and each water type (LCW, Loop Current Water; GCW, Gulf Common Water) and mean (± SD) $\delta^{13}C$, $\delta^{15}N$, and C:N values for each species.

Species	Median nighttime depth (m)	n	2015 LCW	2015 GCW	2016 LCW	2016 GCW	SL range (mm)	$\delta^{13}C$ (‰)	$\delta^{15}N$ (‰)	C:N	Depth Reference
Migrators											
B. suborbitale	80	63	4	17	4	38	16–31	−19.41 ± 0.40	8.05 ± 0.74	3.40 ± 0.70	Gartner, 1987
L. guentheri	80	48	6	17	4	21	21–66	−19.10 ± 0.46	7.18 ± 0.94	3.38 ± 0.23	Gartner, 1987
M. simus	300	45	8	9	4	24	14–27	−19.58 ± 0.48	8.94 ± 0.95	3.44 ± 0.06	Sutton et al., 2017
S. elongatus	175	70	11	17	10	32	49–196	−19.05 ± 0.45	8.70 ± 0.70	3.34 ± 0.05	Lancraft et al., 1988
Non-migrators											
A. hemigymnus	400	41	8	11	7	15	16–37	−18.75 ± 0.45	8.87 ± 0.63	3.40 ± 0.10	Hopkins and Baird, 1985
C. obscura	1950	61	2	16	9	34	28–51	−18.29 ± 0.40	10.61 ± 0.74	3.32 ± 0.05	McEachran and Fechhelm, 1998
S. pseudobscura	850	41	1	13	4	23	14–46	−19.85 ± 0.29	8.27 ± 0.56	3.53 ± 0.07	Hopkins and Baird, 1985

Median nighttime depth distribution data were determined using depth data for adult life stages and excluded depth data for non-migratory juvenile stages. Depth data were derived from primary literature sources that incorporated finer-scale depth-stratified sampling (50–100 m depth bins) to allow for more accurate estimations of depth of occurrence.

multcomp packages (Hothorn et al., 2008; Fox and Weisberg, 2019).

Trophic Position Estimates

Trophic position (TP) estimates were made using both SIA and AA-CSIA data. TP estimations using SIA followed Eq. 1 where $\delta^{15}N_i$ represents the nitrogen signature of an individual, $\delta^{15}N_{base}$ represents the nitrogen signature of the pyrosome, *Pyrosoma atlanticum*, and trophic enrichment factor (TEF) represents the enrichment of ^{15}N with each trophic step (3.15‰ following Valls et al., 2014). Primary consumers are useful when setting isotopic baselines because their slower tissue turnover rates and longer generation times allow for the integration of isotopic baselines over broader spatiotemporal scales (Post, 2002). Pyrosomes are filter-feeding pelagic tunicates known to feed on POM and have been used as model primary consumers in several studies examining pelagic food web structure (Cherel et al., 2010; Ménard et al., 2014). The utility of pyrosomes to delineate isotopic baselines is enhanced in regions like the GOM, which are characterized by low chlorophyll α concentrations and phytoplankton communities dominated by small flagellates rather than diatoms, which have been shown to be unassimilated during pyrosome feeding (von Harbou et al., 2011; Pakhomov et al., 2019). The mean $\delta^{13}C$ (-22.40 ± 0.63) and $\delta^{15}N$ (3.15 ± 0.92) values of 22 *P. atlanticum* collected during this study were higher than $\delta^{13}C$ and $\delta^{15}N$ values of epipelagic POM, suggesting that pyrosomes are suitable for setting the isotopic baseline in the pelagic GOM.

$$TP_{SIA} = \frac{\delta^{15}N_i - \delta^{15}N_{base}}{TEF} + 1 \quad (1)$$

Trophic position estimations using data derived from AA-CSIA followed Eq. 2. In the equation, $\delta^{15}N_{Tr-AA}$ represents the weighted mean of the three trophic amino acids alanine, leucine, and glutamic acid, and $\delta^{15}N_{Src-AA}$ represents the weighted mean of three source amino acids glycine, lysine, and phenylalanine (Bradley et al., 2015; Gloeckler et al., 2018). The terms β, which represents the difference in $\delta^{15}N$ values of trophic and source amino acids of primary producers, and TEF_{Tr-Src}, which represents the average isotopic enrichment between trophic and source amino acids in consumers, were set to 3.6 and 5.7‰, respectively, following Bradley et al. (2015). As mentioned above, AA-CSIA samples and subsequent TP estimations using AA-CSIA were conducted during the 2016 sampling year only.

$$TP_{Tr-Src} = \frac{\delta^{15}N_{Tr-AA} - \delta^{15}N_{Src-AA} - \beta}{TEF_{Tr-Src}} + 1 \quad (2)$$

RESULTS

POM SIA

Particulate organic matter isotope values were variable within each depth zone, with individual $\delta^{13}C$ values spanning 4.0‰ in the bathypelagic zone and varying by as much as 6.69‰ in surface samples. Similarly, individual $\delta^{15}N$ values spanned 4.25‰ in the mesopelagic zone and varied by as much as 6.7‰ in the

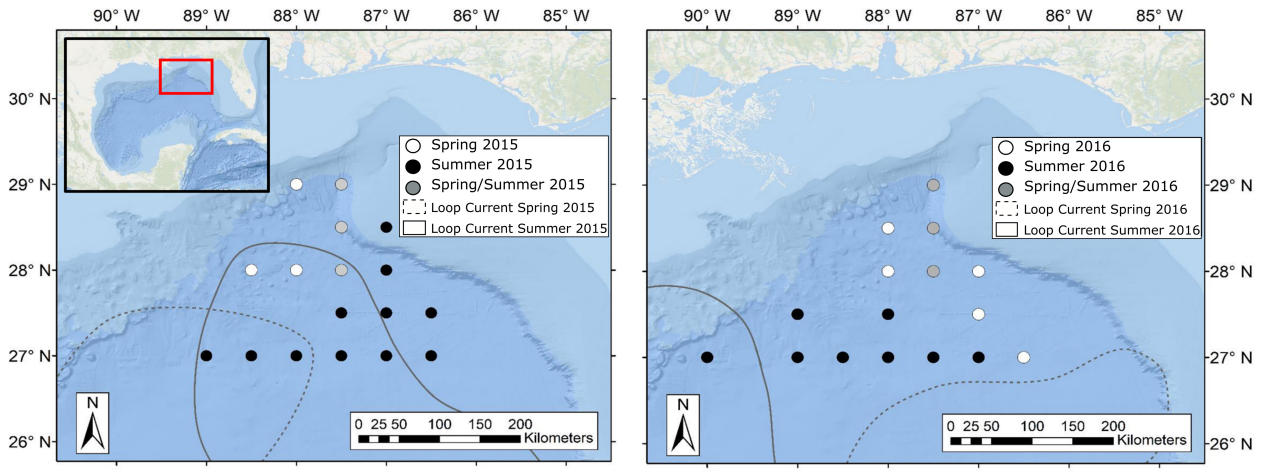

FIGURE 2 | Maps of the northern Gulf of Mexico showing sample collection locations during spring (white circles), summer (black circles), and spring and summer (gray circles) for oceanographic cruises conducted in 2015 (left panel) and 2016 (right panel). Dashed and solid lines represent approximate location of the Loop Current defined by 20-cm sea surface height anomaly (SSHA) during spring and summer sampling periods, respectively. Water surrounding the Loop Current was classified as Gulf Common Water following Johnston et al. (2019). Loop Current positions were created using remotely sensed sea surface height data available through the Copernicus Marine Environmental Monitoring Service.

epipelagic zone. POM $\delta^{13}C$ values differed significantly among depth zones (ANOVA: $F_{3,63} = 17.10$, $p < 0.001$), with differences among zones interacting with year ($F_{3,63} = 8.08$, $p < 0.001$) due to lower $\delta^{13}C$ values for meso- and bathypelagic samples in 2015 relative to 2016 (**Supplementary Tables S1**, **S2**). Generally, POM $\delta^{13}C$ values were lowest in the epipelagic zone and highest in the mesopelagic zone, while surface and bathypelagic samples were intermediate (**Table 2** and **Figure 3A**). POM $\delta^{15}N$ values varied significantly among depth zones (ANOVA: $F_{3,63} = 20.11$, $p < 0.001$) and water types ($F_{1,63} = 5.71$, $p < 0.05$) (**Supplementary Tables S1**, **S2**), with $\delta^{15}N$ values significantly higher in GCW (mean ± SD, 4.25 ± 1.81) relative to LCW (mean ± SD, 2.40 ± 2.60). Among depth zones, $\delta^{15}N$ values of surface and epipelagic samples were similar ($p > 0.05$, Shaffer's MCP) but significantly lower than meso- and bathypelagic samples ($p < 0.05$, Shaffer's MCP for each), while POM $\delta^{15}N$ values from the meso- and bathypelagic zones were statistically similar to each other ($p > 0.05$, Shaffer's MCP) (**Table 2** and **Figure 3A**).

Within each depth zone, the influence of sampling year and water type on POM isotope values differed between $\delta^{13}C$ and $\delta^{15}N$. Differences between sampling years were only observed in $\delta^{13}C$ data, while differences between water types only occurred in $\delta^{15}N$ data (**Table 3**). Significant interannual differences in $\delta^{13}C$ values occurred in all depth zones, with surface and epipelagic POM $\delta^{13}C$ values higher in 2015 relative to 2016, while meso- and bathypelagic samples were higher in 2016 relative to 2015 ($p < 0.05$, Shaffer's MCP for each). Mean $\delta^{15}N$ values from surface and epipelagic samples were lower in LCW relative to samples collected from GCW ($p < 0.05$, Shaffer's MCP for each). No differences in $\delta^{13}C$ and $\delta^{15}N$ values were observed between water types in meso- or bathypelagic samples (**Table 3**).

Deep-Pelagic Fish SIA

Despite feeding on similar prey, there was considerable variation in the $\delta^{13}C$ and $\delta^{15}N$ values of the seven species of fishes examined (**Figure 3**). The $\delta^{13}C$ values of non-migratory fishes were more variable than migratory species, with $\delta^{13}C$ values of non-migrators almost completely separated in isotope space from one another (**Figure 3**). Fish $\delta^{13}C$ values differed significantly among species (ANOVA: $F_{6,347} = 92.16$, $p < 0.001$) and water types ($F_{1,347} = 23.95$, $p < 0.001$), with differences among species varying significantly between GCW and LCW ($F_{6,347} = 5.08$, $p < 0.001$) (**Supplementary Tables S3**, **S4**). In GCW, interspecific differences were driven by high $\delta^{13}C$ values in *C. obscura* and low values in *S. pseudobscura*, with the four migratory species and the non-migratory *A. hemigymnus* displaying intermediate $\delta^{13}C$ values (**Figure 4**). Interspecific differences for $\delta^{13}C$ in LCW differed slightly due to higher $\delta^{13}C$ values in *A. hemigymnus*, *B. suborbitale*, *L. guentheri*, and *S. elongatus* relative to samples from GCW (**Figure 4**).

Individual fish $\delta^{15}N$ values spanned 7.62‰, with mean $\delta^{15}N$ values of non-migratory fishes encompassing a broader range (2.34‰) than migratory species (1.76‰). The $\delta^{15}N$ values of fishes differed significantly among species (ANOVA: $F_{6,347} = 131.24$, $p < 0.001$), with interspecific differences varying between GCW and LCW ($F_{6,347} = 7.28$, $p < 0.001$). $\delta^{15}N$ values of fishes also differed between years ($F_{1,347} = 5.20$, $p < 0.05$), with values slightly lower in 2015 relative to 2016, and differed between water types ($F_{1,347} = 34.42$, $p < 0.001$), with $\delta^{15}N$ values lower in LCW relative to GCW (**Supplementary Tables S3**, **S4**). In both water types, differences among species were primarily driven by high $\delta^{15}N$ values in *C. obscura* and low values in *L. guentheri* and *B. suborbitale* (**Figure 5**), while the migratory *M. simus* and *S. elongatus* and the non-migratory *A. hemigymnus*

TABLE 2 | Summary table depicting sample totals of particulate organic matter for each sampling period and mean (± SD) $\delta^{13}C$, $\delta^{15}N$, and C:N values for each depth zone.

Depth Zone	n	2015 LCW	2015 GCW	2016 LCW	2016 GCW	$\delta^{13}C$ (‰)	$\delta^{15}N$ (‰)
Surface (0–3 m)	20	4	1	2	13	−23.11 ± 1.46	2.54 ± 1.74
Epipelagic (∼76.6 m)	24	4	6	2	12	−24.82 ± 1.49	2.87 ± 1.67
Mesopelagic (∼426.6 m)	17	2	2	1	12	−22.01 ± 1.57	6.05 ± 1.15
Bathypelagic (∼1,500 m)	14	0	2	1	11	−23.62 ± 1.22	4.76 ± 1.75

and *S. pseudobscura* were characterized by intermediate $\delta^{15}N$ values (**Figure 5**).

Standard length was correlated with $\delta^{13}C$ and $\delta^{15}N$ values in both migratory and non-migratory fishes. Specifically, statistically significant relationships between $\delta^{13}C$ and standard length were observed in the migratory *L. guentheri* ($p < 0.05$; $R^2 = 0.11$), *M. simus* ($p < 0.001$; $R^2 = 0.40$), *S. elongatus* ($p < 0.001$; $R^2 = 0.15$), and in the non-migratory *C. obscura* ($p < 0.001$; $R^2 = 0.25$). Similarly, significant relationships between standard length and $\delta^{15}N$ were observed for all migratory species: *B. suborbitale* ($p < 0.01$; $R^2 = 0.12$), *L. guentheri* ($p < 0.001$; $R^2 = 0.43$), *M. simus* ($p < 0.001$; $R^2 = 0.73$), *S. elongatus* ($p < 0.001$; $R^2 = 0.23$), and for the non-migratory *C. obscura* ($p < 0.01$; $R^2 = 0.15$). Subsequent ANCOVA indicated the effect of sampling year and water type on isotope values varied by species, with no consistencies between migrators and non-migrators (**Table 4**). Intraspecific interannual variability was minimal, with no differences in $\delta^{13}C$ observed between sampling years and interannual differences in $\delta^{15}N$ only occurring in the migratory *L. guentheri* and non-migratory *A. hemigymnus* and *S. pseudobscura* ($p < 0.05$, Shaffer's MCP for each). The effect of water type was more pronounced, with the migratory *B. suborbitale*, *L. guentheri*, and *S. elongatus* and the non-migratory *A. hemigymnus* possessing higher $\delta^{13}C$ and lower $\delta^{15}N$ values in LCW relative to GCW ($p < 0.05$, Shaffer's MCP for each) (**Table 4**).

AA-CSIA and Trophic Position Estimates

Mean $\delta^{15}N_{sourceAA}$ values of fishes echoed patterns in $\delta^{15}N$ values, with the migratory *L. guentheri* and *B. suborbitale* displaying the lowest mean $\delta^{15}N_{sourceAA}$ values and the non-migratory and deepest dwelling *C. obscura* displaying the highest (**Figure 6**). The migratory *M. simus* and *S. elongatus* and non-migratory *A. hemigymnus* and *S. pseudobscura* had similar $\delta^{15}N_{sourceAA}$ values that fell between the end members of *L. guentheri* and *C. obscura* (**Figure 6**). Significant positive linear relationships were observed between bulk $\delta^{15}N$ values and $\delta^{15}N_{sourceAA}$ values ($p < 0.01$; $R^2 = 0.90$) (**Figure 6A**) and between mean $\delta^{15}N_{sourceAA}$ values and median nighttime depth ($p < 0.05$; $R^2 = 0.81$) (**Figure 6B**). Mean TP_{SIA} estimates spanned 1.09 trophic levels, with all species except *C. obscura* placed between the third and fourth trophic level (**Table 5**). Comparatively, $TP_{AA-CSIA}$ estimates exhibited a narrower range of 0.62 trophic levels and placed all species between the third and fourth trophic level. Differences in mean TP estimates between the two methods varied by species, with close agreement between estimates for *S. pseudobscura*, *L. guentheri*, and *M. simus* but a relatively large disparity in *C. obscura*, with $TP_{AA-CSIA}$ estimates 0.9 TLs lower than TP_{SIA} estimates (**Table 5**).

DISCUSSION

Variation in POM SIA

The isotopic values of POM varied considerably among and within the vertical depth zones of the northern GOM. The high level of variation is consistent with previous GOM studies that documented POM values collected from similar depths spanning 6–10‰ and 5–13‰ for $\delta^{13}C$ and $\delta^{15}N$, respectively, Fernández-Carrera et al. (2016). Despite the high degree of variation, POM $\delta^{13}C$ and $\delta^{15}N$ values differed among depth zones, with a pattern of enrichment between the epipelagic and meso- and bathypelagic zones. The observed enrichment, particularly in ^{15}N, between epipelagic and deep-pelagic samples (>200 m) is consistent with previous studies, which showed that POM values increase most strongly above 200 m (3–10‰), then remain relatively constant through the meso- and bathypelagic zone, as we found (Altabet, 1988; Altabet et al., 1991; Emeis et al., 2010; Fernández-Carrera et al., 2016).

The isotopic enrichment of POM with depth observed in our samples has been documented in pelagic systems throughout the world's oceans and is attributed to microbial degradation as POM sinks through the water column (Altabet, 1988; Mintenbeck et al., 2007; Hannides et al., 2013). During microbial reworking, bonds containing ^{14}N are preferentially broken, leaving the residual material isotopically heavier and isotopically distinct from newly formed particles in the epipelagic zone (Mintenbeck et al., 2007; Hannides et al., 2013). Additionally, as POM sinks, microbial activity and disturbance from zooplankton swimming and feeding enhances physical degradation resulting in different size fractions that vary from large (>53 μm), fast sinking particles to small (0.7–53 μm), suspended particles (Altabet, 1988; Gloeckler et al., 2018). SIA and AA-CSIA of POM has shown that small suspended particles at depths >200 m have $\delta^{15}N$ and $\delta^{15}N_{sourceAA}$ values that are enriched relative to newly formed particles (of both size classes) near the ocean's surface and to large particles throughout the meso- and bathypelagic zones (Hannides et al., 2013; Gloeckler et al., 2018). The finding that $\delta^{15}N$ and $\delta^{15}N_{sourceAA}$ values of POM undergo distinct changes with depth provides important context, as it suggests that variation among higher-order consumers could reflect variation at the base of the food web and not a change in trophic status.

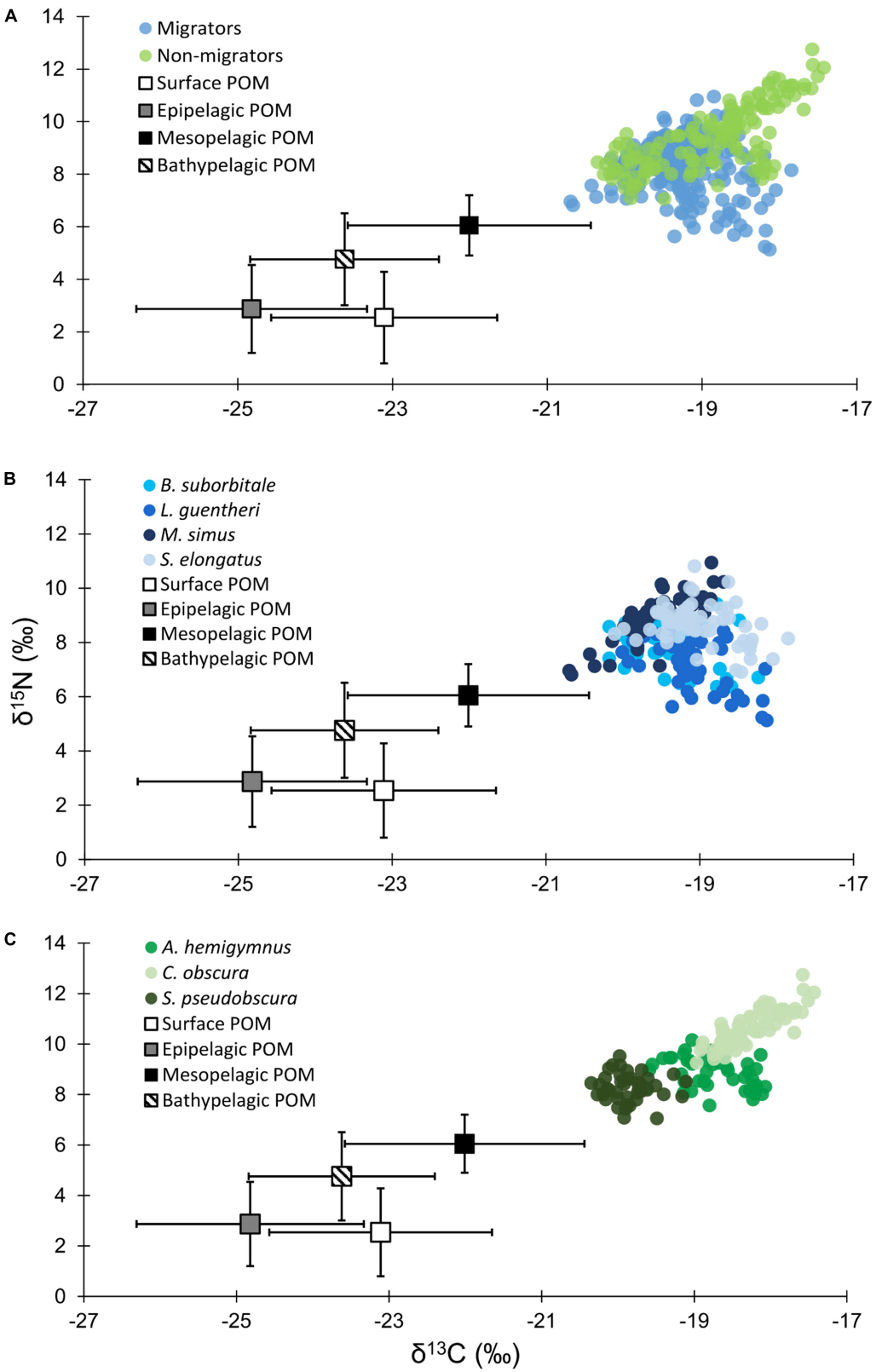

FIGURE 3 | (A) Isotope biplot displaying mean (± SD) $\delta^{13}C$ and $\delta^{15}N$ values for particulate organic matter from each depth zone (squares) and individual $\delta^{13}C$ and $\delta^{15}N$ values for all vertically migrating (blue circles) and non-migrating (green circles) fish species. **(B)** Individual $\delta^{13}C$ and $\delta^{15}N$ values of vertically migrating species. **(C)** Individual $\delta^{13}C$ and $\delta^{15}N$ values of non-migrating species.

TABLE 3 | Mean (± SD) $\delta^{13}C$ and $\delta^{15}N$ stable isotope ratios of particulate organic matter among sampling years (2015/2016) and water types (Loop Current/Common Water).

	$\delta^{13}C$ (‰)	$\delta^{15}N$ (‰)
Surface		
Year (2015/2016)	**−22.18 ± 0.43/**	1.20 ± 1.48/
	−23.42 ± 1.56	2.99 ± 1.63
Water type (Loop/Common)	−23.22 ± 2.42/	**0.83 ± 1.09/**
	−23.06 ± 0.92	**3.27 ± 1.43**
Epipelagic		
Year (2015/2016)	**−23.94 ± 0.85/**	2.21 ± 1.34/
	−25.45 ± 1.55	3.34 ± 1.76
Water type (Loop/Common)	−24. 95 ± 1.99/	**1.37 ± 0.77/**
	−24.78 ± 1.35	**3.37 ± 1.59**
Mesopelagic		
Year (2015/2016)	**−23.20 ± 1.43/**	5.96 ± 1.79/
	−21.64 ± 1.47	6.08 ± 0.98
Water type (Loop/Common)	−21.91 ± 1.17/	6.39 ± 2.21/
	−22.03 ± 1.68	5.98 ± 0.92
Bathypelagic		
Year (2015/2016)	**−25.20 ± 0.28/**	4.18 ± 1.22/
	−23.36 ± 1.10	4.86 ± 1.85
Water type (Loop/Common)	−24.79 ± NA/	6.07 ± NA/
	−23.53 ± 1.22	4.66 ± 1.78

Values in bold represent significant differences.

Variation in Deep-Pelagic Fish SIA

The isotopic values of deep-pelagic fishes differed significantly among species, with variation among species appearing to be depth related. The low $\delta^{13}C$ and $\delta^{15}N$ values among migratory species, which share broadly overlapping depth distributions, suggest a shared reliance on recently formed primary production within the epipelagic zone. In contrast, the variation in $\delta^{13}C$ values of non-migratory species was significant, with minimal isotopic overlap among species. The pattern of ^{13}C enrichment within non-migratory species is interesting, as it did not perfectly align with vertical distributions due to lower $\delta^{13}C$ values in *S. pseudobscura* relative to the shallower dwelling *A. hemigymnus*. The low $\delta^{13}C$ values in *S. pseudobscura*, which were similar to $\delta^{13}C$ values of the migratory *B. suborbitale* and *L. guentheri*, suggest that *S. pseudobscura* uses food webs supported by production derived in the epipelagic zone despite a depth of distribution that centers below 700 m. In contrast, higher $\delta^{13}C$ values in *A. hemigymnus* and *C. obscura* suggests that both species feed within food webs supported by POM with higher $\delta^{13}C$ values within the meso- and bathypelagic zone.

Depth-driven variation in micronekton $\delta^{15}N$ values has been observed in deep-pelagic assemblages in the Atlantic (Parzanini et al., 2017), Pacific (Gloeckler et al., 2018; Romero-Romero et al., 2019), and Mediterranean Sea (Valls et al., 2014), and our data suggest that depth is an important factor influencing the $\delta^{15}N$ values of GOM assemblages as well. For example, $\delta^{15}N$ values were lower in *B. suborbitale* and *L. guentheri*, which have epipelagic nighttime distributions, relative to *M. simus* and *A. hemigymnus*, which have nighttime distributions in the mesopelagic zone. Additionally, the highest $\delta^{15}N$ values belonged to the non-migratory *C. obscura*, which has the deepest depth of occurrence of the species examined. The trend of higher $\delta^{15}N$ values in deeper-dwelling species was not reflected in the values of *S. pseudobscura*, which was isotopically similar to *B. suborbitale* and characterized by lower $\delta^{15}N$ values relative to the shallower dwelling species such as *M. simus*, *S. elongatus*, and *A. hemigymnus*. Despite a center of distribution below 700 m, the $\delta^{15}N$ values for *S. pseudobscura* suggests the use of food webs with similar isotopic baselines to those of migratory species foraging in the upper meso- and epipelagic zones (Hopkins and Baird, 1985; Hopkins et al., 1996). Diet analysis of *S. pseudobscura* in the GOM has shown selection for epipelagic prey, with >90% of the identified copepod species consumed by *S. pseudobscura* possessing population centers above 75 m (Hopkins et al., 1996). To date, there has been no explanation for the occurrence of epipelagic prey in *S. pseudobscura*, but downwelling of prey items, net feeding, and the hypothesis that epipelagic copepods are the prey of *S. pseudobscura's* prey have been ruled out during previous investigations (Hopkins and Baird, 1985; Hopkins et al., 1996). While our results cannot offer a mechanism to link *S. pseudobscura* to epipelagic prey, the isotopic similarities between *S. pseudobscura* and migratory species provides additional support for the assertion that *S. pseudobscura* feeds at depth in the lower meso- and upper bathypelagic zones on prey with $\delta^{15}N$ values indicative of an epipelagic origin and offers an interesting example of vertical connectivity in GOM pelagic food webs.

Interspecific differences in $\delta^{15}N$ values could be influenced by slight differences in the diet compositions of the species examined and should be considered. With the exception of large *S. elongatus* and *S. pseudobscura*, which can feed on decapod crustaceans and fishes, all species have diets composed of small crustaceans, including frequent consumption of copepods from the genus *Pleuromamma* (Hopkins and Baird, 1985; Hopkins et al., 1996; Burghart et al., 2010). Based on available diet data, hypothesized trophic structure would suggest *S. elongatus* and *S. pseudobscura* occupy trophic positions higher than the other five species. Assuming dietary relationships among taxa remain similar to those outlined by Hopkins et al. (1996), observed interspecific variation in $\delta^{15}N$ was greater than, and different from, variation predicted from feeding patterns. Specifically, that *M. simus*, *A. hemigymnus*, and *C. obscura*, which feed on copepods and ostracods, possess $\delta^{15}N$ values similar to *S. elongatus* and elevated relative to *S. pseudobscura*, is counter to known diet data. Interspecific differences in $\delta^{15}N$ values instead suggests differences among species are driven by differential use of food webs supported by isotopically distinct POM pools, with deeper-dwelling species more likely to use food webs at depth supported by small, suspended particles with elevated $\delta^{13}C$ and $\delta^{15}N$ values.

The $\delta^{15}N_{sourceAA}$ values in fishes were variable but reflected trends in $\delta^{15}N$, with lower $\delta^{15}N_{sourceAA}$ values in the shallowest migratory species (*L. guentheri*, *B. suborbitale*) and higher values in the deepest dwelling *C. obscura*. The contrasting $\delta^{15}N_{sourceAA}$ values provides further evidence supporting the assertion that variation among species is underpinned by differential use of food webs supported by POM with isotopically distinct signatures.

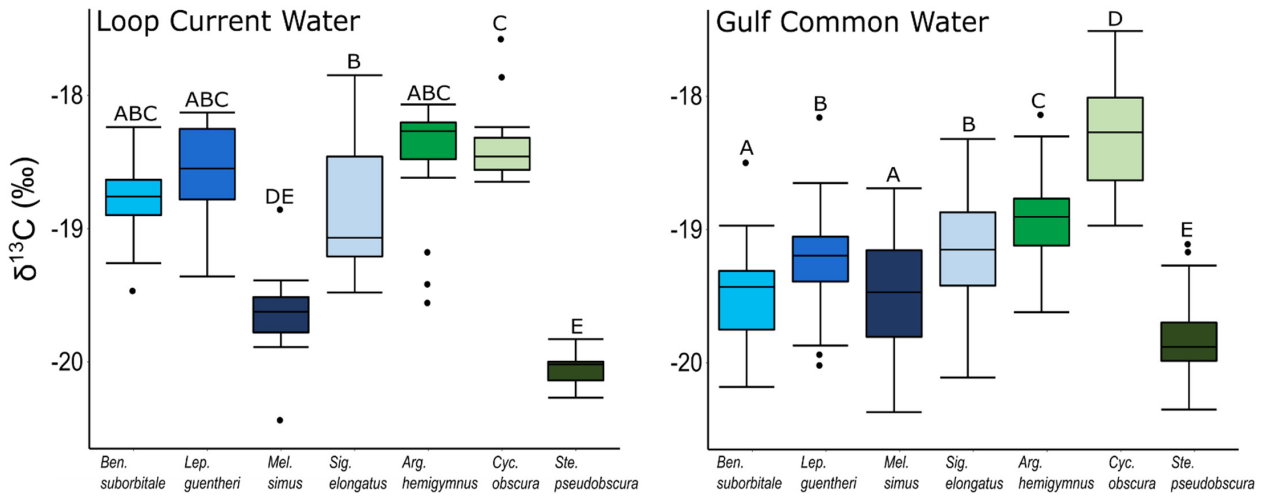

FIGURE 4 | Boxplots depicting interspecific differences in mean (± SD) $\delta^{13}C$ values for migratory (blue shades) and non-migratory (green shades) deep-pelagic fishes collected in Loop Current water and Gulf common water. Differing letters among species denote significant differences.

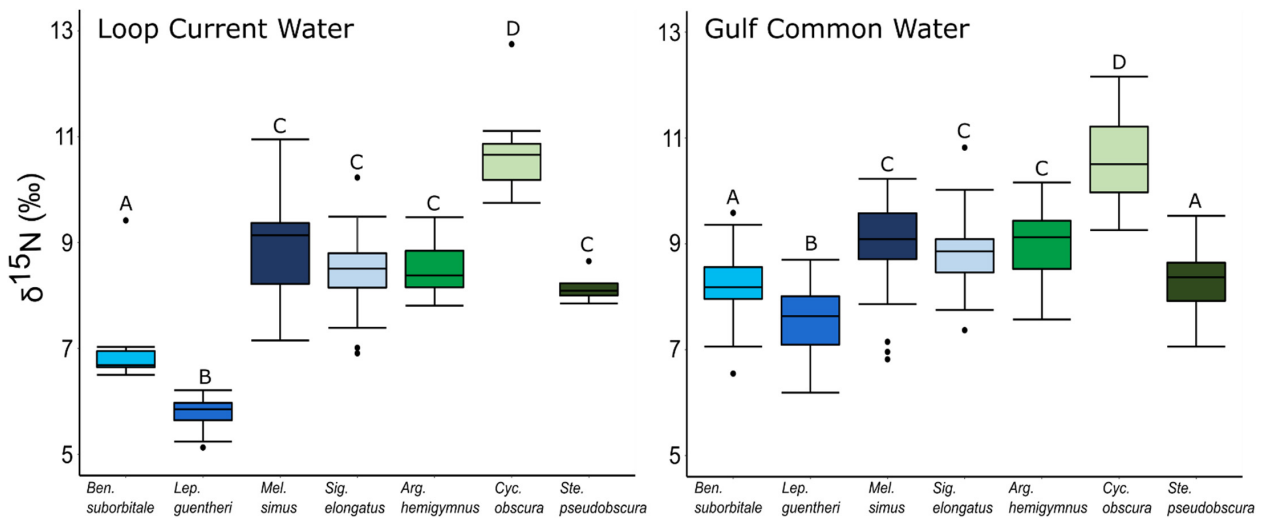

FIGURE 5 | Boxplots depicting interspecific differences in mean (± SD) $\delta^{15}N$ values for migratory (blue shades) and non-migratory (green shades) deep-pelagic fishes collected in Loop Current water and Gulf common water. Differing letters among species denote significant differences.

Similar results were reported in the Pacific by Gloeckler et al. (2018) who found that micronekton $\delta^{15}N_{sourceAA}$ values increased with depth, suggesting that non-migratory species inhabiting the lower meso- and bathypelagic zones increasingly rely on food webs supported by small, suspended particles relative to species in the epi- and upper mesopelagic zones.

It is noteworthy that *C. obscura* appears to receive carbon from deep-suspended particles, as it was the second most abundant species collected during midwater sampling of the GOM behind its congener, *Cyclothone pallida* (Sutton et al., 2017). The $\delta^{15}N_{sourceAA}$ values of *C. pallida*, which has a median depth distribution slightly shallower than *C. obscura*, displayed elevated $\delta^{15}N_{sourceAA}$ values (4.3 ± 2.7) and appeared to be supported by small, suspended particle-based food webs in the Pacific (Gloeckler et al., 2018). Members of the genus *Cyclothone* are one of the most numerous vertebrates on the planet (Nelson et al., 2016), and it is interesting that two highly abundant deep-pelagic species appear to feed within food webs supported by suspended particles at depth, which, until recently, were not known to significantly contribute to the production of deep-pelagic micronekton (Gloeckler et al., 2018). While *C. pallida* and *C. obscura* both appear to utilize suspended particle-based food webs, Gloeckler et al. (2018) found that $\delta^{15}N_{sourceAA}$ values for the upper mesopelagic *Cyclothone braueri* and *C. alba* more closely resembled source values of large, sinking particles in the epi- and mesopelagic zones. The contrasting $\delta^{15}N_{sourceAA}$ values among members of *Cyclothone* again suggests that

TABLE 4 | Mean (± SD) $\delta^{13}C$ and $\delta^{15}N$ stable isotope ratios of deep-pelagic fishes between sampling years (2015/2016) and water types (Loop Current/Common Water).

	$\delta^{13}C$ (‰)	$\delta^{15}N$ (‰)
B. suborbitale		
Year (2015/2016)	−19.42 ± 0.58/	7.94 ± 0.92/
	−19.41 ± 0.27	8.11 ± 0.64
Water type (Loop/Common)	**−18.13 ± 0.38/**	**6.96 ± 1.12/**
	−19.50 ± 0.32	**8.21 ± 0.55**
L. guentheri		
Year (2015/2016	−18.99 ± 0.62/	**6.95 ± 0.91/**
	19.18 ± 0.25	**7.39 ± 0.92**
Water type (Loop/Common)	**−18.60 ± 0.41/**	**5.76 ± 0.35/**
	−19.22 ± 0.39	**7.56 ± 0.62**
M. simus		
Year (2015/2016)	−19.56 ± 0.28/	8.92 ± 0.66/
	−19.58 ± 0.57	8.96 ± 1.10
Water type (Loop/Common)	−19.64 ± 0.37/	8.92 ± 1.08/
	−19.56 ± 0.51	8.95 ± 0.92
S. elongatus		
Year (2015/2016)	−19.00 ± 0.54/	8.48 ± 0.88/
	−19.08 ± 0.38	8.85 ± 0.50
Water type (Loop/Common)	**−18.86 ± 0.49/**	**8.43 ± 0.80/**
	−19.13 ± 0.41	**8.82 ± 0.62**
A. hemigymnus		
Year (2015/2016)	−18.67 ± 0.40/	**8.64 ± 0.61/**
	−18.83 ± 0.49	**9.11 ± 0.56**
Water type (Loop/Common)	**−18.48 ± 0.48/**	**8.55 ± 0.52/**
	−18.92 ± 0.35	**9.01 ± 0.63**
C. obscura		
Year (2015/2016)	−18.36 ± 0.42/	10.42 ± 0.69/
	−18.26 ± 0.39	10.68 ± 0.75
Water type (Loop/Common)	−18.35 ± 0.33/	10.67 ± 0.81/
	−18.27 ± 0.41	10.59 ± 0.73
S. pseudobscura		
Year (2015/2016)	−19.73 ± 0.30/	**8.57 ± 0.60/**
	−19.91 ± 0.27	**8.12 ± 0.48**
Water type (Loop/Common	−20.05 ± 0.16/	8.16 ± 0.30/
	−19.82 ± 0.29	8.29 ± 0.59

Values in bold represent significant differences.

utilization of small particle food webs appears to be primarily driven by differences in depth distribution among species (Gloeckler et al., 2018).

Effects of Water Type on Isotopic Values

The $\delta^{15}N$ values of surface and epipelagic POM and four fish species were significantly lower in LCW relative to samples collected in GCW. The magnitude of isotopic variation between the two water types appeared to be depth related, as differences in POM $\delta^{15}N$ values were greatest at the surface and decreased with increasing depth (**Table 3**). Similarly, differences in fish $\delta^{13}C$ and $\delta^{15}N$ values between water types were greatest for species with epipelagic nighttime distributions (*B. suborbitale* and *L. guentheri)*, less pronounced in species with mesopelagic nighttime distributions (*S. elongatus*, *A. hemigymnus*), and absent for the deepest dwelling *C. obscura*. The pattern of higher $\delta^{13}C$ and $\delta^{15}N$ values in anticyclonic features like the Loop Current is consistent with previous investigations of epipelagic micronekton and zooplankton in the northern GOM (Dorado et al., 2012; Wells et al., 2017). Interestingly, the mean differences in $\delta^{15}N$ values observed between fish collected in LCW and GCW, which ranged from 1.80‰ (*L. guentheri*) to 0.39‰ (*S. elongatus*), were less than the isotopic differences observed in surface-dwelling flying fishes (1.95‰) and *Sargassum*-associated crustaceans (5.4‰) collected from anticyclonic (Loop Current) and cyclonic features by Wells et al. (2017).

Isotopic differences in POM and micronekton collected within cyclonic and anticyclonic features are driven by differences in nitrogen cycling, which result in isotopically distinct nitrogen sources fueling production at the base of the food web (Montoya et al., 2002; Dorado et al., 2012; Wells et al., 2017). The Loop Current and other anticyclonic features in the GOM are areas of convergence, characterized by increased stratification and downwelling, which depresses nitracline depths and limits the amount of isotopically enriched deepwater nitrate entering the photic zone (Biggs et al., 1988; Biggs, 1992). In the absence of new, upwelled nitrate, phytoplankton in the Loop Current and anticyclones have been shown to be supported by regenerated nitrogen and by isotopically light nitrogen derived from diazotrophy (cyanobacteria *Trichodesmium* spp.), resulting in phytoplankton with lower $\delta^{15}N$ values that can then be reflected in the $\delta^{15}N$ values of higher-order consumers (Montoya et al., 2002; Dorado et al., 2012). By contrast, phytoplankton in cyclonic eddies or in neritic waters (i.e., common water) are largely supported by isotopically enriched deepwater nitrate or isotopically enriched dissolved inorganic nitrogen associated with the terrestrial environment and Mississippi River leading to higher $\delta^{15}N$ values in phytoplankton and higher-order consumers (Dorado et al., 2012). Although turnover rates for deep-pelagic fishes are unknown, *B. suborbitale*, *L. guentheri*, and *S. elongatus* have life spans of 1–3 years, so assumed tissue turnover rates of several weeks are reasonable (Lancraft et al., 1988; Gartner, 1991). While the currents associated with the anticyclonic Loop Current are not strong enough to trap micronekton, the Loop Current and associated eddies can be 100 s of kilometers in diameter, persist for months to years, and dominate circulation in the upper layer of the GOM (Vukovich and Crissman, 1986; Biggs, 1992). Thus, due to the persistence of the Loop Current over timescales greater than hypothesized tissue turnover rates, the conservation of isotopic baselines unique to a particular water type in micronekton is feasible, particularly for short-lived species with relatively shallow distributions. Due to a lack of appropriate samples and funding, we were unable to explicitly test the hypothesis that differing sources of nitrogen-drive isotopic differences between water types using AA-CSIA. While these results should be interpreted carefully due to low sample sizes in LCW, our results, combined with those of previous studies in the GOM, suggest that distinct isotopic baselines within mesoscale features can be conserved in deep-pelagic micronekton and should be considered when examining the trophic structure of pelagic assemblages.

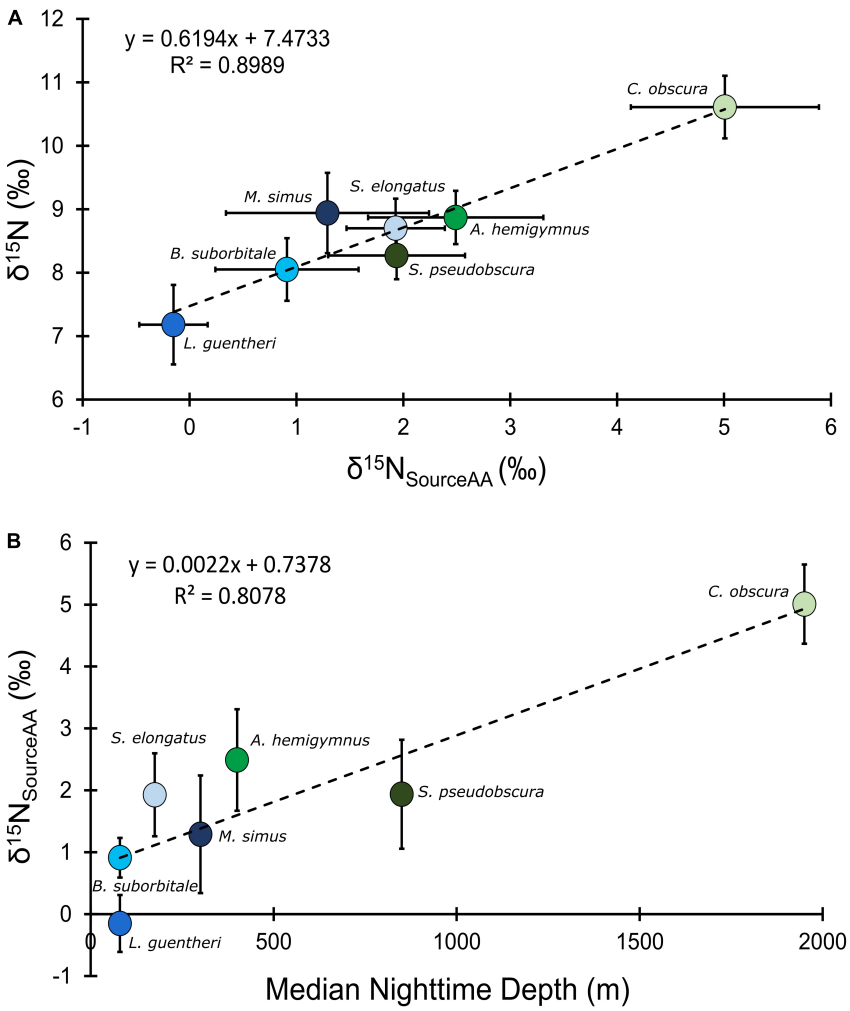

FIGURE 6 | (A) Bulk tissue $\delta^{15}N$ values of deep-pelagic fishes as a function of $\delta^{15}N_{sourceAA}$ values. **(B)** $\delta^{15}N_{sourceAA}$ values as a function of median nighttime depth of occurrence. $\delta^{15}N_{sourceAA}$ represents the averaged value for each fish species. Blue circles represent vertical migrators, green circles represent non-migrators, and error bars represent the standard error for each species.

TABLE 5 | Comparison of mean (± SD) trophic positions for each fish species created using bulk SIA and AA-CSIA.

Species	TP: Bulk	TP: AA-CSIA
Migrators		
B. suborbitale	3.56 ± 0.24	3.11 ± 0.22
L. guentheri	3.28 ± 0.30	3.38 ± 0.22
M. simus	3.84 ± 0.30	3.73 ± 0.35
S. elongatus	3.76 ± 0.22	3.44 ± 0.29
Non-migrators		
A. hemigymnus	3.82 ± 0.20	3.38 ± 0.36
C. obscura	4.37 ± 0.24	3.47 ± 0.26
S. pseudobscura	3.63 ± 0.18	3.61 ± 0.41

In summary, we found marked differences in the $\delta^{13}C$ and $\delta^{15}N$ values of seven micronekton species with similar diet compositions over relatively small vertical and horizontal spatial scales in the pelagic GOM. Variation in $\delta^{13}C$ and $\delta^{15}N$ values among species was related to depth of occurrence and migration type, with deeper-dwelling, non-migratory species typically having higher $\delta^{13}C$ and $\delta^{15}N$ values relative to shallower-dwelling, migratory species. Depth-related trends in $\delta^{15}N$ were similar in $\delta^{15}N_{sourceAA}$ data, with higher $\delta^{15}N_{sourceAA}$ values in species occupying deeper depths. Taken together, the correlation between depth and $\delta^{15}N$ and $\delta^{15}N_{sourceAA}$ data suggests that deeper-dwelling species increasingly rely on food webs supported by small, suspended POM particles, which possess higher $\delta^{15}N$ and $\delta^{15}N_{sourceAA}$ values relative to newly formed particles in the epipelagic zone. Additionally, we observed significant differences in the $\delta^{13}C$ and $\delta^{15}N$ values of epipelagic POM and micronekton collected in the anticyclonic Loop Current relative to surrounding water masses (LCW). Isotopic differences in samples collected from the two water masses is driven by differences in nitrogen cycling, which results in isotopically distinct nitrogen sources fueling production at the base of

the food web. These results suggest the trophic structure of GOM deep-pelagic assemblages is influenced by both feeding relationships and nutrient source dynamics at the base of the food web, which can vary over small spatial scales. By highlighting factors contributing to variation in isotopic values of deep-pelagic species, this study broadens our understanding of deep-pelagic trophic structure and will inform the interpretation of SIA data in future studies of pelagic systems.

DATA AVAILABILITY STATEMENT

The isotope data used in this study are publicly available through the Gulf of Mexico Research Initiative Information & Data Cooperative (GRIIDC) at https://data.gulfresearchinitiative.org (doi: 10.7266/n7-bf8a-hq12; doi: 10.7266/N75D8Q7Z).

ETHICS STATEMENT

The animal study was reviewed and approved by the Institutional Animal Care and Use Committee.

AUTHOR CONTRIBUTIONS

TR, TS, and RW contributed to the concept and initial study design. TR and TS collected samples, while TR conducted laboratory and statistical analyses and data interpretation and wrote the first draft of the manuscript. All authors contributed to the manuscript revisions. TS and RW have read and approved the submitted version of the manuscript.

FUNDING

This research was made possible by a grant from The Gulf of Mexico Research Initiative.

ACKNOWLEDGMENTS

We would like to thank the crew of the r/v *Point Sur* for their help operating the MOCNESS. We thank Charles Kovach, Cole Easson, Jacqueline Long, Shaojie Sun, and Lindsay Freed for their help filtering water for POM. We are grateful to April Cook for her organization of the DEEPEND micronekton database and for her help constructing **Figure 1**.

SUPPLEMENTARY MATERIAL

The Supplementary Material for this article can be found online at: https://www.frontiersin.org/articles/10.3389/fmars.2020.507992/full#supplementary-material

REFERENCES

Altabet, M. A. (1988). Variations in nitrogen isotopic composition between sinking and suspended particles: implications for nitrogen cycling and particle transformation in the open ocean. *Deep Sea Res. Part A Oceanogr. Res. Papers* 35, 535–554. doi: 10.1016/0198-0149(88)90130-6

Altabet, M. A., Deuser, W. G., Honjo, S., and Stienen, C. (1991). Seasonal and depth-related changes in the source of sinking particles in the North Atlantic. *Nature* 354:136. doi: 10.1038/354136a0

Angel, M. V. (1989). Vertical profiles of pelagic communities in the vicinity of the Azores Front and their implications to deep ocean ecology. *Prog. Oceanogr.* 22, 1–46. doi: 10.1016/0079-6611(89)90009-8

Biggs, D. C. (1992). Nutrients, plankton, and productivity in a warm−core ring in the western Gulf of Mexico. *J. Geophys. Res. Oceans* 97, 2143–2154. doi: 10.1029/90jc02020

Biggs, D. C., Vastano, A. C., Ossinger, R. A., Gil-Zurita, A., and Perez-Franco, A. (1988). Multidisciplinary study of warm and cold-core rings in the Gulf of Mexico. *Mem. Soc. Cienc. Nat. La Salle, Venezuela* 48, 12–31.

Boecklen, W. J., Yarnes, C. T., Cook, B. A., and James, A. C. (2011). On the use of stable isotopes in trophic ecology. *Annu. Rev. Ecol. Evol. Syst.* 42, 411–440.

Bradley, C. J., Wallsgrove, N. J., Choy, C. A., Drazen, J. C., Hetherington, E. D., Hoen, D. K., et al. (2015). Trophic position estimates of marine teleosts using amino acid compound specific isotopic analysis. *Limnol. Oceanogr. Methods* 13, 476–493. doi: 10.1002/lom3.10041

Bretz, F., Hothorn, T., and Westfall, P. (2016). *Multiple Comparisons Using R*. London: Chapman and Hall/CRC.

Burghart, S. E., Hopkins, T. L., and Torres, J. J. (2010). Partitioning of food resources in bathypelagic micronekton in the eastern Gulf of Mexico. *Mar. Ecol. Prog. Series* 399, 131–140. doi: 10.3354/meps08365

Cherel, Y., Fontaine, C., Richard, P., and Labatc, J. P. (2010). Isotopic niches and trophic levels of myctophid fishes and their predators in the Southern Ocean. *Limnol. Oceanogr.* 55, 324–332. doi: 10.4319/lo.2010.55.1.0324

Chikaraishi, Y., Ogawa, N. O., Kashiyama, Y., Takano, Y., Suga, H., Tomitani, A., et al. (2009). Determination of aquatic food−web structure based on compound−specific nitrogen isotopic composition of amino acids. *Limnol. Oceanogr. Methods* 7, 740–750. doi: 10.4319/lom.2009.7.740

Chipps, S. R., and Garvey, J. E. (2007). "Assessment of food habits and feeding patterns," in *Analysis and Interpretation of Freshwater Fisheries Data*, eds C. S. Guy and M. L. Brown (Bethesda, MD: American Fisheries Society), 473–514.

Choy, C. A., Portner, E., Iwane, M., and Drazen, J. C. (2013). Diets of five important predatory mesopelagic fishes of the central North Pacific. *Mar. Ecol. Prog. Series* 492, 169–184. doi: 10.3354/meps10518

Davis, R. W., Ortega-Ortiz, J. G., Ribic, C. A., Evans, W. E., Biggs, D. C., Ressler, P. H., et al. (2002). Cetacean habitat in the northern oceanic Gulf of Mexico. *Deep Sea Res. Part I Oceanogr. Res. Papers* 49, 121–142. doi: 10.1016/s0967-0637(01)00035-8

DeNiro, M. J., and Epstein, S. (1978). Influence of diet on the distribution of carbon isotopes in animals. *Geochim. Cosmochim. Acta* 42, 495–506. doi: 10.1016/0016-7037(78)90199-0

Dorado, S., Rooker, J. R., Wissel, B., and Quigg, A. (2012). Isotope baseline shifts in pelagic food webs of the Gulf of Mexico. *Mar. Ecol. Prog. Series* 464, 37–49. doi: 10.3354/meps09854

Emeis, K. C., Mara, P., Schlarbaum, T., Möbius, J., Dähnke, K., Struck, U., et al. (2010). External N inputs and internal N cycling traced by isotope ratios of nitrate, dissolved reduced nitrogen, and particulate nitrogen in the eastern Mediterranean Sea. *J. Geophys. Res. Biogeosci.* 115:G04041.

Fernández-Carrera, A., Rogers, K. L., Weber, S. C., Chanton, J. P., and Montoya, J. P. (2016). Deep Water Horizon oil and methane carbon entered the food web in the Gulf of Mexico. *Limnol. Oceanogr.* 61, S387–S400.

Fox, J., and Weisberg, S. (2019). *An R Companion to Applied Regression*, 3rd Edn. Thousand Oaks CA: Sage.

Gartner, J. V. Jr. (1987). The lanternfishes (Pisces: Myctophidae) of the eastern Gulf of Mexico. *Fish. Bull. US* 85, 81–98.

Gartner, J. V. (1991). Life histories of three species of lanternfishes (Pisces: Myctophidae) from the eastern Gulf of Mexico. *Mar. Biol.* 111, 11–20. doi: 10.1007/bf01986339

Gloeckler, K., Choy, C. A., Hannides, C. C., Close, H. G., Goetze, E., Popp, B. N., et al. (2018). Stable isotope analysis of micronekton around Hawaii reveals suspended particles are an important nutritional source in the lower mesopelagic and upper bathypelagic zones. *Limnol. Oceanogr.* 63, 1168–1180. doi: 10.1002/lno.10762

Hannides, C. C., Popp, B. N., Choy, C. A., and Drazen, J. C. (2013). Midwater zooplankton and suspended particle dynamics in the North Pacific Subtropical Gyre: a stable isotope perspective. *Limnol. Oceanogr.* 58, 1931–1946. doi: 10.4319/lo.2013.58.6.1931

Hopkins, T. L., and Baird, R. C. (1985). Feeding ecology of four hatchetfishes (Sternoptychidae) in the eastern Gulf of Mexico. *Bull. Mar. Sci.* 36, 260–277.

Hopkins, T. L., and Gartner, J. V. (1992). Resource-partitioning and predation impact of a low-latitude myctophid community. *Mar. Biol.* 114, 185–197. doi: 10.1007/bf00349518

Hopkins, T. L., Sutton, T. T., and Lancraft, T. M. (1996). The trophic structure and predation impact of a low latitude midwater fish assemblage. *Prog. Oceanogr.* 38, 205–239. doi: 10.1016/s0079-6611(97)00003-7

Hothorn, T., Bretz, F., and Westfall, P. (2008). Simultaneous inference in general parametric models. *Biometrical J.* 50, 346–363. doi: 10.1002/bimj.200810425

Irigoien, X., Klevjer, T. A., Røstad, A., Martinez, U., Boyra, G., Acuña, J. L., et al. (2014). Large mesopelagic fishes biomass and trophic efficiency in the open ocean. *Nat. Commun.* 5:3271.

Johnston, M. W., Milligan, R. J., Easson, C. G., DeRada, S., English, D. C., Penta, B., et al. (2019). An empirically validated method for characterizing pelagic habitats in the Gulf of Mexico using ocean model data. *Limnol. Oceanogr. Methods* 17, 362–375.

Lancraft, T. M., Hopkins, T. L., and Torres, J. J. (1988). Aspects of the ecology of the mesopelagic fish *Gonostoma elongatum*(Gonostomatidae, Stomiiformes) in the eastern Gulf of Mexico. *Mar. Ecol. Prog. Series Oldendorf.* 49, 27–40. doi: 10.3354/meps049027

Longhurst, A. R., Bedo, A. W., Harrison, W. G., Head, E. J. H., and Sameoto, D. D. (1990). Vertical flux of respiratory carbon by oceanic diel migrant biota. *Deep Sea Res. Part A Oceanogr. Res. Papers* 37, 685–694. doi: 10.1016/0198-0149(90)90098-g

McClain-Counts, J. P., Demopoulos, A. W., and Ross, S. W. (2017). Trophic structure of mesopelagic fishes in the Gulf of Mexico revealed by gut content and stable isotope analyses. *Mar. Ecol.* 38:e12449. doi: 10.1111/maec.12449

McClelland, J. W., and Montoya, J. P. (2002). Trophic relationships and the nitrogen isotopic composition of amino acids in plankton. *Ecology* 83, 2173–2180. doi: 10.1890/0012-9658(2002)083[2173:tratni]2.0.co;2

McEachran, J. D., and Fechhelm, J. D. (1998). *Fishes of the Gulf of Mexico, Volume 1: Myxiniformes to Gasterosteiformes*. Austin: University of Texas Press, 1120.

Mengerink, K. J., Van Dover, C. L., Ardron, J., Baker, M., Escobar-Briones, E., Gjerde, K., et al. (2014). A call for deep-ocean stewardship. *Science* 344, 696–698. doi: 10.1126/science.1251458

Ménard, F., Benivary, H. D., Bodin, N., Coffineau, N., Le Loc'h, F., Mison, T., et al. (2014). Stable isotope patterns in micronekton from the Mozambique Channel. *Deep Sea Res. Part II Top. Stud. Oceanogr.* 100, 153–163. doi: 10.1016/j.dsr2.2013.10.023

Milligan, R. J., Bernard, A. M., Boswell, K. M., Bracken-Grissom, H. D., D'Elia, M. A., DeRada, S., et al. (2018). The application of novel research technologies by the deep pelagic nekton dynamics of the Gulf of Mexico (DEEPEND) consortium. *Mar. Technol. Soc. J.* 52, 81–86. doi: 10.4031/mtsj.52.6.10

Minagawa, M., and Wada, E. (1984). Stepwise enrichment of 15N along food chains: further evidence and the relation between δ15N and animal age. *Geochim. Cosmochim. Acta* 48, 1135–1140. doi: 10.1016/0016-7037(84)90204-7

Mintenbeck, K., Jacob, U., Knust, R., Arntz, W. E., and Brey, T. (2007). Depth-dependence in stable isotope ratio δ15N of benthic POM consumers: the role of particle dynamics and organism trophic guild. *Deep Sea Res. Part I Oceanogr. Res. Papers* 54, 1015–1023. doi: 10.1016/j.dsr.2007.03.005

Montoya, J. P., Carpenter, E. J., and Capone, D. G. (2002). Nitrogen fixation and nitrogen isotope abundances in zooplankton of the oligotrophic North Atlantic. *Limnol. Oceanogr.* 47, 1617–1628. doi: 10.4319/lo.2002.47.6.1617

Moteki, M., Arai, M., Tsuchiya, K., and Okamoto, H. (2001). Composition of piscine prey in the diet of large pelagic fish in the eastern tropical Pacific Ocean. *Fish. Sci.* 67, 1063–1074. doi: 10.1046/j.1444-2906.2001.00362.x

Murawski, S. A., Hollander, D. J., Gilbert, S., and Gracia, A. (2020). "Deepwater oil and gas production in the Gulf of Mexico and related global trends," in *Scenarios and Responses to Future Deep Oil Spills*, eds S. Murawski, et al. (Cham: Springer), 16–32. doi: 10.1007/978-3-030-12963-7_2

Nelson, J. S., Grande, T. C., and Wilson, M. V. (2016). *Fishes of the World*. Hoboken, NJ: John Wiley & Sons.

Pakhomov, E. A., Henschke, N., Hunt, B. P., Stowasser, G., and Cherel, Y. (2019). Utility of salps as a baseline proxy for food web studies. *J. Plankton Res.* 41, 3–11. doi: 10.1093/plankt/fby051

Parzanini, C., Parrish, C. C., Hamel, J. F., and Mercier, A. (2017). Trophic ecology of a deep-sea fish assemblage in the Northwest Atlantic. *Mar. Biol.* 164:206.

Peterson, B. J., and Fry, B. (1987). Stable isotopes in ecosystem studies. *Annu. Rev. Ecol. Syst.* 18, 293–320. doi: 10.1146/annurev.es.18.110187.001453

Popp, B. N., Graham, B. S., Olson, R. J., Hannides, C. C., Lott, M. J., López−Ibarra, G. A., et al. (2007). Insight into the trophic ecology of yellowfin tuna, Thunnus albacares, from compound−specific nitrogen isotope analysis of proteinaceous amino acids. *Terrestrial Ecol.* 1, 173–190.

Post, D. M. (2002). Using stable isotopes to estimate trophic position: models, methods, and assumptions. *Ecology* 83, 703–718. doi: 10.1890/0012-9658(2002)083[0703:usitet]2.0.co;2

Ramirez-Llodra, E., Tyler, P. A., Baker, M. C., Bergstad, O. A., Clark, M. R., Escobar, E., et al. (2011). Man and the last great wilderness: human impact on the deep sea. *PLoS One* 6:e22588. doi: 10.1371/journal.pone.0022588

Richards, T. M., Gipson, E. E., Cook, A., Sutton, T. T., and Wells, R. D. (2018). Trophic ecology of meso-and bathypelagic predatory fishes in the Gulf of Mexico. *ICES J. Mar. Sci.* 76, 662–672. doi: 10.1093/icesjms/fsy074

Romero-Romero, S., Choy, C. A., Hannides, C. C., Popp, B. N., and Drazen, J. C. (2019). Differences in the trophic ecology of micronekton driven by diel vertical migration. *Limnol. Oceanogr.* 64, 1473–1483. doi: 10.1002/lno.11128

Rooker, J. R., Kitchens, L. L., Dance, M. A., Wells, R. D., Falterman, B., and Cornic, M. (2013). Spatial, temporal, and habitat-related variation in abundance of pelagic fishes in the Gulf of Mexico: potential implications of the Deepwater Horizon oil spill. *PLoS one* 8:e76080. doi: 10.1371/journal.pone.0076080

Shaffer, J. P. (1986). Modified sequentially rejective multiple test procedures. *J. Am. Stat. Assoc.* 81, 826–831. doi: 10.1080/01621459.1986.10478341

Sutton, T. T., Cook, A. B., Moore, J. A., Frank, T., Judkins, H., Vecchione, M., et al. (2017). *Inventory of Gulf Oceanic Fauna Data including Species, Weight, and Measurements. Meg Skansi Cruises from Jan. 25–Sept. 30, 2011 in the Northern Gulf of Mexico. Distributed by: Gulf of Mexico Research Initiative Information and Data Cooperative (GRIIDC)*. Corpus Christi, TX: Harte Research Institute, Texas A &M University.

Sutton, T. T., and Hopkins, T. L. (1996). Trophic ecology of the stomiid (Pisces: Stomiidae) fish assemblage of the eastern Gulf of Mexico: strategies, selectivity and impact of a top mesopelagic predator group. *Mar. Biol.* 127, 179–192. doi: 10.1007/bf00942102

Thurber, A. R., Sweetman, A. K., Narayanaswamy, B. E., Jones, D. O., Ingels, J., and Hansman, R. L. (2014). Ecosystem function and services provided by the deep sea. *Biogeosciences* 11, 3941–3963. doi: 10.5194/bg-11-3941-2014

Valls, M., Olivar, M. P., de Puelles, M. F., Molí, B., Bernal, A., and Sweeting, C. J. (2014). Trophic structure of mesopelagic fishes in the western Mediterranean based on stable isotopes of carbon and nitrogen. *J. Mar. Syst.* 138, 160–170. doi: 10.1016/j.jmarsys.2014.04.007

Vereshchaka, A. L., Lunina, A. A., and Sutton, T. (2019). Assessing deep-pelagic shrimp biomass to 3000 m in the Atlantic ocean and ramifications of upscaled global biomass. *Sci. Rep.* 9:5946.

von Harbou, L., Dubischar, C. D., Pakhomov, E. A., Hunt, B. P., Hagen, W., and Bathmann, U. V. (2011). Salps in the Lazarev Sea, Southern Ocean: I. Feeding dynamics. *Mar. Biol.* 158, 2009–2026. doi: 10.1007/s00227-011-1709-4

Vukovich, F. M., and Crissman, B. W. (1986). Aspects of warm rings in the Gulf of Mexico. *J. Geophys. Res. Oceans* 91, 2645–2660. doi: 10.1029/jc091ic02p02645

Wada, E., Mizutani, H., and Minagawa, M. (1991). The use of stable isotopes for food web analysis. *Crit. Rev. Food Sci. Nutr.* 30, 361–371. doi: 10.1080/10408399109527547

Webb, T. J., Berghe, E. V., and O'Dor, R. (2010). Biodiversity's big wet secret: the global distribution of marine biological records reveals chronic under-exploration of the deep pelagic ocean. *PLoS One* 5:e10223. doi: 10.1371/journal.pone.0010223

Wells, R. D., Rooker, J. R., Quigg, A., and Wissel, B. (2017). Influence of mesoscale oceanographic features on pelagic food webs in the Gulf of Mexico. *Mar. Biol.* 164:92.

Winemiller, K. O., and Polis, G. A. (1996). "Food webs: what can they tell us about the world?" in *Food Webs*, eds G. A. Polis and K. O. Winemiller (Boston, MA: Springer), 1–22. doi: 10.1007/978-1-4615-7007-3_1

Yarnes, C. T., and Herszage, J. (2017). The relative influence of derivatization and normalization procedures on the compound−specific stable isotope analysis of nitrogen in amino acids. *Rapid Commun. Mass Spectrom.* 31, 693–704. doi: 10.1002/rcm.7832

Zanden, M. J. V., and Rasmussen, J. B. (2001). Variation in δ15N and δ13C trophic fractionation: implications for aquatic food web studies. *Limnol. Oceanogr.* 46, 2061–2066. doi: 10.4319/lo.2001.46.8.2061

Conflict of Interest: The authors declare that the research was conducted in the absence of any commercial or financial relationships that could be construed as a potential conflict of interest.

frontiers in Marine Science

METHODS
published: 29 December 2020
doi: 10.3389/fmars.2020.548880

A Multidisciplinary Approach to Investigate Deep-Pelagic Ecosystem Dynamics in the Gulf of Mexico Following *Deepwater Horizon*

April B. Cook[1], Andrea M. Bernard[1], Kevin M. Boswell[2], Heather Bracken-Grissom[2], Marta D'Elia[2], Sergio deRada[3], Cole G. Easson[1,4], David English[5], Ron I. Eytan[6], Tamara Frank[1], Chuanmin Hu[5], Matthew W. Johnston[1], Heather Judkins[7], Chad Lembke[5], Jose V. Lopez[1], Rosanna J. Milligan[1], Jon A. Moore[8,9], Bradley Penta[3], Nina M. Pruzinsky[1], John A. Quinlan[10], Travis M. Richards[6], Isabel C. Romero[5], Mahmood S. Shivji[1], Michael Vecchione[11], Max D. Weber[6], R. J. David Wells[6] and Tracey T. Sutton[1]*

[1] Guy Harvey Oceanographic Center, Halmos College of Arts and Sciences, Nova Southeastern University, Dania Beach, FL, United States, [2] Institute of Environment, Department of Biological Sciences, Florida International University – Biscayne Bay Campus, North Miami, FL, United States, [3] United States Naval Research Laboratory, Stennis Space Center, Washington DC, United States, [4] Department of Biology, Middle Tennessee State University, Murfreesboro, TN, United States, [5] College of Marine Science, University of South Florida, Tampa, FL, United States, [6] Department of Marine Biology, Texas A&M University at Galveston, Galveston, TX, United States, [7] Integrative Biology, University of South Florida St. Petersburg, St. Petersburg, FL, United States, [8] Wilkes Honors College, Florida Atlantic University, Jupiter, FL, United States, [9] Florida Atlantic University, Harbor Branch Oceanographic Institute, Fort Pierce, FL, United States, [10] Southeast Fisheries Science Center, National Oceanic and Atmospheric Administration, Miami, FL, United States, [11] NMFS National Systematics Laboratory, National Museum of Natural History, Washington, DC, United States

The pelagic Gulf of Mexico (GoM) is a complex system of dynamic physical oceanography (western boundary current, mesoscale eddies), high biological diversity, and community integration via diel vertical migration and lateral advection. Humans also heavily utilize this system, including its deep-sea components, for resource extraction, shipping, tourism, and other commercial activity. This utilization has had impacts, some with disastrous consequences. The *Deepwater Horizon* oil spill (DWHOS) occurred at a depth of ∼1500 m (Macondo wellhead), creating a persistent and toxic mixture of hydrocarbons and dispersant in the deep-pelagic (water column below 200 m depth) habitat. In order to assess the impacts of the DWHOS on this habitat, two large-scale research programs, described herein, were designed and executed. These programs, ONSAP and DEEPEND, aimed to quantitatively characterize the oceanic ecosystem of the northern GoM and to establish a time-series with which natural and anthropogenic changes could be detected. The approach was multi-disciplinary in nature and included *in situ* sampling, acoustic sensing, water column profiling and sampling, satellite remote sensing, AUV sensing, numerical modeling, genetic sequencing, and biogeochemical analyses. The synergy of these methodologies has provided new and unprecedented perspectives of an oceanic ecosystem with respect to composition, connectivity, drivers, and variability.

Keywords: micronekton, epipelagic, mesopelagic, bathypelagic, sampling, hydrography, acoustics, ecosystem structure

OPEN ACCESS

Edited by:
Jose Angel Alvarez Perez, Universidade do Vale do Itajaí, Brazil

Reviewed by:
Malcolm Ross Clark, National Institute of Water and Atmospheric Research (NIWA), New Zealand
Adela Roa-Varon, National Marine Fisheries Service (NOAA), United States

****Correspondence:***
April B. Cook
acook1@nova.edu

Specialty section:
This article was submitted to Deep-Sea Environments and Ecology, a section of the journal Frontiers in Marine Science

Received: *03 April 2020*
Accepted: *27 November 2020*
Published: *29 December 2020*

Citation:
Cook AB, Bernard AM, Boswell KM, Bracken-Grissom H, D'Elia M, deRada S, Easson CG, English D, Eytan RI, Frank T, Hu C, Johnston MW, Judkins H, Lembke C, Lopez JV, Milligan RJ, Moore JA, Penta B, Pruzinsky NM, Quinlan JA, Richards TM, Romero IC, Shivji MS, Vecchione M, Weber MD, Wells RJD and Sutton TT (2020) A Multidisciplinary Approach to Investigate Deep-Pelagic Ecosystem Dynamics in the Gulf of Mexico Following Deepwater Horizon. Front. Mar. Sci. 7:548880. doi: 10.3389/fmars.2020.548880

INTRODUCTION

Of the ecotypes of the Gulf of Mexico (GoM) affected by the *Deepwater Horizon* oil spill (DWHOS), the open-ocean pelagic ecotype was by far the largest. The spill began on April 20, 2010, about 66 km off the coast of Louisiana, at a depth ∼1,500 m and continued for 87 days (Beyer et al., 2016). Some percentage of oil, other hydrocarbons, and injected dispersant reached the sea surface and seabed, whereas 100% occurred within the deep-pelagic domain (200 m depth to just above the seafloor). During the summer of 2010, a continuous plume of oil over 35 km in length was discovered at approximately 1,100 m depth (Camilli et al., 2010). This plume persisted for several months, prompting concern about the effects of the DWHOS on the meso- and bathypelagic (200–1000 and >1,000 m depths, respectively; deep-pelagic, cumulatively) faunas. Deep-pelagic animals are known to vertically migrate to shallow, epipelagic (0–200 m depth) waters at night to feed (Sutton et al., 2020), a process which ostensibly increases exposure throughout the water column and connects the shallower and deeper parts of the oceanic GoM.

Gaining insight and understanding of pelagic ecosystems over time requires a multidisciplinary approach, given their complex physical (4-D, Lagrangian), biological, and ethological (vertically migratory) nature. Here we describe the sampling, sensing, and analysis methods of two major research programs, both aimed at characterizing effects, or potential effects, of the DWHOS on the epi-, meso-, and bathypelagic faunas of the northern GoM. The first program, ONSAP (Offshore Nekton Sampling and Analysis Program), was supported by the National Oceanic and Atmospheric Administration (NOAA) as part of the DWHOS Natural Resource Damage Assessment (NRDA) conducted in 2010–2015. This program encompassed *in situ* net sampling, water column profiling, and active acoustic sensing (**Supplementary Tables 1,2**) to address the question, "What could have been affected by the DWHOS in the deep-pelagic GoM?" The dearth/lack of pre-DWHOS data and the needs of the NRDA process required this initial approach. The second program was DEEPEND (DEEp PElagic Nekton Dynamics), a research consortium supported by The Gulf of Mexico Research Initiative (GoMRI) from 2015 to 2020. This program, which added satellite remote sensing, AUV sensing, physical oceanographic numerical modeling, pelagic microbial ecology, genetic analysis, biogeochemical analysis, and trophic ecology (**Supplementary Tables 3,4**) was both a continuation and evolution of ONSAP. The additions to DEEPEND, when integrated with foundational information from ONSAP, addressed the questions, "What are the natural drivers of pelagic ecosystem structure in the GoM?" and "Did pelagic faunal abundance variations after DWHOS exceed this 'natural envelope'?"

SURVEY APPROACH

The overall goal of the initial ONSAP project was to survey and quantify the deep-pelagic life forms living within or traveling through the area of the GoM affected by the oil spill (Frank et al., 2020; Sutton et al., 2020). Of interest was the water column fauna at the mesopelagic/bathypelagic interface, the depth stratum containing the deep hydrocarbon plume. The plume was discovered in areas surrounding the Macondo wellhead where the spill originated. To accomplish this goal, a multi-disciplinary approach was used. Acoustic profiles were collected to synoptically quantify organisms distributed throughout the water column. These can easily be repeated for comparisons across space and time. While a very useful tool, acoustics cannot discern between individual species nor can it detect many deep-pelagic organisms without swim bladders or air pockets. Discrete-depth midwater trawling was conducted to identify and quantify the organisms collected during both day and night to account for vertical migration. These results also help to ground truth the acoustic profiles. Environmental factors such as temperature, conductivity, and dissolved oxygen were collected from both trawl-mounted sensors and CTD rosette profiling from 0 to 1500 m depth. Details of survey design and methodologies are described further below.

When planning the DEEPEND program, several additional components were added to the survey approach to fill in data gaps and to expand on research objectives. A remote sensing and satellite imagery component was added to identify mesoscale oceanographic and riverine discharge features to inform planning and execution of field work (e.g., Androulidakis et al., 2019). A glider was deployed to collect oceanographic data that were assimilated in the ocean model which was used to establish DEEPEND cruise tracks. This multidisciplinary methodology, integrating physical oceanographic modeling, satellite observation, and *in situ* sensing, provided the spatiotemporal habitat context by which pelagic faunal composition, abundance and distribution were analyzed (i.e., biophysical coupling; Meinert et al., 2020; Milligan and Sutton, 2020; Pruzinsky et al., 2020).

A biogeochemical component was added to directly measure the amount of petrogenic contamination in animal organs, muscle tissues, and eggs using polycyclic aromatic hydrocarbons (PAHs) as a proxy (Romero et al., 2018, 2020). A molecular taxonomy component (DNA barcoding; Hebert et al., 2003) was added to help identify damaged, cryptic, and juvenile specimens where morphological characters do not yet exist or could not differentiate between species (e.g., Moore et al., 2020). The gene sequences analyzed are well established as robust markers for species identification of marine fishes (Ward et al., 2009) and invertebrates (Mantelatto et al., 2018). A population genomics component was added (double-digest Restriction Associated DNA sequencing; ddRADseq) to study genetic diversity and connectivity of the GoM and adjacent water deep-pelagic fauna (Timm et al., 2020b). Genetic diversity and connectivity can be used as proxies to measure population health and resilience (Oliver et al., 2015). Over a time-series, these measures can show how diversity is maintained and restored in the face of anthropogenic and/or natural disasters. A trophic ecology component, using Stable isotope analysis (SIA), was added to identify feeding relationships among taxa, estimate trophic positions, and delineate energy flow (Richards et al., 2020). Understanding the flow of energy through this deep-sea

ecosystem is essential to be able to identify linkages which may be vulnerable to disasters such as an oil spill. A microbial ecology component was added to help characterize pelagic habitats (along with environmental and ocean modeling data) and to investigate the dynamics of diel vertical migration using acoustic backscatter data and eDNA sampling (Easson et al., 2020).

The time-series aspect of these two programs provides information on the patterns of abundance and distribution of the pelagic fauna, the concentration of PAHs therein, and the pattern of genetic diversity following a major marine disaster. Information such as this also provides a basis against which to compare hindcast-derived abundance estimates using proxies for data that did not previously exist (e.g., larval and adult deep-pelagic fish abundance relationships; the former data were collected prior to the DWHOS, while the latter were not). The multidisciplinary nature of these two programs facilitates an ecosystem-based approach to guide interpretations of assemblage-level data. For example, using ddRADseq in combination with physical oceanographic modeling provided evidence that the Loop Current could be facilitating genetic connectivity in pelagic shrimps, with its concomitant implications for the recovery and resilience of a species (Timm et al., 2020a). In another example, microbial assemblages were characterized using abiotic and biotic data collected via CTD sensing and their dynamics interpreted using MODIS satellite imagery (Easson and Lopez, 2019). In summary, results derived from each component were valuable in their own right, but each also added necessary information for other working groups.

Transect Design

During ONSAP field operations, a subset of the Southeast Area Monitoring and Assessment Program (SEAMAP; Eldridge, 1988) stations surrounding the DWHOS site was sampled (**Figure 1**), with original station nomenclature maintained. Sampling the entire 46-station grid took approximately 3 months, requiring that sampling be divided into several legs for resupply and personnel changes. This necessity dictated that sampling transects be arranged by logistics (time to station, weather, and personnel availability) in lieu of oceanographic and/or ecological considerations. Sampling, acoustic sensing, and water column profiling were conducted twice at each station (day and night). Sampling of the entire grid was conducted three times over a 9-month period, with each station being occupied either three (most stations) or two times over the course of ONSAP (**Figure 1**).

Due to time constraints, only a portion of the stations sampled during ONSAP were sampled during individual DEEPEND cruises, each of which lasted approximately 15 days. DEEPEND cruise tracks were designed to transect as many water masses (Common Water and Loop Current, *sensu* Johnston et al., 2019; Boswell et al., 2020) and mesoscale features (eddies, Mississippi River plumes) as possible during each cruise in order to model faunal assemblage structure, abundance, and distribution as a function of biophysical drivers. Because the location, intensity, and persistence of the GoM's salient oceanographic features are constantly in flux, we considered both hindcasts and forecasts of hydrographic conditions from the United States Naval Research Laboratory's Hybrid Coordinate Ocean Model (HYCOM; see section "Hybrid Coordinate Ocean Model") along with satellite imagery (see section "Remote sensing/chlorophyll") in selecting the location and timing of DEEPEND sampling stations from the original ONSAP sampling grid (**Figure 2**). This "directed sampling" approach allowed statistical analysis of population and assemblage variability as a function of environmental variability,

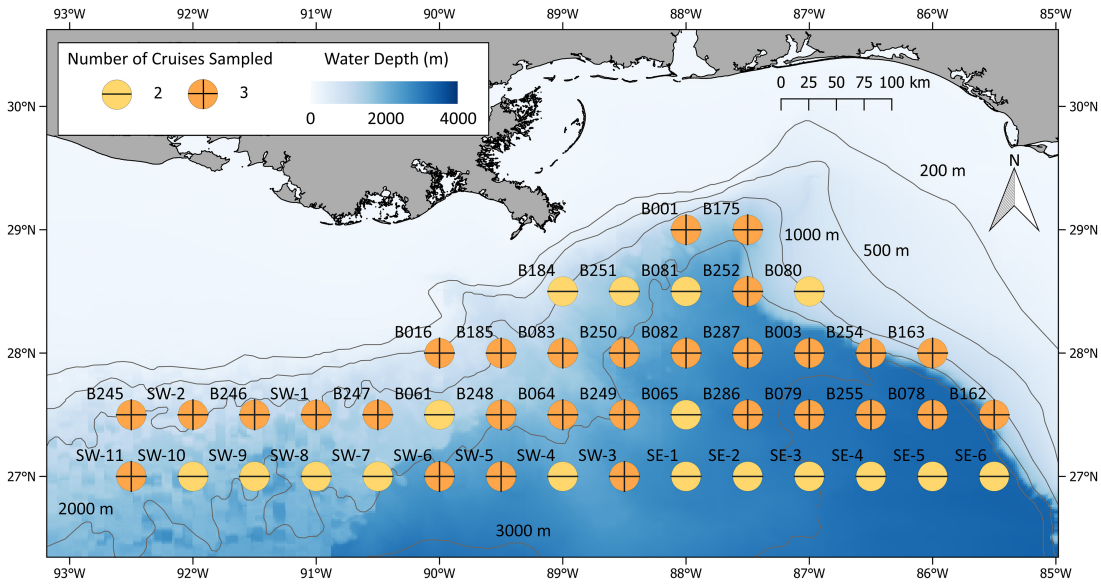

FIGURE 1 | ONSAP MOC10 stations sampled during the winter, spring, and summer 2011. Symbol colors represent the number of seasons (up to three) each location was sampled.

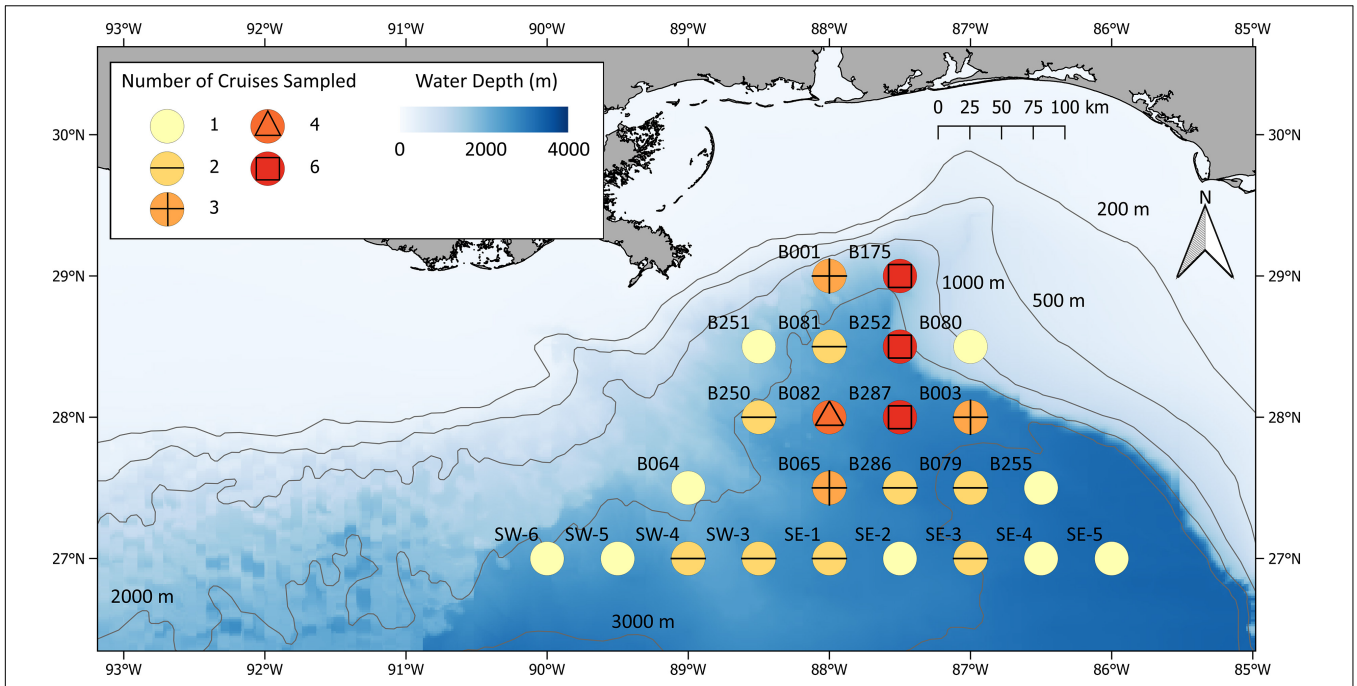

FIGURE 2 | DEEPEND MOC10 stations sampled between 2015 and 2018. Symbol colors represent the number of cruises during which each location was sampled.

a methodology applied to both DEEPEND and the preceding ONSAP data.

Hybrid Coordinate Ocean Model

Hybrid Coordinate Ocean Model (HYCOM), implemented at 1/25° horizontal-resolution for the GoM (18 to 31° N., 77 to 98° W.), was run in "real-time" in the weeks before and during the DEEPEND cruises (DP01 through DP06, **Supplementary Table 3**), providing surface and sub-surface predictions through the pelagic ocean. In order to sample important features, pre-determined cruise tracks and stations were adjusted depending on proximity to these predicted mesoscale oceanographic features (e.g., eddies and fronts). Model predictions were delivered in the form of "first-look" visualizations via web portals. The model was configured with a 32-layer hybrid (σ/z/ρ) time-variant vertical structure, which was post-processed into a time-invariant, 50-level, *z*-vertical structure for end-user dissemination. In this configuration, the model assimilated daily observations using 3-D variational data-assimilation, received (initial) boundary information from the Global Ocean Forecasting System (Metzger et al., 2014), and was forced by 3-h momentum and heat fluxes from the Navy Global Environmental Model (NAVGEM). Tidal boundary conditions for water level and barotropic velocity were provided by the global Ocean Tide Inverse Solution (OTIS), and rivers were implemented as a "precipitation bogus," specified by a monthly climatological database. Further information and detailed documentation about HYCOM can be found at hycom.org.

For the DEEPEND cruise campaigns, the model provided up to 120 h of forecasts, at 3-h frequency, of the 3-D oceanic physical environment (sea surface height, ocean currents, temperature, and salinity). The HYCOM model was initialized on January 1, 2015 and ran continuously through December 31, 2018. Its outputs for 2015 (Cruises DP01 and DP02), 2016 (DP03 and DP04), 2017 (DP05), and 2018 (DP06) were deposited in the Gulf of Mexico Research Initiative Information and Data Cooperative (GRIIDC; **Supplementary Table 5**).

Remote Sensing/Chlorophyll

In the GoM, the location and intensity of mesoscale features can change dramatically in a few days, requiring that ocean color imagery be used to determine the precise location of surface features (e.g., **Figure 3**), especially the location of Mississippi River plumes and the Loop Current. While the location of surface fronts may not coincide with water mass boundaries at bathypelagic depths, the material and energetic relationships between euphotic and deeper waters were considerations when planning DEEPEND sampling transects.

Ocean color satellite images from the Moderate Resolution Imaging Spectroradiometer (MODIS) satellite were processed at the University of South Florida (USF) Optical Oceanography Laboratory through a Virtual Antenna System (VAS; Hu et al., 2013). Ocean color imagery is based on spectral reflectance of the surface ocean, which depends on the absorption and scattering of sunlight in near surface waters and therefore carries information on surface water constituents such as phytoplankton chlorophyll and colored dissolved organic matter (CDOM). The chlorophyll imagery was derived using NASA standard algorithms to remove atmospheric effects and convert surface reflectance to chlorophyll (Hu et al., 2012). Clouds, sunlight, and limited viewing angles can reduce the area of reliable ocean color satellite data. Thus, multi-day composites of MODIS ocean color imagery were created

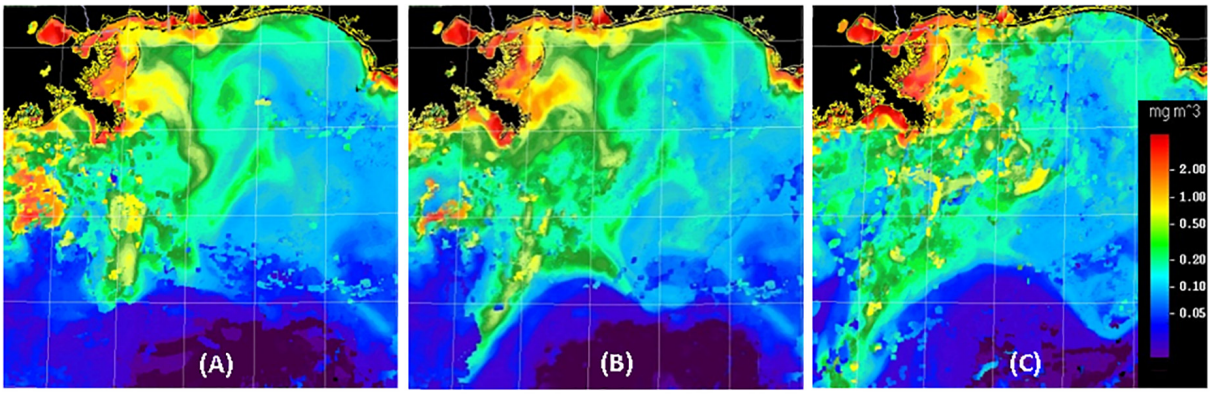

FIGURE 3 | Examples of MODIS ocean-color composite images created for the DEEPEND study region (26–30°N, 85–91°W) during DP06 (**A–C** for July 22, 25, and 30, 2018, respectively). Imagery from several days was combined to emphasize recent surface feature locations. In agreement with HYCOM model predictions, features in the left portion of these images tended to move toward the southwest at more than 20 km per day, while features in the lower central portion of the images were influenced by the Loop Current and moved to the east-southeast at about 50 km per day.

to decrease the fraction of the cruise area imagery that would otherwise have been masked or obscured. Due to the movement of surface fronts (sometimes more than 20 km over several days; **Figure 3**), satellite images from several days (up to a week) were combined such that the locations of ocean color features in the most recent images would be emphasized. The composites were sent to the Chief Scientist aboard the ship and the supervisor of glider operations so that transects could be adjusted to avoid or examine particular features. While sea surface temperature (SST) imagery was also examined, solar heating of the surface waters diminished the practical use of SST imagery to monitor the changing location of mesoscale features during the late-season (August) cruises.

FIELD SAMPLING AND WATER-COLUMN SENSING

Net Sampling

The vertical distribution of micronekton in the water column from the surface to 1,500 m was quantified by sampling discrete-depth intervals using a Multiple Opening Closing Net and Environmental Sensing System (Wiebe et al., 1985; Sutton et al., 2010) with an effective mouth area of 10 m^2 (referred to as MOC10 hereafter; **Figure 4**) when towed at a 45^o angle. The MOC10 (3.41 × 4.69 m mouth opening) was equipped with six nets of 3-mm uniform mesh which were opened and closed at specific depth intervals on command from the ship through conducting trawl wire. This procedure yielded one oblique sample from the surface to the maximum depth sampled (net 0) and five discrete-depth samples (nets 1–5, **Table 1**). The rationale for these depth intervals, following Sutton (2013) and listed from deep to shallow, was: Net (1) sample the bathypelagic fauna living below the deep hydrocarbon/dispersant plume [i.e., below 1,200 m depth; Net (2)] sample the bathypelagic fauna within the stratum occupied by the deep plume (1,000 to 1,200 m depth); Net (3) sample the deep mesopelagic fauna (600 to 1,000 m, the daytime depths of occurrence of most vertically migrating taxa and persistent depth of occurrence of non-migrating mesopelagic taxa); Net (4) sample the fauna within the upper mesopelagic zone (200–600 m, daytime depths of shallow mesopelagic migrators and nighttime depth of weakly migrating taxa); and Net (5) sample the fauna of the epipelagic zone (0–200 m, the nighttime depths of most vertically migrating mesopelagic taxa and persistent depth of non-migrating surface fauna). Trawling was conducted twice at each station, centered at solar noon and midnight, to quantify diel vertical migration. Instruments were mounted to the trawl frame to measure depth, temperature, and salinity [conductivity], as well as the mouth angle of the net through the water. The volume of water filtered by each MOC10 net was measured by a Tsurumi-Sikie-Kosakusho Co., Ltd. flowmeter mounted on the MOC10 frame (adjusted for towing angle) facing directly into the flow of water. The trawl was towed at 1.5–2.5 knots and retrieved at a rate of 5 m min^{-1}. The total volume of water filtered varied by net depth stratum and ranged from 6,500 to 70,000 m^3 (**Supplementary Tables 1,3**). During the ONSAP, MOC10 sampling on the M/V *Meg Skansi* occurred almost continuously from January to September 2011 (**Figure 1**). In total, 241 trawl deployments were conducted at 58 stations, yielding 936 quantitative, discrete-depth samples (**Supplementary Table 1**). During DEEPEND, sampling occurred in either May or August (the height of dry and wet seasons in the GoM, respectively) aboard the R/V *Point Sur* from 2015–2018 (**Figure 2**). In total, 122 trawl deployments were conducted at 24 stations, yielding 470 quantitative, discrete-depth samples (**Supplementary Table 3**). A quantitative sample was defined as having been collected within the depth bins detailed in **Table 1** as well as having a valid measurement of the volume of seawater filtered by that net.

The MOC10 system was chosen for its discrete-depth sampling capability (versus non-closing nets), a key consideration for quantifying the abundance of vertically migrating taxa. The 10 m^2 MOCNESS was chosen over a 1 m^2 MOCNESS, as the former selects for micronekton (2–20 cm body

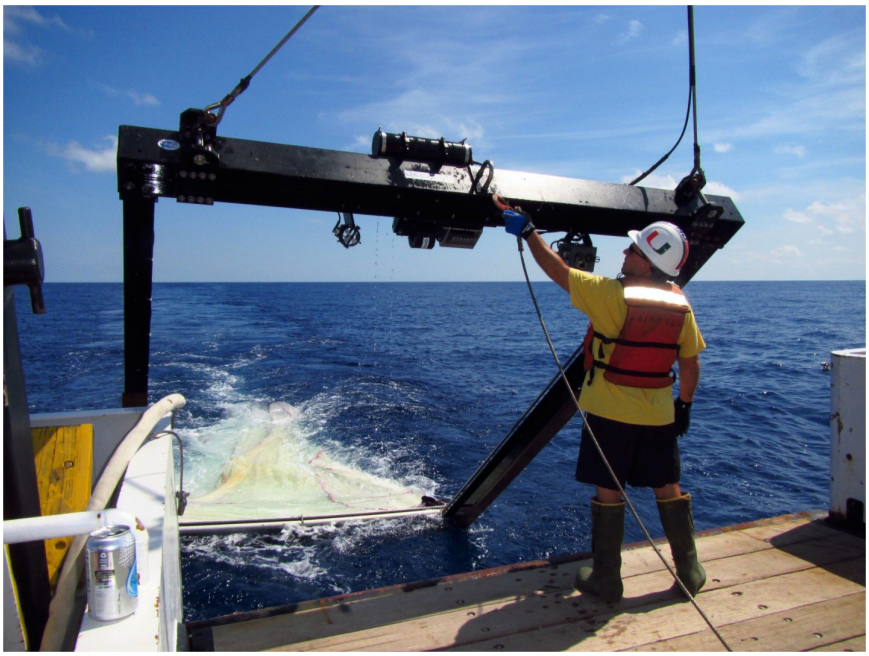

FIGURE 4 | MOC10 unit used to quantitatively sample discrete-depth strata during ONSAP and DEEPEND cruises. Image courtesy of DEEPEND/Danté Fenolio. Written informed consent was obtained from the individual for the publication of any potentially identifiable images included in this article.

length) as opposed to plankton (Wiebe and Benfield, 2003). The fixed mouth area and the integrated flow meter allow for precise quantitative sampling, a prerequisite for time-series analysis. Lastly, the MOC10 can be deployed from an intermediate (regional-class) research size vessel with a single aft winch and conducting cable. Larger, dual-warp trawls require larger, fisheries-capable research vessels whose expense and availability are often prohibitive. That said, there are caveats with any sampling system, including the MOC10. The mouth and mesh size of rectangular midwater trawls limit the speed at which they can be towed, allowing for net avoidance by larger, more mobile taxa (Pearcy, 1983; Kaartvedt et al., 2012; Kwong et al., 2018). The multiple opening/closing nets may also be prone to "net contamination," where animals from non-target strata can squeeze through the mouth bars of a closed net. We found the latter to be infrequent, and readily recognizable when it occurred. Taking all these factors into consideration, the MOC10 was determined to be the best gear to sample deep-pelagic micronekton/nekton in the GoM in a quantitative fashion in order to accomplish the goals of ONSAP and DEEPEND.

TABLE 1 | Discrete-depth ranges targeted for sampling via MOC10 during both ONSAP and DEEPEND cruises.

Net number	Depth range (m)
Net 0	0–1500
Net 1	1500–1200
Net 2	1200–1000
Net 3	1000–600
Net 4	600–200
Net 5	200–0

Midwater Trawl Sample Processing

ONSAP

After each MOC10 deployment and retrieval, individual nets were washed down with seawater and the contents of each codend were rinsed into separate numbered containers. Specimens from each codend sample were then concentrated with a sieve and placed into labeled collection jars and preserved. Larger specimens were curated separately in labeled jars. Nets 1–5 were preserved with buffered 10% formalin: seawater, while net 0's were preserved in 95% non-denatured ethanol (EtOH) for genetic analyses. When the size or amount of gelatinous zooplankton exceeded storage capacity, individuals of each taxon were sorted into a graduated beaker, the volume and weight recorded, and the animals discarded at sea. The remaining gelatinous individuals were preserved with the rest of the catch. No subsampling occurred during at-sea processing. After each cruise, the samples were transported to Nova Southeastern University's (NSU) Oceanic Ecology Laboratory, where they were sorted by major taxon, and distributed to the appropriate laboratory for species-level identifications by experts within each major taxonomic group. Specimens were then enumerated, weighed, and measured. Data were entered and stored as described in section "Biotic databases."

DEEPEND

Midwater trawl sample processing at sea was more involved during DEEPEND than ONSAP (i.e., there was extensive subsampling for genetic and biogeochemical analyses), requiring

additional handling and data management procedures. Upon retrieval of the MOC10, catches from each net were rinsed into separate containers and kept in cold (4°C) seawater during shipboard processing. This step is extremely important; deep-pelagic animals tend to degrade quickly at room temperature due to their chemical composition. Samples were sorted separately and sequentially to avoid mixing specimens from different collection nets (i.e., depth strata). While each sample was being processed, all others were stored in a refrigerator at 4°C.

Fishes, crustaceans, and cephalopods were rough-sorted by higher taxon and then identified to lower taxonomic levels (usually species) by onboard taxonomic specialists. Identified animals were counted and weighed to the nearest gram on a motion-compensating scale in batches per lowest taxonomic unit. Up to 25 specimens of each taxonomic unit were measured to the nearest millimeter per sample. All data were entered directly into the DEEPEND Nekton Database at sea (see section "Biotic databases" for biotic database description). Animals that were not subsampled for other analyses (described below) were preserved and brought back to the lab. Animals that were not identified to species at sea were examined in the lab post-cruise for further identification.

Genetics sub-sampling

As part of DEEPEND's initiative to catalog the species diversity of the deep-pelagic waters of the GoM, a ∼650 bp segment of the mitochondrial Cytochrome c oxidase I (COI) gene and/or a ∼550 bp segment of the large mitochondrial subunit 16 or 28S genes were sequenced from a subset of fishes, crustaceans, and cephalopod species. This method, "DNA barcoding," allows researchers to use a partial DNA sequence to identify an organism to the species level. It is particularly helpful in cases where the specimen represents an undescribed, "cryptic" species, an undescribed early-life-history form, or when definitive morphological characters are not available (e.g., male anglerfishes, trawl-damaged specimens, etc.).

Tissue samples for genetic barcoding were taken from up to 10 specimens of each fish species and up to five specimens of each crustacean and cephalopod species collected during DEEPEND cruises. Initial morphological identifications were conducted at sea, and subsequently checked by COI, 16S, and/or 28S barcoding (depending on taxonomic group). Tissues were preserved in either 95% non-denatured EtOH or RNALater. In addition to these samples, up to 50 tissue samples per cruise were collected for temporal population genomics studies (ddRADseq; Peterson et al., 2012) of eight fish species and six crustacean species (Timm et al., 2020b, **Supplementary Table 6**). Additionally, tissue samples from three species of cephalopods were used to compare the genetic connectivity of each species between the GoM (**Supplementary Table 6**) and the Bear Seamount region of the northern Atlantic Ocean (Timm et al., 2020a). In all cases, paired plastic identification tags were kept with each tissue sample and the corresponding individual voucher specimen to maintain data integrity before, during, and after barcoding procedures.

These methods have proven useful for the study of diversity, health and resilience in the GoM (Judkins et al., 2016, 2020; Timm et al., 2019, 2020a,b). A major challenge of the DNA barcoding method was matching the genetic sequences with those already submitted by other researchers in the Barcode of Life Database. There were many instances where either one genetic sequence had more than one species name assigned to it, multiple sequences were attributed to the same species, or the species name listed in the database conflicted with the identification made by DEEPEND taxonomic experts.

Stable isotope analysis sub-sampling

A thorough understanding of deep-pelagic ecosystems requires detailed knowledge of food webs including descriptions of feeding relationships among taxa, estimations of trophic position, and delineations of energy flow. Food webs have traditionally been examined through gut content analysis (GCA) which can require thousands of samples, a high level of taxonomic expertise, and is best suited for organisms that ingest prey whole. SIA is a powerful complement to GCA, as it is not as dependent on taxonomic expertise, can be applied to a range of taxa regardless of feeding mode, and can be conducted with fewer samples. However, interpretation of SIA data can be difficult due to significant spatiotemporal variation in the isotopic signatures of primary producers (isotopic baseline) which can be conserved in higher-order consumers resulting in misinterpretation of feeding relationships and incorrect trophic position estimates. Amino acid compound-specific isotope analysis (AA-CSIA) is a more refined technique that can help distinguish between variation in consumer isotopic signatures caused by changes in the isotopic baseline and changes in the diets and feeding habits of consumers (Popp et al., 2007). The method uses "source" amino acids that accurately reflect the isotope values of primary producers and "trophic" amino acids that can be used as indicators of change in consumer feeding and diet (McClelland and Montoya, 2002; Chikaraishi et al., 2009). Given the advantages of SIA, and because several high quality GCA datasets currently exist for deep-pelagic assemblages in the GoM (Flock and Hopkins, 1992; Hopkins et al., 1996), SIA and AA-CSIA were employed to provide a complementary description of the trophic structure of deep-pelagic assemblages in the GoM (Richards et al., 2019, 2020). To better inform the study design, catch data from MOC10 sampling and prior GCA investigations in the GoM were leveraged to identify numerically dominant species that represent important energy vectors connecting primary and secondary production with higher-order consumers. These species encompassed an array of migratory strategies (synchronous vertical migrators, asynchronous vertical migrators, and non-migrators) and feeding modes (**Supplementary Table 6**). Additionally, data from the HYCOM and MODIS were used to ensure specimens were collected from salient mesoscale features (e.g., cyclonic and anticyclonic eddies, Mississippi River plume), providing as complete a representation of deep-pelagic trophic structure as possible.

Following collection through MOC10 sampling, specimens for SIA and AA-CSIA were identified and enumerated at sea, with specimens selected for bulk SIA frozen whole at −20°C, while specimens selected for AA-CSIA were frozen whole in liquid nitrogen before transport to Texas A&M University at Galveston.

SIA and AA-CSIA specimens were kept in long-term storage at −20 and −80°C, respectively. Muscle tissue used for SIA and AA-CSIA was dissected from the lateral musculature of fishes, from the anterior portion of the mantle from cephalopods, and from the dorsal portion of the abdomen in decapod crustaceans. Samples were then rinsed with deionized water to remove trace carbonates, freeze dried, and homogenized using mortar and pestle. Information on remaining procedures during SIA and AA-CSIA can be found in Richards et al. (2019) and Richards et al. (2020).

Polycyclic aromatic hydrocarbon analysis sub-sampling

Polycyclic aromatic hydrocarbon (PAH) analyses were conducted on GoM deep-pelagic micronekton to determine the extent and persistence of DWHOS-derived oil contamination. Smaller fishes (<15 mm), cephalopods, and shrimp samples collected for PAH analysis were stored whole in pre-combusted (450°C for 4 h) glass vials and frozen in a −20°C freezer. The larger fishes (>15 mm) were dissected at sea to remove internal organs (liver, stomach, heart, and intestines), gills, muscle tissue, and eggs (if present). Each dissected tissue was stored separately and frozen. All samples were transported on dry ice to USF (**Supplementary Table 6**). Whole-body samples were dissected at USF to collect internal organs, muscle tissue, and eggs (if present) from fishes and shrimps, and mantle tissue and eggs (if present) from cephalopods. For a complete description of methods and findings for fishes see Romero et al. (2018) and for cephalopods see Romero et al. (2020).

In situ Sensing

Abiotic Sensing

MOC10 sensors

The MOC10 was outfitted with pressure (depth), temperature, and conductivity (salinity) sensors, which were calibrated annually. The sensors recorded a reading once every four seconds during the entire tow.

CTD sensors

ONSAP. A Sea-Bird SBE 19 plus V2 CTD profiling package was deployed at each station to at least 1,500 m (when the bottom depth was greater than 1600 m). Stations with water depths less than 1,600 m were profiled to full water column depth within 100 m of the bottom (**Supplementary Table 2**). The CTD was mounted to a 12-Niskin bottle (12-L) rosette and equipped with a dissolved oxygen sensor (Sea-Bird SBE-43), two fluorometers (WET Labs CDOM and WET Labs ECO-AFL/FL), and a turbidity meter (WET Labs ECO-NTU). The CTD data were processed following the DWH-NRDA CTD processing protocol. Calibrated data from each sensor were averaged in 1-m bins within Sea-Bird's SBE Processing software. For all deployments, only data from the downcasts were used in characterizing the water column structure.

DEEPEND. A 12-Niskin bottle (12-L) rosette with CTD was deployed from the R/V *Point Sur* at DEEPEND stations (**Figure 2**), usually to depths greater than 1,000 m. There were 106 CTD profiles collected during the DEEPEND cruises (**Supplementary Table 4**). The Sea-Bird 911plus CTD on the sampling rosette combined measurements of conductivity, temperature, and pressure, with additional sensors connected to the CTD on a per-cruise basis. These sensors included one or more dissolved oxygen sensors (Sea-Bird SBE-43), a transmissometer (WET Labs C-Star), and fluorometers (WET Labs ECO CDOM, ECO chlorophyll *a*, or Chelsea UV Aquatracka). The number and type of sensors varied between cruises, but information from the dissolved oxygen sensor and chlorophyll fluorometer was available at almost all of the DEEPEND stations. The CTD data were post-processed using Sea-Bird's SBE Data Processing software, which converted the data to engineering units as well as computed salinity and dissolved oxygen concentrations. To increase the consistency of *in situ* chlorophyll *a* fluorometer results between the DEEPEND cruises, the measurements of water-sample chlorophyll *a* and CDOM absorbance were used to scale the CTD's *in situ* fluorometer measurements. The measurements were binned (using median values) into 1-m depth intervals. Both the raw and binned CTD data for each DEEPEND cruise are available through the GRIIDC data repository (**Supplementary Table 5**).

Slocum glider sensing

During select DEEPEND cruises, a 1000-m depth-rated Slocum Electric Glider (**Figure 5**) was used to characterize the upper 400 m (on average) of the GoM water column. The glider was equipped with a Seabird SBE41CP CTD, two WET Labs fluorometers, two Satlantic radiometers, and an Aanderaa dissolved oxygen sensor. The fluorometers were equipped to sample for chlorophyll, CDOM, backscatter at 660 and 880 nm, and turbidity. All sensors sampled at 0.25 Hz. The radiance and irradiance sensors sampled at four wavelengths: ∼412, 443, 556, and 683 nm. The glider transited vertically between 2 m and max depth (ranging from 400–800 m) at ∼0.1 m/s which resulted in a vertical sample resolution of ∼0.4 m. The measurements were taken at various depths and included conductivity, temperature, depth, chlorophyll fluorescence, gelbstoff fluorescence, dissolved oxygen, and light field measurements. While the glider was

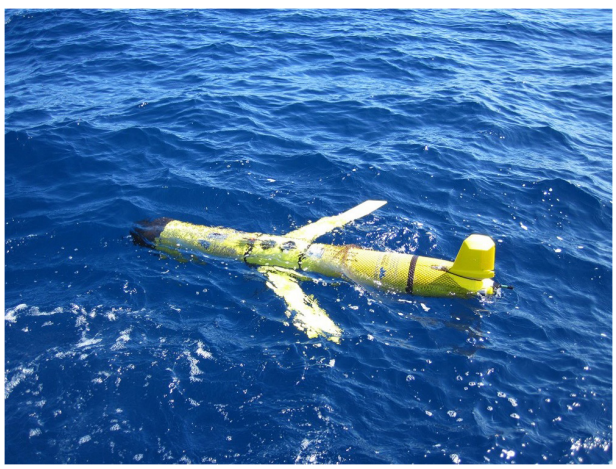

FIGURE 5 | Slocum glider during DP02 cruise deployment.

deployed at sea, it surfaced and communicated to an onshore control station at predetermined intervals, typically every 3 h. Launch, transit progress, and recovery of the glider position were planned and conducted, in part, by utilizing the HYCOM to provide context of the predicted current structure of the Loop Current and eddies. Model input for mission planning allowed glider adaptive sampling of features and assisted piloting to avoid unfavorable currents wherever possible. Once recovered, the complete measurement suite was downloaded from the vehicle, processed, and made available through USF and national data archives, including GRIIDC. The glider temperature and salinity data were assimilated into the HYCOM to assist in analyses of subsurface water characteristics and validation of ocean models, which was used to support the DEEPEND cruises.

Biotic Sensing

Acoustic backscatter

Two different vessels collected hydroacoustic data during the ONSAP and DEEPEND sampling programs. Simrad split-beam echosounder systems (EK60 and EK80) were used on both vessels; however, the transmitted frequencies varied according to vessel (**Table 2**). Transducers were mounted from a pole mount on both the M/V *Meg Skansi* and R/V *Point Sur*. While both vessels transmitted at 18 and 38 kHz, the higher frequencies were intermittently available. During each survey, the echosounder system was calibrated following the standard sphere method described by Demer et al. (2015). Measured gains and offsets derived from the Simrad lobe calibration program were recorded and input into the data analysis process. The echosounders were operated consistently among the surveys to ensure comparability over time. Multifrequency backscatter data were recorded simultaneously from each transceiver with a ping rate set to 0.2 Hz.

Analyses of raw backscatter data were processed in Echoview (PTY. Ltd.). Data were manually scrutinized for interference, noise, and other artifacts, and data processing routines were applied to reduce the effects of these on the processed data following methods outlined in D'Elia et al. (2016). Specifically, data were corrected for the effects of attenuation due to propagation losses and absorption. Intermittent noise spikes and transient noise were removed with Echoview (Ryan et al., 2015). Following that, a background noise removal process was applied (De Robertis and Higginbottom, 2007). Data were re-sampled at 500 m × 5 m (horizontal by vertical) elementary distance sampling units (EDSU) to generate analysis cells in which the echo integral was derived for each transect. Multifrequency comparisons were drawn to examine water-column backscatter between 18 and 38 kHz (D'Elia et al., 2016; Boswell et al., 2020).

The main limitation or bias associated with this method is attributing the backscatter to specific taxa. Using "ground-truth" data from direct biological sampling (i.e., nets) to interpret the backscatter patterns is the ideal methodology and was employed in both ONSAP and DEEPEND. Another potential limitation when using acoustic data across wide depth ranges is the potential effect of resonance when vertically migrating animals with gas bladders change depth. This effect occurs because backscattering intensity changes as a function of the surface area of a gas bladder. Therefore, it is important to interpret acoustic data carefully to account for this possibility (Davison et al., 2015; Proud et al., 2019).

Water Sampling

During DEEPEND cruises, CTD profiles were used to identify the depths of four "features of interest" at each station where water samples were collected. The features of interest included the surface layer, the chlorophyll-maximum layer, the oxygen-minimum zone, and the maximum trawl depth at each station. The depths of the chlorophyll maximum and oxygen-minimum zone, which varied by station, were determined visually during the CTD downcast using real-time data collected by fluorometer and oxygen sensors. Once the station-specific water collection depths were determined, three Niskin bottles were fired at each of the four targeted depths during the CTD upcast, yielding 36 L per depth.

Optical Absorption of Particulate and Dissolved Material and Determination of Chlorophyll a Concentration

The absorption of light within the surface waters is a dominant factor in determining ocean color. Measurements of the optical absorption spectra for particulates and dissolved material in water samples were collected because they provide information for the validation of ocean color imagery (e.g., section "Remote sensing/chlorophyll"), information about the pigment composition of phytoplankton in a water sample, and a measurement of the concentration of chlorophyll and dissolved material in that water sample. Samples from waters near the sea surface (<5 m depth) and the chlorophyll maximum were used not only to estimate the chlorophyll *a* concentration, but also to separate the water's optical absorption spectra into contributions from the sample's particulate material, $a_p(\lambda)$, detrital material, $a_d(\lambda)$, and CDOM, $a_{CDOM}(\lambda)$. Shortly after collection, samples were filtered through a glass fiber filter to separate the particulate constituents from a water sample, with additional filtration to partition the dissolved material. Both the filter pad and filtrate were then stored for additional processing and analysis ashore.

The chlorophyll *a* and CDOM measurements from the water samples were used to standardize the *in situ* fluorometry values as mentioned in section "DEEPEND". While the variability in the relationship between *in situ* fluorometric measurements and

TABLE 2 | Echosounder system properties used during multi-vessel studies in the GoM.

Program and date range	Vessel	Frequency (kHz)	Pulse duration [kHz]	Pulse rate (pps)
ONSAP, 2011	M/V *Meg Skansi*	18, 38, 70, 120, 200	4 ms [18, 38]; 1 ms [120]	0.2
DEEPEND, 2015–2018	R/V *Point Sur*	18, 38, 70, 120	4 ms [18, 38]; 1 ms [70,120]	0.2

chlorophyll *a* concentrations and the necessity of validation measurements is often acknowledged, the normalization of the fluorometric data is frequently omitted in presentations of the *in situ* fluorometry (Roesler et al., 2017). Not only was the *in situ* environment during the DEEPEND cruises different than those used for factory fluorometer calibrations, different fluorometers were used with the CTD on different cruises. The optical absorption information from the filter pads was used to improve the consistency of *in situ* fluorometric measurements between different casts and cruises.

The determination of optical absorption using this filter pad method requires several liters of sample water for the clear waters found throughout much of the DEEPEND sampling region. This relatively large volume of sample water, and the time and effort needed to filter and process that water, limits the number of water sampling depths that can be practically collected from a CTD cast. Though the samples were intended to capture representative waters from CTD profile features (e.g., chlorophyll maximum depth intervals), unsampled variations in planktonic composition and optical properties may occur within features. Chlorophyll *a* concentration and optical absorption spectra data are available through the GRIIDC data repository (**Supplementary Table 5**).

Microbial Community Characterization

Seawater microbial sampling followed routine methods, as described in Easson and Lopez (2019), to capture the dynamics of microbial plankton communities in relation to a host of biotic and abiotic factors. Briefly, seawater samples from all four targeted depths (surface, chlorophyll maximum, oxygen minimum, and maximum depth) were passed through 0.45-um hydrophilic mixed cellulose ester filters, which were then frozen and stored at −20°C for subsequent DNA extractions post-cruise. Subsequent next-generation sequencing and microbial community analyses were conducted following the methods of Easson and Lopez (2019). During seawater collection, environmental metadata were simultaneously collected with instruments on the CTD. These metadata provided context for determining function and structure of the subsequently described microbial communities.

The two main limitations of this method are that it does not directly identify the function of community members or provide an absolute abundance estimation (only relative abundance). Assumptions are made based on substantial literature evidence that these communities are responding directly to a particular influence. Despite these limitations, these data remain useful in capturing how microbial plankton dynamics are related to several biological and oceanographic variables.

Stable Isotope Analysis of Particulate Organic Matter

Because a consumer's isotopic signature is determined by both its position in the food web and the isotope value of primary producers, isotopic variation in primary producers can lead to isotopic variation in consumers not reflective of a change in diet or trophic status. Thus, when conducting SIA it is essential to characterize the isotopic signatures of relevant primary producers so that variation in consumer isotope values caused by shifting isotope values in primary producers can be distinguished from changes caused by differences in the feeding habits of consumers. In order to establish an isotopic baseline in the pelagic GoM, we conducted SIA on samples of particulate organic matter (POM) to serve as a proxy for phytoplankton primary production in the region. Water samples for POM were initially collected from 12-L Niskin bottles deployed during CTD casts and then transferred to clean 1-L Nalgene bottles, which were inverted into 500-ml Pall magnetic filter funnels. Samples of POM were then obtained by filtering 5 – 20 L of water through pre-combusted (2 h at 450°C) 47-mm (surface and chlorophyll maximum) and 25-mm (oxygen minimum and maximum trawl depth) glass microfiber filters (GF/F) under low pressure. Once sufficient material had been obtained, filters were stored frozen at −20°C until processing for SIA.

COLLECTIONS AND DATABASES

Specimen Collections

The majority of specimens (fishes, crustaceans, and gelatinous zooplankton) collected during both ONSAP and DEEPEND are housed at the Guy Harvey Oceanographic Center, Nova Southeastern University, Dania Beach, FL and tracked through the biotic databases described in section "Biotic databases." Molluscan specimens were deposited in the National Museum of Natural History, Washington, DC, United States, or at the USF St. Petersburg, St. Petersburg, FL, United States. All crustacean specimens used for genetics, including tissue and DNA extracts, were assigned catalog numbers (HBG#) in curated, databased research collections. All voucher specimens and tissues were archived in the Florida International Crustacean Collection (FICC), which currently houses over ∼10,000 curated crustacean specimens.

The holotypes and paratypes for new species discovered during these projects (e.g., Pietsch and Sutton, 2015; Judkins et al., 2020) were deposited in museum collections appropriate for each taxonomic group. Crustaceans and cephalopods were deposited at the National Museum of Natural History, Washington, DC, United States. Fishes will be deposited in one of several museums based on the specific taxon: Lophiiformes will be deposited at the Burke Museum, University of Washington, Seattle, WA, United States; Stomiiformes will be deposited at the Museum of Comparative Zoology, Harvard University, Cambridge, MA, United States; and representative subsets of the entire collection, or select specimens, will be deposited at the Scripps Institution of Oceanography, the Louisiana State University Ichthyology Collection, the Tulane Ichthyology Collection, the Virginia Institute of Marine Science Ichthyology Collection, the Yale Peabody Museum of Natural History, and the Florida Museum of Natural History.

Biotic Databases

All biotic data are stored in Microsoft Access databases at the Oceanic Ecology Laboratory at NSU (T. Sutton).

Data collected during the ONSAP are stored as "Nekton_Database_DDMMYY.accdb" and data collected during DEEPEND are stored as "DEEPEND_Nekton_Database_DDMMYY.accdb." These are relational databases stored on NSU's servers with replication. There are three main tables: (1) Field Sample/Trawl Field Data table containing the station and sampling depth information, (2) Nekton Database table containing the catch information (taxon, catch in numbers, weight, etc.), and (3) Taxon List table containing the hierarchical taxonomic information (class, order, family, etc.).

In addition, there are other tables to look up and combine data. A Primary Key connects these tables to one another.

Database Availability

DIVER

Biotic and abiotic data collected during the ONSAP are publicly available through NOAA's Data Integration Visualization Exploration and Reporting (DIVER) tool found at https://www.diver.orr.noaa.gov/. DIVER is a data warehouse and query tool that allows public access to NOAA's Damage Assessment, Remediation, and Restoration Program data. These data are collected in response to, and/or restoration of, environmental damage caused by oils spills, releases of hazardous waste, or vessel groundings. The DIVER Explorer query tool can be used to search, filter, and download these data using links to popular datasets, guided queries, or keyword searches. Data mentioned in this paper can be located by linking to the popular dataset "*Deepwater Horizon* NRDA data" and performing a keyword search for "*Meg Skansi*."

GRIIDC

Biotic (ONSAP and DEEPEND) and abiotic (DEEPEND only) data are also publicly available through the GRIIDC, housed at the Harte Research Institute for GoM Studies at Texas A&M University, Corpus Christi. GRIIDC is a team of researchers, data and topic specialists, and information technology professionals who have developed a data management system to organize, store, and disseminate data collected by GoM researchers as part of the Master Research Agreement between British Petroleum (BP) and the GoM Alliance. GRIIDC has secured a funding agreement with the GoMRI, the funding body of the GoM Alliance, to continue providing data management and the dissemination of datasets to the scientific community (both GoMRI funded and non-GoMRI funded research) for a minimum of 10 years beyond the conclusion of formal GoMRI funding in 2020 (i.e., through the year 2030, at a minimum).

All data produced by GoMRI-funded individuals and research consortia (such as DEEPEND) are required to be submitted to the GRIIDC repository in a timely fashion, typically within one year of data collection and/or processing. Upon submission, all datasets undergo a rigorous vetting process led by GRIIDC subject matter experts who work with researchers and the Data Manager to ensure data integrity, organization, and discovery, including descriptive, ISO-19115-2 compliant metadata. All datasets housed by GRIIDC are assigned Digital Object Identifiers (DOIs) in the same manner as publications to allow future researchers to use and cite the data. See **Supplementary Table 5** for a list of datasets and their corresponding DOIs. All datasets are available at https://data.gulfresearchinitiative.org/.

NCEI

Most environmental data, such as CTD and ship along-track measurements, were submitted on behalf of DEEPEND to the National Centers for Environmental Information (NCEI) through a proprietary process developed between NCEI and GRIIDC. Calibrated water column acoustic backscatter data, including associated metadata, collected during the DEEPEND program are also archived at NCEI. The archive includes raw acoustic backscatter data for each station that has corresponding net tow data (**Supplementary Table 5**).

NCBI

DNA sequences obtained from barcoding were submitted on behalf of DEEPEND to the National Center for Biotechnology Information (NCBI) database. A compendium of specimen information that includes ID Number, Cruise Number, Collection Date, Collection Location, Taxonomic Species Identity (Order, Family, Genus, and Species), and NCBI GenBank Accession Numbers have been deposited into GRIIDC (**Supplementary Table 5**). Additionally, the small subunit rRNA gene was sequenced from samples collected in the water column to identify the microbial community. These sequences were deposited in the NCBI Short Read Archive where bioproject accession numbers were assigned.

DATA AVAILABILITY STATEMENT

Data are publicly available through the Gulf of Mexico Research Initiative Information & Data Cooperative (GRIIDC) at https://data.gulfresearchinitiative.org (doi: 10.7266/N7R49P43; 10.7266/N7MC8XDC; 10.7266/n7-ceq1-5g82; 10.7266/N7GM85P1; 10.7266/N73R0QSX; 10.7266/N7PV6HS1; 10.7266/N7Q52N08; 10.7266/N7KD1W8J; 10.7266/N7VM49MP; 10.7266/N7QR4VK0; 10.7266/N7X065FZ; 10.7266/N70K26W5; 10.7266/n7-77gs-w736; 10.7266/N7FF3QFK; 10.7266/N7610XD5; 10.7266/N72805Q8; 10.7266/N7XG9P7F; 10.7266/N7JD4V45; 10.7266/n7-j3c9-4s47; 10.7266/N7TM78J6; 10.7266/N7ZC818X; 10.7266/N7NC5ZK6; 10.7266/N7ZK5F24; 10.7266/n7-bhzk-nh73; 10.7266/N7CN729W; 10.7266/N7H41PX6; 10.7266/N7474871; 10.7266/N76T0K11; 10.7266/N7BK19RB; 10.7266/n7-ac8e-0240; 10.7266/N70P0X3T; 10.7266/N7VX0DK2; 10.7266/N7XP7385; 10.7266/N7902234; 10.7266/n7-dd3p-t155; 10.7266/n7-05f6-th15; 10.7266/N7ZG6QQ9; 10.7266/N7XP73B2; 10.7266/N7HM56TD; 10.7266/N71C1TZC; 10.7266/n7-1xs7-4n30; 10.7266/n7-3p3y-g470; 10.7266/n7-hhnq-kh83; 10.7266/N75M63Q3; 10.7266/n7-c56k-dp86; 10.7266/N7VX0F19;

10.7266/n7-9yq3-3177; 10.7266/n7-rg4t-2k74; 10.7266/n7-67wg-mz19; 10.7266/n7-ws46-0612; 10.7266/n7-rmfn-4d68; 10.7266/N7GF0RW0; 10.7266/N7Z036HF; 10.7266/n7-k9tp-y248; 10.7266/n7-033n-s709; 10.7266/n7-awwx-4g13; 10.7266/N79K48MZ; 10.7266/N7P55KWX; 10.7266/N7833QCP; 10.7266/N7XD1026; 10.7266/N7QZ28B4; 10.7266/n7-jxss-1s14; 10.7266/n7-bf8a-hq12; 10.7266/n7-bzef-0e24; 10.7266/N7ZS2V04; 10.7266/N75D8Q7Z; 10.7266/n7-3t9h-8p38; 10.7266/N7319T92; 10.7266/N7ZP44GF; 10.7266/N73B5XHK; 10.7266/N7TX3CQ8; and 10.7266/N70Z71NN).

ETHICS STATEMENT

The animal study was reviewed and approved by the Florida Atlantic University Institutional Animal Care and Use Committee.

AUTHOR CONTRIBUTIONS

All authors conducted the research, analyzed the data, and contributed to the manuscript. AC and TS oversaw all aspects of this research, including specimen, sample, and data collection, analysis and data management. All authors have agreed to being listed as such and approve of the submitted version of this manuscript.

FUNDING

This research was funded in part by the NOAA Office of Response and Restoration and in part by a grant from The Gulf of Mexico Research Initiative (GoMRI).

ACKNOWLEDGMENTS

We thank the captains and crews of the M/V *Meg Skansi* and R/V *Point Sur* for their excellent shipboard services. We are thankful for the shore-based support from Continental Shelf Associates, particularly Gray Lawson and Eddie Hughes, and from the Louisiana Universities Marine Consortium. We thank Okeanus Science and Technology and Sea-Gear Corporation for equipment support. Our sincerest thanks to all of the students, laboratory techs, and research scientists who have helped collect and process an enormous sample set. This is contribution #230 from the Center for Coastal Oceans Research in the Institute of Water and Environment at Florida International University.

SUPPLEMENTARY MATERIAL

The Supplementary Material for this article can be found online at: https://www.frontiersin.org/articles/10.3389/fmars.2020.548880/full#supplementary-material

REFERENCES

Androulidakis, Y., Karourafalou, V., Le Hénaff, M., Kang, H. S., Sutton, T. T., Chen, S., et al. (2019). Offshore spreading of Mississippi waters: pathways and vertical structure under eddy influence. *J. Geophys. Res. Oceans* 124, 5952–5978. doi: 10.1029/2018JC014661

Beyer, J., Trannum, H. C., Bakke, T., Hodson, P. V., and Collier, T. K. (2016). Environmental effects of the *Deepwater Horizon* oil spill: a review. *Mar. Poll. Bull.* 110, 28–51. doi: 10.1016/j.marpolbul.2016.06.027

Boswell, K. M., D'Elia, M., Johnston, M. W., Mohan, J. A., Warren, J. D., Wells, R. J., et al. (2020). Oceanographic structure and light levels drive patterns of sound scattering layers in a low-latitude oceanic system. *Front. Mar. Sci.* 7:51. doi: 10.3389/fmars.2020.00051

Camilli, R., Reddy, C. M., Yoerger, D. R., Van Mooy, B. A. S., Jakuba, M. V., Kinsey, J. C., et al. (2010). Tracking hydrocarbon plume transport and biodegradation at Deepwater Horizon. *Science* 330, 201–204. doi: 10.1126/science.1195223

Chikaraishi, Y., Ogawa, N. O., Kashiyama, Y., Takano, Y., Suga, H., Tomitani, A., et al. (2009). Determination of aquatic food-web structure based on compound-specific nitrogen isotopic composition of amino acids. *Limnol. Oceanogr.-Meth.* 7, 740–750. doi: 10.4319/lom.2009.7.740

Davison, P. C., Koslow, J. A., and Kloser, R. J. (2015). Acoustic biomass estimation of mesopelagic fish: backscattering from individuals, populations, and communities. *ICES J. Mar. Sci.* 72, 1413–1424. doi: 10.1093/icesjms/fsv023

De Robertis, A., and Higginbottom, I. (2007). A post-processing technique to estimate the signal-to-noise ratio and remove echosounder background noise. *ICES J. Mar. Sci.* 64, 1282–1291. doi: 10.1093/icesjms/fsm112

D'Elia, M., Warren, J. D., Rodriguez-Pinto, I., Sutton, T. T., Cook, A., and Boswell, K. M. (2016). Diel variation in the vertical distribution of deep-water scattering layers in the Gulf of Mexico. *Deep Sea Res. Part I* 115, 91–102. doi: 10.1016/j.dsr.2016.05.014

Demer, D. A., Berger, L., Bernasconi, M., Bethke, E., Boswell, K., Chu, D., et al. (2015). Calibration of acoustic instruments. *ICES Coop. Res. Rep. No.* 326:133. doi: 10.25607/OBP-185

Easson, C. G., Boswell, K. M., Tucker, N., Warren, J. D., and Lopez, J. V. (2020). Combined eDNA and acoustic analysis reflects diel vertical migration of mixed consortia in the Gulf of Mexico. *Front. Mar. Sci.* 7:552. doi: 10.3389/fmars.2020.00552

Easson, C. G., and Lopez, J. V. (2019). Depth-dependent environmental drivers of microbial plankton community structure in the northern Gulf of Mexico. *Front. Microbiol.* 9:3175. doi: 10.3389/fmicb.2018.03175

Eldridge, P. J. (1988). The Southeast Area Monitoring and Assessment Program (SEAMAP): a state-federal-university program for collection, management, and dissemination of fishery-independent data and information in the southeastern United States. *Mar. Fish. Rev.* 50, 29–39.

Flock, M. E., and Hopkins, T. L. (1992). Species composition, vertical distribution, and food habits of the sergestid shrimp assemblage in the eastern Gulf of Mexico. *J. Crust. Biol.* 12, 210–223. doi: 10.2307/1549076

Frank, T. M., Fine, C. D., Burdett, E. A., Cook, A. B., and Sutton, T. T. (2020). The vertical and horizontal distribution of deep-sea crustaceans in the order Euphausiacea in the vicinity of the *Deewater Horizon* oil spill. *Front. Mar. Sci.* 7:99. doi: 10.3389/fmars.2020.00099

Hebert, P. D. N., Cywinska, A., Ball, S. L., and deWaard, J. R. (2003). Biological identifications through DNA barcodes. *Proc. R. Soc. Lond. B* 270, 313–321. doi: 10.1098/rspb.2002.2218

Hopkins, T. L., Sutton, T. T., and Lancraft, T. M. (1996). The trophic structure and predation impact of a low latitude midwater fish assemblage. *Prog. Oceanogr.* 38, 205–239. doi: 10.1016/s0079-6611(97)00003-7

Hu, C., Barnes, B. B., Murch, B., and Carlson, P. R. (2013). Satellite-based virtual buoy system to monitor coastal water quality. *Opt. Eng.* 53:051402. doi: 10.1117/1.OE.53.5.051402

Hu, C., Lee, Z., and Franz, B. (2012). Chlorophyll a algorithms for oligotrophic oceans: a novel approach based on three-band reflectance difference. *J. Geophys. Res.* 117:C01011. doi: 10.1029/2011JC007395

Johnston, M., Milligan, R., Easson, C., DeRada, S., Penta, B., and Sutton, T. (2019). An empirically-validated method for characterizing pelagic habitats in the Gulf

of Mexico using ocean model data. *Limnol. Oceanogr.-Meth.* 17, 362–375. doi: 10.1002/lom3.10319

Judkins, H., Lindgren, A., Villanueva, R., Clark, K., and Vecchione, M. (2020). A description of three new bathyteuthid squid species from the North Atlantic and Gulf of Mexico. *Bull. Mar. Sci.* 96, 281–296. doi: 10.5343/bms.2019.0051

Judkins, H., Vecchione, M., and Rosario, K. (2016). Morphological and molecular evidence of Heteroteuthis dagamensis in the Gulf of Mexico. *Bull. Mar. Sci.* 92, 51–57. doi: 10.5343/bms.2015.1061

Kaartvedt, S., Staby, A., and Aksnes, D. L. (2012). Efficient trawl avoidance by mesopelagic fishes causes large underestimation of their biomass. *Mar. Ecol. Prog. Ser.* 456, 1–6. doi: 10.3354/meps09785

Kwong, L. E., Pakhomov, E. A., Suntsov, A. V., Seki, M. P., Brodeur, R. D., Pakhomova, L. G., et al. (2018). An intercomparison of the taxonomic and size composition of tropical macrozooplankton and micronekton collected using three sampling gears. *Deep Sea Res. Part I* 135, 34–45. doi: 10.1016/j.dsr.2018.03.013

Mantelatto, F. L., Terossi, M., Negri, M., Buranelli, R. C., Robles, R., Magalhães, T., et al. (2018). DNA sequence database as a tool to identify decapod crustaceans on the São Paulo coastline. *Mitochondrial DNA Part A* 29, 805–815. doi: 10.1080/24701394.2017.1365848

McClelland, J. W., and Montoya, J. P. (2002). Trophic relationships and the nitrogen isotopic composition of amino acids in plankton. *Ecology* 83, 2173–2180. doi: 10.1890/0012-9658(2002)083[2173:tratni]2.0.co;2

Meinert, C. R., Clausen-Sparks, K., Cornic, M., Sutton, T. T., and Rooker, J. R. (2020). Taxonomic richness and diversity of larval fish assemblages in the oceanic Gulf of Mexico: links to oceanographic conditions. *Front. Mar. Sci.* 7:579. doi: 10.3389/fmars.2020.00579

Metzger, E. J., Smedstad, O. M., Thoppil, P. G., Hurlburt, H. E., Cummings, J. A., Wallcraft, A. J., et al. (2014). US Navy operational global ocean and Arctic ice prediction systems. *Oceanography* 27, 32–43. doi: 10.5670/oceanog.2014.66

Milligan, R. J., and Sutton, T. T. (2020). Dispersion overrides environmental variability as a primary driver of horizontal assemblage structure of the mesopelagic fish family *Myctophidae* in the northern Gulf of Mexico. *Front. Mar. Sci.* 7:15. doi: 10.3389/fmars.2020.00015

Moore, J. A., Fenolio, D. B., Cook, A. B., and Sutton, T. T. (2020). Hiding in plain sight: elopomorph larvae are important contributors to fish biodiversity in a low-latitude oceanic ecosystem. *Front. Mar. Sci.* 7:169. doi: 10.3389/fmars.2020.00169

Oliver, T. H., Heard, M. S., Isaac, N. J., Roy, D. B., Procter, D., Eigenbrod, F., et al. (2015). Biodiversity and resilience of ecosystem functions. *Trends Ecol. Evol.* 30, 673–684.

Pearcy, W. G. (1983). Quantitative assessment of the vertical distributions of micronektonic fishes with opening/closing midwater trawls. *Biol. Oceanogr.* 2, 289–310.

Peterson, B. K., Weber, J. N., Kay, E. H., Fisher, H. S., and Hoekstra, H. E. (2012). Double digest RADseq: an inexpensive method for de novo SNP discovery and genotyping in model and non-model species. *PLoS One* 7:e37135. doi: 10.1371/journal.pone.0037135

Pietsch, T. W., and Sutton, T. T. (2015). A new species of the ceratioid anglerfish genus *Lasiognathus* Regan (*Lophiiformes*: *Oneirodidae*) from the northern Gulf of Mexico. *Copeia* 103, 429–432. doi: 10.2307/1446097

Popp, B. N., Graham, B. S., Olson, R. J., Hannides, C. C., Lott, M. J., López-Ibarra, G. A., et al. (2007). Insight into the trophic ecology of yellowfin tuna, *Thunnus albacares*, from compound-specific nitrogen isotope analysis of proteinaceous amino acids. *Terr. Ecol.* 1, 173–190. doi: 10.1016/s1936-7961(07)01012-3

Proud, R., Handegard, N. O., Kloser, R. J., Cox, M. J., and Brierley, A. S. (2019). From siphonophores to deep scattering layers: uncertainty ranges for the estimation of global mesopelagic fish biomass. *ICES J. Mar. Sci.* 76, 718–733. doi: 10.1093/icesjms/fsy037

Pruzinsky, N. M., Milligan, R. J., and Sutton, T. T. (2020). Pelagic habitat partitioning of late-larval and juvenile tunas in the oceanic Gulf of Mexico. *Front. Mar. Sci.* 7:257. doi: 10.3389/fmars.2020.00257

Richards, T. M., Gipson, E. E., Cook, A., Sutton, T. T., and Wells, R. D. (2019). Trophic ecology of meso-and bathypelagic predatory fishes in the Gulf of Mexico. *ICES J. Mar. Sci.* 76, 662–672. doi: 10.1093/icesjms/fsy074

Richards, T. M., Sutton, T. T., and Wells, R. D. (2020). Trophic structure and sources of variation influencing the stable isotope signatures of meso- and bathypelagic micronekton fishes. *Front. Mar. Sci.* 7:507992. doi: 10.3389/fmars.2020.507992

Roesler, C., Uitz, J., Claustre, H., Boss, E., Xing, X., Organelli, E., et al. (2017). Recommendations for obtaining unbiased chlorophyll estimates from in situ chlorophyll fluorometers: a global analysis of WET Labs ECO sensors. *Limnol. Oceanogr.-Meth.* 15, 572–585. doi: 10.1002/lom3.10185

Romero, I. C., Judkins, H., and Vecchione, M. (2020). Temporal variability of polycyclic aromatic hydrocarbons in deep-sea cephalopods of the northern Gulf of Mexico. *Front. Mar. Sci.* 7:54. doi: 10.3389/fmars.2020.00054

Romero, I. C., Sutton, T. T., Carr, B., Quintana-Rizzo, E., Ross, S. W., Hollander, D. J., et al. (2018). Decadal assessment of polycyclic aromatic hydrocarbons in mesopelagic fishes from the Gulf of Mexico reveals exposure to oil-derived sources. *Envir. Sci. Tech.* 52, 10985–10996. doi: 10.1021/acs.est.8b02243

Ryan, T. E., Downie, R. A., Kloser, R. J., and Keith, G. (2015). Reducing bias due to noise and attenuation in open-ocean echo integration data. *ICES J. Mar. Sci.* 72, 2482–2493. doi: 10.1093/icesjms/fsv121

Sutton, T. T. (2013). Vertical ecology of the pelagic ocean: classical patterns and new perspectives. *J. Fish Biol.* 83, 1508–1527. doi: 10.1111/jfb.12263

Sutton, T. T., Frank, T. M., Romero, I. C., and Judkins, H. (2020). "As Gulf oil extraction goes deeper, who is at risk? Community structure, distribution, and connectivity of the deep-pelagic fauna," in *Scenarios and Responses to Future Deep Oil Spills – Fighting the Next War*, eds S. A. Murawski, C. Ainsworth, S. Gilbert, D. Hollander, C. B. Paris, M. Schlüter, et al. (Cham: Springer), 403–418. doi: 10.1007/978-3-030-12963-7_24

Sutton, T. T., Wiebe, P. H., Madin, L., and Bucklin, A. (2010). Diversity and community structure of pelagic fishes to 5000 m depth in the Sargasso Sea. *Deep Sea Res. Part II* 57, 2220–2233. doi: 10.1016/j.dsr2.2010.09.024

Timm, L., Browder, J. A., Simon, S., Jackson, T. L., Zink, I. C., and Bracken-Grissom, H. D. (2019). A tree money grows on: the first inclusive molecular phylogeny of the economically important pink shrimp (*Decapoda*, *Farfantepenaeus*) reveals cryptic diversity. *Invertebr. Syst.* 33, 488–500.

Timm, L., Bracken-Grissom, H., Sosnowski, A., Breitbart, M., Vecchione, M., and Judkins, H. (2020a). Population genomics of three deep-sea cephalopod species reveals connectivity between the Gulf of Mexico and northwestern Atlantic Ocean. *Deep Sea Res. Part I* 158:103222. doi: 10.1016/j.dsr.2020.103222

Timm, L., Isma, L. M., Johnston, M. W., and Bracken-Grissom, H. (2020b). Comparative population genomics and biophysical modeling of shrimp migration in the Gulf of Mexico reveals current-mediated connectivity. *Front. Mar. Sci.* 7:19. doi: 10.3389/fmars.2020.00019

Ward, R. D., Hanner, R., and Hebert, P. D. (2009). The campaign to DNA barcode all fishes, FISH-BOL. *J. Fish Biol.* 74, 329–356. doi: 10.1111/j.1095-8649.2008.02080.x

Wiebe, P. H., and Benfield, M. C. (2003). From the Hensen net toward four-dimensional biological oceanography. *Progr. Oceanogr.* 56, 7–136. doi: 10.1016/s0079-6611(02)00140-4

Wiebe, P. H., Morton, A. W., Bradley, A. M., Backus, R. H., Craddock, J. E., Barber, V., et al. (1985). New development in the MOCNESS, an apparatus for sampling zooplankton and micronekton. *Mar. Biol.* 87, 313–323. doi: 10.1007/BF00397811

Conflict of Interest: The authors declare that the research was conducted in the absence of any commercial or financial relationships that could be construed as a potential conflict of interest.

Advantages of publishing in Frontiers

OPEN ACCESS
Articles are free to read for greatest visibility and readership

FAST PUBLICATION
Around 90 days from submission to decision

HIGH QUALITY PEER-REVIEW
Rigorous, collaborative, and constructive peer-review

TRANSPARENT PEER-REVIEW
Editors and reviewers acknowledged by name on published articles

Frontiers
Avenue du Tribunal-Fédéral 34
1005 Lausanne | Switzerland

Visit us: www.frontiersin.org
Contact us: frontiersin.org/about/contact

REPRODUCIBILITY OF RESEARCH
Support open data and methods to enhance research reproducibility

DIGITAL PUBLISHING
Articles designed for optimal readership across devices

FOLLOW US
@frontiersin

IMPACT METRICS
Advanced article metrics track visibility across digital media

EXTENSIVE PROMOTION
Marketing and promotion of impactful research

LOOP RESEARCH NETWORK
Our network increases your article's readership